THE APPLICABILITY OF PUBLISHED PAVEMENT DETERIORATION MODELS FOR NATIONAL ROADS

L KANNEMEYER

THE APPLICABILITY OF PUBLISHED PAVEMENT DETERIORATION MODELS FOR NATIONAL ROADS

LOUW KANNEMEYER

A dissertation submitted in partial fulfilment
of the requirements of the degree of

MASTER IN ENGINEERING (TRANSPORTATION ENGINEERING)

in the

FACULTY OF ENGINEERING

UNIVERSITY OF PRETORIA

December 1993

DISSERTATION SUMMARY

THE APPLICABILITY OF PUBLISHED PAVEMENT DETERIORATION MODELS FOR NATIONAL ROADS

L KANNEMEYER

Supervisor: Professor Doctor AT Visser
Department: Civil Engineering
University: University of Pretoria
Degree: Master of Engineering (Transportation Engineering)

The growing interest in pavement management systems (PMSs), both in South Africa and internationally, has been in response to a shift in importance from the construction of new roads to the maintenance of the existing paved network coupled with increasingly restrictive road funding. In order to develop a balanced expenditure programme for the national roads of South Africa there is a need to predict the rate of deterioration of a pavement and the nature of the changes in its condition so that the timing, type and cost of maintenance needs could be estimated. Internationally these expected changes in pavement condition are predicted by pavement deterioration models, which normally are algorithms developed mathematically or from a study of pavement deterioration.

Since no usable pavement deterioration models existed locally, it was necessary to evaluate overseas literature on pavement deterioration prediction models with the aim of identifying models possibly applicable to the national roads of South Africa. Only deterioration models developed from the deterioration results of in-service pavements under a normal traffic spectrum were evaluated. Models developed from accelerated testing were avoided since these models virtually eliminated long-term effects (these are primarily environmental but also include effects of the rest periods between loads), and that the unrepresentative traffic loading regimes can distort the behaviour of the pavement materials, which is often stress dependent. Models developed from the following studies were evaluated:

- AASHO Road Test
- The Kenya study
- Brazil-UNDP study (HDM-III models)
- Texas study

Of all the above models studied that were developed from major studies it was concluded that the incremental models developed during the Brazil study, were the most appropriate for further evaluation under South African conditions. A sensitivity analysis was conducted on the HDM-III models to evaluate their sensitivity to changes in the different parameters comprising each model. The results obtained from the sensitivity analysis indicate that the incremental roughness prediction model incorporated into the HDM-III model tends to be insensitive to changes in most parameters. Accuracy ranges for input data were, however, also identified for parameters which indicated an increase in sensitivity in certain ranges.

The local applicability of the HDM-III deterioration models were finally evaluated by comparing HDM-III model predictions with the actually observed deterioration values of a selected number of national road pavement sections. To enable the above comparison, a validation procedure had to be developed according to which the format of existing data could be transformed to that required by the HDM-III model, as well as additional information be calculated.

From the comparison it was concluded that the HDM-III models are capable of accurately predicting the observed deterioration on South African national roads, but that for most models calibration is needed for local conditions. Guidelines regarding recommended calibration factor ranges for the different HDM-III models are given.

Finally it is recommended that the HDM-III models should be considered for incorporation into a balanced expenditure programme for the national roads of South Africa.

SAMEVATTING VAN VERHANDELING

DIE TOEPASLIKHEID VAN GEPUBLISEERDE PLAVEISEL AGTERUITGANG MODELLE VIR NASIONALE PAAIE

L KANNEMEYER

Promotor:	Professor Doktor AT Visser
Departement:	Siviele Ingenieurswese
Universiteit:	Universiteit van Pretoria
Graad:	Magister in Ingenieurswese (Vervoeringenieurwese)

Die groeiende belangstelling in plaveisel bestuurstelsels (PBSs) beide in Suid-Afrika en internasionaal is die gevolg van 'n verskuiwing in prioriteit van die konstruksie van nuwe paaie na die instandhouding van die bestaande padnetwerk tesame met 'n vermindering in fondse beskikbaar vir paaie. Ten einde 'n ekonomies gebalanseerde bestedingsprogram vir die nasionale paaie van Suid-Afrika te ontwikkel, bestaan daar 'n behoefte om die tempo van agteruitgang van 'n plaveisel sowel as die veranderings in sy toestand met tyd te voorspel. Internasionaal word hierdie verwagte veranderinge in plaveisel toestand voorspel deur plaveisel agteruitgang modelle, wat meestal algoritmes gebaseer op wiskundige vergelykings of 'n plaveisel agteruitgang studie is.

Aangesien geen bruikbare plaveisel agteruitgang modelle plaaslik beskikbaar was nie, was dit nodig om oorsese literatuur te bestudeer ten einde plaveisel ageteruitgang modelle te identifiseer wat moontlik van toepasing kan wees op die nasionale paaie van Suid-Afrika. Slegs plaveisel agteruitgang modelle ontwikkel vanaf die agteruitgang resultate van plaveisels onder normale verkeer, is oorweeg. Agteruitgang modelle ontwikkel vanaf versnelde toetse met stilstaande toestelle is vermy. Hierdie modelle is vermy aangesien langtermyn effekte (meestal omgewingsfaktore, asook die effek van rusperiodes tussen lasaanwendings), glad nie ingesluit word nie. Verder kan die onverteenwoordigende lasaanwending die gedrag van sekere plaveisel materiale wat spanningsensatief is, beïnvloed. Modelle ontwikkel vanaf die volgende studies is geëvalueer:

- AASHO Padtoets
- Die Kenia studie
- Die Brasilië-UNDP studie (HDM-III modelle)
- Texas studie

Van al die bogenoemde modelle is die inkrementele modelle ontwikkel tydens die Brasilië studie geïdentifiseer as mees toepaslike vir verdere evaluasie onder Suid-Afrikaanse toestande. 'n Sensitiwiteitsanalise is op die HDM-III modelle uitgevoer om die sensitiwiteit van die modelle vir veranderinge in hulle parameters te bepaal. Die resultate van die sensitiwiteitsanalise dui daarop dat die inkrementele ongelykheidsmodel van die HDM-III model meestal onsensatief is vir veranderinge in meeste van sy parameters. Akkuraatheidsintervalle is egter geïdetifiseer vir die parameters wat 'n toename in sensitiwiteit in sekere gebiede getoon het.

Ten einde die plaaslike toepaslikheid van die HDM-III modelle te evalueer, is model voorspellings vergelyk met werklik waargenome toestande op 'n gekose aantal plaveiselseksies op nasionale paaie. Ten einde bogenoemde moontlik te maak moes 'n werkswyse ontwikkel word waarvolgens data omgeskakel kon word na die formaat wat deur die HDM-III model benodig word, sowel as addisionele inligting bereken kon word.

Vanaf bogenoemde vergelyking met waargenome waardes is tot die slotsom gekom dat die HDM-III modelle wel instaat is om die waargenome agteruitgang op nasionale paaie akkuraat te voorspel, maar dat kalibrasie van die modelle eers nodig is. Riglyne met betrekking tot kalibrasiegrense vir die verskillende HDM-III modelle is ook ingesluit.

Ten slotte word aanbeveel dat die HDM-III modelle oorweeg moet word vir insluiting in 'n ekonomies gebalanseerde bestedingsprogram vir die nasionale paaie van Suid-Afrika.

ACKNOWLEDGEMENT

I wish to express my appreciation to the following organisations and persons who made this dissertation possible:

- This dissertation is based on a research project of the South African Roads Board. Permission to use the material is gratefully acknowledged. The opinions expressed are those of the author and do not necessarily represent the policy of the board.

- Professor AT Visser, my supervisor for his assistance, guidance, support and understanding.

- VIAED, for providing the facilities that enabled me to carry out this study.

- The Catholic University of Santiago, Chile, for making the HDM-III calibration program available for use in this study.

- The assistance of the following persons is gratefully acknowledged during the course of the study:

  Mr JEB Basson, Division of Roads and Transport Technology, CSIR

  Mr A Caroca Baeza, VIAED

  Mr MJ Kemp, Division of Roads and Transport Technology, CSIR

  Prof SC van AS, VIAED

  Mr G van Zyl, Division of Roads and Transport Technology, CSIR

  Mr S van Wyk, Van Niekerk and Associates

TABLE OF CONTENTS

LIST OF TABLES

LIST OF FIGURES

CHAPTER 1

INTRODUCTION

1.1 BACKGROUND

The primary road network in South Africa has been established over the last half century and has been planned, constructed and maintained to provide as good a level of service as possible. However, the acute shortage of funds available for roads in South Africa is endangering the integrity of this network, putting a considerable emphasis on rationalising planning in the area of pavement maintenance and rehabilitation. Thus pavement management defined as *the total range of activities required to provide the pavement portion of the public works programme* (Draft TRH12 CSRA, 1991) has become more important.

An essential activity of pavement management is the modelling of the changes in pavement condition with accumulated use, generally known as pavement deterioration. These pavement deterioration models play a crucial role in several aspects of pavement management , and are included into international pavement management systems with the aim (George *et al*, 1989):

- To predict the time and type of maintenance required for individual road sections, and to prioritise the different pavement sections competing for maintenance.

- To enable the owner agency to estimate long-range funding requirements for pavement preservation and to analyse the consequences of different budgets on the future condition of the pavement network.

- To relate the influence of pavement exposure variables to pavement distress or to a combined performance index, to be used for design as well as the life-cycle economic evaluation of new pavements.

During the last two decades several major experiments were conducted internationally with the aim of developing pavement deterioration prediction

models. Some of the developed models or principles were incorporated into the latest pavement management systems used internationally. The pavement management system used in South Africa on national roads does not yet incorporate these pavement deterioration prediction models. At present the current condition of a pavement is used as a trigger for action to identify maintenance or rehabilitation projects in terms of the type of maintenance and the urgency (Walker and Curtayne, 1986).

The urgency ratings are defined according to a five point scale where 1 indicates a need for immediate attention and 5 a case where maintenance is unlikely to be required for a number of years. The parameters denoting the condition of a pavement are allocated according to the dominant strategy approach whereby the condition of the road is tested against a number of criteria . The criteria are based on expert opinion and Departmental policy.

The projects identified as requiring attention are verified by a panel of experts through a field inspection from which the projects are divided into a resurfacing programme and a priority list for rehabilitation. As illustrated in Figure 1.1 this method has a low probability of selecting the optimum rehabilitation strategy if the expected future deterioration of a pavement is not considered.

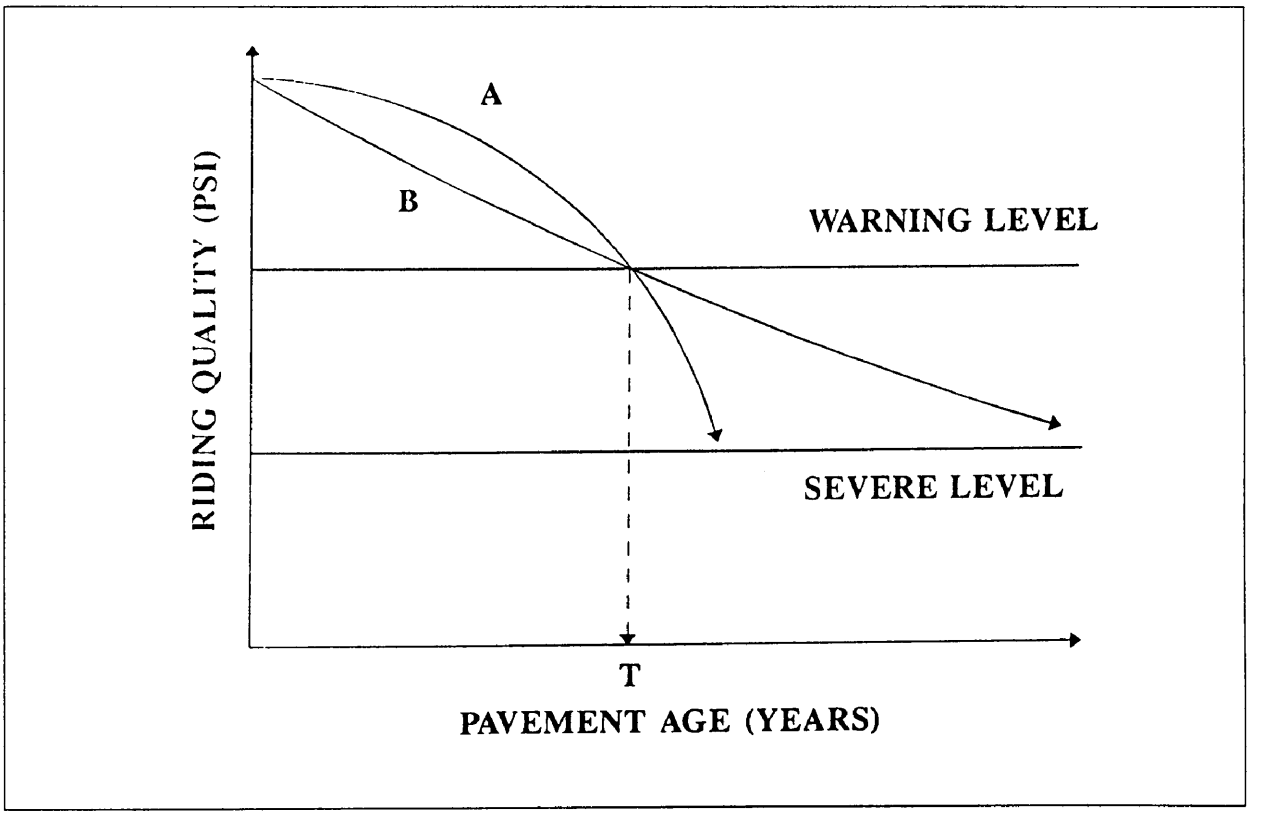

Figure 1.1: Expected future pavement deterioration.

Although both pavements A and B in Figure 1.1 have the same level of riding quality after T years, their expected future deterioration differs to a large extent. This demonstrates the need to use deterioration prediction models in pavement management systems to predict the timing, type and cost of future maintenance needs.

1.2 OBJECTIVES OF THE STUDY

The objective of the study is to use the information on flexible pavements obtained from the Department of Transport's extensive pavement management database, covering the deterioration of the national road network over the past 15 years, to achieve the following:

- To evaluate the applicability of models developed internationally for predicting the deterioration of the national road network in terms of roughness, cracking and rutting under the normal traffic and environmental conditions experienced on the in-service pavements.

- To develop calibration factors from long term observations, for the models identified as applicable for South African conditions if the models are inappropriate for predicting the deterioration trends observed on the South African national road network.

1.3 SCOPE OF THE STUDY

The study is directed towards the review of available literature on international deterioration models developed from the deterioration results of in-service pavements under the normal traffic spectrum, avoiding models developed from accelerated testing with stationary devices. The reasons for avoiding these models are that the long-term effects are virtually eliminated (these are primarily environmental but also include effects of the rest periods or vehicle headway), and that the unrepresentative traffic loading regimes can distort the behaviour of the pavement materials, which is often stress dependent (Paterson, 1987). Only flexible pavement types were included in the study.

Since the data from the Department of Transport's database are network level data, the models identified will only incorporate the distress types and severity

generally observed during routine visual inspections on a network level. The models will be calibrated for use on the network level of planning to address the need for trade-offs in project selection, and aim to provide the necessary information for the effective funding and planning of operations needed to protect the integrity of the network. The resulting deterioration models identified or calibrated would only be applicable to roads with the same pavement type, traffic loading and environmental conditions as studied.

1.4 METHODOLOGY

At first a study on available literature of internationally developed models will be conducted. The aim of this study is to identifying models possibly applicable for South African conditions. The model or models identified as possibly applicable for South African conditions will then be evaluated, and if needed calibrated, through an analytical approach using the deterioration observed during the past 15 years on the flexible pavements of the national road network of South Africa. No additional field observations will be conducted at any phase of the study.

1.5 ORGANISATION OF THE REPORT

The report is organised into the following chapters:

- In Chapter 1 the background to the problem is discussed and the aims of the study and the methodology in achieving them are outlined.
- The different deterioration prediction models in use internationally are discussed briefly in Chapter 2 and the model or models applicable to South African conditions are identified.
- The results of a sensitivity analysis performed on the model or models identified as applicable to South Africa are discussed in Chapter 3.
- The methods used for the processing of the data obtained from the database are discussed in Chapter 4.
- In Chapter 5 the results obtained from the comparison of observed values with predicted values are discussed.
- Chapter 6 presents the conclusions and recommendations of the study.

CHAPTER 2

REVIEW OF PAVEMENT DETERIORATION PREDICTION MODELS

2.1 INTRODUCTION

During the last two decades many attempts have been made by researchers and highway agencies to develop models that could predict the deterioration of a pavement, over time. As a result of this several models are available today to predict the deterioration of a pavement over time. Each model however, has certain inherent limitations due to the assumptions made during the development of the model.

Thus a study of all the available prediction models, developed from the deterioration results of in-service pavements was necessary to identify models that could possibly be implemented in South Africa, for further evaluation. The results obtained from the study are summarised in this chapter.

2.2 PREDICTION MODEL CATEGORIES

During the last two decades researchers attempted to develop the ideal pavement deterioration prediction model. This model would be able to consider the evolution of various distresses and how they may be affected by both routine and special maintenance. This ideal model was so highly complex that a compromise procedure combining a strong empirical base and mechanistic approach was adopted to achieve a reliable model. These compromise pavement deterioration prediction models may either be categorised as (George *et al*, 1989):

- **Deterministic models**: These models ignore the possibilities of a better-than or worse-than scenarios, and only consider the predicted deterioration. These models may either be empirical, implying that they were developed through regression analysis using in-situ field deterioration data or mechanistic-empirical implying that they were based on the mechanistic modelling of pavement response parameters.

- **Probabilistic models**: These models accept that the future deterioration of a pavement cannot be predicted with certainty, and employ probabilities

for predicting the expected future condition of a pavement, given the current condition. Typical models are based on Markovian and Baysian modelling techniques. The Markov process can be used to predict the "after" state for as many time steps as are desired, if the "before" condition or state of the pavement is known. Survivor curves describe pavement deterioration in the form of a cumulative distribution, as illustrated in Figure 2.1 for a cracking model.

As seen in Figure 2.1 the survivor curve (cumulative distribution curve) indicate the probability that a pavement is still "surviving" at a certain age, meaning that the pavement is still uncracked. From this survivor curve a transition probability matrix could be developed.

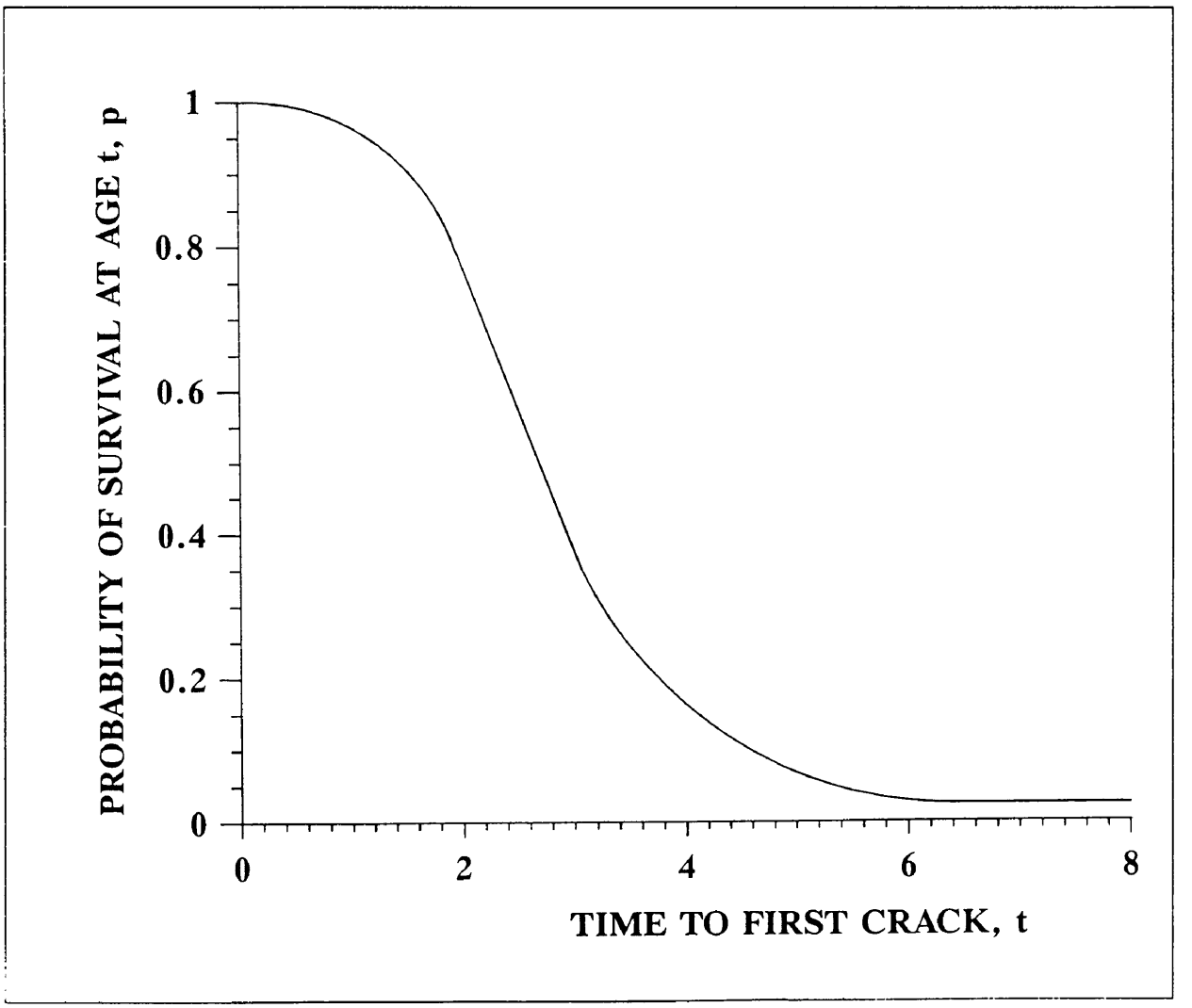

Figure 2.1: Survivor function for a cracking model (After Paterson, 1987).

Both deterministic and probabilistic models are further subdivided into the following two categories:

- **Functional deterioration prediction models**: These models predict changes in the functional condition of a pavement, which is an indication as to what extent a pavement serves its purpose of providing a safe and comfortable ride to the road user at an acceptable speed.

- **Structural deterioration prediction models**: These models predict changes in the physical or structural condition of a pavement and gives an indication of the remaining bearing capacity of the pavement. This is of great importance to engineers, since it allows them to timeously maintain the pavement structure to ensure that it remains serviceable.

2.2.1 Functional deterioration prediction models

The main functional distress modelled is roughness, but other types of distress such as ravelling, potholing and rutting (this is also a structural distress) should also be considered.

- **Roughness**: Roughness is the irregularity of the road surface that road users experience as vibrations and the prediction of its progression over the life-cycle of a pavement is the most critical of the various pavement deterioration predictions (Paterson, 1987). Roughness determines the road user's perception of the riding quality and thus the service provided by a road. Paterson (1987) further also states that roughness affects the dynamics of moving vehicles, increasing the wear on vehicle parts and the handling of a vehicle and has an appreciable impact on vehicle operating costs and the safety, comfort and speed of travel.

  Roughness also increases the dynamic loadings imposed by vehicles on the surface, which leads to an acceleration of the deterioration of the pavement structure. All the above mentioned contribute to roughness forming the basis for the determination of vehicle operating costs, which is one of the key elements in the evaluation of road policies.

- **Ravelling**: Ravelling is the loss of stone particles from the surface which results either from the mechanical fracture of the binder film or the loss of adhesion between binder and stone (stripping). Mechanical fracturing occurs when the binder film becomes too brittle or is too thin to sustain the

stresses imposed by the tyre contact area of a moving vehicle (Paterson, 1987). Ravelling of the surface could affect the functional deterioration of a pavement in respect of vehicle safety through the decrease in skid resistance and an increase in the aquaplaning potential.

Ravelling has however a negligible effect on roughness and holds serious structural implications only when the surface layer is thin and prone to potholing, it usually only triggers preventative measures like the repair of potholes and resurfacing. In severe cases of ravelling the resealing of the pavement may also be required. As a result of the maintenance activity on national roads in South Africa, ravelling is not a major problem.

- **Potholing**: Potholing is the most visible and severe form of distress and results from the disintegration and loss of surfacing material and, subsequently, base material due to deferred maintenance of severe cracking or ravelling (Paterson, 1987). Left untended extreme costs can be incurred by the road user through a tire blowout, or damage to the vehicle. For these reasons the Department of Transport places a high urgency on the patching of potholes within days after their occurrence on national roads. This action limits, to a large extent the severe influence of potholes on roughness and with the diversity in material and construction properties makes the prediction of potholing in most instances not useful, and even not feasible.

- **Rutting**: Rutting is the accumulation of deformation within pavement layers visible in the wheeltracks on the surface. This traffic-associated permanent deformation is the result of a rather complex combination of densification and plastic flow mechanisms (Paterson, 1987). The rutting is significantly influenced by material characteristics and induced stresses and strains which are a function of wheel loads, tire pressures and pavement stiffness.

  Rutting is one of the main criteria of pavement deterioration used in many pavement design methods to indicate an end of life situation. Rutting may increase road roughness, thus influencing road user costs, dynamic loads, riding quality and safety due to possible ponding of water on the road surface that could cause aquaplaning. Thus where data is available it should be included in a deterioration prediction model.

2.1.2 Structural deterioration prediction models

The main distress being modelled is cracking (especially crocodile cracking) although other distress types such as rutting also need to be considered.

- **Cracking**: The cracking of bituminous surfacings during their life under the combined action of traffic and environment is a defect in the surfacing which weakens the pavement and allows water to penetrate and cause further weakening. After a pavement has cracked the rate of deterioration usually accelerates with particular impact on the rates of rutting and roughness progression, making cracking an important criterion for maintenance intervention. (Watanatada *et al*, 1987).

All these pavement deterioration prediction models express the deterioration of a pavement as a function incorporating some or all of the parameters in Table 2.1. The parameters listed in Table 2.1 are those identified through numerous tests over the years as having a significant influence on pavement deterioration. The parameters to be included in a pavement deterioration prediction model depend on whether the model is used at a network or a project level, and whether the model is a functional or a structural deterioration prediction model.

Various approaches have been used over the years to quantifying the predictions of these pavement deterioration models in an easy to use indicator, which

Table 2.1: Parameters influencing pavement deterioration (George *et al*, 1989).

Pavement Characteristics	Materials	Surface type and thickness Material type used in base Thickness of different layers
	Structural	Modified structural number Benkelman Beam Deflection Age of the pavement Subgrade CBR Cracking
	Functional	Pavement surface roughness Ravelling Patching Rutting
Traffic Characteristics	Cumulative standard axle load in E80's Percentage of heavy vehicles Average daily traffic Traffic growth rate	
Environmental Variables	Freeze or non-freeze cycles Average yearly rainfall Average temperature	

incorporates a combination of the parameters listed in Table 2.1. Some of the indicators defined are:

- The pavement serviceability index (PSI) with a 0-5 scale on which 5 indicates an excellent pavement and 0 an impassable pavement.
- The pavement condition index (PCI) with a 0-100 scale on which 100 is a excellent pavement and 0 is a impassable pavement.
- The pavement quality index with a 0-10 scale on which 10 is a excellent pavement and 0 an impassable pavement.

2.3 AASHO ROAD TEST

2.3.1 Background

The AASHO Road Test was an accelerated trafficking experiment conducted under the auspices of the American Association of State Highway Officials (AASHO) using typical road vehicles on specially-constructed pavements in Illinois between 1958 and 1960. The primary objective was to determine the relationship between the number of axle passes of different loadings and the deterioration of flexible and rigid pavements, and with this known, develop instrumentation, design procedures and formulas to aid engineers in future designs.

The design of the experiment met the objective by trafficking 10 lanes on 5 tests loops separately by ten different axle loads ranging from 9 kN on single-tire axles to 213 kN on tandem axles, at a rate of approximately one vehicle per minute over the two year period with a total of 1 114 000 axle applications on each loop. A total of 368 flexible pavement sections were located on the six independent test loops of which one was not trafficked as a measure of climatic effects.

2.3.2 Major contributions to the field of pavement deterioration prediction

The analysis of the data obtained from the test resulted in the following major contributions to the field of pavement deterioration prediction:

- Deterioration classification : The test was the first to define and quantify the many facets of pavement condition and their progressive change over time known as road deterioration. Deterioration was quantified as the fractional loss of serviceability relative to the defined

limits of serviceability for new and terminal pavement conditions. Serviceability was quantified in a comprehensive index known as the Present Serviceability Index (PSI), which was a measure of the current condition of the experimental road pavements during the test. The Present Serviceability Index (PSI) was obtained by firstly quantifying the subjective ratings of a panel of road users, including road engineers, in the Present Serviceability Rating (PSR). To obtain a rating for a pavement the raters travelled over the test sections in vehicles of their choice, assessing the serviceability of a road on a scale of 0 to 5, where 0 indicates an impassable pavement and 5 and perfect pavement. The PSR is primarily a measure of the ability of the road to carry a road user safely and comfortably.

Secondly, a measure of serviceability was obtained by correlating the combined PSR statistically through multiple regression with the following three physical measurements of the state of the flexible pavement surface:

- Longitudinal slope variance (a measure of riding quality).
- Rut depth.
- Percentage of area of the road surfaced that was either cracked or patched.

For flexible pavements the following equation was derived (Highway Research Board, 1962):

$$PSI = 5{,}03 - 1{,}91 \log_{10}(1+SV) - 1{,}38\ RD^2 - 0{,}01\ (c + p)^{½}$$

where:

SV = Slope variance, a measure of longitudinal roughness.
RD = Average rut depth in inches.
c = Area of cracking in feet / 1000 sq feet.
p = Area of patching in feet / 1000 sq feet.

The deterioration of a pavement was expressed in terms of the rate of change of the serviceability of the pavement under trafficking. This expressed the deterioration of the pavement in relation to two standards, the quality of original construction or initial condition (p_o) and the terminal level of distress at which maintenance or rehabilitation is deemed necessary (p_r). The deterioration was related to the axle load, axle configuration and number of passes by the mathematical model, as follows:

$$g = \frac{p_o - p_t}{p_o - p_r} = \left(\frac{N_t}{n}\right)^{\beta}$$

where:

g = Dimensionless damage parameter defining the fractional loss of serviceability incurred prior to time t.

p_o = Present Serviceability Index at time t = 0.

p_t = Present Serviceability Index at time t.

p_r = The terminal serviceability index at which condition the pavement is deemed to require rehabilitation or reconstruction.

N_t = Number of axle load applications at the end of time t.

n = A function of design and load variables that denotes the expected number of axle load applications to a serviceability index of 1,5.

ß = A function of design and load variables that influence the shape of the p versus N serviceability curve, and related to the load and pavement variables for flexible pavements as follows:

$$= 0{,}40 + \frac{0{,}081\ (L_1 + L_2)^{3{,}23}}{(SN+1)^{5{,}19}\ L_2^{3{,}23}}$$

L_1 = Load on one single axle or on one tandem-axle set in kips.

L_2 = Axle code (1 for single axle and 2 for tandem axle).

SN = Structural number (See definition on page 2-9).

Through the years continuous research on the data obtained from the AASHO Road Test led to improvements and modifications to the original models developed. In the 1986 AASHTO Pavement Design Guide a simplification of the "serviceability progression" function was included. The roughness prediction given by the model is illustrated in Figure 2.2 under the Kenya study. The simplified model is:

$$\log N_{t18} = Z_R S_o + 9{,}36 \log_{10}(SN + 1) - 0{,}20 + \frac{G_t}{0.40 + 1094\ (SN + 1)^{-5{,}19}}$$

$$+ 2{,}32 \log_{10}(M_R) - 8{,}07$$

where:

$$G_t = \log_{10}\left(\frac{p_o - p_t}{4{,}2 - 1{,}5}\right)$$

N_{t18} = Number of 80 kN single axle load applications to time t.
Z_R = Standard normal deviate.
S_o = Combined standard error of the traffic prediction and performance prediction.
SN = Structural number, see discussion later on.
p_o = Initial present serviceability index.
p_t = Present serviceability index at time t.
M_R = Resilient modulus of the subgrade (psi).

- **Equivalent standard axle concept**: Another contribution was the definition of the equivalent standard axle concept. This was achieved by comparing the deterioration of a pavement test section across lanes, with each lane being associated with a single axle load category. The equivalent standard axle (E80) concept defines the damage caused by any axle relative to the standard axle load. The standard axle load was defined as a dual-tire single axle load of 80 kN. The adoption of the 80 kN single axle as a standard reference has historical ties to North America since it approximated the legal limits prevailing at the time of the test in the 1960's (This load is also adopted as the standard axle load in South Africa). Furthermore to reduce mixed traffic loadings to a single unit of equivalent standard axle loadings (E80), which is the number of standard axle loads that cause the same amount of damage as the mixed traffic, the relative damage was represented in the simplest form by:

$$F_j\ (E80) = \left[\frac{P_j}{P_s} \right]^n$$

where:

F_j = Damage caused by axle load P_j relative to the standard axle load.
P_j = Axle load expressed in kN.
P_s = Standard axle load in kN.
n = Load equivalency exponent.

The load equivalency exponent values varied in the range of 3,8 to 4,5, with an average of 4,2, over the range of pavement strengths and terminal pavement conditions and it soon came to be known for convenience as the "fourth-power law", the law being mathematical rather than physical.

- **Structural number**: During the test the definition of the structural number (SN) as an index of pavement strength was developed. This allowed the representation of a semi-infinite pavement comprising layers of materials with often greatly differing properties and behaviour under load in some uniform basis as required in predictive models (See modification under Kenya study to allow for subgrade strength). The structural number was defined as follows:

$$SN = 0{,}04 \Sigma a_i h_i$$

where:

SN = Structural number.

a_i = Material and layer strength coefficients, per inch.

h_i = Layer thickness, mm (where $\Sigma h_i \leq 700$ mm).

2.3.3 Discussion

The AASHO Road Test was the first major study carried out to evaluate the existing design methods that were developed in the period from the 1930's to the start of the test. The results obtained from the test made major contributions in the field of pavement deterioration predictions. Despite these contributions the applicability of the original deterioration models to roads in southern Africa is severely limited by the following factors (AASHTO, 1986):

- The freezing environment in Illinois, which had a major influence on deterioration, is distinctly different from the semi-arid and subtropical environment in South Africa.

- The pavement types evaluated during the test mainly consist of thick asphalt concrete and rigid surfacings constructed from only one set of materials on a single subgrade type, which is not representative of the thin surfacings and materials used in South Africa.

- Uncertainty about the applicability of the accelerated experimentally controlled loading since it provided very little information on long term environmental effects and no direct indication of the deterioration of roads under mixed traffic volumes.

- It is desirable to predict the trends of deterioration for cracks, rut depth and roughness separately rather than in the serviceability index.

2.4 THE WORLD BANK'S HIGHWAY DESIGN AND MAINTENANCE STANDARDS STUDIES

2.4.1 Background

Most of the early pavement research was conducted in Europe and North America where high traffic volumes, and high standards of road design and maintenance are evident. In developing countries, which are the focus of World Bank activities, the traffic volumes are typically much lower, incomes and values attached to travel time savings are lower and there is usually an acute shortage of financial resources (Watanatada *et al*, 1987).

These differences suggest that the optimal design and maintenance standards could be quite different for developing countries. To address these differences the World Bank in 1969 initiated the Highway Design and Maintenance Standards study in several countries to develop a new quantitative basis for decision making in the highway sector of these countries. This research led to the development of a conceptual framework and a first prototype model for interrelating the life-cycle costs of highway construction, maintenance and vehicle operation.

Though the conceptual model developed showed great promise the absence of sound empirical evidence from previous research made it impossible to establish the fundamental cost relationships quantitatively. Consequently, subsequent phases of the research concentrated on empirical quantification involving field collection of new primary data on the underlying physical and economic relations to ensure that the theoretical models conform to the real world as closely as possible (Watanatada *et al*, 1987).

Four such studies have been carried out in Kenya, the Caribbean, Brazil, and India. These studies were designed to collect data on the changes of roughness, cracking and rut depth of flexible and semirigid pavements in nonfreezing climates, over a wide range of pavement strengths and mixed traffic loadings, and under different maintenance standards. From the results obtained from the different studies only the results from the Kenya and Brazil studies are summarised in more detail in this chapter as they are the most comprehensive of the four studies, and also have the largest potential for application on South African national roads.

2.4.2 The Kenya study

2.4.2.1 Background

The study was conducted by the Transport and Road Research Laboratory (TRRL) of the United Kingdom from 1971 to 1974 in Kenya. The objective of the study was to develop models to predict deterioration of paved and unpaved roads with structural compositions typically used in Kenya, as a function of regional design and construction standards, environmental factors, traffic loading and maintenance policies (Hodges *et al*, 1975). Road deterioration was studied under normal operating conditions, rather than through accelerated testing. This study method is know as the "window monitoring" technique since it provides a "window" or "snapshot" of part of the lifecycle of the pavements studied. According to Watanatada *et al* (1987) this method of study had the following advantages:

- Roads normally constructed are more representative of the network than experimental sections which tend to be more closely controlled during construction.

- It permits the obtaining of results within a reasonable time since it allows both the monitoring of road test sections from the initial construction to their ultimate defined state of failure (time-series analysis), and secondly by allowing the sampling of the road population at any instant of time to include a representative collection of roads in the sample at different stages of their lives (cross-section analysis).

- Much cheaper to use existing roads with normal traffic than to build separate experimental sections.

The paved sections were selected by experimental design, making up the partial factorial of major variables listed in Table 2.2. The flexible pavement study included a total of 49 in-service sections of which 39 were surface dressed roads on cement stabilised bases, and the remaining 10 had granular bases. As seen in Table 2.2 pavement type, vertical and horizontal geometry and rainfall were used as factorial parameters for the Kenya study.

Table 2.2: Sampling factorial for paved roads in Kenya study (After Hodges *et al*, 1975).

	Geometric Classification	Low rainfall < 1000 mm/year			High rainfall > 1000 mm/year		
	Vertical / Horizontal	Flat	Inter mediate	Steep	Flat	Inter mediate	Steep
Premix surfaced roads (P)	Low	P8	-	-	P2	P7	P6
	Medium	P10	-	-	P3	P1	P4
	High	-	P9	-	-	-	P5
New Surface-dressed roads (NB)	Low	NB10	NB12	NB13	NB2	NB4	NB3
	Medium	-	NB11	NB14	NB1	NB9	NB8
	High	-	-	-	NB5	NB6	NB7
Old surface-dressed roads (OB)	Low	OB17* OB18	OB20** OB24	OB21 -	OB7* OB10	OB5 OB11*	OB2* OB3
	Medium	OB23* OB25	OB19* OB22	- -	OB8*	OB13 OB9	OB1* OB4
	High	-	-	-	-	OB6	OB12* OB15

Where:

Low	< 30°/km	Flat	< 1,5%
Medium	30°/km ≤ and < 90°/km	Intermediate	1,5% ≤ and ≤ 3,5%
High	≥ 90°/km	Steep	≥ 3,5%

* Nil maintenance sections

** Surfaced dressed in error

Cell numbers indicate the section numbers

Most of the cement-stabilised base pavements covered a narrow range of pavement strengths with modified structural numbers (SNC) between 2,7 and 3,7. The modified structural number (SNC) includes the contribution of the subgrade (SN_{sg}) defined as follows (Hodges *et al*, 1975):

$$SNC = 0{,}04 \Sigma a_i h_i + SN_{sg}$$

where:

SNC = Modified structural number.

a_i = Material and layer strength coefficients.

h_i = Layer thickness, mm (where $\Sigma h_i \leq 700$ mm).

SN_{sg} = Contribution of the subgrade after Hodges *et al* (1975):

= $3.51 \log_{10} CBR - 0.85 (\log_{10} CBR)^2 - 1.43$.

CBR = In situ California Bearing Ratio of subgrade in %.

The traffic volumes were sufficiently high on some sections to allow almost complete deterioration records to be obtained during the study period . The climatic region was classified as arid to subhumid with a rainfall varying from 400 mm to 2000 mm per annum.

2.4.2.2 Major contributions to the field of pavement deterioration prediction

The chosen study method resulted in strict demands on analytical and statistical data treatment during the analysis of the data obtained from the study. The results obtained had the following major contributions to the field of pavement deterioration prediction:

- **Prediction of roughness**: One of the major contributions was the discovery of the large effect of road roughness on vehicle operating costs for both paved and unpaved roads (Hide *et al*, 1975). This discovery was corroborated in subsequent studies in the Caribbean, Brazil and India. The Kenya study also reasserted the findings of the AASHO Road Test that roughness progression was an entirely structural phenomenon depending on pavement strength (the modified structural number), and cumulative traffic loading with no allowance for environmental factors. However, the following important differences existed between this test and the AASHO Road Test (Paterson, 1987):

  - The direct use of roughness instead of serviceability.
  - Observations under actual mixed traffic loading and not under experimentally controlled conditions.
  - A variety of pavement types on various subgrade strengths, which eliminated the problem of a single subgrade or set of materials of the AASHO Road Test.

A variety of pavement ages giving "windows" at different stages of the deterioration trend of a pavement in comparison with the new pavements of the AASHO Road Test.

The following roughness prediction model was developed from the data:

$$R_t = R_o + m\,NE_t$$

where:

R_t = Predicted roughness at time t (mm/km Bump Integrator trailer).

R_o = Initial roughness at time t = 0, constant for given range of modified structural number , SNC.

NE_t = Cumulative traffic at time t, in millions of equivalent 80 kN standard axle loads (million E80).

m = Constant for a given range of pavement structural number.

At first the values for the parameters were fixed for ranges of SNC, but in 1982 Parsley and Robinson modelled m as a continuous function as follows:

$$m = \frac{1250}{\text{antilog}_{10}(a - b - 1{,}3841)}$$

where:

$a = [(0.20209 + 23{,}1318\,c^2)^{0{,}5} - 4{,}8096\,c]^{0{,}33}$

$b = [(0.20209 + 23{,}1318\,c^2)^{0{,}5} + 4{,}8096\,c]^{0{,}33}$

$c = 2{,}1989 - SNC$

This continuous model for m was however limited to the range of $2{,}75 < SNC < 3{,}75$. Due to rapid changes in the prediction of m by the model for SNC values less than 3, the model was modified as follows:

$$m' = m_3 \left(\frac{3}{SNC}\right)^4$$

where:

m' = modified value of m valid for $1{,}5 < SNC < 3$, and

m_3 = value of m for SNC = 3.

The exponent of 4 and the inverse proportionality were adopted from the Brazil study. Predictions given by the model are illustrated in Figure 2.2 along with the predictions given by the AASHTO Pavement Design Guide of 1986.

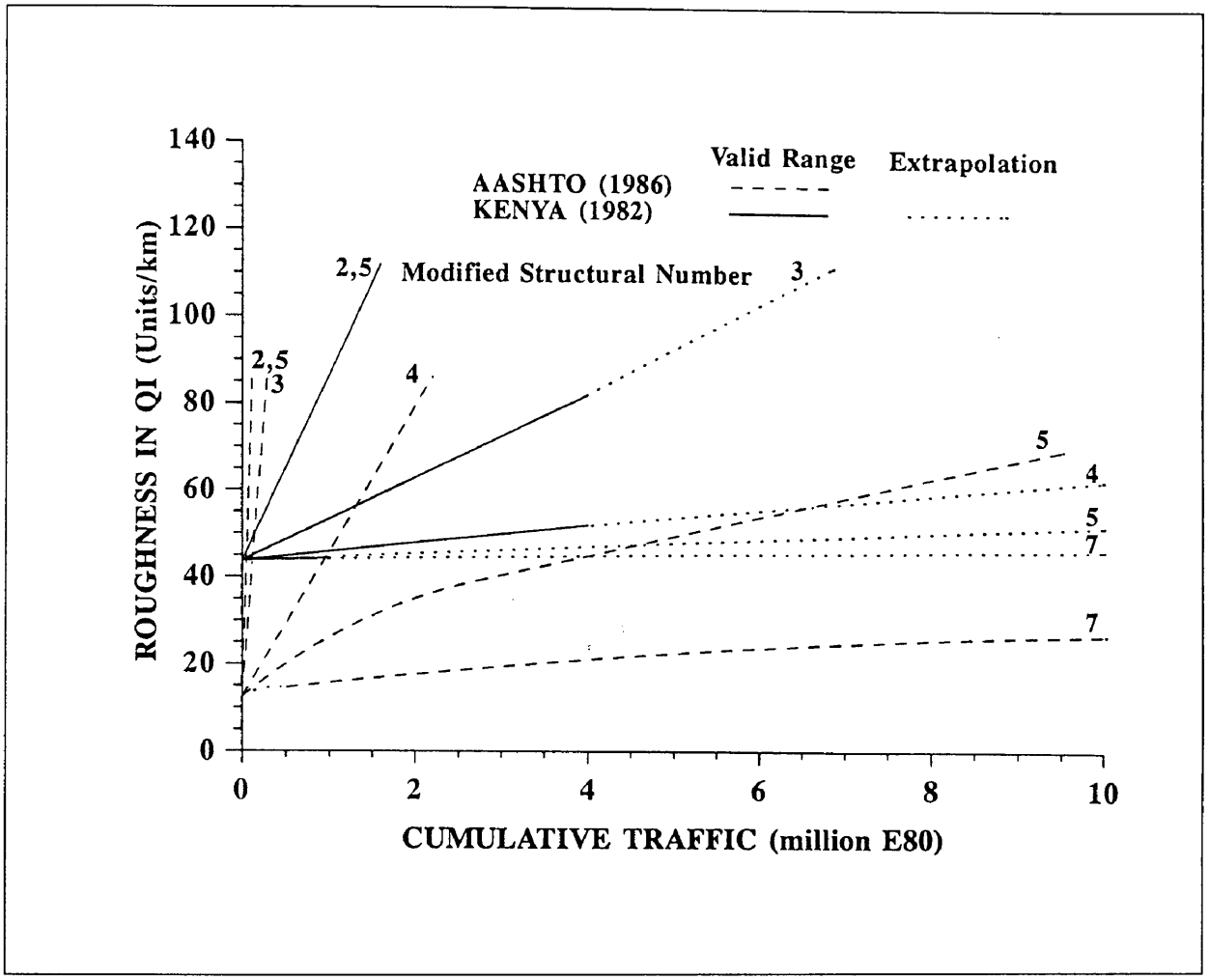

Figure 2.2: Roughness predictions given by the AASHTO Pavement Design Guide (1986) and the Kenya models (After Paterson, 1987).

From Figure 2.2 it is evident that the Kenya model predicts a slower rate of roughness progression than the AASHTO model. According to Paterson (1987) the difference is equivalent to a 60 % increase in the structural number. Since the modification for the subgrade strength is already included it is believed that the difference could be ascribed to the environmental difference between the harsh cold climatic conditions in Illinois and the warm arid climatic conditions in Kenya. Furthermore each model assumes a different initial value for roughness. The Kenya model is independent of the initial value, but in the AASHTO model the rate of progression is influenced slightly by the initial value according to Paterson (1987).

- **Prediction of cracking**: Another contribution was the development of a model from which the expected life of a pavement in E80's could be determined before the threshold cracking condition of 5 m/m², where base failure was assumed, was reached. Cracking was however classified by an average intensity, without classifying severity. The cracking was measured in one metre square samples of the road surface at 100 m intervals in each wheel path of a 1000 m long section. The model developed combines cracking initiation and progression in one relationship expressed in terms of cracking plus patching, as follows:

  For SNC < 4,0 and C + P ≥ 0:

  $$(C + P)_i = 21600\ NE_s\ SNC^{-SNC}$$

  By reduction the occurrence of cracking initiation is expressed in terms of the cumulative number of E80's applied, as follows:

  $$NCA = \max \{[((\frac{4}{SNC}) - 1) (SNC^{(1 + SNC)})] / 72 ; 0\}$$

  where:

  (C + P) = Sum of areas of cracking of intensity exceeding 5 m/m² and patching (m²/km/lane).

  SNC = Modified structural number.

  NE_s = Cumulative traffic loadings since latest resurfacing (million E80).

  NCA = Cumulative E80's applied during the period before cracking initiation (million E80).

2.4.2.3 Discussion

The study pioneered the development of basic measurement methodologies (Abaynayaka, 1976) and researchers were able to establish simple statistical relationships in linear form between the various operating cost components (for example fuel, tires, vehicle maintenance) and the principal road characteristics for example surface type, roughness and vertical alignment. This initiated further studies throughout the world, which resulted in major contributions to the field of pavement deterioration predictions. The study further adopted a

more versatile approach by modelling the major modes of distress individually. This approach permits the analysis of a variety of design and maintenance strategies under different scenarios, without assumptions as to environment, pavement type, design standards or maintenance standards (Paterson, 1987). A further advantage of the study was that it was conducted under an actual mixed traffic loading. Despite these contributions the applicability of the original deterioration models developed to roads in southern Africa is limited by the following factors:

- The narrow range of the pavement strengths ($2{,}75 \leq SNC \leq 3{,}75$) for which the relationship were developed limits the extrapolation of the relationships beyond this range.

- Furthermore 80 percent of the pavements in the Kenya study were of cement-treated base construction which under moderate and high traffic loadings, cracked within the first year. Consequently the rate of roughness progression may have been dominated by the block cracking and disintegration process (Paterson, 1987).

- The fact that the roughness predicted by the model is insensitive to the initial roughness value, indicates another limitation in the model, since it is generally accepted that the rate of roughness progression increases with an increase in roughness. This increase in roughness progression is influenced for example by the dynamic effect of heavy vehicles on the pavement (Van Niekerk, 1992).

2.4.3 Brazil-UNDP study

2.4.3.1 Background

The Brazil study was conducted between 1975 and 1984 on the central plateau of Brazil by a joint team of specialists from Brazil and nine other countries. The main objective of the study was to develop models predicting the life-cycle costs (construction, maintenance and road user costs) for both paved and unpaved roads as a function of pavement design, maintenance standards and other policy options that may be considered (GEIPOT, 1982). The development of these models incorporated the establishment of road deterioration relationships for both road maintenance and operating costs.

The road deterioration study was, as in the case of the Kenya study, conducted on existing in-service pavements under normal mixed traffic conditions. The pavement sections were also selected by experimental design, using the central factorial of major parameters given in Table 2.3. The central factorial was supplemented by the "star point" factorial in Table 2.4, which added sections having intermediate values of the main parameters. As illustrated in Table 2.3 the Brazil study included vertical geometry, traffic flow, pavement type and pavement age (breakdown by surfacing, base and rehabilitation status) as factorial parameters. The study included a total of 116 sections of which 74 were surface dressed roads on granular bases, and 11 on cement stabilised bases. The remaining 33 sections were overlaid and included the rehabilitation effects.

Table 2.3: Central factorial of Brazil-UNDP study (After Paterson, 1987).

Surface type			Asphaltic concrete				Surface treatment (Double)			
Base type			Gravel		Crushed Stone		Gravel		Crushed Stone	
Traffic (ADT)			50-500	>1000	50-500	>1000	50-500	>1000	50-500	>1000
Vertical geometry (%)										
Age (years)										
State rehab.										
Overlaid	≥ 6	≥ 6	128	129						
		0 - 1,5				158		109 009		
	0-2	≥ 6		125			035	032		
		0 - 1,5		006			034	031		159
As Constructed	≥ 12	≥ 6		119			123 172	110 008		
		0 - 1,5		003 113		166	173	007		121
	0 - 4	≥ 6	022	025	151	162	002	024 111	155	103 165
		0 - 1,5	001 021	033 112	152	161 026	004 023	106	101	102

Where:

Cell numbers indicate the section numbers.

Table 2.4: Star point factorial used in Brazil-UNDP study (After Paterson, 1987).

Traffic ADT (veh\day)	Vertical geometry as Percentage	Pavement Age(years)						Asphalt concrete				Surface treatment			
								Gravel Base		Crushed stone		Gravel Base		Crushed stone	
		<2	<4	3-5	>6	8-10	>12	Co	Ov	Co	Ov	Co	Ov	Co	Ov
<500	3-5					*						1			
600-900	3-5		*					1				2		2	
600-900	3-5	*							1						1
600-900	0-1,5					*		1				1			
600-900	3-5		*									2			
600-900	3-5						*					1			
600-900	>6					*		1				1			
>1000	3-5					*		1		1		1		1	
>1000	3-5			*									1		

Where:

Co = As constructed

Ov = Overlaid

Cell numbers indicate the number of road sections.

The total of 116 pavement sections virtually covered the whole range of pavement strengths currently used in most developing countries (Paterson, 1987). The pavement construction generally comprised asphalt surfacings less than 100 mm in thickness and a basecourse of natural gravel, crushed stone or cemented gravel materials. Inverted designs with granular base and cemented subbase were not included. The traffic loading varied between 300 and 1,2 million equivalent 80 kN single axle loads per lane per year. The climate in the central plateau where the study was conducted was classified as almost entirely humid with small areas classified as moist subhumid to perhumid. The rainfall varied between 1200 and 2000 mm per annum.

2.4.3.2 Major contributions to the field of pavement deterioration prediction

The chosen study method also resulted in strict demands on analytical and statistical data treatment during the analysis of the data obtained from the study. The results obtained provided the following major contributions to the field of pavement deterioration prediction:

- **Prediction of roughness**: The influence of roughness on vehicle operating costs as indicated by previous studies made the modelling of

roughness the most important aspect of the Brazil study. The roughness prediction models developed during previous studies included only structural effects, or only time and environmental effects. In the Brazil study however, the models were developed beyond simple correlation models by incorporating the following major mechanistic effects (Paterson, 1987):

- Structural and traffic related factors.
- Time-related environmental mechanisms.
- Effects of surface distress such as cracking, patching and potholing.

From the study two empirical models were developed to suit different applications. The first model was a comprehensive and fairly sophisticated incremental model intended for the life-cycle simulation of discrete construction and maintenance activities. The model incorporates the interacting effects on roughness progression of the following individual modes of distress:

- Maintenance
- Traffic
- Pavement age and strength.
- Environment

The second model was a simple aggregate roughness model developed for the more general deterioration model applications such as road transport pricing and cost allocation studies. This model only predicts the trend of the absolute level of roughness as a function of the following primary parameters, namely cumulative traffic loading in E80, pavement age, pavement strength, and a generalised environmental coefficient. The two models were (Paterson, 1987):

Incremental Roughness model

$$\delta RI = K_{gp} [134\, e^{m\,t}\, SNCK^{-5,0}\, \delta NE_4 + 0,114\, \delta RDS + 0,0066\, \delta A_{crx} + 0,003\, H_p\, \delta A_{pat} + 0,16\, \delta V_{pot}] + K_{ge} m\, RI(t)\, \delta t$$

$$SNCK = 1 + SNC - 0,000758\, H_c\, A_{crx}$$

Aggregate roughness model

$$RI(t) = [RI_o + 725\,(1 + SNC)^{-5,0}\,NE_4(t)]\,e^{0,0153t}$$

where:

δRI = Incremental change in roughness over time period t, m/km IRI.
IRI = International Roughness Index with, 1 IRI = 13 Quarter car index units (QI).
K_{gp} = User specified deterioration factor for roughness progression.
K_{ge} = User specified deterioration factor for environmental related annual fractional increase in roughness.
m = Environmental coefficient.
t = Age of pavement or overlay since rehabilitation or construction in years.
δNE_4 = Incremental number of equivalent axle loads in period δt, million E80 / lane.
δRDS = Increase in rut depth standard deviation of wheelpaths, mm.
δA_{crx} = Increase in indexed area of cracking, in percent (see prediction of cracking).
H_p = Average protrusion of patch from original surface profile, mm.
δA_{pat} = Increase in the area of surface patching, as a percentage.
δV_{pot} = Change in the total volume of potholing in m^3/lane/km.
RI(t) = Roughness at time t, m/km IRI.
SNC = Modified structural number of the pavement.
H_c = Total thickness of cracked layers of bound materials mm.
A_{crx} = Area of indexed cracking (see prediction of cracking).
$NE_4(t)$ = Cumulative traffic loading at time t, million E80 (with load damage factor of 4).
δt = Incremental value of time t, in years.

The environmental coefficient (m) is an environment-age component representing the annual average effect of all non-traffic-related environmental factors, including for example temperature changes, seasonal and drainage related moisture variations, freeze-thaw effects, foundation movements (Paterson, 1987). No major quantified estimates are available yet, but recommended values to be assigned to the m - coefficient for various climates are given in Table 2.5. The moisture classification is done according to the Thornthwaite moisture index. Although these values are based on relatively few evaluations so far, the fact that the values fall into a pattern across widely different countries and regions

Table 2.5: Recommended values for the environmental coefficient m (After Paterson, 1987).

Moisture Classification	Temperature classification		
	Tropical nonfreezing	Subtropical nonfreezing	Temperate freezing
Arid	0,005	0,010	0,025
Semiarid	0,010	0,016	0,035
Subhumid	0,020	0,030	0,065
Humid, wet	0,025	0,040	0,10 - 0,23

lend a strong credibility to the values.

The area of indexed cracking (CRX) was defined as a percentage of the total surface area with the objective of combining all severities of cracking, and thus reducing the number of predictive relationships to be both estimated and applied. The area of indexed cracking is defined as follows (Paterson, 1987):

$$CRX = \sum_{j=1,4} \frac{(i\ CL_j)}{4}$$

where:

CRX = Area of indexed cracking, as a percentage of the surfaced area.

CL_j = Area cracked of class j, j = 1 to 4 (see prediction of cracking).

i = Weighting factor, taken as a crack width equal to i mm.

The roughness prediction by both models are illustrated in Figure 2.3 for the incremental model, and Figure 2.4 for the aggregate model. The different trends shown in Figure 2.3 by the generally convex curves indicate the effects of traffic loading and surface distress on roughness progression. Furthermore the effect of the environment-age component is evident in the increase in roughness at extremely low traffic levels. For the aggregate model in Figure 2.4 it is evident that the model is less concave than the incremental model. However the model still incorporates both age and cumulative traffic, thus overcoming the deficiencies of previous traffic-only and time-only models (Paterson, 1987). Since both models are based on well established theories of physical and behavioural phenomena, and incorporates most of the major determining factors and mechanisms in sufficient detail (especially the incremental model), the models are transferable across diverse environments. This was evident in the verification of both models within experimental error on eight other data bases from studies conducted throughout the world (Paterson, 1987).

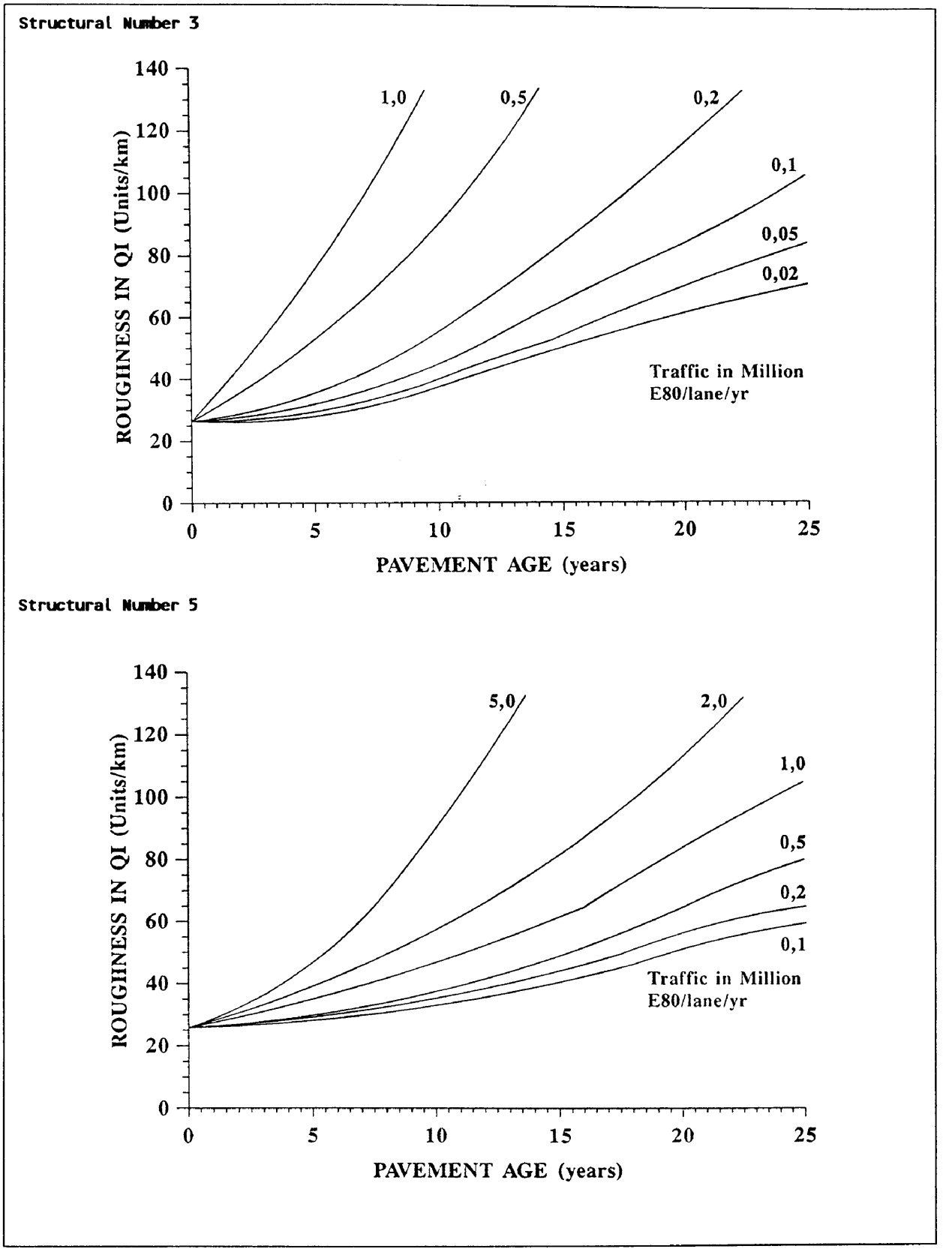

Figure 2.3: Illustration of the roughness prediction given by the incremental model (After Paterson, 1987).

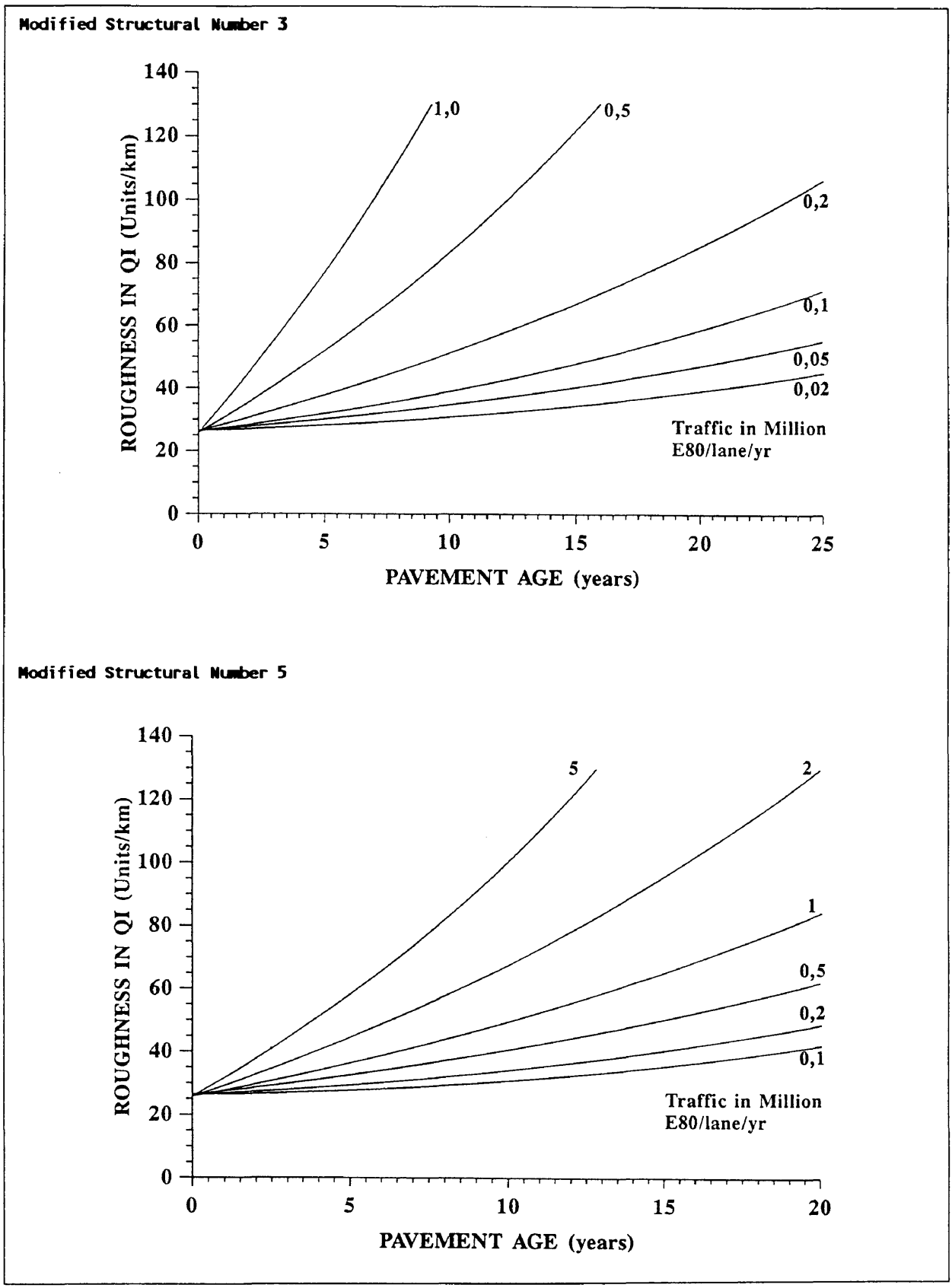

Figure 2.4: Illustration of the roughness prediction given by the aggregate model (After Paterson, 1987).

- **Prediction of rutting**: The empirical model developed from the Brazil study was the first model to incorporate both mechanisms of traffic-associated deformation. The two mechanisms are densification and plastic flow. Densification according to Paterson (1987) is the change in the volume of material as a result of the tighter packing of the material particles and sometimes also the degradation of particles into smaller sizes. The rutting in this case is usually fairly wide and uniform in the longitudinal direction with heaving on the surface occurring seldomly. The degree of densification depends greatly on compaction specifications during construction, and the subsequent degree of compaction obtained. Plastic flow is usually associated with shear displacements in which both depression and heave are usually manifested and occurs when the shear stresses imposed by traffic exceed the inherent shear strength of the pavement layers.

The modern pavement design methods and predominantly thin asphalt surfacings (less than 100 mm thick) used in Brazil resulted in 95 percent of the rut depth values being less than 8 mm with the maximum ranging up to 16 mm measured manually with a 1,2 m straight edge at 80 m intervals. This severely restricts the applicability of the developed models to cases of extreme behaviour, as evident from the under-prediction of mean rut depth at high rut depth values during validation studies. A strong relationship between the standard deviation of the rut depth and the mean rut depth was found and both were nonlinear functions of cumulative equivalent standard axle loadings, modified structural number, average relative compaction and cracking. The models developed were (Paterson, 1987):

Mean Rut Depth

$$RDM = t^{0,166}\, SNC^{-0,502}\, COMP^{-2,30}\, NE_4^{\,ERM}$$

$$ERM = 0,0902 + 0,0384\, DEF - 0,009\, RH + 0,00158\, MMP\, A_{crx}$$

Rut Depth Standard Deviation

$$RDS = 2,06\, RDM^{0,532}\, SNC^{-0,422}\, COMP^{-1,66}\, NE_4^{\,ERS}$$

$$ERS = -0,009\, RH + 0,00116\, MMP\, A_{crx}$$

where:

RDM = Mean rut depth in both wheelpaths, mm.

RDS = Standard deviation of rut depth in both wheelpaths, mm.

t = Age of pavement since rehabilitation or construction in year.

SNC = Modified structural number of pavement strength.

COMP = Compaction index of flexible pavements.

$NE_4(t)$ = Cumulative traffic loading at time t, million E80 (with load damage power 4).

DEF = Pavement surface deflection by Benkelman beam, mm.

RH = Rehabilitation state (= 1 if pavement overlay, = 0 otherwise).

MMP = Mean monthly precipitation, m per month.

A_{crx} = Area of indexed cracking (see prediction of cracking).

The compaction index of flexible pavements (COMP) was defined as a reference compaction standard because the compaction achieved in a pavement at the time of construction is expected to influence the densification occurring under traffic (Paterson, 1987). The COMP is defined as the average relative compaction weighted by layer thickness, over a 1m depth as follows (Paterson, 1987):

$$COMP = \sum_{i=2,n} RC_i \left(\frac{H_i}{\sum_{i=2,n} H_i}\right)$$

$$RC_i = \min\left[1, \frac{C_i}{C_{nom,i}}\right]$$

$$C_{nom,i} = 1.02 - 0.14\, z_i$$

where:

C_i = The compaction of layer i defined by $C_i = DD_i / MDD_i$.

DD_i = In-situ dry density of layer i.

MDD_i = Maximum dry density of material in layer i determined in the laboratory to the relevant compaction standard.

$C_{nom,i}$ = The nominal specification of compaction to be achieved in layer i with respect to the relevant standard, as a fraction.

RC_i = Relative compaction, that is the ratio of the compaction measured in the field to the nominal compaction, as a fraction.

z_i = Depth at the bottom of layer i, in meters, where $z_i \leq 1$ metre.

The predictions given by the models for the mean and standard deviation of rut depth are illustrated in Figure 2.5. The prediction for the mean rut depth shows a generally diminishing concave rate of rut depth progression

over time as a function of the cumulative equivalent axle loading and various structural parameters (Paterson, 1987). The high initial rates indicate a degree of early densification under traffic. This is explained through the fact that when stresses induced in the pavement are within the elastic range of the material, the rut depth tends towards an ultimate value determined largely by the amount of densification and pavement strength. When plastic flow occurs through weakening due to for example cracking, the trend of deformation becomes more linear with traffic increase. Paterson (1987) stated that it was apparent from validation studies that the models are applied best to thin-surfaced asphalt pavements (asphalt thickness less than 100 mm). The average rate of progression in relation to mixed traffic loading was generally well-validated, but the variance of absolute rut depth about the predicted mean may be high as a result of the limited range from which the models were developed.

- **Prediction of cracking**: Another contributions of the Brazil study was that it was the first major study in which the approach was adopted to model cracking in two phases, namely the time before initiation of cracking, and the rate of progression of the area cracked. The advantages of such a model which separate the predictions of initiation and progression are (Paterson, 1987):

  - It allows independent determination of the two phases, thus improving the applicability in pavement management applications were the data obtained from network monitoring can be used.

  - It is more adaptable to the prediction of maintenance effects.

  To enable the development of the model the cracking was classified by severity, area and type as follows (Paterson, 1987):

  Severity:
  - Class 1 : Hairline cracks, width 1 mm or less.
  - Class 2 : Crack widths 1 to 3 mm.
  - Class 3 : Crack widths greater than 3 mm without spalling.
  - Class 4 : Spalled cracks, i.e., fragments of the surfacing adjacent to the crack were lost.

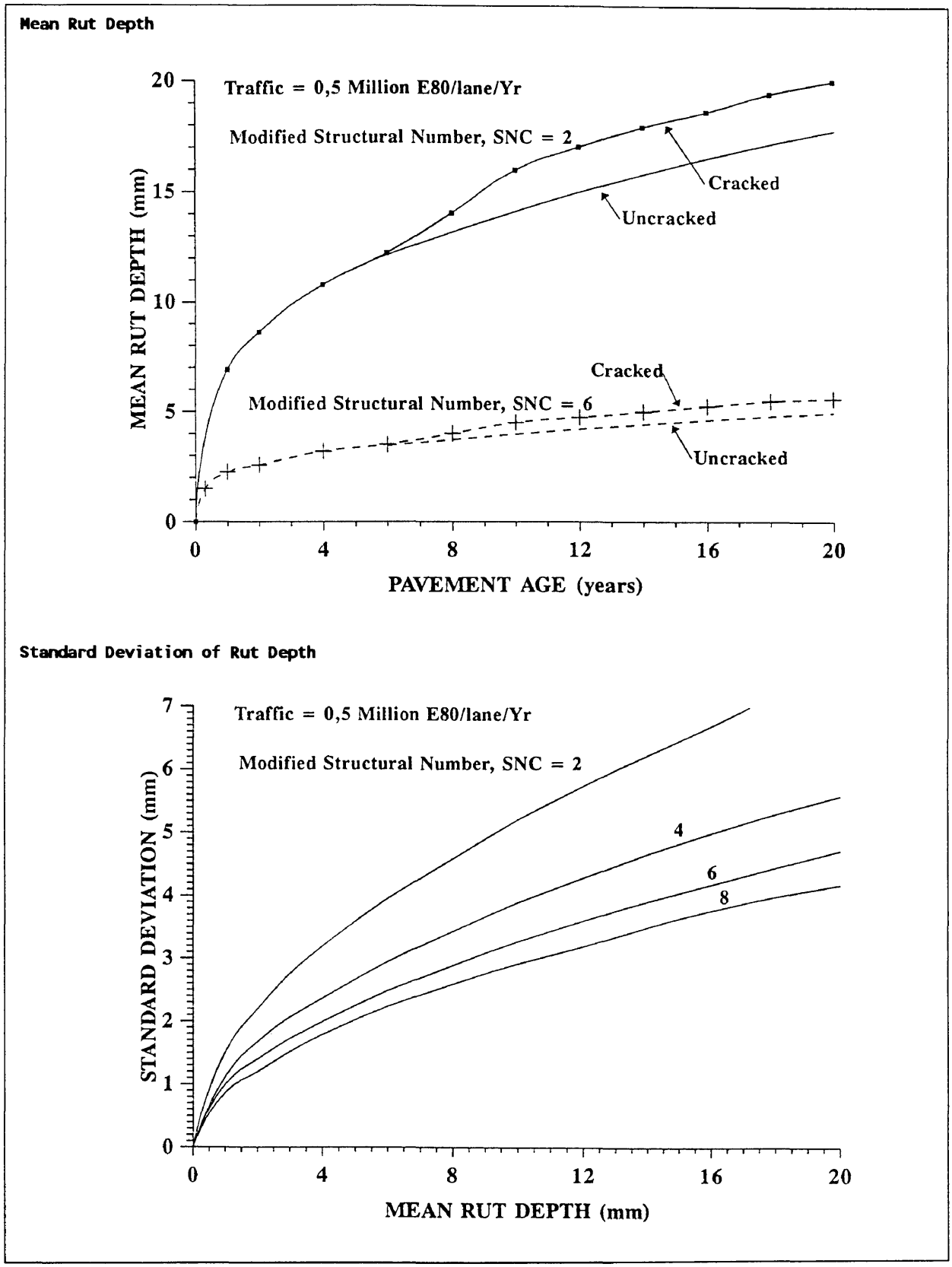

Figure 2.5: Predictions of the progression of the mean and standard deviation of rut depth (After Paterson, 1987).

Area:

The sum in square metres, of rectangular areas surrounding the individual cracking networks reported as a percentage of the total area of the test section. For linear cracks it was defined as an 0,5 m wide strip extending the length of the crack.

Type:

Crocodile, irregular, block, transverse or longitudinal.

The Brazil study only included crocodile and irregular cracking. Other types of cracking like longitudinal, transverse and map cracking were not considered for further evaluation during the study. These types of cracking were deemed to be largely determined by material characteristics and temperature regime, resulting in a large number of variables that made it not practicable to model these types of cracking for network analysis (Paterson, 1987). Since both initiation and progression models were needed for each severity level, it was decided to reduce the number of models needed, by rationalising the severity levels to only two, namely:

CR_2 = Area of all cracking (narrow and wide, classes 2, 3 and 4) as a percentage of the surfaced area.

CR_4 = Area of wide cracking (class 4), as a percentage of the total surfaced area.

a) Initiation of all cracking: The cracking initiation phase was defined as the time to reach a cracked area of 0,5 percent or more for each particular pavement section. The diversity in the initiation of cracking, (cracking occurred at different times at various locations along a normally homogeneous road) indicated that not all physical factors affecting the initiation of cracking could be included in the experimental data. In order to evaluate these effects a special estimation procedure based on failure-time analysis principles were developed for asphalt pavements (Paterson, 1987). Analysis of the data resulted in the following two models for the prediction of the initiation of all cracking for asphalt concrete pavements:

$$TY_{cr2} = 4{,}21 \exp (0{,}139\ SNC - 17{,}1\ YE_4 / SNC^2) \quad (a)$$

$$TY_{cr2} = 8{,}61 \exp (- 24{,}4\ YE_4 / SNC^2) \quad (b)$$

where:

TY_{cr2} = Expected (mean) age of surfacing at initiation of all cracking in years.

SNC = Modified structural number.

YE_4 = Annual traffic loading, million E80/lane/year, with n=4.

The predictions given by both models are illustrated in Figure 2.6 Both models indicate the strong effects of aging at low traffic loading rates because the life predicted is finite and does not tend towards infinity as purely mechanistic models would indicate. Model (a) had the best statistical fit to the data, but model (b) despite its focal point for no traffic is however more readily transferable to other regimes (Paterson, 1987).

For surface treatments a number of models were also developed by using the maximum likelihood procedure. Of all the models developed the following model had the best fit to the data:

$$TY_{cr2} = 13{,}2 \exp [-20{,}7 (1 + CQ) YE_4 / SNC^2]$$

where:

TY_{cr2}, YE_4 and SNC as defined previously.

CQ = Construction quality indicator, where CQ = 0 if construction of the surfacing was not faulty, and CQ = 1 if construction was faulty (poor binder distribution, contaminated stone, early stripping of binder, etc.)

An illustration of the prediction capabilities of the model are shown in Figure 2.7. From the illustration it is evident that the model also verifies the effect of aging by indicating a maximum probable life of 13 years for a double surface treatment without any traffic load. Furthermore the model predicts a longer life for a surface treatment under light traffic (loadings smaller than 0,6 million/E80/lane/year) than for an asphalt concrete pavement as was experienced in Brazil. But for traffic loadings exceeding 0,6 million/E80/lane/year the asphalt concrete pavement proved to be better. The reason for this is probably the influence of other factors such as an increase in ravelling due to the higher traffic loading on the life of the surface treatment.

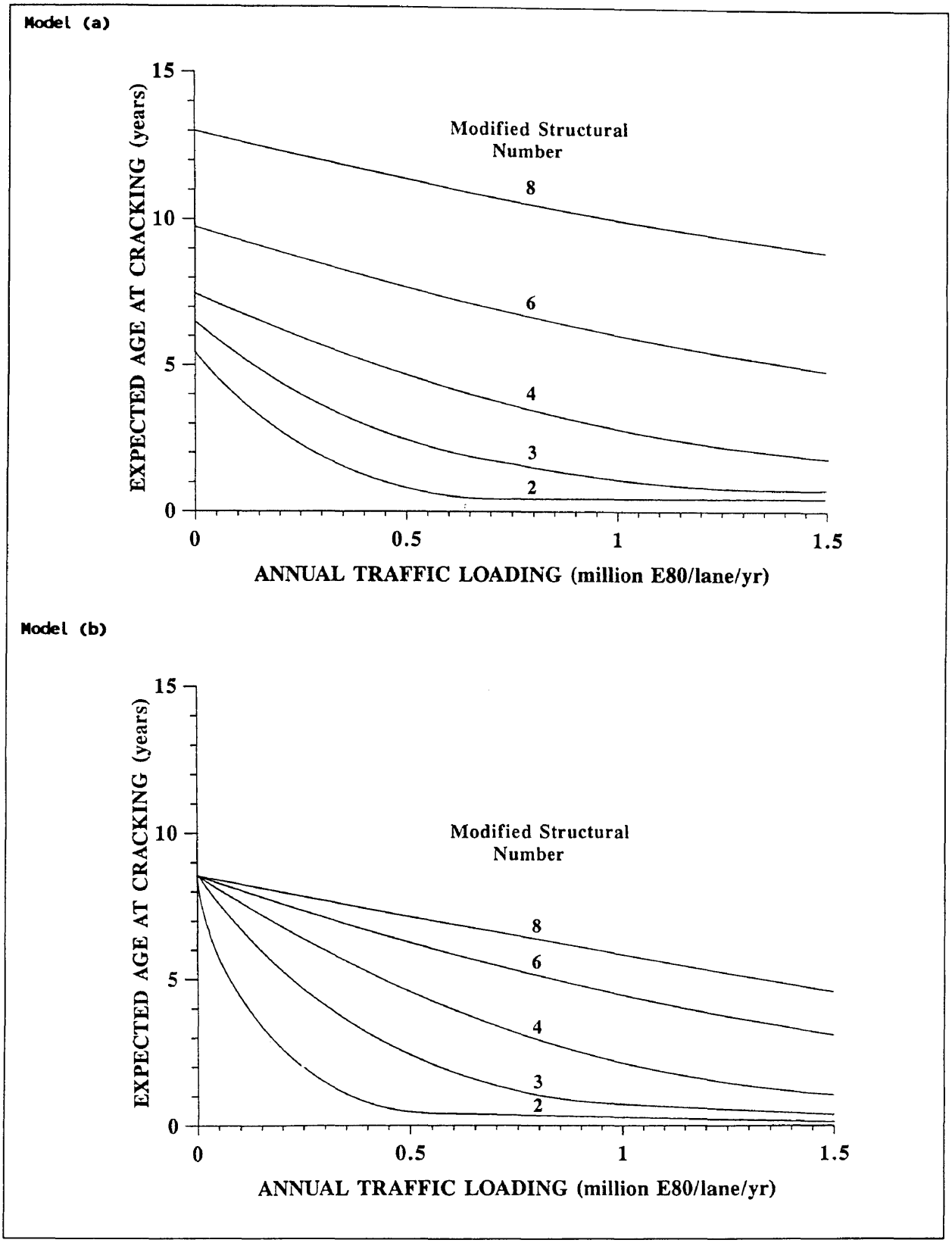

Figure 2.6 : Prediction of the expected age of asphalt concrete original surfacings at the initiation of all cracking (After Paterson, 1987).

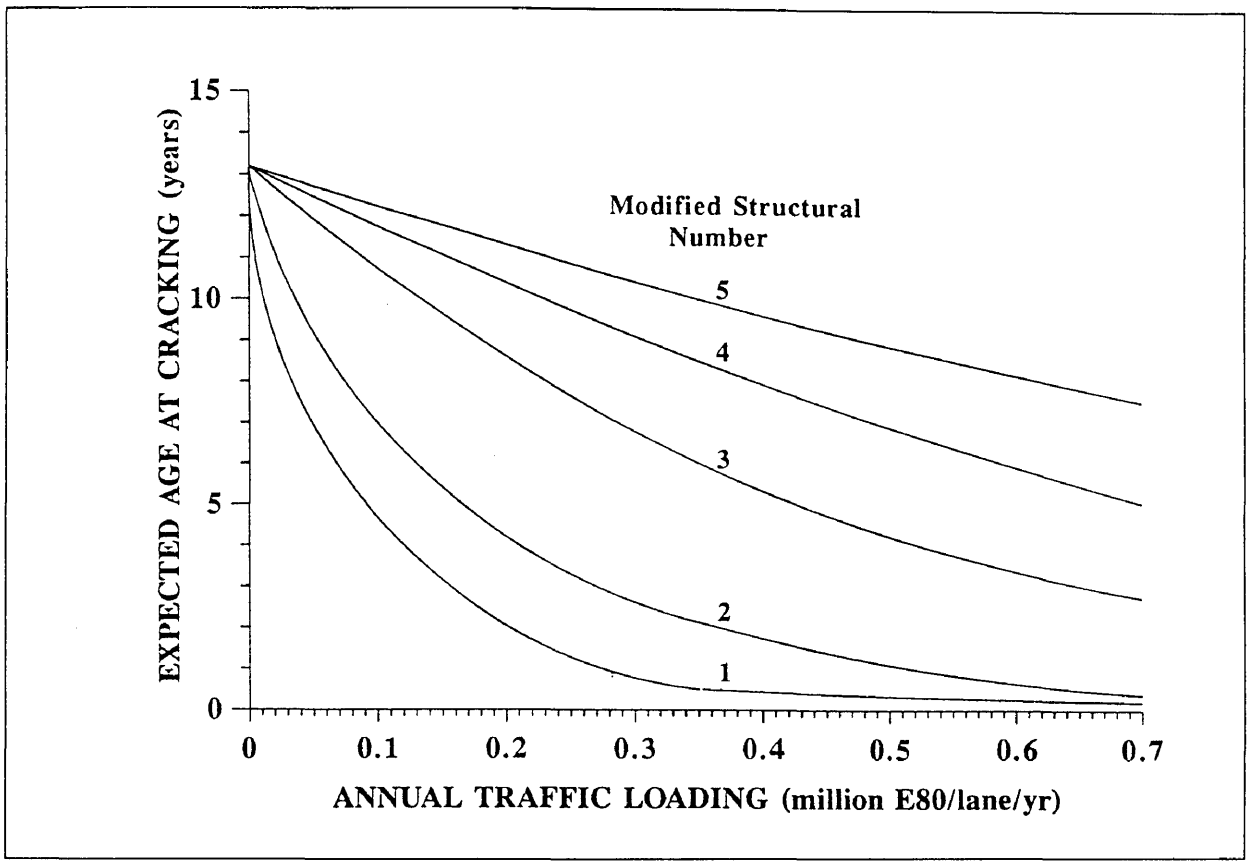

Figure 2.7: Prediction of the expected age of a double surface treatment at the initiation of all cracking (After Paterson, 1987).

For surfacings on cemented roads a crack initiation model was also developed using the maximum likelihood procedure. During the development of this model it became evident that the structural number was not as strong a predictor of cracking initiation as deflection. The model was:

$$TY_{cr2} = 1{,}11 \exp(0{,}035\ H_s + 0{,}371 \ln CMOD - 0{,}418 \ln DEF - 2.87\ YE_4 / SNC^2)$$

where:

TY_{cr2}, SNC and YE_4 as previously defined.

H_s = Thickness of bituminous layers, mm.

CMOD = Resilient modulus of cemented base in GPa.

DEF = Benkelman beam deflection under 80 kN single axle load, mm.

The prediction given by the model is illustrated in Figure 2.8 From the illustration it is evident that as the deflection of the pavement decreases, the effect of traffic loading also decreases due to the effect of pavement stiffness. The stiffer the pavement the longer the expected life. The model developed is however not valid when a strain relieving inter layer is present between the base and the surfacing.

b) Initiation of wide cracking : The prediction of the initiation of wide cracking (that is the time to reach class 4 cracking with an extent of 0,5 percent of the area) was expressed as a function of the initiation of all cracking. This decision made the prediction more reliable since it did not allow the initiation of wide cracking before the initiation of all cracking. The models were simply linear models assuming that the same factors affecting the all cracking models, were affecting the development of wide cracking. The model generally predicted a reasonable constant period of 2

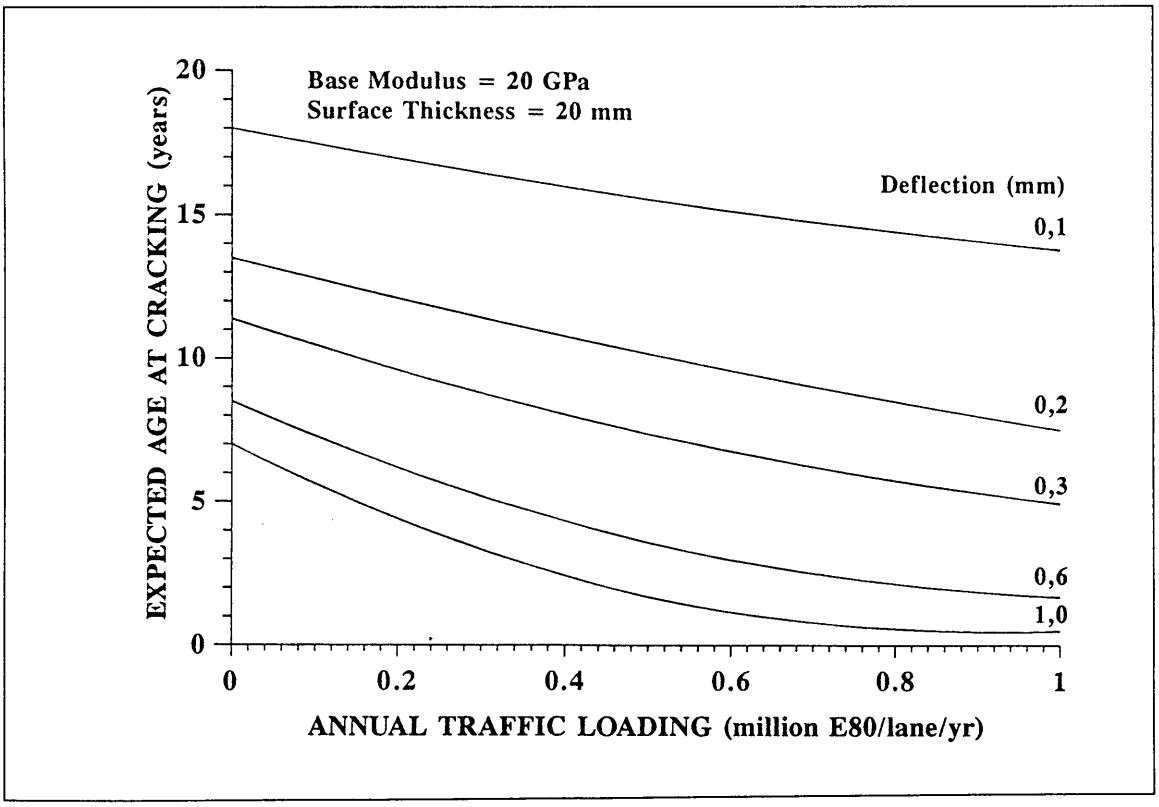

Figure 2.8: Prediction of the expected age of a semirigid pavement at the initiation of all cracking (After Paterson, 1987).

to 2,5 years difference between the initiation of all cracking and the initiation of wide cracking. The model for asphalt concrete pavements is:

$$TY_{cr4} = 2,46 + 0,93\ TY_{cr2}$$

where:

TY_{cr4} = Time since surface construction to the initiation of wide cracking.

TY_{cr2} = Expected (mean) age of surfacing at the initiation of all cracking in years.

For the prediction of the initiation of wide cracking on double surface treatments, the same assumptions were made as for asphalt concrete pavements, and two models were developed. The models predicted a period of 2,7 years from the initiation of all cracking to the initiation of wide cracking for new surfacings (Paterson, 1987). The models were:

$$TY_{cr4} = 2,66 + 0,88\ TY_{cr2}$$
$$TY_{cr4} = 1,16\ TY_{cr2}$$

where:

TY_{cr4} and TY_{cr2} are as previously defined.

The same assumptions were also made for the prediction of the initiation of wide cracking on pavements with cemented layers the same assumptions were made as for asphalt overlays, and the following model was developed:

$$TY_{cr4} = 1,46 + 0,98\ TY_{cr2}$$

With TY_{cr4} and TY_{cr2} as previously defined.

The model predicted an interval of about 1,5 years for cemented base pavements between the initiation of all cracking and the initiation of wide cracking. According to Paterson (1987) the daily thermal movements in the pavement dominated the cracking mechanisms.

Models were also developed for asphalt overlays, surface reseals and slurry seals, but according to Paterson (1987) the models are not very reliable because of the partial lack of data on the pavement condition prior to the overlay and the clear indication that the prior condition is a factor influencing the deterioration. The models developed are summarised in Table 2.6.

Table 2.6: Models for initiation of cracking for overlays and reseals (After Paterson, 1987).

Pavement Type	Time until the initiation of all cracking
Asphalt Overlay	$TY_{cr2} = 10,8 \exp(-1,21\ DEF - 1.02\ YE_4\ DEF)$
Reseal on Uncracked surface	$TY_{cr2} = 13,2 \exp[-20,7\ (1 + CQ)\ YE_4 / SNC^2]$
Reseal on Cracked surface	$TY_{cr2} = 0,4\ Ho$ or $TY_{cr2} = 0,2\ Ho$
	Time until the initiation of wide cracking
Asphalt Overlay	$TY_{cr4} = 2,04 + 0,98\ TY_{cr2}$
Both Reseals	$TY_{cr4} = 1,85 + 1,00\ TY_{cr2}$

Where:

TY_{cr2}, SNC, YE_4, DEF, CQ and TY_{cr4} as previously defined.

Ho = Average thickness of the seal, mm.

c) Progression of area cracked: These models predict the progression of the cracked area once cracking has initiated. Separate models were developed for the progression of all cracking and for wide cracking. The slow progression of cracking during the study period limited the information collected on the progression of cracking. As a result of the limited data collected, especially for a cracked area above 30 percent of the pavement area, statistical manipulation methods had to be used to enable the use of all collected data. An approach using linear regression on the transformations of all individual observations of incremental area allowed the use of all data. Five nonlinear recursive model forms were evaluated. The following model was however selected because of its symmetry and flexibility of curvature. The model was:

$SA' = aSA^b$

where:

A = Decimal fraction of area.

SA = min (A, 1-A)

SA' = Rate of change of SA with respect to t.

a = Coefficient to be estimated as a function of pavement type, strength and traffic.

b = Constant.

With the redefinition of b in the above formula as follows:

$$dSCR_{it} = a\, SCR_{it}^{1-b}\, dt,$$

the area of cracking at time t, CR_{it}, is derived by integration, i.e.:

$$CR_{it} = (1-z)50 + z[z\, a\, b\, t_{ci} + z\, 0{,}5^b + (1-z)\, 50^b]^{1/b}.$$

The incremental area of cracking during the period δt, δCR_{it}, is given by:

$$\delta CR_{it} = zz\{[\, z\, a\, b\, \delta t + SCR_{it}^{\,b}\,]^{1/b} - SCR_{it}\}$$

where:

CR_{it} = The area of cracking at time t.

δCR_{it} = The incremental area of cracking during period δt.

a,b = As previously defined.

SCR_{it} = Minimum [CR_{it}, 100 - CR_{it}]

t_{ci} = Time since the initiation of CR_i cracking (years) in time-base models, or traffic loadings since initiation (million E80) in traffic-base models.

z = 1 When $t_{ci} \leq t^{50}$ and z = -1 otherwise,

t^{50} = $(50^b - 0{,}5^b)/a\, b$; i.e., the time to 50% area cracked.

zz = 1 when $CR_{it} \leq 50$; otherwise zz = -1.

For each pavement type two sets of coefficients for a and b were derived, firstly for time-based models where cracking progression was defined as a function of time and independent of the strength or traffic variables, and

secondly for traffic-based models where cracking progression was defined as function of traffic loading and strength. The results are summarised in Table 2.7. Usually there was only a small difference in the goodness of fit between the two dimensions, though the traffic-based models were generally superior (Paterson, 1987). However traffic-based models were

Table 2.7: Recommended values for the coefficients a and b (After Paterson, 1987).

Cracking class and surfacing	Time-base		Traffic-base	
	a	b	a	b
All cracking				
Asphalt Concrete	1,84	0,45	$450\ SNC^{-2,27}$	0,65
Surface Treatment	1,76	0,32	$1,760\ SNC^{-3,23}$	0,28
On Cemented Base	2,13	0,36	$0,005\ DEF^{0,64}\ CMOD^{0,90}$	0,41
Asphalt Overlays	1.07	0,28	-	-
Reseals and slurry seals	2,41	0,34	-	-
Wide cracking				
Asphalt Concrete	2,94	0,56	$718\ SNC^{-2,52}$	0,72
Surface Treatment	2,50	0,25	$160\ DEF^{1,48}$	0,45
On Cemented Base	3,67	0,38	$0,061\ CMOD^{0,56}$	0,22
Asphalt Overlays	2,58	0,45	-	-
Reseals	3,40	0,35	-	-

not always applicable for some surface types. An illustration of the prediction by both models are shown in Figure 2.9. From Figure 2.9 it is evident that the rates of progression of wide cracking are generally faster than the rates of all cracking, but the area of wide cracking never exceeded the area of all cracking as a result of the assumptions made during the development of the models (Paterson, 1987). Furthermore strong similarities are evident among groups of surface types, for example between asphalt concrete and asphalt overlays, which take twelve to fourteen years for the development of cracks over the whole pavement section area.

- **Prediction of ravelling**: As with the prediction of cracking, ravelling is also modelled in two phases, namely the time before initiation of ravelling, and the rate of progression of the area ravelled once initiated. The area of ravelling was defined the same as for cracking. The modelling was however simplified by the fact that there was only one severity class.

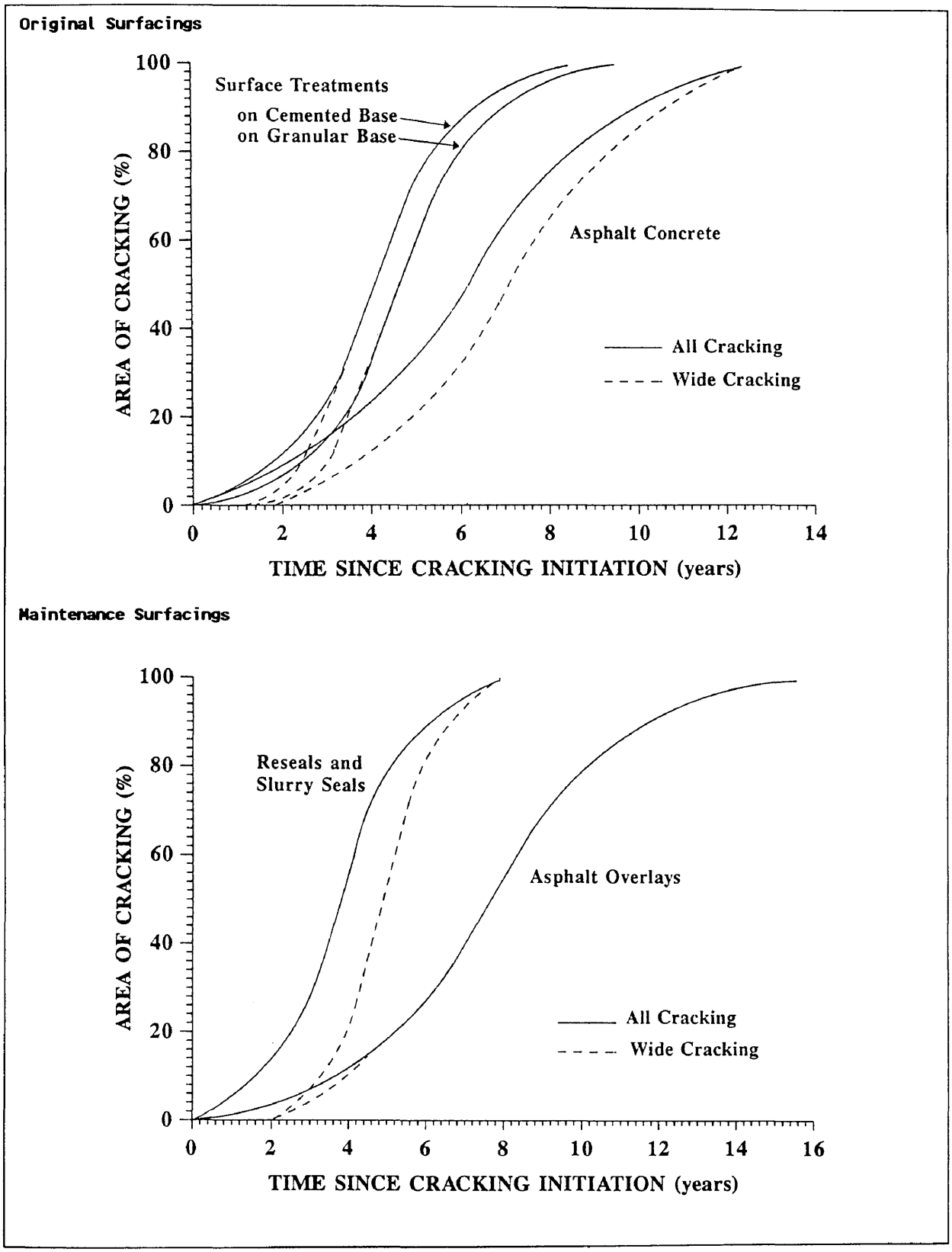

Figure 2.9: Predicted cracking progression for original and maintenance surfacings (After Paterson, 1987).

During the study of the pavements used in the development of the model, it was evident that in some instances ravelling could confidently be attributed to problems that manifested during construction (Paterson, 1987). As a result of this a construction quality code (CQ) was defined as follows:

CQ = 1 In the cases where the seal appeared to be streaky due to faulty binder distribution, or 100 percent loss of stone occurred within one to three years due apparently to loss of adhesion.

CQ = 0 In the absence of identifiable surfacing construction problems.

The models developed are only applicable to surface treatments, since ravelling was not assumed to be a problem on asphalt concrete surfaces.

a) Initiation of ravelling: The initiation of ravelling was defined as the time to reach a cracked area of 0,5 percent or more for each pavement section. The prediction model was developed by using the probabilistic failure-time method of analysis. The following simple model containing only three explanatory variables was developed (Paterson, 1987):

$$TY_{rav}(sp) = K_{sp}\, a_s \exp(-0.655\, CQ - 0{,}156\, YAX)$$

where:

$TY_{rav}(sp)$ = Predicted age of surface treatments at the initiation of ravelling, with probability of survival sp, in years.

CQ = Construction quality (0 if no faults, 1 if faulty).

YAX = Annual flow of all vehicle axles, million axles/lane/year.

a_s = Constant related to surfacing type, as follows:
= 10,5 for Chip seal
= 14,1 for Slurry seal
= 8,0 for Cold-mix

K_{sp} = Factor depending on probability of survival, sp, as illustrated in Figure 2.10. K_{sp} = 1 for mean value.

As seen in the model, no strength parameter was found that had a significant influence on ravelling initiation, traffic flow did however seem to have more of an influence. An illustration of the model prediction is shown in Figure 2.10 as a function of traffic flow and construction quality. From the Figure it is evident that the expected life before ravelling is diminishing with an increase in traffic. The life is however not highly sensitive to traffic flow, decreasing by approximately 14 percent per million vehicle axles per lane (Paterson, 1987). According to Paterson (1987) the difference indicated for the three surfacing types is directly related to the binder film thickness and void content of these surfacings, since these two factors determine the relative susceptibility of the materials to oxidation. Taking for example the open-graded cold mixed asphalt which has a short diffusion path through the binder film, and much of the film exposed to air through the inter connecting voids, it is obvious that the binder is susceptible to faster oxidation, resulting in an increase in the probability of ravelling.

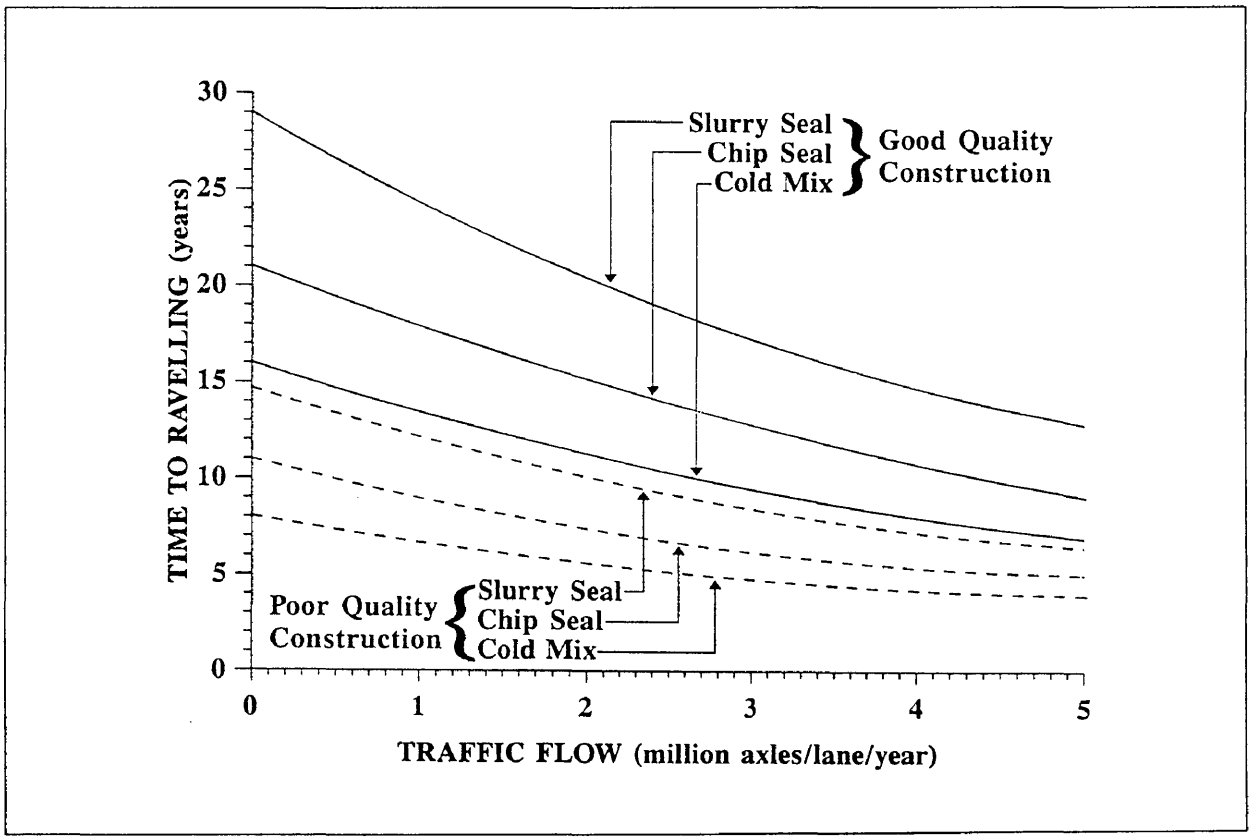

Figure 2.10: Model predictions for the initiation of ravelling for various surface treatment types (After Paterson, 1987).

Another observation from the illustration is the influence of construction quality on the life of a pavement, indicating nearly a 50 percent decrease in case of faulty construction. According to Paterson (1987) the inclusion of this parameter allows the economic evaluation of the influence of quality control on pavement deterioration.

b) Progression of ravelling: It was found that the progression of the area ravelled was best represented by a sigmoidal (S-shaped) function, with the area being normalised as a percentage of the pavement section (Paterson, 1987). The rate of ravelling progression was computed as the difference in area ravelled between consecutive surveys. From the analysis of the data the following model was developed:

$$dARAV_t = 4{,}42\ SRAV_t^{0{,}648}\ dt$$

where:

$dARAV_t$	=	Increment of ravelled area, percentage of carriageway area.
dt	=	Incremental time, years.
$SRAV_t$	=	Sigmoidal function of ravelled area, $ARAV_t$ at time t,
	=	min ($ARAV_t$, 100 - $ARAV_t$).

When integrated the model yields the following expression for the absolute area of ravelling at time t since initiation:

$$ARAV_t = (1\text{-}z)50 + z[z\ a\ b\ t + z\ 0{,}5^b + (1\text{-}z)\ 50^b]^{1/b}$$

where:

a	=	4,42
b	=	0,352
z	=	1 if $t < T_c$; and z = -1 otherwise.
T_c	=	$(50^b - 0{,}5^b)/a\ b$; this is the time to 50% area ravelled.
t	=	Time since initiation, in years.

The prediction given by the model is illustrated in Figure 2.11. As seen it is a single curve independent of traffic flow and pavement characteristics that applies to all surfacing types studied. The model predicts a time of roughly 4 years between the initiation of ravelling and the extension of ravelling over 100% of the area.

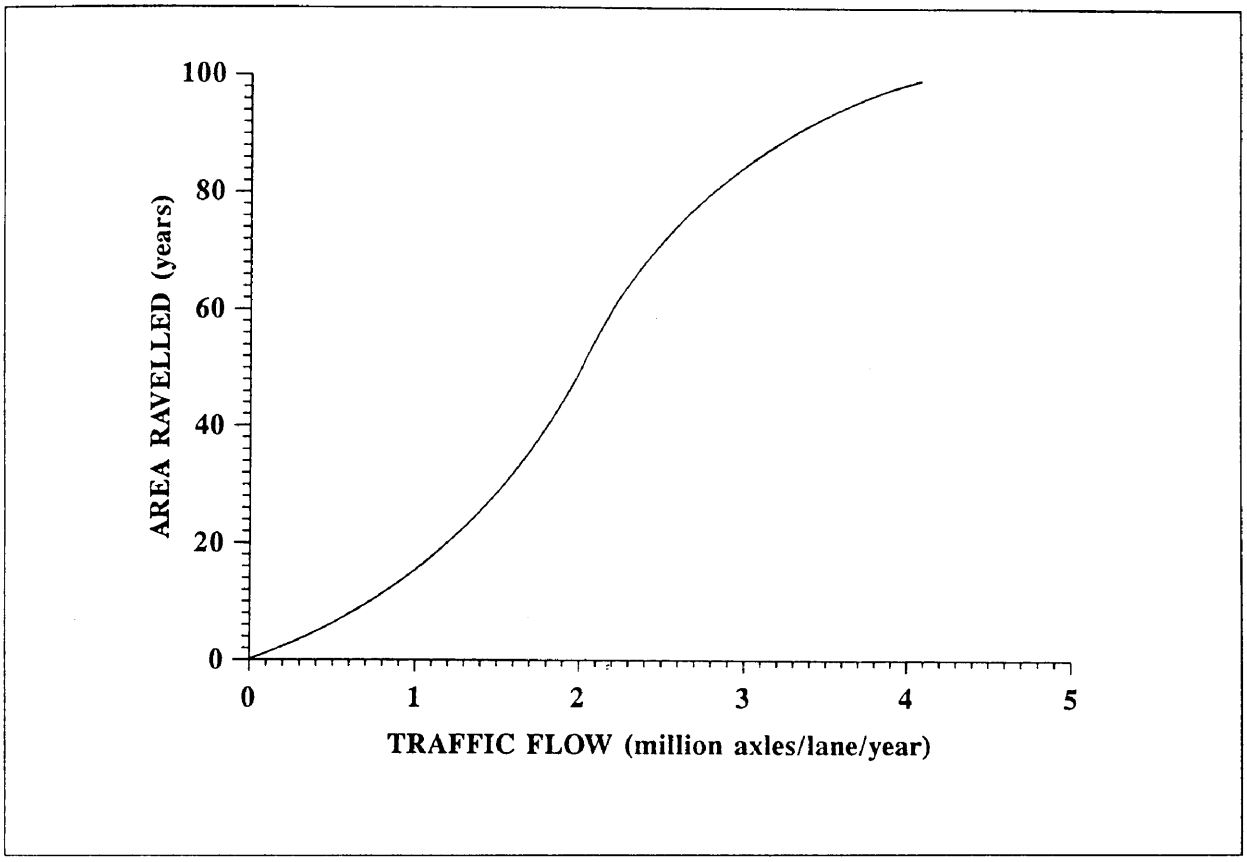

Figure 2.11: Model prediction for the progression of area of ravelling for all surface treatments over time (After Paterson, 1987).

- Potholing: Despite the fact that potholing is probably the least predictive form of distress, it is necessary to include some prediction of potholing and its impact on vehicles in an economic evaluation model to serve as the economic penalty of deferred or neglected maintenance (Paterson, 1987). In order to distinguish potholing from ravelling, a pothole is defined as follows (Paterson, 1987):

  A pothole is a cavity in the road surface which is 150 mm or more in diameter and 25 mm or more in depth.

  These dimensions are the minimum that affect the motion of a car wheel and the measured roughness significantly according to Hide and Keith (1979). As a result of the insufficient data available, the most appropriate procedure of statistical estimation could not be employed to develop models. Instead simple models had to be constructed based on considerable engineering judgment and supposition using the available data.

a) **Initiation of potholes**: The available data showed considerable variability, but in general it appeared reasonable to state that the probability of potholes developing becomes significant when the area of wide cracking exceeds 20 percent or the area of ravelling exceeds 30 percent (Paterson, 1987). The time (TMIN) from the initiation of the triggering distress (wide cracking or ravelling) to the initiation of potholing is expressed by (Paterson, 1987):

TMIN = max [2 + 0,04 HS - 0,5 YAX; 2] if base is not cemented
TMIN = max [6 - YAX; 2] if base is cemented

Because maintenance may have been undertaken during this time, the initiation of potholing at time TMIN is made conditional upon the time since initiation and the area of distress must satisfy the following:

Wide cracking:
$AGES - TY_{cr4} > TMIN$ and $CR_4 > 20$

Ravelling:
$AGES - TY_{rav} \geq TMIN$ and $ARAV \geq 30$

Potholing:
When potholing has been observed at any time during the current surfacing period, TMIN is automatically applicable recardless whether the requirements for wide cracking or ravelling is satisfied.

where:

TMIN = Predicted time between the initiation of either wide cracking or ravelling, whichever occurs earliest, and the probable initiation of potholing, in years.
HS = Total thickness of bituminous surfacing, mm.
YAX = Annual number of vehicle axles, million axles/lane/year.
AGES = Age of the most recent surfacing, in years.
TY_{cr4} = Predicted surfacing age (year) at the initiation of wide cracking.
TY_{rav} = Predicted surfacing age (year) at the initiation of ravelling.
CR_4 = Area of wide cracking as a percentage of pavement area.
ARAV = Area of ravelling as a percentage of pavement area.

The prediction of the initiation of potholes for wide cracking by the algorithm is illustrated in Figure 2.12. From the illustration it can be seen that the delay before potholing occurs, increases by one year per 25 mm thickness of surfacing and by one year per reduction of 2 million axles/lane/year. It is also obvious that the chances of potholes occurring on thick bituminous-base pavements are much smaller than for a thin single surface treatment.

b) **Progression of potholes**: By relating the available data to mechanistic parameters such as traffic flow, surfacing thickness and base quality, a group of algorithms were constructed from which the incremental area of potholing could be derived from one of three sources, namely from wide cracking, ravelling or from the enlargement of existing potholes, as follows (Paterson, 1987):

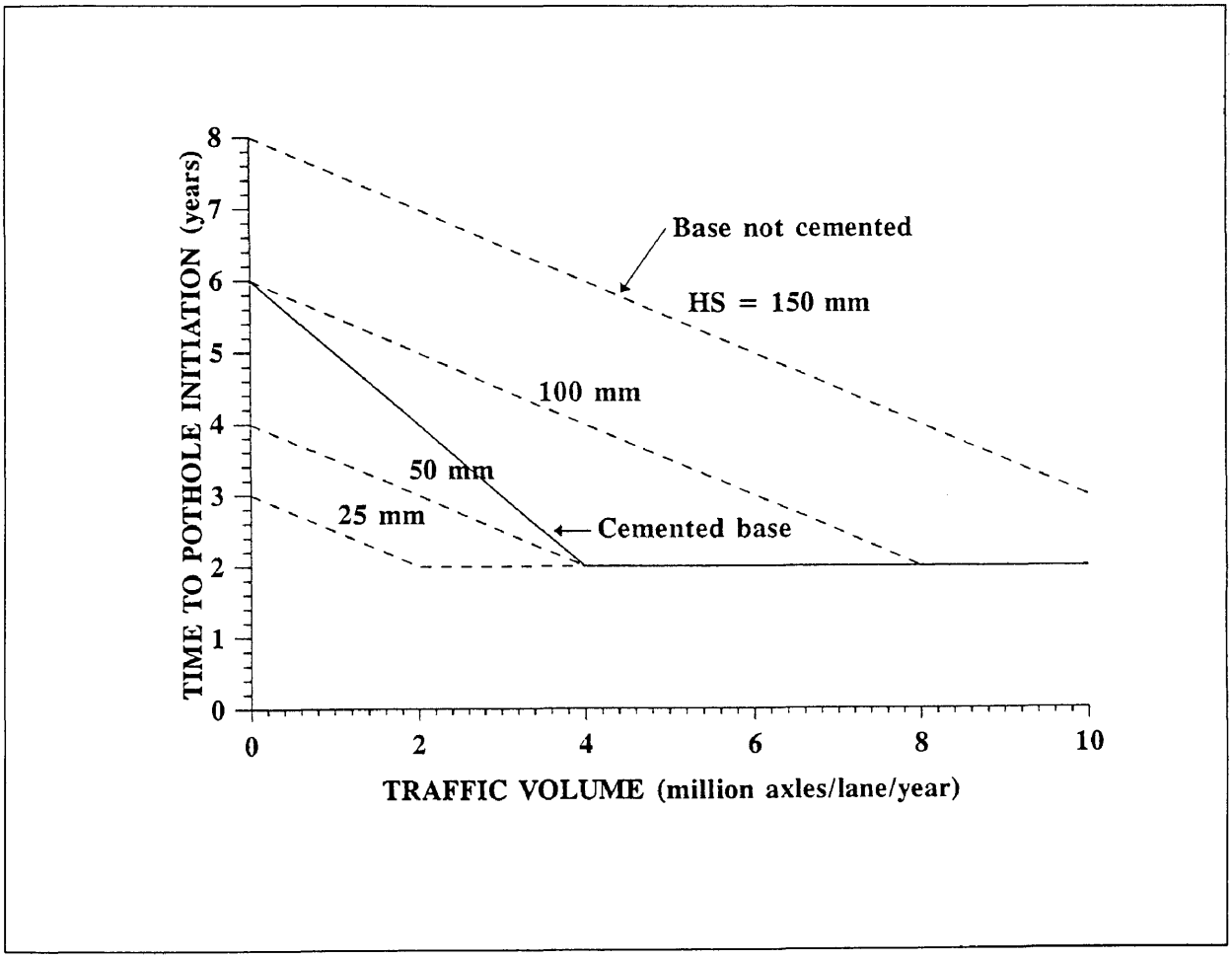

Figure 2.12: Model predictions for the time to pothole initiation (After Paterson, 1987).

$$\delta APOT = \min \{\delta APOT_{cr} + \delta APOT_{rv} + \delta POT_{pe}; 10\}$$

where:

$\delta APOT$ = The predicted change in the total area of potholes during the analysis year due to road deterioration (limited to a maximum of 10 percent per year), as a percentage.

$\delta APOT_{cr}$ = The predicted change in the area of potholes during the analysis year due to cracking;

= $\min (2\ CR_4\ U; 6)$

$\delta APOT_{rv}$ = The predicted change in the area of potholes during the analysis year due to ravelling;

= $\min (0{,}4\ ARAV\ U; 6)$

$$U = \frac{(1 + CQ)\ (YAX/SNC)}{2{,}7\ HS^{5}}$$

CQ = Construction quality factor.

YAX = Annual number of vehicle axles, million axles/lane/year.

SNC = Modified structural number.

HS = Total thickness of bituminous surfacing, mm.

$\delta APOT_{pe}$ = The predicted change in the equivalent area of potholes during the analysis year due to pothole enlargement as a result of the scouring action of water, traffic removing material from a pothole, and the erosion of the surfacing by spalling;

= $\min \{\delta APOT\ [K_{base}\ YAX\ (MMP + 0{,}1)]; 10\}$

K_{base} = $\max [2 - 0{,}02\ HS; 0{,}3]$ if base is granular.

= 0,6 if base is cemented.

= 0,3 if base is bituminous.

MMP = Mean monthly precipitation in meters.

An illustration of the algorithm predictions for a granular base pavement is shown in Figures 2.13 and 2.14. The rate of pothole progression is modelled to increase linearly with an increase in the total area of distress.

As seen in Figure 2.13 the same applies as the traffic volume increases. According to Paterson (1987) the basecourse and surfacing quality are

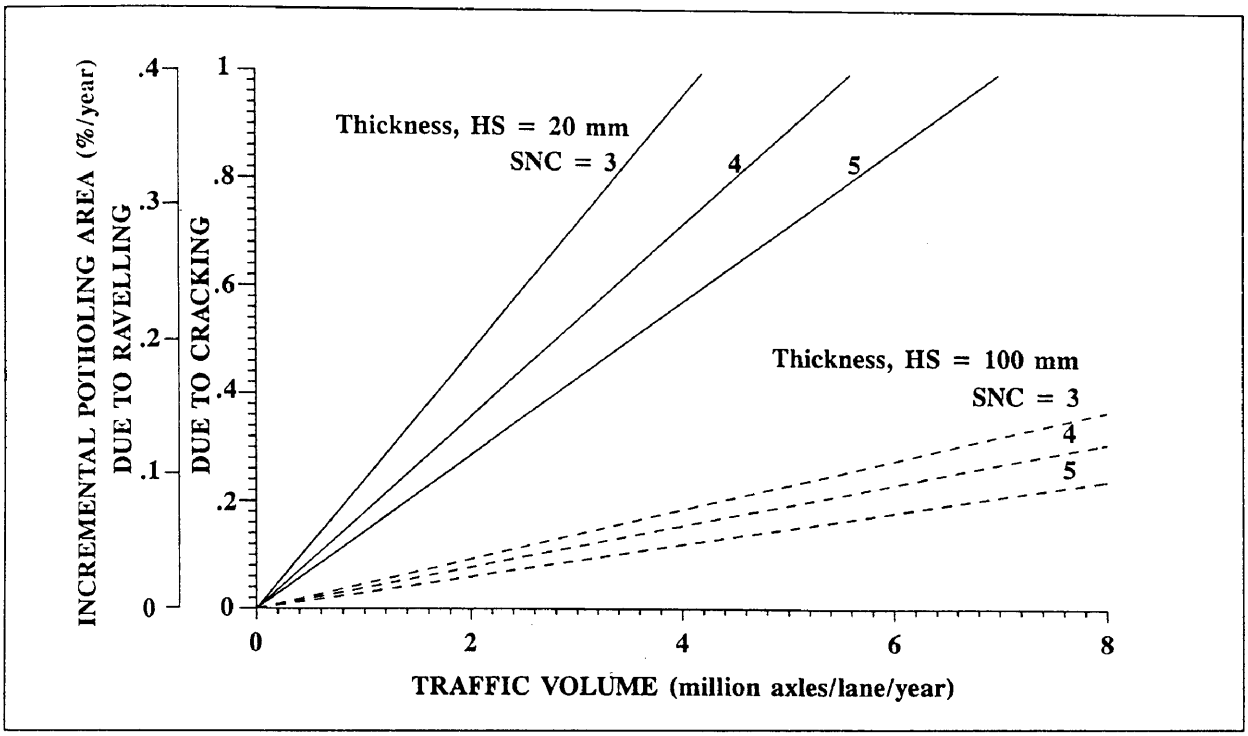

Figure 2.13: Model predictions for the progression of area of potholing due to wide cracking and ravelling (After Paterson, 1987).

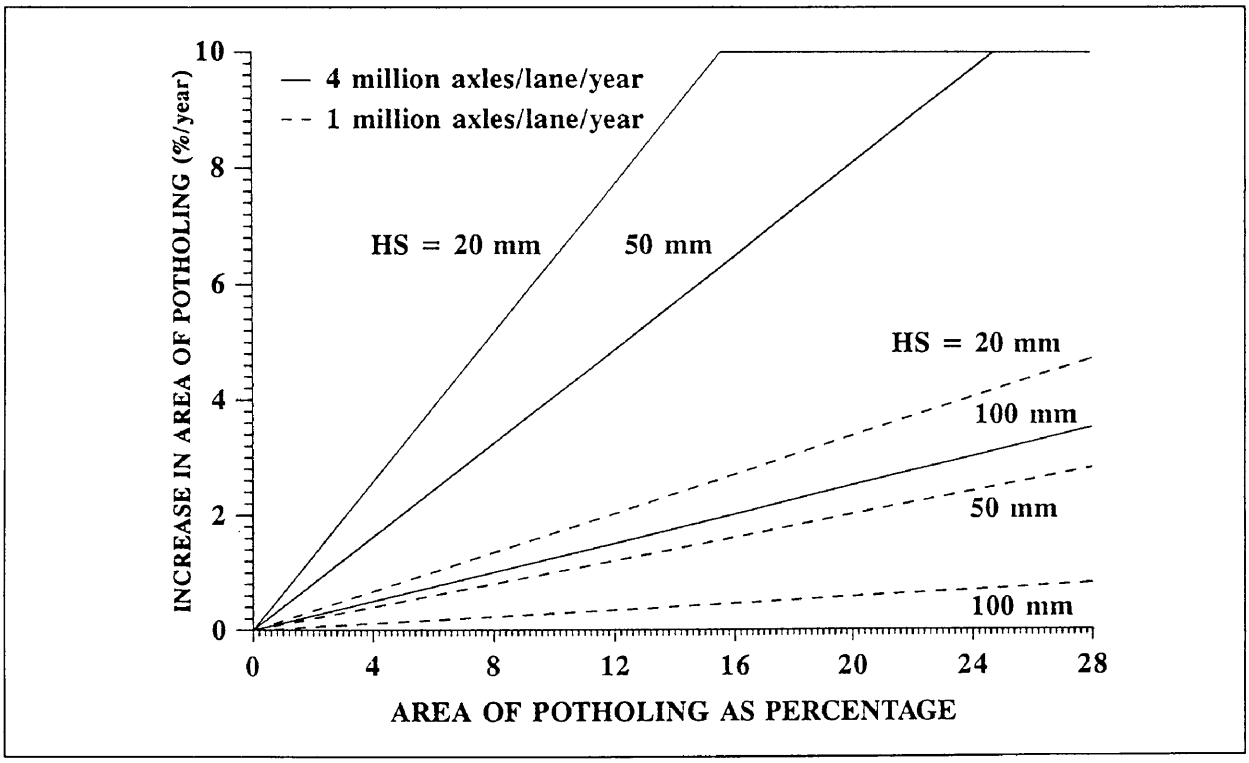

Figure 2.14: Model predictions for the progression of area of potholing due to enlargement of potholes (After Paterson, 1987).

important factors in the prediction of potholing but difficult to quantify, as result of this the construction quality factor (CQ) and modified structural number were used as surrogates of quality. This does not imply that the rate of potholing is physically related to pavement strength, but rather that this is as mentioned a convenient surrogate of base quality that is typically higher for high standard pavements. It is further also evident that thick surfacings are modelled to be less sensitive to pothole progression. Figure 2.14 provides an accelerating rate of pothole progression as a function of the area of potholing, in the absence of routine maintenance.

2.4.3.3 Discussion

The Brazil study conducted from 1976 to 1984 surpassed most of the previous attempts undertaken to quantify the deterioration of a pavement. The models developed out- classed most of the previous models developed elsewhere in the world, and some models resulted in major contributions to the field of pavement deterioration. The incremental roughness model developed was the first model incorporating structural, surface distress and environment-age conditions factors. This alone ranked the Brazil study in importance with the AASHO Road Test. The Brazil study differs however from the AASHO test in that (Paterson, 1987):

- The use of actual mixed traffic instead of controlled traffic.
- Pavement types varied considerably in age, modulus, layer thickness, subgrade support and surface type in contrast with the uniform type of experimental pavements used at AASHO.
- The pavements covered a vast range of ages in contrast with the relatively young pavements in the AASHO Road Test.

All these factors allowed for the easier adoption of the Brazil models to other climatic regions. This was illustrated by the strong validation of the models across the following eight major data sets from Kenya Costs Study, Kenya Network Sample, Arizona Network Sample, Texas Network Sample, AASHO Road Test in Illinois, Ordway Base Experiment in Colorado, as well as network sample data from Tunisia and South Africa. The climate varied across data sets from arid nonfreezing to wet freezing climates. Thus the models developed in Brazil are appropriate for further evaluation under South African conditions.

2.5 TEXAS STUDY

2.5.1 Background

The study was conducted on data collected intermittently in Texas over a period of seven years from 1972 to 1980 on 337 road sections, each section in one lane and 2 miles long (Texas Research and Development Foundation, 1980). The condition data included into the study were collected according to a rating method and quantified by a score. Maintenance activities were also included but the roughness data were difficult to interpret because large fluctuations existed that were often not explained by the maintenance records.

2.5.2 Major contributions to the field of pavement deterioration prediction

- **Prediction of roughness**: The study resulted in the introduction of a variable sigmoidal shape to the basic AASHO Road Test damage model. This modification allowed the condition of a pavement to approach an asymptotic value, and changes to take place in the deterioration rate over the life of a pavement. The modified pavement damage function was as follows:

$$g' = \frac{p_i - p}{p_i - p_f} = \exp\left[-\left(\frac{\alpha}{N}\right)^{\beta}\right]$$

where:

g' = Dimensionless damage function with values $g' = e^{-1}$ at $\alpha = N$, and asymptotic to 1 as $n \rightarrow$ infinity.

p_i = Initial serviceability (PSI).

p = Current serviceability (PSI).

p_f = The asymptotic value of terminal serviceability (PSI).

α = A magnitude parameter to be estimated as a function of pavement and traffic variables (See discussion later on).

β = A shape parameter of the condition trend curve to be estimated as a function of pavement and traffic variables (See figures 2.15).

N = Number of 80 kN equivalent single axle load applications.

Figure 2.15 indicates the main advantage of the modification to the damage function, since as illustrated the modification allows a variety of trend shapes that could be applied. During the study it was assumed that ß = 1 for all pavements, and α and p_f were estimated as follows (Lytton, Michalak and Scullion, 1982) :

For surface treatments:

$$\alpha = [0,29 - 0,0076\ TI + 0,015\ H2 + 0,0004\ FTC - 0,035\ DMD]\ 10^6$$
$$p_f = 0,84$$

For asphalt concrete on bituminous base:

$$\alpha = [0,34 + 0,0075\ H' - 0,032\ PI]\ 10^6$$
$$p_f = 0,055\ (H')^{-1}\ PI^{0,867}$$

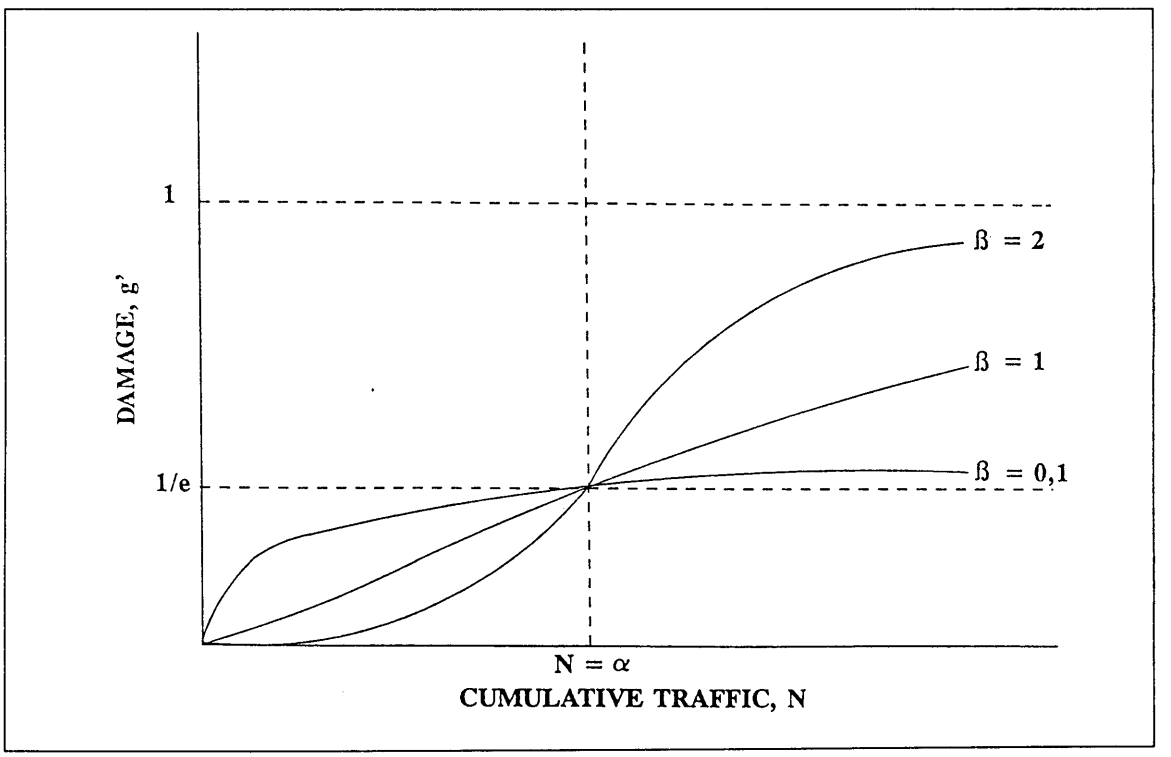

Figure 2.15: Influence of ß on shape of damage function g'(After Lytton, Michalak and Scullion, 1982).

where:

TI = Thornthwaite Index of 1948 + 50.
H2 = Thickness of base layer in inch.
FTC = Number of annual freeze-thaw cycles.
DMD = Dynaflect maximum deflection in 0,001 inch.
PI = Plasticity index of subgrade soil as percentage.
H' = Transformed total thickness of pavement above rigid base in inch.

- **Prediction of cracking**: In this study cracking was modelled by the following dimensionless score (S) (Lytton, Michalak and Scullion, 1982):

$$S = \exp\left[-\left(\frac{\alpha}{NE}\right)^{\beta}\right]$$

where:

S = Decimal severity score of cracking ranging in value from 0 at no cracking, to 1 at the maximum defined score.
NE = Cumulative equivalent standard axle load since most recent surfacing, million E80.
α,ß = Functions of pavement and environmental parameters, where the value of ß determines the shape of the sigmoidal curve, and hence also determines the period elapsing until effective initiation and the rate of progression simultaneously.

For crocodile cracking in surface treatments:

$$\alpha = [-0,97 + 0,039\,T + 0,0034\,TI + 0,018\,H2 + 0,0066\,FTC + 0,0056\,PI - 0,0046\,LL]\,10^{6}$$

$$\beta = 0,39\,PI^{-0,63}\,DMD^{0,54}\,T^{1,02}$$

where:

T = Mean monthly air temperature less 10 °C.
LL = Liquid limit of subgrade soil as percentage.

For longitudinal and transverse cracking the variable NE in the equation was defined as the number of months since the previous major maintenance or reconstruction.

The score rating system (S) was an approximately linear function that combines the area and severity (class) of cracking (each were grouped into four ratings), into a single decimal score for each pavement as follows:

$$\text{Cracking score} = \text{Area score} + \text{Severity score}$$
$$\leq 1$$

The decimal scores used in the Texas study to convert the different numerical ratings for both area and severity are listed in Table 2.8. As seen in Table 2.8 the maximum decimal score is 0,5 for a cracked area greater than 30 percent, or a severity level of 3 which are then summarised to give a maximum value of 1. Table 2.8 also contains the values assumed to convert the numerical ratings into the format required for HDM-III, allowing the use of the data . The conversion factor used was:

$$CRX = A_{TX}\, S_{TX}$$

where:

CRX = Area of indexed cracking as percentage of the surface area.

A_{TX} = Area assumed as percentage of surface area.

S_{TX} = Value assumed for severity numerical rating.

Table 2.8: Decimal score of cracking, used in combining area and severity in Texas (After Lytton, Michalak and Scullion, 1982).

Area				Severity			
Percentage of area	Numerical rating	Decimal score	ATX as a percentage	Severity rating	Numerical rating	Decimal score	STX as a factor
0 - 1	0	0,005	0,50	None	0	0,005	0,00
1 - 15	1	0,080	8,00	Slight	1	0,167	0,50
16 - 30	2	0,230	23,0	Moderate	2	0,333	0,75
> 30	3	0,500	50,0	Severe	3	0,500	1,00

2.5.3 Discussion

Although the roughness model developed was a improvement over the AASHO model it still could not be compared with the model developed from the Brazil study. The models developed are however not applicable to South African conditions as a result of (Paterson, 1987):

- The fact that the function implies that the serviceability tends to an asymptotic boundary defined by g' =1. Such a plateau-effect predicted by the sigmoidal curve for roughness would be indicative of the permanent deformation trends. Thus the function would therefore only apply under conditions where the induced shear stresses do not exceed the shear strength threshold. Under other circumstances, the shape may simply reflect proximity to the lower boundary of the serviceability scale.

- The fact that support for the S-shape in the Texas data base appears somewhat questionable, and the presence of unexplainable difference in the data set.

- The difficulty to parametrise such model forms so that changes in the pavement structure, traffic flow or maintenance will cause the predictions to respond correctly.

- The fact that these model forms constrain the rate of progression by the time to initiation of distress, resulting in long-surviving pavements to have a rapid rate of progression once cracking initiates.

2.6 CONCLUSIONS

The main conclusion from the literature survey was that the accurate prediction of pavement deterioration is of world wide concern. This is evident in the number of studies conducted over the years with each of these studies contributing towards the better understanding of the deterioration of pavements. Of all the models studied that were developed from major studies it was concluded that the incremental models developed during the Brazil study, were the most appropriate for further evaluation under South African conditions. These models were selected because:

- they were developed from the large comprehensive source of data obtained from the Brazil-UNDP study which employed more advanced and theoretical and statistical methodologies to generate a database covering a broader range of road characteristics and vehicle types;

- they were validated across eight major independent data sets from widely differing climates, ranging from arid nonfreezing to wet freezing, indicating the fundamental plausibility of the models and their transferability (Paterson, 1987);

- the incremental form of the models allowed the year-by-year simulation of pavement deterioration, thus making the models excellent for application in a pavement management system, and

- they are the deterioration models incorporated into the HDM-III model because they provided the best representation of time and traffic interactions.

CHAPTER 3

SENSITIVITY ANALYSIS OF MODEL PARAMETERS

3.1 INTRODUCTION

To enable the local adoption of the road deterioration and maintenance submodel developed during the Brazil study and incorporated into the Highway Design and Maintenance Standards Model (HDM-III), it was necessary to evaluate the sensitivity of the HDM-III model to changes in the different parameters composing the road deterioration and maintenance submodel. This evaluation of the sensitivity of the road deterioration and maintenance submodel was conducted by substituting different values within the allowable range specified by the HDM-III submodel for each parameter, and plotting the results over a twenty year analysis period. These plotted results allowed the identification of the sensitivity of the road deterioration and maintenance submodel to changes in a specific parameter.

This investigation of the sensitivity of the submodel to changes in its parameters was necessary to determine whether the data obtainable from the Department of Transport database was sufficient for use in the evaluation of the applicability of the HDM-III relationships to local conditions. The results obtained from the sensitivity analysis of the road deterioration and maintenance submodel are discussed in this chapter.

3.2 SENSITIVITY ANALYSIS PROCEDURE

The sensitivity of the road deterioration and maintenance submodel to changes in the different combinations of parameters listed in Table 3.1 were evaluated by using the HDM-III model. Each combination of parameters was individually evaluated and the following general values were assumed where applicable:

- Initial roughness of 30 quarter-car index (QI) units/km, to allow for most of pavements constructed.
- Subgrade California Bearing Ratio (CBR) of 10 percent. This minimised the influence of the subgrade on deterioration, but still allowed for most of the pavements constructed.

Table 3.1: Sensitivity analysis factorial

		Surfacing type		Asphalt Concrete / Surface Treatment											
		Base type		Granular						Cemented					
		Traffic 10^6 E80/lane/yr		0,1			1,0			0,1			1,0		
		Structural number SN		1	3	6	1	3	6	1	3	6	1	3	6
MODEL EVALUATED FOR SENSITIVITY	CRACKING	Modulus of cemented basecourse (GPa)	0,1 0,4 1 3												
		Thickness of Bituminous layers in mm	30 50 150 300												
		Deflection in mm	0,1 1 3 5												
		Construction quality	Good Poor												
	RAVEL	Construction quality	Good Poor												
	POTHOLE	Thickness of Bituminous layers in mm	30 50 150 300												
		Construction quality	Good Poor												
	RUT	Deflection in mm	0,1 1 3 5												
		Percentage of compaction	85 90 95 100												
	INCREMENTAL ROUGHNESS	Initial area all cracking as % of area	0 0,1 10 20 50 100												
		Initial area wide cracking as % of area	0 0,1 10 20 50 100												
		Initial area of ravelling as % of area	0 0,1 10 20 50 100												
		Mean rut depth value in mm	0 5 10 20 50												
		Rut depth standard deviation mm	0 5 10 20												
		Subgrade CBR as %	2 5 10 20 50 80												
		Initial Roughness in QI	26 39 52 65 78 91 104												

- Maintenance activity included routine maintenance and 100 percent patching of potholes in line with Department of Transport policy.
- Layer thickness of 30 mm for asphalt concrete layers, and 15 mm for surface treatments.
- Resilient modulus of 0,4 GPa for a cement stabilised basecourse, since it was assumed that the cemented layer is broken up into an equivalent granular state.

The empty cells indicate options that are not available, since that parameter was found to have no significant influence on the specific model during its development. The structural number (SN) and traffic values included in Table 3.1 were selected to evaluate the HDM-III roughness prediction submodel at the limit of the recommended range for each parameter. It must be noted that the HDM-III model uses the modified structural number (SNC), which includes the contribution of the subgrade CBR. The incorporation of the specific subgrade CBR of 10 % results in an increase of 1,21 structural units to the structural number specified. Thus for a pavement with structural number (SN) of 1, the modified structural number (SNC) calculated equals 2,21. The percentages included in Table 3.1 were selected to give an acceptable indication of the sensitivity of the specific model to changes in that parameter.

3.3 RESULTS FROM THE SENSITIVITY ANALYSIS

The results obtained from the HDM-III model were plotted against each input parameter to obtain graphs denoting the sensitivity of the submodel to changes in that specific parameter over a 20 year analysis period. The following results were obtained from the sensitivity analysis for the different pavement models.

3.3.1 Cracking model

The evaluation of the sensitivity of the cracking model to changes in its parameters were conducted for both all and wide cracking. As mentioned in Chapter 2 the area of all cracking only includes crocodile and irregular cracks wider than 1 mm, excluding longitudinal, transverse and irregular cracking that were deemed not practicable to be modelled for network analysis (Paterson, 1987). The area of wide cracking only includes the percentage area of class 4 cracks, that is spalled cracks greater than 3 mm in width. The sensitivity of

both all and wide cracking were evaluated individually for the resilient modulus of a cemented basecourse, thickness of bituminous surfacing layers, deflection of the pavement structure and construction quality in collaboration with the structural number, traffic load and basecourse type. The following results were obtained.

3.3.1.1 Resilient modulus of cemented basecourse

The resilient modulus (M_R or as in this case CMOD) of a cemented layer describes the elasticity of material under a repeating axle load better than the static elasticity modulus (E), since it is recognising certain nonlinear characteristics of the elastic properties of soil. The results obtained from the sensitivity analysis for a twenty year study period are illustrated in Figures 3.1 to 3.4 for all cracking and Figures 3.5 to 3.8 for wide cracking. As seen the sensitivity analysis were conducted for four different resilient modulus values. These values were chosen to enable the analysis to represent all three phases during the life of a cement treated basecourse.

From Figure 3.1 and 3.2 it is evident that the increase in structural number from 1 to 3 does affect the predicted area of all cracking, especially for the higher resilient modulus values. The reason for this is that most of the relative strength of a pavement with cement treated layers are usually contained within these layers. Thus an increase in resilient modulus of the cemented layer accompanied by the increase in pavement structural strength (which indicate larger support from the subbase to the cemented layer), made the cemented layer more rigid. Since the layer is more rigid it is more resistant to the stresses induced by traffic, and this accompanied by one of the benefits of cementation, namely a reduction in linear shrinkage, results in a longer life before the initiation of cracking on pavements with a higher resilient modulus for the cemented basecourse. The reason why the above two factors lengthen the life of a pavement before cracking, is that block cracking which develops due to shrinkage early in the life of the cemented layer are reflected through to the surface of the pavement.

From the two Figures it is evident that once initiated the rate of progression is the same for all the resilient modulus strengths. The reason for this is that the HDM-III model only incorporates the time-based progression models described in

Chapter 2, which are not susceptible to either traffic or structural number (SN). As seen from Figures 3.3 and 3.4 similar conclusions can be made between medium (SN = 3) and strong (SN = 6) pavements under heavy traffic load of 1,0 million E80/lane/year.

From Figures 3.2 and 3.3 it can be concluded that with an increase in traffic load, the predicted age before the initiation of cracking tends to decrease, especially for the cemented layers with higher resilient modulus values. As previously mentioned it is believed that this behaviour under a heavy traffic load (1,0 million E80/lane/year) is the result of the fact that the cemented layers with higher resilient modulus values are more rigid, and tend to concentrate a larger percentage of the total pavement strength within them. This accompanied by the fact that the pavement strength tends to be slightly inadequate for the heavy traffic load, results in the cemented layer being more sensitive when over-stressed because it is less flexible, resulting in the decrease in life before cracking initiation.

From Figure 3.5 to 3.8 it is evident that exactly the same applies for wide cracking except for the fact that the initiation of wide cracking tends to be delayed until approximately two years after the initiation of all cracking, also resulting in a slightly higher initial increase in area of wide cracking. These differences are the direct result of the fact that the HDM-III model expresses the initiation of wide cracking as a function of the initiation of all cracking.

It can be concluded from the analysis that the sensitivity of the cracking model to the resilient modulus of cemented layers is minimal and would have no major influence on the cracking predictions given by the HDM-III model for South African pavements. The reasons for this are:

- Pavement designs in South Africa tend to be structurally more balanced in design, resulting in good support for the cemented layers.
- Most of the pavements are structurally adequate for the loads applied.
- The fact that the construction of cemented layers is usually accurately controlled.

3.3.1.2 Thickness of bituminous layers

The thickness of bituminous layers refers to the thickness of the bituminous surfacing of a pavement. As with the previous parameter this one is also only

applicable for pavements with cemented basecourse layers, since it is only incorporated into the cracking models of a cemented layer. The results obtained from the sensitivity analysis for a twenty year study period are illustrated in Figures A.1 to A.4 for all cracking, and Figures A.5 to A.8 in Appendix A, for wide cracking. As seen the analysis was conducted for four pavement thicknesses namely 30, 50, 150 and 300 mm. These values were chosen to provide a good representation of the thickness of the bituminous layers used on roads.

As seen from the Figures A.1 to A.4 for all cracking, and Figures A.5 to A.8 for wide cracking, the same is applicable for the sensitivity of cracking to the thickness of asphalt layers, than to the resilient modulus of the basecourse. This behaviour is expected because traffic-associated cracking usually initiates in the cemented basecourse and propagates through to the surfacing. The thicker the surface layer the larger the contribution to pavement strength, resulting in a decreased stress induced on the cemented layer, and secondly the longer the path for the crack to propagate to the top, thus extending the time until the crack is noted on the surface.

It can be concluded from the analysis that the slight increase in sensitivity observed for the cracking model to the thickness of bituminous layers would have no major influence on the cracking predictions given by the HDM-III model. The reasons for this being the same as previously mentioned, and also the fact that the thickness of bituminous layers are normally very accurately measured after construction, eliminating errors in thickness measurements to a large extent.

3.3.1.3 Pavement deflection

The deflection refers to the Benkelman beam deflection (mm) of the pavement measured under a 80 kN single axle load. As with the previous two parameters the pavement deflection was only included into the cracking model of cemented layers. The results obtained from the sensitivity analysis are illustrated in Figures 3.9 to 3.12 for all cracking and Figures A.9 to A.12 for wide cracking in Appendix A. As seen from Figures 3.9 to 3.12 the area of all cracking predicted does not change with a change in the structural number of the pavement. The reason for this is the fact that when both the deflection and structural number (SN) are specified, the deflection value specified is used instead of calculating it

from the correlation between the two parameters included in the HDM-III model. As seen in Figures A.9 to A.12 in Appendix A, the same applies for wide cracking. It is however evident from the Figures that for deflection values of 1 mm and greater the model predictions tend not to differ much. As seen there is a substantial difference between 0,1 mm and 1 mm deflection. This difference can be related directly to the correlation (see below) between the modified structural number and deflection, where deflection values of 1 mm indicate a flexible pavement controlled by materials in the granular state usually with low modulus (< 200 MPa) values. Thus the rigid cemented layer has little or no support from the other pavement layers, resulting in the quick development of cracks as a result of the stress induced within the cemented layer by the traffic load. These cracks then reflect through to the surface of the pavement. The opposite is indicated by a deflection value of 0,1 mm which is the typical deflection value of a very stiff pavement controlled by layers acting as slabs. This indicates that the pavement is strong and that the cemented basecourse layer is well supported by the other pavement layers, which results in lower induced stresses within the cemented basecourse layer as well as in the surface layer. As a result a longer period before the initiation of cracking occurs, although the rate of progression stays unchanged.

As a result of the fact that the deflection measurements are not frequently conducted on national roads, very little deflection data is available. Thus in most instances the deflection value used would be calculated from the following correlation between modified structural number (SNC) and deflection included into the HDM-III model for cemented base pavements:

$$Def = 3{,}5\ SNC^{-1{,}6}$$

It can be concluded from the analysis that the sensitivity of the cracking model to deflection observed may have some influence on the cracking predictions given by the HDM-III model. The reasons for this being:

- Limited deflection measurements are available on South African national roads.
- The use of correlations, that have not been locally verified, to determine deflection measurements from the modified structural number.
- The fact that accurate details on pavement strength is also difficult to obtain.

3.3.1.4 Construction quality

As mentioned in Chapter 2 a construction quality indicator (CQ) was included for surface treatment models, since surface treatments showed an obvious sensitivity to the quality of construction. The reason for only including such a parameter for surface treatments is that they are less forgiving to construction errors than asphalt concrete surfacings. The results obtained for the sensitivity of the area of all cracking on a surface treatment to construction quality are illustrated in Figure 3.13 and 3.14 for a granular basecourse, and in Figures 3.15 and 3.16 for a cemented basecourse. For the area of wide cracking on a surface treatment the results are illustrated in Figures A.13 and A.14 for granular basecourse and in Figures A.15 and A.16 for cemented basecourse in Appendix A.

From Figure 3.13 it is evident that under a light traffic load of 0,1 million E80/lane/year the initiation and progression of all cracking on a granular basecourse seemed to be affected by both the quality of construction and the structural number. This is evident in the shorter time to the initiation of ravelling for poor construction quality, and the fact that the difference in time predicted between good and poor construction quality tends to decrease with an increase in the strength of the pavement. The reason for this may be the fact that the structurally stronger the pavement, the less flexible it is. This results in a decrease of the flexural stress on the binder film of the surfacing, which tends to decrease the influence of construction quality on the initiation of cracking. It is also believed that the kneading action of the light traffic might produce a beneficial effect, through the binder film being raised around the stone particles, as they are embedded and thus countering the oxidation effects which influences the aging of the layer.

From Figures 3.14 and 3.16 it is evident that at a heavy traffic load of 1,0 million E80/lane/year construction quality and basecourse type also seem to have an influence on the initiation and progression of all cracking. Figure 3.14 illustrates a large difference in the area of all cracking for the medium (SN = 3) to strong (SN = 6) pavements, indicating the influence of construction quality on the behaviour of a surface treatment on a granular basecourse. The behaviour of pavement with structural number (SN) of 1 was ignored since it was assumed that the pavement strength was totally inadequate for the traffic load applied,

and usually the pavement structure will fail very fast when the induced stresses exceed the shear strength of the upper pavement layers, resulting in the crushing of the surfacing layer. Since a surface treatment has a very small contribution to the structural strength of a pavement it does not matter whether the construction quality of the surface layer was good or poor.

However the structurally stronger the pavement the larger the effect of construction quality as seen for a structural number (SN) of 3 and 6. The reason for this is the fact that these pavement structures are structurally adequate to withstand the stresses induced within the pavement layers, and as a result of that any weakness with the construction quality of the surfacing layer would be highlighted. For example, a weakness like poor binder distribution or overheating of binder during construction will result in the mechanical fracture of the binder film because it is too thin or too brittle to sustain the stresses imposed through the tyre contact area of a moving vehicle. The decrease in area of all cracking observed for some of the pavements is the result of the fact that the maximum surface distress area are not allowed to exceed 100 %. Thus if potholes start to initiate and progress, the area of all cracking has to decrease to adhere to the above mentioned requirement. This usually happens when the area of new potholes during a year exceeds the maintenance capacity. This is usually an indication that the surfacing is in need of urgent rehabilitation.

Evaluating Figures 3.13 and 3.14 it is evident that for an increase in traffic on the medium (SN = 3) to strong (SN = 6) pavements the life to initiation of cracking tends to decrease. It is also obvious that the difference between good and poor construction quality tends to increase. It is believed that this is the result of the higher stresses induced within the binder film resulting in any weakness within the layers being highlighted.

From Figures 3.15 and 3.16 it is evident that for a pavement with a cemented basecourse under both a light (0,1 million E80/lane/year) and a heavy (1,0 million E80/lane/year) traffic load no difference in area of all cracking between good or poor construction seems to exist. It must however be noted that the life until the initiation and progression of all cracking is in general much less on cemented bases than for granular pavements, and tends to be slightly less under the heavy traffic load. The probable cause of both the similar behaviour between good and poor construction quality and the much shorter life until cracking

initiation is block cracking within the cemented layer due to shrinkage. These cracks usually initiate soon after construction within the cemented layer and will probably reflect through the thin surfacing layer with little resistance. This usually happens before construction quality could have any major influence.

From Figures A.13 to A.16 in Appendix A, it is evident that the same conclusions apply for wide cracking, except for the later initiation of the area of wide cracking. This behaviour is in line with the definition of wide cracking as a function of all cracking in the HDM-III model. During the definition it was assumed that the same factors affecting all cracking is influencing wide cracking.

It is believed that the construction quality of surface treatments would not be a problem on the national road pavements as a result of the fact that asphalt concrete is used most of the time, and when a surface treatment is used the control over construction quality is usually of a high standard.

3.3.2 Ravelling model

As mentioned in Chapter 2 ravelling refers to the loss of stone particles from the surface which either results from the mechanical fracture of the binder film or the loss of adhesion between the binder and stone. The first is influenced by traffic while the second factor is influenced by construction quality. The ravelling models developed are only applicable to surface treatments, since ravelling was not considered to be a problem on asphalt concrete pavements during the Brazil study. The sensitivity of ravelling was evaluated for construction quality in collaboration with traffic loading, structural number and basecourse type. The following results were obtained.

3.3.2.1 Construction quality

The results obtained for the sensitivity of the area of ravelling on a surface treatment to construction quality is illustrated in Figures 3.17 and 3.18 for pavements with a granular basecourse, and in Figures 3.19 and 3.20 for cemented basecourse pavements.

From Figures 3.17 and 3.19 it is evident that under light traffic of 0,1 million

E80/lane/year the initiation and progression of ravelling seemed to be affected by both the quality of construction and the basecourse. As seen the life until the initiation of ravelling is nearly halved by poor construction quality for both granular and cemented basecourse pavements. As previously mentioned when poorly constructed the binder film of the surface treatment around the stone particles are too brittle or too thin to sustain the stresses imposed through the tyre contact area of a moving vehicle. The stresses impart fractures the binder film, and then by a combination of horizontal stresses in the tyre contact area, and suction, the tyre plucks the stone out of the bituminous matrix (Paterson, 1987).

From Figures 3.17 and 3.19 it is also obvious that the predicted area of ravelling is much higher for granular basecourse pavements than for cemented basecourse pavements. The reason for this is that in the HDM-III model the maximum area of surface distress allowed is 100 %. This area of surface distress includes contributions from cracking, ravelling and potholing. In the HDM-III model the sequence of modelling these three parameters is firstly cracking, then ravelling and finally potholing. Cracking therefore has a higher priority than ravelling. Thus for pavements on which cracking initiates before ravelling, as for a cemented basecourse pavement, the progression of ravelling is automatically limited to a value less than 100 %, to adhere to the above-mentioned requirement. For pavements with granular basecourse layers where the initiation of cracking seems to be much later, ravelling is allowed to progress over a much larger area of the surfacing. The decrease in area of ravelling observed can be explained by the same argument, with the area of potholing affecting both area of cracking and ravelling.

Figures 3.18 and 3.20 indicate that under a heavy traffic load of 1,0 million E80/lane/year the same as mentioned for light traffic (0,1 million E80/lane/year) is applicable. Except that in this instance the ravelling tends to initiate earlier under the heavy traffic load, and the difference between good and poor construction quality is less. As previously mentioned it is believed that this is the result of the higher stresses induced on the binder film, which fractures the binder film earlier and as such limits the influence of poor construction quality to a certain extent. Under these high traffic loads the behaviour of the pavement with a structural number (SN) of one was again ignored since it is believed that the pavement is structurally inadequate for the applied load.

Figures 3.17 and 3.18 illustrate the effect of traffic on ravelling on a granular pavement, with a decrease in the time to ravelling, even for pavements with a good construction quality. This behaviour indicates that under a high traffic load, a surface treatment is not the most appropriate surfacing to be used, since even a good constructed surface treatment has problems to withstand the stresses of a heavy traffic load. It is also evident that the weaker the pavement the lower the area of ravelling reached. This is the result of the fact that the weaker the pavement, the sooner it is over-stressed, resulting in the shear failure of the granular material which leads to earlier cracking under the heavy traffic of 1,0 million E80/lane/year, which limits the progression of ravelling.

Thus despite the obvious sensitivity of ravelling to the construction quality of a surface treatment, it is believed that construction quality would not have such a significant influence on the ravelling predicted. The reasons for this being the fact that when a surface treatment is constructed the supervision and quality control during construction and the subsequent maintenance is of a very high standard. Secondly the traffic load on pavements with surface treatments in South Africa is normally much lower than 1,0 million E80/lane/year.

3.3.3 Potholing

Potholing is the most severe form of pavement deterioration and is usually the result of deferred or neglected maintenance. As mentioned in Chapter 2 it is the least predictable form of distress, which is only included into the HDM-III model to serve as the economic penalty of deferred or neglected maintenance. To distinguish potholing from ravelling a pothole is defined as a cavity in the road surface which is 150 mm or more in average diameter and 25 mm or more in depth (Paterson, 1987). The sensitivity of potholing to bituminous layer thickness and construction quality were evaluated in collaboration with the traffic load and the following results were obtained.

3.3.3.1 Thickness of bituminous layers

The thickness of bituminous layers refer to the thickness of the bituminous surfacing of a pavement with a granular basecourse. The sensitivity to thickness of bituminous layers was only evaluated for asphalt on granular basecourse since it was only included into the granular model as a parameter. The results

obtained from the sensitivity analysis for a twenty year study period are illustrated in Figures A.17 to A.20 in Appendix A, for all cracking. As seen the study were conducted for four surfacing thicknesses namely 30, 50, 150 and 300 mm. These values were chosen to provide a good representation of the thickness of the bituminous layers used on roads.

From Figures A.17 to A.20 it is evident that the area of potholing seemed totally insensitive to the thickness of the surfacing. This behaviour is believed to be the combination of the following two factors, firstly the maintenance activity specified of patching all potholes which exceed the pothole initiation rate and as such limits the progression of potholes. Secondly potholes usually initiate from wide cracking, whose progression is severely limited by the thickness of the layers as previously described.

Thus from the analysis it can be concluded that the thickness of the bituminous layers seemed to have no effect on the initiation and progression of potholes on roads. Even if the thickness of bituminous layers does influence potholes, the thickness is normally measured accurately resulting in an elimination of any possible error.

3.3.3.2 Construction quality

The sensitivity to construction quality is illustrated in Figures 3.21 and 3.22 for surface treatment on granular basecourse and Figures A.21 and A.22 in Appendix A, for surface treatment on cemented basecourse. From Figures 3.21 and A.21 it is evident that at a low traffic loading (0,1 million E80/lane/year) neither the structural number or construction quality seem to have an effect on the initiation and progression of potholes. The reason for this may be the fact that for surface treatments potholes usually developed from ravelling which has exposed the basecourse, or from wide cracking which has reached such intensity that fragments are easily removed. As mentioned previously both these actions are dependent on traffic loading to highlighted any construction quality deficiencies. From Figures 3.22 and A.22 it seems that the same applies under a traffic load of 1,0 million E80/lane/year, except for pavements with a structural number of 1. It is believed that this pavement is totally inadequate for the traffic load applied. From the analysis it is believed that the influence of construction quality on pothole initiation and progression is limited under the maintenance activity specified for national roads.

3.3.4 Rutting

Rutting refers to the accumulation of deformation within pavement layers visible in the wheeltracks on the surface which is normally traffic-associated permanent deformation. In the HDM-III model rutting is divided into two different parameters, namely the mean rut depth and the rut depth standard deviation. The sensitivity of the mean rut depth and the rut depth standard deviation to deflection and percentage of compaction were evaluated in conjunction with traffic loading and structural number. The following results were obtained.

3.3.4.1 Pavement deflection

As previously mentioned deflection refers to the Benkelman Beam deflection (mm) of the pavement measured under a 80 kN single axle load. The results obtained from the sensitivity analysis are illustrated in Figures 3.23 to 3.26 for the mean rut depth and Figures A.23 to A.26 in Appendix A, for the rut depth standard deviation. As seen deflection values of up to 5 mm were specified. Although these values may not normally occur on national roads, they were included into the study to evaluated the HDM-III model at the limit of its allowable range.

From Figures 3.23 to 3.26 it is evident that for the normal range of deflections between 0,01 to 1 mm measured on national roads the rut depth predicted is not that sensitive, with the predicted values lower than the 10 mm used to indicate a warning level. From the Figures it is also evident that when the deflection exceeds 1 mm, the mean rut depth increased at a faster rate, indicating some increase in the sensitivity of the rutting model to deflection. From Figures 3.23 and 3.24 it is evident that under a light traffic load (0,1 million E80/lane/year) this increase in sensitivity tends to be lower for a pavement with a higher structural strength. As seen from Figures 3.25 to 3.26 the same is applicable under a heavy traffic load of 1,0 million E80/lane/year, although not to the same extent. This behaviour is expected since an increase in deflection above 1,0 mm, indicates that the pavement behaviour is controlled by flexible materials in the granular state (Freeme, 1983). The higher deflection values indicate poor pavement structure quality, which results from a combination of poor materials and inadequate compaction during construction. This give rise to post-

construction compaction under traffic, resulting in the higher rut depth values measured within four years after construction. The factors mentioned in combination with an increase in moisture content (as result of water ingress through the cracked surface), results in the earlier shear failure of the granular material. The end result of this is a fast increase in rut depth, especially under heavy traffic.

From Figures A.23 to A.26 it is evident that the influence of deflection on the standard deviation of rut depth seems to be far less, even at the higher deflection values. Although the values predicted are lower than the mean rut depth values, the roughness predictions are more sensitive to the standard deviation as seen later in the chapter under the incremental roughness model.

From the sensitivity analysis it can be concluded that the influence of deflection on rutting for the range of deflection values between 0,1 to 0,6 mm are limited. The range of deflection values are determined by the correlation within the HDM-III model, for the structural strengths observed on national roads. Although the rutting model is not that sensitive for the typical range of structural numbers observed on national roads, these structural values must still be determined as accurately as possible.

3.3.4.2 Percentage of compaction

The percentage of compaction refers to the percentage of the specified compaction obtained during construction in the field. As mentioned in Chapter 2 this term was included because it is believed that the compaction achieved in a pavement at the time of construction will influence the densification occurring under traffic, and thus the rutting. The results obtained from the sensitivity analysis for a twenty year study period are illustrated in Figures A.27 to A.30 for the mean rut depth, and Figures A.31 to A.34 in Appendix A, for the rut depth standard deviation.

From Figures A.27 and A.29 it is evident that the pavement structures that are on the line of being inadequate for the applied traffic load, seems to be affected the most by the compaction achieved during construction. As seen in Figure A.27 the influence is the largest for the weak pavement (SN=1) under a light traffic load (0,1 million E80/lane/year). It is believed that for such a weak

pavement most of the material used is of such a poor quality, that the pavement strength is dependent on the compaction obtained during construction. Thus, if poorly compacted during construction the pavement will be susceptible to densification under the traffic load, resulting in the mean rut depth values observed being higher for the lower compaction achieved. It must be noted that for a structural number of one the deflection determined by the correlation within HDM-III is the main contribution factor to the high deflection values observed, as seen at 100 % compaction.

As seen the structurally stronger the pavement the lower the predicted mean rut depth. As seen from Figure A.30 even for structurally strong pavements, the compaction does seem to have a influence on rutting, although it is smaller.

From Figures A.31 to A.34 it is evident that the influence of compaction on rut depth standard deviation is even less. Only a small difference is noticeable, indicating that although compaction is affecting the rut depth standard deviation, it is minimal.

From the analysis it can be concluded that the compaction achieved during construction do seem to have an influence on the rut depth measured on roads structurally just adequate for the applied traffic load. However if the observed sensitivity is compared with the influence of deflection on rutting, it seems that the influence of compaction is minimal. Thus it is believed that the influence of compaction achieved during construction on rutting predictions would be negligible, as there is accurate control over compaction during construction on national roads.

3.3.5 Incremental roughness model

The incremental roughness model refers to the model that combines the predictions of the previous models into a single value, known as roughness. The model contains three groups of components, dealing with structural, surface distress and environment-age condition parameters. Of all the models evaluated the incremental roughness model is the most important, because it forms the basis for determining vehicle operating costs, which is one of the key elements in the evaluation of road policies. The sensitivity of the incremental roughness model to the parameters listed in Table 3.1 were evaluated and the following results were obtained.

3.3.5.1 General deterioration predictions

The difference in roughness predictions given by the HDM-III roughness prediction submodel for the various pavement types are illustrated in Figures 3.27 and 3.28 for light traffic (0,1 million E80/lane/year) and heavy traffic (1,0 million E80/lane/year) respectively. The pavement types included are:

- Surface treatment on granular base with SN of 1 (SurSN1Gran).
- Surface treatment on granular base with SN of 6 (SurSN6Gran).
- Surface treatment on cemented base with SN of 1 (SurSN1Cem).
- Surface treatment on cemented base with SN of 6 (SurSN6Cem).
- Asphalt layer on granular base with SN of 1 (AsSN1Gran).
- Asphalt layer on granular base with SN of 6 (AsSN6Gran).
- Asphalt layer on cemented base with SN of 1 (AsSN1Cem).
- Asphalt layer on cemented base with SN of 6 (AsSN6Cem).

For pavements with a cemented base only the post-cracked phase (phase 3), where the cemented layer is broken up in an equivalent granular state was evaluated. The reason for this was that the breaking down of a cemented layer from phase 1 (pre-cracked) to phase 3 usually happens relatively quickly (Jordaan, 1992), thus the material spends the largest part of its life in phase 3.

From Figures 3.27 and 3.28 it is evident that the prediction of roughness for the different pavement types follows the same general trend. This was also confirmed during the evaluation of the different pavement types. As a result of this general trend, only the results obtained from an asphalt surfacing on a granular base are discussed in more detail, since it represented the pavement type for which the most information was available on the Department of Transport database. Where noticeable differences in behaviour between the different pavement types exists, it will be mentioned. All the parameters were evaluated in combination with the modified structural number and the traffic load. These two parameters were included as general parameters as a result of their influence on pavement behaviour. The following results were obtained from the evaluation of the different parameters.

3.3.5.2 Initial traffic load and traffic growth rate

The sensitivity of the HDM-III roughness prediction submodel to traffic load is illustrated by the large difference in roughness predictions seen in Figures 3.27 and 3.28, especially for the pavement group with a structural number of one. This sensitivity to traffic load decreases with an increase in pavement strength as seen for the pavements with a structural number of 6. This large difference observed in predicted roughness for weak to medium strength pavements with a change in traffic is expected since based on the results of the AASHO Road Test. The sensitivity of the HDM-III roughness prediction submodel to traffic load (E80) indicate that traffic and traffic growth rate is still one of the major influences on pavement deterioration. Thus the initial traffic (E80) and the expected growth rate should be determined as accurately as possible. To determine the traffic load as accurately as possible it is recommended that the traffic load (E80) and the growth rate be determined from traffic surveys conducted with a Traffic Axle Weight Classifier (TAWC) on the road section under evaluation, or a nearby section with more or less the same traffic load.

3.3.5.3 Area of all cracking

As mentioned previously the area of all cracking only includes crocodile and irregular cracks wider than 1 mm. The results obtained from the sensitivity analysis of roughness to the area of all cracking for a twenty year study period, are illustrated in Figures 3.29, 3.30 and Figures A.35 to A.36 in Appendix A, at four year intervals. From these illustrations it is evident that the model for the prediction of roughness is sensitive for whether a pavement is cracked (0,1 % of pavement area cracked) or not cracked (0 % of pavement area cracked). Although the initiation of cracking was defined as an cracked area of 0,5 % or more, the value of 0,1 % was used to indicate the sensitivity of the HDM-III roughness prediction submodel for cracks. Once a pavement is cracked the roughness model seems insensitive for the initial area of all cracking specified. Thus it should only be defined as accurately as possible whether a pavement is cracked or not cracked.

Some of the Figures indicate an initial increase, although very small, in the predicted roughness until a area of all cracking of 10 percent is reached. Once this area of cracking is exceeded, the predicted roughness tends to decrease.

According to Watanatada *et al* (1987) patching not exceeding 10 % of the evaluated surfaced area in any year tends to increase the roughness. However if the patched area is larger it tends to have a net corrective rather than adverse impact on roughness. This is however contrary to South African experience where the roughness always increases despite the area patched. To evaluate the explanation given by Watanatada *et al* (1987) the pothole progression factor was adjusted to slow down the prediction of potholing, and thus decrease the area to be patched. This will have the net effect of increasing the roughness according to the theory of Watanatada *et al* (1987). The results obtained after the adjustments remained the same as previously, and did not decrease as expected. The factor for cracking progression was also adjusted, at first on its own and then in combination with the pothole progression factor. Both these adjustments had no effect on the roughness prediction, and in some instances even resulted in a further decrease in roughness. Since no explanation was obtained from the evaluations, the reason given for the decrease in roughness with an increase in area of initial cracking seems highly questionable.

3.3.5.4 Area of wide cracking

The area of wide cracking only includes the percentage area of class 4 cracks, that is spalled cracks larger than 3 mm in width. The results obtained from the sensitivity analysis of roughness to the area of wide cracking for a twenty year study period, are illustrated in Figures A.37 to A.40 in Appendix A, at four year intervals. From these Figures it is evident that the same applies as for the area of all cracking regarding the sensitivity of the HDM-III roughness prediction submodel between no cracking (0 % of the area) and a cracked pavement (0,1 % of the area). The roughness values predicted for wide cracking by the HDM-III roughness prediction submodel for the same pavement conditions and traffic load are higher than the values predicted for all cracking. Another noticeable difference is that the predicted roughness values for wide cracking decrease at a faster rate than the roughness values predicted for the equivalent percentage of all cracking.

This may be ascribed to the more severe influence of wide cracking on roughness progression in the HDM-III roughness prediction submodel where roughness values tends to increase more for a percentage point increase in wide cracking than for a percentage point increases in all cracking, resulting in higher

roughness values. The area to be patched also increases more for an equal percentage change in wide cracking than for all cracking. The end result of this is a faster rate of decrease in roughness according to the previously mentioned theory of Watanatada *et al* (1987). As mentioned the investigations conducted did not support this theory.

3.3.5.5 Area of ravelling

The results obtained from the analysis of the sensitivity of the HDM-III roughness prediction submodel to the initial area of ravelling are illustrated at 4 year intervals for a 20 year study period in Figures A.41 and A.42 in Appendix A. The sensitivity illustrated is that of a surface treatment on granular material since ravelling was considered not to be a problem on pavements with asphalt surfaces as previously mentioned. As seen both Figures A.41 and A.42 indicate that the HDM-III roughness prediction submodel is insensitive to the initial percentage of ravelling specified at the beginning of the period. According to Paterson (1987) the sensitivity to ravelling is influenced:

- To a certain extent by problems that manifested during the construction of the layer. As a result of this the HDM-III roughness prediction submodel includes a construction quality code to distinguish between good and poor quality of construction as discussed previously.

- By the fact that ravelling has serious structural implications only when the surface layer is thin and prone to potholing, and usually only triggers preventative measures like the repair of potholes and resurfacing.

Most of the national road sections included in the study had asphalt surfaces, and those with surface treatments were generally constructed under strict supervision ensuring good construction quality. This in conjunction with the specified maintenance activity of patching of all potholes ensures that ravelling would not be of major concern on national roads. Thus the accuracy needed when calculating the area of ravelling at the beginning seems to have no influence on the roughness predicted later on.

3.3.5.6 Mean rut depth

The results obtained from the analysis of the sensitivity of the HDM-III roughness prediction submodel to the mean rut depth are illustrated at 4 year intervals for a 20 year study period in Figures A.43 and A.44. From these

Figures it seems evident that the prediction of roughness by the HDM-III submodel seems relatively insensitive to an error in the specified mean rut depth, especially for values above 10 mm. This is the result of a combination of the following factors which affect the roughness predictions given by the model:

- The influence of densification in the model predicting rutting, the higher the initial compaction during construction the lower the rut depth predicted. Research indicated that a 5 percent reduction in density achieved during construction can increase rut depths by 15 percent or more (Paterson, 1987). In South Africa the compaction achieved during construction on national roads is usually of a high quality, thus limiting compaction under traffic to a great extent, and thus rutting.

- The fact that when the pavement deflection is less than 1 mm or the structural number (SN) is larger than 3, the maximum rut depth is not likely to exceed 10 mm even under heavy traffic of up to 2 million E80/lane/year (Paterson, 1987). Most of the national road pavements evaluated have modified structural numbers (SNC) of 3 or more.

- The fact that the mean rut depth is not used as a maintenance intervention criterion in the HDM-III roughness prediction model, but is used as a means to estimate the variation of rut depth standard deviation which contributes directly to roughness (Watanatada *et al*, 1987).

Thus it can be concluded that the prediction of roughness by the HDM-III model would not be that sensitive to an error in the mean rut depth calculated for South African conditions. Despite this the mean rut depth still has to be calculated as accurate as possible for the reason explained in 3.3.5.7.

3.3.5.7 Rut depth standard deviation

The results obtained from the analysis of the sensitivity of the HDM-III roughness prediction submodel to the rut depth standard deviation (across both wheelpaths in a lane) are illustrated at 4 year intervals for a 20 year study period in Figures 3.31 and 3.32. For the evaluation of rut depth standard deviation a mean rut depth of 20 mm was selected. The value of 20 mm was selected based on the recommended performance criteria in Table 13 of TRH12 (1991), where 20 mm is used to indicate the change from a warning level (< 20 mm) to a severe level (≥ 20 mm) of distress.

From Figures 3.31 and 3.32 it seems that for deviations up to 10 mm and for analysis periods up to 12 years the sensitivity to errors in the input is small. For larger deviations and longer periods the sensitivity tends to increase. From these Figures it seems that the HDM-III roughness prediction submodel is more sensitive for errors in the rut depth standard deviation than for errors in the mean rut depth. This may be explained by the fact that in the HDM-III roughness prediction models the rut depth standard deviation is used to express the influence of rutting on roughness and not the mean rut depth. As mentioned under 3.3.5.6 the mean rut depth should be determined as accurately as possible since it is used to calculate the rut depth standard deviation, for which the HDM-III roughness prediction model seems more sensitive.

3.3.5.8 Structural number

In the empirical research conducted by Paterson (1987), the modified structural number (SNC) was found to be the most statistically significant measure of the pavement strength affecting the deterioration of pavements, and is thus the primary strength parameter in the roughness prediction relationship. This superiority of the structural number over other strength parameters like surface deflection lies in the fact that the structural number accounts for both the shear strength and the induced stress level within the pavement layers, through the material coefficients utilised in it's computation.

In this analysis the sensitivity of the HDM-III roughness prediction model the two components of the modified structural number, namely structural number (SN) and subgrade California Bearing Ratio (CBR) were evaluated separately. The results obtained from the analysis of the sensitivity of the HDM-III roughness prediction submodel to the structural number are illustrated at 4 year intervals for a 20 year study period in Figures 3.33 and 3.34.

From these Figures it seems that the prediction of roughness by the HDM-III submodel is very sensitive for a pavement structural number under 3,5. However for a structural number above 3,5 the model is less sensitive to an error in the input data. Thus for a pavement with a structural number below 3,5 additional information such as for example deflection measurements should be used when available to determine the structural strength as accurately as possible. Most pavements evaluated on national roads do however have structural values above 3,5, limiting the influence of the structural number on roughness.

3.3.5.9 Subgrade California Bearing Ratio

The results obtained from the analysis of the sensitivity of the HDM-III roughness prediction submodel to the subgrade California Bearing Ratio (CBR) are illustrated at 4 year intervals for a 20 year study period in Figures 3.35 to 3.37. From these Figures it seems that the prediction of roughness by the HDM-III model is relatively insensitive for a CBR above 20 %. The model does however seem sensitive for an error in the CBR value if it is below 20 % for weak pavements (SN = 1) under a light traffic loading as illustrated in Figure 3.35. The same applies for medium pavements (SN = 3) under a heavy traffic loading, as illustrated in Figure 3.36. From Figure 3.37 it is evident that the sensitivity to subgrade CBR decreases with an increase in the strength of the pavement.

This decrease in sensitivity is explained by the fact that as the strength of the pavement increases, the protection given to the subgrade by the pavement layers also increases, resulting in a decrease in the sensitivity of the subgrade to the traffic load applied. Thus the accuracy required when determining the CBR value decreases with an increase in pavement strength. The CBR values of the subgrade should however be determined as accurately as possible for weak to medium pavements with CBR values below 20 %. To ensure accurate determination of the subgrade CBR it is recommended that subgrade CBR values be determined from in situ measurements conducted on the section under evaluation.

3.3.5.10 Initial roughness value

The results obtained from the analysis of the sensitivity of the HDM-III roughness prediction submodel to the initial roughness value is illustrated at four year intervals for a 20 year study period in Figures 3.38 to 3.40. From these Figures it is evident that the prediction of roughness by the HDM-III model is sensitive to the initial roughness specified. This sensitivity does not differ much for the different pavement strengths and traffic loads. The sensitivity observed is expected since the initial value determines the predicted rate of deterioration. The higher the initial value the faster the rate of deterioration predicted. The reason for this is that as the roughness increases, the dynamic load applied by heavy vehicles on the pavement also increases, thus increasing the deterioration of the pavement. Thus the initial roughness value of a pavement should be determined as accurately as possible for each specific pavement. It is recommended that where available riding quality measurements conducted within a year or two from the completion of the pavement be used. If

unavailable the average value determined from similar pavements that were measured, should be used in conjunction with later measurements on the specific pavement as a guideline in determining an initial roughness value.

3.4 CONCLUSIONS FROM SENSITIVITY ANALYSIS

As mentioned only the HDM-III models were evaluated, since these models were identified as the most appropriate for further evaluation under South African conditions. From the sensitivity analysis conducted the results obtained for the incremental roughness model is the most important as a result of the influence of roughness on vehicle operating costs. The results obtained from the sensitivity analysis indicate that the incremental roughness prediction model incorporated into the HDM-III model tends to be insensitive to changes in most parameters. There are, however, parameters for which changes in a certain range of the parameter require greater accuracy. In some instances the accuracy depends on the length of the analysis period, with the prediction of roughness being more sensitive the longer the period. Despite the insensitivity of the model all input data should be determined as accurately as possible. The following accuracy requirements are applicable when determining the input data:

- The correlation between deflection and structural number needs to be evaluated for South African conditions, as a result of the noticeable influence of deflection on cracking and especially rutting. Where available measured deflection values should be employed.
- One should determine as accurately as possible whether cracking has initiated on a pavement for both all and wide cracking. For cracked pavements the model seems insensitive to the area of cracking.
- The structural number should be determined as accurately as possible if it is under 3,5, and where available additional information should be used for these weaker pavement types.
- Subgrade CBR values below 20 % should be determined as accurately as possible for in situ conditions for pavements with a modified structural number below 4.
- The prediction of roughness is sensitive to the traffic loading. This indicates that both the initial number of vehicles, as well as the expected traffic growth rate should be determined as accurately as possible.
- The initial roughness measurement for each pavement should be determined as accurately as possibly.

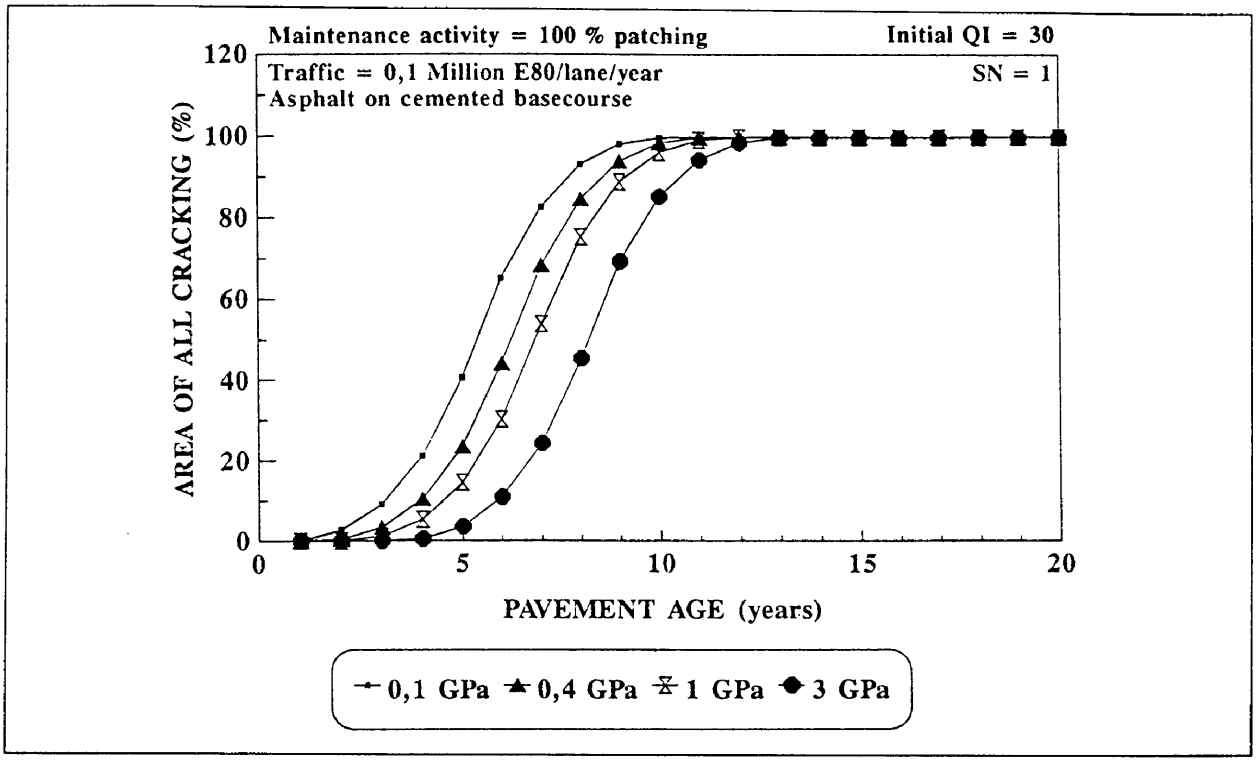

Figure 3.1: Sensitivity of all cracking model to resilient modulus of basecourse for SN = 1 under light traffic.

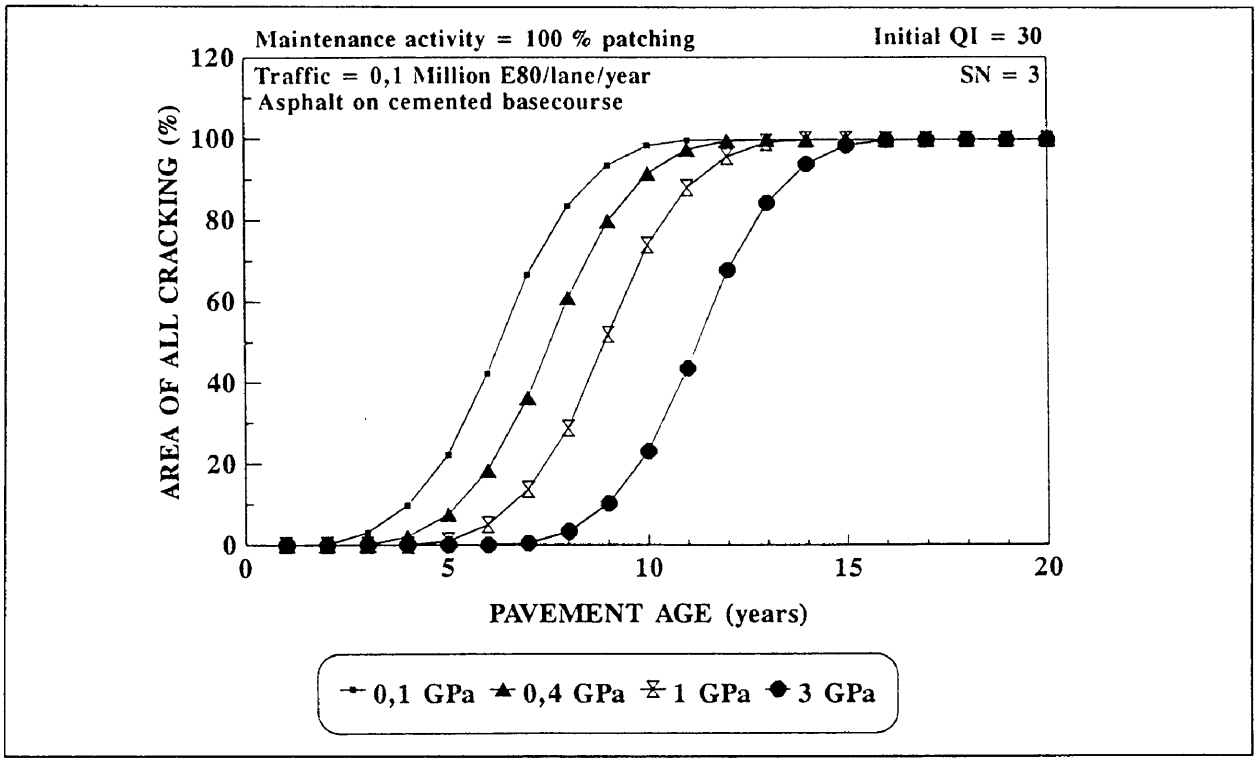

Figure 3.2: Sensitivity of all cracking model to resilient modulus of basecourse for SN = 3 under light traffic.

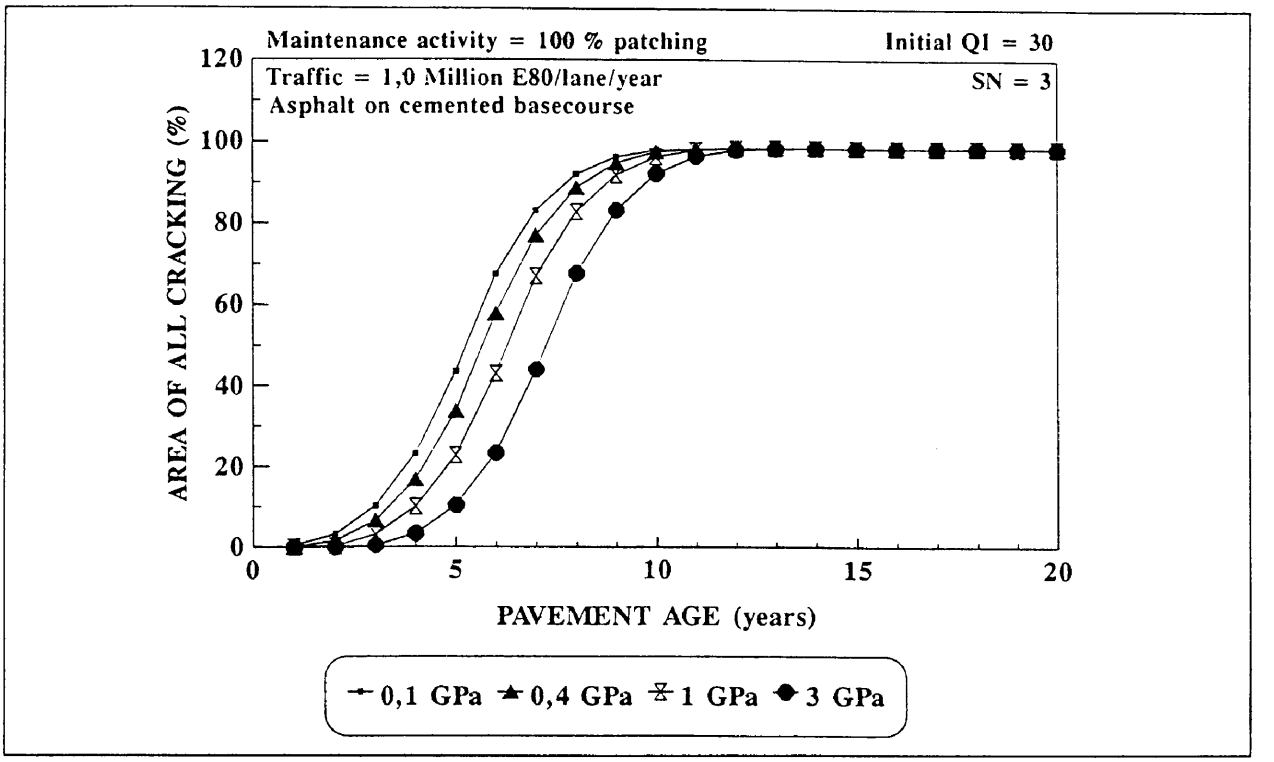

Figure 3.3: Sensitivity of all cracking model to resilient modulus of basecourse for SN = 3 under heavy traffic.

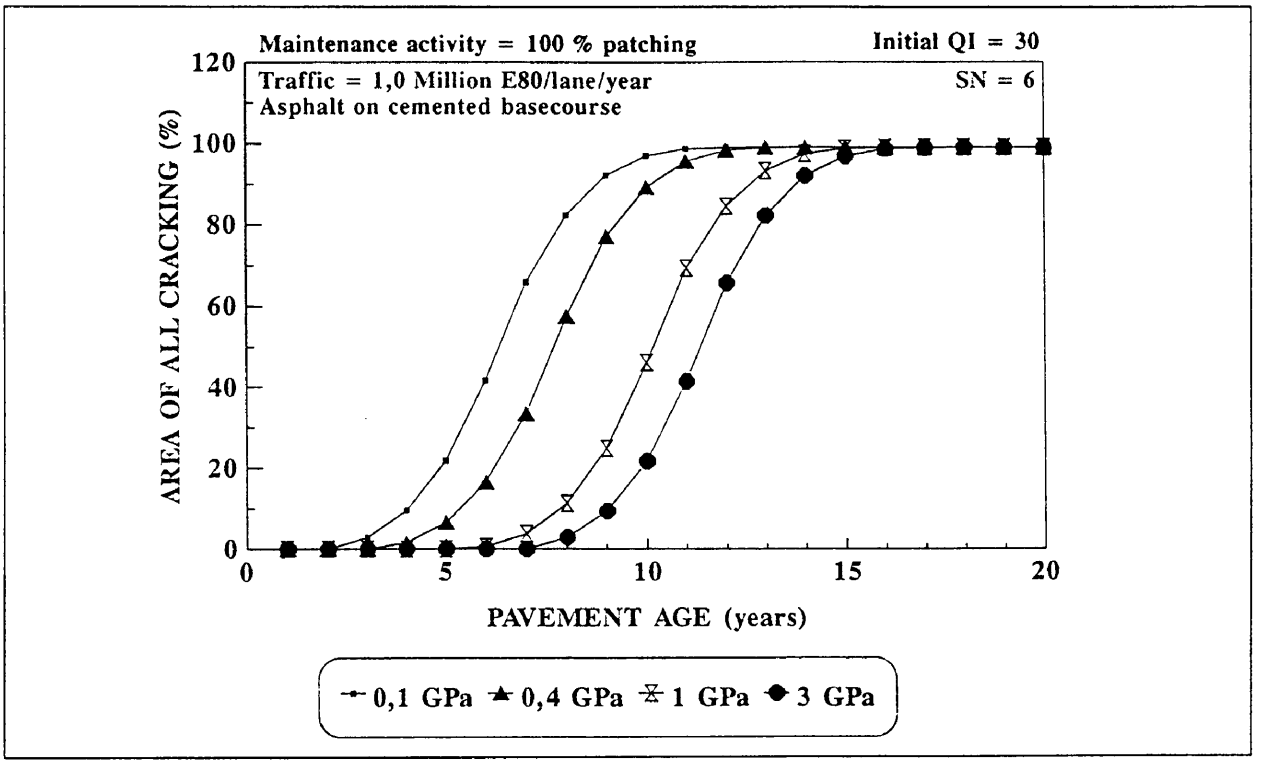

Figure 3.4: Sensitivity of all cracking model to resilient modulus of basecourse for SN = 6 under heavy traffic.

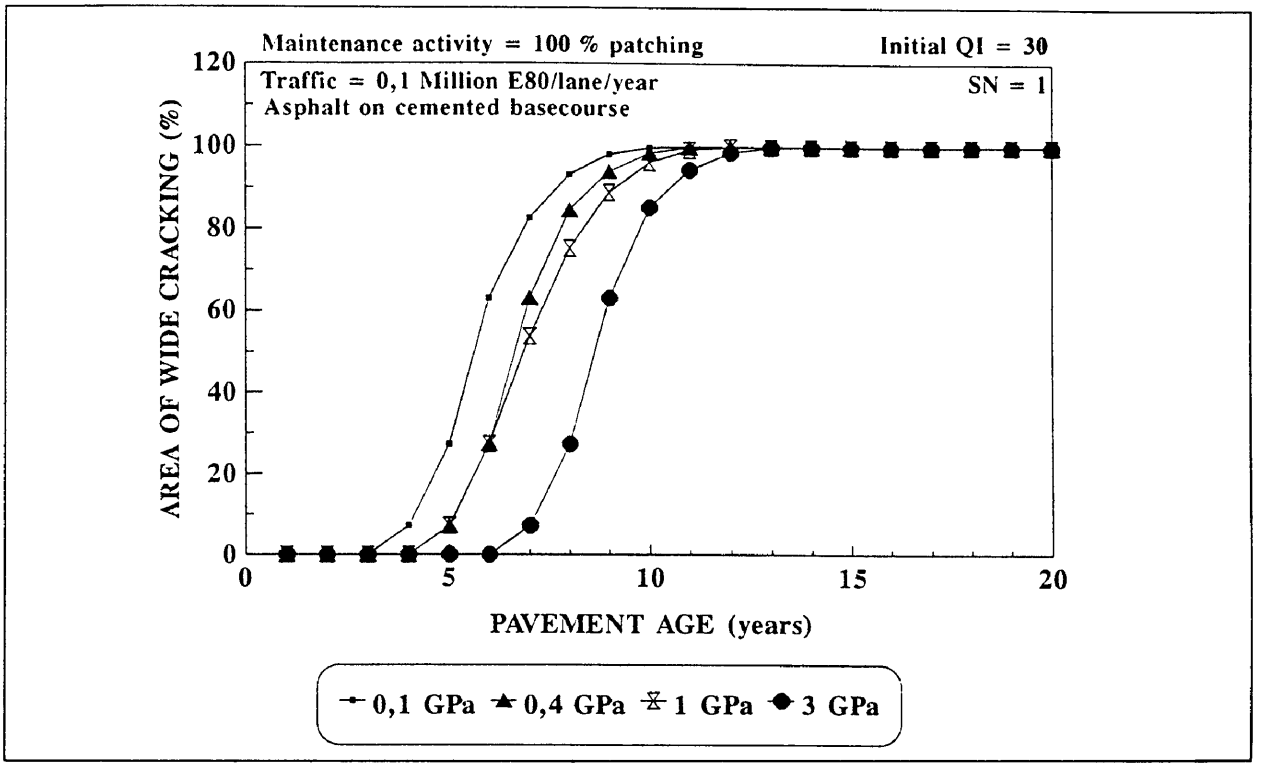

Figure 3.5: Sensitivity of wide cracking model to resilient modulus of basecourse for SN = 1 under light traffic.

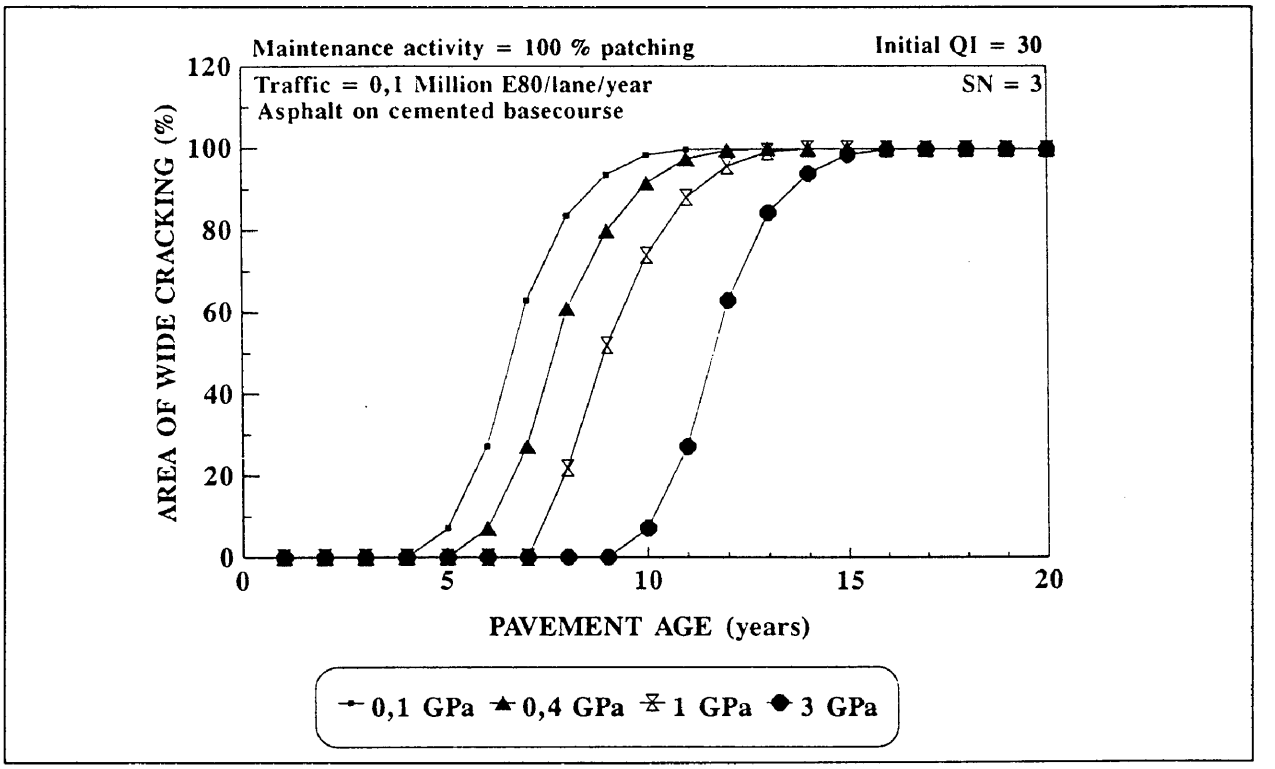

Figure 3.6: Sensitivity of wide cracking model to resilient modulus of basecourse for SN = 3 under light traffic.

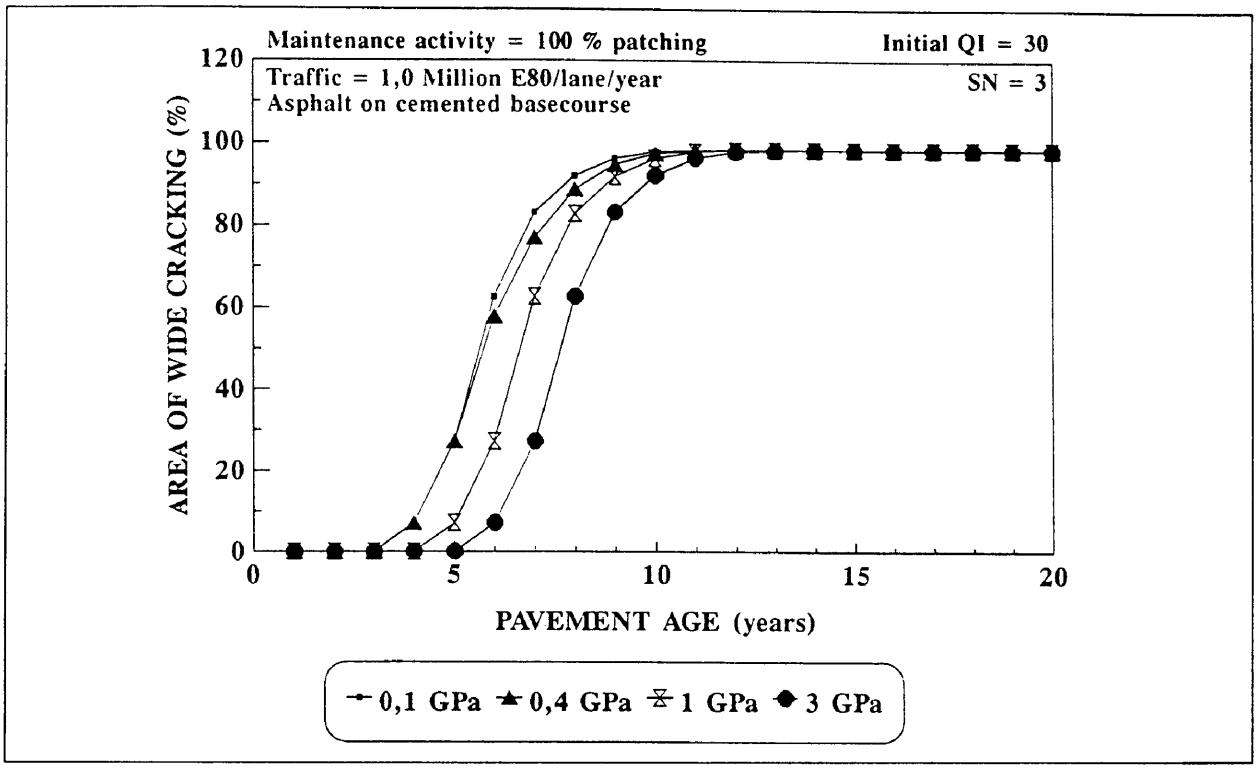

Figure 3.7: Sensitivity of wide cracking model to resilient modulus of basecourse for SN = 3 under heavy traffic.

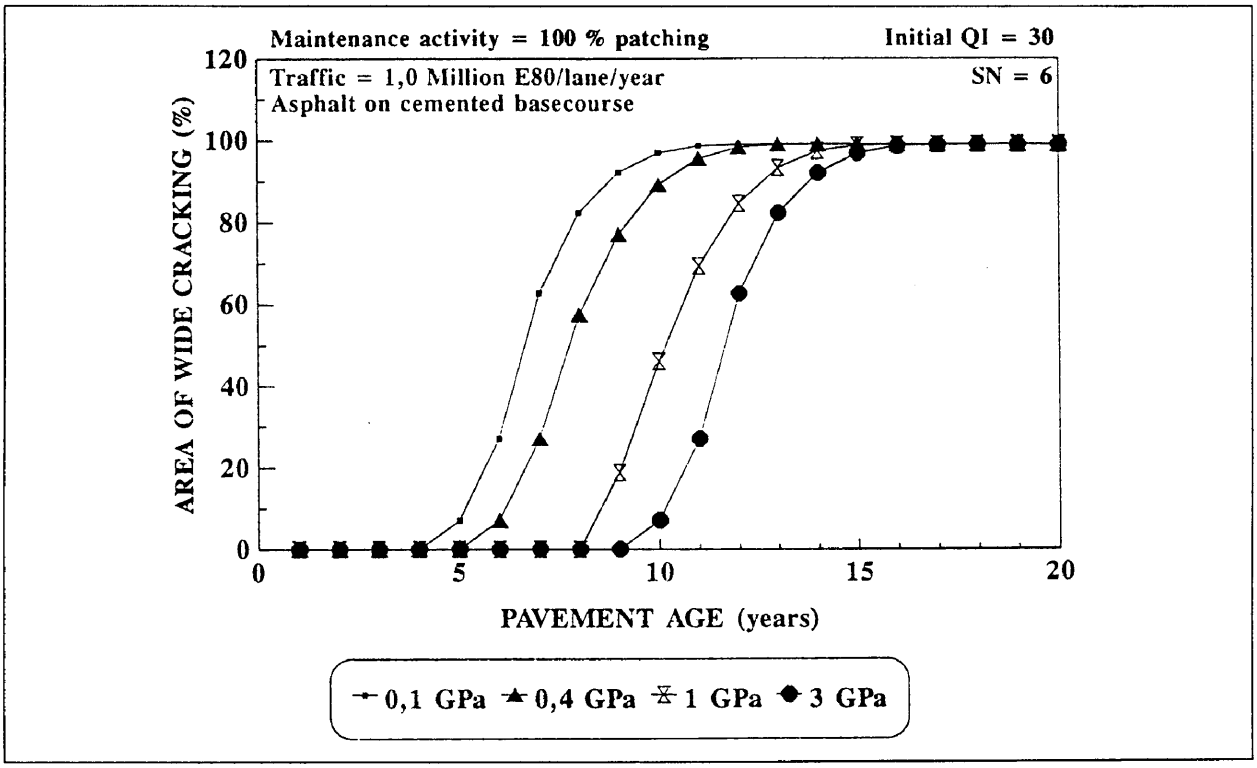

Figure 3.8: Sensitivity of wide cracking model to resilient modulus of basecourse for SN = 6 under heavy traffic.

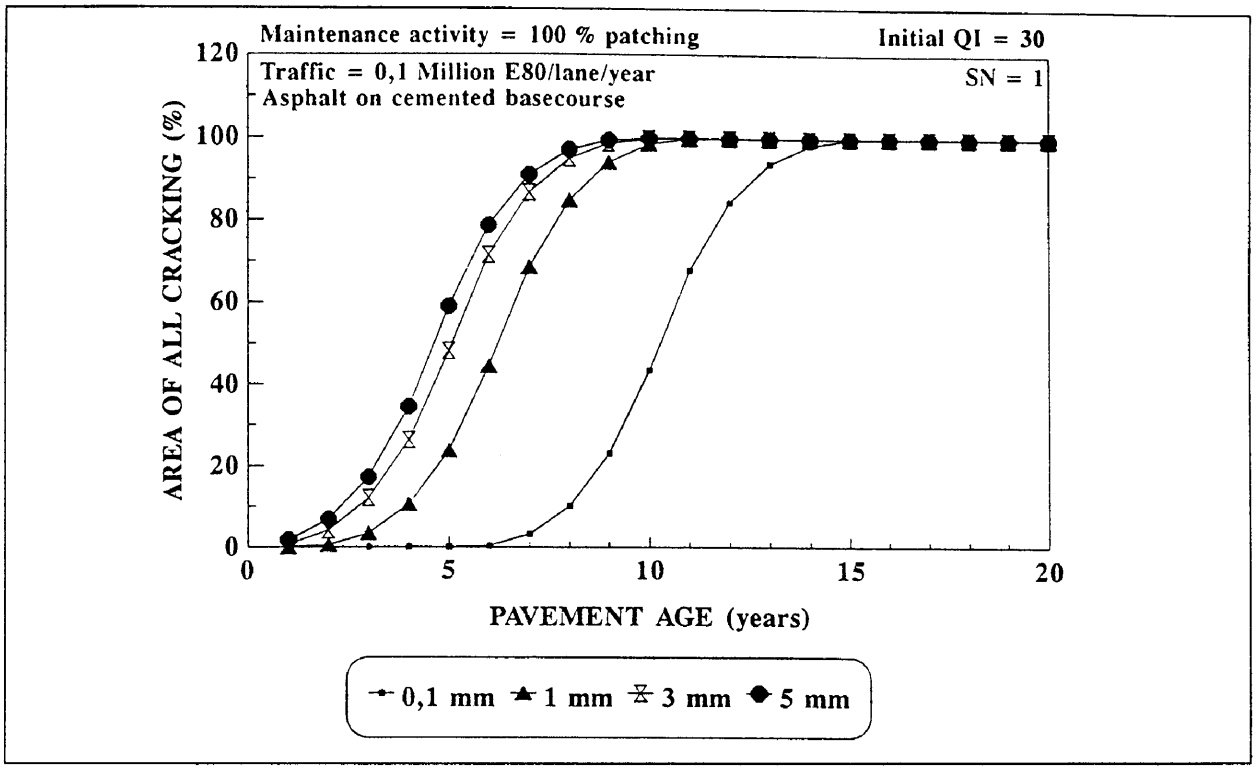

Figure 3.9: Sensitivity of all cracking model to deflection of the pavement for SN = 1 under light traffic.

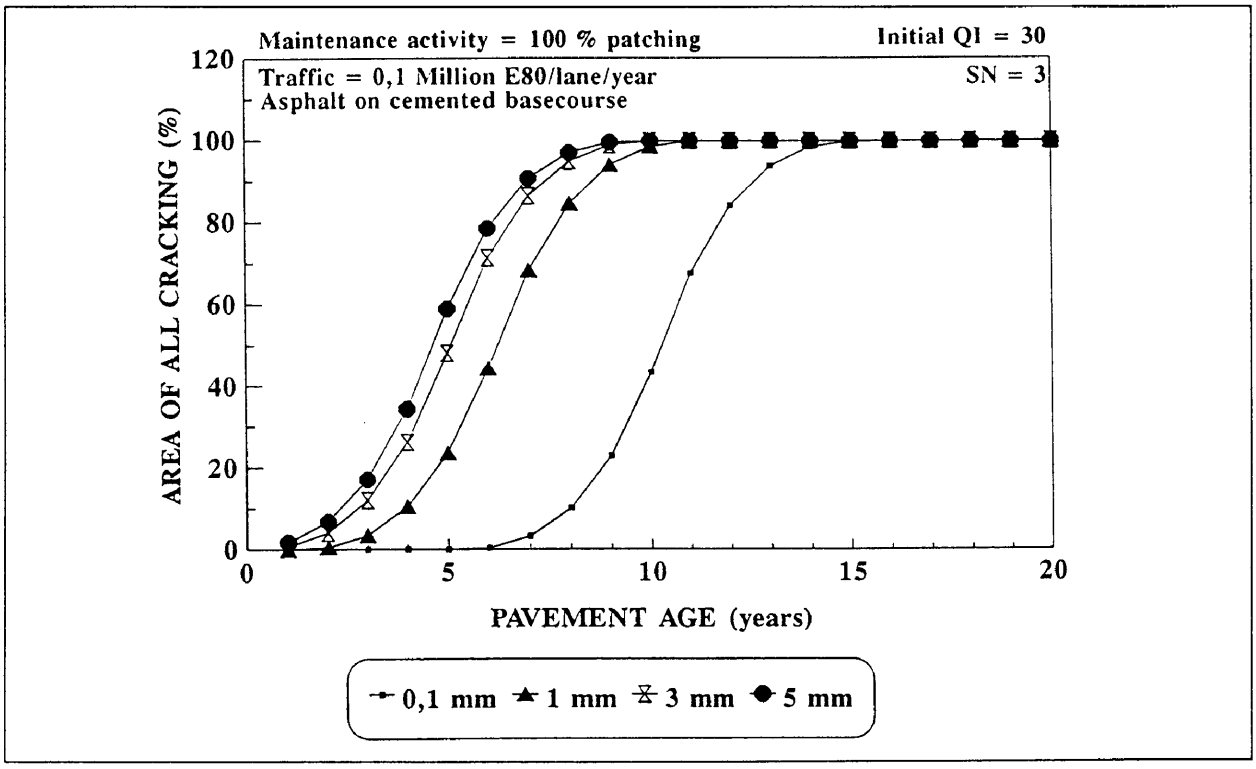

Figure 3.10: Sensitivity of all cracking model to the deflection of the pavement for SN = 3 under light traffic.

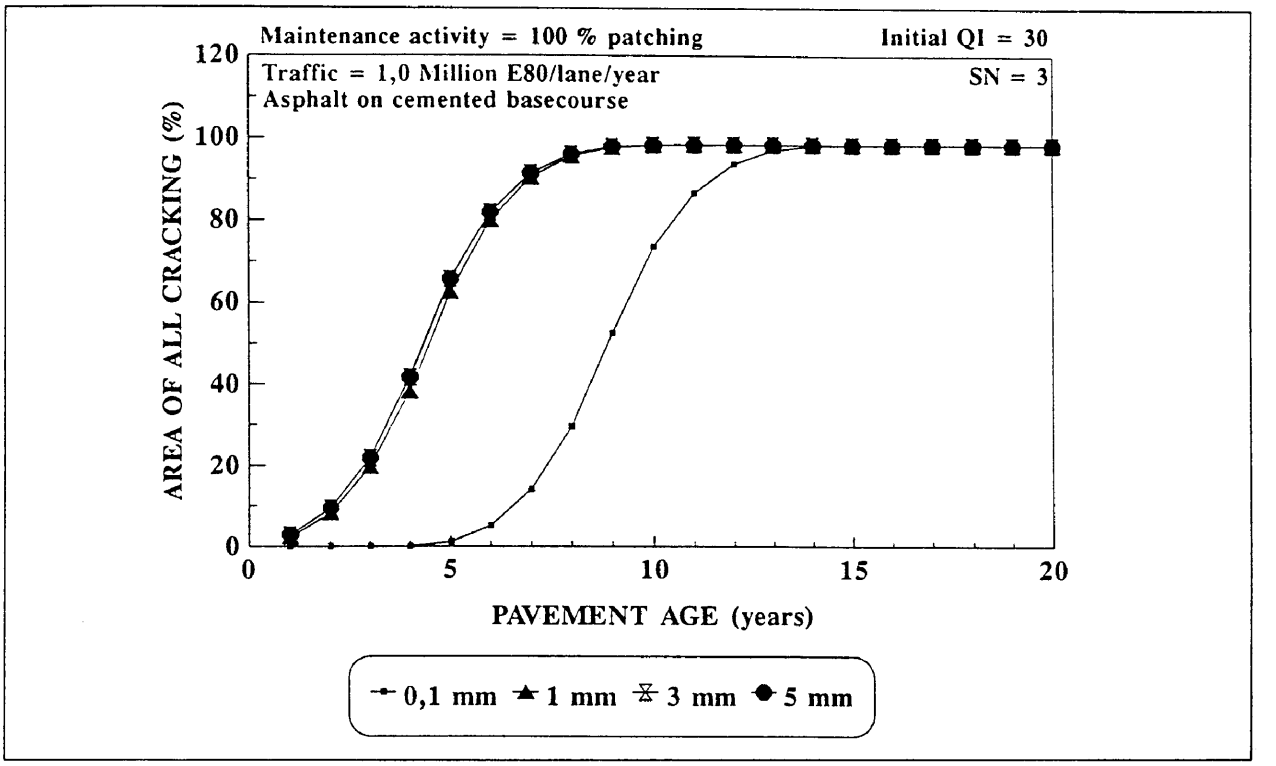

Figure 3.11: Sensitivity of all cracking model to the deflection of the pavement for SN = 3 under heavy traffic.

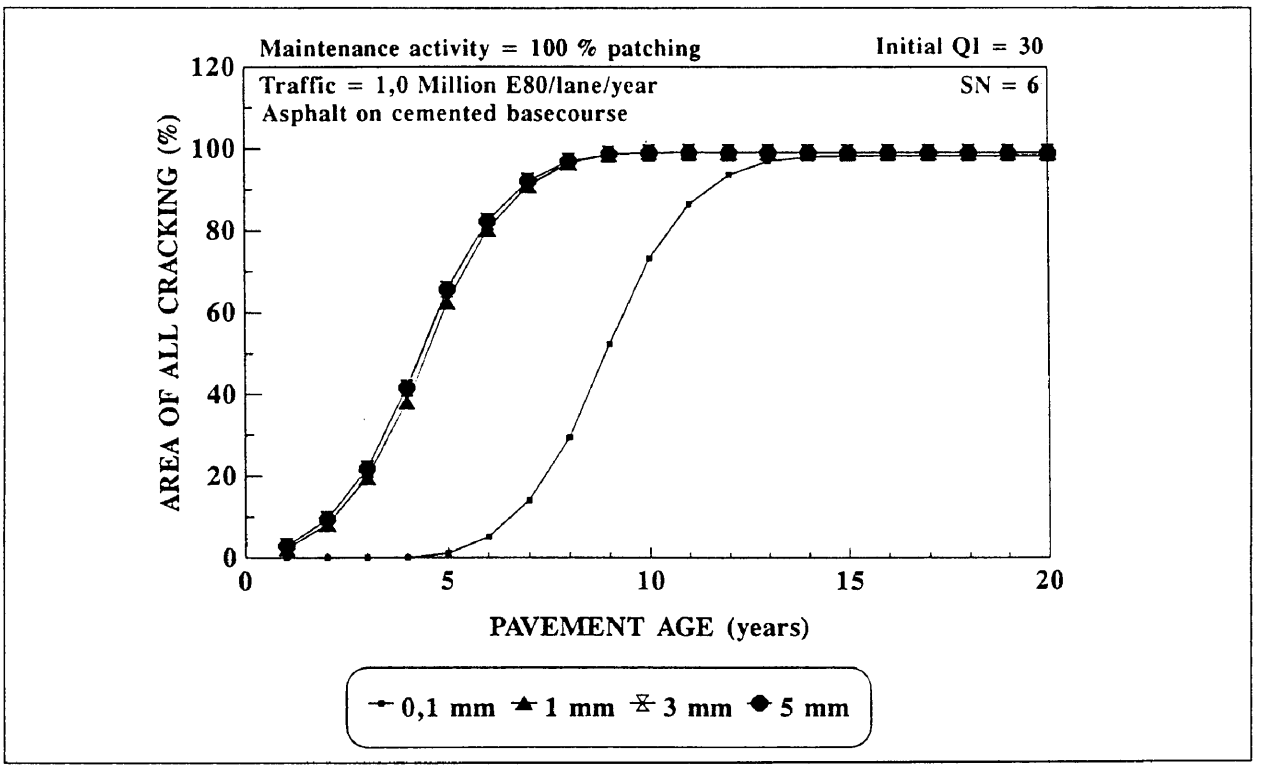

Figure 3.12: Sensitivity of all cracking model to the deflection of the pavement for SN = 6 under heavy traffic.

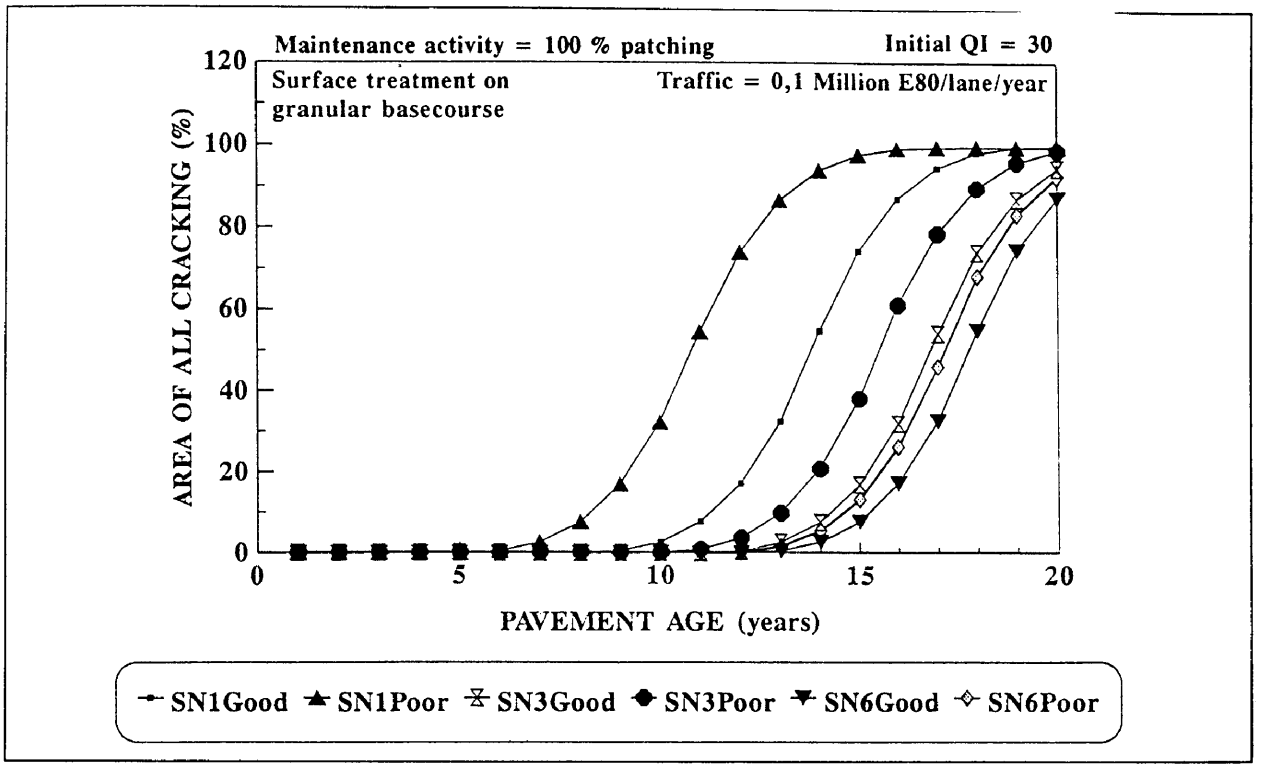

Figure 3.13: Sensitivity of all cracking model to the construction quality of a surfacing on a granular basecourse under light traffic.

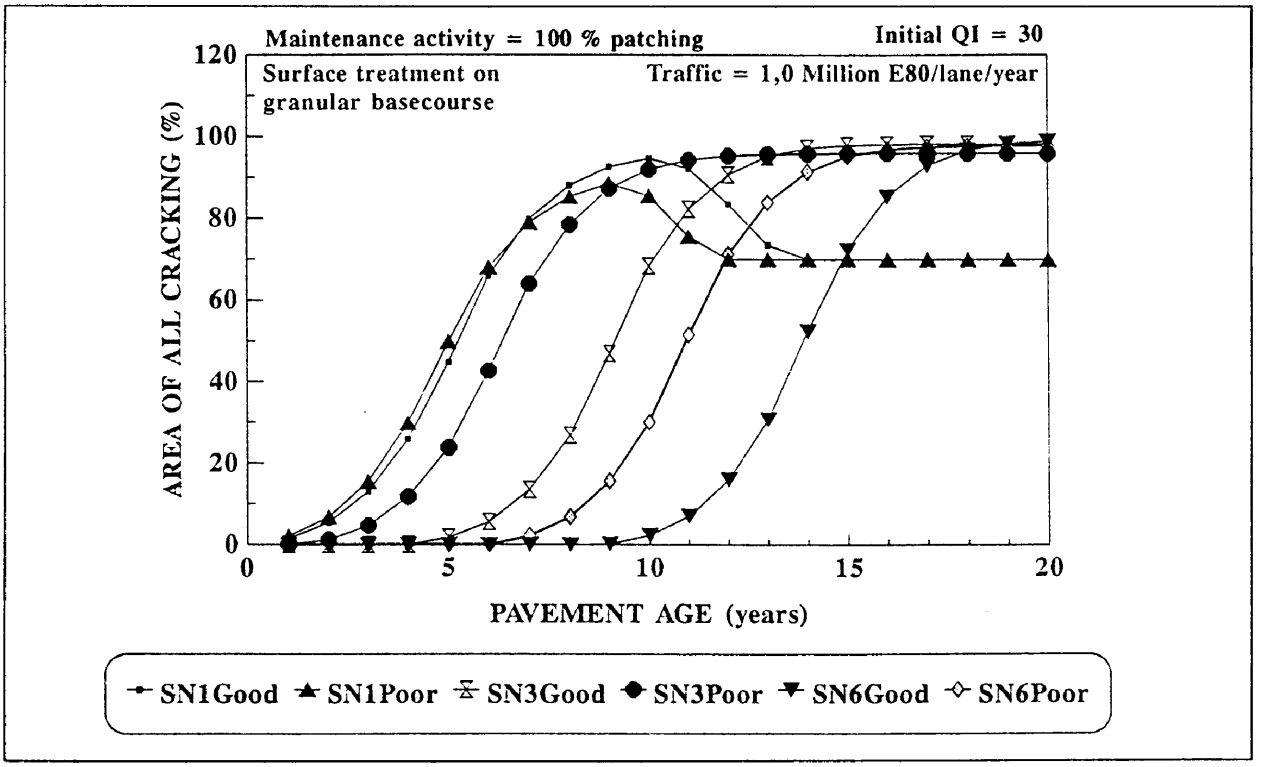

Figure 3.14: Sensitivity of all cracking model to the construction quality of a surfacing on a granular basecourse under heavy traffic.

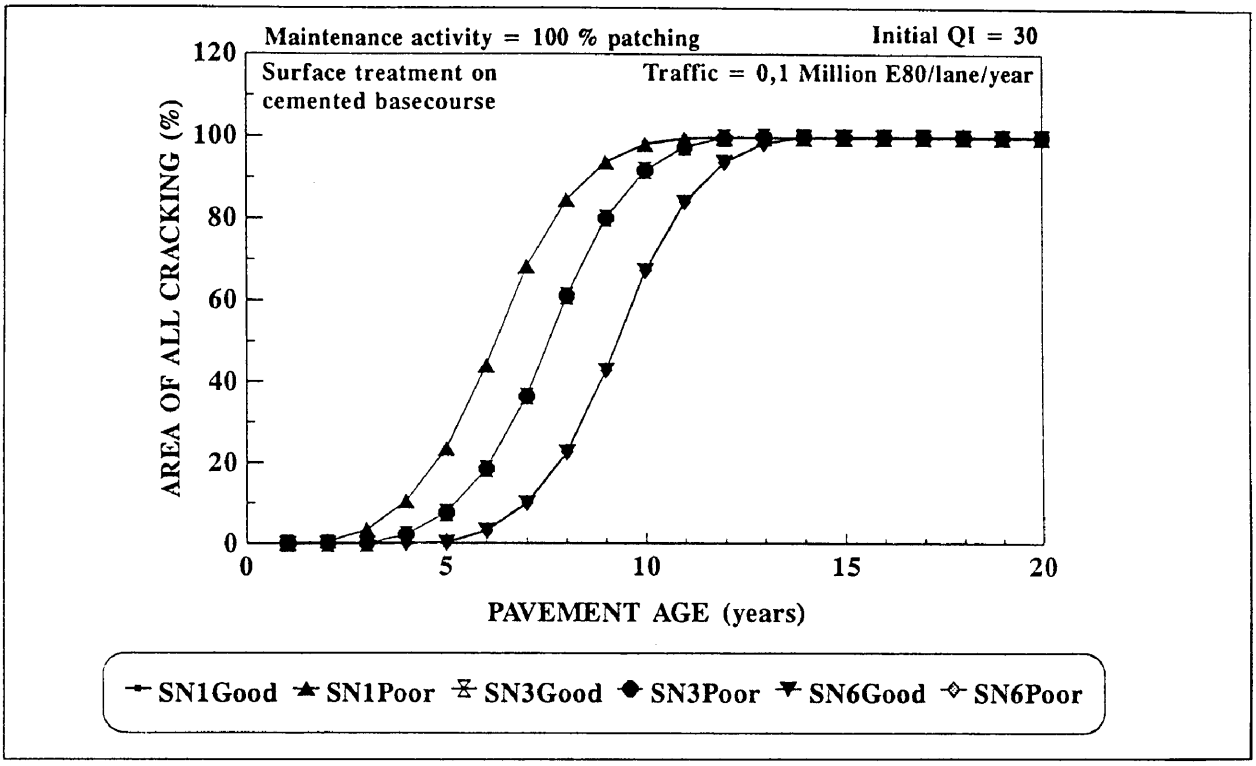

Figure 3.15: Sensitivity of all cracking model to the construction quality of a surfacing on a cemented basecourse under light traffic.

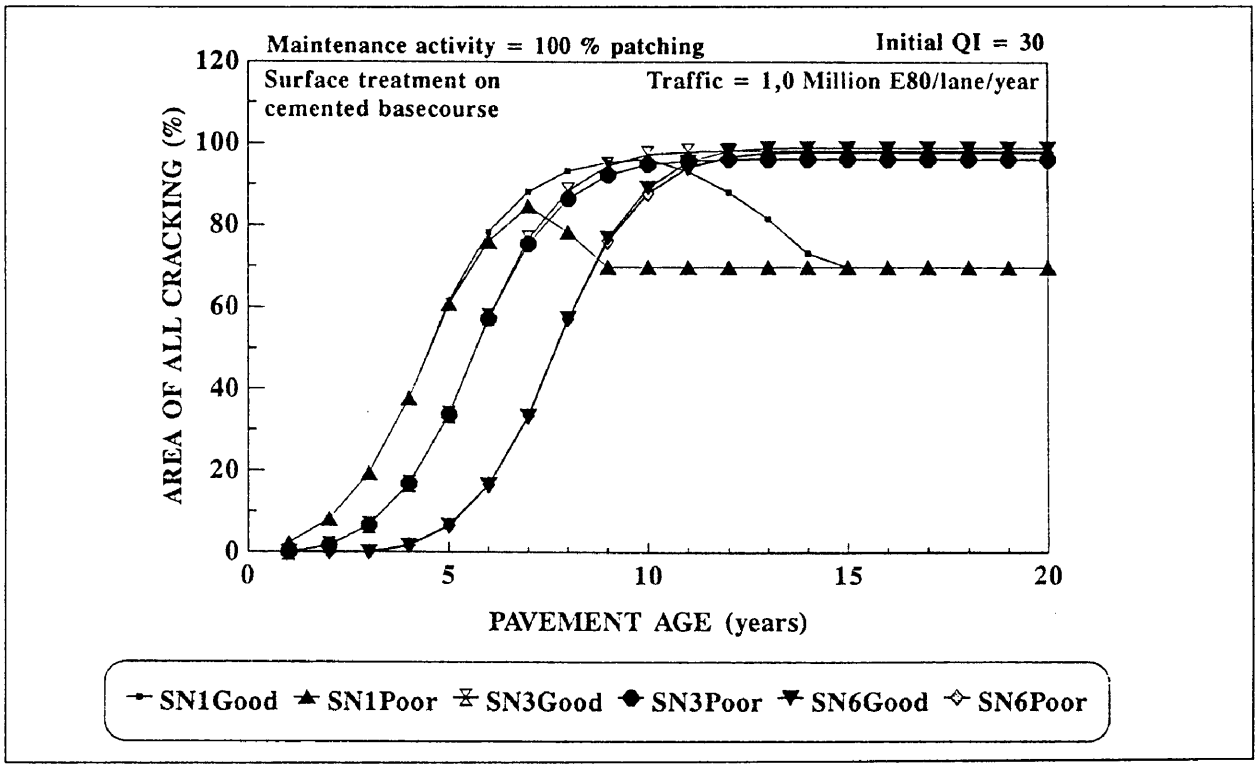

Figure 3.16: Sensitivity of all cracking model to the construction quality of a surfacing on a cemented basecourse under heavy traffic.

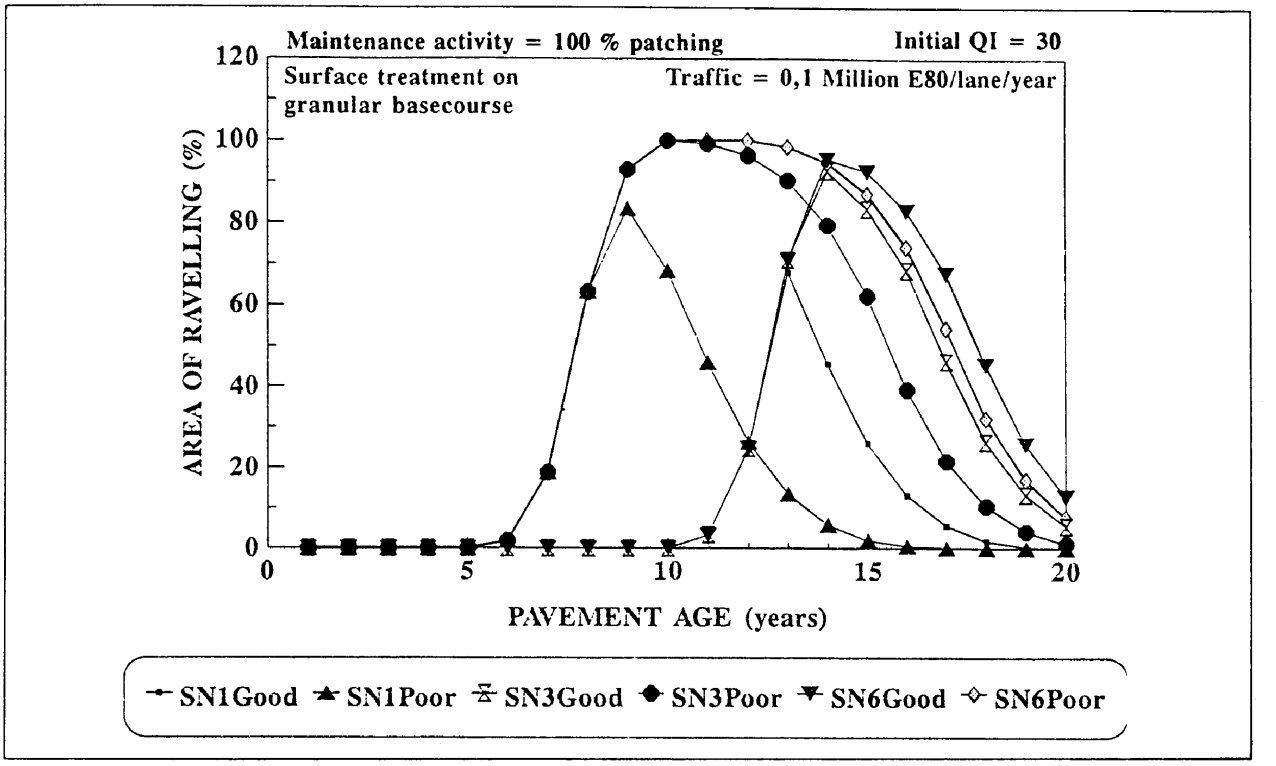

Figure 3.17: Sensitivity of ravelling model to the construction quality of a surface treatment on a granular basecourse under light traffic.

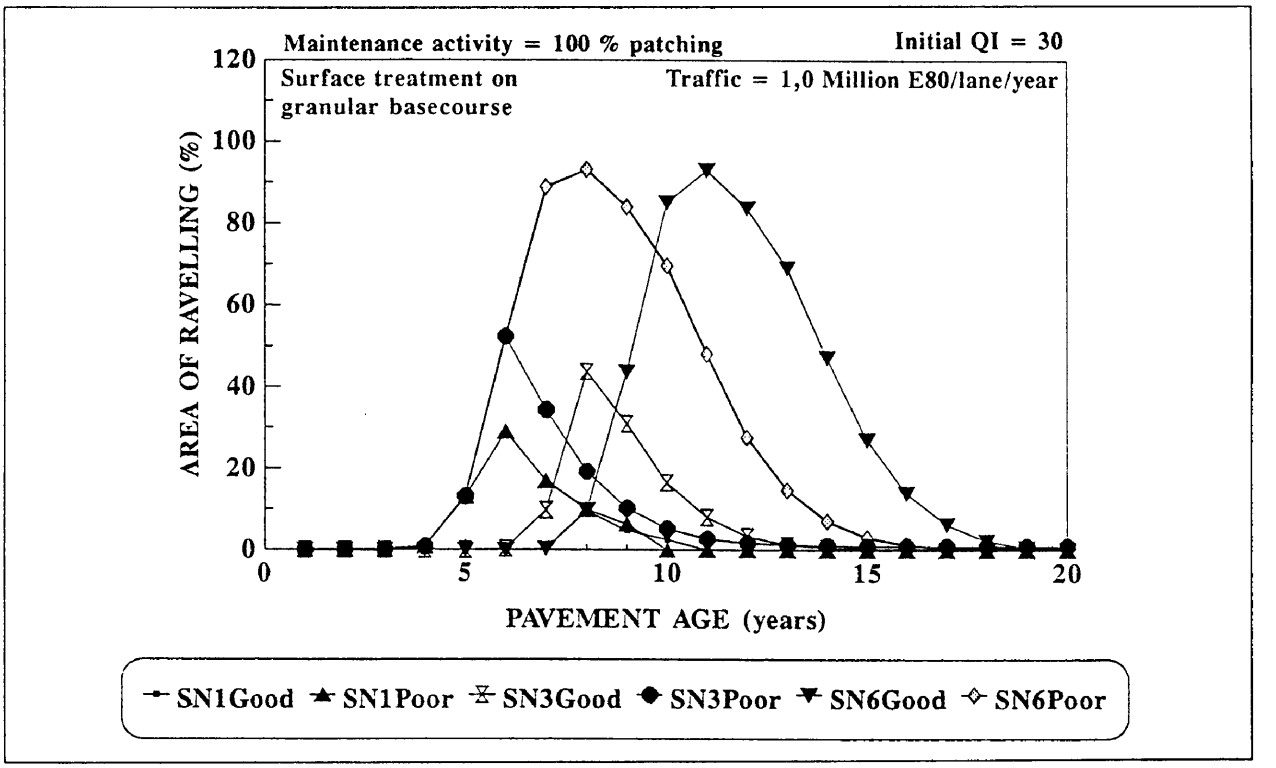

Figure 3.18: Sensitivity of ravelling model to the construction quality of a surface treatment on a granular basecourse under heavy traffic.

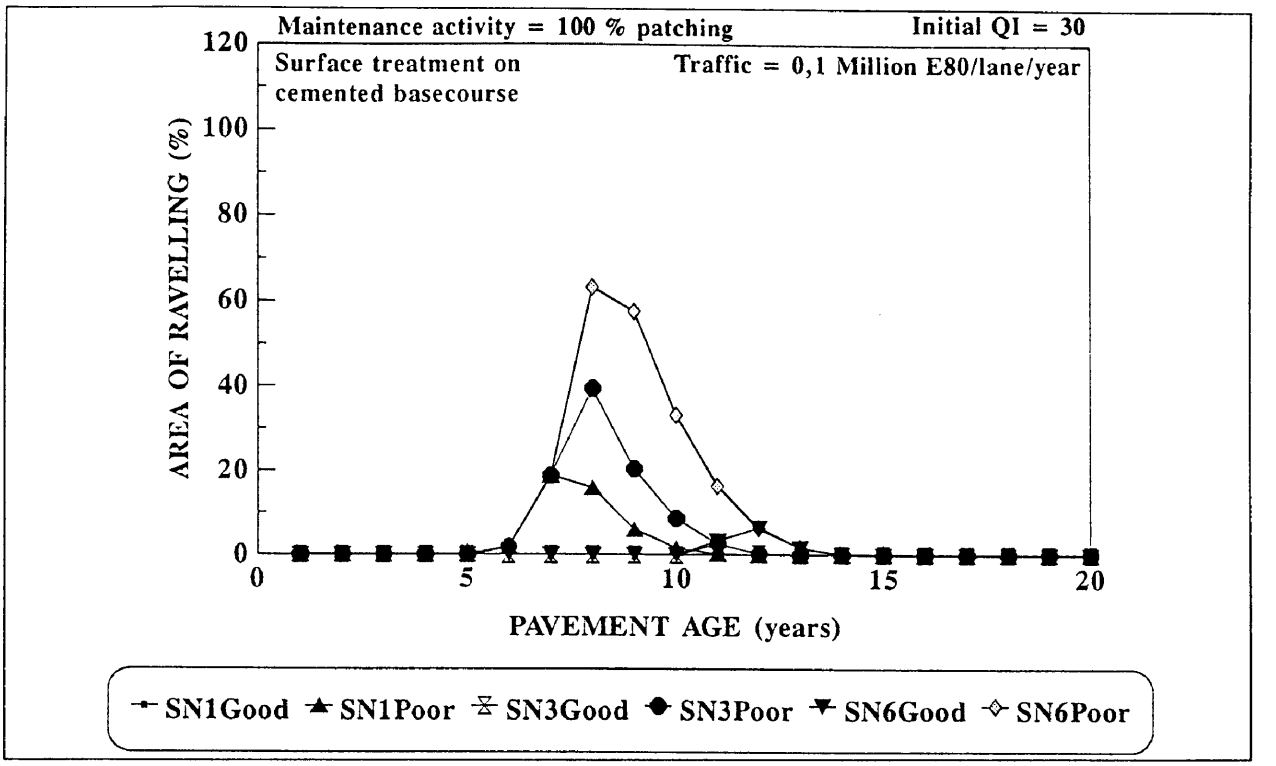

Figure 3.19: Sensitivity of ravelling model to the construction quality of a surface treatment on a cemented basecourse under light traffic.

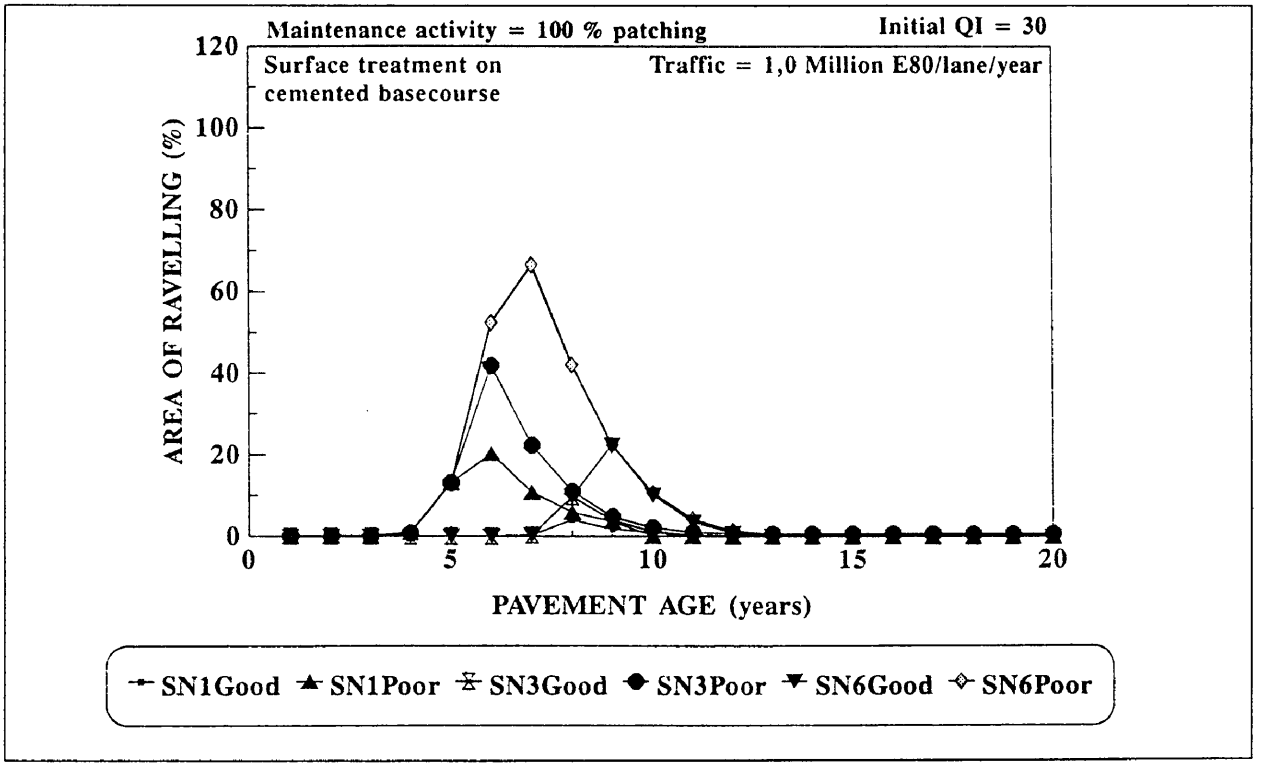

Figure 3.20: Sensitivity of ravelling model to the construction quality of a surface treatment on a cemented basecourse under heavy traffic.

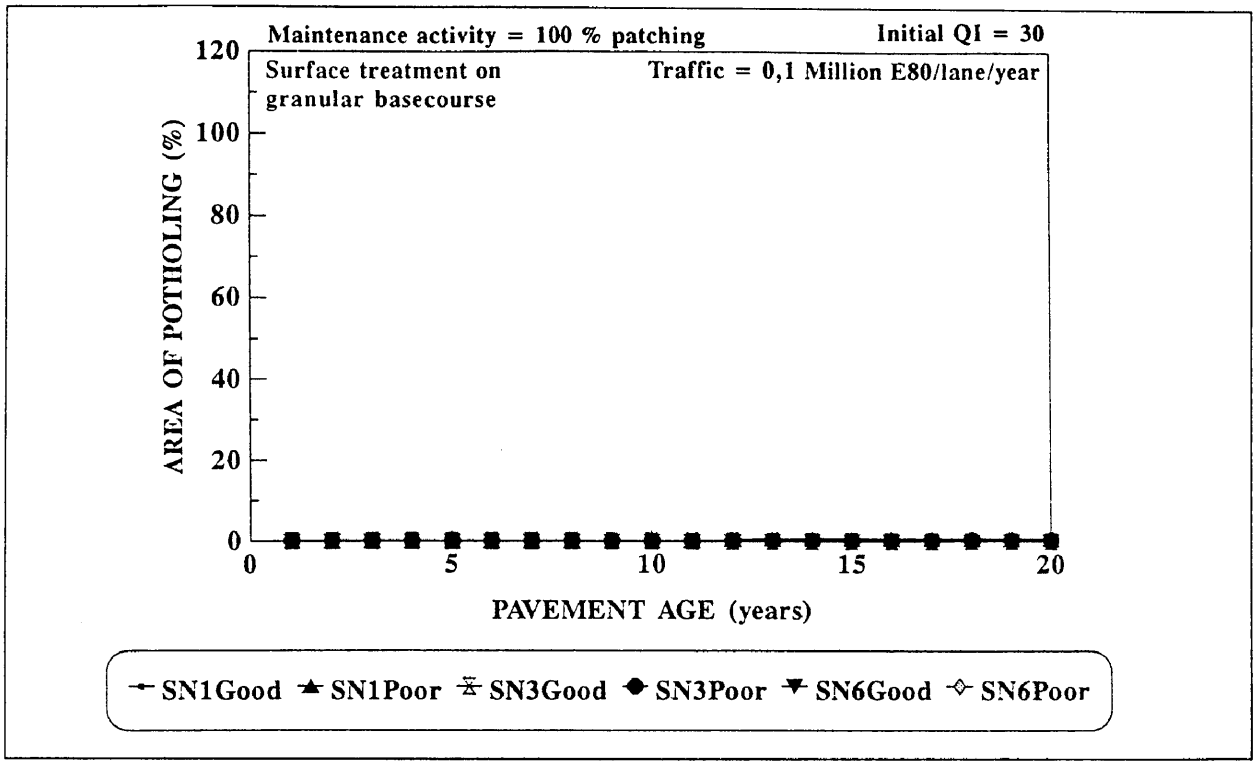

Figure 3.21: Sensitivity of potholing model to the construction quality of a surface treatment on a granular basecourse under light traffic.

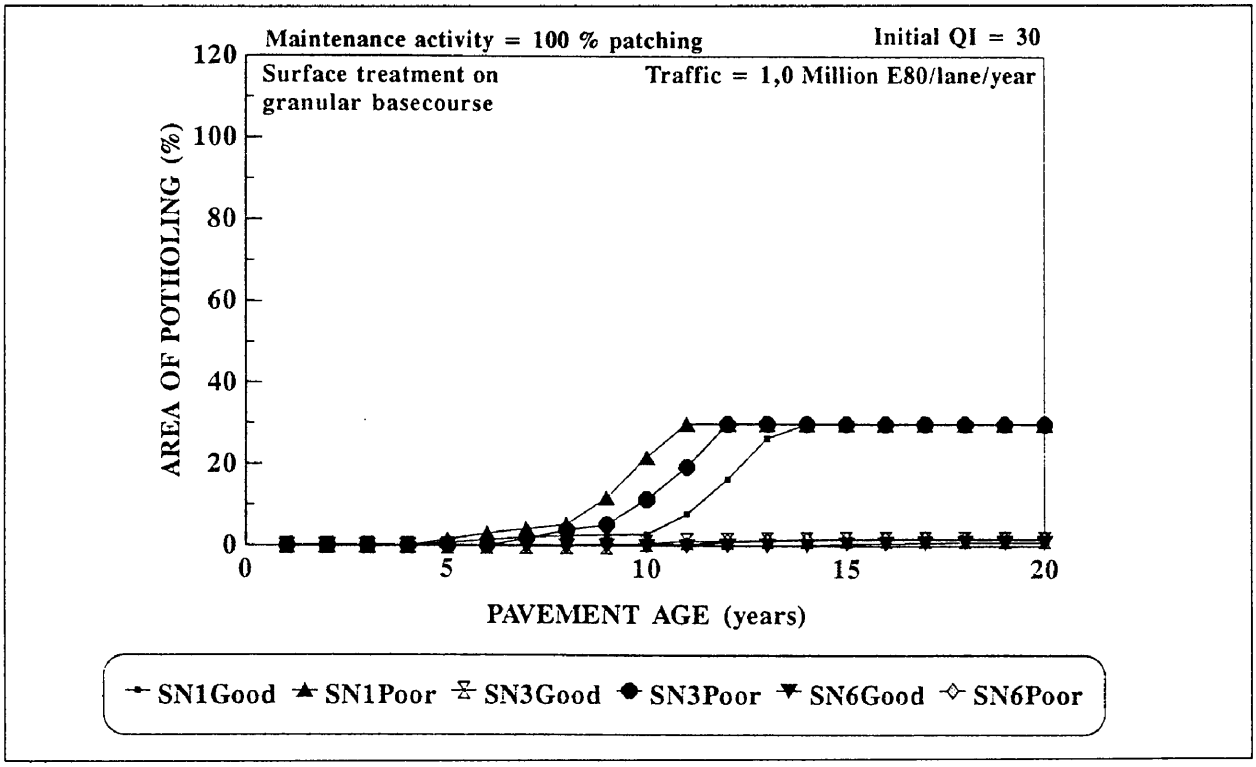

Figure 3.22: Sensitivity of potholing model to the construction quality of a surface treatment on a granular basecourse under heavy traffic.

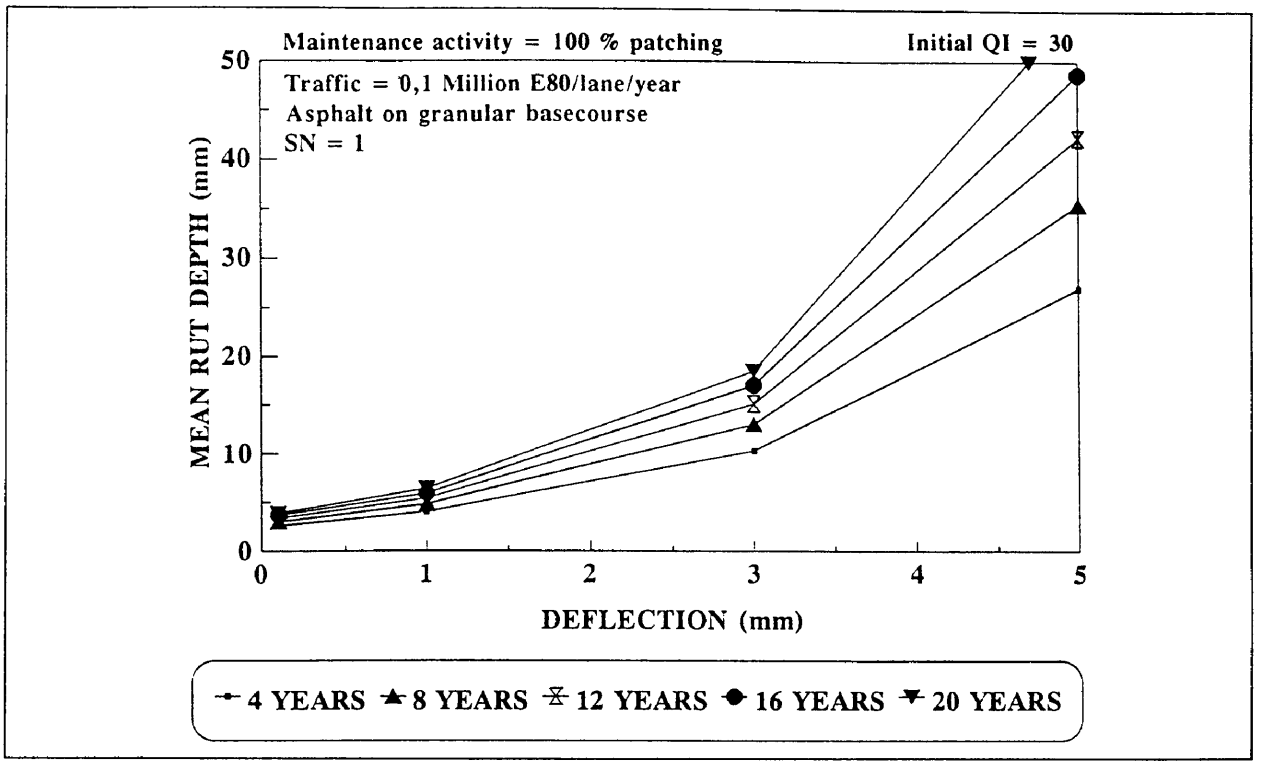

Figure 3.23: Sensitivity of mean rut depth model to pavement deflection for SN = 1 under light traffic.

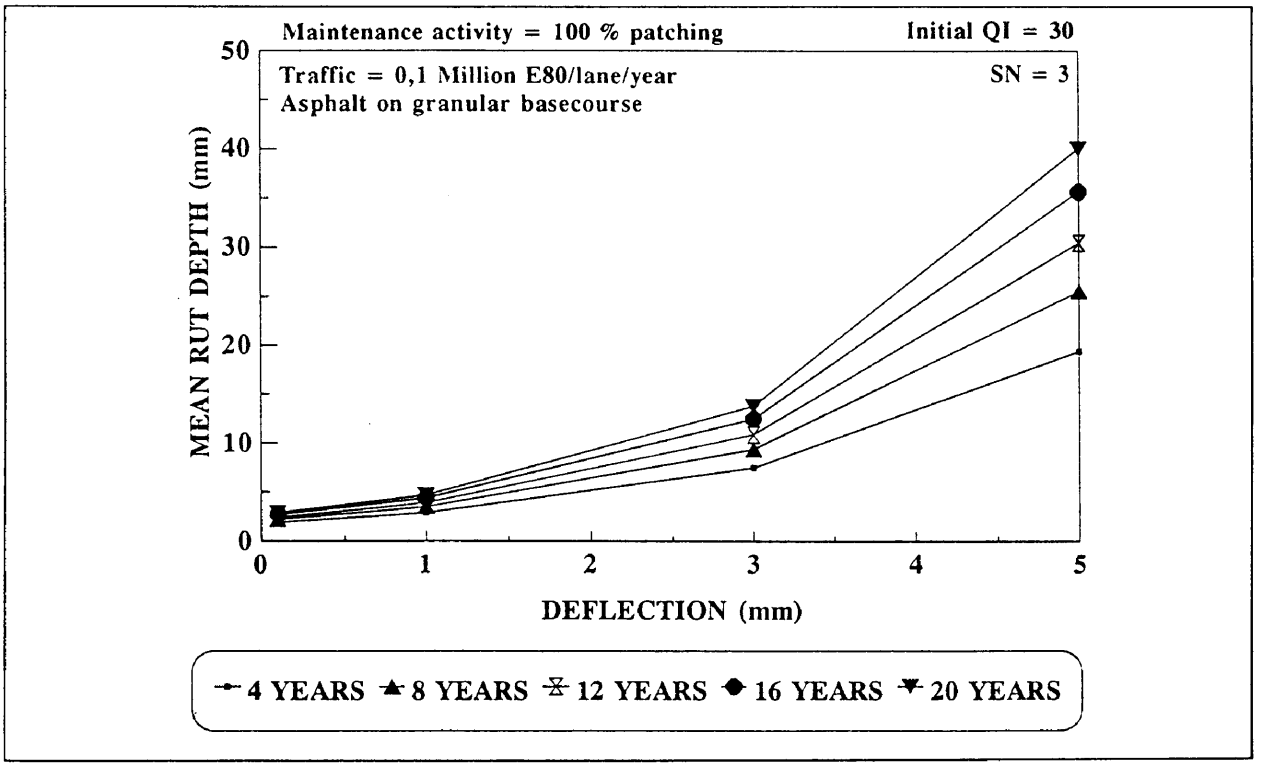

Figure 3.24: Sensitivity of mean rut depth model to pavement deflection for SN = 3 under light traffic.

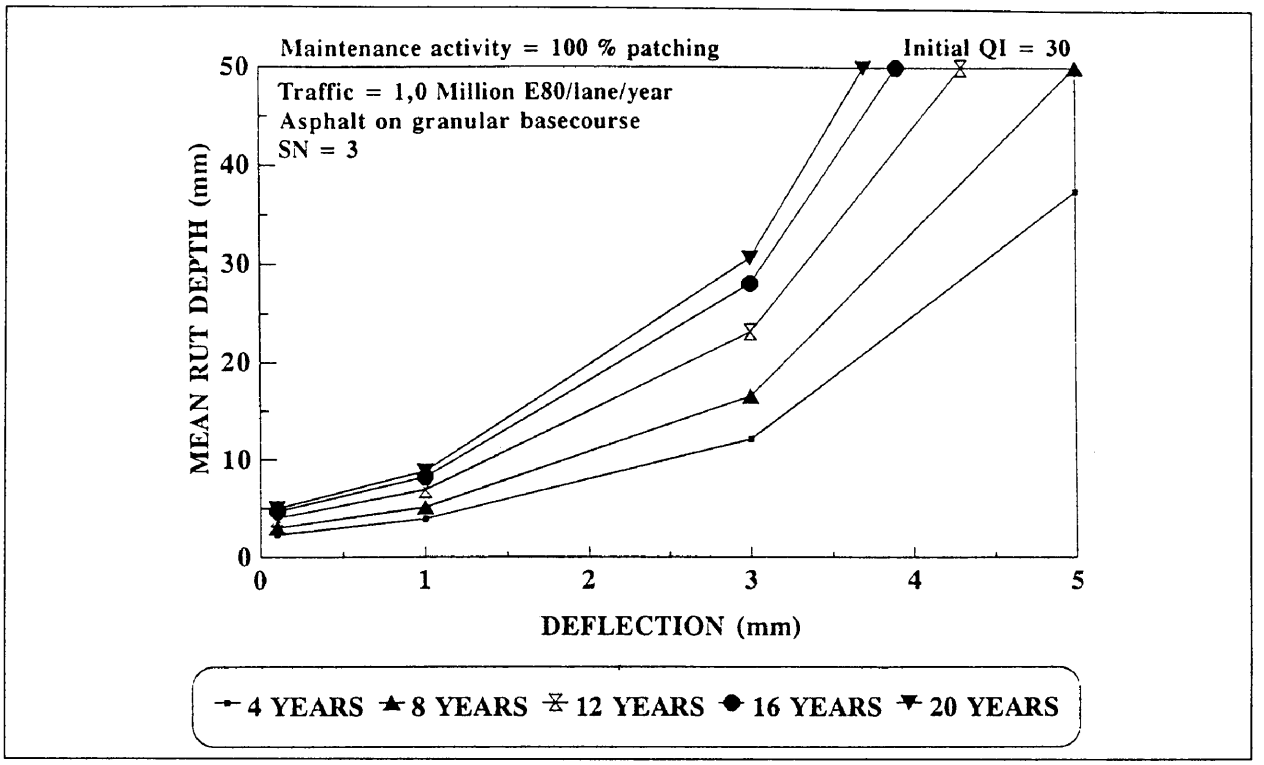

Figure 3.25: Sensitivity of mean rut depth model to pavement deflection for SN = 3 under heavy traffic.

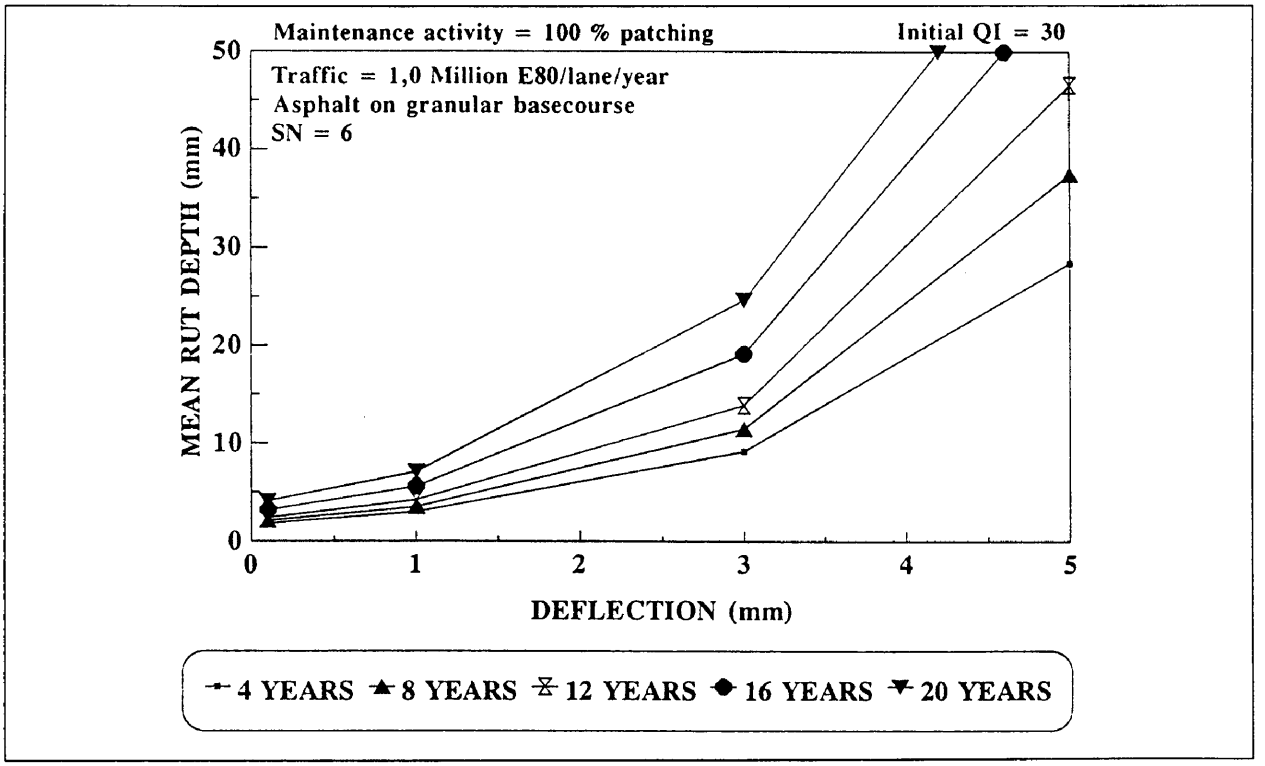

Figure 3.26: Sensitivity of mean rut depth model to pavement deflection for SN = 6 under heavy traffic.

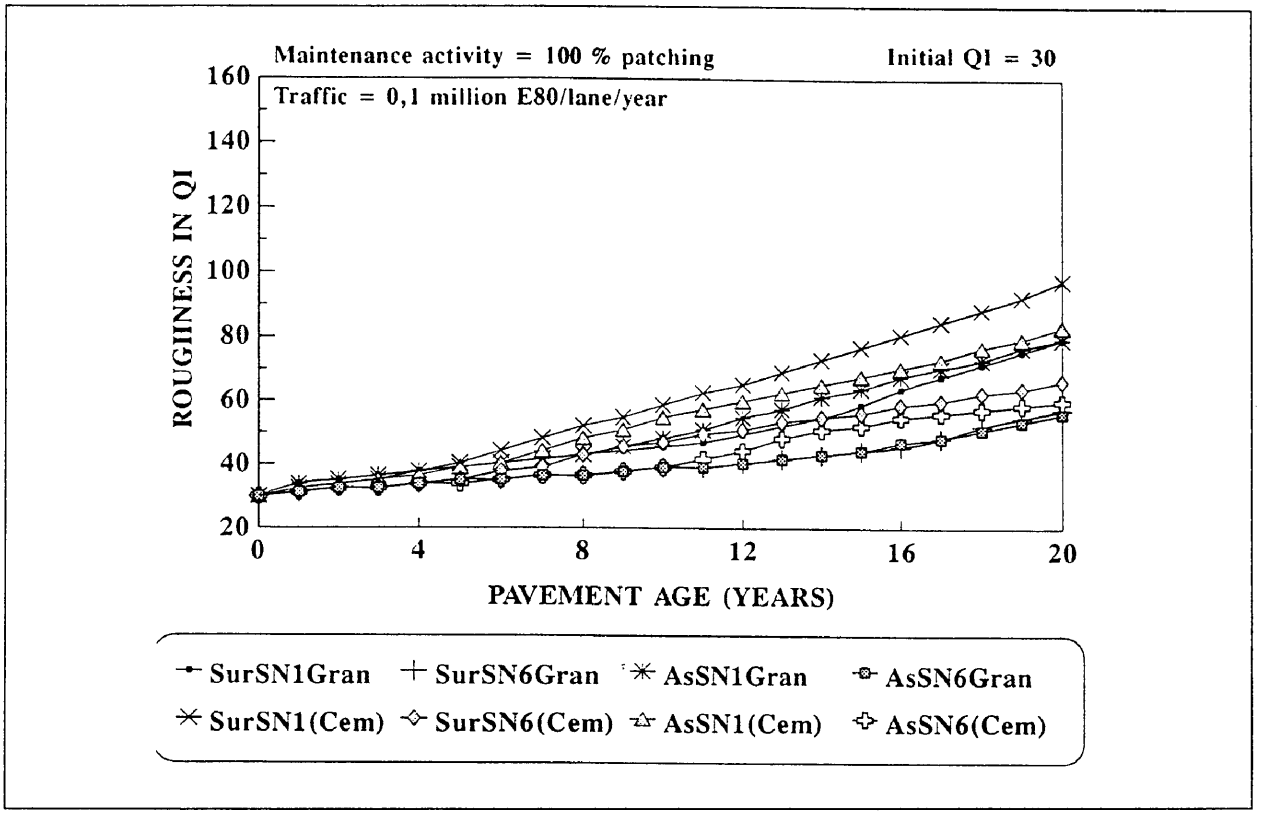

Figure 3.27: Roughness predictions for various pavement types under light traffic.

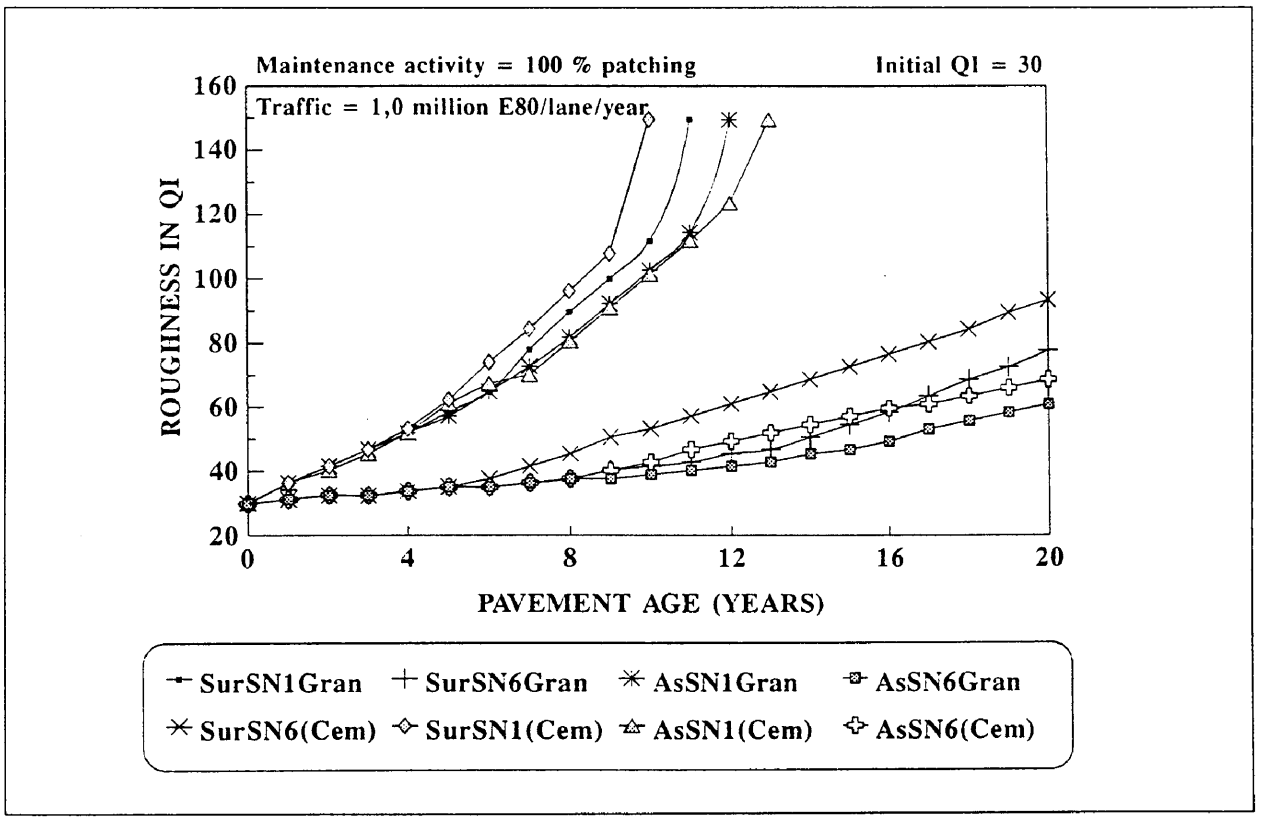

Figure 3.28: Roughness predictions for various pavement types under heavy traffic.

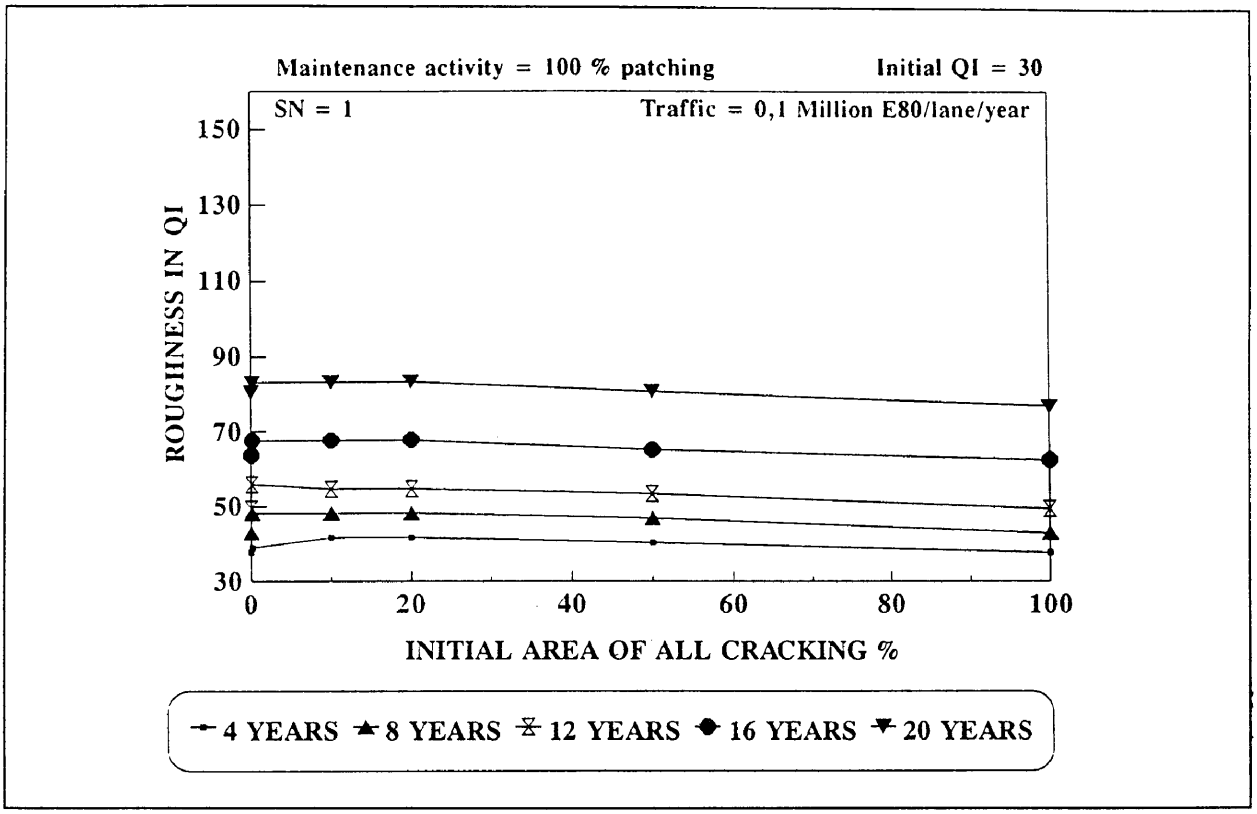

Figure 3.29: Sensitivity to initial area of all cracking for SN = 1 and light traffic.

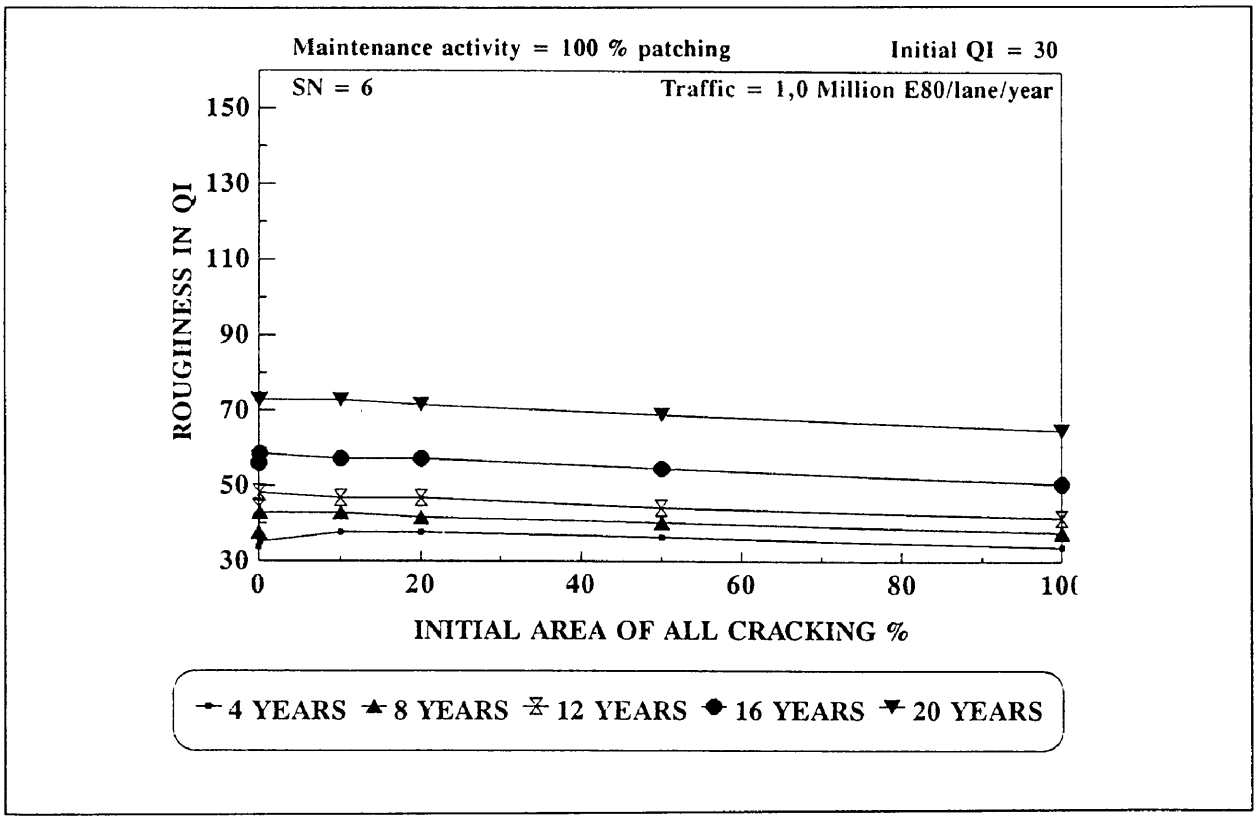

Figure 3.30: Sensitivity to initial area of all cracking for SN = 6 and heavy traffic.

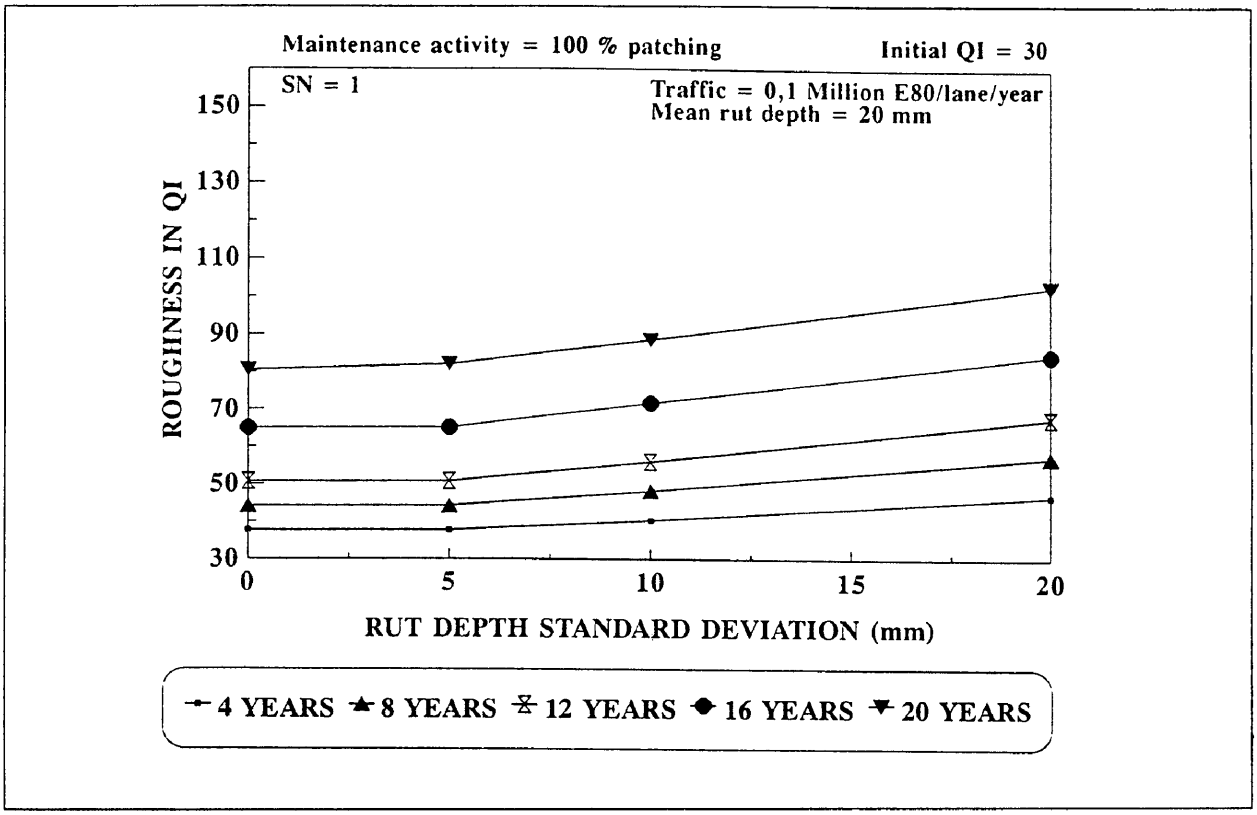

Figure 3.31: Sensitivity to rut depth standard deviation for SN = 1 and light traffic.

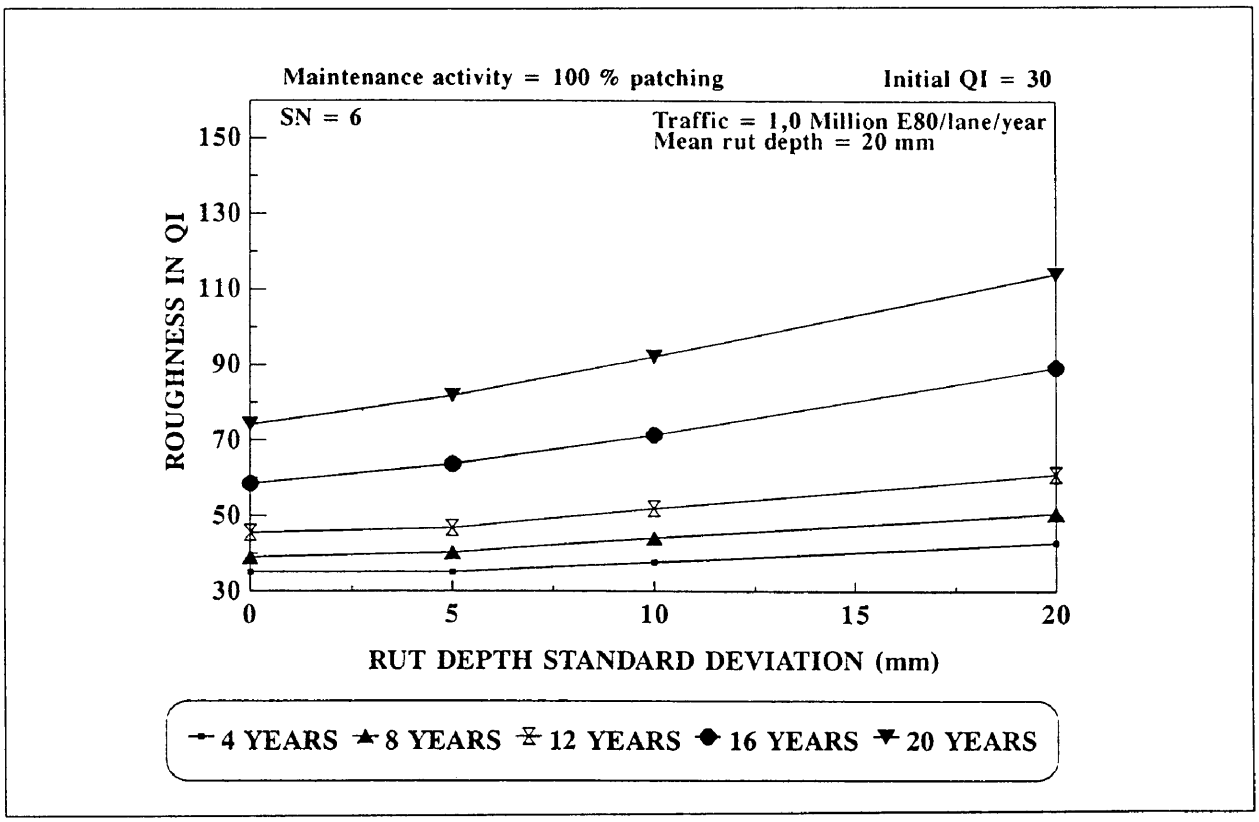

Figure 3.32: Sensitivity to rut depth standard deviation for SN = 6 and heavy traffic.

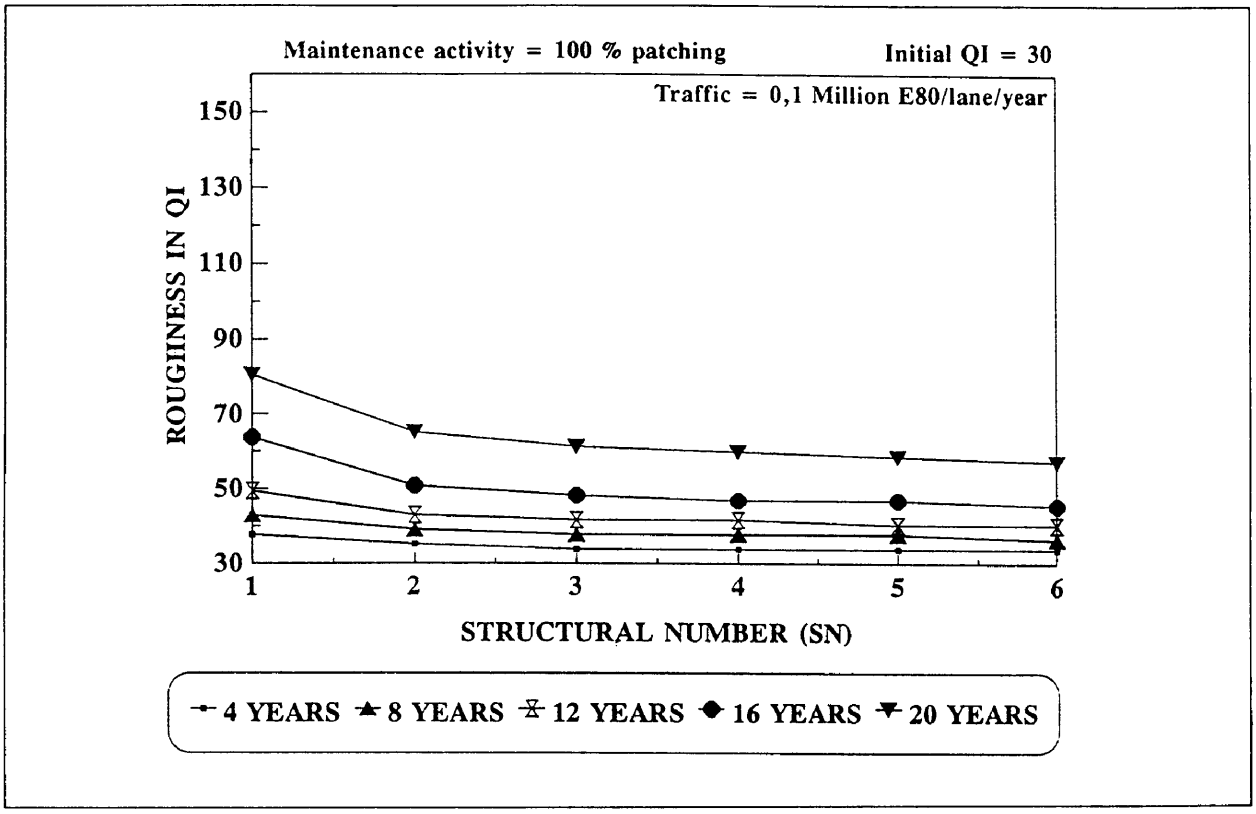

Figure 3.33: Sensitivity to structural number under light traffic.

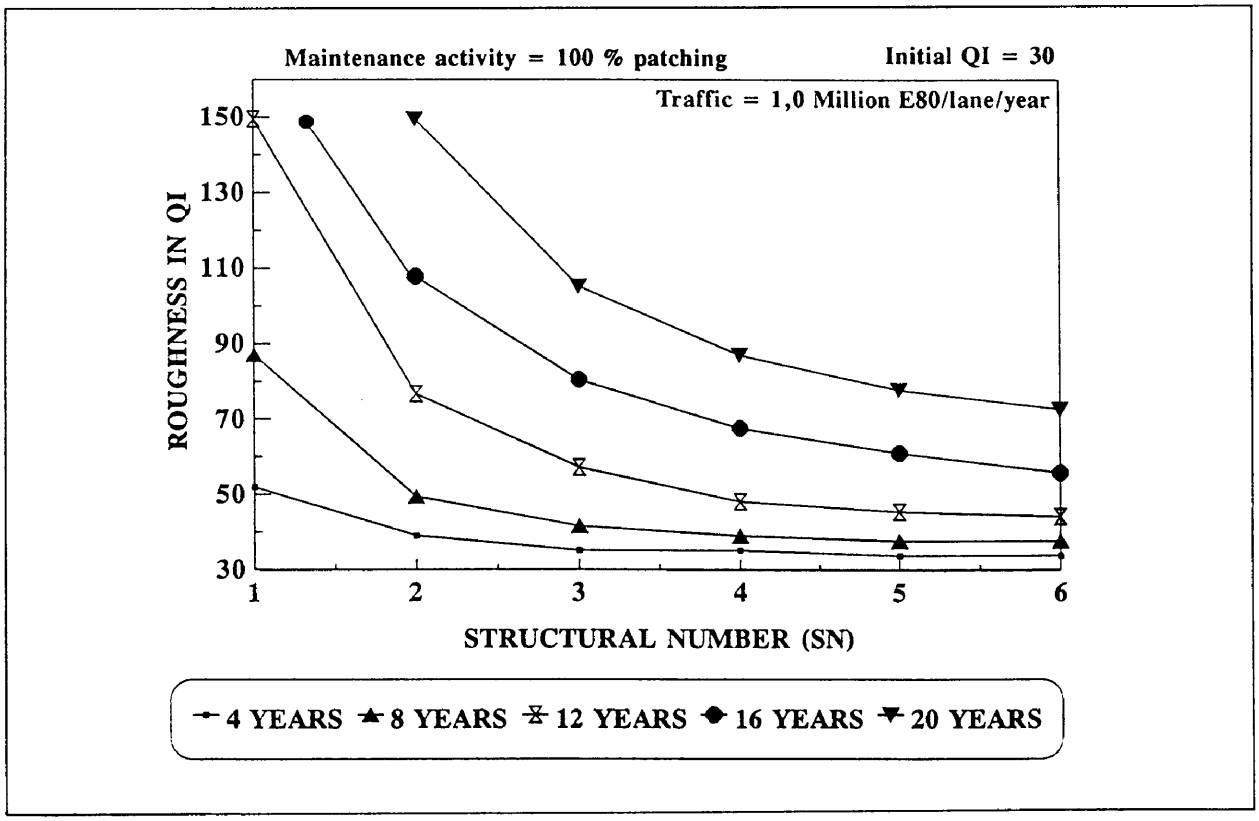

Figure 3.34: Sensitivity to structural number under heavy traffic.

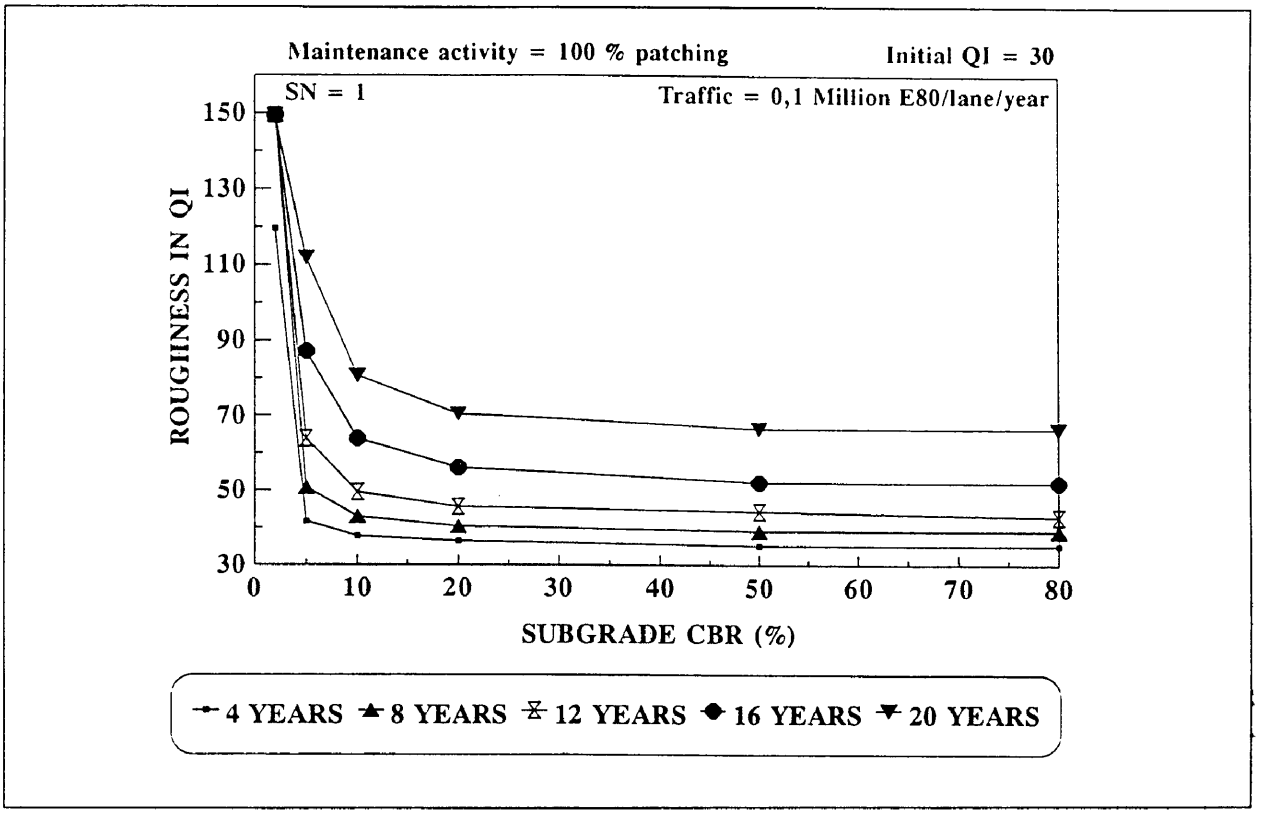

Figure 3.35: Sensitivity to subgrade CBR for SN = 1 under light traffic.

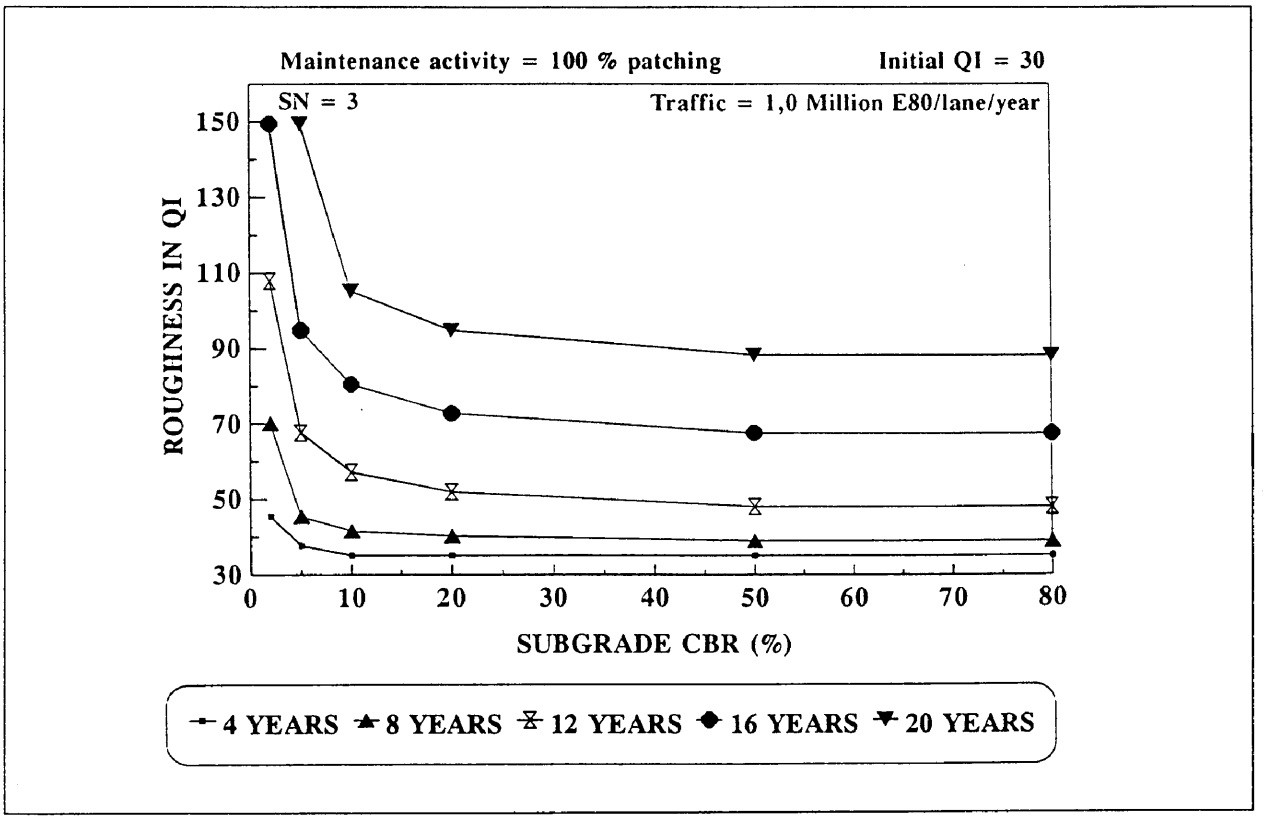

Figure 3.36: Sensitivity to subgrade CBR for SN = 3 under heavy traffic.

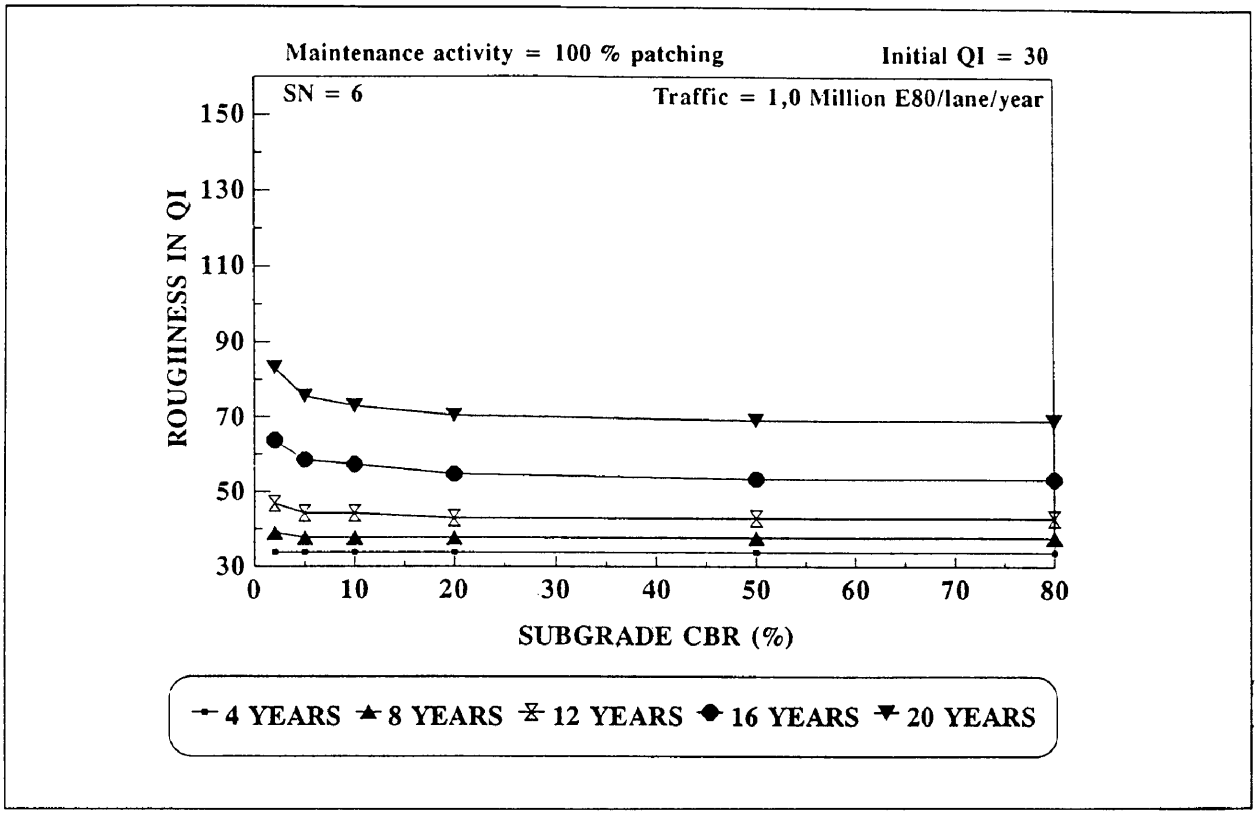

Figure 3.37: Sensitivity to subgrade CBR for SN = 6 under heavy traffic.

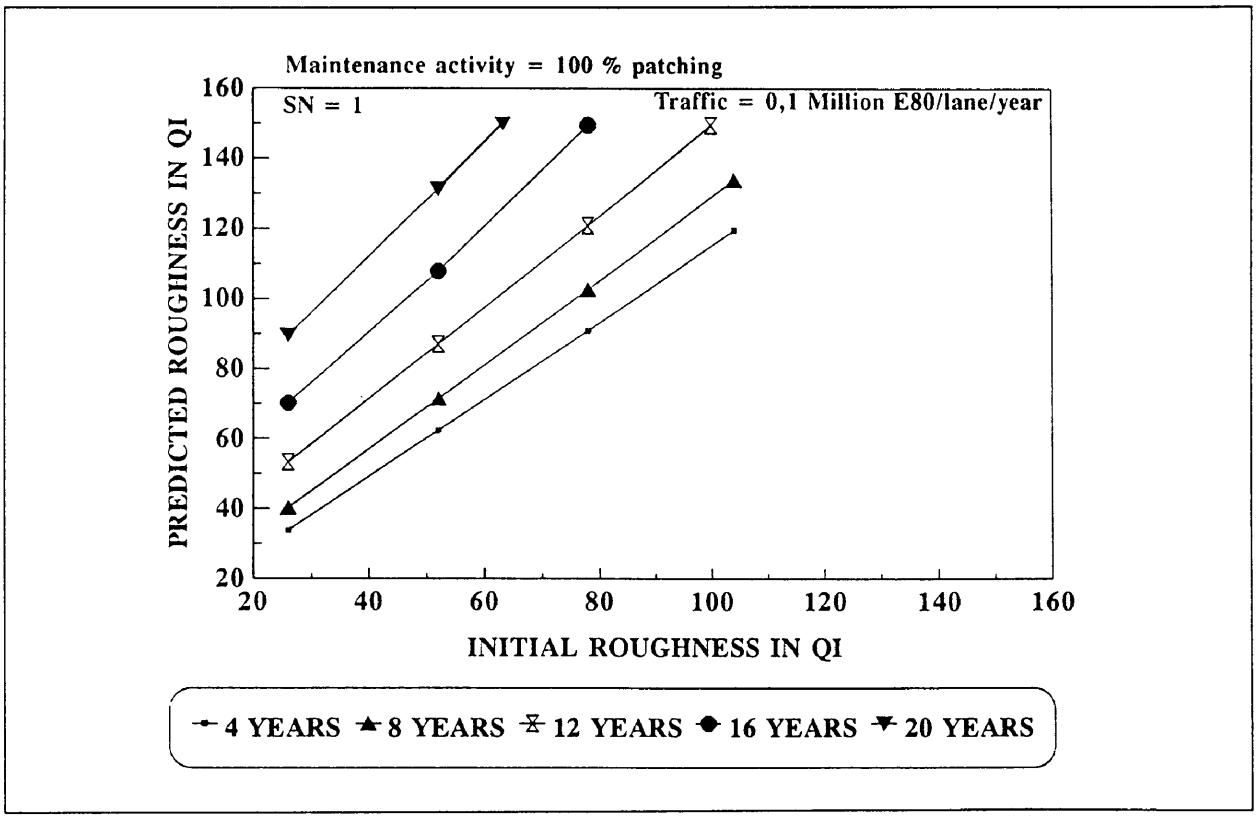

Figure 3.38: Sensitivity to initial roughness for SN = 1 under light traffic.

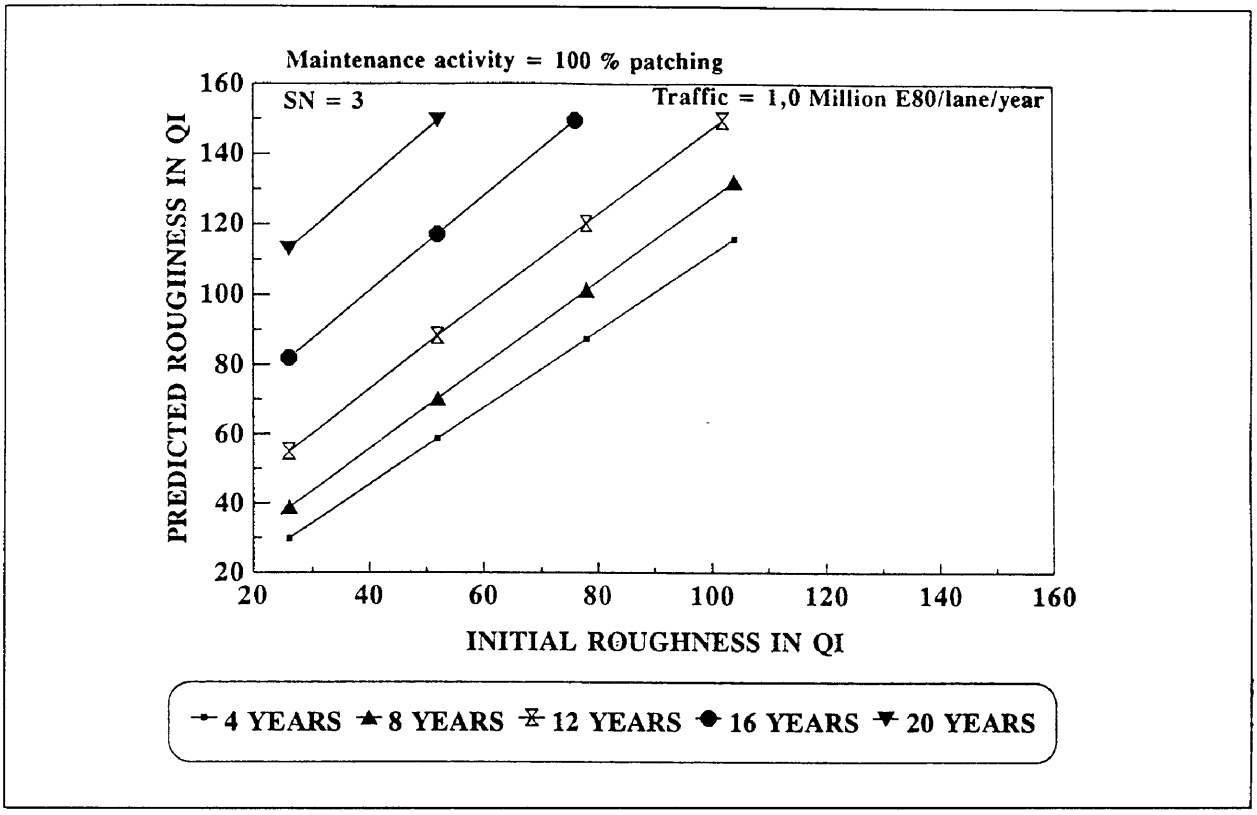

Figure 3.39: Sensitivity to initial roughness for SN = 3 under heavy traffic.

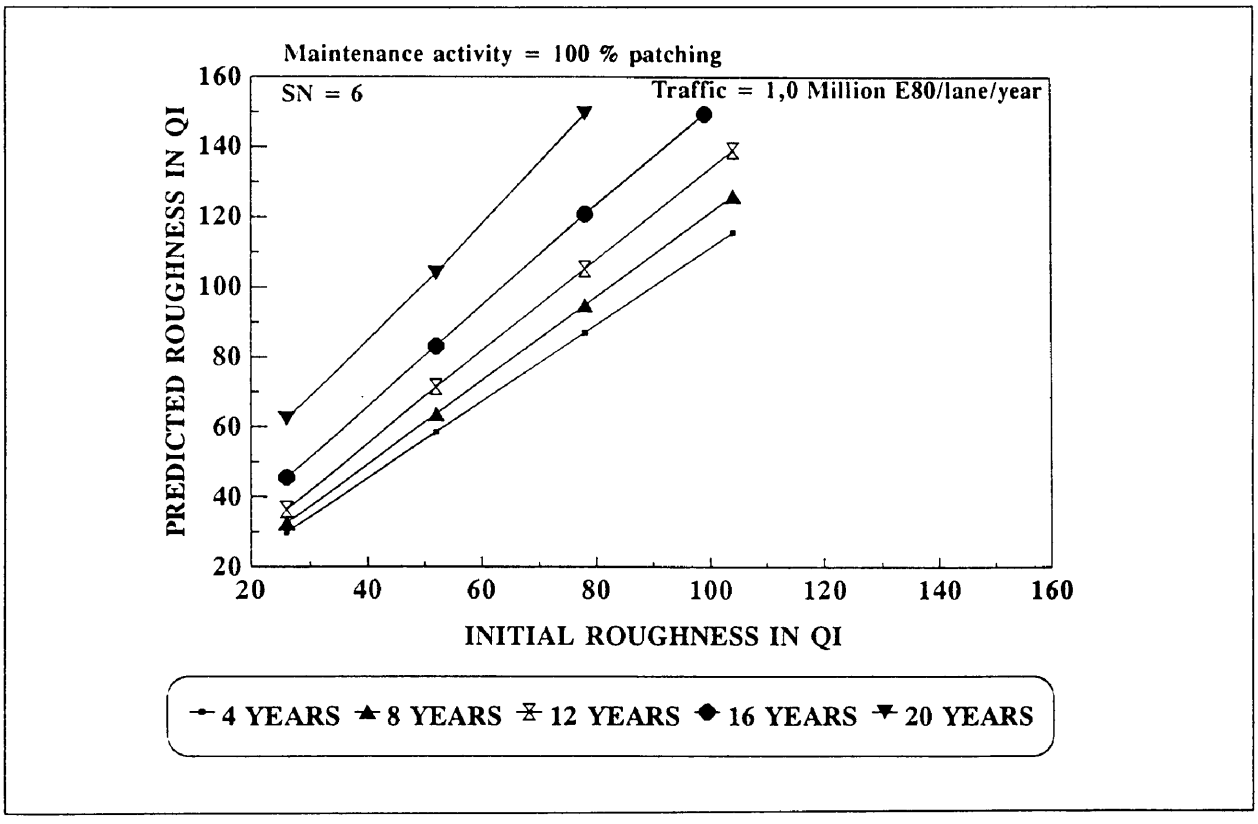

Figure 3.40: Sensitivity to initial roughness for SN = 6 under heavy traffic.

CHAPTER 4

DEVELOPMENT OF A VALIDATION METHODOLOGY

4.1 INTRODUCTION

To investigate the local applicability of the HDM-III deterioration and maintenance submodel, which is based on empirically derived equations mainly from measurements conducted in Brazil, its predictions must be compared against the locally observed values. This comparison would not only indicate the applicability of the HDM-III model, but also whether calibration of the individual models are needed for local conditions.

Since this study is only evaluating the deterioration observed on national roads, the HDM-III models would only be evaluated by using the information available on the Department of Transport pavement management database. All the recorded data on the pavement management database is however not in a format suitable for direct incorporation into the HDM-III models. The methodology assumed to change the format of this data, as well as to calculate the additional information not included in the database, but needed for the comparison process, are discussed in this chapter.

4.2 VALIDATION METHODOLOGY

To enable the successful comparison of the HDM-III model predictions with the observed values it is crucial to define a validation methodology for the exercise. Previous research conducted on the subject in South Africa concentrated only on the comparison of the predicted incremental change in roughness between two measurements, with the measured change in roughness (Kemp, 1991). The results obtained were disappointing with a large amount of scatter, and even the use of roughness data obtained from rod and level measurements did not improve the results. Possible factors contributing to these disappointing results were:

- The correlation factor used to convert the cracking and ravelling extent measurements from their numerical scale to a percentage of pavement area, as required by the HDM-III model.

- The fact that the analysis did not incorporate the contribution of the subgrade CBR in the calculation of the modified structural number of the pavement section evaluated.

- The method of incremental analysis did not allow for the incorporation of the long term aging effects of pavements.

- The m variable accounting for seasonal changes was used incorrectly.

- The fact that only the roughness model of the HDM-III model was considered for calibration by using a single value. This is in contrast with the fact that the HDM-III model allow for a total of seven calibration values, of which five is for the cracking, ravelling, potholing and rutting models which all contribute to the roughness model. The result of not determining calibration values for these individual models, is a large scatter in the roughness model calibration values, since it had to compensate for the all the models.

The approach embarked on in this study was to first calibrate the environmental coefficient(m) for the different moisture regimes, and then to simulate the deterioration of each pavement from the year the pavement was opened to traffic, and then to compare the predicted value for each individual model with the value measured for that year. The decision to employ this method of analysis was based on:

- The disappointing results obtained by the previous studies which aimed at only calibrating the incremental roughness model.

- The limited amount of riding quality measurements available for each pavement section, making it necessary to use each individual value instead of just the incremental change between the two measured values.

- The sensitivity of predictions to the initial values in collaboration with the fact that this method of analysis had the advantage that no initial values of visually recorded distress were needed, since the pavements were new.

This method of analysis led to an increase in accuracy of correlations, and also allowed the comparison of the predicted values for cracking, rutting, ravelling and potholing for a certain year with the measured values for that year.

Based on the fact that the equations defining the different models are of the exponential type it follows that the accuracy of any prediction tends to decline as the time period increases. Thus the value of the local calibration factor determined for each model, would only be valid over the medium term. Based on this it was decided to employ the same approached used in Chile to adapt the HDM-III models to their local conditions (Videla *et al*, 1991). The approach involved the periodic calibration of the models to correct the deterioration curves in such a way that they maintained good predictions over the pavement life. Since this was a very time consuming process, the algorithm developed in Chile that performs the calibration was adopted for local conditions, to automatically determine the calibration factor for each deterioration model of an individual pavement section.

The algorithm employed in the calibration model was developed by isolating the deterioration and maintenance submodel of the HDM-III model. Thus the sequence and method of modelling pavement deterioration is exactly the same as in the HDM-III model. The calibration model has the advantage that since only pavement deterioration is modelled, it is operationally faster than the HDM-III model which is modelling all the submodels.

The calculation method employed in the algorithm is base on the minimisation of the difference between the values predicted by the HDM-III models, and those measured (Videla *et al*, 1991). The procedure of calibration involves the prediction of the change in a specific parameter over time for different calibration factor "ki" values, and then to calculate the corresponding difference between the predicted and measured values for each calibration factor value. These calculated differences are then used to determine the sum of the square of the differences which are then plotted against the specific calibration factor value. When plotted the sum of squared differences are distributed in a parabolic shape, with a minimum at the optimum calibration factor value, as illustrated in Figure 4.1 for the cracking progression calibration factor (kcp). A parabolic curve is then fitted to the sum of squared differences (SSD) incorporating the calibration factor (ki) as follows (Videla *et al*, 1991):

$$SSD = aki^2 + bki + c$$

where:

SSD = Sum of the squared differences.
ki = Calibration factor.
a,b,c = Constants of equation obtained during the fitting of the curve.

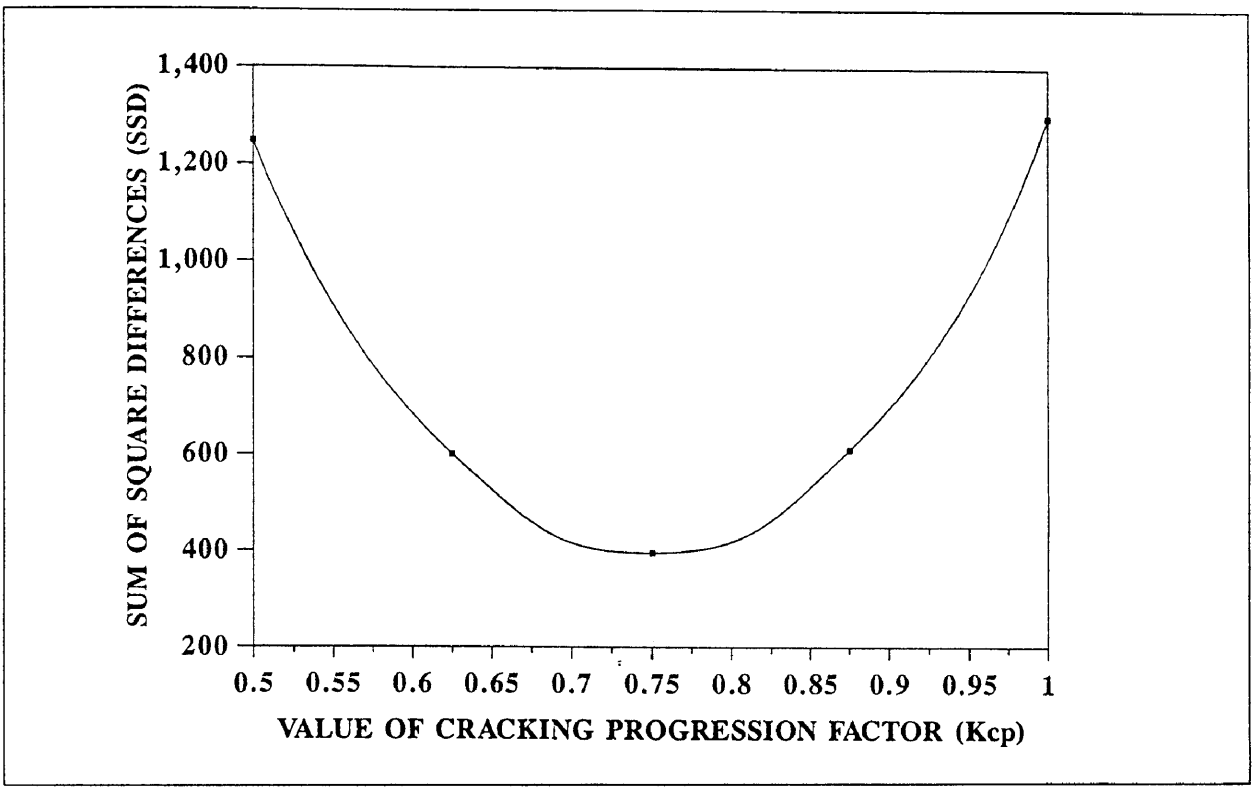

Figure 4.1:Illustration of sum of squared differences against calibration factor values

The value obtained by taking the derivative of the above equation, equals the calibration factor (ki) for which the SSD is the least, namely:

$$ki = \frac{-b}{2a}$$

where:

ki = Calibration factor for which SSD is a minimum.

a,b = Constants obtained during the fitting of the parabolic curve.

The above procedure was repeated for all prediction models for each individual pavement section evaluated.

4.3 SELECTION OF PAVEMENT SECTIONS

All the major studies conducted internationally on existing pavements over the last two decades employed a sampling factorial that incorporated certain parameters according to which pavement sections were selected. As a result of

the limited suitable data available on national roads no factorial could be successfully employed for the selection of pavement sections in this study. For this study the pavement sections were initially selected based on the availability of three or more riding quality measurements before 1985, and:

- An uniform pavement structure over the section with information available on the pavement structure and the subgrade CBR.
- An uniform traffic load over the total pavement section length with the availability of Traffic Axle Weight Classifier (TAWC) data.
- The availability of visually recorded distress measurements.
- Where possible no major rehabilitation work must have been conducted in the period from 1978 to 1985.

The above selection criteria were applied to minimise the number of factors influencing especially the prediction of roughness, which as mentioned in Chapter 3, is the most important variable, since it forms the basis for determining vehicle operating costs. The length of the sections selected were not fixed to a certain length, but instead the longest length that satisfied the previously mentioned requirements were selected. This ensured that the measurements conducted on a pavement section were more representative of the interaction between the pavement material, environment and the applied traffic load, limiting the influence of localised material and construction problems to a large extent. Although a large number of pavement sections are available with a total of three or more measurements during there life, only a limited number of them had three or more measurements before 1985. The reason why it was crucial for three or more measurements before 1985, was that the measured riding quality values in the period from 1982 to 1991, was expected to be inaccurate as a result of the large difference observed between the 1991 and 1992 riding quality measurements. The probable cause of this inaccuracy was an error incurred during the calibration of roughness measuring devices. The probable cause of this error was the lack of evaluation of the calibration sections with the rod and level procedure, from which the calibration coefficients for each measuring device were determined.

The year 1985 was selected as an upper limit based on the assumption that the error incurred as a result of the incorrect calibration would be within acceptable limits, since it was within three years of the last evaluation of the calibration

sections. It was assumed that within these three years the deterioration of the calibration sections were within acceptable limits. The calibration sections were again evaluated by the rod and level procedure in 1992, allowing the use the measurements from this year onwards. With the availability of the 1993 riding quality measurements on national roads it became evident, as illustrated in Figure 4.2, that instead of the riding quality measurements between 1982 and 1991 being questionable, it seemed that the 1992 measurements were inaccurate. Thus meant that most of the national road sections had three or more usable riding quality measurements, increasing the number of pavement sections available for evaluation dramatically. Based on this additional pavement sections without three or more riding quality measurements before 1985, that satisfied the other requirements, were also incorporated into the study.

The pavement sections selected are summarised in Table 4.1, from which it is evident that only a small number of sections on national roads met the selection requirements. Combinations for which no sections were selected do not necessarily indicate that no such pavement section exist on national roads, but rather that no such section met the selection requirements, as illustrated in Figure 4.3, of this study. The sections selected with their general information are listed in Table B.1 of Appendix B.

Table 4.1: Summary of pavement sections selected for the comparison

Wearing Course	Base Course	Classification of moisture regime			
		Arid	Semi-arid	Subhumid	Humid
Asphalt Concrete	Bituminous			8	9
	Cemented			2	2
	Granular		1	13	2
Surface Treatment	Bituminous				
	Cemented				
	Granular		19	2	7

Cell numbers indicate the number of selected sections.
Moisture classification according to Thornthwaite moisture index.

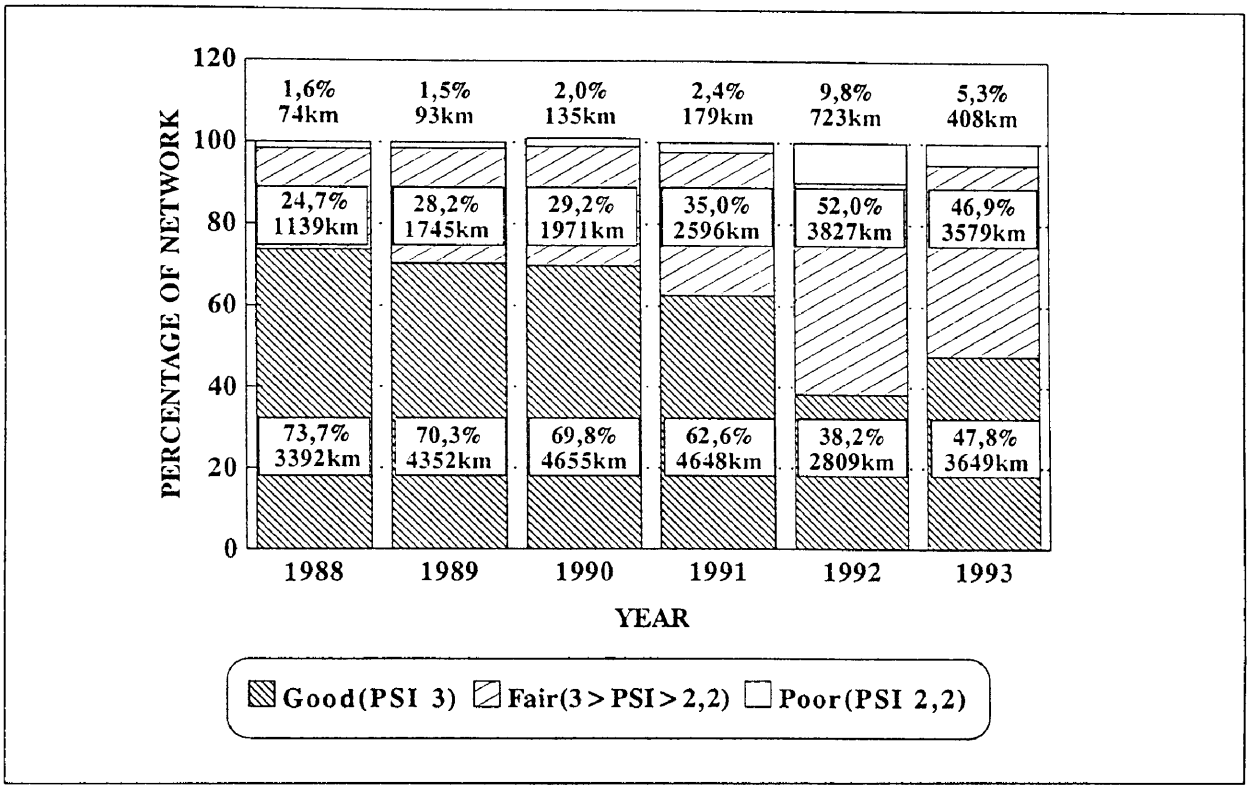

Figure 4.2: Riding quality condition of national road network from 1988.

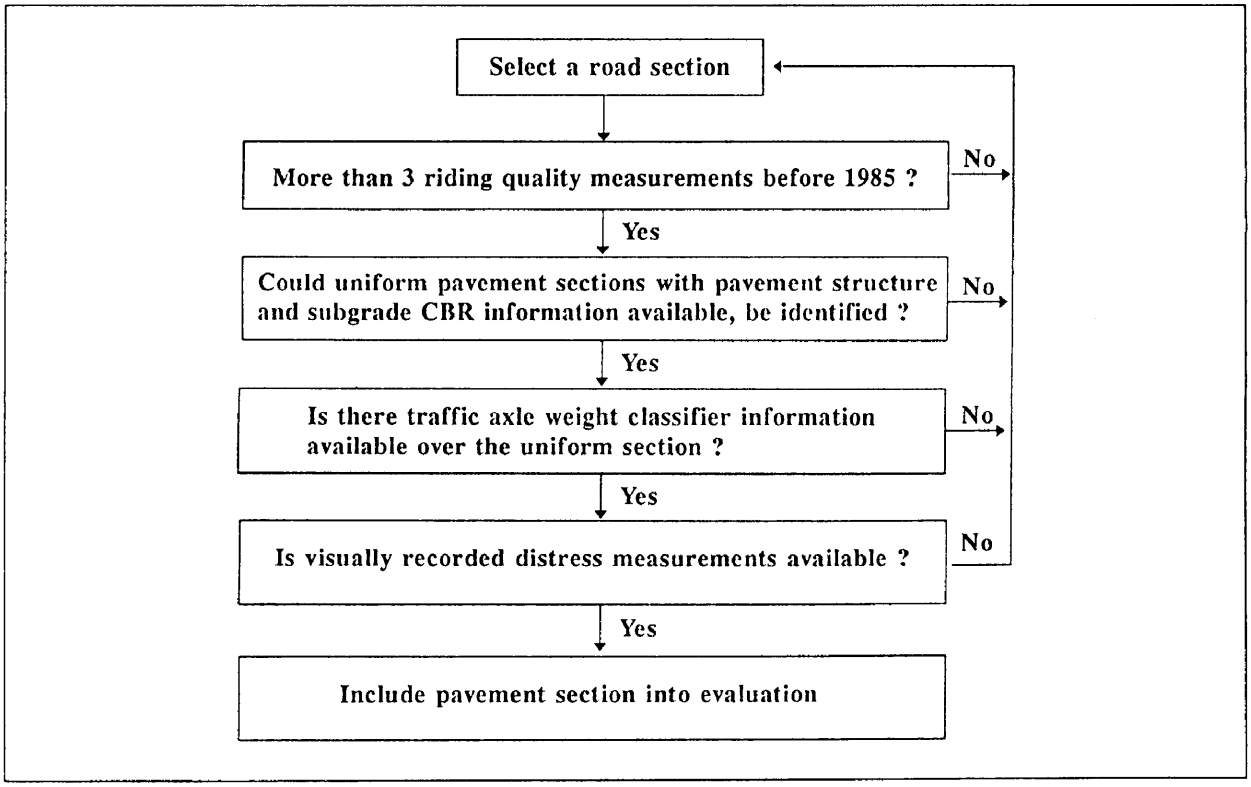

Figure 4.3: Initial procedure for selecting pavement sections.

4.4 CORRELATION OF DISTRESS MEASUREMENTS

The data available on the Department of Transport database that were not in a format suitable for direct incorporation into the HDM-III model had to be changed by correlation to allow their incorporation into the evaluation procedure. The data is obtained from pavement assessments conducted to determine the current condition of a pavement at a network level. The current condition of a pavement is needed to allow the pavement management system developed for national roads to provide the necessary information, for the effective funding and planning of the operations needed to protect the integrity of the network. Methods employed by the Department of Transport to asses the current condition of a pavement at a network level include:

- Visual assessment of pavement condition.
- Mechanical pavement surveillance measurements.

The data obtained is captured onto the Department of Transport pavement management database from where the data is used to determine maintenance and rehabilitation projects by algorithms in terms of the type of maintenance and urgency (Walker and Curtayne, 1986). Not all of this recorded data is in a suitable format for direct incorporated into the HDM-III model. The change of format required for some of the recorded parameters to be allowable for use in the HDM-III model, are discussed in more detail in the following subsections.

4.4.1 Visual assessments

The visual assessment of a pavement at a network level involves recording of visible signs of distress such as cracking, deformation, disintegration and smoothing of the surface. The visual assessments at a network level are done to give an indication of the structural as well as the functional adequacy of the pavement in terms of its current condition (Jordaan and Van As, 1992). The visual assessment of the distress types mentioned are needed because no effective mechanised method or apparatus exists in South Africa that could be used for the evaluation of these distress types.

The visual assessment of the pavement network is conducted by qualified assessors and to ensure consistency in the visual evaluation of the pavement network by assessors, rigid definitions of rating classes and assessment methods are used. Most of the road authorities have formal manuals containing their prescribed guidelines for the assessment of the pavements under their authority

(Walker and Curtayne, 1986). The Department of Transport also employs their own guidelines for the evaluation of there pavements. The aim of these guidelines are to ensure consistency of evaluation between the different assessors.

4.4.1.1 Format of data

As mentioned the network level data is obtained from assessments by qualified assessors according to prescribed guidelines. From the end of 1983 when visual assessments were first conducted on national roads, two sets of guidelines were applicable for the visual inspection of national roads. These guidelines were:

- M3-1 from 1984 to 1990.
- TMH 9 from 1991 onwards.

The guidelines in M3-1 only allowed the assessment of the parameters included on the visual inspection form shown in Figure 4.4. The visual assessments were conducted for a standard pavement sample length of 200 metres, and as seen provision was only made for recording the two most extensive crack patterns. The distress observed was described and quantified by the following parameters:

- **Type**: This parameter described the type of cracking observed, as contained in Table 4.2. It was permissible for both crack patterns to be of the same type when the spacing of a crack type differed substantially.

- **Extent**: Once the type or types of cracking were identified, the extent of various degrees for each crack type was assessed independently, and expressed as the percentage length of a 200 m section over which they appeared. Two degrees of cracking were defined namely (M3-1, 1984):

  - Open cracks: These cracks were generally greater than 1 mm in width and easily discernible from a slow-moving vehicle.

  - Sealed cracks: These were cracks which had been individually sealed with materials such as bitumen or epoxy. Sealed cracks which had reopened were regarded as open cracks.

CHIEF DIRECTORATE : NATIONAL ROADS

FLEXIBLE PAVEMENT FIELD INSPECTION

PAVEMENT MANAGEMENT SYSTEM

Option	Route	Section	Direction

Date
Y Y Y Y - M M - D D

Crack type
C Crocodile
B Block
L Longitudinal
T Transverse
R Random

Position
G General
S Shoulders
R Riding surface
W Wheel path

Stone loss
1 Sound 2 Warning 3 Severe

Coded by : _____

Date : _____

Range of observation		Crack pattern A					Crack pattern B							Patching				
			Extent					Extent										
Start distance (km)	End distance (km)	Type	Open	Sealed	Spacing (m)	Position	Type	Open	Sealed	Spacing (m)	Position	Extent of pumping	Stone loss severity	Extent	Average area (m^2)	Binder condition	Skid Assessment	Extent of rut depth > 10 mm
23	27	31	32	34	36	38	39	40	42	44	46	47	49	51	52			

General comments : _____

Figure 4.4: Example of the flexible pavement management field evaluation form of M3-1.

- **Spacing**: Spacing was defined as the average distance in metres between cracks. Cracks with a spacing of greater than 9,9 m were ignored, and the minimum distance recorded was 0,1 m, even if it was less. In the event a single longitudinal crack, a value of 5,0 m was recorded for the spacing.

- **Position**: The position of each crack pattern was recorded according to the categories contained in Table 4.2.

- **Pumping**: The extent of pumping was assessed in terms of the percentage of all visible cracks (irrespective of type) exhibiting definite signs of pumping.

- **Stone loss**: Stone loss or ravelling was assessed as the percentage of the area of the carriageway exhibiting loss of stone. Three classes of severity, namely sound, warning and severe were defined. The criteria for assigning severity classes differed for the different types of surfacing. The definition of these classes are summarised in Table 4.3 and Figures 4.5 and 4.6.

- **Patching**: Patching refers to the routine maintenance operations conducted to rectify local defects, and were taken into account irrespective of their condition or how well they were performing. Patches over the full width of the carriageway and longer than 100 m were not recorded since they were considered as special maintenance. It is important to note that since no provision was made for recording potholes, potholes were recorded as patches during the assessment. Patching was quantified by the following two variables, namely:

Table 4.2: Cracking types and position according to M3-1.

Cracking type		Position of crack pattern	
Type	Code	Description of position	Code
Crocodile cracks	C	Pattern occurs generally over carriageway	G
Block cracks	B	Pattern occurs on shoulders	S
Longitudinal cracks	L	Pattern occurs on riding surface	R
Transverse cracks	T	Pattern mainly occurs within the wheel tracks	W
Random cracks	R		

Table 4.3: Definition of severity levels for the different surfacings.

Severity	Area of stone loss for different surfacing types			
	Single seal	Double seal	Open graded Asphalt	Area of rolled in chips missing
Sound	area < 10%	See Figure 4.3	See Figure 4.4	< 30% of chips
Warning	10% ≤ area < 40%			30% ≤ chips < 60%
Severe	area ≥ 40 %			Chips ≥ 60%

- Extent: This was the total number of patches in the 200 m section being evaluated. Where two patches overlapped they were counted as separate patches.

- Average area: This is the average area of patches over the section being evaluated in square metres.

The guidelines contained in M3-1 were replaced by the improved guidelines of TMH 9 in 1991. As seen from Figure 4.7 the guidelines in TMH 9 included an extended number of parameters on the visual inspection form. The most noticeable differences included in TMH 9 are:

- The standard sampling section lengths evaluated on national roads are now increased to 1 kilometre and sometimes even up to 5 kilometre for national roads in rural areas.

- Provision is made for a large variety of surface only distress problems, under the surfacing assessment heading.

- Provision is made for four basic crack patterns, in comparison with only the two most occurring patterns previously.

- Allowance is also made for recording rutting, as well as potholing and patching separately.

- Certainly the most important difference are that most of the distress parameters are now classified by two factors, which are both recorded according to a six point severity scale, namely:

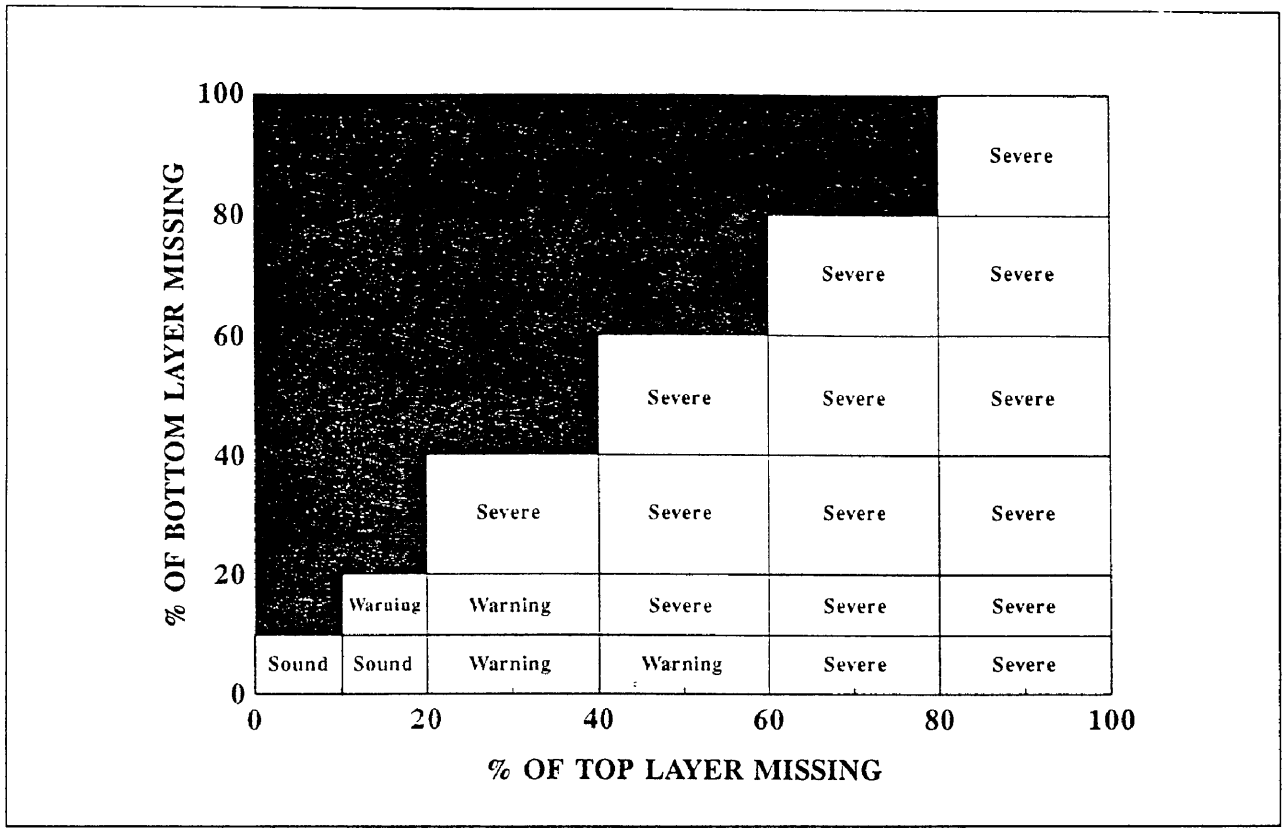

Figure 4.5: Stone loss severity classes for double seals (After M3-1, 1984).

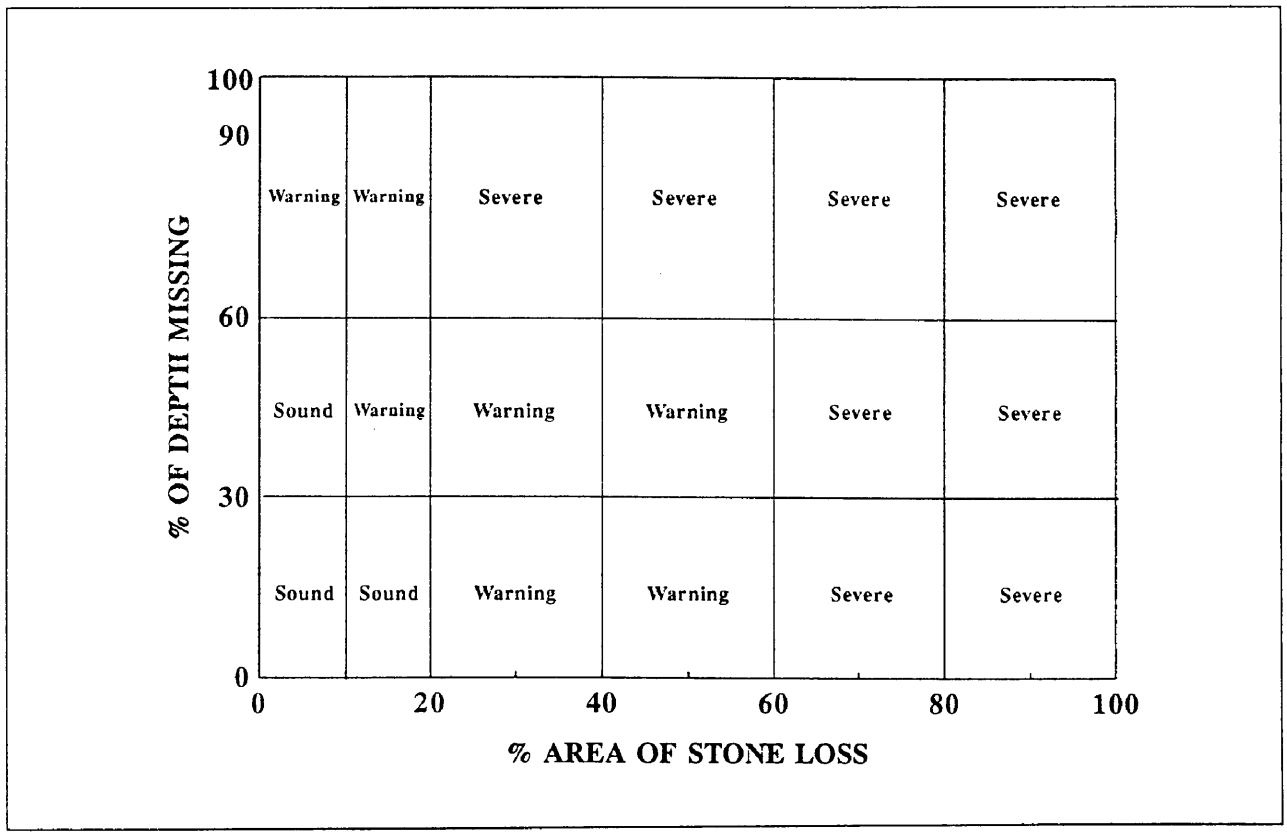

Figure 4.6: Stone loss severity classes for asphalt surfacings (After M3-1, 1984).

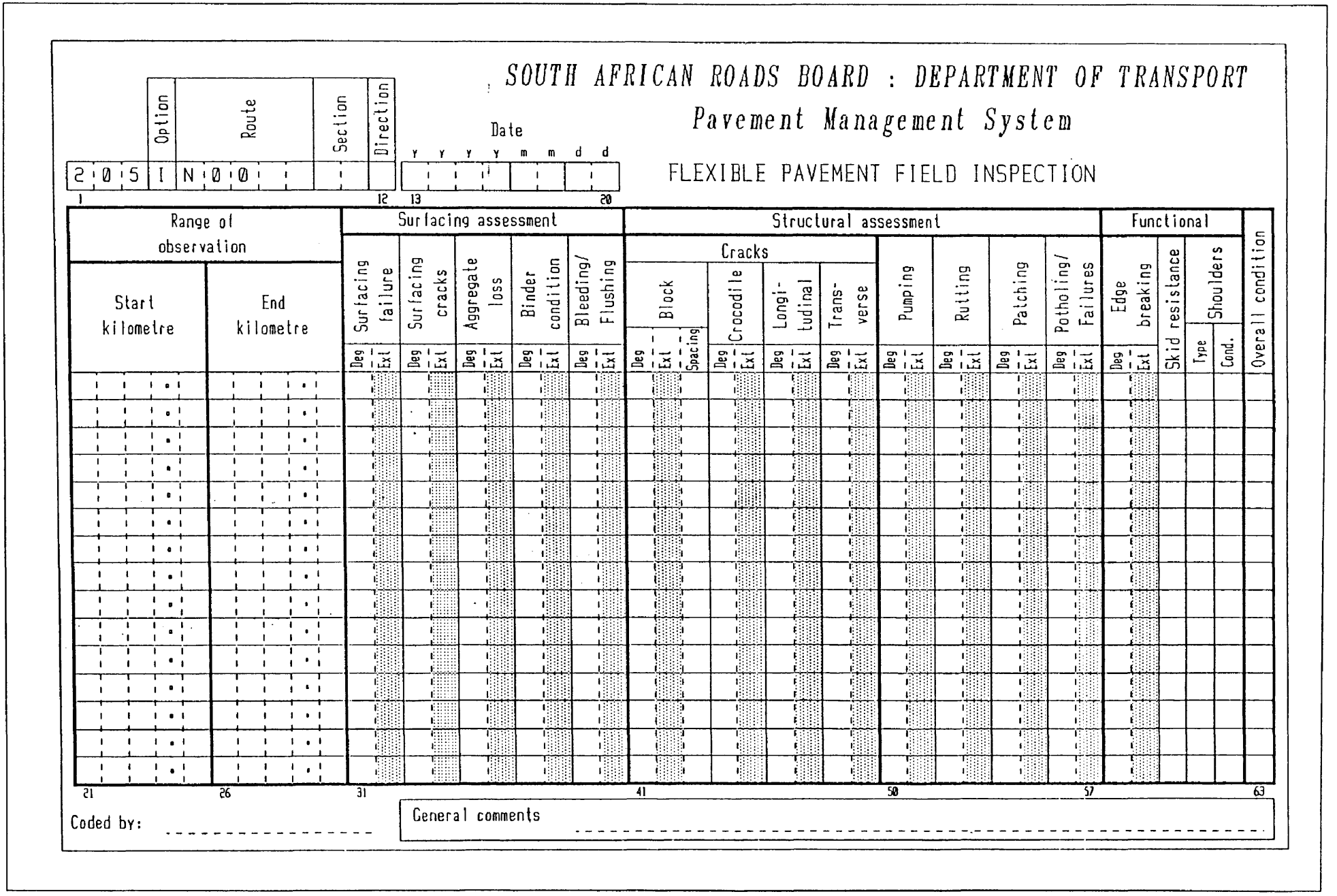

Figure 4.7: Example of the flexible pavement management field evaluation form for TMH 9.

- Degree: It is the measure of severity of a particular distress, and represents the best average assessment of the seriousness of that distress. As mentioned it is defined by the six point severity scale in Table 4.4. As seen degree is indicated by a numerical number between 0 and 5, where 0 indicates no occurrence of the distress and 5 indicates the need for immediate maintenance or rehabilitation (TRH 9, 1992).

- Extent: It is the measure of how widespread the distress is over the length of the road segment under evaluation. It is defined by the six point severity scale in Table 4.5. As seen extent is also indicated by a numerical number between 0 and 5, where 0 indicates no occurrence of the particular distress, and 5 extensive occurrence of the particular distress.

According to the TMH 9 (1992) manual the most important categories for degree are 1, 3 and 5. If there is any uncertainty regarding the condition between for example a degree of 1 or 3, and 3 or 5, the defect may be marked as 2 or 4, respectively.

Table 4.4: General description of degree classification (After TMH 9, 1992).

Degree	Severity	Description
0	None	No distress visible.
1	Slight	Distress difficult to discern. Only the first signs of distress are visible.
2	Between slight and warning	Easily discernible distress but of little immediate consequences.
3	Warning	Distress is distinct. Start of secondary defects. (Distress notable with respect to possible consequences, maintenance may be required in the near future).
4	Between warning and severe	Distress is serious with respect to possible consequences. Secondary defects noticeable and/or primary defect is serious.
5	Severe	Distress is extreme. Secondary defects are well developed (high degree of secondary defects) and/or extreme severity of primary defect (Urgent attention required).

Table 4.5: General description of extent classification (After TMH 9, 1992).

Extent	Description
0	No occurrence visible.
1	Isolated occurrence, not representative of the segment length being evaluated (seldom).
2	Scattered occurrence over parts of the segment length(more than isolated)
3	Scattered occurrence over most of the segment length (general), or extensive occurrence over a limited portion of the segment length.
4	More frequent occurrence over a major portion of the segment length.
5	Extensive occurrence

4.4.1.2 Correlation of visual assessments

Since the HDM-III model requires the area affected by cracking (all and wide) and ravelling as a percentage value, the correlation of visual data is needed to convert numerical ratings into percentage of area. The HDM-III model only required the conversion of the extent numerical rating into a percentage value. It was however decided in this study to combine both the extent and degree ratings into a single value, defined as the area of indexed distress. The reason for adopting this approach is that it is believed that by incorporating both degree and extent in a single value, the value obtained will more accurately portray the pavement condition. Based on research conducted in Texas (Lytton, Michalak and Scullion, 1982) the following conversion factor was used to convert the numerical ratings of M3-1 into the format required for HDM-III model for each pavement section:

$$CRX = \frac{\Sigma A_{TX} S_{TX}}{A} \times 100$$

where:

CRX = Total area of indexed distress as a percentage of the surface area of the pavement section under evaluation.

A_{TX} = Area of surface distress for a certain degree in square metres.

S_{TX} = Decimal factor assumed for converting the degree rating.

A = Total area of the pavement section under evaluation in square metres.

For visual assessments conducted according to M3-1 this meant only the determination of correlation values for the degree ratings. As mentioned

previously the extent was already measured as a percentage of pavement area for stone loss, and as percentage of pavement length for cracking. This only required the conversion of percentage of pavement length to percentage of pavement area. The conversion to area was obtained by multiplying the calculated length in metres affected, with the width of the affected area. The width defined for the affected area are summarised in Table 4.6.

The correlation values assumed for converting the recorded degree ratings are summarised in Table 4.7. As previously mentioned there was no direct numerical classification for degree, but rather a description of the crack type and the condition of the crack, namely whether the crack was open or sealed. As seen in Table 4.7 only crocodile, and random cracking were included in the calculation of the area of indexed cracking. This is in line with the definition of the HDM-III model in which cracking predominantly comprises crocodile and irregular cracking related to traffic and oxidation effects (Watanatada *et al*, 1987).

Table 4.6: Width assumed for different cracking positions.

Description of position of cracking pattern	Width assumed for affected area
Pattern occurs generally over carriageway	Lane width plus shoulder width*
Pattern occurs on shoulders	Shoulder width
Pattern occurs on riding surface	Lane width*
Pattern mainly occurs within the wheel tracks	A width of 1,5 metre assumed

* = Lane width being the width of the lane for pavement sections with only one lane in the direction of travel. Where more than one lane existed in the direction of travel, only the width of the slow lane was used in the calculations. The reason for this being the fact that during the visual inspection the assessors travel on the shoulder of the road for safety reasons, thus any minor distress in the fast lane is difficult to discern, especially on heavily trafficked sections. Thus the distress recorded is more representative of the slow lane, which is normally in a more severe condition.

Table 4.7: Correlation values assumed for degree based on position of crack pattern.

Cracking type	Position of crack pattern	STX
Crocodile cracks, and Random cracks	Pattern occurs generally over carriageway	0,5
	Pattern occurs on shoulders	0,5
	Pattern occurs on riding surface	1,0
	Pattern mainly occurs within the wheel tracks	1,0

Longitudinal, block and transverse cracking were not considered for further evaluation during the study. As previously mentioned in Chapter 2 these types of cracking were deemed to be largely determined by material characteristics and temperature regime, resulting in a large number of variables that made it impracticable to model these types of cracking at a network level (Paterson, 1987). Secondly these types of cracking, especially longitudinal and transverse, are normally repaired individually, making their inclusion in the total area of cracking questionable. If for example one or more severe longitudinal cracks exist on a section, and they are included into the calculation of the total area of cracking, the HDM-III model may predict a need for resurfacing for the pavement section, when indeed only crack sealing is required.

It is believed that the exclusion of these crack types would not seriously affect the deterioration predictions of the HDM-III model, since these crack types do not necessarily indicate a significant deterioration of the pavement, but only a potential for future deterioration. If these crack types led to the formation of severe secondary cracking under traffic, the resulting crack patterns will normally be recorded as random cracking, and if very severe as crocodile cracking, thus any severe influence of the excluded crack types on pavement deterioration would be included into area calculations as either random or crocodile cracks.

As seen from Table 4.7, the position of the crack pattern was also defined as a parameter affecting the degree, since it is for example generally assumed that a crocodile crack within the wheel tracks, is more critical than when the same crack occurs on the shoulder. The value of 0,5 assumed for cracks occurring either on the shoulder, or over the whole carriageway were based on the assumption that cracks occurring in these positions are an indication of a dry or brittle surfacing layer, rather than an inability of the pavement to carry the traffic load. Thus, although the potential influence on future deterioration might be high as a result of water ingress, it was decided that the immediate consequences are not that severe on pavement deterioration.

The last assumption made regarding the conversion of visual data obtained according to M3-1 was that all open cracks were classified as wide cracking, while both open and sealed cracks were classified as all cracking. As previously

mentioned the HDM-III models classify cracking either as all or wide cracking. Wide cracking was generally defined as spalled cracks greater than 3 mm in width. All cracking included all crack widths larger than 1 mm. The reasons for classifying open cracks as wide cracking are:

- To be able to identify an unsealed crack from a slow moving vehicle (10 - 20 km/h), the crack must be at least between 2-3 mm in width.
- Water can penetrate the pavement through the open crack, resulting in the faster deterioration of the pavement. This potential influence of open cracks is similar to the faster deterioration of a pavement observed in Chapter 3, for the area of wide cracking.

For the visual assessments conducted according to TMH 9 manual correlation values had to be determined for both degree and extent numerical ratings. For the TMH 9 numerical values the following conversion factor was used to convert the numerical ratings into the format required by the HDM-III model for each pavement section:

$$CRX = \frac{\sum_{N} A_{TX} S_{TX}}{N}$$

where:

CRX, S_{TX} As previously defined.

A_{TX} = Area of surface distress for a certain degree as a percentage.

N = Number of visual segments included in the pavement section under evaluation.

The preliminary correlation values assumed for converting the extent numerical ratings of TMH 9 into percentage of carriageway area are summarised in Table 4.8. These preliminary correlation values were assumed within the ranges of pavement length previously defined (See Table B.2 Appendix B), by the TMH 9 committee for the different extent numerical ratings of TMH 9. The reason for assuming the previously defined percentage of pavement length now as a percentage of carriageway area, was that no other method of determining the carriageway area for TMH 9 definitions existed.

Table 4.8: Recommended preliminary correlation values for converting extent.

TMH 9 extent classification	Percentage of pavement area assumed for HDM-III models		
	All cracking	Wide cracking	Ravelling
0	0	0	0
1	2,5	2,5	2,5
2	7,5	7,5	7,5
3	15	15	15
4	30	30	30
5	60	60	60

As seen from Table 4.8 the difference in area assumed between two successive extent numerical ratings increases with an increase in the numerical extent rating. The reason for this, except for the assumed values being within the previously defined ranges, is that it is based on the results of the sensitivity analysis of Chapter 3 which indicate that the sensitivity of the roughness model to changes in area of distress, is at it's highest if the distress just initiated. Thus the values assumed aim to allow for this change in sensitivity. The maximum percentage value of 60 assumed is also based on the results of the sensitivity analysis. It is believed that the selected maximum value would not have a significant influence on the calibration of the HDM-III models, because the roughness model seemed insensitive to a change in the area cracked or ravelled, once either has initiated.

The correlation values are defined as preliminary, since it is believed that these preliminary correlation values would decrease if an official correlation study is conducted. The reason being that South African roads are normally repaired long before they reach such severe levels of cracking. Thus the visual assessors may easily overestimate the extent of cracking, since they are not used to such severe levels of cracking.

The preliminary correlation values for the degree numerical ratings could not be determined on their own. The reason for this is that to be able to determine accurate calibration factors for the different deterioration models, there must be

a correlation between the areas of indexed distress determined by both visual assessments methods. Based on the above mentioned and the fact that a limited number of sections were available on which visual assessments were conducted according to both manuals in the same year, it was decided to determine the preliminary degree numerical ratings of TMH 9 by using the area of indexed distress determine according to M3-1 as guideline. The reasons for using the area of indexed distress determined according to the M3-1 as guideline are:

- The M3-1 more accurately defined the area of distress, as a result of the fact that the length of distress was recorded as a percentage of the sample length of 200 metres. The sample length of 200 metre also contributed to the accuracy.
- The M3-1 defined the position of the distress, giving a better indication of the severity (degree) of the distress.

The determination of the preliminary correlation values for degree involved a process by which different decimal values were assumed for degree numerical ratings, the area of indexed distress were then calculated by using these assumed values. The calculated area of indexed distress was then plotted against the area of indexed distress determined according to the M3-1 guidelines. The sum of the squared differences between the plotted data points and the line of equality was then determined. The process was repeated until the sum of squared differences were a minimum, or in other words the R-squared value a maximum.

The above mentioned procedure was firstly conducted for pavement sections with only surface cracks. This allowed the determination of the preliminary correlation values for the degree numerical ratings of surface only cracks. With the preliminary correlation values for surface cracking determined, the procedure was repeated for sections which had both surface and crocodile cracking. This allowed the determination of calibration values for the degree numerical ratings of crocodile cracking. Figure 4.8 illustrates the area indexed cracking calculated from M3-1 assessments, in comparison with the area of indexed cracking calculated by using the preliminary correlation values obtained for TMH9 assessments. An acceptable correlation was obtained between the two areas, resulting in a R-squared value of 0,78.

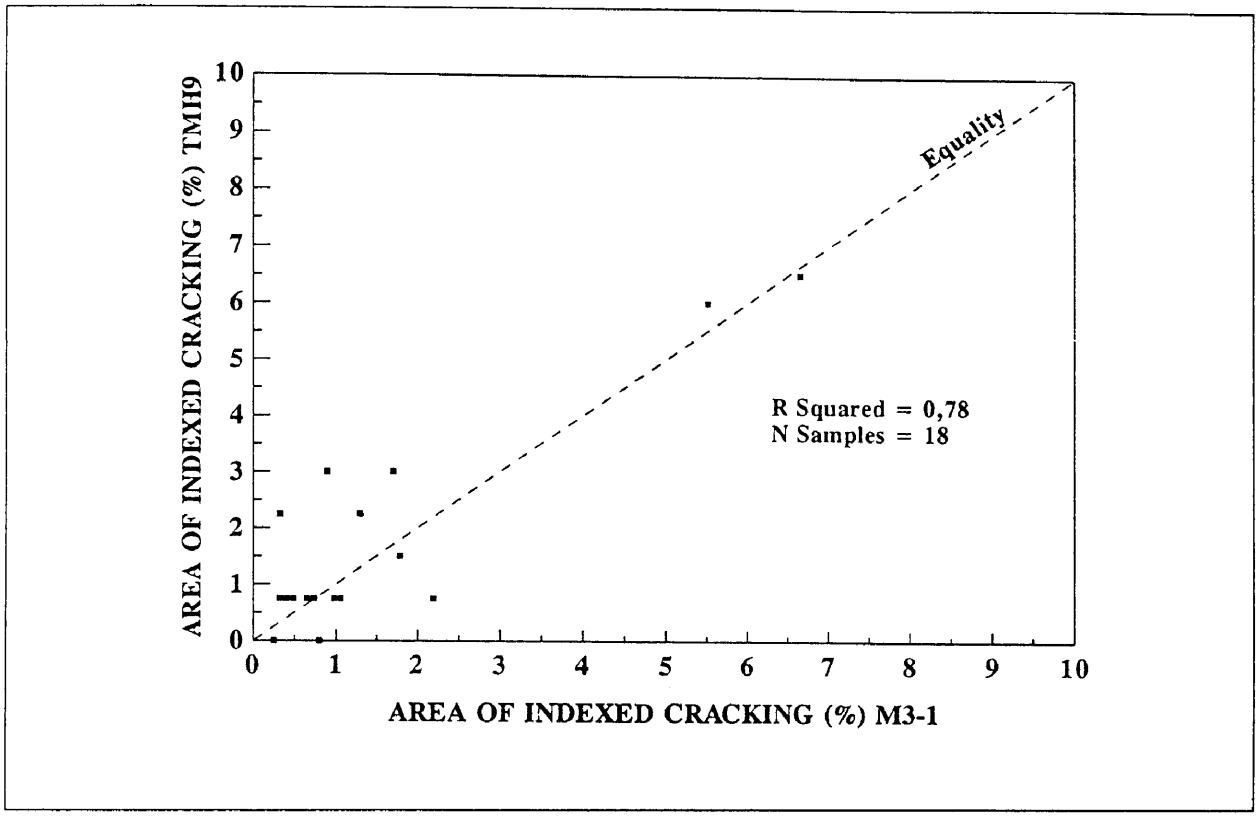

Figure 4.8: Correlation between areas of indexed cracking of M3-1 and TMH 9.

The preliminary correlation values obtained for the conversion of the degree numerical ratings of TMH9, are summarised in Table 4.9. These preliminary correlation values are used along with the once obtained for extent numerical ratings to convert both numerical ratings into percentage of area, as previously mentioned. As seen in Table 4.9 some of the preliminary correlation values are also used to calculate the area of wide cracking. These values were assumed based on the definition of area of wide cracking, since there existed no data to evaluate degree numerical ratings for wide cracking.

The maximum value obtained of 0,5 for surfacing cracking is based on the previously mentioned assumption that this crack type does not necessarily indicate a significant deterioration of the pavement, but only a potential for future deterioration, and as such is not serious. The correlation values for ravelling are simply based on those for surfacing cracking; the reason for this is that both visual assessment methods use a numerical rating for ravelling, making it impossible to determine any correlation, especially for the M3-1 method which defined an area of cracking between 0 and 30% as sound.

Table 4.9: Preliminary correlation values determined for degree numerical ratings of TMH 9.

TMH 9 degree classification	Decimal factor assumed for calculation of area of indexed distress		
	Surface cracking	Crocodile cracking	Ravelling
0	0,0	0,0	0,0
1	0,1	0,1	0,1
2	0,2	0,2	0,2
3	0,3	(0,3)	0,3
4	(0,4)	(0,6)	0,4
5	(0,5)	(1,0)	0,5

( ) = Indicates the degree ratings that were also assumed to represent the area of wide cracking. This means that when the area of indexed cracking is calculated by using one of the indicated degree ratings, the area calculated is also recorded as wide cracking.

It must however be noted that these preliminary correlation values for degree numerical ratings are based on the limited data available, and also that none of the sections included in the calculations had severe distress. Thus the usage of the preliminary correlation values at severe distress levels may be limited. It is recommended that these preliminary correlation values should only be used until the results of a detail correlation study is available.

4.4.2 Mechanical pavement surveillance measurements

Mechanical pavement surveillance measurements refer to the assessments made by special or purpose-built apparatus or machines that increase the speed of assessment as well as the consistency of the evaluations. These mechanical measurements measure the performance indicators of a pavement at high speed ensuring the feasibility of a pavement management system (Walker and Curtayne, 1986). Mechanical pavement measurements can be divided into two categories, namely:

- Measurements conducted to assess the functional performance.
- Measurements conducted to assess the structural performance.

Parameters measured mechanically to assess the functional performance of a pavement include (Draft TRH 12, 1991):

- Riding quality in present serviceability index (PSI).
- Rut depth in mm (Also used to assess the structural performance).
- Skid resistance as the sideways force coefficient at a speed of 80km/h.

Parameters measured mechanically for the assessment of the structural performance include (Draft TRH 12, 1991):

- Maximum surface deflection measurements (mm).
- Radius of curvature in metre using a 80 kN single axle load, or Falling Weight Deflectometer (FWD) measurements.
- Dynamic Cone Penetrometer (DCP) measurements (mm/blow).

The results obtained from the mechanical measurements are used in collaboration with the visually recorded distress to evaluate the functional and structural condition of a pavement.

4.4.2.1 Format of data

One of the most important mechanical measurements is riding quality, which is the primary measure of the functional performance of a pavement. The two instruments most often used for the riding quality measurements in South Africa are both response type road roughness measuring systems. This type of instrument has the advantage that it is easy to use and relatively inexpensive to operate at high speeds (80 km/h). The two instruments employed are:

- **Modified PCA meter**: The modified PCA meter is based on the same principles as the original PCA meter, but with the following modifications by the National Institute for Transport and Road Research (Visser, 1982):

  - Displacements are measured with optical sensors.
  - Inclusion of a self zeroing device allowing for fluctuations in zero associated with road alignment and other factors.
  - Output in PSI.

The output in PSI, from the modified PCA meter is the result of the sum of the squares of the amplitude of the movement between the rear axle and the body of a sedan car determined according to the following equation:

$$PSI = A + B \log_e D$$

where:

A,B = Calibration constants.

D = Sum of squares of axle to body deviations.

The calibration constants were obtained by correlating the sum of the squares of axle to body deviations with the present serviceability rating (PSR) determined for each test section by a panel of 20 raters.

- **Linear Displacement Integrator (LDI)**: The Linear Displacement Integrator (LDI) was developed after the Mays meter principle by the National Institute for Transport and Road Research (NITRR), namely the sum of the axle-body deviations. It is still used today to evaluate the riding quality on the national road network. The LDI measures riding quality in terms of PSI as the cumulative vertical movement of the rear axle relative to the body of the vehicle.

The calibration of the above mentioned instruments is of utmost importance for reliable information. The reason is that the response varies from vehicle to vehicle as a result of suspension stiffness, tyre pressure, vehicle loading and displacement of the load within the vehicle. Both devices are calibrated on a calibration section by correlating the roughness value measured with the device, with the roughness value generated by rod and level measurements at 100 mm intervals over the 200 metre calibration section.

4.4.2.2 Correlation of mechanical measurements

Of the three mechanical measurements of importance on national roads, rutting as well as deflection were already in the right format for inclusion in the HDM-III model. The most important of these measurements the riding quality had to be converted from present serviceability index (PSI) to Quarter Car Index (QI_m). It is important to note that the HDM-III model uses QI_m (Roadmeter-estimate of

QI roughness (Counts/km)), whereas the correlation developed by Visser (1982) is only converting the measured PSI to QI_r (Profile RMSVA-function of QI roughness (counts/km)). Thus QI_r determined according to the correlation by Visser (1982), has to be changed to QI_m by using the relationship provided in Table 2.5 of Paterson (1987), before it could be incorporated into the HDM-III model.

The roughness measurements in PSI, available on the database were used to calculate the mean PSI value for each section for a specific survey date. These mean PSI values were then correlated to the quarter car index (QI_r) by using the correlation developed by Visser (1982), and then to QI_m by using the relationship in Table 2.5 of Paterson (1987).

$$QI_r = 92{,}63 - 56{,}93\ln(PSI)$$
$$QI_m = 9{,}5 + 0{,}9QI_r$$

where:

QI_r = Quarter-car index (Profile RMSVA-function of QI roughness (counts/km)).

QI_m = Quarter-car index (Roadmeter-estimate of QI roughness (counts/km)).

PSI = Mean PSI value calculated for each pavement section.

These calculated roughness values in QI_m were then used in the comparison of the observed values with the roughness values predicted by the HDM-III model, the HDM-III model allows for both the International Roughness Index (IRI) and the Quarter-car index (QI_m).

Since the HDM-III model only predicts the roughness at either the beginning or end of a year, it was decided to compare the observed value with the HDM-III model value predicted at the end of a year. The reason for this being that the effect of any routine maintenance predicted by the HDM-III for a year, would be included into the roughness prediction of the HDM-III model. This would compare more favourably with the measured values, because roughness measurements are normally conducted early in a year, allowing the incorporation of the maintenance activities of the previous year. For a year in which rehabilitation was conducted on a pavement, both the predicted value at the beginning and end of a year were included to give an indication of whether the riding quality measurement was conducted before or after rehabilitation. The riding quality, deflection and rut depth measurements of each individual pavement section used in the study are summarised in Table B.3 of Appendix B.

4.5 MODIFIED STRUCTURAL NUMBER

The modified structural number (SNC) was the only strength parameter available for the HDM-III model due to the lack of Benkelman Beam deflection measurements. This posed no major problem since as discussed in Chapter 3 Paterson (1987) found that of the two, the modified structural number was the most statistically significant measure of pavement strength. The modified structural number (SNC) which includes the contribution of the subgrade (SN_{sg}), was calculated by using the following equation:

$$SNC = SN_i + SN_{sg}$$

where:

SNC = Modified structural number.

SN_i = Initial structural number in first year of modelling.

SN_{sg} = Contribution of the subgrade after Hodges *et al* (1975):

= $3.51 \log_{10} CBR - 0.85 (\log_{10} CBR)^2 - 1.43$.

CBR = In situ California Bearing Ratio of subgrade in %.

The initial structural number (SN_i) was determined by using correlations developed by Rohde (1994), whereby a pavement's structural number (SN) can be determined from its total thickness and the shape of the measured surface deflection bowl obtained from a Falling Weight Deflectometer (FWD). The correlations are based on the general "two thirds rule" of thumb suggested by Irwin (1983) to explain the stress distribution and thus origin of deflections as found below a FWD. This rule is based on the fact that approximately 95% of the deflection measured on the surface of a pavement originates below a line deviating 34° from the horizontal. Based on this simplification it can be assumed that the surface deflection measured at an offset of 1,5 times the pavement thickness originates entirely in the subgrade. By comparing this deflection with the peak deflection, the following index associated with the magnitude of deformation that occurs within the pavement structure was defined by Rohde (1994):

$$SIP = D_0 - D_{1.5Hp}$$

where:

SIP = Structural Index of the pavement.

D_0 = Peak deflection measured under a standard 40 kN FWD impulse load.

$D_{1.5Hp}$ = Surface deflection measured at an offset of 1,5 times Hp under a standard 40 kN FWD impulse load.

Hp = Total pavement thickness.

To develop a relationship between FWD measured surface deflection and a pavement's structural number (SN), a total number of 7776 pavement structures were analysed using layered elastic theory. The SN for each pavement was calculated by using the following approach suggested by AASHTO (1986):

$$SN = 0{,}04 \; \Sigma \, a_g h_i (E_i/E_g)^{1/3}$$

where:

SN = Structural number.

a_g = Material and layer strength coefficients, per inch.

h_i = Layer thickness, mm (where $\Sigma h_i \leq 700$ mm).

E_i = Resilient modulus of pavement layer.

E_g = Resilient modulus of standard materials in the AASHO Road Test.

By comparing the calculated SN with the parameters previously defined, Rohde (1994) obtained the following relationship between SN and SIP:

$$SN = k_1 SIP^{k2} \, HP^{k3}$$

where:

SN = Structural number.

SIP = Structural Index of the pavement (in μm).

HP = Total pavement thickness (in mm).

ki = Coefficients as listed in Table 4.10.

The acceptability of SN determined according to the above procedure was continuously verified by using the approach suggested by AASHTO (1986). Where noticeable differences existed between the two methods (eg. unrealistic high SN predicted according to above procedure, normally associated with unrealistic low deflections), the SN determined according to the AASTHO (1986) approach was used.

Table 4.10: Coefficients for SN vs SIP relationships (After Rohde, 1994).

Surfacing type	k1	k2	k3
Surface Seals	0,1165	-0,3248	0,8241
Asphalt concrete	0,4728	-0,4810	0,7581

Finally the initial structural number SN_i was defined as the structural number SN calculated according to above procedure less the contribution of any maintenance actions within the period between the date of the FWD measurements and the date used as the initial year of modelling:

$$SN_i = SN - 0{,}04 \Sigma a_i h_i$$

where:

SN_i = Initial structural number in first year of modelling.

SN = Structural number.

a_i = Material and layer strength coefficients, per inch.

h_i = Thickness of overlay, reseal etc. in mm.

Pavement structure data were obtained from as-built drawings, and the strength coefficients recommended by Paterson (1987) were used. These coefficients were the result of an adaptation of the results obtained in Kenya, Brazil and South Africa. The in situ subgrade CBR values were obtained from Falling Weight Deflection measurements conducted on the network. For each pavement section the deflection bowl that represented the average condition was selected. The average deflection bowl was selected because during network deterioration predictions using HDM-III, the average condition of a pavement is predicted, and not a certain percentile value.

To select the representative deflection bowl the average of all deflections measured on the pavement section were calculated individually at each FWD sensor offset. The calculated average deflections at each FWD sensor offset represented the average deflection bowl of the pavement section. The actual measured deflection bowl that fitted the calculated average deflection bowl the closest over all the sensors, was then selected as the representative deflection bowl for that section. It was decided to employ this method due to the nature of

deflection measurements. The frequency at which the deflection measurements were conducted were such that according to Jordaan and Van As (1992) these values could incorporate an error of 40 % at a 95 % confidence interval. The use of complex mathematical equations would thus only be time consuming, with no additional benefit.

To determine the layer moduli a deflection bowl was fitted to the selected measured bowl by using backcalculating techniques based on linear elastic theory (Rohde, 1992). With the subgrade elastic modulus known the following simplified conversion was used to determine the subgrade CBR value (Jordaan, 1993):

$$CBR = 10 \times E_S$$

where:

CBR = Subgrade CBR value as a percentage.

E_S = Subgrade elastic modulus (MPa).

Although the use of the above mentioned correlation is highly questionable, no other unique relationship between CBR and E-modulus existed. Thus it was decided to use the above correlation since it is generally used and accepted as a rule of thumb indication of subgrade CBR. The structural number as well as the subgrade CBR value in calculating the modified structural number (SNC) of each pavement section used in the study, are summarised in Table B.4 of Appendix B.

4.6 STRUCTURAL NUMBER AND DEFLECTION RELATIONSHIP

During the Brazil-UNDP study a relationship between the modified structural number and surface deflection was developed. The correlation obtained between the two was acceptable, but not that good, because the two parameters measure different attributes of the pavement (Paterson, 1987). The modified structural number measures the strength of a pavement, by correlating permanent deformation under repeated loading to material characteristics that are related to shear strength. The peak deflection, which depends on the load and loading period, measures the stiffness of the pavement and that depends on the resilient stiffness and thickness of the material in each layer. The two are related only insofar as the resilient characteristics correlate with the permanent deformation behaviour of the component materials (Paterson, 1987).

The following inverse nonlinear relationships were observed for granular and cemented base pavements during the Brazil-UNDP study:

For granular base pavements:

$DEF = 6{,}5\ SNC^{-1{,}6}$

For cemented base pavements:

$DEF = 3{,}5\ SNC^{-1{,}6}$

where:

DEF = Benkelman beam deflection in mm

SNC = Modified structural number

The relationship between the modified structural number and deflection was evaluated using the limited deflection data available on some of the national route pavements. The reasons for evaluating the relationship were:

- The fact that most of the pavements used on South African national roads are so called inverted-design pavements, meaning that the cemented subbase layer is below a stress relieving granular basecourse. This pavement type was not included in the Brazil-UNDP study, thus the relationship between the modified structural number and deflection is unknown for this pavement type.

- The fact that when only the modified structural number is specified, the deflection is computed endogenously according to the applicable relationship. This may have an effect on roughness predictions since the deflection is used in the calculation of the mean rut depth, which is in turn used to calculated the rut depth standard deviation, for which roughness predictions did seem sensitive as shown in Chapter 3.

The results obtained for a surfacing on a granular basecourse with a cemented subbase, which is a so called inverted design, are illustrated in Figure 4.9, and for a surfacing on a granular basecourse with a granular subbase in Figure 4.10. From Figure 4.9 it is evident that no correlation between deflection and modified structural number for pavements with a inverted design seems to exist. This behaviour is normally expected for a pavement with a rigid layer, since most of the pavement strength is located within the rigid layer which acts as a

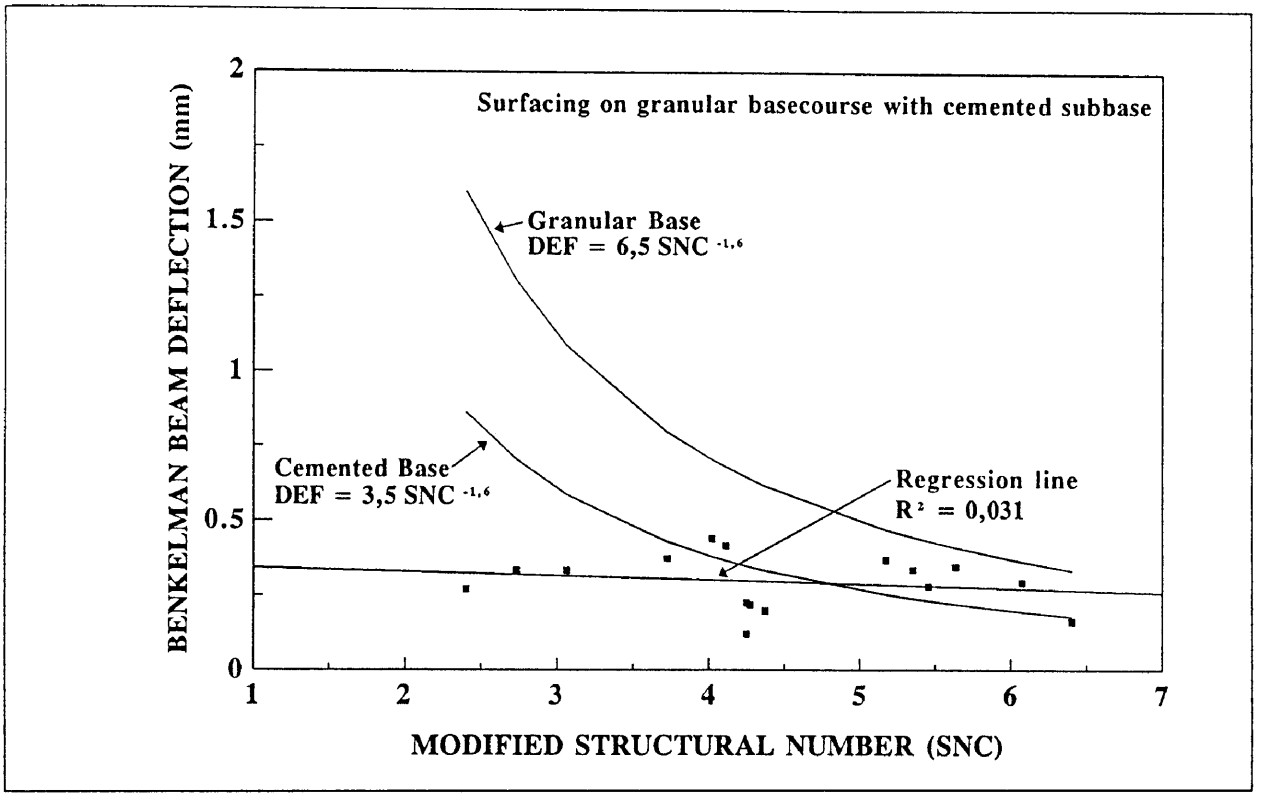

Figure 4.9: Correlation between SNC and deflection for inverted design pavement.

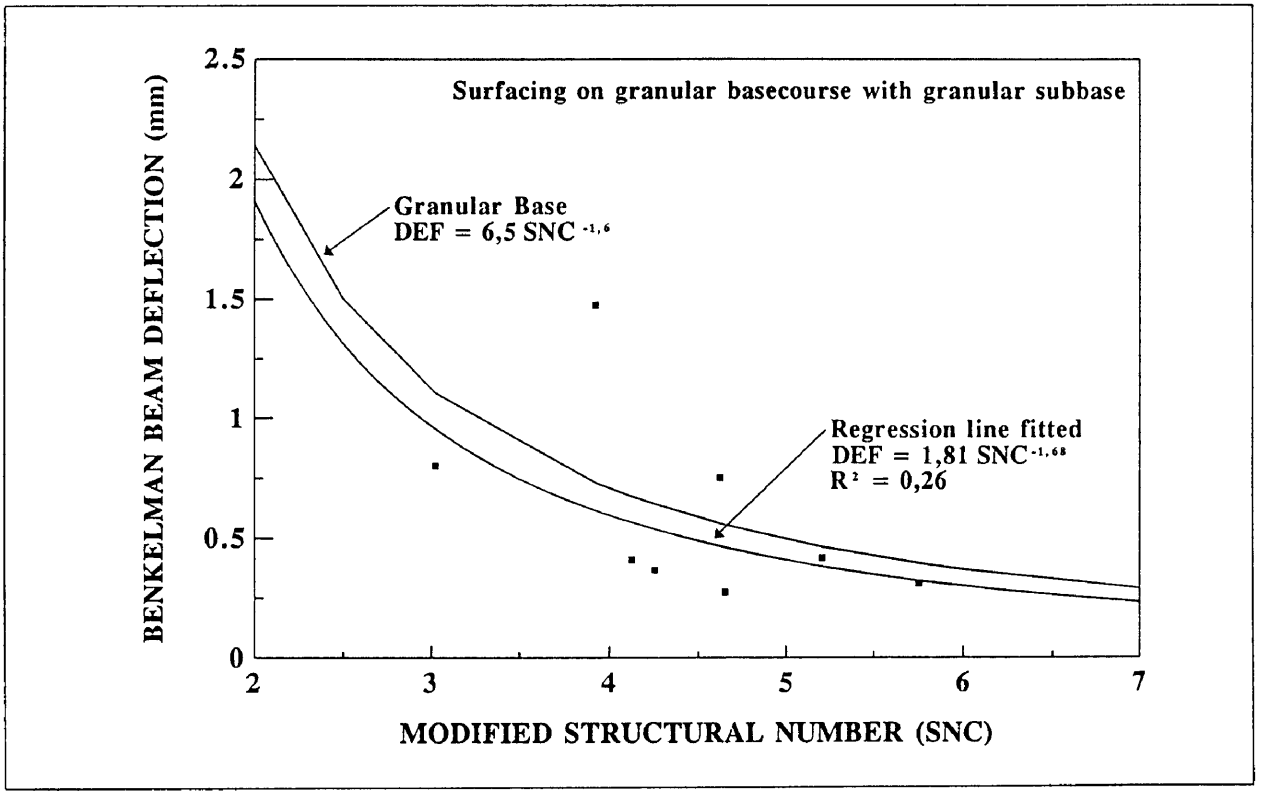

Figure 4.10:Correlation between SNC and deflection for granular base and subbase pavements.

slab resisting deflections. For the higher structural strength pavements the behaviour seemed to be more accurately predicted by the correlation used for a cemented base pavement, than the correlation used for a granular base pavement. Although the presence of a cemented subbase below a granular base does seem to affect the correlation between the deflection and modified structural number, it is not recommended that the correlation for a cemented base should be used for pavements with a inverted design. The reasons for this are:

- The effect of the incorrect correlation is limited to the rutting models, which did not seem that sensitive to the typical range of deflection values measured on the high strength national road pavements. If the cemented base correlation is used all the cracking initiation and progression models as well as the maintenance activities will be affected, resulting in a larger effect on roughness.

- The quality of the data employed in the study is of such a nature that no fundamental changes to the model can be based on it. The reason for this being that the modified structural number was calculated from as-built results which do not necessarily correspond to the pavement condition at the day of the deflection measurements.

From Figure 4.10 it does however seem that for the limited data available the correlation between deflection and modified structural number for granular base and subbase pavements seems applicable (The deflection measurements used are summarised in Table B.3 of Appendix B). Both comparisons do however indicate the need for further research using data obtained under experimentally controlled conditions. It is believed that this research must be conducted to correlate Falling Weight Deflection measurements with structural number, instead of Benkelman beam deflections. One of the reasons for this is that the speed at which Falling Weight Deflection measurements are conducted is making the use of this type of apparatus far more acceptable for network level management than the Benkelman beam.

4.7 RUTTING

A limited number of rut depth measurements were available on some of the national route sections. These measurements were however taken under a straight edge with a length of 2 metres. The straight edge length used in the Brazilian study was only 1,2 metre. Available rut depth measurements will be included into the comparison process, but it is expected that the correlation coefficient between the predicted value and the measured value would be influenced by the difference in length of the straight edge.

For pavements with no measurements it is assumed that rutting is a function of the pavement age and structural number. The standard deviation was assumed to be a function of the mean rut depth as suggested by Paterson in the HDM-III manual. The rut depth measurements available are summarised in Table B.3 of Appendix B.

4.8 MAINTENANCE

Only routine maintenance and the patching of all potholes were scheduled to occur throughout the analysis period at the end of each year. This was in line with the routine maintenance policy of the Department of Transport. Where special maintenance or rehabilitation was conducted during a year, it was specified within the HDM-III model to occur at the end of the specific year. This allowed the HDM-III model to incorporate the changes in any affected parameter, in future predictions.

4.9 INITIAL RIDING QUALITY

For pavement sections where riding quality measurements were taken within a year after the section was opened to traffic, the value measured was taken as the initial roughness value for that pavement section. Where no measurements were taken within a year after construction, the average values in Table 4.11, determined from the limited number of pavement sections evaluated within one year after the road was opened to traffic, were used as an indication of the initial roughness. If the predicted values differed meaningfully from the measured values, the initial roughness value was adjusted accordingly. During the study it was found that the initial values differed to a large extent, even for the same

pavement type. This emphasised the need to introduce a bonus-penalty scheme for contractors during construction, to ensure that the finished product met the necessary requirements. This will have the added advantage that the actual initial roughness value of the pavement will be known for future use as well as for research (Geldenhuys *et al*, 1992).

Table 4.11: Initial roughness values

Surfacing type	Asphalt concrete	Surface treatment
Mean Initial QI_m (counts/km)	23.2	34.9
Standard deviation in QI	5,8	6,6
Number of pavement sections	13	9

4.10 INITIAL TRAFFIC LOAD AND GROWTH RATE

As a result of the methodology employed for predicting the deterioration of a pavement from the date it was initially opened to traffic, it was necessary to determine the initial traffic loading as well as the growth rate experienced over the years for each pavement section evaluated, for both:

- the equivalent number of 80 kN axles (E80's), and
- the total number of axles.

The equivalent number of 80 kN axles are needed for the incremental roughness, mean rut depth, rut depth standard deviation and cracking initiation models. The total number of axles are needed for the ravelling and potholing models.

Both the equivalent number of 80 kN axles and the total number of axles were determined by using the results of traffic axle weight classifier (TAWC) surveys conducted over the years by request on a specific route. The quality of the information available for analysis was influenced by the following factors:

- The limited number of traffic surveys conducted on each route, and the fact that where more than one survey was conducted, they were seldomly performed at the same location.

- Most of the sections included in the study had only one traffic survey conducted during their life, and it is consequently impossible to determine the initial traffic loading and traffic growth rate for these sections in isolation.

As a result of the limited information available assumptions had to be made to allow the use of measurements conducted at different locations on a route, in the determination of the traffic load and growth rate for a specific pavement section. These assumptions were only made for sections on which no major difference in traffic patterns between the different locations existed.

Despite the assumptions made no pavement section had three or more measurements conducted on it from the date the road was opened to traffic. As a result of this the more acceptable method of fitting curves to the data through linear square regression techniques could not be applied. Based on previous traffic studies in South Africa, it was assumed that the E80 as well as the growth rate in total number of axles, followed an exponential form as recommended in TRH 16 (1991). Based on the above assumption the following equation was employed to determine the exponential growth rate between two measurements:

$$t = \frac{LN\left\{\frac{E80a}{E80b}\right\}}{(a-b)}$$

where:

t = Exponential growth rate between two measurements.
E80a = Total number of E80's or axles in year a.
E80b = Total number of E80's or axles in year b.

The results obtained were compared with the recommended values in Table 14 of TRH 16 (1991), to ensure that the obtained values were not unrealistically low or high. With the growth rate known the above equation was then employed to calculate the assumed initial traffic loading.

If a section had only one measurement, the assumed initial traffic load was obtained by either using an E80 growth rate obtained on a road section with a similar traffic loading, or by using one of the recommended values in Table 14 of TRH 16 (1991). The results obtained for the pavement sections included in the study are summarised in Table B.5 of Appendix B.

4.11 CONCLUSIONS FROM VALIDATION METHODOLOGY

The main conclusion from the development of a validation methodology for evaluating the applicability of HDM-III model predictions for South African conditions is that the HDM-III environmental roughness coefficient (Kge) should first be calibrated for local moisture regimes, there after each model of the HDM-III deterioration and maintenance submodel should be evaluated and calibrated individually, and not just the incremental roughness model. Furthermore, the deterioration of a pavement section should be predicted from the year it was opened to traffic, allowing the incorporation of all measured values, as well as the long term aging effects.

During the development of a validation procedure it was evident that the availability of suitable data for the development of accurate correlations between the format of South African visual data and the HDM-III model input requirement, was limited. It is recommended that urgent attention be given to the following:

- It is of utmost importance that traffic axle weight classification studies be conducted more frequently at the same location on all major roads, and not only on request. This will benefit both future predictions, as well as the evaluation of the performance of existing pavement designs.

- Roughness measurements be conducted just after construction, special maintenance or rehabilitation, as this will allow more accurate future deterioration predictions. It will also be of benefit to future research regarding the influence of initial roughness on pavement deterioration.

- Research should be conducted to determine a more accurate correlation between deflection and the modified structural number (SNC) for typical South African pavement designs. The research should especially be directed towards correlating Falling Weight Deflection measurements and should include the evaluation of the influence of temperature, moisture and asphalt thickness on the deflection measurements.

- Research should be conducted into the determination of correlation values for converting the degree and extent numerical ratings used in South Africa, to percentage of pavement area.

CHAPTER 5

RESULTS OBTAINED FROM THE COMPARISON OF PREDICTED VALUES WITH OBSERVED VALUES

5.1 INTRODUCTION

As mentioned previously to investigate the local applicability of the HDM-III model its predictions must be compared against the locally observed values. To enable this a validation methodology was defined in Chapter 4, according to which the environmental roughness coefficient (Kge) would first be calibrated for the different moisture regimes observed on South Africa national roads. After calibration for environmental regimes, an autocalibration procedure would be employed to evaluate the applicability of the HDM-III model for predicting the locally observed deterioration on national roads, and to determine calibration factors if needed.

The results obtained from the application of the above mentioned procedure are discussed in this Chapter for each individual model of the HDM-III deterioration and maintenance submodel.

5.2 ENVIRONMENTAL ROUGHNESS CALIBRATION FACTOR (Kge)

The environmental roughness calibration factor (Kge) is the exponential yearly rate of increase in roughness due to environmental effects. The environmental roughness calibration factor (Kge) is calculated from the environmental coefficient (m) as follows:

$$Kge = m/0{,}023$$

where:

Kge = Environmental roughness calibration factor.

m = Environmental coefficient.

Advice as to recommended values for the environmental coefficient (m) for various climatic regions are given in Table 8.7 of Paterson (1987). It is however mentioned by Paterson (1987) that these recommended values are based on relatively few evaluations. Based on this and the advice given by Paterson

during the Botswana calibration of HDM-III, it was decided to follow the method recommended by him for determining a value for the environmental coefficient (m) from roughness measurements.

The recommended procedure is to firstly run HDM-III with the environmental roughness calibration factor set to zero. This establishes the contribution of traffic to the increase in roughness. The environmental coefficient (m) is then approximated by dividing the difference between the total increase and the increase due to traffic by the product of the mean roughness and the number of years since construction. In mathematical terms:

$$m = \frac{(Rm - Ri) - (Rp - Ri)}{(Rm + Ri) \times (T/2)}$$

where:

Rm = Measured roughness.

Ri = Initial roughness

Rp = Predicted roughness with Kge = 0 = m.

T = Number of years between measurement date and construction date.

For this study the pavement sections under evaluation were subdivided into the different Thornthwaite moisture regimes occurring on South African national roads (See Figure C.1 in Appendix C). Since multiple observations existed under each moisture regime, the best estimate for m was given by the quotient of the sums of the individual numerators and denominations. The results obtained for the different moisture regimes are summarised in Table 5.1 (See Table B.6-B.8 in Appendix B for full list).

Table 5.1: Environmental coefficient (m) for different moisture regimes.

Moisture regime	Semi-Arid	Subhumid	Humid
Calculated value for m	0,009	0,014	0,020
Calculated value for Kge	0,392	0,607	0,886
No of observations	20	25	20
Recommended value for Kge	0,70	1,30	1,74

As seen the calculated environmental roughness calibration factor (Kge) in each instance is nearly half of the value recommended by Paterson (1987) for that moisture regime. Thus the influence of the environment on the pavement deterioration observed on national roads, is only about half of what is predicted by the HDM-III model. Possible factors contributing to this is:

- The generally more balanced deep pavement structures used in South Africa, resulting in more support for the surface layer, and as such decreasing the induced stresses within the upper layers. This results in a longer period before initiation of for example cracking. This is in contrast with the shallow pavements used during the development of the models. As a result of this most of the pavements included in the study were structurally stronger than the pavements used during the development of the HDM-III model, resulting in a lower sensitivity to environmental influences.

- The design and quality control during construction in South Africa, resulting in a high quality finish with adequate provision for surface as well as subsurface drainage.

- The maintenance activity employed on South African national roads, which include routine activities such as crack sealing and periodic overlays or reseals, which decreases the environmental influences, thus increasing the life of a pavement.

The calculated environmental roughness calibration factors (Kge), summarised in Table 5.1 were used in the calibration procedure of the other HDM-III models.

5.3 CRACKING MODEL

The cracking model is the first model evaluated in the modelling sequence of HDM-III model. As mentioned in previous Chapters the cracking model is subdivided into two phases, namely:

- The time until the initiation of cracking, which was defined as an area of all cracking of 0,5% or more, over the pavement section under evaluation.
- The rate of progression of the area cracked.

Both the above phases are further subdivided into either all cracking or wide cracking, with all cracking being the area of crocodile and irregular cracks wider than 1 mm. Wide cracking only includes the two mentioned crack patterns if they were spalled and larger than 3 mm in width.

To enable the local adoption of the cracking model, the HDM-III model allowed for two user defined calibration factors for the area of all cracking, namely:

- Factor for cracking initiation, kci.
- Factor for cracking progression, kcp.

The reason for not having calibration factors for wide cracking, is that the initiation of wide cracking was defined as a function of the initiation of all cracking.

Initially the pavement sections were evaluated individually based on the surfacing type, basecourse type and climatic area. No noticeable difference in performance between the different surfacing layers or basecourse layers existed. It is believed that for the surfacing this is the result of the fact that the asphalt layers used on South African national roads are normally thin (30-40 mm) and the surface treatments used are Cape seals. The Cape seal differs from a normal seal in that it has a one or more slurry seals on top of the single seal aggregate. This improves the impermeability of the layer and also limits ravelling to a large extent, which leads to an improvement in the performance of the seal. For these reasons similar performance of the surfacing types were found.

For the different climatic areas there also existed no noticeable difference in the cracking initiation and progression calibration factor values. Thus the calibration values for cracking initiation and progression were evaluated for all pavement sections irrespective of surfacing type, basecourse type or climatic area. The only noticeable difference that existed was between original constructed pavements, and those with overlays or reseals. The distribution of the calibration values obtained for cracking initiation are illustrated in Figure 5.1 for original constructed pavements and Figure 5.2 for overlays and reseals. A full list of all calibration values obtained for each individual section is summarised in Table C.1, in Appendix C.

As seen from Figure 5.1 the cracking initiation calibration values for original constructed pavements follow a normal distribution with an average value of

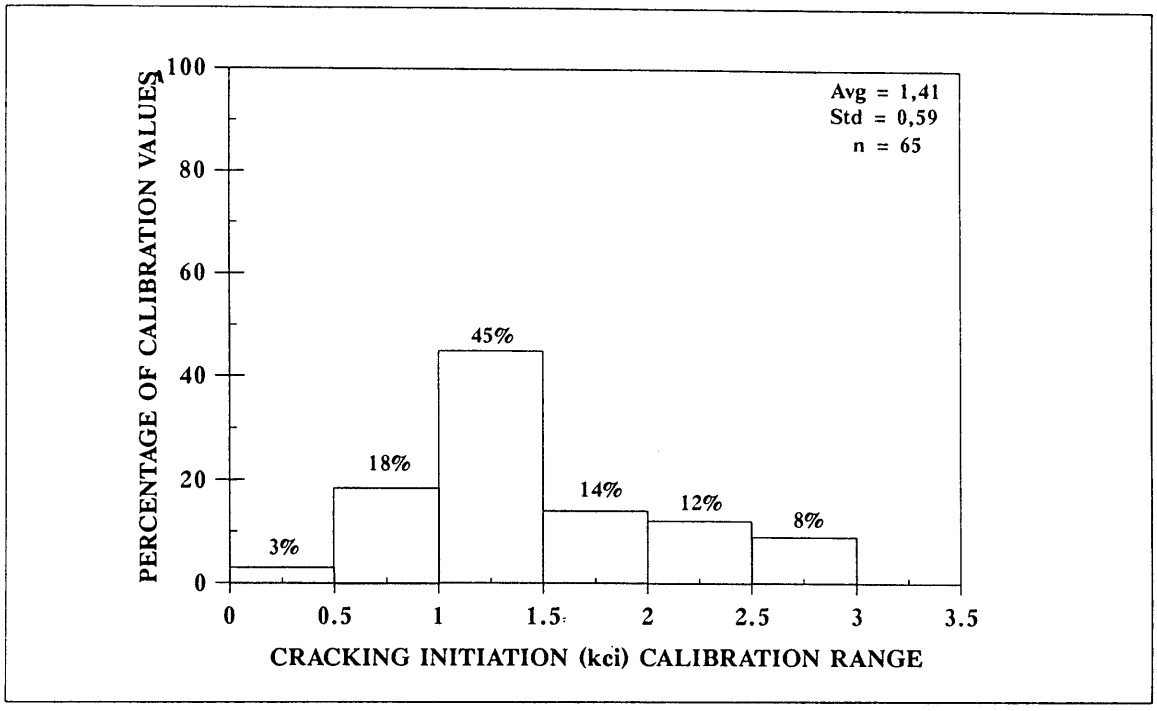

Figure 5.1: **Distribution of cracking initiation calibration (kci) values for original surfacings.**

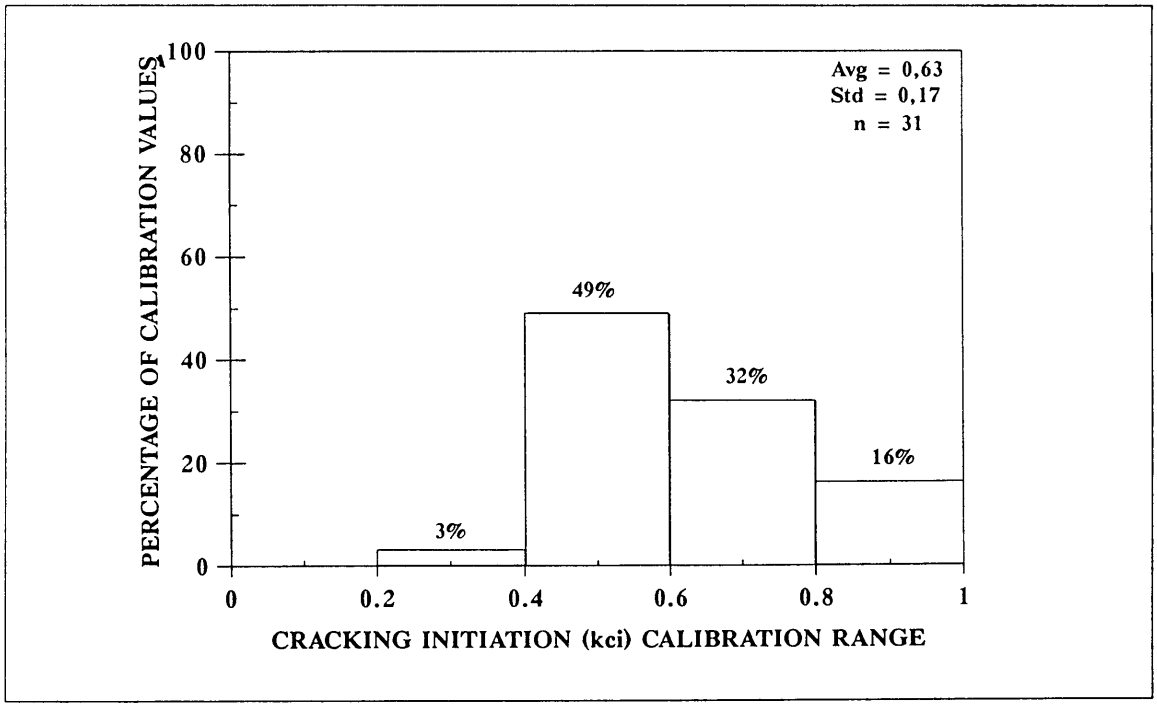

Figure 5.2: **Distribution of cracking initiation calibration (kci) values for overlays and reseals.**

1,41. This indicates that the period until the initiation of cracking on South African national roads is longer than the period predicted by the HDM-III model for the same volume of traffic. The high observed calibration values in the range 2,0 to 3,0 is believed to be the result of maintenance activities that were not recorded, and as such it seemed that the surface layer survived longer. Since no way of proving the above mentioned existed, all values were included in the calculation of the average mentioned.

From Figure 5.2 it is evident that for pavements with overlays or reseals the cracking initiation calibration values also follow a normal distribution, with an average value of 0,63. This indicates that the expected life until cracking initiation tends to be lower for an overlay than the value predicted by the HDM-III model for the same traffic volume. It is believed that this is the result of the fact that the average overlay thickness of between 30-40 mm generally used in South Africa is less than the average overlay thickness of between 50-125 mm used in the Brazil study, from which the cracking models were developed. This thinner layer thickness results in a shorter propagation length for cracks, with a subsequent faster rate of cracking initiation for South African overlays.

The distribution of the calibration values obtained for cracking progression (kcp) is illustrated in Figure 5.3 for original constructed pavements and Figure 5.4 for overlays and reseals (See Table C.1 in Appendix C for full list). From Figure 5.3 it is evident that the cracking progression calibration values for original surfacings also seem to follow a normal distribution, as previously observed for the cracking initiation calibration values. The average value of 0,21 indicates that the progression of cracking observed on national roads is lower than the rate of progression predicted by the HDM-III model for the same volume of traffic. As seen from Figure 5.4 the same seems to be applicable for overlays and reseals, the average value of 0,59 is however higher than the value for original surfacings, but still lower than the value predicted by the HDM-III model for the same traffic volume. The relatively faster rate of cracking propagation for overlays above original surfacings is expected since the original surfaces of the pavement is already cracked, making the propagation of cracks through the overlay easier.

In general it can be concluded that for the pavements used on South African national roads the period before cracking initiation seems to be longer than the

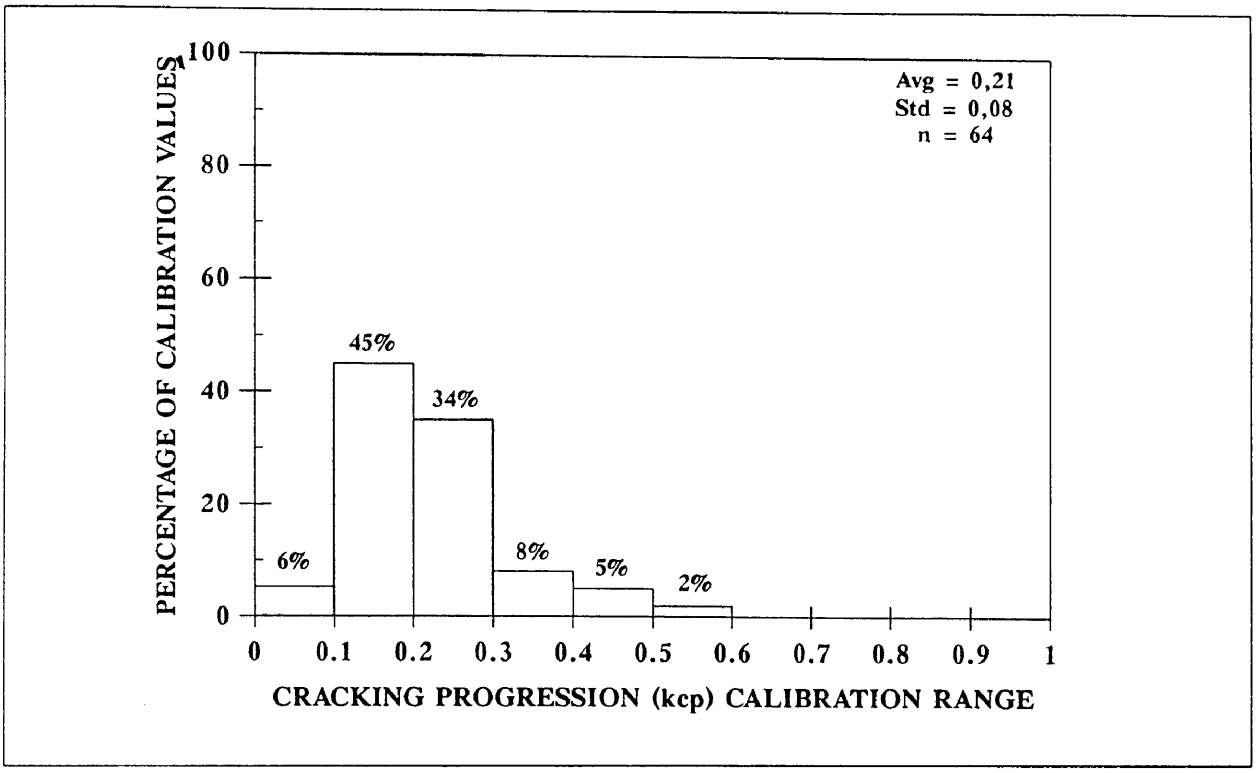

Figure 5.3: Distribution of cracking progression calibration (kcp) values for original surfacings.

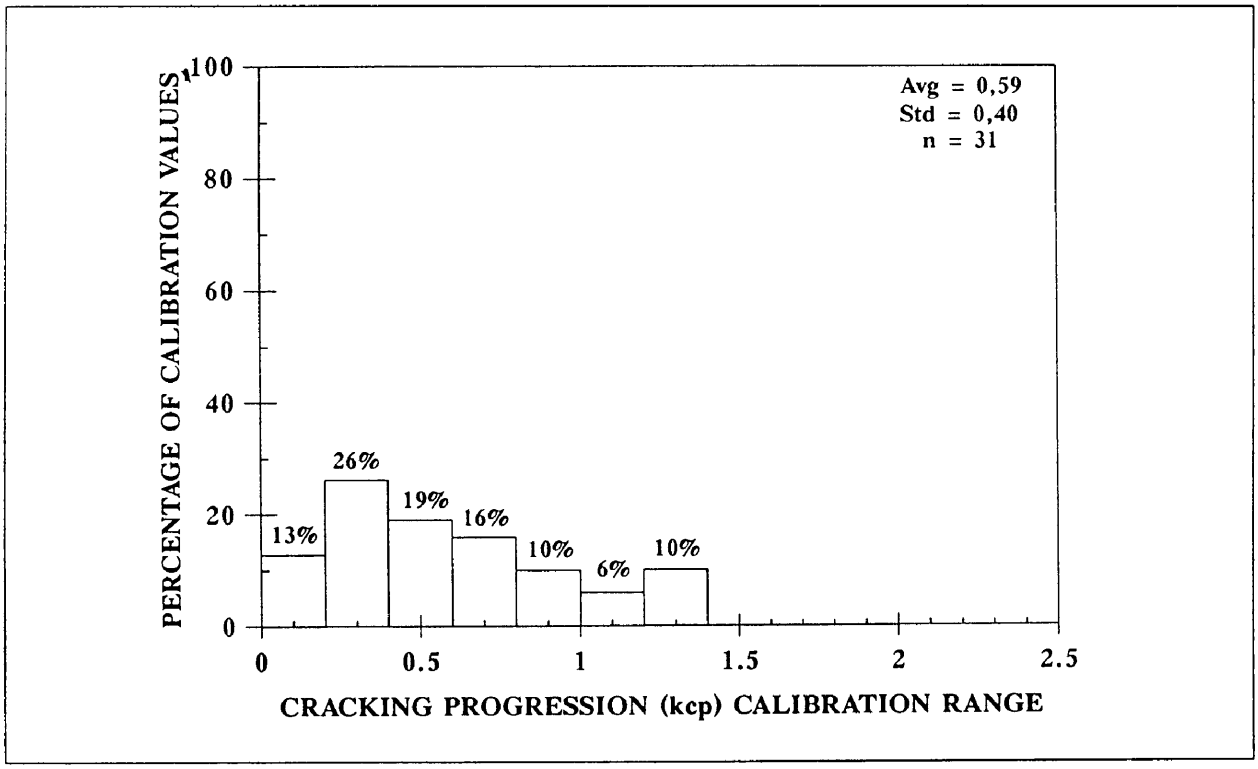

Figure 5.4: Distribution of cracking progression calibration (kcp) values for overlays and reseals.

predicted period, and once cracked, the rate of cracking progression is lower than the values predicted by the HDM-III model for the same traffic volume. Possible factors contributing to the above mentioned observations are:

- The routine maintenance program employed which ensures that a road is sealed or overlaid within 8 years. This activity severely limits the probability for cracking initiation and progression to the severe rates observed during the Brazil study, as is evident in the low areas of cracking observed.

- The fact that only crocodile and surface cracking were included in the calculation of the area of indexed cracking. This may have an influence on the area calculated, since the M3-1 method only allowed the recording of the two most extensive crack patterns, which most of the time were either longitudinal, transverse or block cracking for the type of pavements used on South African national roads.

- In South Africa the asphalt type used is of a semi-gap grading, whereas the type generally used in the Brazil study was continuously graded. It is known that a semi-gap graded asphalt is more resistant to fatigue than the continuously graded, resulting in a longer period before the initiation of cracking and a slower rate of progression once initiated.

The ability of the HDM-III model, once calibrated, to predict the cracking observed on national roads are illustrated in Figure 5.5 for original surfacings, and Figure 5.6 for overlays and reseals. Only the area of all cracking is compared, since wide cracking seldomly occurred on South African national roads. As seen from Figure 5.5 the area of all cracking observed on the pavement sections evaluated were generally very low, not even reaching 10 %. The predictions by the HDM-III model after calibration compares favourably with the observed values as is evident from the R-Squared value of 0,91 obtained from the comparison. From Figure 5.6 it is evident that the same is applicable for overlays and reseals, with even a higher R-Squared of 0,94 being obtained. It seems however from the two figures that the HDM-III model tends to over-predict the area of cracking for larger areas of cracking, as seen from the slope of the line fitted to the data. Since only a limited number of sections with relatively larger areas of cracking were available, it was impossible to evaluate this observation in detail.

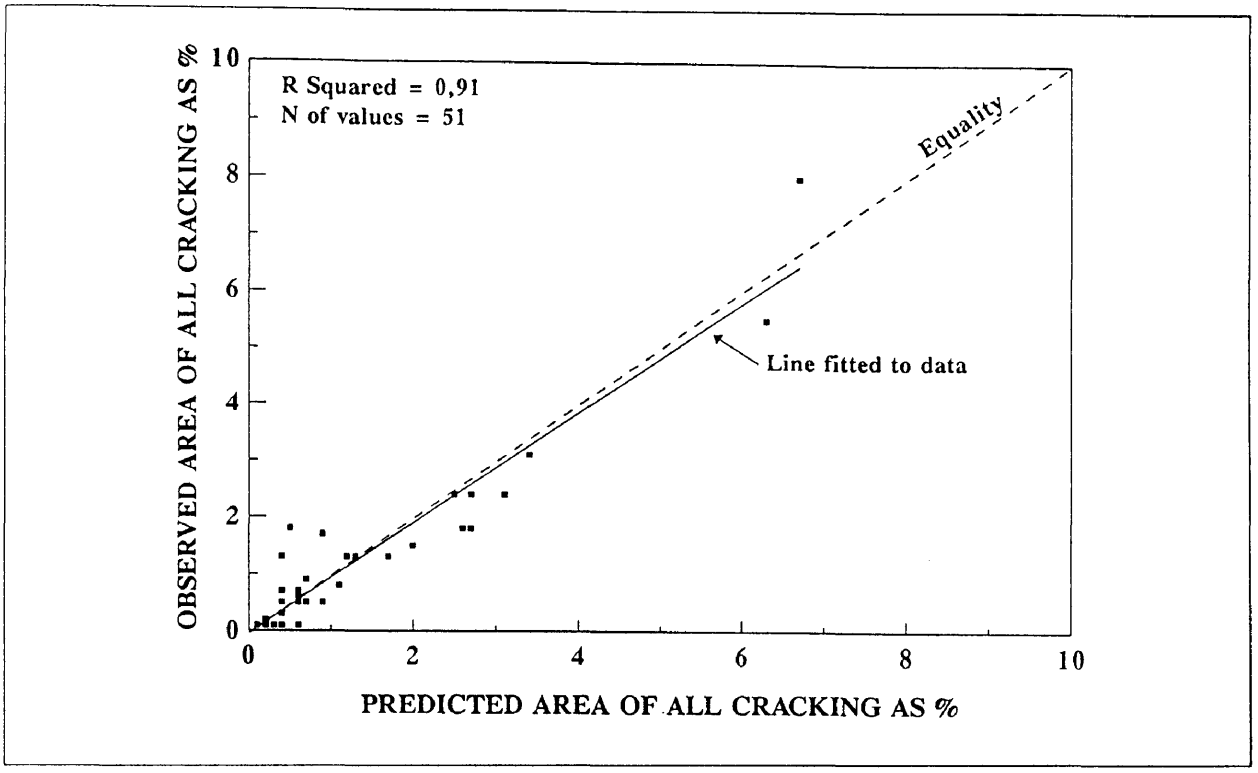

Figure 5.5: Comparison between predicted and observed values for area of all cracking for original surfacings.

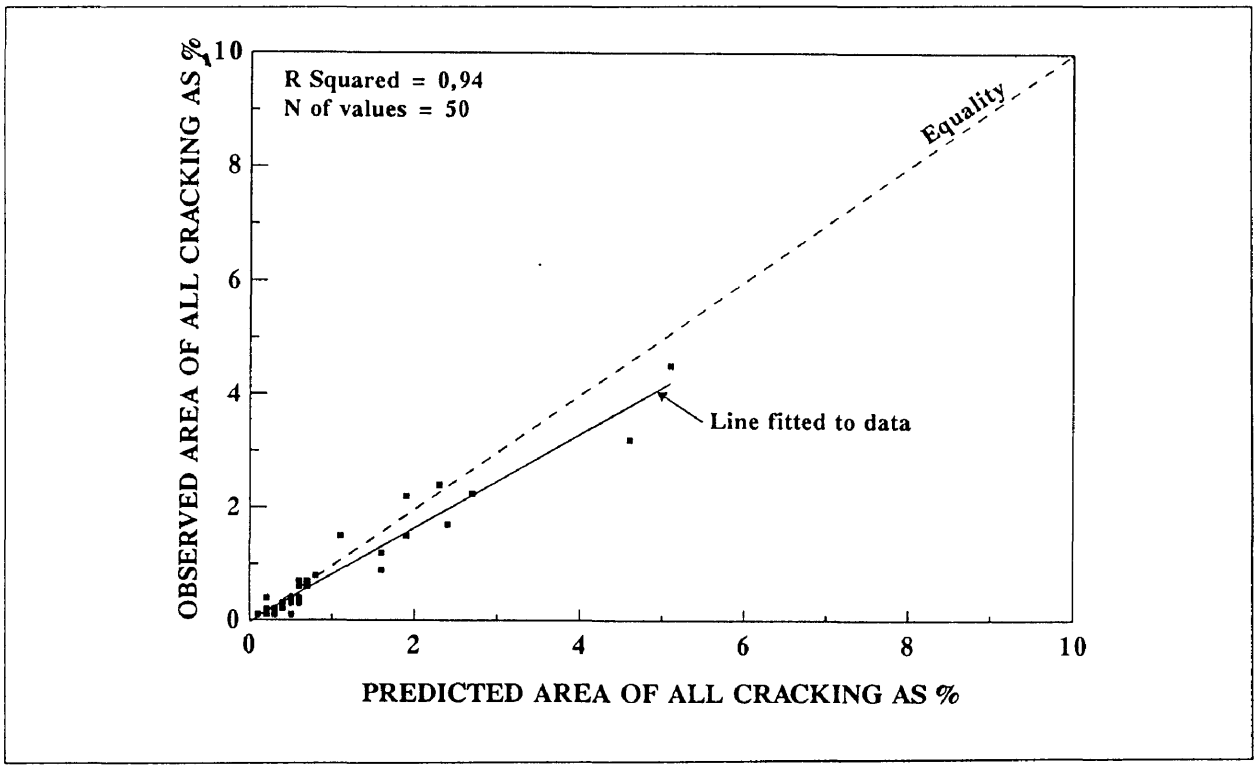

Figure 5.6: Comparison between predicted and observed values for area of all cracking for overlays and reseals.

It must however be remembered from the sensitivity analysis in Chapter 3 that the roughness model was extremely sensitive to whether a pavement was cracked or not cracked; once cracked the roughness model seemed insensitive to the area of cracking. This indicates that despite the fact that the cracking model was not evaluated for larger areas of all cracking, the results obtained would still be acceptable for the roughness model. Thus it can be concluded that for the low areas of cracking observed on national roads the HDM-III model predictions after calibration do seem reasonable. It is however recommended that further research be conducted on the correlation between the TMH9 degree and numerical ratings and the percentage of area used in the HDM-III model. Until such research is conducted, it is recommended that the ranges in Table 5.2 should be used in the selection of a calibration factor value, if an individual value is not determined for the specific section.

Table 5.2: Recommended range for calibration factor values of the cracking model.

Pavement type	Cracking initiation (kci)	Cracking progression (kcp)
Original surfacings	1,00-1,50	0,1-0,3
Overlays and reseals	0,4-0,8	0,3-0,7

5.4 RAVELLING MODEL

As mentioned in Chapter 2, ravelling is also modelled in two phases, namely:

- The time before the initiation of ravelling.
- The progression of the area ravelled, once initiated.

The HDM-III model only allowed for one user defined calibration factor for the initiation of ravelling, namely kvi. As mentioned in Chapter 4, no method to use the information obtained according to the M3-1 method in the calibration procedure existed. The reason is the fact that a numerical rating of 1 was used to indicate an area of ravelling ranging from no ravelling to 30% of area ravelled, making it impossible to determine any correlation for ravelling. The data obtained according to the TMH9 method, was usable although the correlation values for extent and degree numerical ratings were not tested. But

since the ravelling models in the HDM-III model were developed for original and maintenance surfacings of double surface treatments, slurry seals and open graded cold-mix asphalt, most of the pavement sections could not be evaluated. The reason for this is that most of the pavement sections had semi-gap or continuously graded asphalt surfacings, asphalt overlays or Cape seals, for which the ravelling model was not developed as they normally do not ravel.

Thus no correlation values could be determined for the ravelling model of the HDM-III model. It is believe that this would not adversely affect the calibration values of the other models, since the influence of ravelling on potholing is only of importance once the area of ravelling exceeds 30%, which never occurred on the sections evaluated. Secondly the influence of ravelling on roughness, as may be recalled from the sensitivity analysis in Chapter 3, is negligible. Thus it is recommended that for ravelling initiation a default value of 1 should be used, until calibration values are determined from a more accurate source of information.

5.5 POTHOLING MODEL

The potholing model is the third model in the modelling sequence. The reason for this being the fact that potholing was considered to develop from the spalling of wide cracks or the ravelling of thin surface treatments (Watanatada *et al*, 1987). As with the previous two models the potholing model is also divided into two phases, namely:

- The initiation of potholing defined as a function of the time since the initiation of the triggering distress, which is either wide cracking for a asphalt surfacing, or ravelling for a surface treatment.
- The progression of potholes which is the result of new potholes caused by wide cracking or ravelling, and the enlargement of existing potholes.

The HDM-III model only allowed for a user-specified calibration factor for the progression of potholes, namely kpp. No user specified calibration factor existed for pothole initiation. It is believed that this is the result of the fact that since pothole initiation is depended on either wide cracking or ravelling, which both have initiation factors, the initiation of potholing is controlled by the initiation factors of these two parameters.

The initiation and subsequent progression of potholes is thus controlled by either wide cracking or ravelling. The minimum requirements for the initiation of the pothole models were defined as a minimum area of wide cracking of 20% for asphalt surfacings, or a minimum ravelled area of 30% for surface treatments. As a result of the maintenance activity of patching of all potholes, and the fact that the area of wide cracking never exceeded 20% for asphalt surfacings or the area of ravelling never exceeded 30% for surface treatments, the pothole models were never initiated within the HDM-III model. Thus no method of determining calibration factor values for the pothole models existed, since no predictions were made by the HDM-III model.

Thus it is recommended that for the pothole progression calibration factor (kpp) a default value of 1 should be used. It is also recommended that further research be conducted on the triggering requirements for the pothole models. The reason for this is that it seemed evident that potholes initiated at lower areas of wide cracking and ravelling on South African national roads, than required by the HDM-III model.

5.6 RUTTING MODEL

The rutting model consisted of two models, namely:

- Mean rut depth model.
- Rut depth standard deviation model.

The mean rut depth model is not used directly in the HDM-III model, but instead is used as a means to estimate the variation of rut depth (standard deviation) which contributes directly to the roughness model. For the rutting model the HDM-III model only allowed for a user defined calibration factor for the progression of rutting, krp. A limited number of rut depth measurements were available with often only one measurement available on a pavement section.

The distribution of the calibration values obtained for rutting are illustrated in Figure 5.7 for originally constructed pavements. No rut depth measurements were available on pavements with overlays or reseals. As seen the calibration values for rut depth progression also seem to follow a normal distribution with an average value of 1,57. It is believed that this average value does not necessarily indicate a faster rate of rut depth progression for South African pavements. The reason for this higher than 1 value is the fact that in South Africa a 2 metre straight edge is used in comparison with a 1,2 metre straight

edge used in the development of the model. The rut depth measured under a 2 metre straight edge will be larger than the same rut depth measured with a 1,2 metre straight edge, especially if the rut is wide due to subgrade failure.

In Figure 5.8 the comparison between predicted values and observed values are illustrated for the mean rut depth, and in Figure 5.9 for rut depth standard deviation. From Figure 5.8 it is evident that for the limited number of rut depth measurements available on national roads, the predictions given by the HDM-III model after calibration is not that favourable, with a R-Squared of 0,68 being obtained. As seen from the slope of the fitted line the HDM-III model tends to over predict for rut depth values below 5mm, and under predict for rut depth values above 5 mm. The limited data available as well as the difference in straight edge length is believed to be contributing to the poor correlation.

From Figure 5.9 it is evident that the correlation obtained for rut depth standard deviation is even worse, with a R-Squared value of 0,28 being obtained. It is believed that this is the result of the fact that the relationship between mean rut depth and rut depth standard deviation is a nonlinear relationship. With the

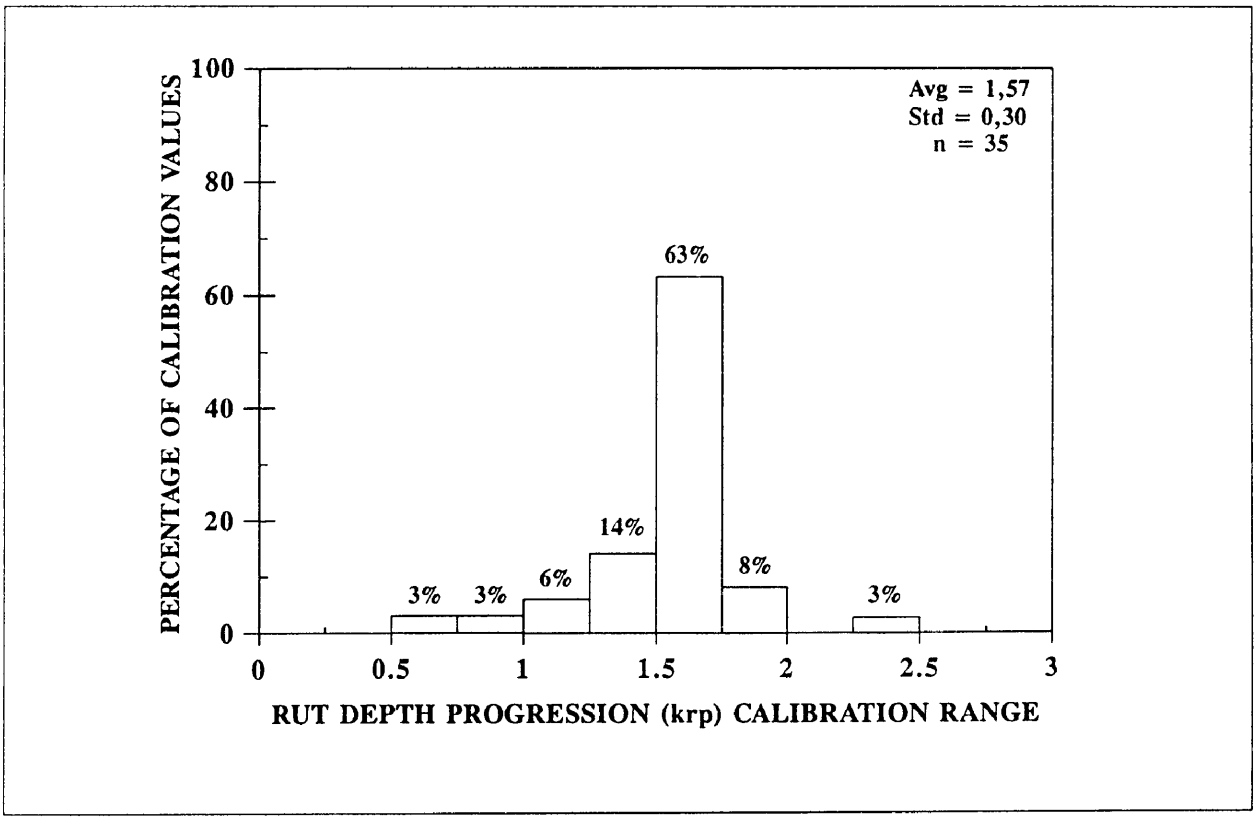

Figure 5.7: Distribution of rut depth progression calibration values for original surfacings.

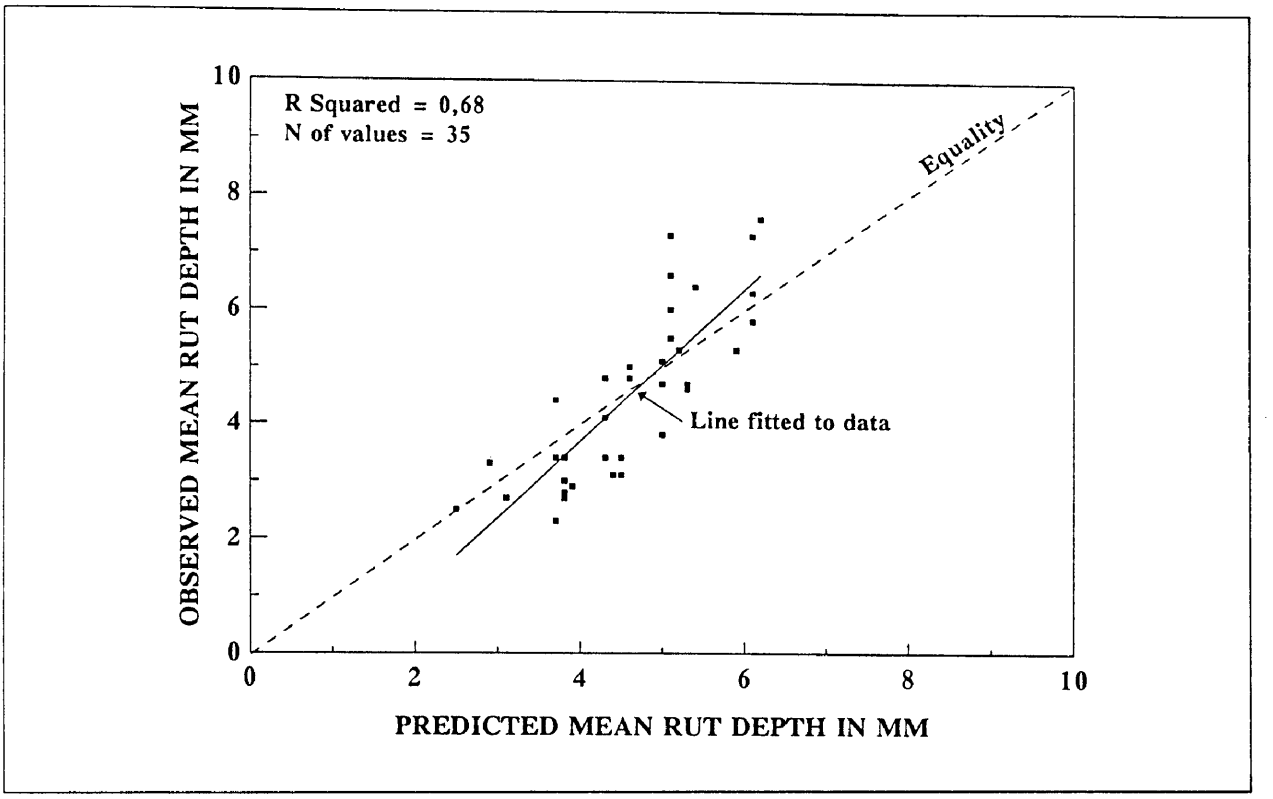

Figure 5.8: Comparison between predicted and observed values for mean rut depth.

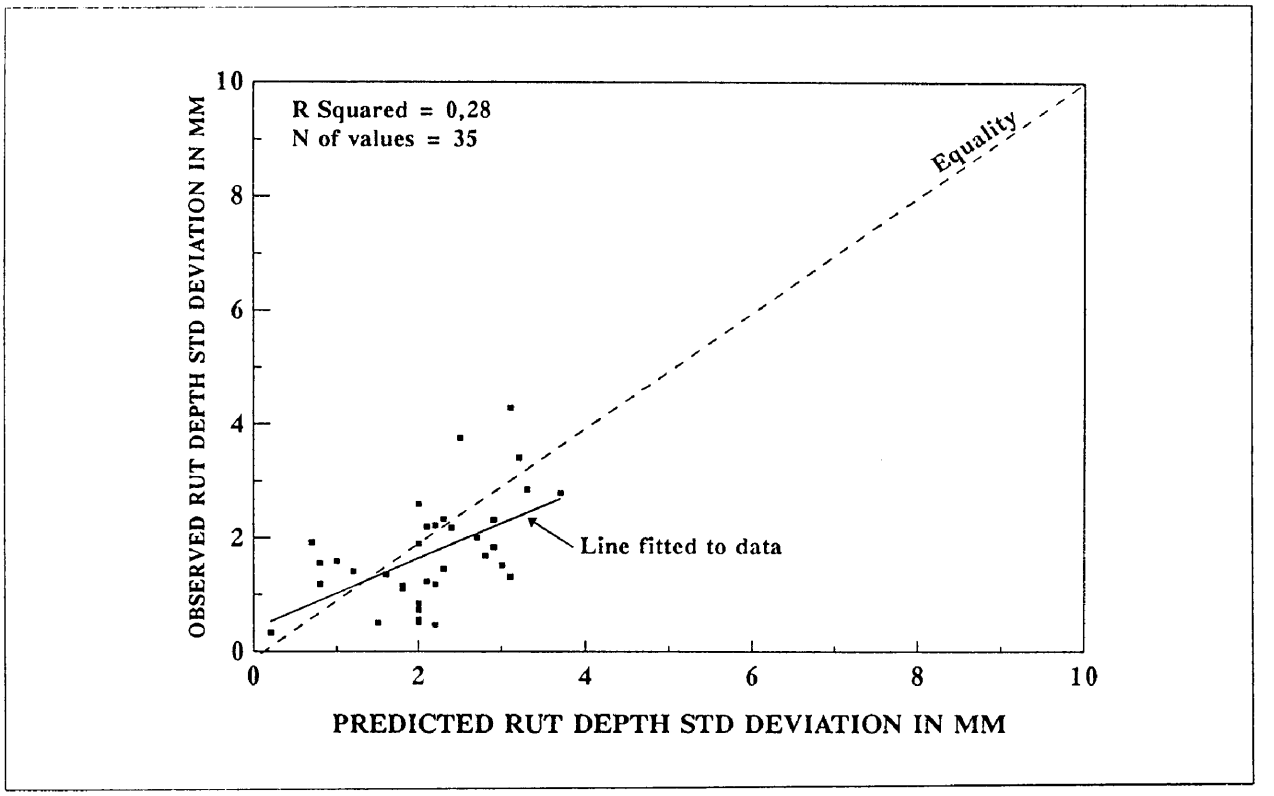

Figure 5.9: Comparison between predicted and observed values for rut depth standard deviation.

relationship being influenced by the fact that higher rut depth values have to be predicted by the HDM-III model to compensate for the difference in straight edge length.

The use of large scale rut depth measurements on a network level on national roads ceased in 1987. Since then the use of rut depth measurements were mainly limited to project level investigations due to time and cost considerations. From 1991 onwards rut depth is simply visually recorded over the network according to the definitions in the TMH-9 visual assessment manual, which resulted in data not being accurate.

Based on this and the results obtained during the sensitivity analysis in Chapter 3, which indicated that the roughness model was not that sensitive for variations in the mean rut depth measurements and only sensitive to a small extent for rut depth standard deviation, it is recommended that the calibration range in Table 5.3 be used for the rut depth progression factor (krp).

Table 5.3: Recommended range for calibration factor values of the rut depth model.

Pavement type	Rut depth progression (krp)
Original surfacings	1,5-1,75
Overlays and reseals	1,0

5.7 ROUGHNESS MODEL

As roughness is the last model in the modelling sequence, it gives an indication of the importance of the roughness model. This model combines the predictions of all the previous mentioned models into a single value, which forms the basis for the determination of vehicle operating costs. The HDM-III model allowed for two user specified calibration factors for the roughness model, namely:

- For roughness progression, kgp.
- For the environment related annual fractional increase in roughness, kge.

The environment related calibration factor, kge is fixed to certain values, defined on the basis of Thornthwaite moisture index, as summarised in Table

5.1. These environmental roughness calibration factors (Kge) determined for South African conditions, were used in the evaluation of the other models as mentioned previously. Since these environmental roughness calibration factors (Kge) are divided into different moisture regimes, it was decided to also evaluate the roughness progression calibration factor (kgp) for the different climatic areas. The climatic areas applicable for the study according to Thornthwaite's moisture classification were semi-arid, subhumid and humid.

Initially the pavement sections were evaluated individually based on the surfacing type, basecourse type and whether it was an original constructed surface layer or an overlay or reseal. No noticeable difference in performance existed between the different surfacing layers, basecourse layers or between original surfacings or overlays and reseals. Thus the calibration values for roughness progression (Kgp) were evaluated for all pavements irrespective of surfacing type, basecourse type or whether the surfacing was an original layer, overlay or reseal.

The results obtained for semi-arid areas are illustrated in Figure 5.10 for the pavement sections evaluated. From Figure 5.10 it is evident that for the number of sections evaluated, the roughness progression calibration factor (Kgp) followed a normal distribution with 85% of the calibration factor values falling within the range 0,8 to 1,2, with an average of 1,02. The average value obtained indicates that the observed roughness deterioration on South African national roads is equal to the value predicted by the HDM-III model.

Thus after calibrating the HDM-III model for local environmental conditions it seems that little or no calibration is needed for the roughness progression model. Thus the deterioration predicted by the HDM-III for traffic related distress seems to be similar to the deterioration observed on South African national roads. Furthermore the maintenance activity mentioned previously, employed on South African national roads did not allow the evaluation of the exponential nature of the roughness deterioration model. The reason being that when maintenance is conducted timeously, the deterioration of a pavement is kept to a more or less linear progression as seen in Figures C.2 to C.65 of Appendix C.

The results obtained for subhumid areas are illustrated in Figure 5.11 for the pavement sections evaluated. From Figure 5.11 it is evident that for the number

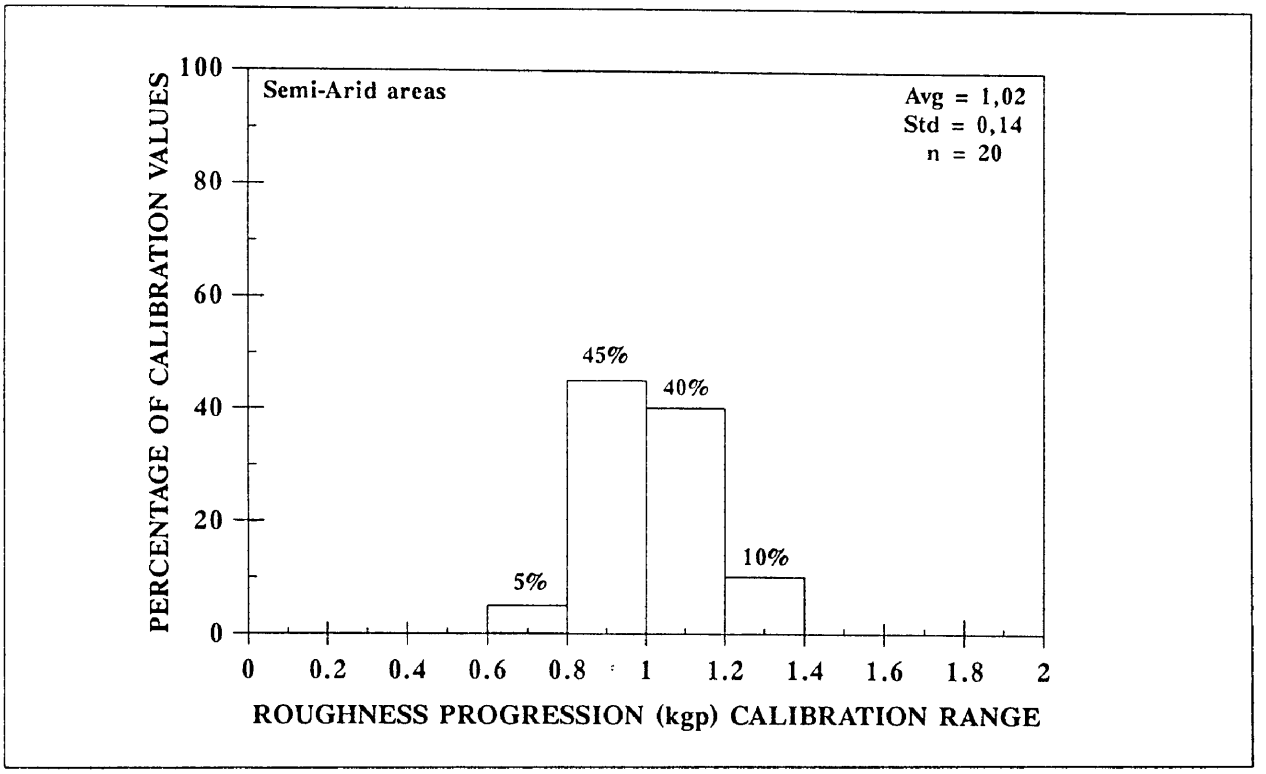

Figure 5.10: Distribution of roughness progression calibration values for semi-arid areas.

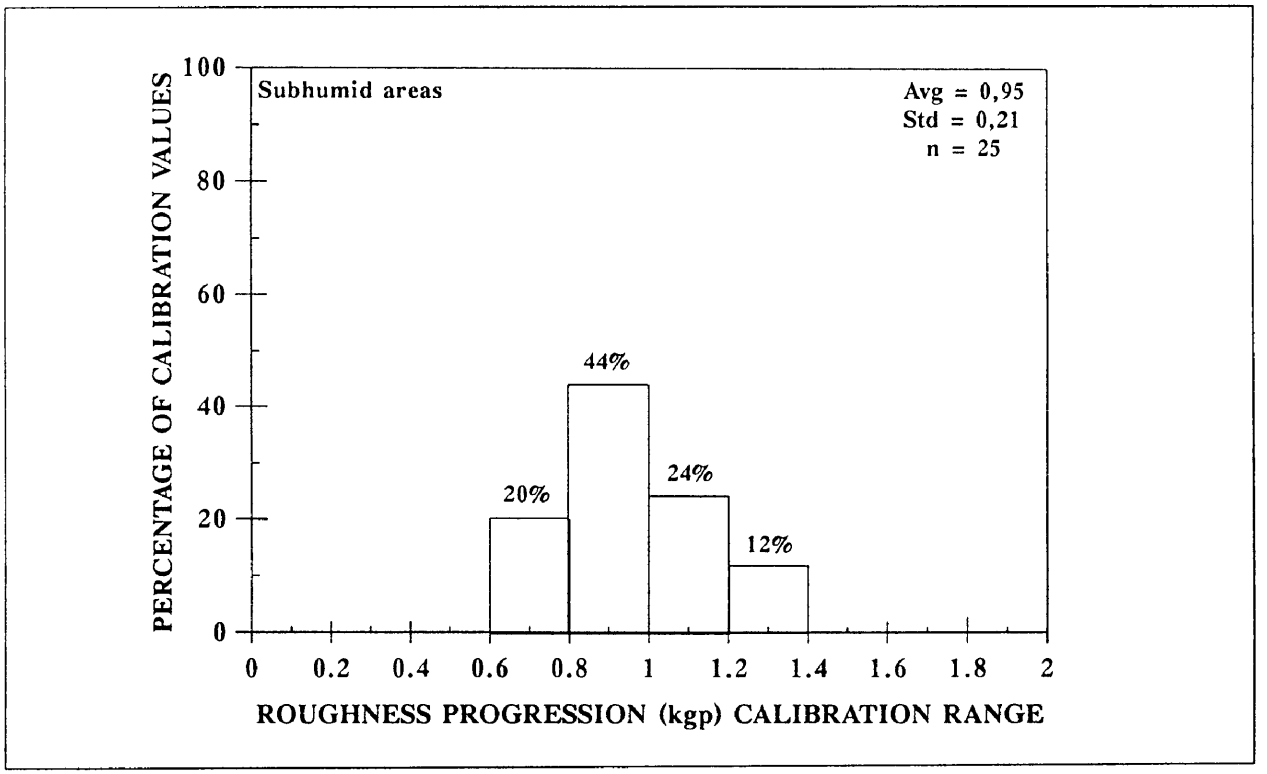

Figure 5.11: Distribution of roughness progression calibration values subhumid areas.

of sections evaluated, the roughness progression calibration factor (Kgp) followed a normal distribution with 88% of the calibration factor values falling within the range 0,6 to 1,4, with an average of 0,95. As with the semi-arid areas, the average value obtained for subhumid areas indicates that the observed roughness deterioration on South African national roads is more or less equal to the value predicted by the HDM-III model. Thus after calibrating the HDM-III model for local environmental conditions it once again seems that little or no calibration is needed for the roughness progression model.

The results obtained for humid areas are illustrated in Figure 5.12 for the pavement sections evaluated. From Figure 5.12 it is evident that for the number of sections evaluated, the roughnes progression calibration factor (Kgp) followed a normal distribution with 70% of the calibration factor values falling within the range 0,8 to 1,2, with an average of 0,99. As with the previous two moisture areas the average value obtained indicates that the observed roughness deterioration on South African national roads is more or less equal to the value predicted by the HDM-III model. Thus after calibrating the HDM-III model for local environmental conditions it once again seems that little or no calibration is needed for the roughness progression model.

Figure 5.13 illustrates the distribution of the roughness progression calibration (kgp) values for all climatic areas. As expected a normal distribution is obtained with 74% of roughness progression calibration factor (Kgp) values falling within the range 0,8 to 1,2. The average of all these pavement sections of 0,98 correlates well with the average values determined for the individual climatic areas. From this it can be concluded that in general it seems that no calibration is needed for the roughness progression calibration factor (kgp), after calibrating the environmental roughness progression factor. This indicates that the expected difference in behaviour between the different climatic areas are taken into consideration by the environmental roughness calibration factor (kge), which increases or decreases the rate of deterioration as required. The roughness progression calibration factor (kgp) value of 1,0 indicates that no decrease in roughness progression is needed for traffic related distress.

Based on the results obtained it is recommended that after calibrating the HDM-III model for local environmental conditions (Kge), little or no calibration is

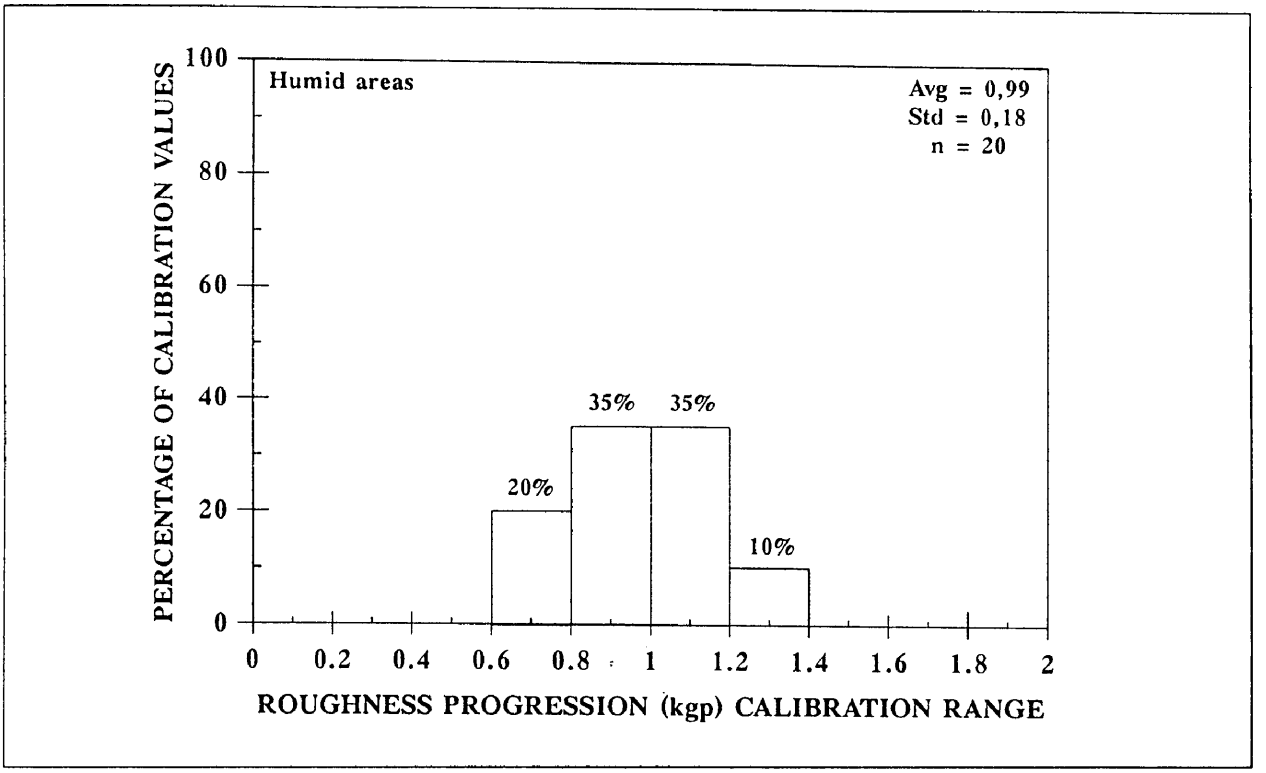

Figure 5.12: Distribution of roughness progression calibration values for humid areas.

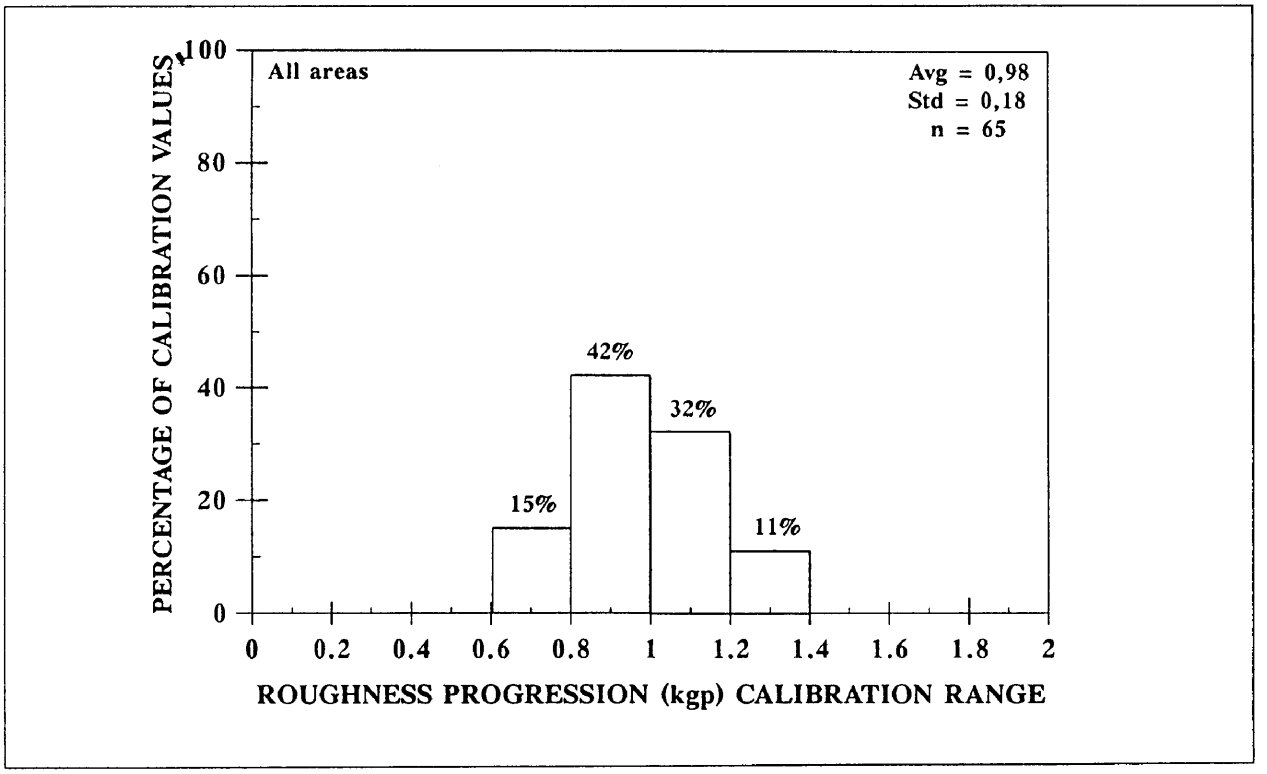

Figure 5.13: Distribution of roughness progression calibration values for all areas.

needed for traffic related distress. Thus a Kgp value of 1 is recommended for all moisture regimes. The calibration of each individual pavement section is still recommended, but being very time consuming the further refinement appears unjustifiable and unlikely to improve the closeness of fit significantly.

The ability of the HDM-III model to predict the roughness observed on national roads after calibration is illustrated in Figures 5.14 to 5.16 for each moisture regime, and in Figure 5.17 for all pavement sections evaluated. As seen from the Figures a R-Squared value of 0,88 and higher was obtained. This indicated that after calibration, the HDM-III model is capable of very accurately predicting the roughness deterioration observed on South African national roads. Thus the use of the HDM-III deterioration models for predicting the deterioration observed on South African national roads is highly recommended, as is evident in Figure 5.18 (Also see C.2 to C.65 in Appendix C), in which the observed roughness is compared with the predicted roughness for each individual pavement section evaluated. It is also obvious from these Figures that as mentioned previously the maintenance activity employed on South African national roads did not allow the evaluation of the exponential nature of the HDM-III models.

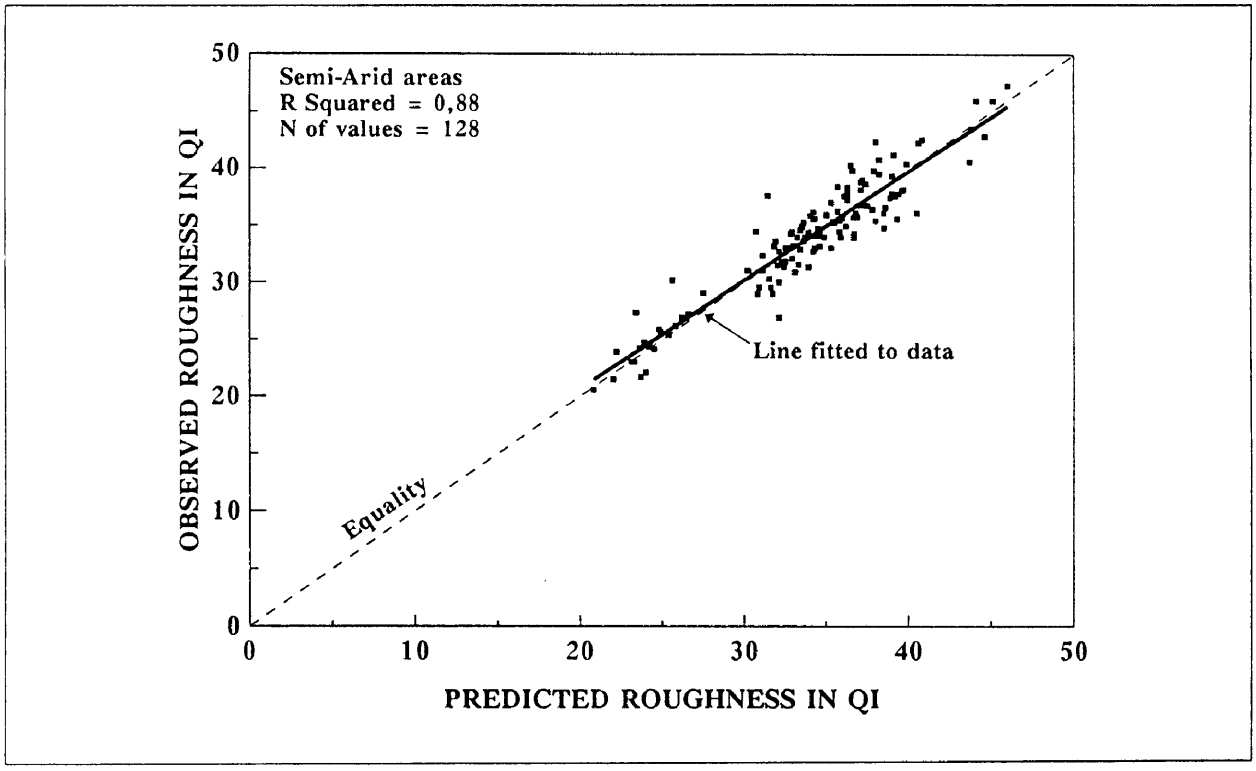

Figure 5.14: Comparison between predicted and observed roughness values for semi-arid areas.

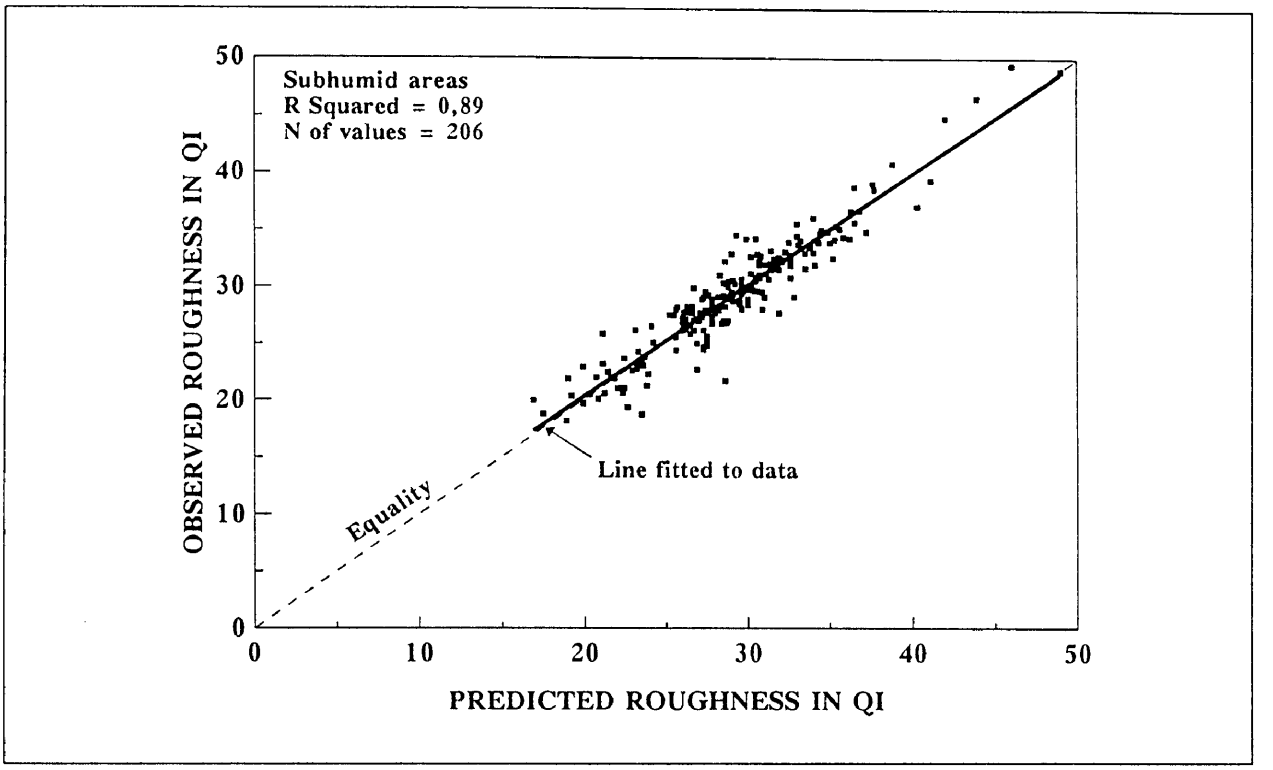

Figure 5.15: Comparison between predicted and observed roughness values for subhumid areas.

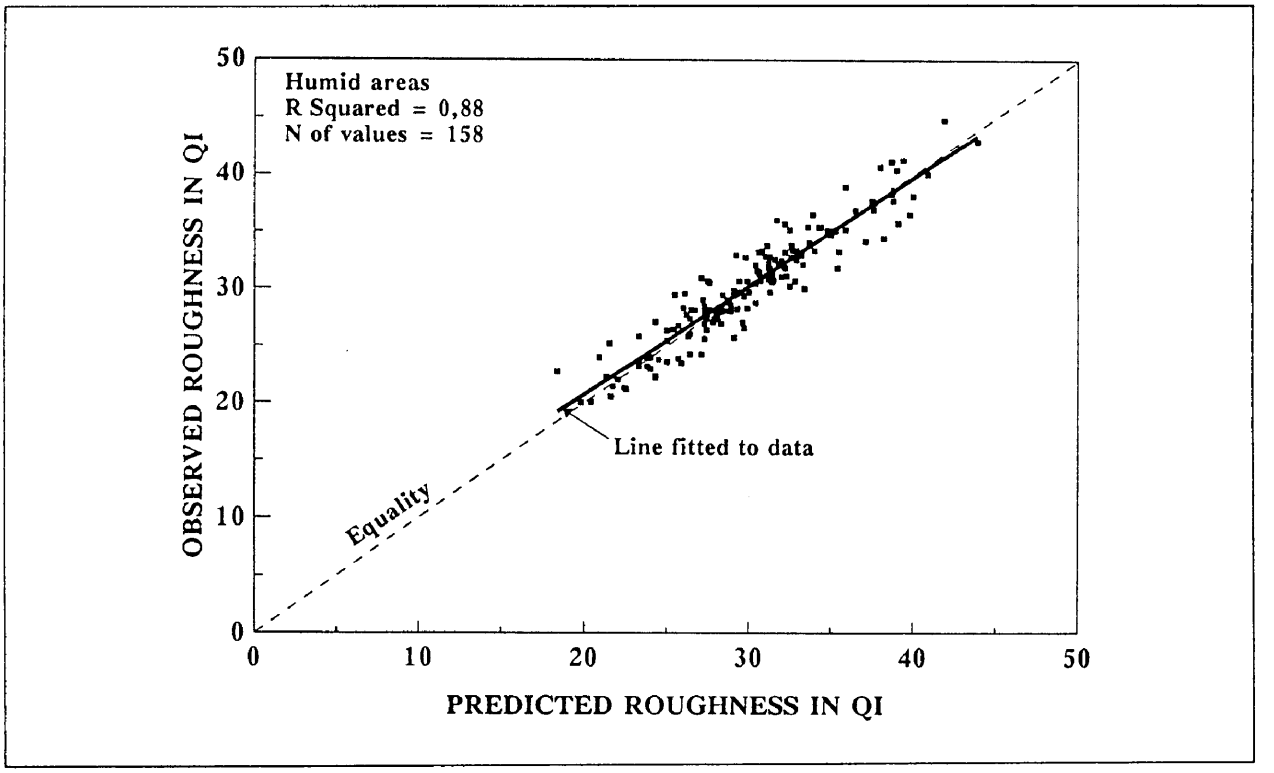

Figure 5.16: Comparison between predicted and observed roughness values for humid areas.

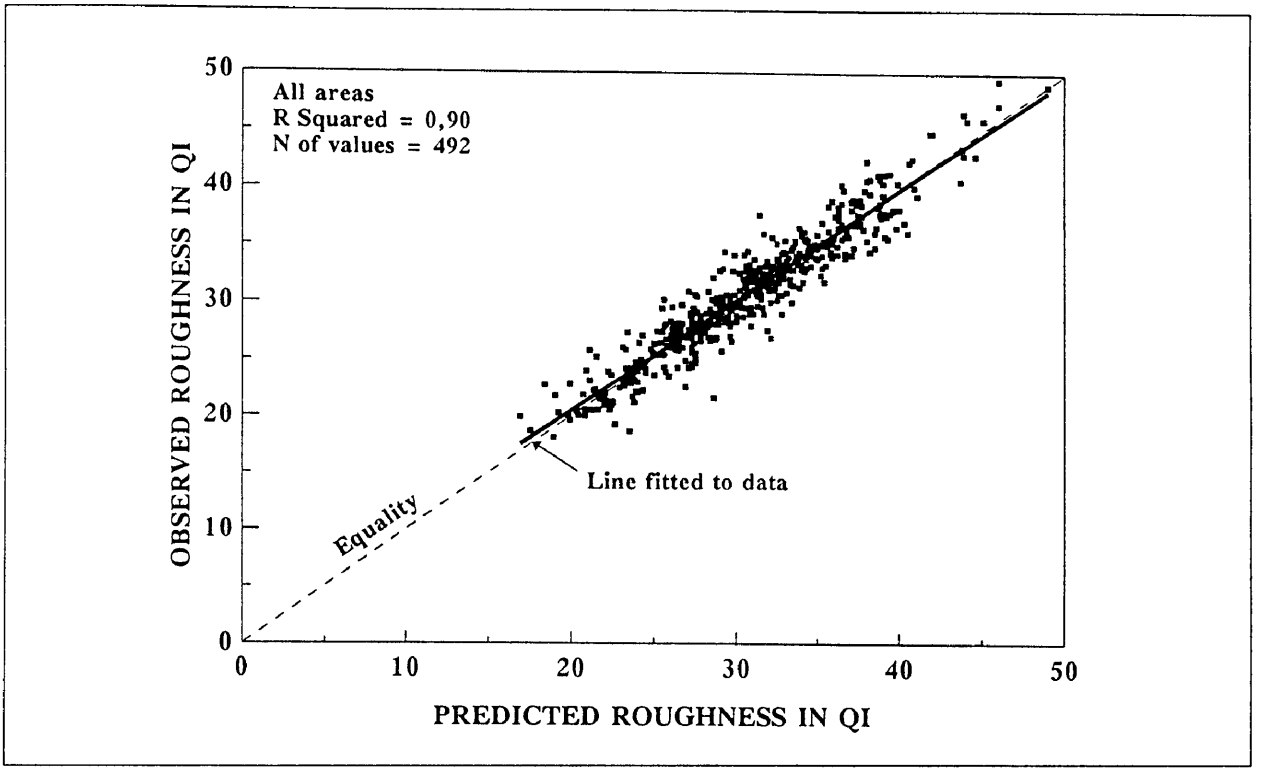

Figure 5.17: Comparison between predicted and observed roughness values for all areas.

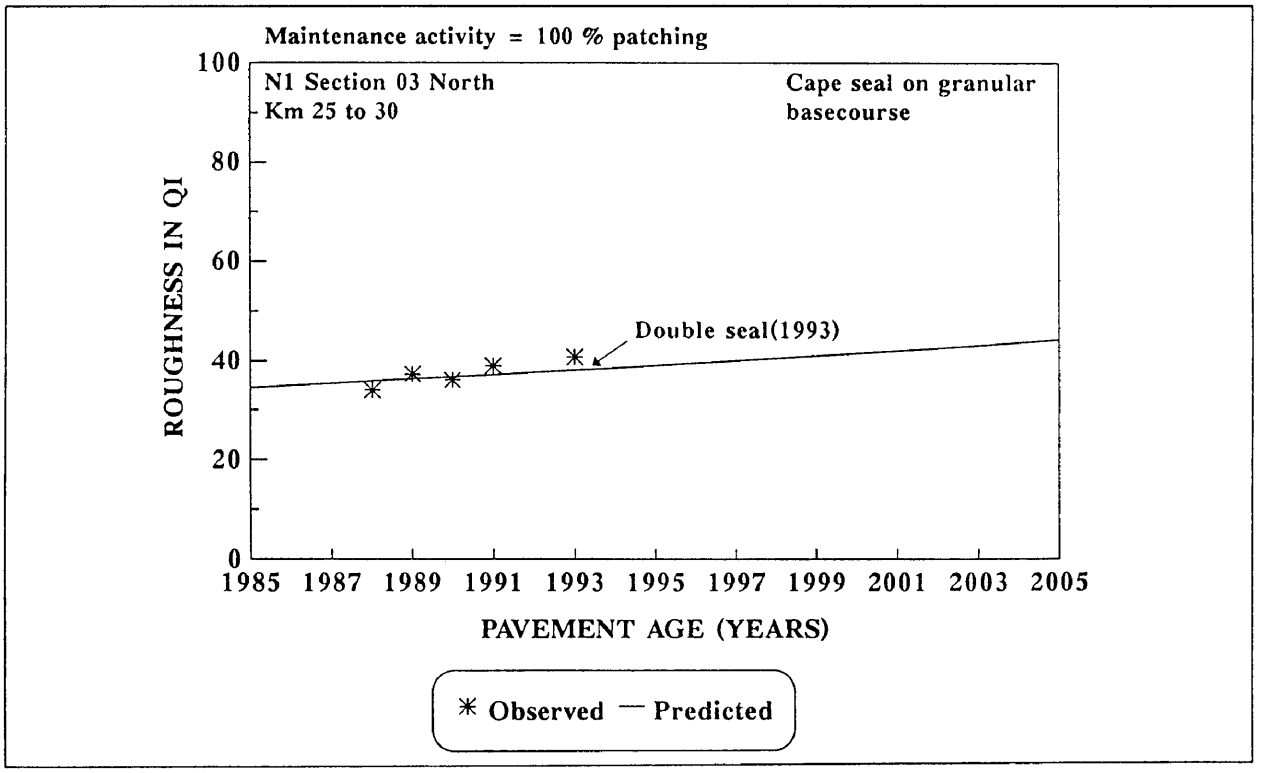

Figure 5.18: Typical illustration of comparison between observed and predicted roughness values for national route 1 section 03 north.

5.8 CONCLUSIONS FROM COMPARISON

The main conclusion from the comparison of observed values with predicted values, is that the HDM-III models are capable of very accurately predicting the observed deterioration on South African national roads, but that for most models calibration is needed for local conditions, especially the environmental roughness calibration factor (Kge).

Despite the favourable correlations obtained for some of the HDM-III models, others could not be calibrated as a result of the lack of suitable South African deterioration data. Thus for the ravelling, potholing, and to certain extent cracking models additional research should be conducted in determining calibration values for some models, and for other models more accurate calibration values.

The recommended calibration ranges obtained for the different calibration factor values are summarised in Table 5.4, where a value of 1 indicates a default value (Except for roughness progression (Kgp)).

Table 5.4: Recommended calibration factor ranges for the different HDM-III models.

HDM-III model	Climatic area	Original surfacings	Overlays & Reseals
Environmental (Kge)	Semi-arid Subhumid Humid	0,39 0,61 0,87	0,39 0.61 0,87
Cracking (kci) Initiation	All	1,00-1,50	0,4-0,8
Cracking (kci) Initiation	All	0,75-1,25	0,4-0,8
Cracking (kcp) Progression	All	0,1-0,3	0,3-0,7
Ravelling (kvi)	All	1,0	1,0
Potholing (kpp)	All	1,0	1,0
Rutting (krp)	All	1,50-1,75	1,0
Roughness (kgp)	All	1,0	1,0

As seen from Table 5.4 it can be concluded that the environmental roughness calibration factor (Kge) in each instance is nearly half of the value recommended by Paterson (1987) for that climatic area. Thus the influence of the environment on the pavement deterioration is only about half of what is predicted by the HDM-III model. Furthermore it can be concluded that for the pavements used on South African national roads the period before cracking initiation seems to be longer than the period predicted for original surfacings, and shorter for overlays and reseals. Once cracked, the rate of cracking progression is lower, than the values predicted by the HDM-III model for the same traffic volume. As seen for rutting a value greater than 1 was obtained. It is believed that this is result of the fact that in South Africa a 2 metre straight edge is used in comparison with a 1,2 metre straight edge used in the development of the model.

For roughness progression (Kgp) it can be concluded that the different climatic areas seem to have a similar calibration value. This indicates that the expected difference in behaviour between the different climatic areas are taken into consideration by the environmental roughness calibration factor (kge), which increases or decreases the rate of deterioration as required.

Finally it can be concluded that after calibration the HDM-III model has excellent capabilities for predicting the observed deterioration on South African national roads, although the exponential nature of the models could not be evaluated due to maintenance activity employed on national roads.

CHAPTER 6

CONCLUSIONS AND RECOMMENDATIONS

6.1 CONCLUSIONS

The objective of the study was to use the information on flexible pavements obtained from the Department of Transport's extensive pavement management database, covering the deterioration of the national road network over the past 15 years, to achieve the following:

- To evaluate the applicability of models developed internationally for predicting the deterioration of the national road network in terms of roughness, cracking and rutting under the normal traffic and environmental conditions experienced on the in-service pavements.

- To develop calibration factors from long term observations, for the models identified as applicable for South African conditions if the models are inappropriate for predicting the deterioration trends observed on the South Africa national road network.

6.1.1 Literature review

The literature review only included international deterioration models developed from the deterioration results of in-service pavements under the normal traffic spectrum, avoiding models developed from accelerated testing with stationary devices. The reasons for avoiding these models are that the long-term effects are virtually eliminated (these are primarily environmental but also include effects of the rest periods or vehicle headway), and that the unrepresentative traffic loading regimes can distort the behaviour of the pavement materials, which is often stress dependent (Paterson, 1987). Models developed from the following studies were evaluated:

- AASHO Road Test
- The Kenya study
- Brazil-UNDP study
- Texas study

The main conclusion from the literature survey was that the accurate prediction of pavement deterioration is of world wide concern. This is evident in the number of studies conducted over the years with each of these studies contributing towards the better understanding of the deterioration of pavements. Of all the models studied that were developed from major studies it was concluded that the incremental models developed during the Brazil study, were the most appropriate for further evaluation under South African conditions. These models were selected because:

- they were developed from the large comprehensive source of data obtained from the Brazil-UNDP study which employed advanced theoretical and statistical methodologies to generate a database covering a broad range of road characteristics and vehicle types;

- they were validated across eight major independent data sets from widely differing climates, ranging from arid nonfreezing to wet freezing, indicating the fundamental plausibility of the models and their transferability (Paterson, 1987);

- the incremental form of the models allowed the year-by-year simulation of pavement deterioration, thus making the models excellent for application in a pavement management system, and

- they are the deterioration models incorporated into the HDM-III model because they provided the best representation of time and traffic interactions.

6.1.2 Sensitivity analysis of model parameters

To enable the local adoption of the road deterioration and maintenance submodel developed during the Brazil study and incorporated into the Highway Design and Maintenance Standards Model (HDM-III), it was necessary to evaluate the sensitivity of the HDM-III model to changes in the different parameters composing the road deterioration and maintenance submodel.

From the sensitivity analysis conducted the results obtained for the incremental roughness model is the most important as a result of the influence of roughness

on vehicle operating costs. The results obtained from the sensitivity analysis indicate that the incremental roughness prediction model incorporated into the HDM-III model tends to be insensitive to changes in most parameters. There are, however, parameters for which changes in a certain range of the parameter require greater accuracy. In some instances the accuracy depends on the length of the analysis period, with the prediction of roughness being more sensitive the longer the period. Despite the insensitivity of the model all input data should be determined as accurately as possible. The following accuracy requirements are applicable when determining the input data:

- The correlation between deflection and structural number needs to be evaluated for South African conditions, as a result of the noticeable influence of deflection on cracking and especially rutting. Where available measured deflection values should be employed.
- One should determine as accurately as possible whether cracking has initiated on a pavement for both all and wide cracking. For cracked pavements the model seems insensitive.
- The structural number should be determined as accurately as possible if it is below 3,5, and where available additional information should be used for these weaker pavement types.
- Subgrade CBR values below 20 % should be determined as accurately as possible for in situ conditions for pavements with a modified structural number below 4.
- The prediction of roughness is sensitive to the traffic loading. This indicates that both the initial number of vehicles, as well as the expected traffic growth rate should be determined as accurately as possible.
- The initial roughness measurement for each pavement should be determined as accurately as possibly.

6.1.3 Development of validation procedure

To investigate the local applicability of the HDM-III deterioration and maintenance submodel, which is based on empirically derived equations mainly from measurements conducted in Brazil, its predictions must be compared against the locally observed values. To enable this a validation procedure was needed according to which the format of existing data could be changed, to the format required by HDM-III model. In addition information not available on the database, could be generated.

The main conclusion from the development of a validation methodology for evaluating the applicability of HDM-III model predictions for South African conditions is that:

- The HDM-III environmental roughness calibration factor (Kge) should first be calibrated for local moisture regimes. Thereafter, each model of the HDM-III deterioration and maintenance submodel should be evaluated and calibrated individually, and not just the incremental roughness model.

- The deterioration of a pavement section should be predicted from the year it was opened to traffic, allowing the incorporation of all measured values, as well as the long term aging effects.

- The availability of suitable data for the development of accurate correlations between the format of South African visual data and the HDM-III model input requirement, is limited.

6.1.4 Comparison of observed values with predicted values

The main conclusion from the comparison of observed values with predicted values, is that the HDM-III models are capable of very accurately predicting the observed deterioration on South African national roads, but that for most models calibration is needed for local conditions, especially for the environmental roughness calibration factor (Kge).

Despite the favourable correlations obtained for some of the HDM-III models, others could not be calibrated as a result of the lack of suitable South African deterioration data. Thus for the ravelling, potholing, and to certain extent cracking models additional research should be conducted for determining calibration values for some models, or more accurate calibration values for other models.

The recommended calibration ranges obtained for the different calibration factor values are summarised in Table 6.1, where a value of 1 indicates a default value (Except for roughness progression) As seen from Table 6.1 it can be concluded that for the pavements used on South African national roads the period before cracking initiation seems to be delayed for a longer period, and once cracked, the rate of cracking progression is lower, than the values predicted by the HDM-III model for the same traffic volume.

Table 6.1: Recommended calibration factor ranges for the different HDM-III models.

HDM-III model	Climatic area	Original surfacings	Overlays & Reseals
Environmental (Kge)	Semi-arid Subhumid Humid	0,39 0,61 0,87	0,39 0,61 0,87
Cracking (kci) Initiation	All	1,00-1,50	0,4-0,8
Cracking (kcp) Progression	All	0,1-0,3	0,3-0,7
Ravelling (kvi)	All	1,0	1,0
Potholing (kpp)	All	1,0	1,0
Rutting (krp)	All	1,50-1,75	1,0
Roughness (kgp)	All	1,0	1,0

As seen for rutting a value greater than 1 was obtained. It is believed that this is result of the fact that in South Africa a 2 metre straight edge is used in comparison with a 1,2 metre straight edge used in the development of the model.

For roughness progression (Kgp) it can be concluded that the different climatic areas seem to have a similar calibration value. This indicates that the expected difference in behaviour between the different climatic areas are taken into consideration by the environmental roughness calibration factor (kge), which increases or decreases the rate of deterioration as required.

6.2 RECOMMENDATIONS

Based on the results obtained for the limited number of sections included into the study, it is recommended that the HDM-III models should be considered for incorporation into a balanced expenditure programme for the national roads of South Africa. The incorporation of these models would be simple, since most of the models only need calibration for them to be applicable to local conditions. The incorporation of these models would allow for the prediction of the rate of deterioration of a pavement, and the nature of the changes so that the timing, type and cost of maintenance needs could be estimated.

Before the full scale incorporation of these models it is however recommended that urgent attention be given to the following:

- It is of utmost importance that traffic axle weight classification studies be conducted more frequently at the same location on all major roads, and not only on request. This will benefit both future predictions, as well as the evaluation of the performance of existing pavement designs.

- Roughness measurements be conducted just after construction, special maintenance or rehabilitation, as this will allow more accurate future deterioration predictions. It will also be of benefit to future research regarding the influence of initial roughness on pavement deterioration.

- Research should be conducted to determine a more accurate correlation between deflection and the modified structural number (SNC) for typical South African pavements designs. The research should especially be directed towards correlating Falling Weight Deflection measurements and should include the evaluation of the influence of temperature and asphalt thickness on the deflection measurements.

- Research should be conducted into the determination of correlation values for converting the degree numerical ratings used in South Africa, to percentage of pavement area.

CHAPTER 7

REFERENCES

AASHO ROAD TEST: Report 5, 1962, Pavement Research, Highway Research Board, Special report 61E, National Academy of Science, Washington D.C.

AMERICAN ASSOCIATION OF STATE HIGHWAY AND TRANSPORTATION OFFICIALS (AASHTO), 1986, AASHTO interim guide for the design of pavement structures, AASHTO, Washington D.C.

ABAYNAYAKA, S.W., 1976, Some techniques for measuring vehicle operating cost and road deterioration parameters - With particular reference to developing countries, TRRL supplementary report 193 UC, Transportation and Road Research Laboratory, England.

COMMITTEE OF STATE ROAD AUTHORITIES (CSRA), 1984, Structural design of interurban and rural pavements, TRH 4, Department of Transport, Pretoria.

COMMITTEE OF STATE ROAD AUTHORITIES (CSRA), 1991, Flexible pavement rehabilitation investigation and design , Draft TRH 12 (unpublished), Department of Transport, Pretoria.

COMMITTEE OF STATE ROAD AUTHORITIES (CSRA), 1991, Traffic loading for pavement and rehabilitation design, TRH 16, Department of Transport, Pretoria.

COMMITTEE OF STATE ROAD AUTHORITIES (CSRA), 1992, Pavement management systems: Standard visual assessment manual for flexible pavements, TMH 9, Department of Transport, Pretoria.

DEPARTMENT OF TRANSPORT, 1984, Pavement management systems: Manual for the visual assessment of pavement distress, M3-1, Department of Transport, Pretoria.

FREEME, C.R., 1983, Evaluation of pavement behaviour for major rehabilitation of roads, NITRR Technical Report RP/19/83, CSIR, Pretoria.

GEIPOT, 1982, Research on the interrelationships between costs of highway construction, maintenance and utilisation. Final Report, Ministry of Transport, Brasilia.

GELDENHUYS, J., JORDAAN, G.J., GRÄTER, S.F., LOURENS, J.P.. and STRAUSS, P.J., April 1992, An initial evaluation of the bonuses and penalties for contractors as related to the riding quality of newly constructed roads, South African Roads Board, RDAC PR 91/255, Pretoria.

GEORGE, K.P., RAJAGOPAL, A.S. and LIM, L.K., 1989, Models for predicting pavement deterioration, Transportation Research Record 1215, Washington, D C.

HIDE, H, ABAYNAYAKA, S.W., SAYER, I. and WYATT, R., 1975, The Kenya Road Transport Study: Research on vehicle operating costs, TRRL Report LR 674, Transportation and Road Research Laboratory, England.

IRWIN, L.H., 1983, Users guide to MODCOMP2: Version 2.1, Local Roads Programme, Cornell University, Ithaca, New York.

HODGES, J.W., ROLT, J. and JONES, T.E., 1975, The Kenya Road Transport Cost Study: Research on road deterioration, Laboratory Report 673, Transportation and Road Research Laboratory, England.

JORDAAN, G.J. and VAN AS, S.C., 1993,A practical approach for the determination of deflection test frequencies for pavement evaluations, Paper 4C/3, 1993 Annual Transportation Convention, Pretoria.

JORDAAN, G.J., April 1993, Users manual for the South African mechanistic pavement rehabilitation design method, South African Roads Board, RDAC IR 91/243, Pretoria.

LYTTON, R.L., MICHALAK, C.H. and SCULLION, T., 1982, The Texas Flexible Pavement System. Proceedings Fifth International Conference on Structural Design of Asphalt Pavements. Vol 1, The University of Michigan and the Delft University of Technology, Ann Arbor.

PARSLEY, L. and ROBINSON, R., 1982, The TRRL road investment model for developing countries (RTIM2), Laboratory Report 1057, Transport and Road Research Laboratory, England.

PATERSON, W.D.O., December 1987, Road deterioration and maintenance effects: Models for planning and management, World Bank, Washington D.C.

ROHDE, G.T., July 1992, Bowler users guide: Version 2, BIS (Pty) Ltd, Pretoria.

ROHDE, G.T., July 1994, Determining a pavements structural number and the subgrade strength from falling weight deflection testing, Paper 4D/5, 1994 Annual Transportation Convention, Pretoria.

TEXAS RESEARCH AND DEVELOPMENT FOUNDATION, 1980, Final Report V: Pavement and Maintenance studies, Research on the interrelationships between costs of highway construction, maintenance and utilisation, Empresa Brasileria de Planejamento de Transportes-GEIPOT, Brasillia.

VAN NIEKERK, P.E. and VISSER, A.T., March 1992, Dynamic effects of heavy vehicles on road pavements, South African Roads Board, RDAC PR 91/280, Pretoria.

VISSER, A.T., 1982, A correlation study of roughness measurements with an index obtained from a road profile measured with rod and level, Technical Report RC/2/82, National Institute for Transport and Road Research, Pretoria.

VIDELA, C., ECHEVERRIA, G. and GAETE, R., 1991, Calibration of asphalt pavement behaviour models in Chile, Paper 4B/4, 1991 Annual Transportation Convention, Pretoria.

WALKER, R.N. and CURTAYNE, P.C., 1986, Status of pavement management in South Africa, Paper 3B/II, 1986 Annual Transportation Convention, Pretoria.

WATANATADA, T, HARRAL, C.G., PATERSON, W.D.O., DHARESHWAR, A.M., BHANDARI, A. and TSUNOKAWA, K., December 1987, The highway design and maintenance standards model: Volume 1-Description of the HDM-III Model, World Bank, Washington D.C.

APPENDIX A

Sensitivity analysis results

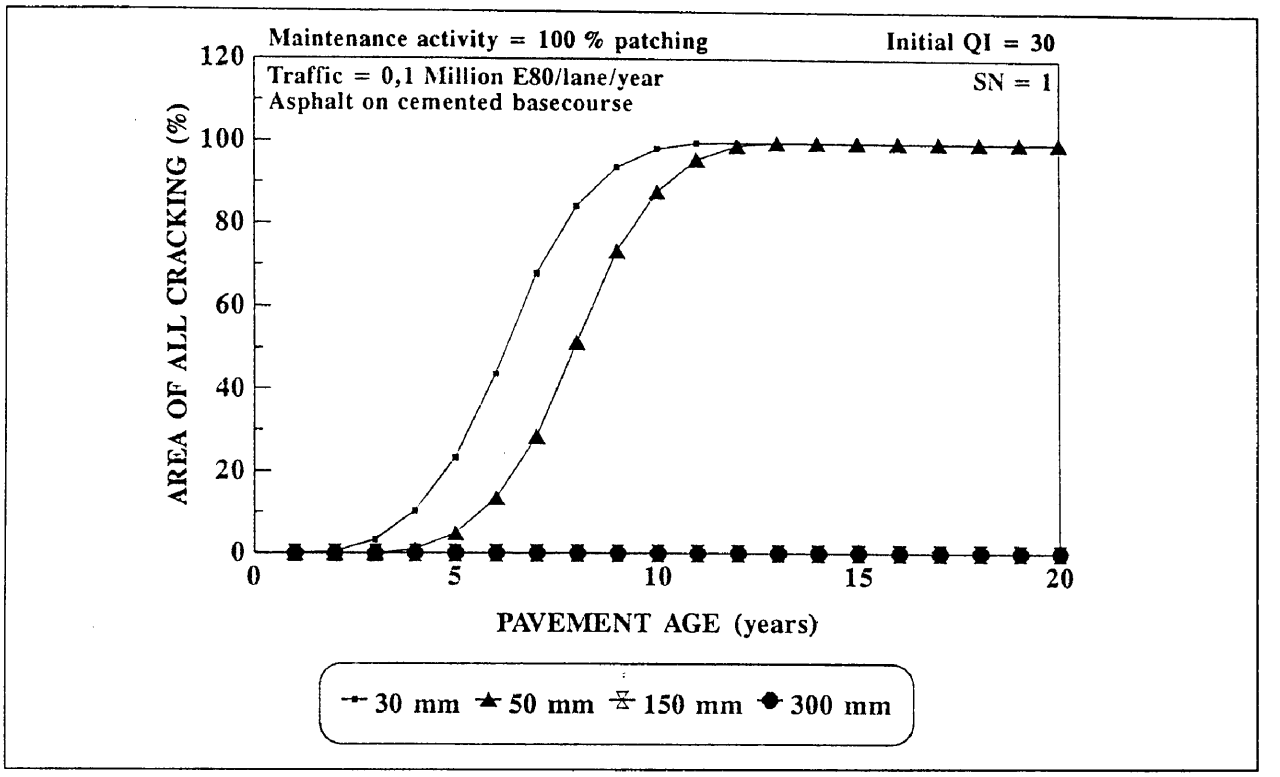

Figure A.1: Sensitivity of all cracking model to the thickness of bituminous surfacing for SN = 1 under light traffic.

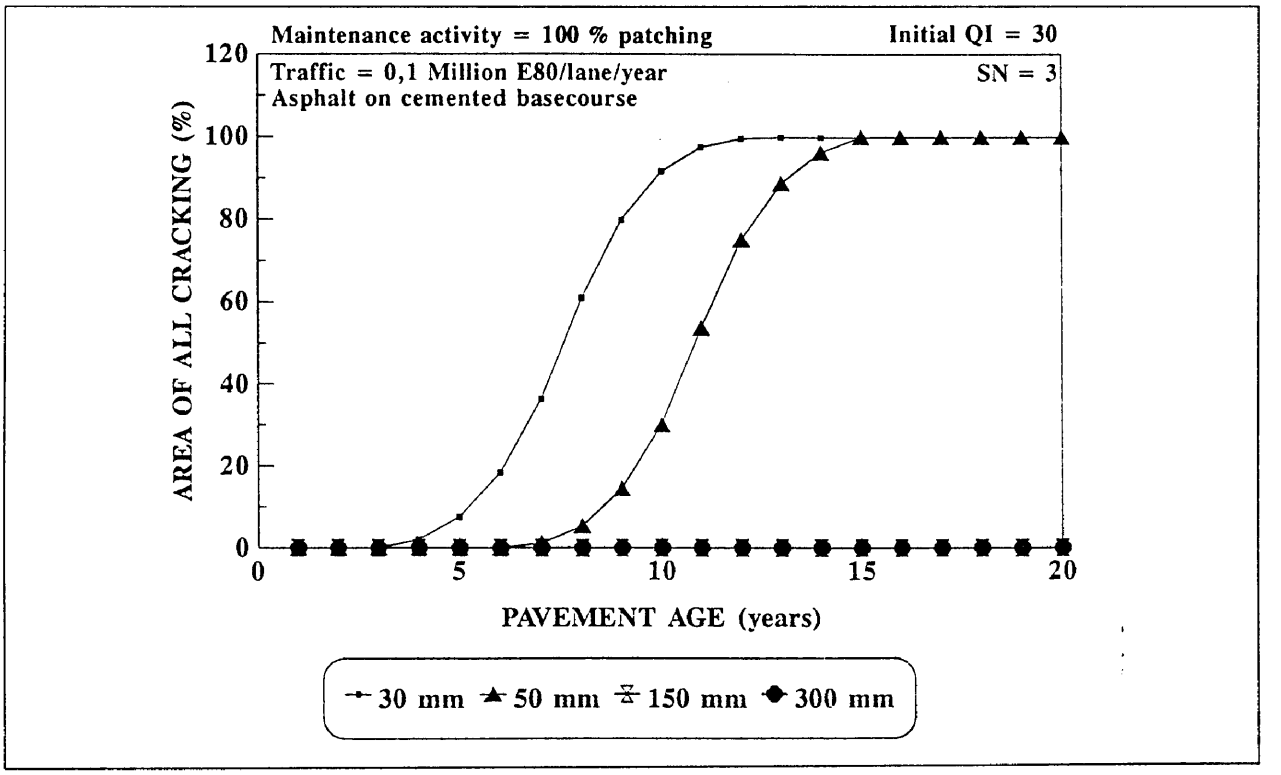

Figure A.2 Sensitivity of all cracking model to the thickness of bituminous surfacing for SN = 3 under light traffic.

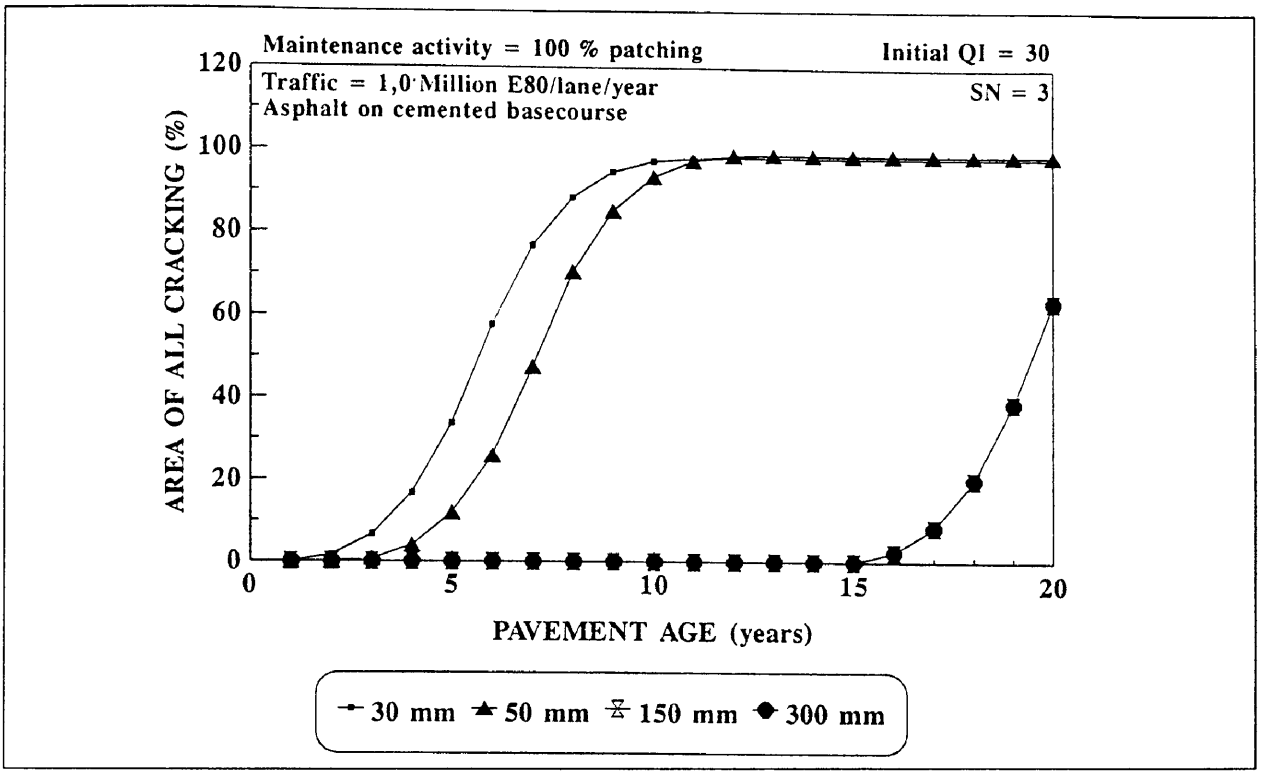

Figure A.3: Sensitivity of all cracking model to the thickness of bituminous surfacing SN = 3 under heavy traffic.

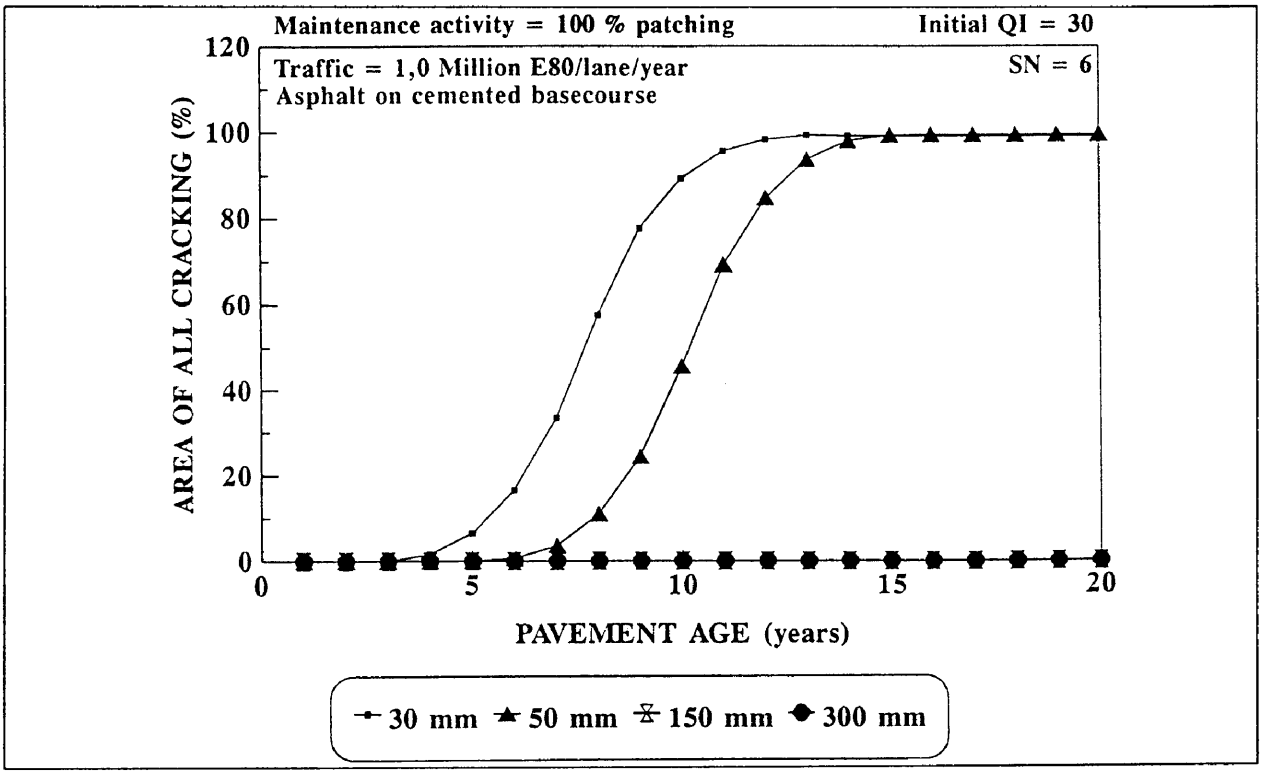

Figure A.4: Sensitivity of all cracking model to the thickness of bituminous surfacing for SN = 6 under heavy traffic.

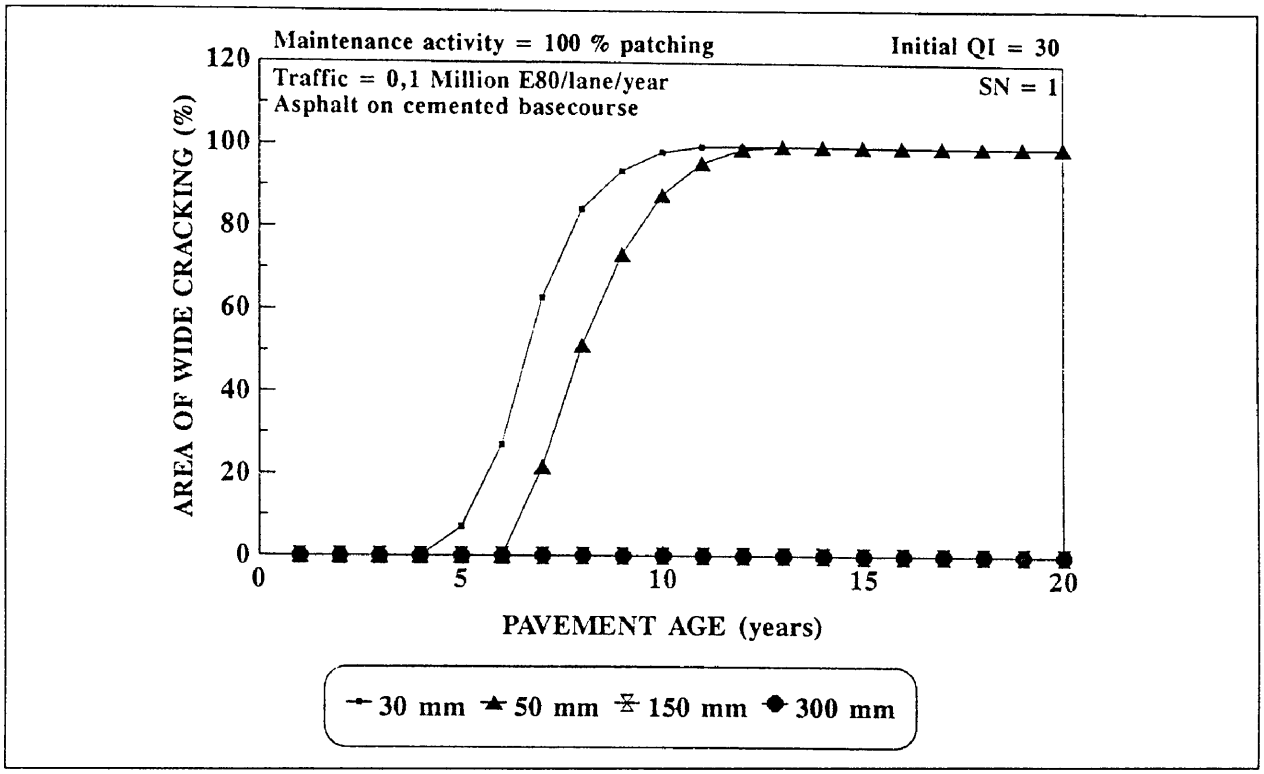

Figure A.5: Sensitivity of wide cracking model to the thickness of bituminous surfacing for SN = 1 under light traffic.

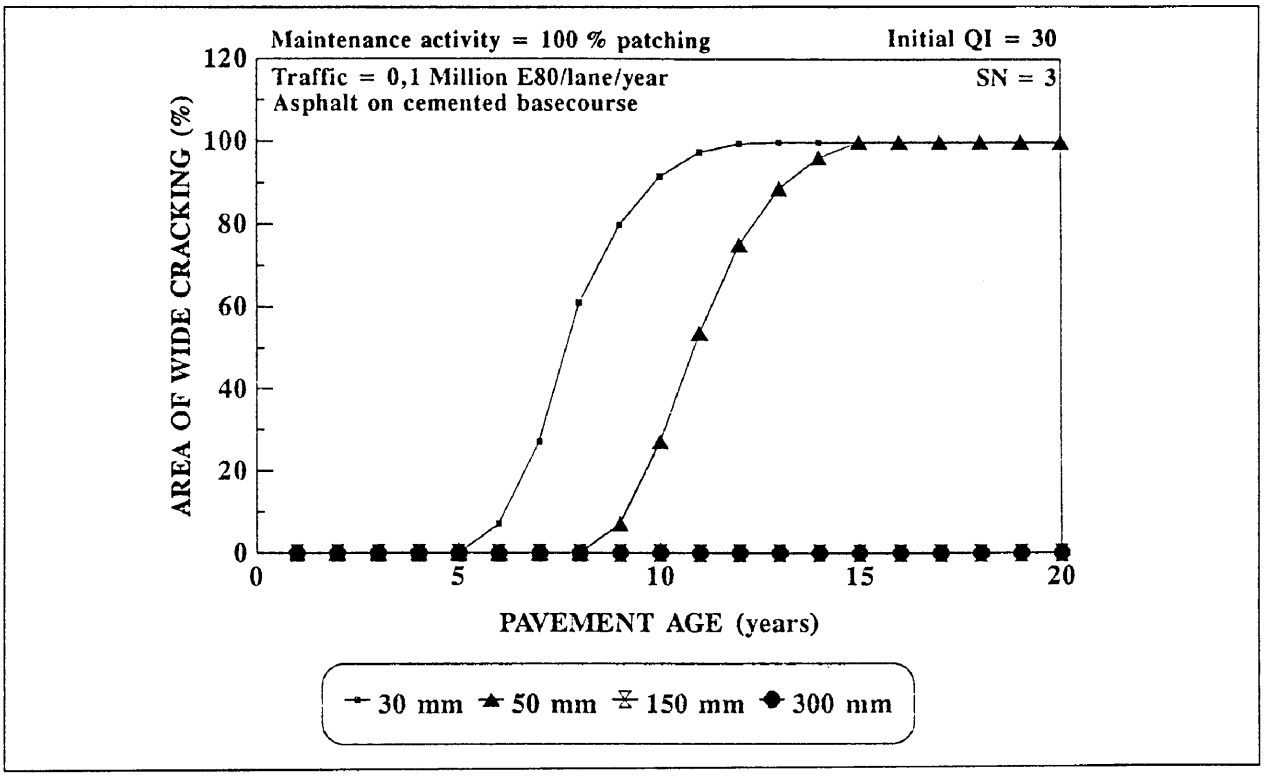

Figure A.6: Sensitivity of wide cracking model to the thickness of bituminous surfacing for SN = 3 under light traffic.

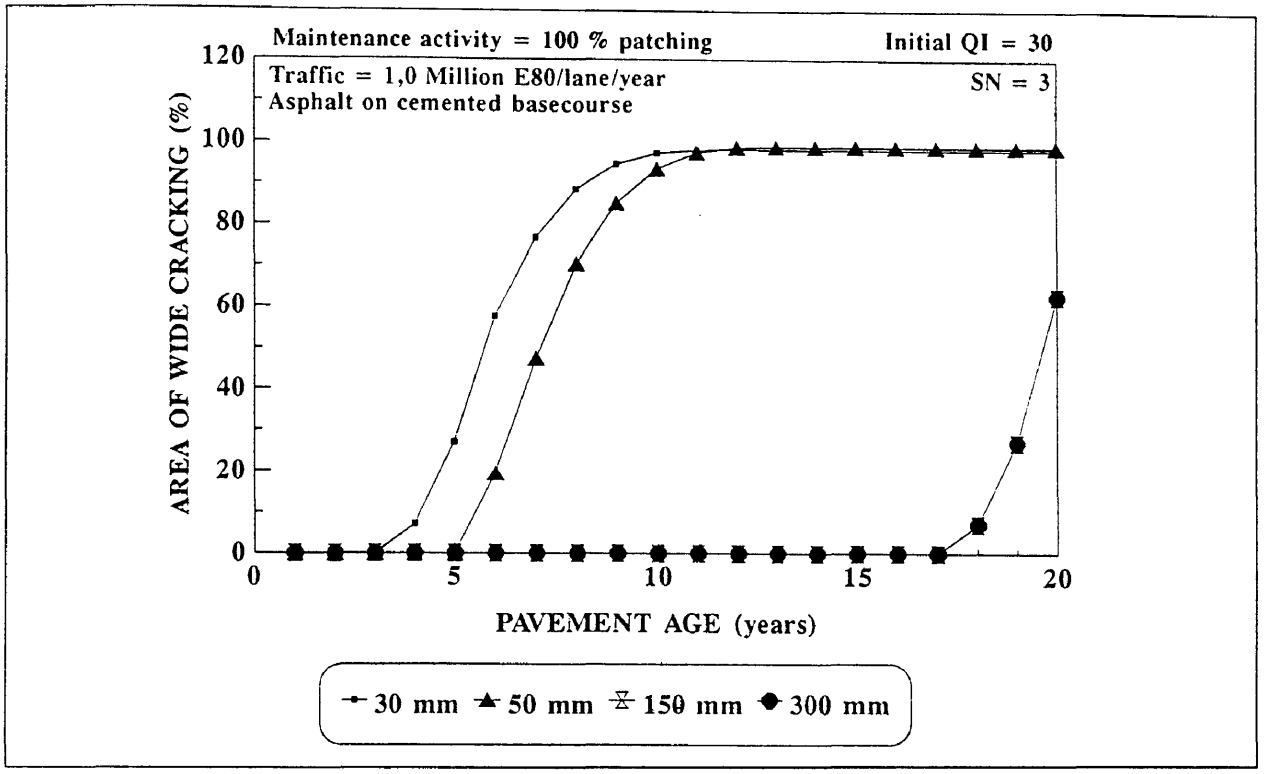

Figure A.7: Sensitivity of wide cracking model to the thickness of bituminous surfacing for SN = 3 under heavy traffic.

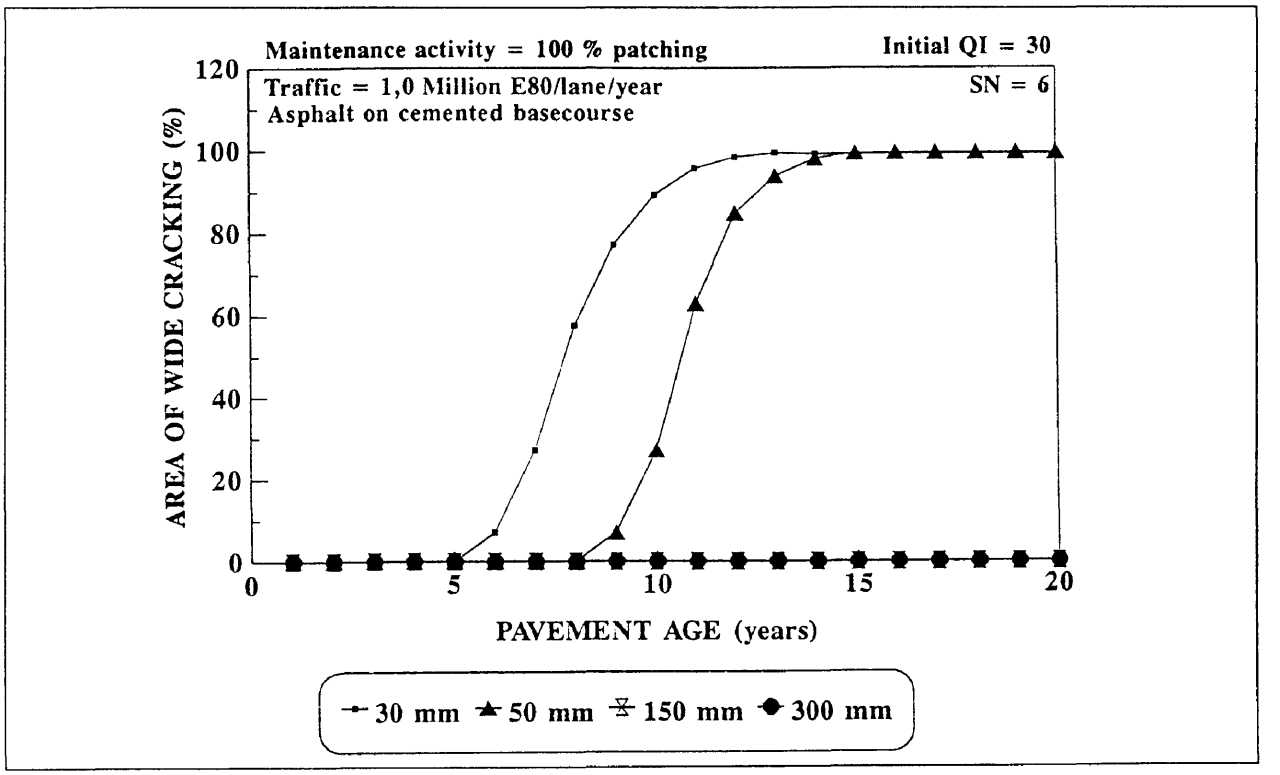

Figure A.8: Sensitivity of wide cracking model to the thickness of bituminous surfacing for SN = 6 under heavy traffic.

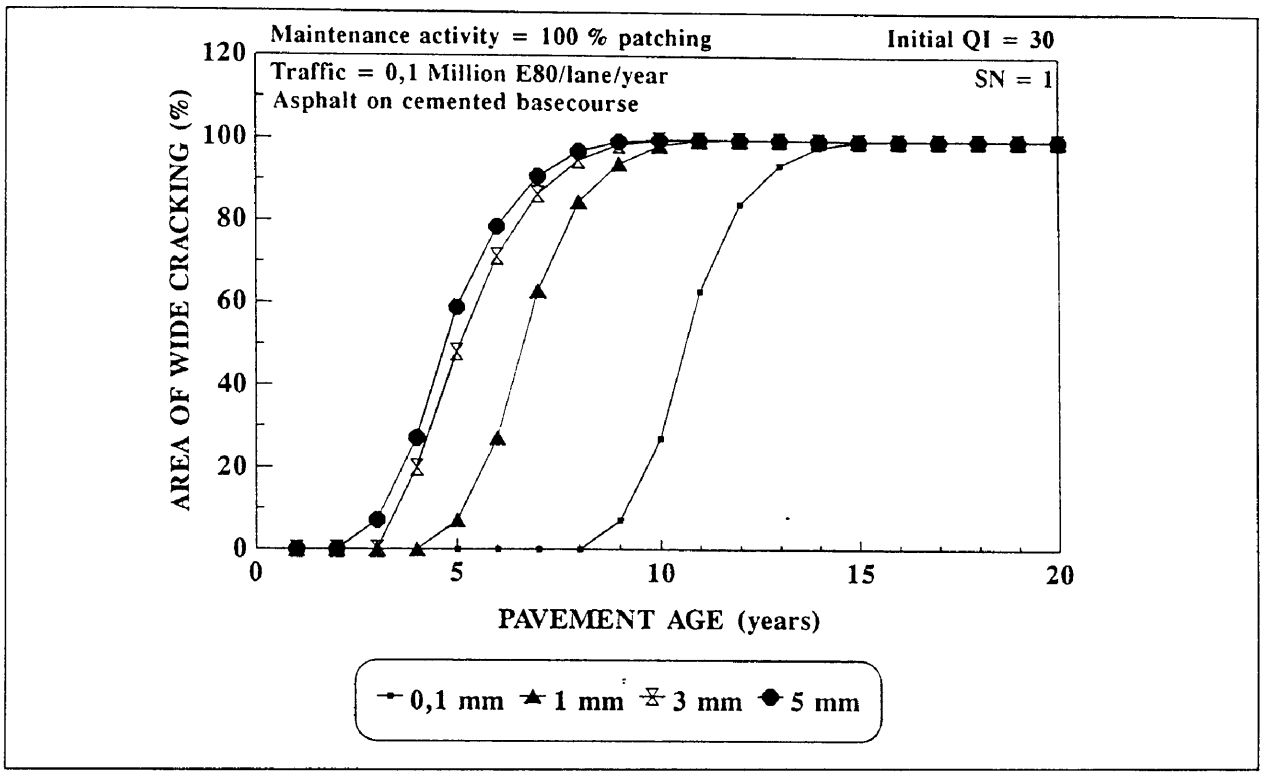

Figure A.9: Sensitivity of wide cracking model to deflection of the pavement for SN = 1 under light traffic.

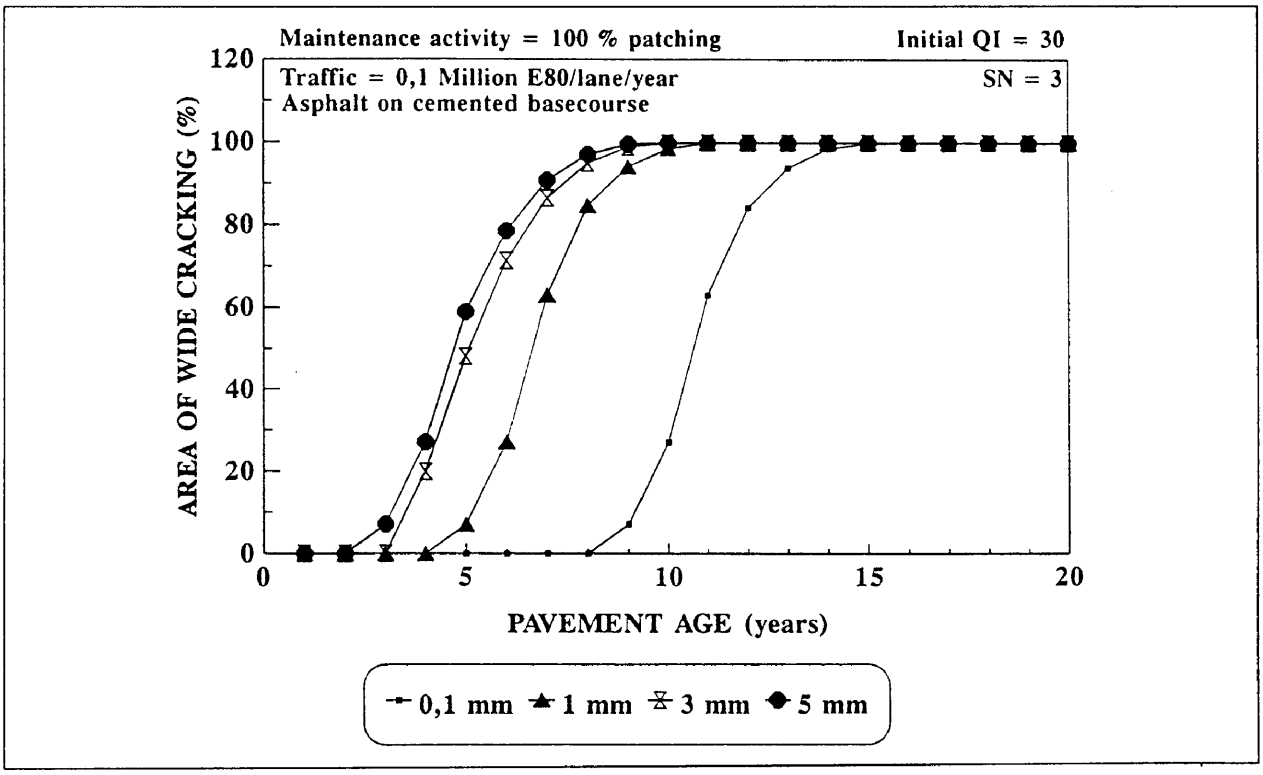

Figure A.10: Sensitivity of wide cracking model to the deflection of the pavement for SN = 3 under light traffic.

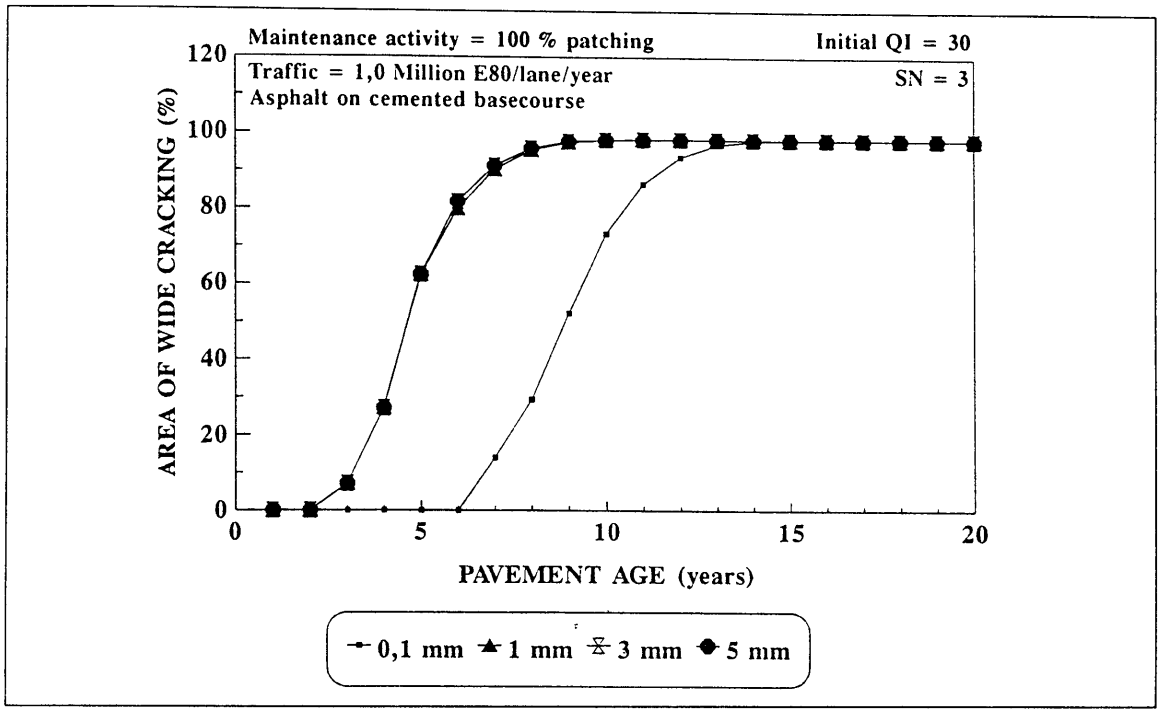

Figure A.11: Sensitivity of wide cracking model to the deflection of the pavement for SN = 3 under heavy traffic.

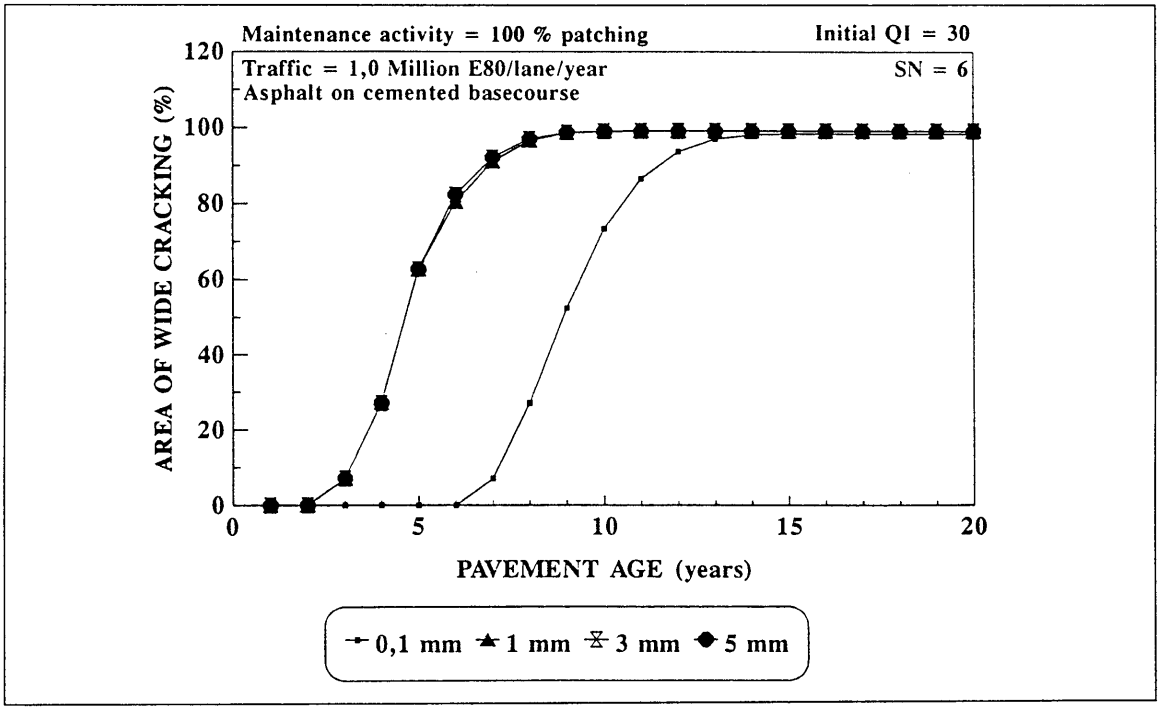

Figure A.12: Sensitivity of wide cracking model to the deflection of the pavement for SN = 6 under heavy traffic.

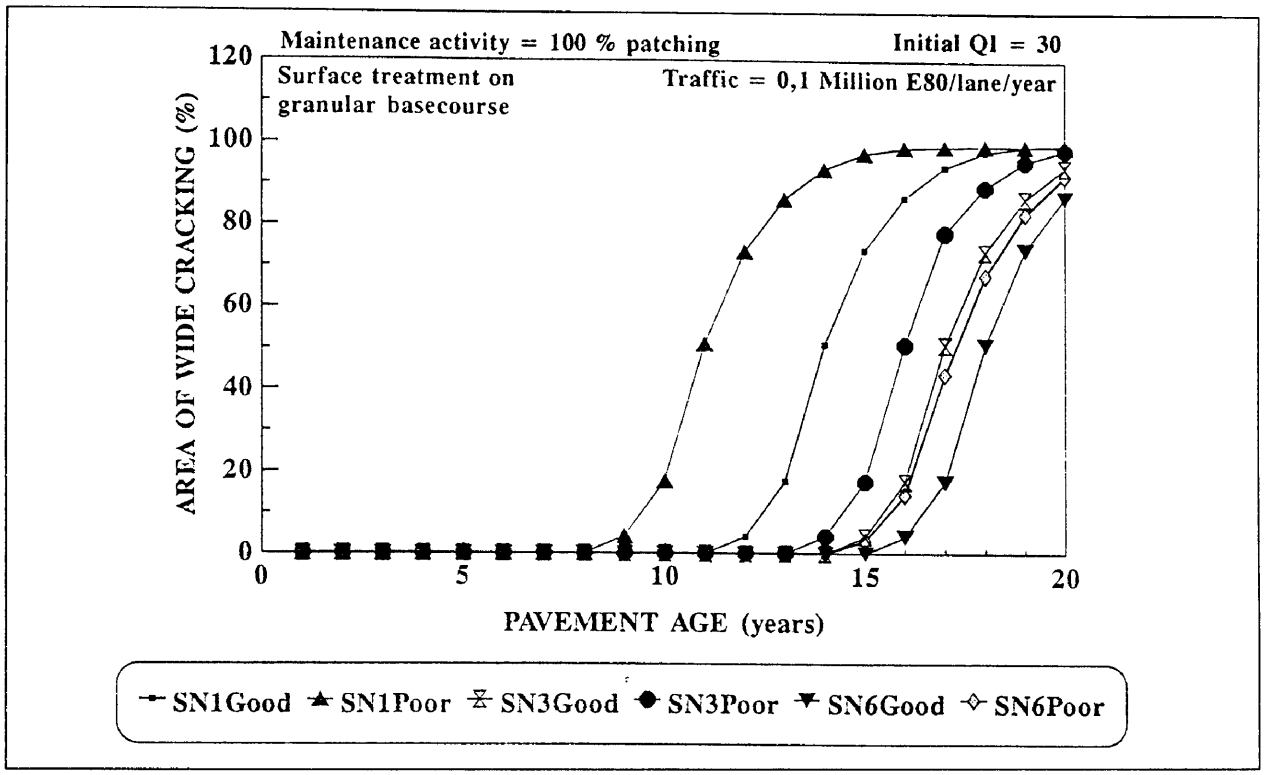

Figure A.13: Sensitivity of wide cracking model to the construction quality of a surfacing on a granular basecourse under light traffic.

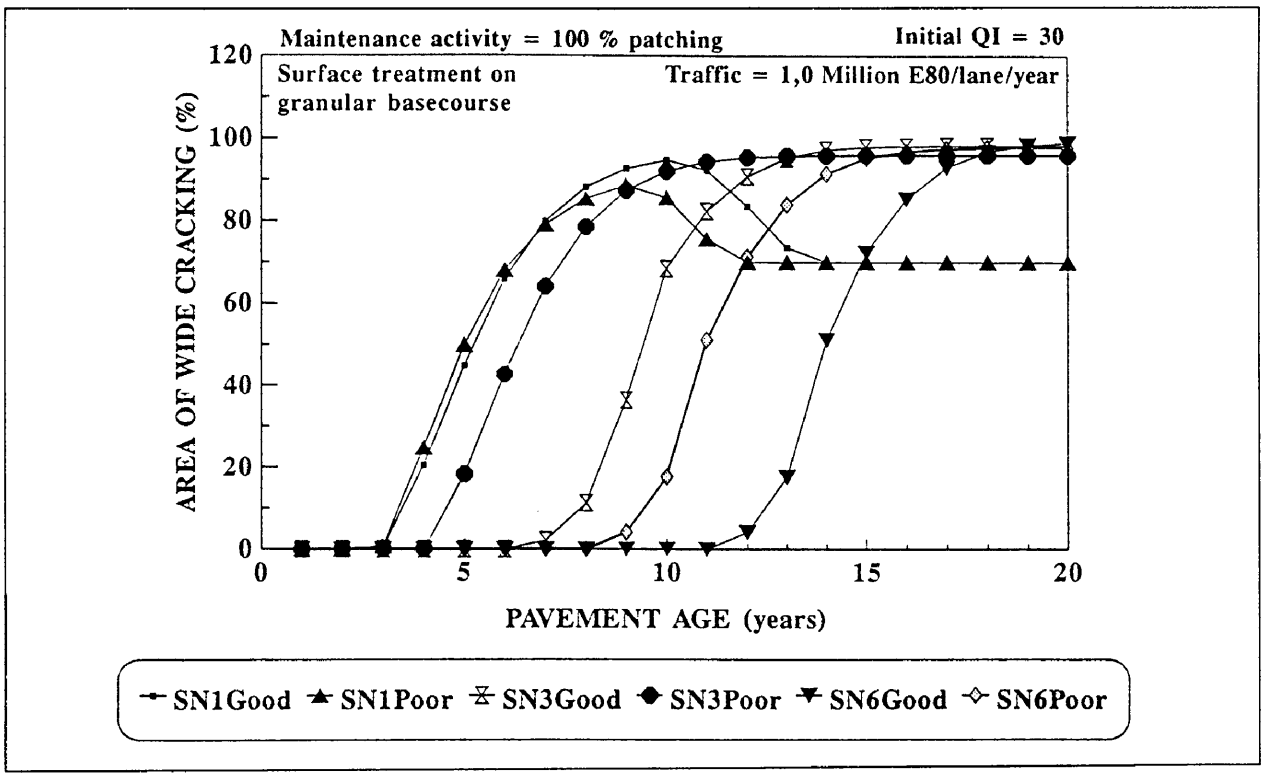

Figure A.14: Sensitivity of wide cracking model to the construction quality of a surfacing on a granular basecourse under heavy traffic.

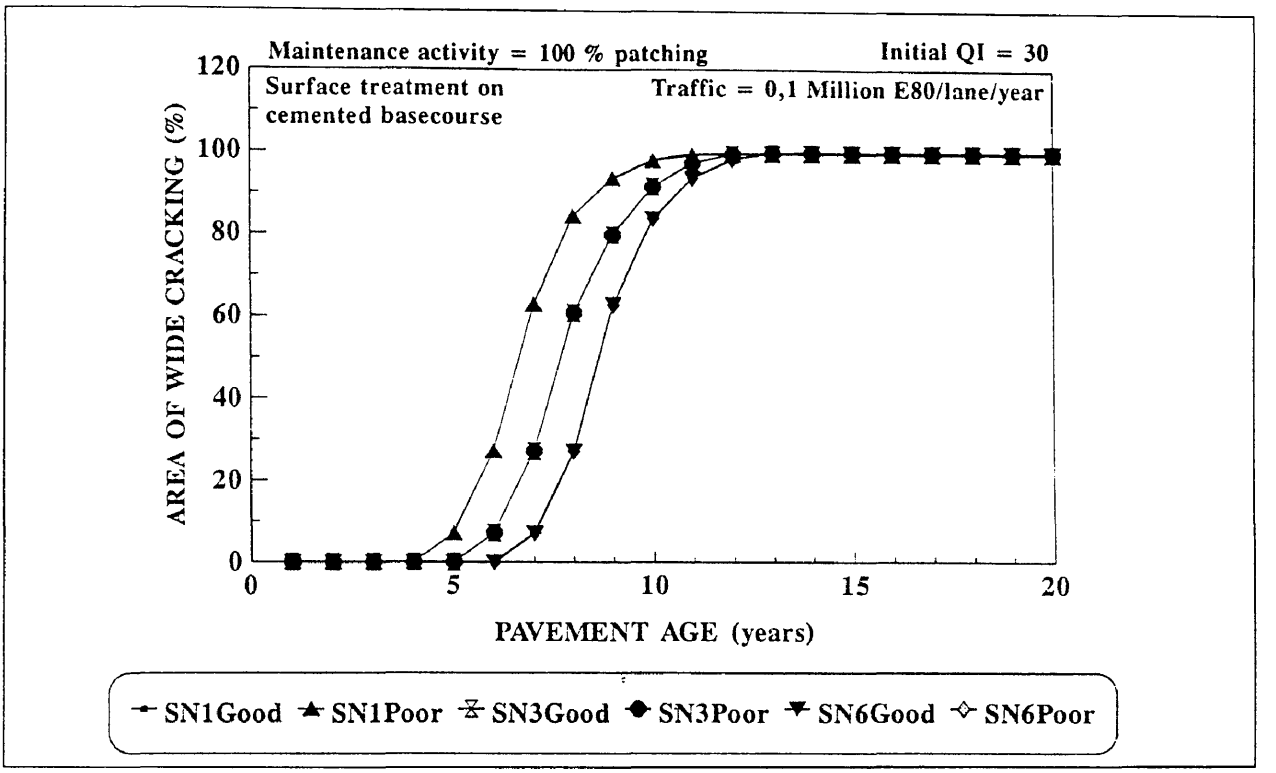

Figure A.15: Sensitivity of wide cracking model to the construction quality of a surfacing on a cemented basecourse under light traffic.

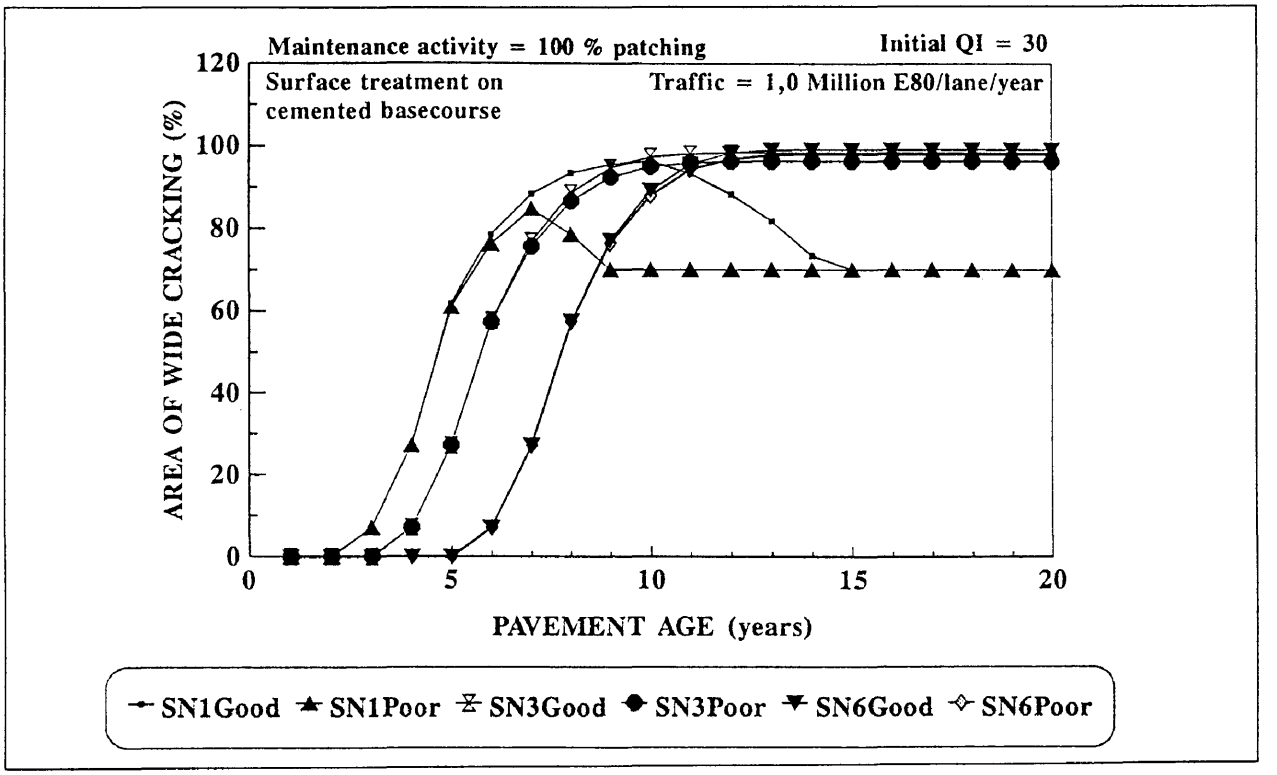

Figure A.16: Sensitivity of wide cracking model to the construction quality of a surfacing on a cemented basecourse under heavy traffic.

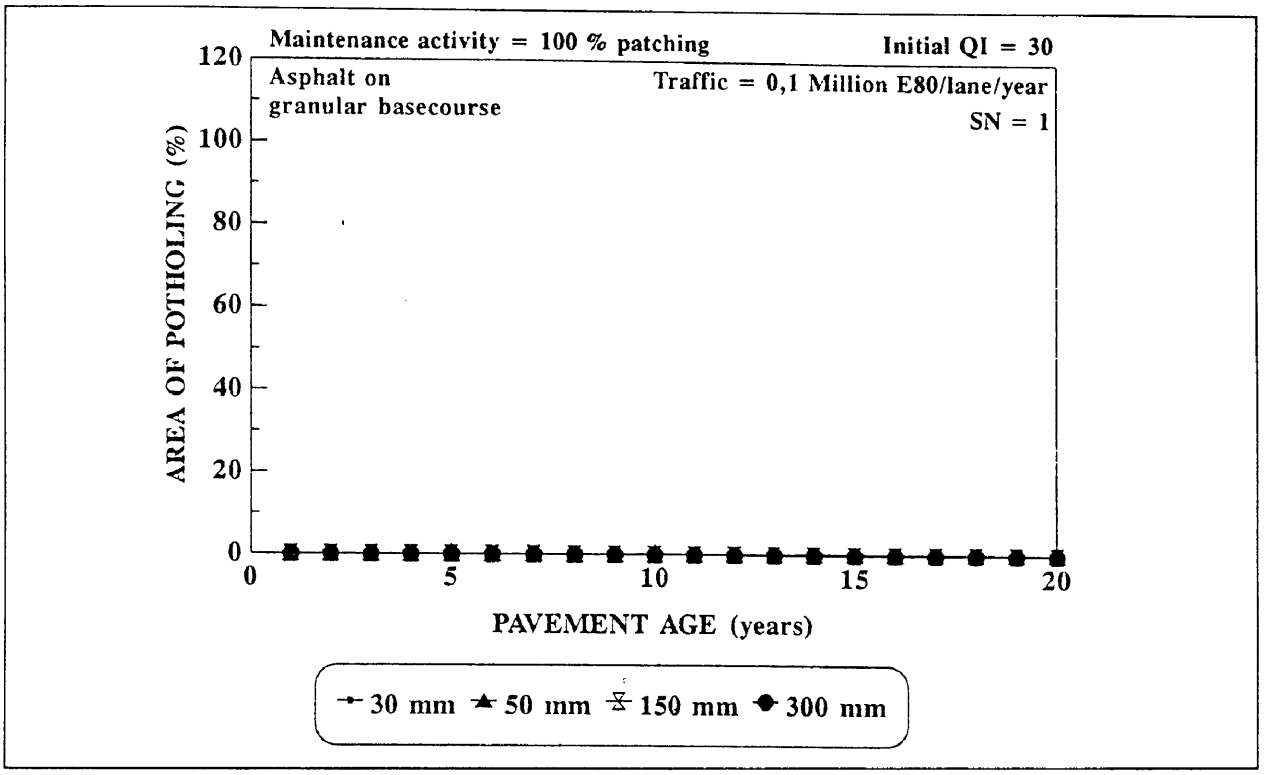

Figure A.17: Sensitivity of potholing model to thickness of surfacing for SN = 1 under light traffic.

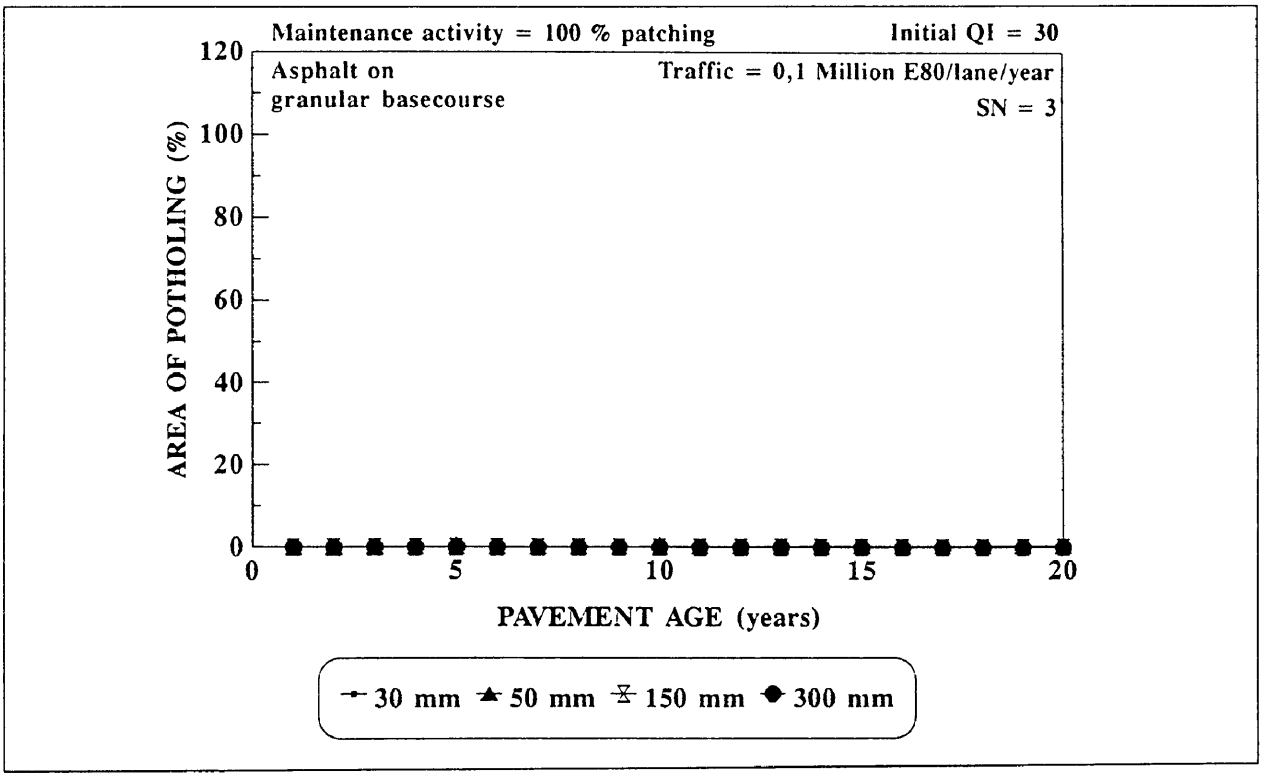

Figure A.18: Sensitivity of potholing model to the thickness of surfacing for SN = 3 under light traffic.

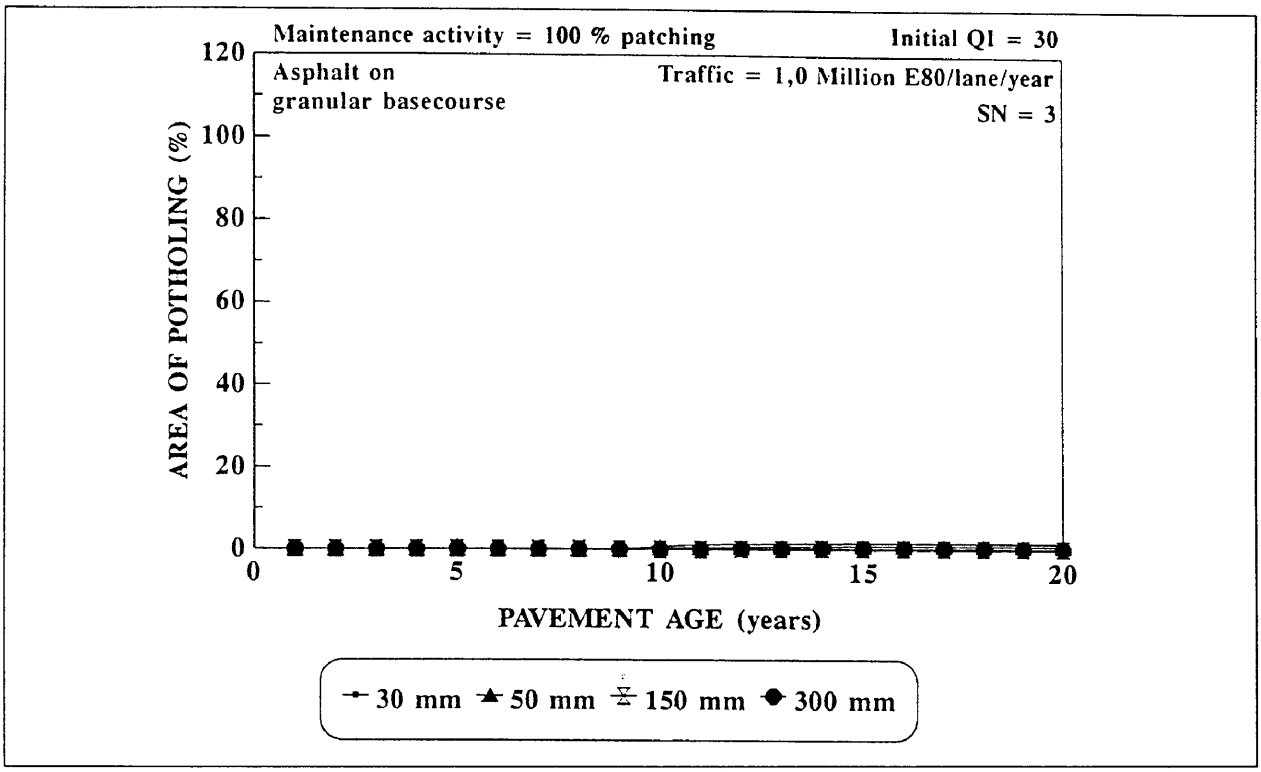

Figure A.19: Sensitivity of potholing model to the thickness of surfacing for SN = 3 under heavy traffic.

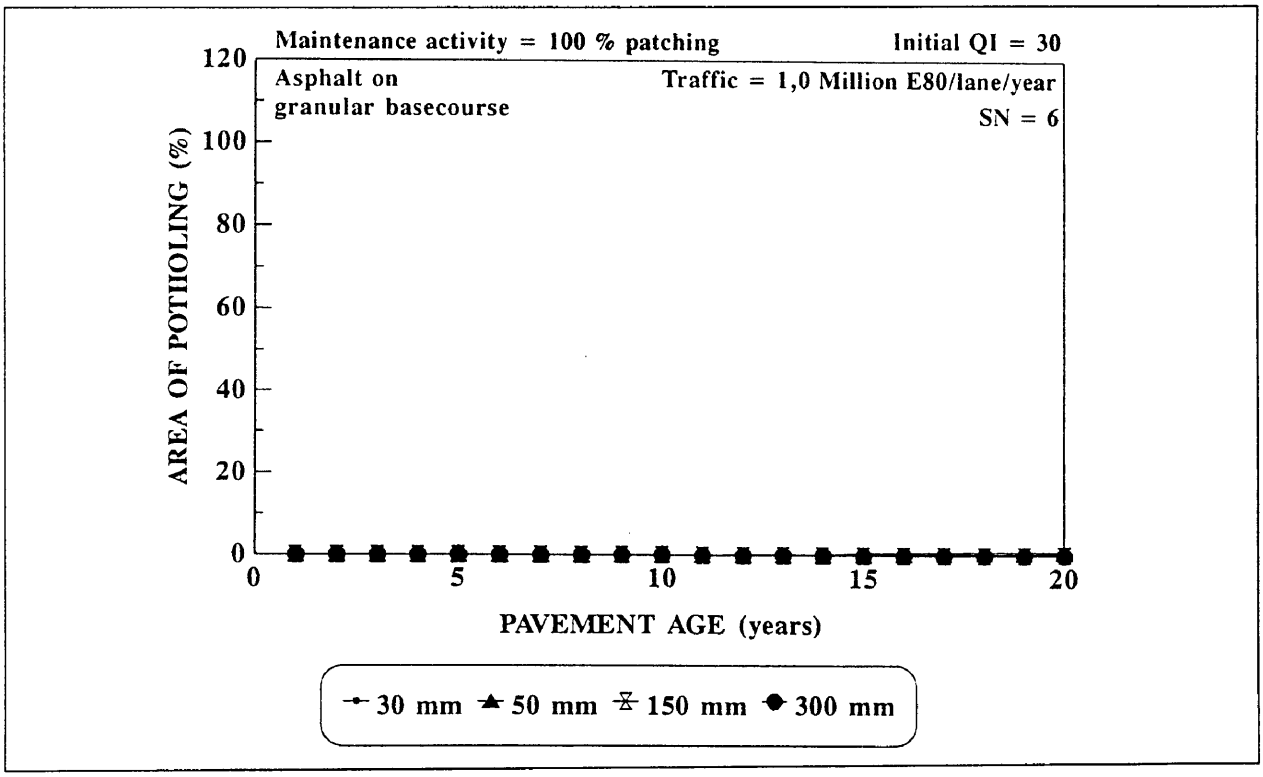

Figure A.20: Sensitivity of potholing model to the thickness of surfacing for SN = 6 under heavy traffic.

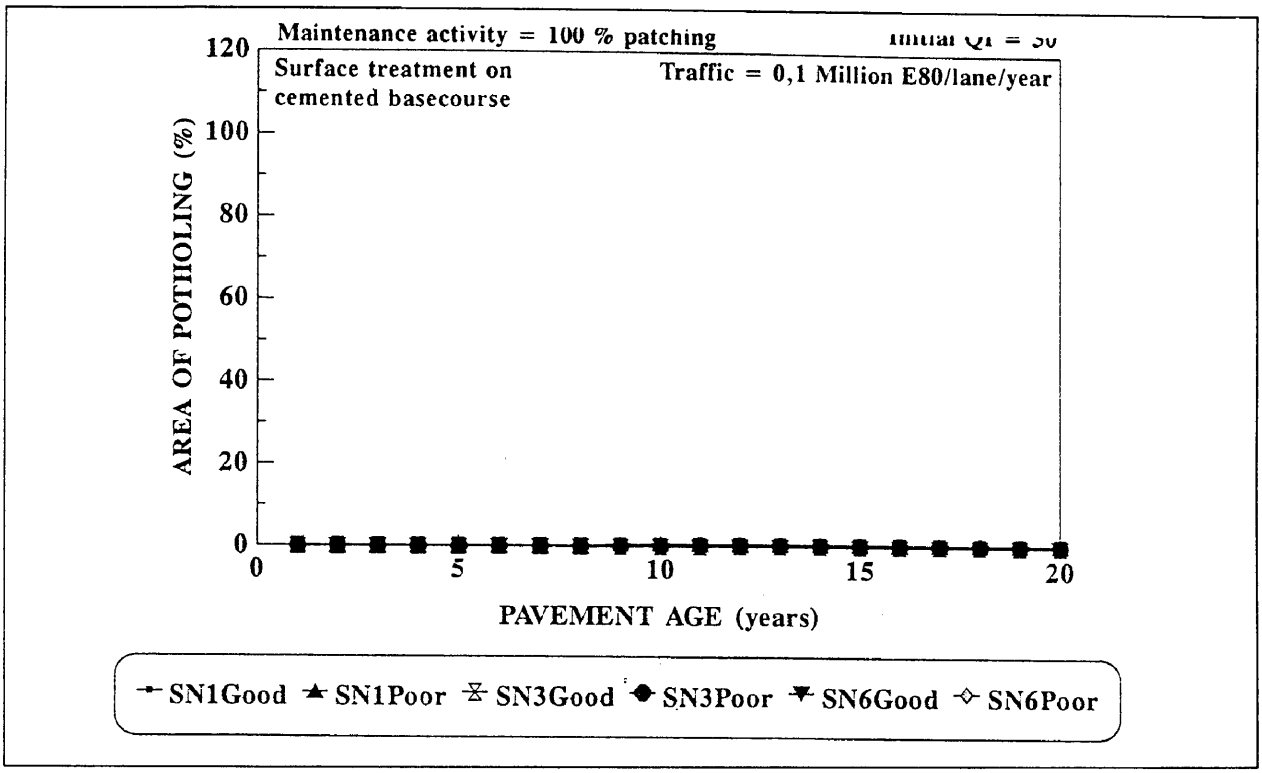

Figure A.21: Sensitivity of potholing model to the construction quality of a surface treatment on a cemented basecourse under light traffic.

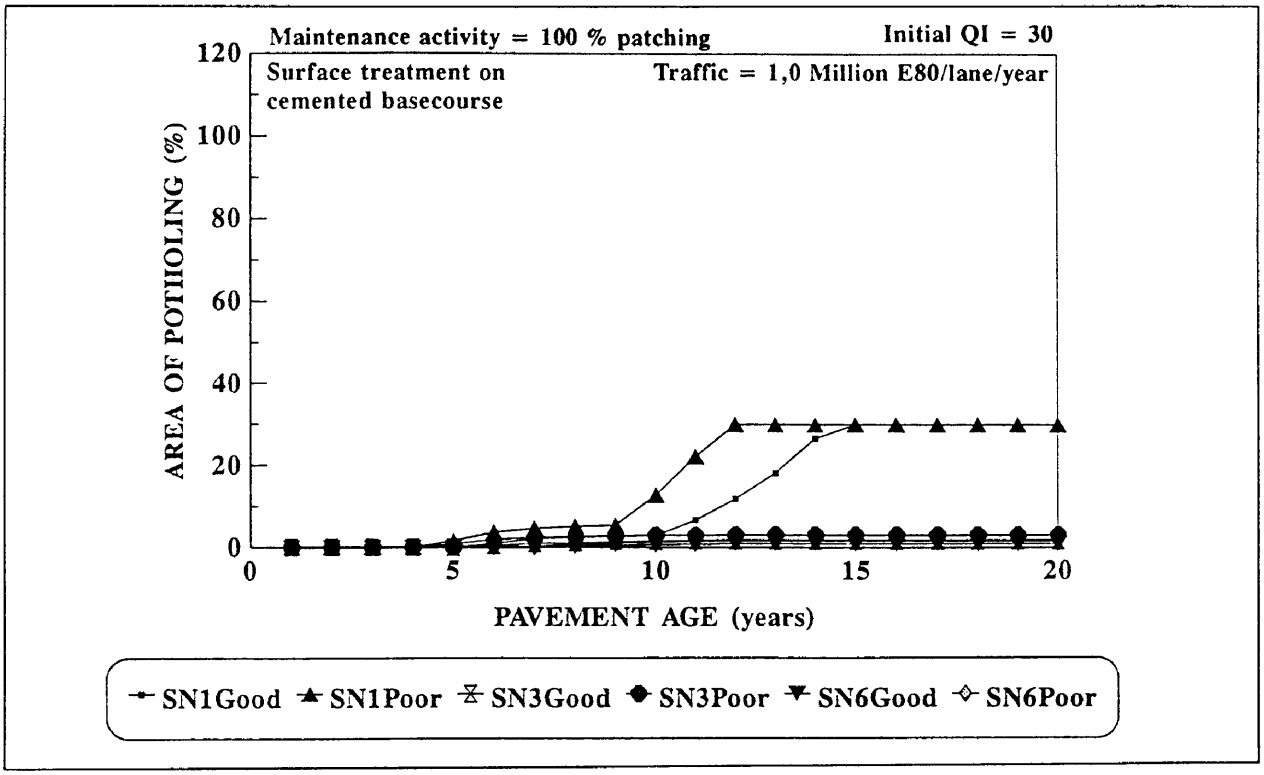

Figure A.22: Sensitivity of potholing model to the construction quality of a surface treatment on a cemented basecourse under heavy traffic.

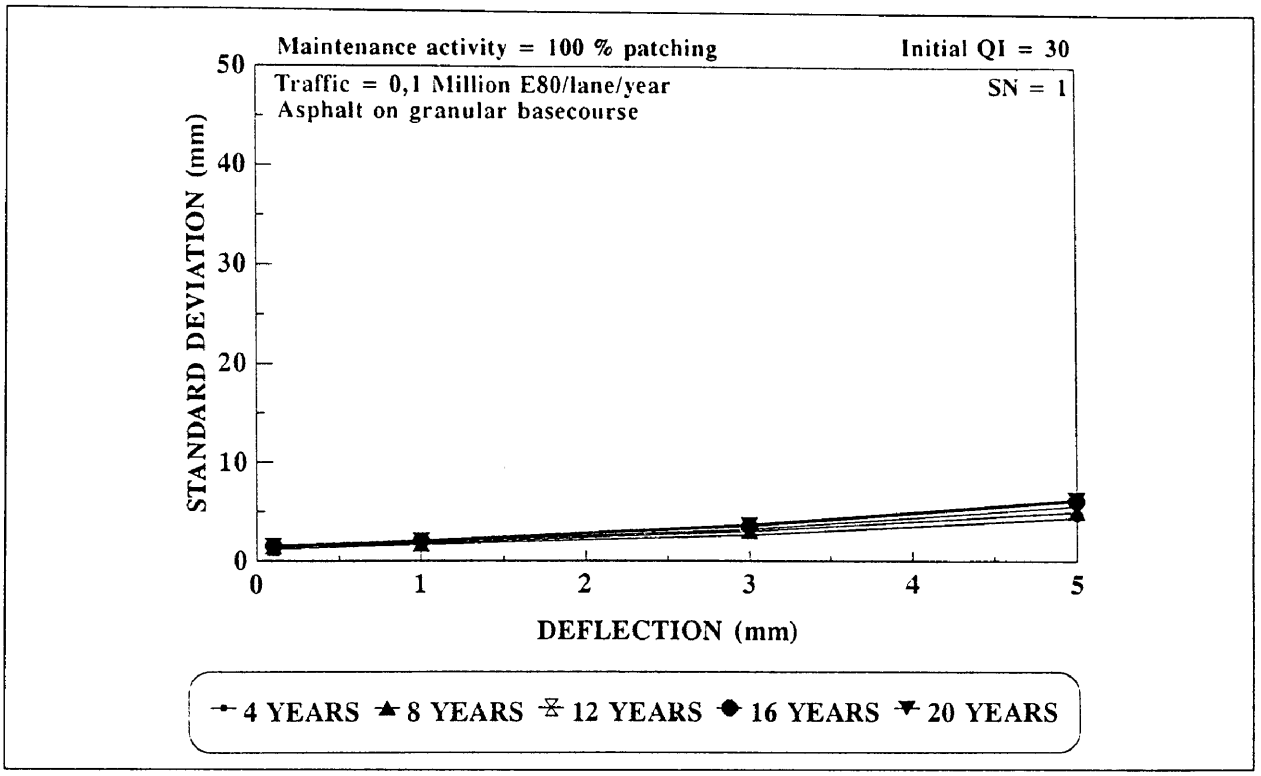

Figure A.23: Sensitivity of rut depth standard deviation model to pavement deflection for SN = 1 under light traffic.

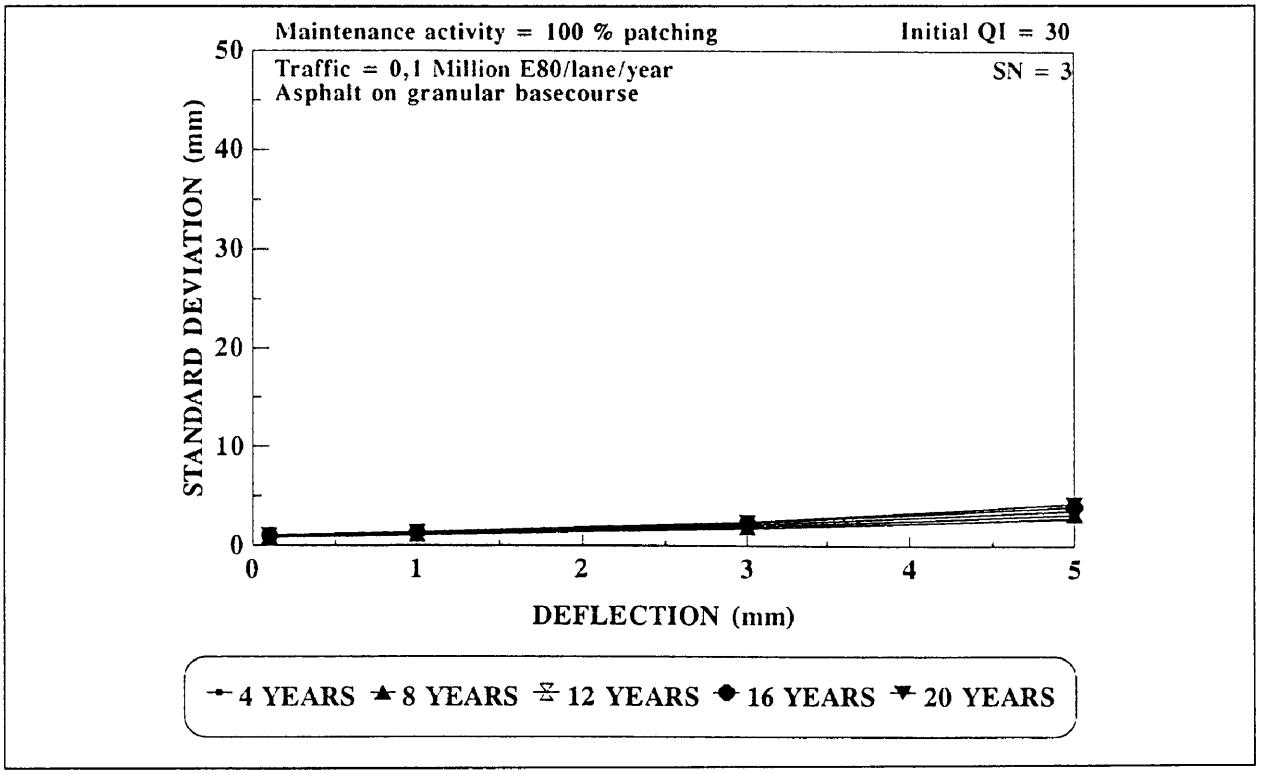

Figure A.24: Sensitivity of rut depth standard deviation model to pavement deflection for SN = 3 under light traffic.

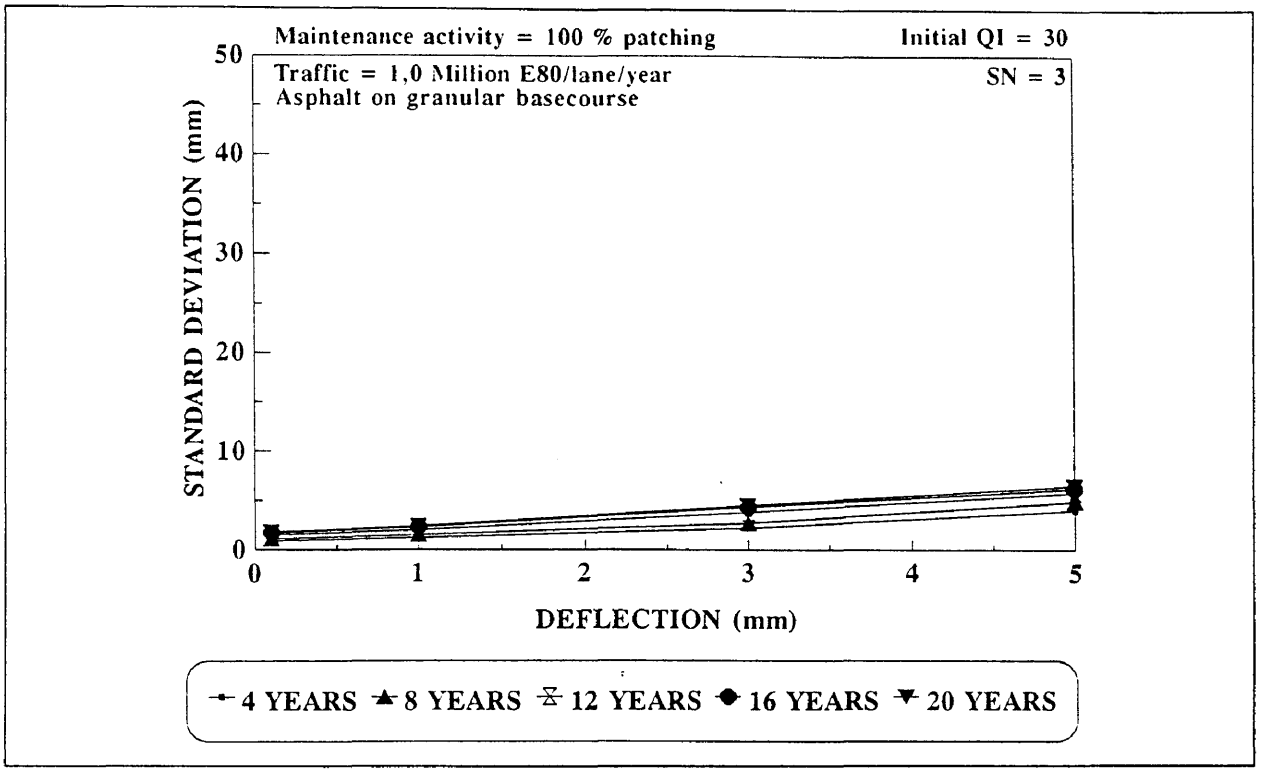

Figure A.25: Sensitivity of rut depth standard deviation model to pavement deflection for SN = 3 under heavy traffic.

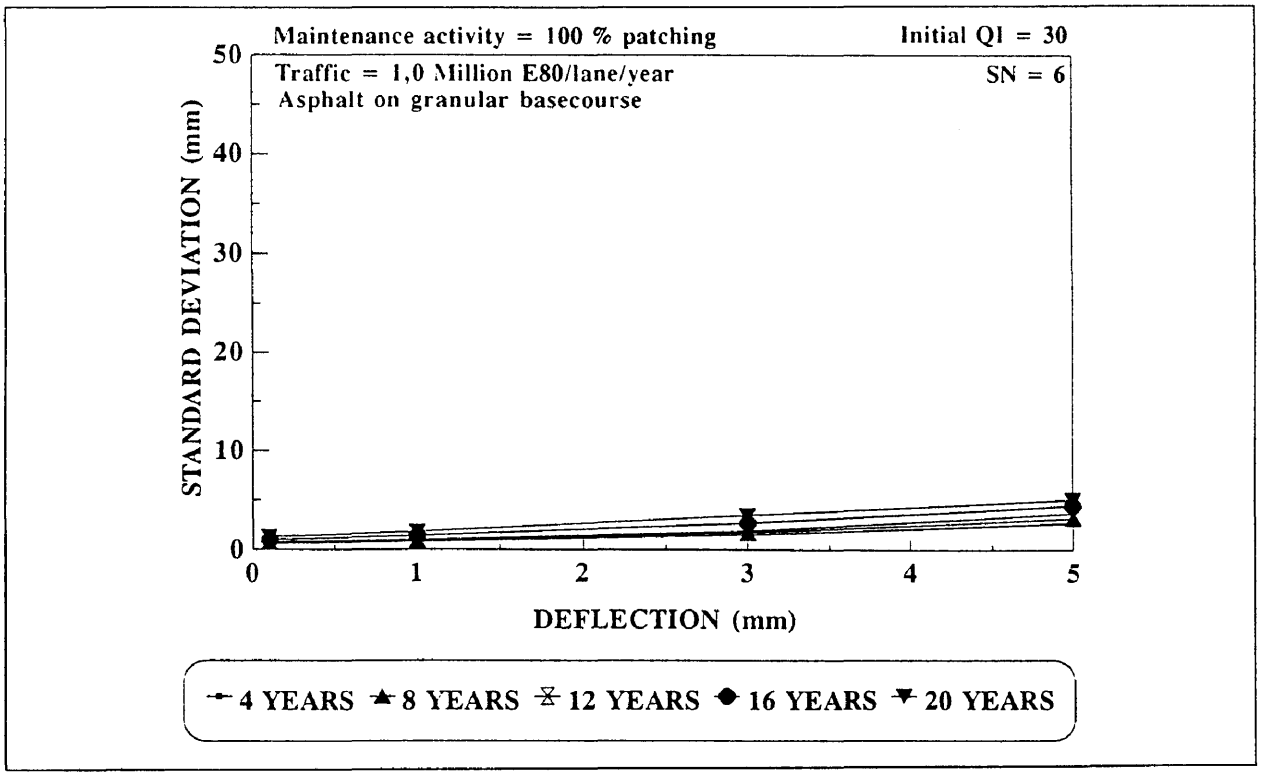

Figure A.26: Sensitivity of rut depth standard deviation model to pavement deflection for SN = 6 under heavy traffic.

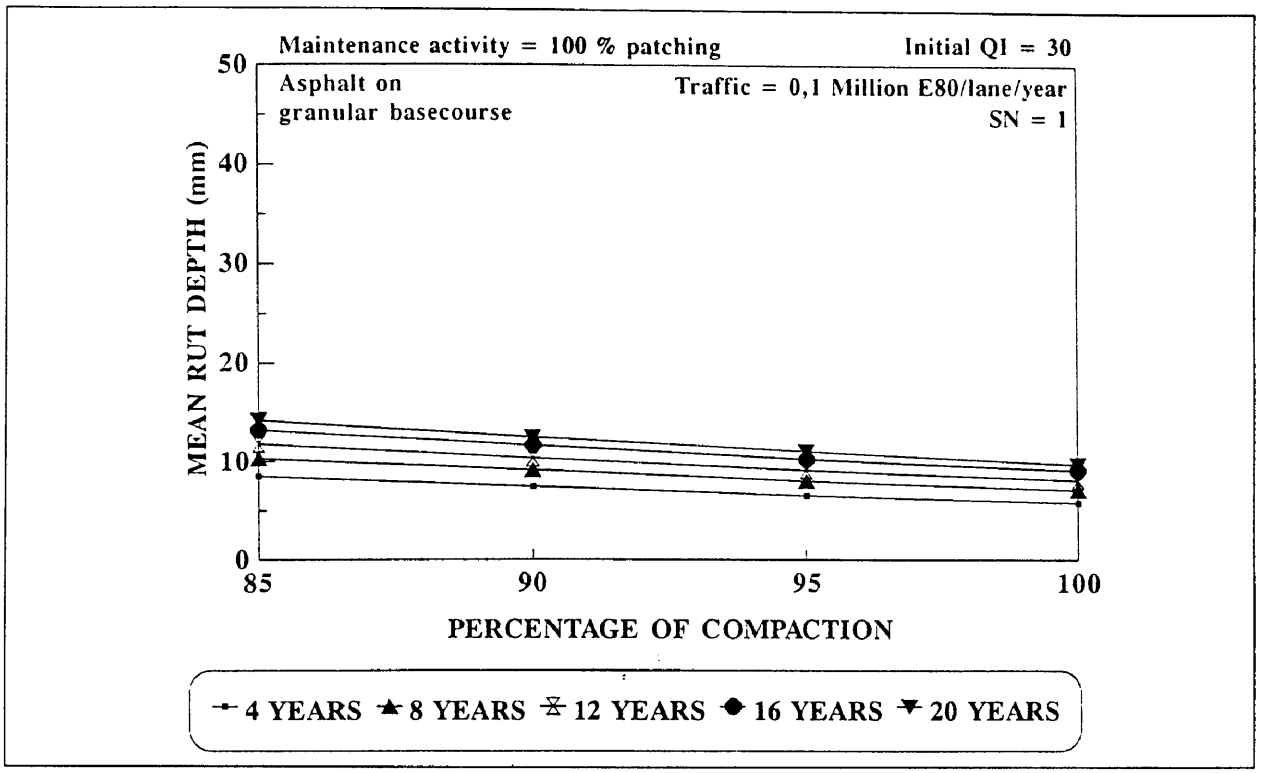

Figure A.27: Sensitivity of mean rut depth model to pavement compaction for SN = 1 under light traffic.

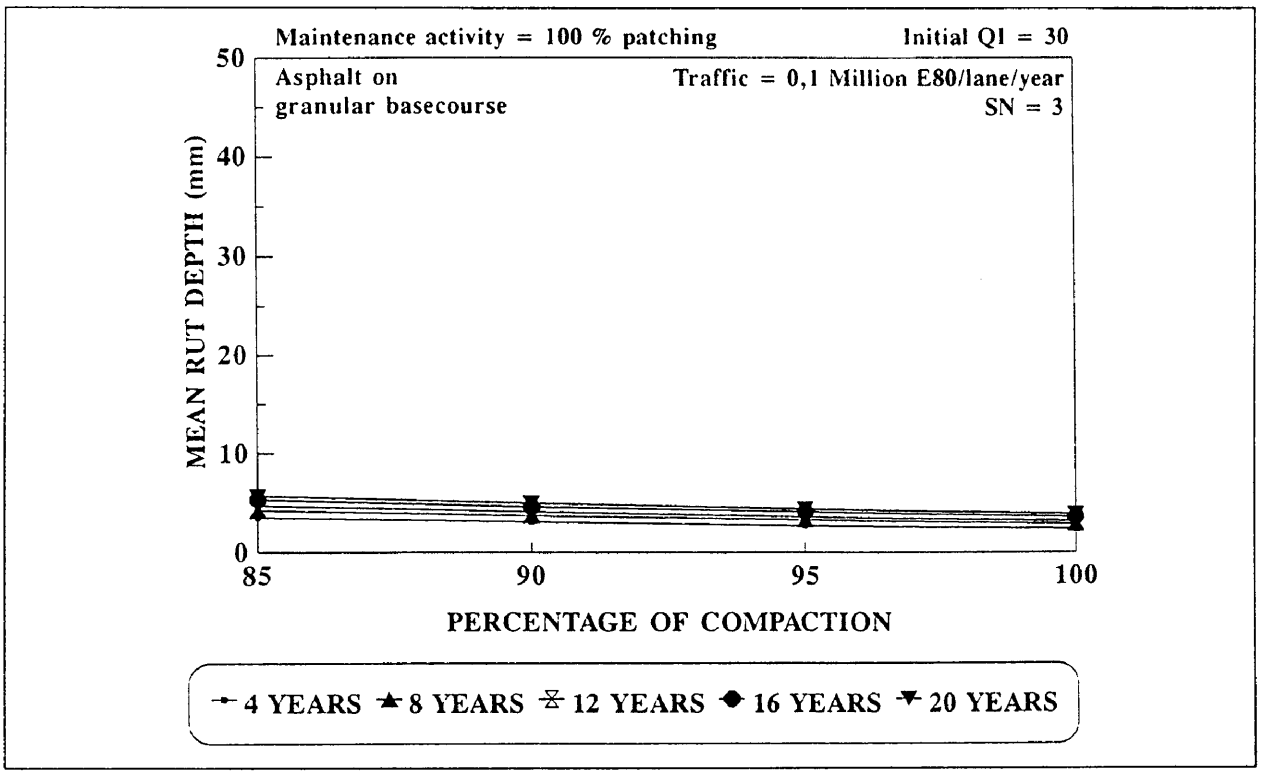

Figure A.28: Sensitivity of mean rut depth model to pavement compaction for SN = 3 under light traffic.

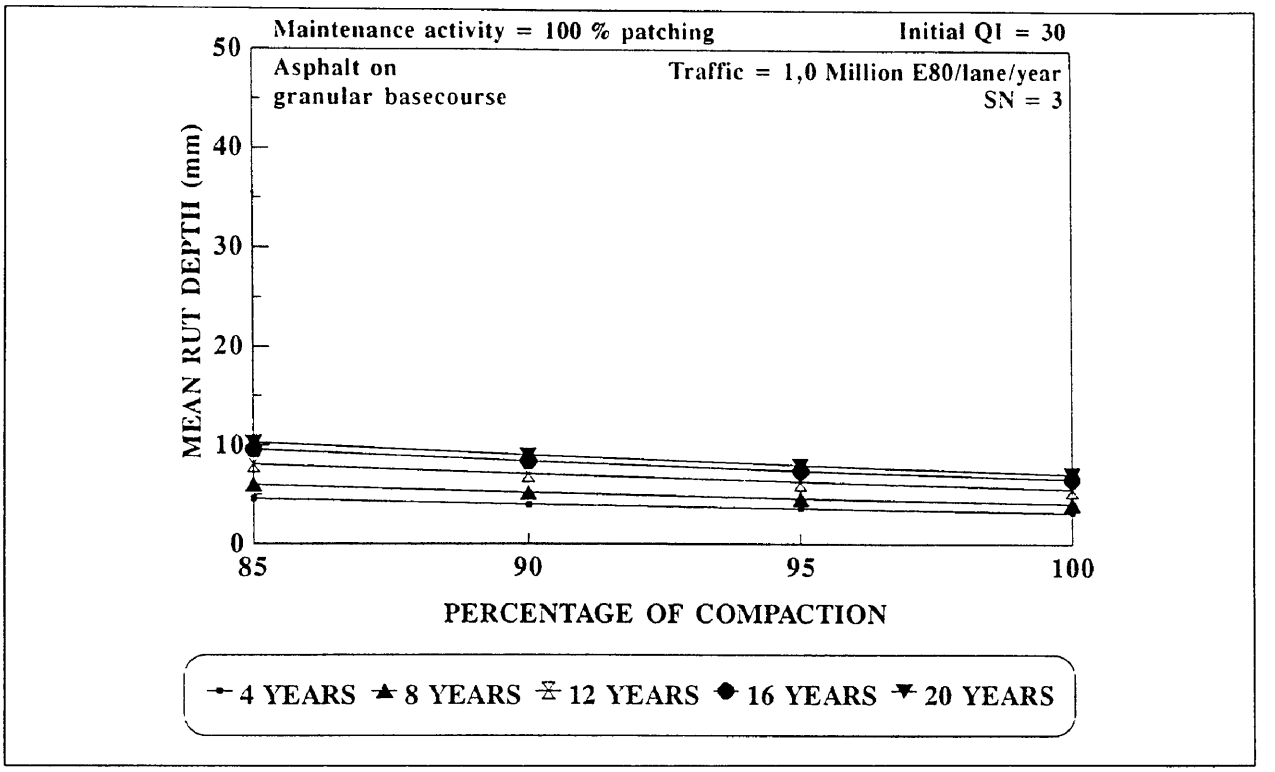

Figure A.29: Sensitivity of mean rut depth model to pavement compaction for SN = 3 under heavy traffic.

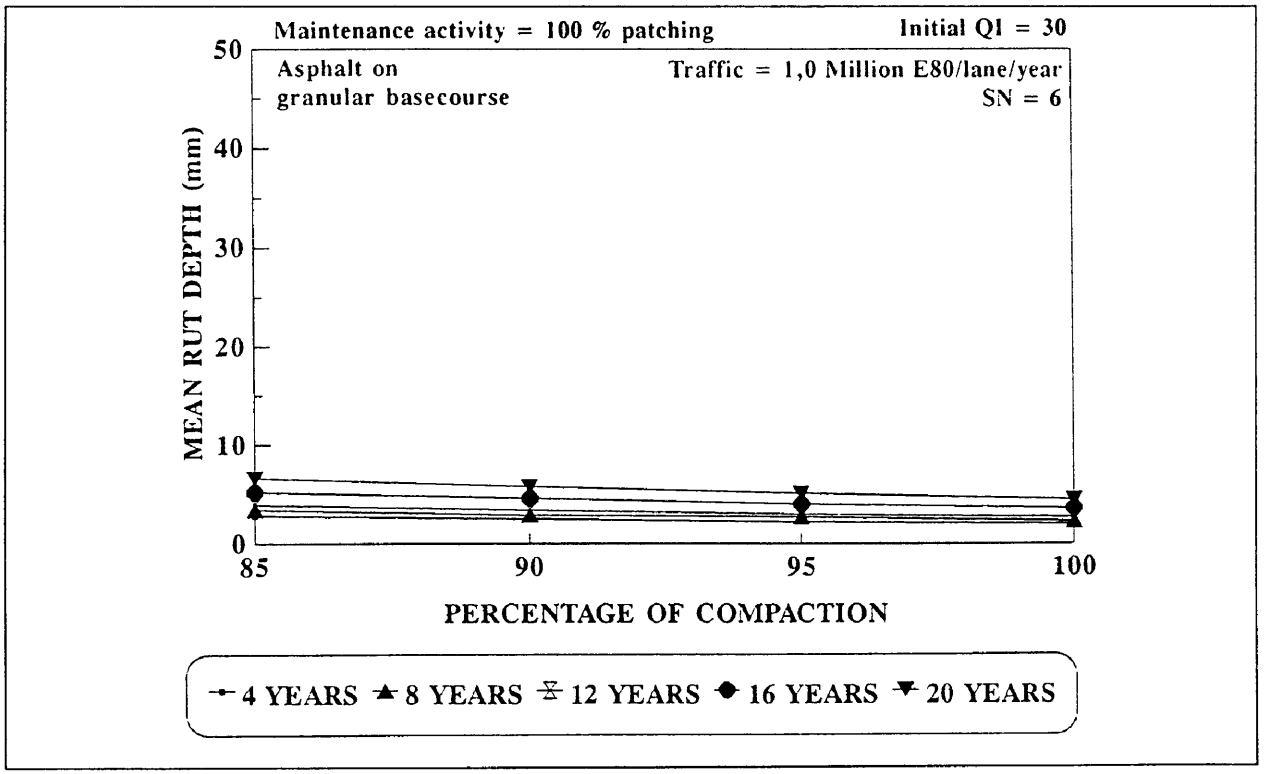

Figure A.30: Sensitivity of mean rut depth model to pavement compaction for SN = 6 under heavy traffic.

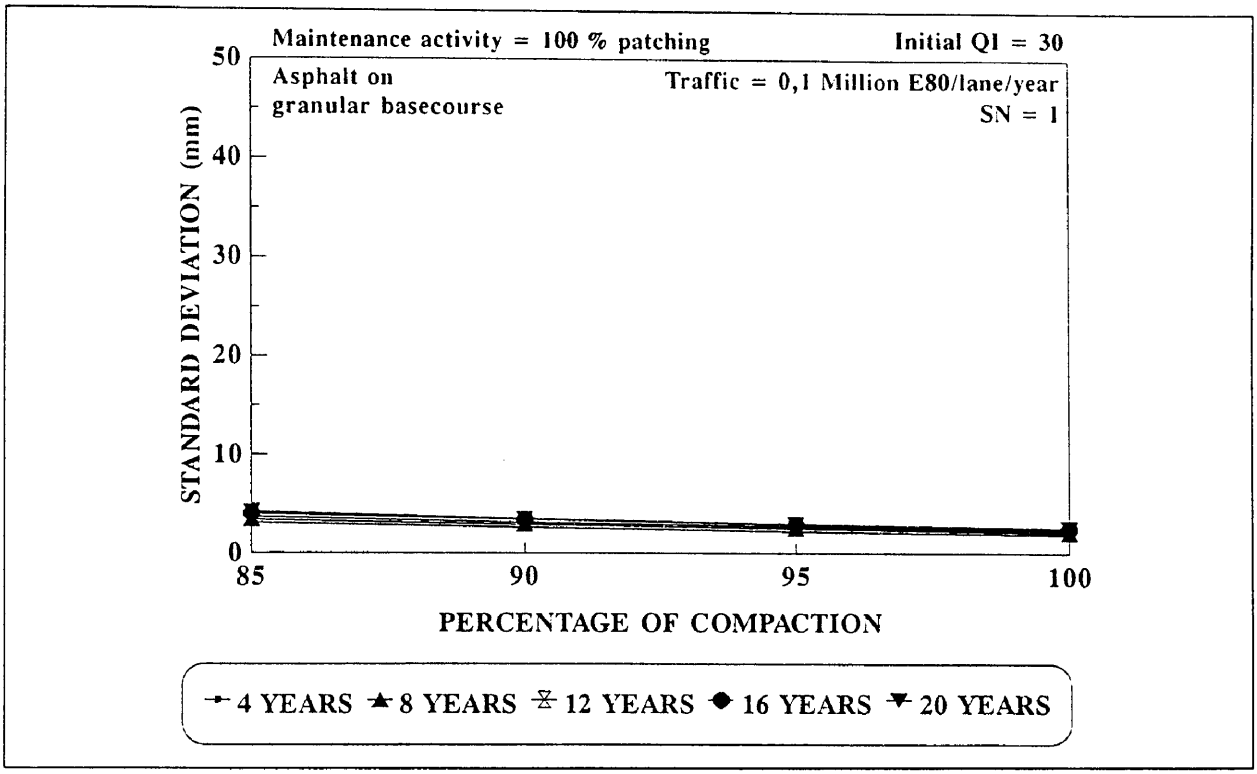

Figure A.31: Sensitivity of rut depth standard deviation model to pavement compaction for SN = 1 under light traffic.

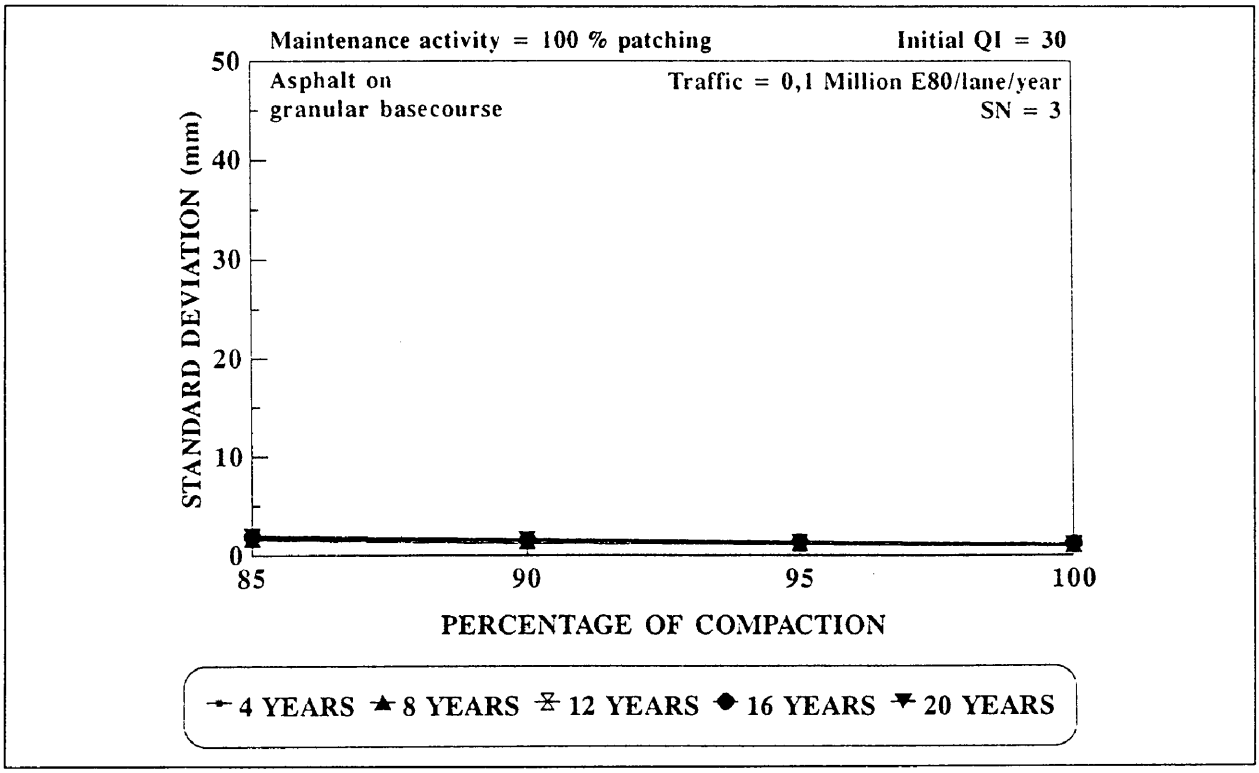

Figure A.32: Sensitivity of rut depth standard deviation model to pavement compaction for SN = 3 under light traffic.

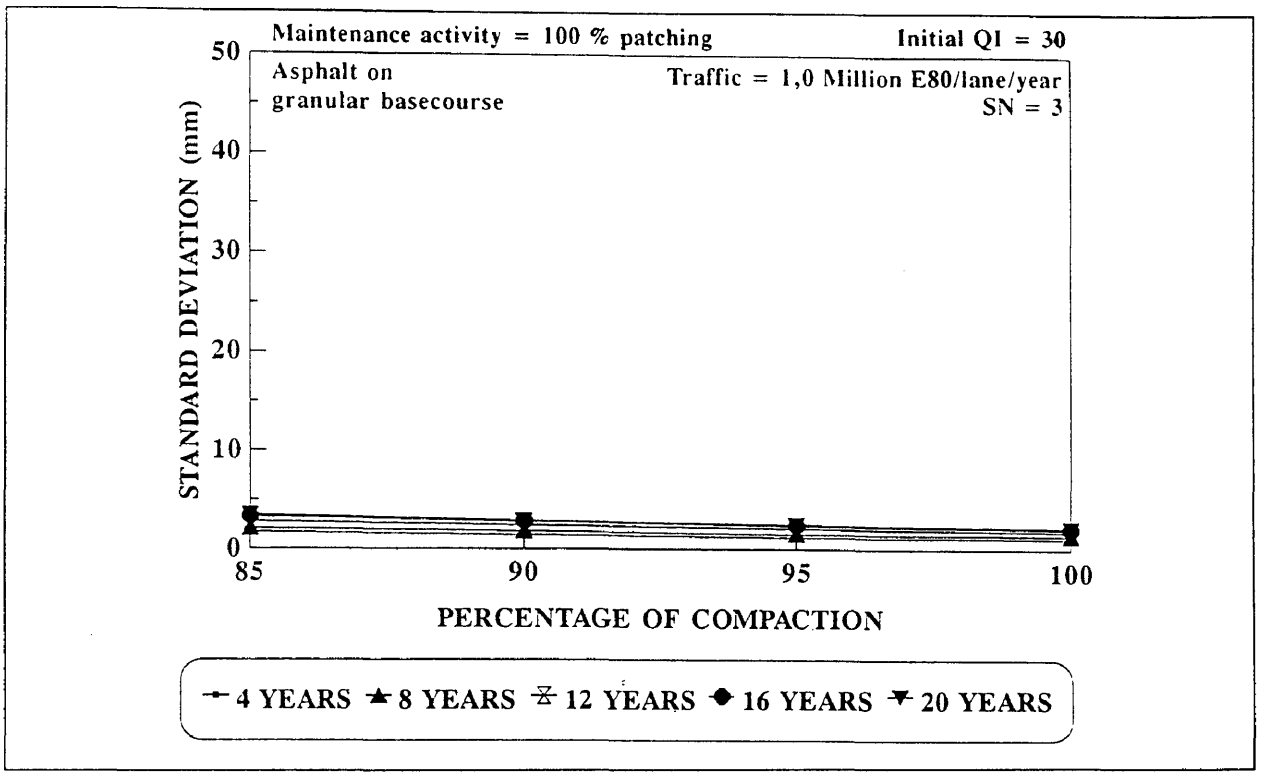

Figure A.33: Sensitivity of rut depth standard deviation model to pavement compaction for SN = 3 under heavy traffic.

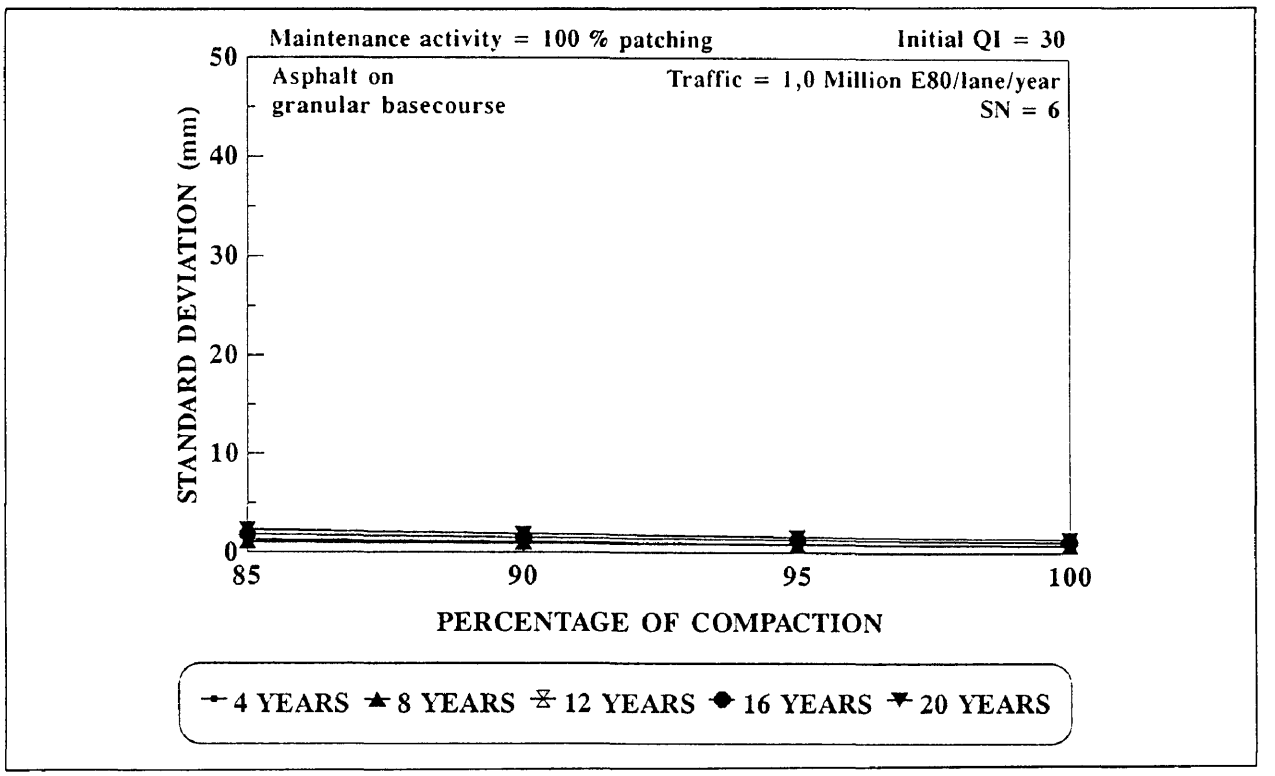

Figure A.34: Sensitivity of rut depth standard deviation model to pavement compaction for SN = 6 under heavy traffic.

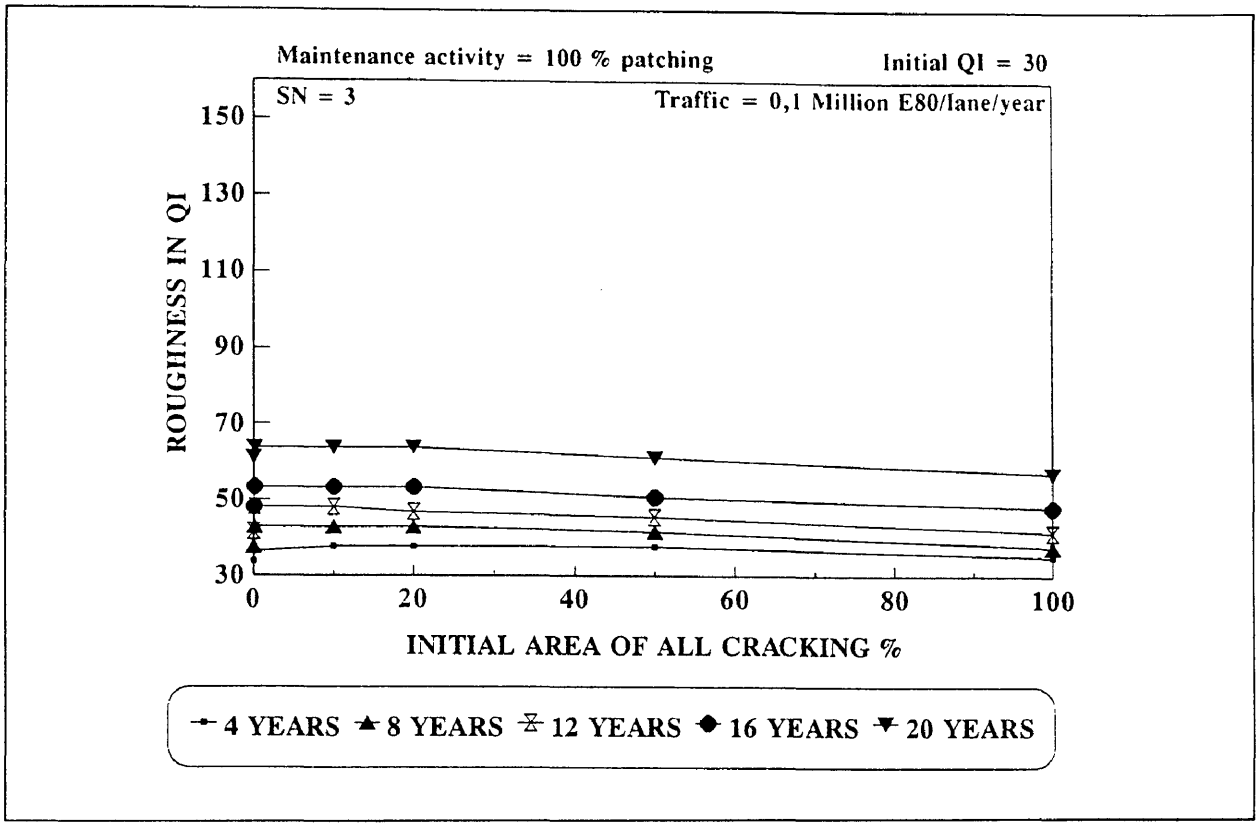

Figure A.35: Sensitivity to initial area of all cracking for SN = 3 and light traffic.

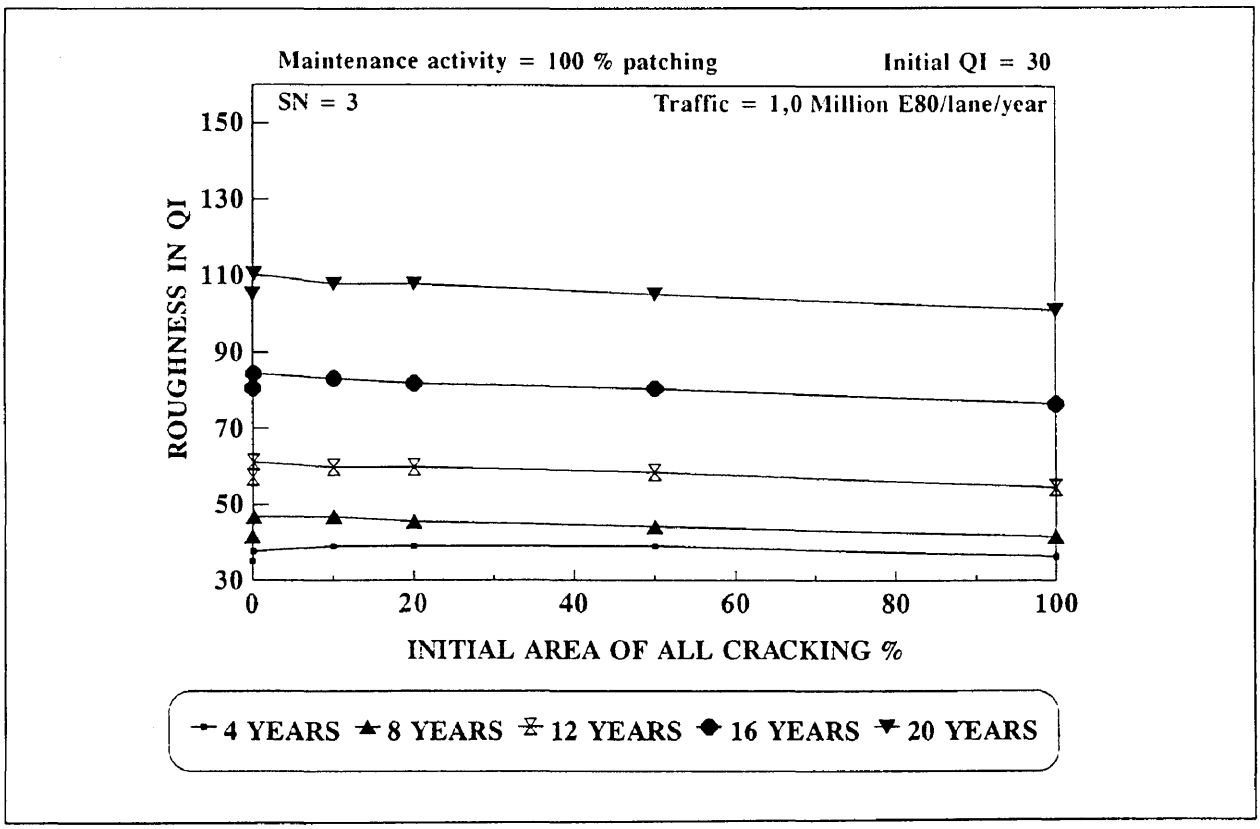

Figure A.36: Sensitivity to initial area of all cracking for SN = 3 and heavy traffic.

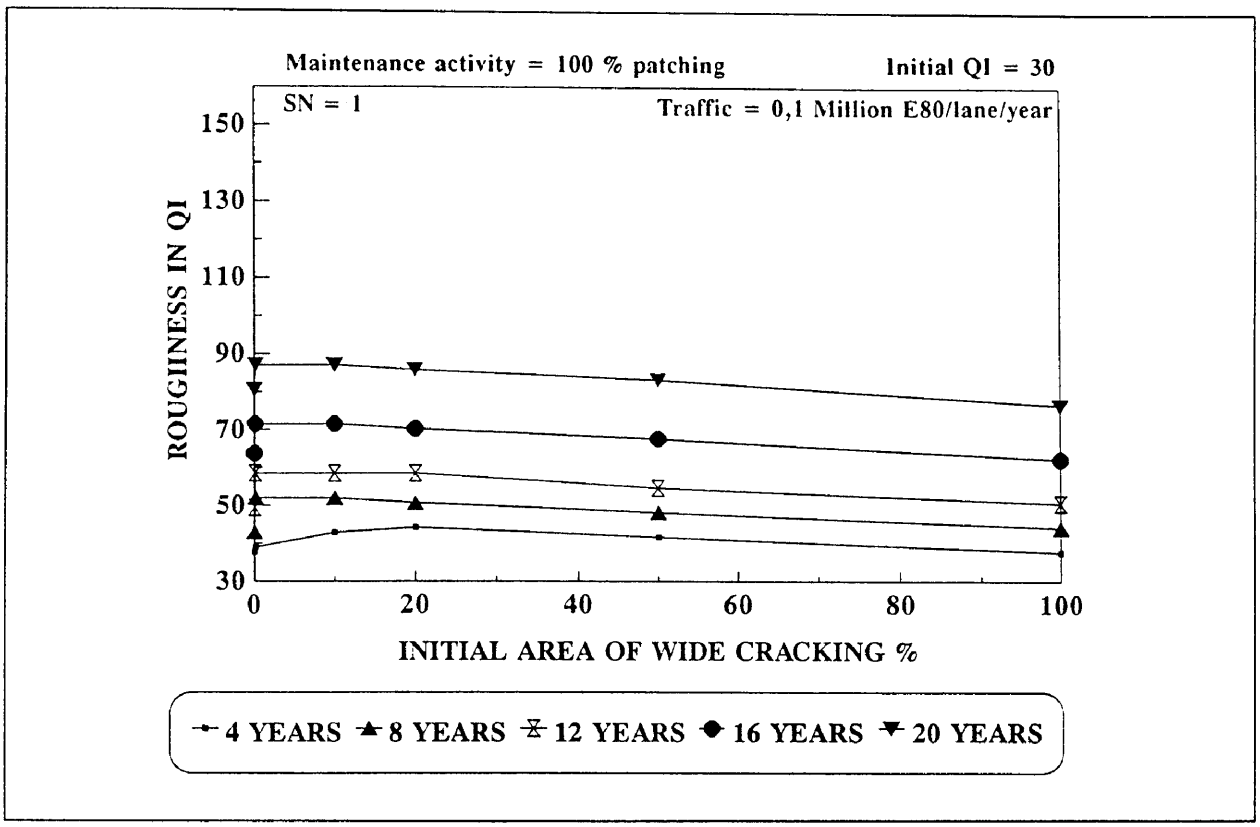

Figure A.37: Sensitivity to initial area of wide cracking for SN = 1 and light traffic.

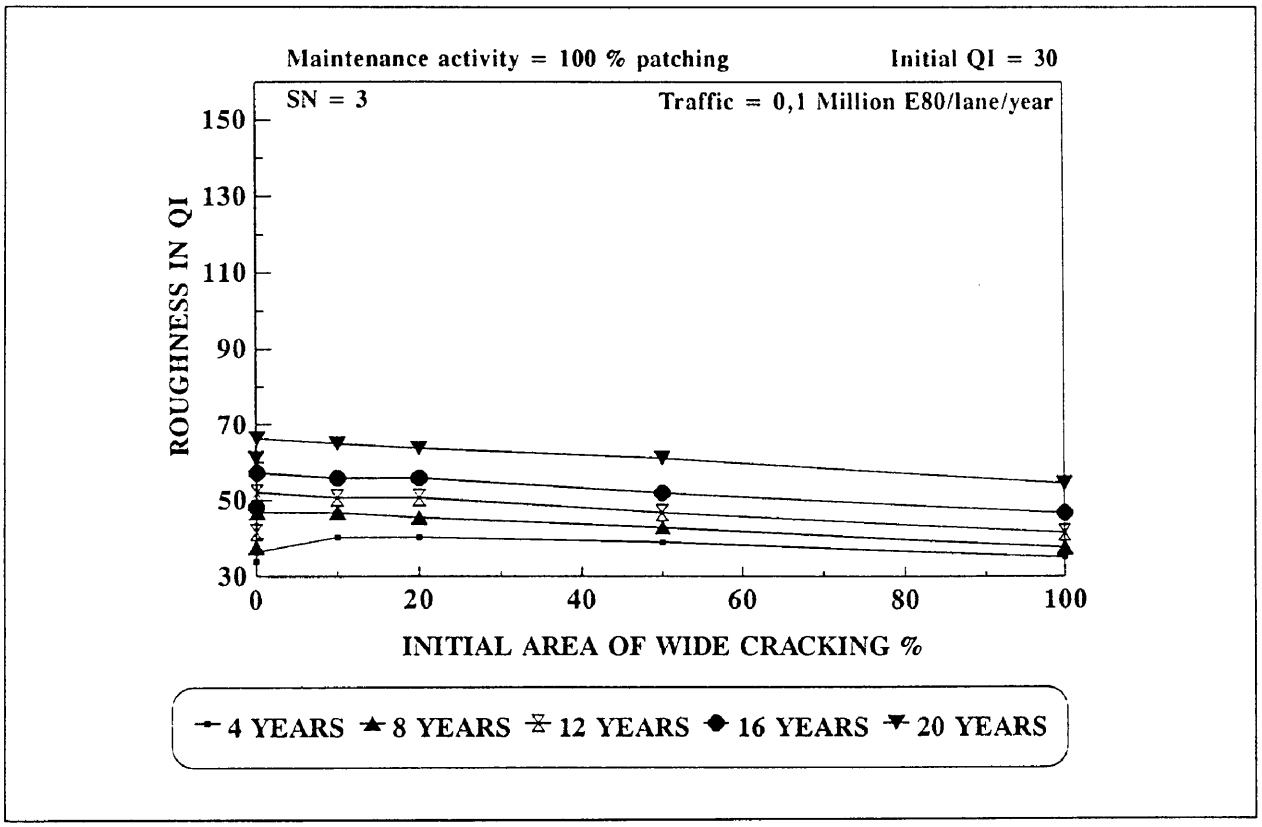

Figure A.38: Sensitivity to initial area of wide cracking for SN = 3 and light traffic.

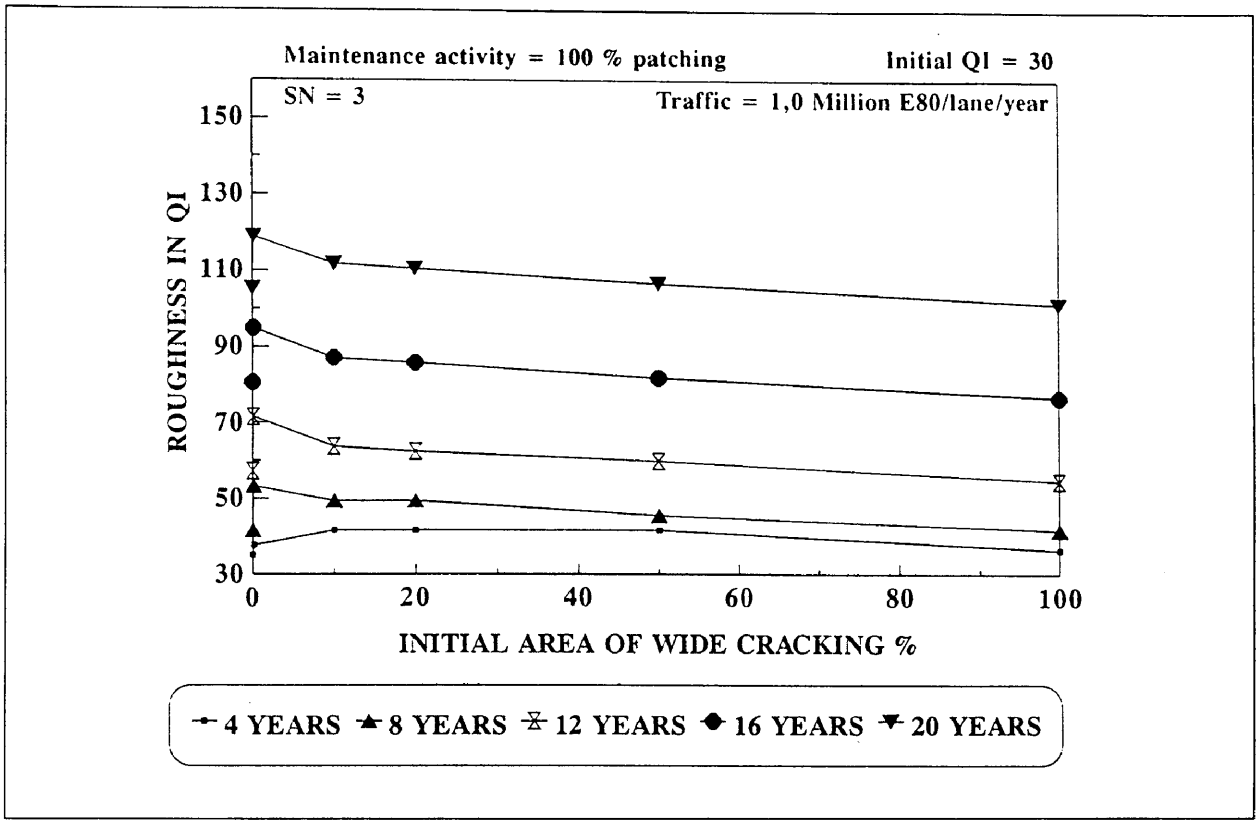

Figure A.39: Sensitivity to initial area of wide cracking for SN = 3 and heavy traffic.

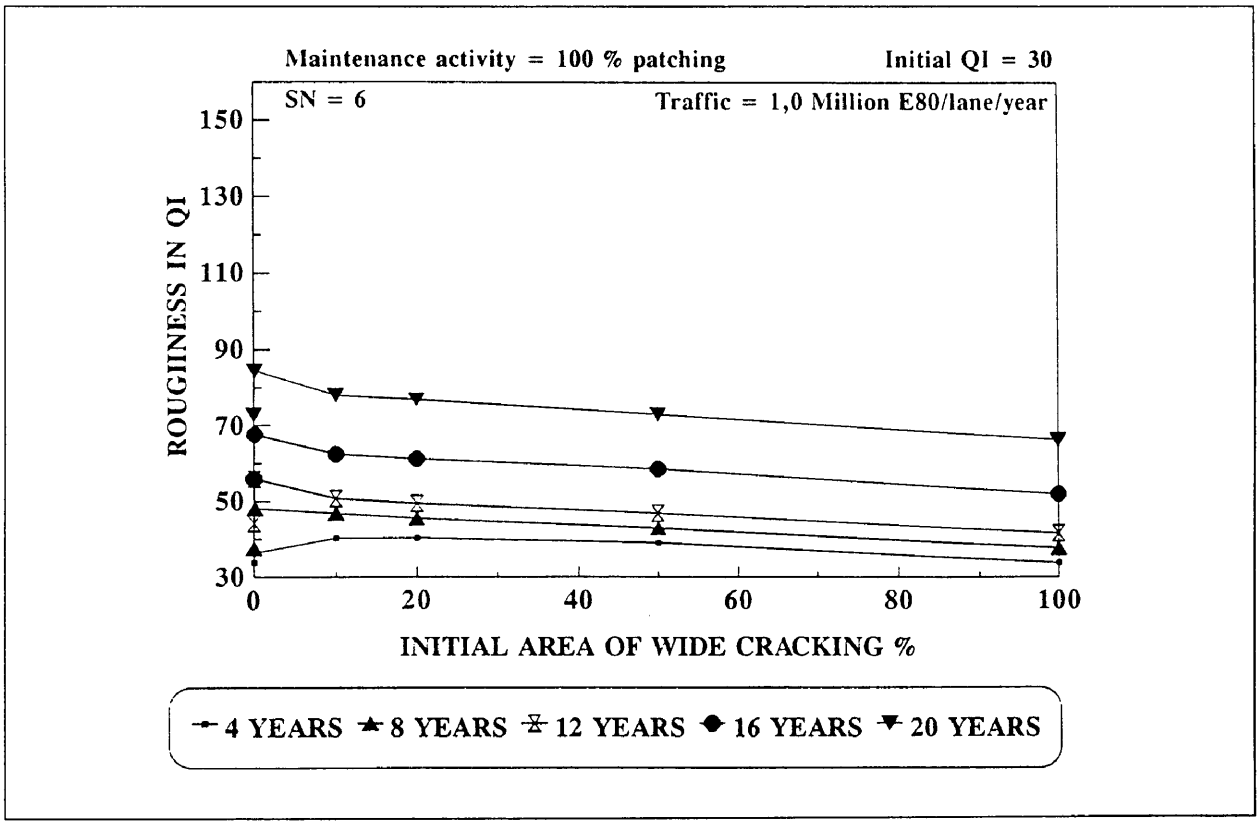

Figure A.40: Sensitivity to initial area of wide cracking for SN = 6 and heavy traffic.

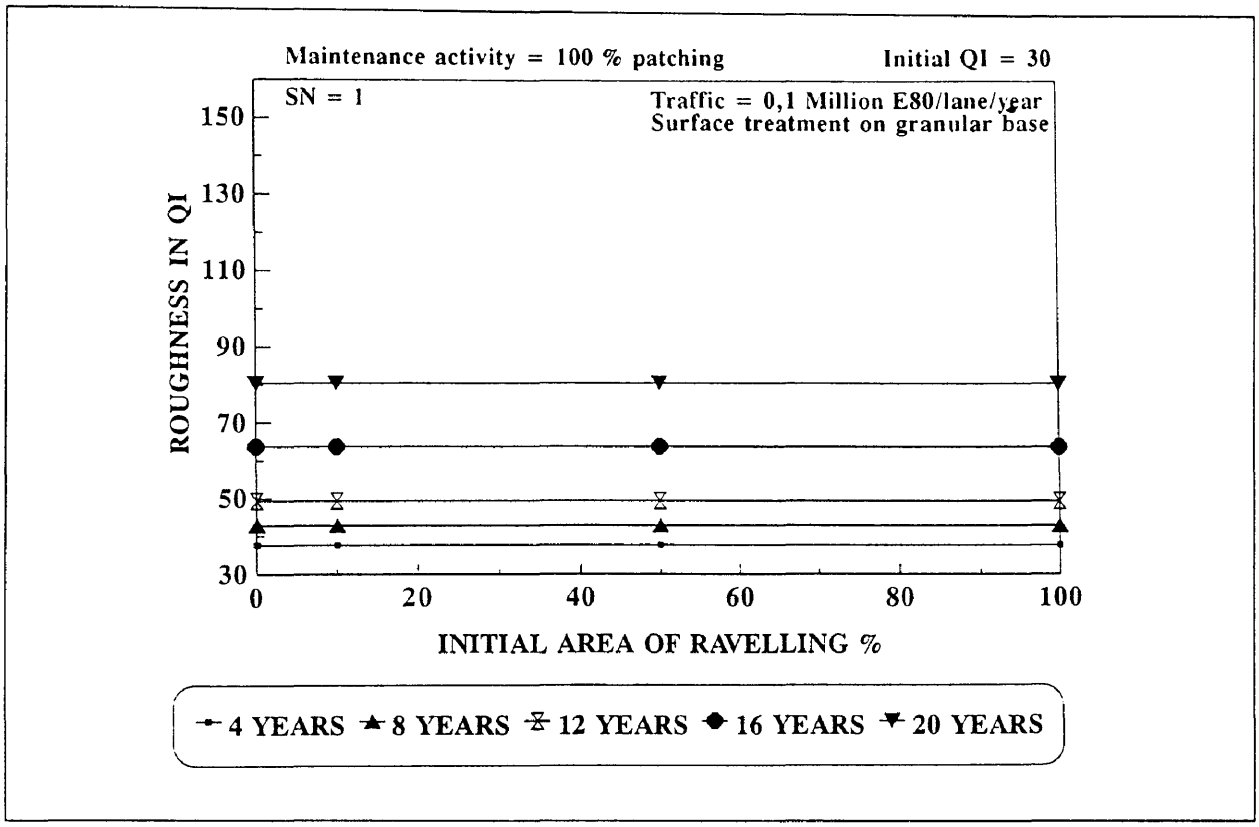

Figure A.41: Sensitivity to initial area of ravelling for SN = 1 and light traffic.

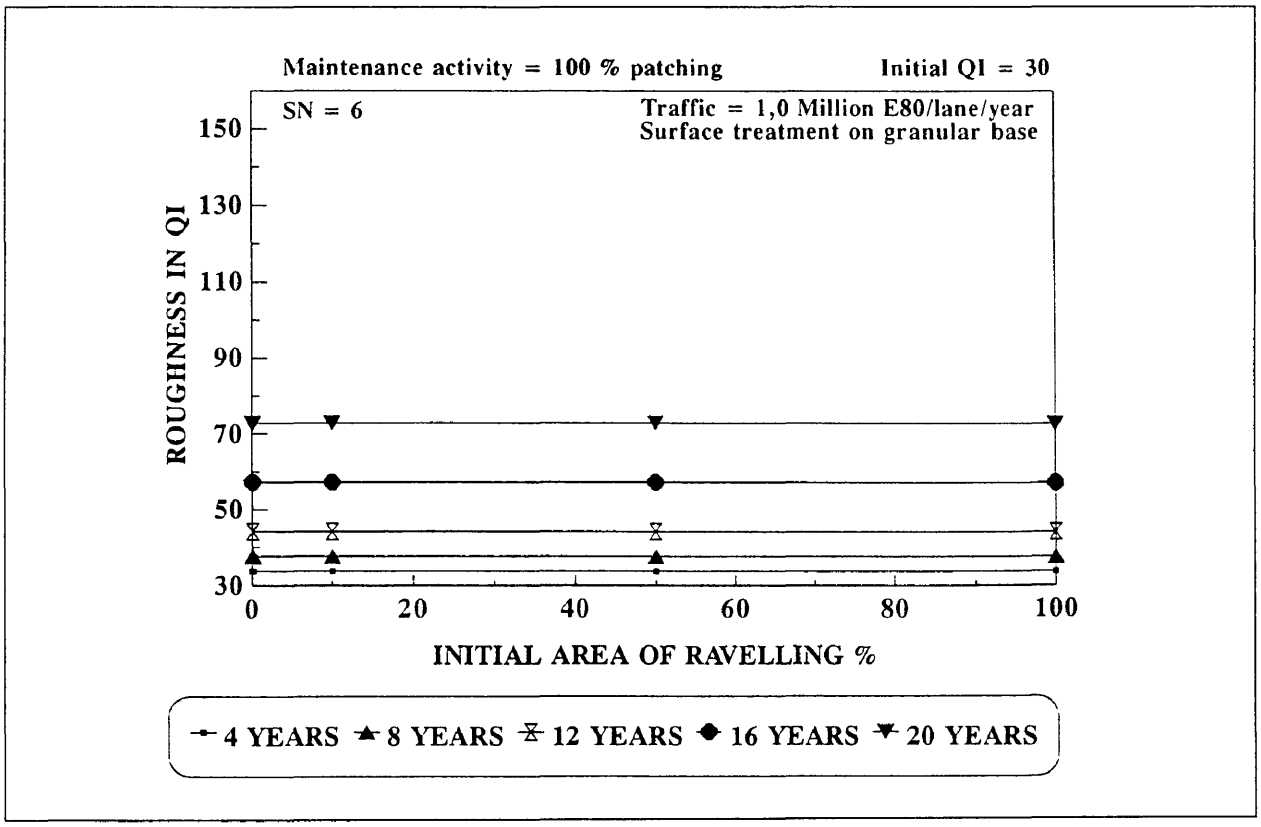

Figure A.42: Sensitivity to initial area of ravelling for SN = 6 and heavy traffic.

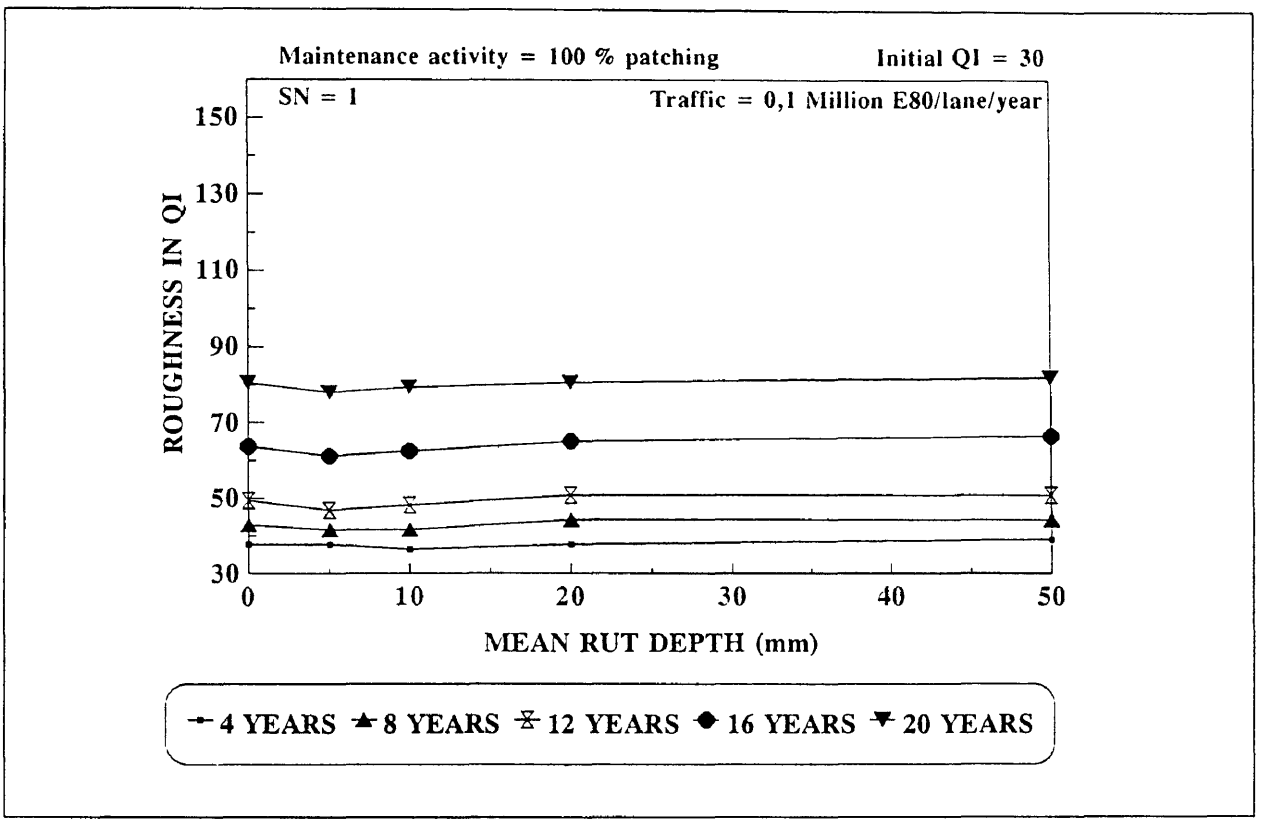

Figure A.43: Sensitivity to initial rut depth for SN = 1 and light traffic.

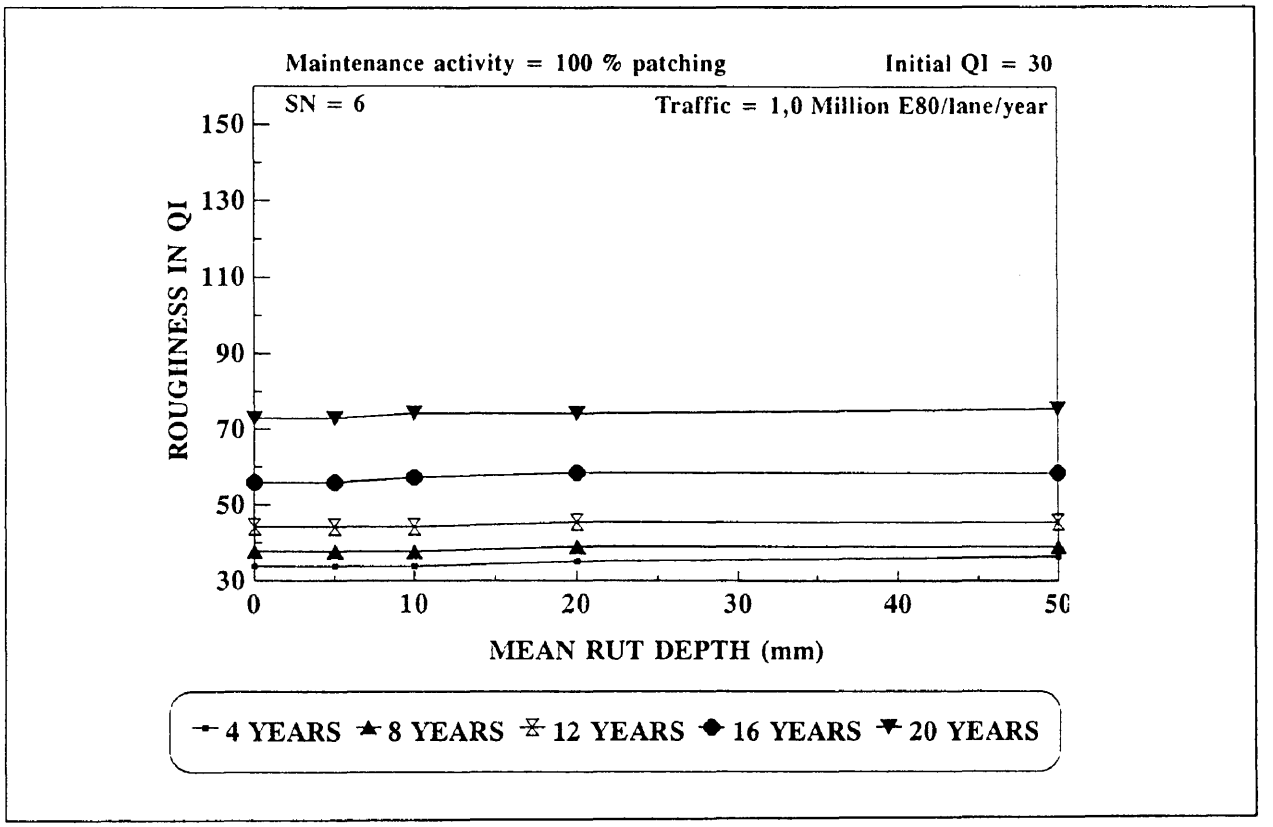

Figure A.44: Sensitivity to initial rut depth for SN = 6 and heavy traffic.

APPENDIX B

General information of sections used in study

Table B.1: General information of pavement sections used in study.

Route	Section	Direction	Construc Date	Lenght of section		Wearing coarse		Base coarse		Subbase		Top selected layers		Bottom selected layers		Site	Thornthwaite	Monthly Rainfall mm
				From	To	Material	Thickness	Material	Thickness	Material	Thickness	Material	Thickness	Material	Thickness			
N0001	3	N	85	25	30	S4	19	G2	200	G5	150	G7	150	NONE		Level	Semi-arid	20
N0001	4	N	84	10	15	S4	19	G2	200	G5	150	G8	250	NONE		Level	Semi-arid	20
N0001	4	N	83	60	65	S4	19	G2	200	G5	150	G8	250	NONE		Level	Semi-arid	20
N0001	5	N	75	20	25	S4	19	G2	200	G5	100	G7	250	NONE		Level	Semi-arid	20
N0001	6	N	78	20	25	S4	19	G2	200	G5	100	G7	250	NONE		Level	Semi-arid	20
N0001	7	N	75	20	25	S4	19	G2	200	G5	150	G8	250	NONE		Level	Semi-arid	20
N0001	7	N	75	40	45	S4	19	G2	200	G5	150	G8	250	NONE		Level	Semi-arid	20
N0001	8	N	80	20	25	S4	13	G2	200	G5	150	G8	250	NONE		Level	Semi-arid	20
N0001	8	N	83	65	70	S4	19	G2	200	G5	150	G8	250	NONE		Level	Semi-arid	20
N0001	9	N	82	11	16	S2	19	G2	200	G5	100	G7	250	NONE		Level	Semi-arid	20
N0001	9	N	87	80	85	S4	19	G2	200	G5	100	G7	250	NONE		Level	Semi-arid	20
N0001	10	N	80	10	15	S4	19	G1	200	G5	150	G7	250	NONE		Level	Semi-arid	30
N0001	10	N	80	40	45	S4	19	G1	200	G5	150	G7	250	NONE		Level	Semi-arid	30
N0001	11	N	88	30	35	S4	19	G1	150	C3	150	G7	250	NONE		Level	Semi-arid	30
N0001	15	N	12/76	31	39	AS	50	G3	200	C3	150	G7	300	NONE		Level	Semi-arid	45.8
N0001	18	N	12/77	70	77	AS	40	BS	90	C3	300	G7	125	G7	125	Level	Subhumid	60
N0001	21	N	74/75	19	25	AC	30	G1	200	C2	150	G5	150	G7	150	Level	Subhumid	60
N0001	21	N	74/75	29	33	AG	60	G1	200	C2	100	G5	125	G7	150	Level	Subhumid	60
N0001	21	N	74/75	35	40	AG	30	G1	200	C2	150	C2	125	G9	125	Level	Subhumid	60
N0001	22	N	05/75	0	4	AS	30	G1	200	C1	150	C2	125	G9	125	Level	Subhumid	60
N0001	22	N	05/75	18	22	AS	25	BC	125	C2	150	G7	150	NONE		Level	Subhumid	60
N0001	23	N	12/77	14	28	AS	40	BS	80	C3	200	C4	150	G7	150	Rolling	Subhumid	60
N0001	1	S	73	20	23	AC	25	BS	125	G5	150	G5	150	G9	150	Rolling	Subhumid	80
N0001	12	S	08/73	4	10	S4	19	G3	200	G5	150	G7	125	G9	150	Rolling	Semi-arid	37.5
N0001	12	S	08/73	20	25	S4	19	G3	200	G5	150	G7	125	G9	150	Rolling	Semi-arid	37.5
N0001	14	S	03/75	29	48	S4	19	G3	200	C3	150	G5	250	G9	150	Level	Semi-arid	45.8
N0001	15	S	03/75	10	20	S4	19	G3	200	C3	150	G7	300	NONE		Level	Semi-arid	45.8
N0001	16	S	10/73	67	78	S4	19	G1	150	C3	300	G7	150	G7	150	Level	Semi- arid	45.8
N0002	6	E	73	1	10	AG	45	G2	200	G5	150	G7	125	NONE		Rolling	Subhumid	80
N0002	6	E	73	15	22	S4	19	G2	200	G5	150	G7	250	NONE		Rolling	Subhumid	80
N0002	6	E	80	40	45	S4	19	G2	200	G5	150	G7	250	NONE		Rolling	Subhumid	80
N0002	6	E	78	60	65	S4	19	G2	200	G5	150	G7	125	NONE		Rolling	Subhumid	80
N0002	6	W	78	85	90	AG	45	G2	200	G5	150	G7	125	NONE		Rolling	Subhumid	80
N0002	7	E	88	20	25	S4	19	G1	150	C3	300	G6	300	G7	300	Rolling	Subhumid	80
N0002	10	E	72	0	8	S4	19	G2	200	G5	150	G6	250	G7	150	Rolling	Subhumid	80
N0002	10	E	78	40	52	AS	40	G2	150	C2	300	G6	150	G7	150	Rolling	Subhumid	80
N0002	10	E	79	13	25	S4	19	G2	200	G5	150	G6	250	G7	150	Rolling	Subhumid	80
N0002	10	E	74	61	65	AC	30	G2	200	G5	150	G6	300	G7	150	Rolling	Subhumid	80
N0002	11	E	83	24	30	AC	30	G2	200	G5	150	G7	300	NONE		Rolling	Subhumid	60
N0002	11	E	71	31	32	AC	30	BC	150	G5	150	G7	300	NONE		Rolling	Subhumid	60
N0002	11	E	71	43	45	AC	60	G2	200	G5	150	G7	300	NONE		Rolling	Subhumid	60
N0002	11	E	71	60	68	AC	25	C2	150	G5	150	G7	250	NONE		Rolling	Subhumid	60
N0002	16	E	77	0	5	AS	30	BC	150	C4	150	G5	250	G7	250	Level	Subhumid	100
N0002	16	E	78	9	14	AS	30	BC	150	C2	150	G5	250	G7	250	Level	Subhumid	100
N0002	16	E	75	16	22	AC	30	G2	200	G4	150	G5	250	G7	250	Level	Subhumid	100
N0002	16	E	56	50	60	AC	30	G2	110	G5	250	G7	250	NONE		Mountain	Subhumid	100
N0002	23	E	75	7	13	AG	50	BC	120	C3/C4	150/150	G9	150	NONE		Rolling	Humid	100
N0002	23	E	79	33	41	AS	40	BC	120	C3/C4	150/150	G7	150	G9	150	Rolling	Humid	100
N0002	23	W	75	27	32	AG	50	BC	120	C3/C4	150/150	G7	150	G9	150	Rolling	Humid	100
N0002	24	E	72	14	18	AS	40	BC	110	C3/C4	150/150	G7	150	G9	150	Rolling	Humid	100
N0002	25	W	76	18	22	AS	38	BS	150	C3/C4	150/150	C3	150	G7	150	Rolling	Humid	100
N0002	26	W	78	4	10	AS	40	BC	90	C3/C4	150/150	G7	150	G9	150	Rolling	Humid	100
N0002	29	E	65	0	5	AS	30	C2	200	G6	150	G9	250	NONE		Rolling	Humid	100
N0002	30	E	74	66	74	S1+S6	15	G2	200	C3	150	G9	300	NONE		Rolling	Humid	100
N0003	1	N	74	9	16	AS	40	BC	125	C3/C4	150/150	G7	100	G9	125	Rolling	Humid	100
N0003	1	N	74	20	25	AS	40	BC	125	C3/C4	150/150	G7	100	G9	125	Rolling	Humid	100
N0003	1	N	74	25	30	AS	40	BC	125	C3/C4	150/150	G7	100	G9	125	Rolling	Humid	100
N0003	2	N	72	12	20	AS	30	C2	200	G5	150	G7	300	NONE		Rolling	Humid	100
N0003	3	S	75	16	18	AS	40	G2	200	G5	200	G8	200	NONE		Rolling	Humid	95
N0003	4	N	75	53	58	AS	50	G2	200	C3	150	G7	300	G9	150	Rolling	Humid	95
N0003	11	N	73	29	36	AG	30	G1	200	C2	150	G5	150	G7	150	Rolling	Subhumid	60
N0003	12	S	05/76	0	8	AS	40	G1	150	C3/C4	150/150	G7	150	G9	150	Rolling	Subhumid	60
N0003	12	S	03/77	17	20	AS	30	BC	150	C2	150	C2	125	G9	150	Rolling	Subhumid	60
N0003	12	S	07/75	24	25	AS	50	BC	125	C1	175	G1	150	G5/G7	150/150	Rolling	Subhumid	60
N0004	1	W	69	21	25	AC	25	C1	100	C1	100	C3	100	G5/G7	125/125	Rolling	Subhumid	60

Abbreviations according to TRH 4 (1985) classification.

Table B.2: General description of extent classification.

Extent	Description	% of length of segment
1	Isolated occurrence and is not representative of the link that is being evaluated (Seldom).	0 - 5
2	Intermittent occurrence (more than isolated).	5 - 15
3	Regular occurrence, but not over full length.	15 - 30
4	More frequent occurrence, occurs over a major portion of the link.	30 - 60
5	Extensive occurrence.	> 60

The above Table is obtained from the Committee of State Road Authorities (CSRA) proposal of 1990.

Table B.3: Roughness, rut depth and deflection measurements used in study.

Route	Section	Direction	Kilometre distance		Riding quality						Rut depth in mm			Deflection in mm		
			From	To	Year	Ave PSI	Std deviation	Qlr	Qlm	Ave IRI	Year	Avg	Std deviation	Year	Avg	Std deviation
N0001	3	N	25.00	30.00	88	3.19	0.25	27.22	33.99	2.61						
					89	2.99	0.22	30.87	37.28	2.87						
					90	3.06	0.22	29.56	36.11	2.78						
					91	2.89	0.24	32.79	39.01	3.00						
					92	2.56	0.32	39.62	45.16	3.47						
					93	2.79	0.29	34.77	40.79	3.14						
N0001	4	N	10.00	15.00	88	3.16	0.16	27.75	34.47	2.65						
					89	2.96	0.15	31.44	37.79	2.91						
					90	3.17	0.20	27.57	34.31	2.64						
					91	2.94	0.19	31.82	38.14	2.93						
					92	2.61	0.21	38.53	44.18	3.40						
					93	2.79	0.19	34.77	40.79	3.14						
N0001	4	N	60.00	65.00	88	2.80	0.16	34.57	40.61	3.12						
					89	2.52	0.19	40.51	45.96	3.54						
					90	2.68	0.20	37.04	42.84	3.30						
					91	2.52	0.17	40.51	45.96	3.54						
					92	2.12	0.22	50.26	54.73	4.21						
					93	2.36	0.20	44.21	49.29	3.79						
N0001	5	N	20.00	25.00	88	3.08	0.15	29.20	35.78	2.75						
					89	2.91	0.15	32.40	38.66	2.97						
					90	3.04	0.17	29.93	36.44	2.80						
					91	2.86	0.16	33.37	39.54	3.04						
					92	2.51	0.20	40.74	46.16	3.55						
					93	2.66	0.19	37.46	43.22	3.32						
N0001	6	N	20.00	25.00	89	2.87	0.22	33.18	39.36	3.03						
					90	2.96	0.25	31.44	37.79	2.91						
					91	2.81	0.21	34.37	40.43	3.11						
					92	2.44	0.31	42.33	47.60	3.66						
					93	2.54	0.28	40.07	45.56	3.50						
N0001	7	N	20.00	25.00	88	3.14	0.20	26.11	34.80	2.68						
					89	2.98	0.24	31.06	37.45	2.88						
					90	3.09	0.22	29.01	35.61	2.74						
					91	2.94	0.25	31.82	38.14	2.93						
					92	2.59	0.25	38.97	44.57	3.43						
					93	2.71	0.27	36.41	42.27	3.25						
N0001	7	N	40.00	45.00	88	3.36	0.24	24.29	31.36	2.41						
					89	3.09	0.23	29.01	35.61	2.74						
					90	3.24	0.22	26.34	33.21	2.55						
					91	3.07	0.21	29.38	35.94	2.76						
					92	2.78	0.30	34.97	40.98	3.15						
					93	2.81	0.27	34.37	40.43	3.11						
N0001	8	N	20.00	25.00	89	3.19	0.16	27.22	33.99	2.61						
					90	3.25	0.17	26.17	33.05	2.54						
					91	3.05	0.16	29.75	36.27	2.79						
					92	2.62	0.22	38.32	43.98	3.38						
					93	2.71	0.21	36.41	42.27	3.25						
N0001	8	N	65.00	70.00	89	3.19	0.20	27.22	33.99	2.61						
					90	3.27	0.21	25.82	32.74	2.52						
					91	3.15	0.23	27.93	34.64	2.66						
					92	2.72	0.30	36.20	42.06	3.24						
					93	2.89	0.22	32.79	39.01	3.00						
N0001	9	N	11.00	16.00	88	3.52	0.13	21.67	29.00	2.23						
					89	3.27	0.19	25.82	32.74	2.52						
					90	3.35	0.13	24.46	31.51	2.42						
					91	3.17	0.17	27.57	34.31	2.64						
					92	2.86	0.27	33.37	39.54	3.04						
					93	2.99	0.21	30.87	37.28	2.87						
N0001	9	N	80.00	85.00	88	3.48	0.18	22.31	29.58	2.28	81.00	1.06	0.33	81	0.37	0.07
					89	3.35	0.16	24.46	31.51	2.42						
					90	3.36	0.19	24.29	31.36	2.41						
					91	3.25	0.17	26.17	33.05	2.54						
					92	2.91	0.24	32.40	38.66	2.97						
					93	3.01	0.25	30.49	36.94	2.84						
N0001	10	N	10.00	15.00	88	3.52	0.15	21.67	29.00	2.23	85	3.03	1.15	85	0.26	0.15
					89	3.38	0.13	23.95	31.06	2.39						
					90	3.43	0.13	23.13	30.31	2.33						
					91	3.24	0.13	26.34	33.21	2.55						
					92	3.01	0.18	30.49	36.94	2.84						
					93	3.04	0.18	29.93	36.44	2.80						
N0001	10	N	40.00	45.00	88	3.45	0.17	22.80	30.02	2.31	83	1.38	1.35	83	0.12	0.04
					89	3.25	0.15	26.17	33.05	2.54						
					90	3.31	0.19	25.13	32.12	2.47						
					91	3.19	0.15	27.22	33.99	2.61						
					92	2.84	0.25	33.77	39.89	3.07						
					93	2.97	0.22	31.25	37.62	2.89						
N0001	11	N	30.00	35.00	88	3.33	0.21	24.79	31.81	2.45	82	3.08	0.52	82	0.32	0.06
					89	3.25	0.21	26.17	33.05	2.54						
					90	3.39	0.20	23.79	30.91	2.38						
					91	3.26	0.20	25.99	32.89	2.53						
					92	2.92	0.30	32.20	38.48	2.96						
					93	3.02	0.26	30.30	36.77	2.83						
N0001	15	N	31.00	39.00	77	4.09	0.45	13.27	21.44	1.65	81	1.06	0.33	81	0.37	0.07
					78	3.89	0.79	16.03	23.93	1.84						
					82	3.96	0.63	15.02	23.02	1.77						
					83	3.64	0.42	19.84	27.35	2.10						
					84	4.07	0.31	13.53	21.68	1.67						
					85	4.04	0.34	13.97	22.07	1.70						
					87	4.16	0.25	12.27	20.55	1.58						
					88	3.67	0.37	19.36	26.92	2.07						
					89	3.16	0.35	27.70	34.43	2.65						
					90	3.18	0.33	27.34	34.11	2.62						
					91	3.18	0.36	27.39	34.15	2.63						
					92	2.73	0.47	36.06	41.95	3.23						
					93	2.98	0.48	31.00	37.40	2.88						

Table B.3: Continued.

Route	Section	Direction	Kilometre distance		Riding quality						Rut depth in mm			Deflection in mm		
			From	To	Year	Ave PSI	Std deviation	Qlr	Qlm	Ave IRI	Year	Avg	Std deviation	Year	Avg	Std deviation
N0001	14	S	29.00	48.00	77	2.97	0.50	31.21	37.59	2.89						
					78	2.84	0.45	33.69	39.82	3.06						
					79	3.02	0.44	30.36	36.82	2.83						
					82	3.03	0.39	30.10	36.59	2.81						
					83	2.96	0.37	31.47	37.83	2.91						
					84	2.94	0.30	31.76	38.08	2.93						
					88	3.96	0.17	15.01	23.01	1.77						
					89	3.87	0.16	16.35	24.22	1.86						
					90	3.83	0.16	16.90	24.71	1.90						
					91	3.86	0.18	16.52	24.37	1.87						
					92	3.83	0.23	16.91	24.72	1.90						
					93	3.74	0.22	18.22	25.90	1.99						
N0001	15	S	10.00	20.00	77	3.38	0.45	23.97	31.07	2.39	81	3.09	0.84	81	0.33	0.11
					78	3.16	0.45	27.75	34.47	2.65						
					79	3.30	0.34	25.39	32.35	2.49						
					82	3.33	0.35	24.81	31.83	2.45						
					83	3.24	0.43	26.43	33.28	2.56						
					84	3.15	0.26	27.91	34.62	2.66						
					88	3.78	0.33	17.66	25.40	1.95						
					89	3.72	0.38	18.55	26.19	2.01						
					90	3.67	0.35	19.36	26.92	2.07						
					91	3.65	0.37	19.65	27.19	2.09						
					92	3.51	0.60	21.84	29.18	2.24						
					93	3.52	0.47	21.75	29.07	2.24						
N0001	16	S	67.00	78.00	77	3.48	0.45	22.31	29.58	2.28	81	4.79	1.84	81	0.29	0.11
					78	2.97	0.51	31.23	37.60	2.89						
					79	3.21	0.46	26.81	33.63	2.59						
					82	3.34	0.55	24.56	31.60	2.43						
					83	3.19	0.50	27.20	33.98	2.61						
					84	3.06	0.38	29.65	36.19	2.78						
					88	3.09	0.34	29.09	35.68	2.74						
					89	3.02	0.39	30.30	36.77	2.83						
					90	3.87	0.16	16.31	24.17	1.86						
					91	3.76	0.16	17.93	25.64	1.97						
					92	3.42	0.42	23.34	30.51	2.35						
					93	3.30	0.53	25.24	32.21	2.48						
N0002	6	E	1.00	10.00	77	3.88	0.40	16.13	24.02	1.85	82	4.40	0.50	82	0.41	0.08
					78	3.72	0.56	18.56	26.21	2.02						
					79	4.04	0.50	13.90	22.01	1.69						
					82	3.95	0.56	15.19	23.18	1.78						
					83	3.65	0.48	19.57	27.12	2.09						
					88	3.70	0.29	18.81	26.43	2.03						
					89	3.61	0.29	20.18	27.66	2.13						
					90	3.52	0.29	21.71	29.04	2.23						
					91	3.47	0.30	22.46	29.71	2.29						
					92	3.29	0.44	25.48	32.43	2.49						
					93	3.23	0.39	26.46	33.32	2.56						
N0002	6	E	15.00	22.00	77	3.66	0.38	19.42	26.98	2.08	85	4.06	1.63	85	0.41	0.10
					78	3.42	0.48	23.34	30.51	2.35						
					79	3.63	0.36	19.87	27.38	2.11						
					82	3.59	0.49	20.62	28.06	2.16						
					83	3.57	0.41	20.85	28.27	2.17						
					88	3.26	0.24	25.94	32.85	2.53						
					89	3.33	0.25	24.79	31.81	2.45						
					90	3.28	0.25	25.60	32.54	2.50						
					91	3.10	0.22	28.83	35.45	2.73						
					92	2.81	0.31	34.39	40.45	3.11						
N0002	6	E	40.00	45.00	88	3.24	0.23	26.34	33.21	2.55						
					89	3.47	0.20	22.47	29.72	2.29						
					90	3.38	0.18	23.95	31.06	2.39						
					91	3.23	0.20	26.51	33.36	2.57						
					92	3.00	0.24	30.68	37.11	2.85						
					93	2.81	0.19	34.37	40.43	3.11						
N0002	6	E	60.00	65.00	88	3.20	0.21	27.04	33.84	2.60						
					89	3.31	0.21	25.13	32.12	2.47						
					90	3.23	0.22	26.51	33.36	2.57						
					91	3.12	0.18	28.47	35.12	2.70						
					92	2.84	0.26	33.77	39.89	3.07						
					93	2.77	0.21	35.18	41.16	3.17						
N0002	7	E	20.00	25.00	89	3.16	0.27	27.75	34.47	2.65						
					90	3.08	0.28	29.20	35.78	2.75						
					91	2.94	0.28	31.82	38.14	2.93						
					92	2.57	0.32	39.40	44.96	3.46						
					93	2.43	0.29	42.56	47.81	3.68						
N0002	10	E	0.00	8.00	79	3.53	0.46	21.46	28.81	2.22						
					82	3.54	0.49	21.41	28.77	2.21						
					84	3.33	0.27	24.83	31.85	2.45						
					88	3.72	0.23	18.55	26.19	2.01						
					89	3.73	0.21	18.40	26.06	2.00						
					90	3.73	0.20	18.40	26.06	2.00						
					91	3.65	0.21	19.62	27.16	2.09						
					92	3.62	0.26	20.09	27.58	2.12						
					93	3.46	0.29	22.63	29.67	2.30						
N0002	10	E	13.00	25.00	79	3.43	0.41	23.08	30.27	2.33	87	2.91	2.60	87	0.42	0.11
					82	3.48	0.49	22.26	29.54	2.27						
					84	3.28	0.25	25.58	32.52	2.50						
					88	3.42	0.26	23.29	30.46	2.34						
					89	3.38	0.27	23.95	31.06	2.39						
					90	3.35	0.24	24.46	31.51	2.42						
					91	3.31	0.22	25.13	32.12	2.47						
					92	2.96	0.33	31.44	37.79	2.91						
					93	2.91	0.25	32.40	38.66	2.97						
N0002	10	E	40.00	52.00	79	3.59	0.36	20.51	27.96	2.15	87	5.00	1.92	87	0.16	0.13
					82	3.59	0.38	20.51	27.96	2.15						
					84	3.36	0.25	24.37	31.44	2.42						
					88	3.23	0.24	26.51	33.36	2.57						
					89	3.20	0.28	27.04	33.84	2.60						
					90	3.14	0.27	28.11	34.80	2.68						
					91	3.11	0.26	28.65	35.28	2.71						
					92	2.75	0.34	35.59	41.53	3.19						
					93	2.74	0.32	35.79	41.71	3.21						

Table B.3: Continued.

Route	Section	Direction	Kilometre distance		Riding quality						Rut depth in mm			Deflection in mm		
			From	To	Year	Ave PSI	Std deviation	Qlr	Qlm	Ave IRI	Year	Avg	Std deviation	Year	Avg	Std deviation
N0002	10	E	61.00	65.00	77	3.39	0.41	23.79	30.91	2.38	87	5.84	2.32	87	0.60	0.15
					78	3.27	0.57	25.85	32.77	2.52						
					79	3.41	0.46	23.41	30.57	2.35						
					82	3.36	0.54	24.37	31.44	2.42						
					84	3.33	0.37	24.74	31.77	2.44						
					88	3.29	0.29	25.48	32.43	2.49						
					89	3.17	0.31	27.57	34.31	2.64						
					90	3.09	0.32	29.01	35.61	2.74						
					91	3.14	0.33	28.11	34.80	2.68						
					92	2.65	0.43	37.67	43.41	3.34						
					93	2.63	0.34	38.10	43.79	3.37						
N0002	11	E	24.00	30.00	77	3.58	0.61	20.67	28.10	2.16						
					78	3.58	0.69	20.71	28.14	2.16						
					79	3.66	0.58	19.42	26.98	2.08						
					82	3.52	0.68	21.75	29.07	2.24						
					84	3.53	0.44	21.47	28.83	2.22						
					88	3.47	0.76	22.52	29.77	2.29						
					89	3.64	0.25	19.73	27.25	2.10						
					90	3.60	0.30	20.43	27.89	2.15						
					91	3.57	0.26	20.82	28.24	2.17						
					92	3.38	0.39	24.00	31.10	2.39						
					93	3.48	0.36	22.26	29.54	2.27						
N0002	11	E	31.00	32.00	77	3.51	0.92	21.83	29.14	2.24	77	3.40	1.90	77	0.25	0.03
					78	3.60	1.11	20.40	27.85	2.14						
					79	3.44	0.72	22.96	30.17	2.32						
					82	2.94	0.95	31.82	38.14	2.93						
					84	3.62	0.70	20.09	27.58	2.12						
					88	2.94	0.41	31.82	38.14	2.93						
					89	3.42	0.39	23.29	30.46	2.34						
					90	3.48	0.20	22.31	29.58	2.28						
					91	3.48	0.18	22.31	29.58	2.28						
					92	3.19	0.29	27.22	33.99	2.61						
					93	3.32	0.29	24.95	31.97	2.46						
N0002	11	E	43.00	45.00	77	4.05	0.54	13.76	21.88	1.68	82	5.30	1.26	82	0.75	0.18
					78	3.75	0.43	18.10	25.79	1.98						
					79	4.05	0.52	13.76	21.88	1.68						
					82	4.00	0.48	14.41	22.47	1.73						
					84	4.11	0.27	12.97	21.17	1.63						
					88	3.98	0.12	14.74	22.77	1.75						
					89	3.50	0.08	21.99	29.29	2.25						
					90	3.45	0.09	22.86	30.09	2.31						
					91	3.39	0.61	23.67	30.98	2.38						
					92	3.13	0.21	28.29	34.96	2.69						
					93	3.33	0.65	24.88	31.89	2.45						
N0002	11	E	60.00	68.00	77	3.52	0.50	21.70	29.03	2.23	82	6.49	1.45	82	0.43	0.15
					78	3.26	0.46	25.98	32.88	2.53						
					79	3.33	0.40	24.83	31.85	2.45						
					82	3.18	0.35	27.45	34.20	2.63						
					84	2.92	0.35	32.24	38.52	2.96						
					88	2.41	0.31	43.10	48.29	3.71						
					89	2.58	0.41	39.23	44.81	3.45						
					90	2.49	0.46	41.19	46.57	3.58						
					91	2.35	0.45	44.38	49.44	3.80						
					92	1.89	0.46	56.70	60.53	4.66						
					93	1.95	0.42	55.00	59.00	4.54						
N0002	16	E	0.00	5.00	78	3.65	0.32	19.56	27.10	2.08						
					79	3.62	0.30	20.16	27.65	2.13						
					82	3.79	0.32	17.45	25.21	1.94						
					84	3.69	0.22	19.07	26.66	2.05						
N0002	16	E	9.00	14.00	77	3.61	0.54	20.24	27.72	2.13	82	6.63	1.69	82	6.63	1.69
					78	3.52	0.50	21.63	28.97	2.23						
					79	3.31	0.46	25.13	32.12	2.47						
					82	3.40	0.56	23.56	30.70	2.36						
					84	3.51	0.40	21.76	29.09	2.24						
					88	3.66	0.22	19.44	26.99	2.08						
					89	3.45	0.40	22.73	29.95	2.30						
					90	3.41	0.19	23.46	30.61	2.35						
					91	3.30	0.19	25.30	32.27	2.48						
					92	3.05	0.24	29.82	36.34	2.80						
					93	3.23	0.20	26.60	33.44	2.57						
N0002	16	E	16.00	22.00	78	3.27	0.72	25.85	32.77	2.52	82	4.40	1.18	82	0.37	0.16
					79	3.15	0.70	27.87	34.59	2.66						
					82	3.77	0.43	17.87	25.58	1.97						
					84	3.53	0.27	21.52	28.87	2.22						
					88	3.47	0.34	22.47	29.72	2.29						
					89	3.38	0.29	23.95	31.05	2.39						
					90	3.28	0.29	25.70	32.63	2.51						
					91	3.25	0.26	26.22	33.10	2.55						
					92	2.92	0.41	32.16	38.45	2.96						
					93	3.02	0.58	30.36	36.82	2.83						
N0002	16	E	50.00	60.00	78	3.44	0.39	22.93	30.14	2.32	82	6.09	1.32	82	0.80	0.25
					79	3.44	0.34	22.96	30.17	2.32						
					82	3.49	0.26	22.18	29.46	2.27						
					84	3.30	0.25	25.37	32.34	2.49						
					88	3.15	0.30	27.95	34.65	2.67						
					89	3.20	0.21	27.04	33.84	2.60						
					90	3.13	0.23	28.34	35.01	2.69						
					91	3.03	0.20	30.06	36.56	2.81						
					92	2.57	0.28	39.47	45.02	3.46						
					93	2.89	0.25	32.81	39.02	3.00						
N0002	23	E	7.00	13.00	79	4.02	0.44	14.16	22.25	1.71	88	4.65	2.33	88	0.27	0.07
					81	4.11	0.44	12.98	21.18	1.63						
					84	4.02	0.23	14.20	22.28	1.71						
					85	3.92	0.20	15.67	23.60	1.82						
					87	3.75	0.24	18.17	25.85	1.99						
					89	3.58	0.20	20.76	28.18	2.17						
					90	3.49	0.17	22.15	29.43	2.26						
					91	3.48	0.18	22.26	29.54	2.27						
					92	3.21	0.32	26.85	33.66	2.59						
					93	3.38	0.22	23.90	31.01	2.39						

Table B.3: Continued.

Route	Section	Direction	Kilometre distance		Riding quality						Rut depth in mm			Deflection in mm		
			From	To	Year	Ave PSI	Std deviation	Qir	Qlm	Ave IRI	Year	Avg	Std deviation	Year	Avg	Std deviation
N0002	23	E	33.00	41.00	79	3.98	0.56	14.68	22.71	1.75	88	7.28	3.42	88	0.31	0.07
					81	4.20	0.48	11.67	20.00	1.54						
					84	4.09	0.23	13.25	21.43	1.65						
					85	4.10	0.21	13.11	21.30	1.64						
					87	3.88	0.27	16.12	24.00	1.85						
					89	3.70	0.19	18.85	26.47	2.04						
					90	3.57	0.23	20.90	28.31	2.18						
					91	3.58	0.19	20.71	28.14	2.16						
					92	3.44	0.29	22.91	30.12	2.32						
					93	3.59	0.27	20.51	27.96	2.15						
N0002	24	E	14.00	18.00	77	3.33	0.37	24.81	31.83	2.45						
					78	3.28	0.39	25.60	32.54	2.50						
					79	3.10	0.28	28.83	35.45	2.73						
					81	3.14	0.38	28.07	34.76	2.67						
					84	2.97	0.36	31.28	37.66	2.90						
					87	3.53	0.35	21.44	28.80	2.22						
					89	3.47	0.30	22.47	29.72	2.29						
					90	3.35	0.32	24.42	31.48	2.42						
					91	3.34	0.34	24.69	31.72	2.44						
					92	3.08	0.42	29.27	35.84	2.76						
					93	3.27	0.38	25.85	32.77	2.52						
N0002	29	E	0.00	5.00	77	3.35	0.64	24.52	31.57	2.43						
					78	3.37	0.62	24.09	31.16	2.40						
					79	3.31	0.57	25.13	32.12	2.47						
					81	3.26	0.47	26.03	32.92	2.53						
					84	3.33	0.38	24.83	31.85	2.45						
					88	3.40	0.99	23.59	30.73	2.36						
					89	3.03	0.26	30.04	36.54	2.81						
					90	2.97	0.24	31.21	37.59	2.89						
					91	2.93	0.23	32.05	38.34	2.95						
					92	2.54	0.26	40.15	45.64	3.51						
					93	2.68	0.26	37.12	42.91	3.30						
N0002	30	E	66.00	74.00	78	3.39	0.30	23.79	30.91	2.38	83	6.28	1.32	83	0.27	0.11
					79	3.65	0.34	19.56	27.10	2.08						
					81	3.41	0.36	23.52	30.67	2.36						
					84	3.07	0.20	29.45	36.01	2.77						
					85	3.43	0.18	23.06	30.25	2.33						
					88	3.12	0.36	28.45	35.10	2.70						
					89	3.12	0.20	28.54	35.19	2.71						
					90	3.01	0.21	30.44	36.89	2.84						
					91	3.01	0.20	30.51	36.96	2.84						
					92	2.56	0.23	39.67	45.20	3.48						
					93	2.61	0.21	38.64	44.28	3.41						
N0002	6	W	85.00	90.00	88	3.63	0.25	19.93	27.44	2.11						
					89	3.45	0.27	22.80	30.02	2.31						
					90	3.38	0.28	23.95	31.06	2.39						
					91	3.38	0.29	23.95	31.06	2.39						
					92	3.14	0.42	28.11	34.80	2.68						
					93	3.13	0.34	28.29	34.96	2.69						
N0002	23	W	27.00	32.00	79	3.75	0.30	18.16	25.84	1.99						
					81	4.03	0.70	14.09	22.18	1.71						
					84	3.92	0.26	15.60	23.54	1.81						
					85	3.73	0.22	18.40	26.06	2.00						
					87	3.41	0.24	23.49	30.64	2.36						
					89	3.58	0.32	20.68	28.11	2.16						
					90	3.26	0.21	26.03	32.92	2.53						
					91	3.27	0.23	25.82	32.74	2.52						
					92	2.92	0.30	32.20	38.48	2.96						
					93	3.08	0.29	29.20	35.78	2.75						
N0002	25	W	18.00	22.00	79	3.95	0.50	15.17	23.15	1.78	87	4.12	2.22	87	0.07	0.09
					81	3.90	0.54	15.91	23.82	1.83						
					84	3.86	0.31	16.42	24.28	1.87						
					85	3.86	0.42	16.42	24.28	1.87						
					87	3.66	0.37	19.42	26.98	2.08						
					89	3.50	0.41	22.07	29.36	2.26						
					90	3.31	0.39	25.06	32.07	2.47						
					91	3.26	0.36	25.94	32.85	2.53						
					92	2.92	0.49	32.20	38.48	2.96						
					93	3.12	0.50	28.50	35.15	2.70						
N0002	26	W	4.00	10.00	79	4.20	0.37	11.71	20.04	1.54	87	2.31	1.10	87	0.21	0.02
					81	4.16	0.40	12.25	20.52	1.58						
					84	3.92	0.27	15.60	23.54	1.81						
					85	3.89	0.18	16.06	23.95	1.84						
					87	3.71	0.22	18.73	26.36	2.03						
					89	3.63	0.22	19.88	27.40	2.11						
					90	3.40	0.30	23.59	30.73	2.36						
					91	3.37	0.24	24.12	31.21	2.40						
					92	3.11	0.30	28.68	35.32	2.72						
					93	3.27	0.26	25.79	32.71	2.52						
N0003	1	N	9.00	16.00	78	3.89	0.35	16.01	23.91	1.84	87	3.03	1.55	87	0.16	0.06
					79	3.61	0.58	20.26	27.73	2.13						
					81	3.59	0.60	20.62	28.06	2.16						
					84	3.75	0.37	18.04	25.73	1.98						
					85	3.69	0.34	19.01	26.61	2.05						
					87	3.96	0.37	14.97	22.97	1.77						
					89	3.77	0.24	17.74	25.46	1.96						
					90	3.49	0.29	22.16	29.45	2.27						
					91	3.48	0.25	22.29	29.56	2.27						
					92	3.22	0.37	26.62	33.46	2.57						
					93	3.36	0.30	23.89	31.00	2.38						
N0003	1	N	20.00	25.00	89	3.40	0.21	23.62	30.76	2.37						
					90	3.24	0.22	26.34	33.21	2.55						
					91	3.23	0.22	26.51	33.36	2.57						
					92	2.90	0.26	32.59	38.83	2.99						
					93	3.10	0.25	28.83	35.45	2.73						
N0003	1	N	25.00	30.00	89	3.57	0.45	20.87	28.28	2.18						
					90	3.36	0.46	24.29	31.36	2.41						
					91	3.33	0.49	24.79	31.81	2.45						
					92	3.03	0.59	30.12	36.61	2.82						
					93	3.21	0.57	26.86	33.68	2.59						

Table B.3: Continued.

Route	Section	Direction	Kilometre distance		Riding quality						Rut depth in mm			Deflection in mm		
			From	To	Year	Ave PSI	Std deviation	QIr	QIm	Ave IRI	Year	Avg	Std deviation	Year	Avg	Std deviation
N0003	2	N	12.00	20.00	77	3.56	0.41	21.06	28.45	2.19	82	7.28	2.76	82	0.67	0.37
					78	3.63	0.44	19.99	27.49	2.11						
					79	3.66	0.36	19.53	27.07	2.08						
					81	3.54	0.43	21.41	28.77	2.21						
					84	3.41	0.55	23.54	30.68	2.36						
					85	3.19	0.66	27.30	34.07	2.62						
					87	3.12	0.51	26.40	35.05	2.70						
					89	3.18	0.42	27.43	34.19	2.63						
					90	2.69	0.45	36.67	42.68	3.28						
					91	2.65	0.48	37.67	43.41	3.34						
					92	2.08	0.61	51.25	55.63	4.28						
					93	3.06	0.38	29.51	36.05	2.77						
N0003	4	N	53.00	58.00	77	3.68	0.46	19.19	26.77	2.06	82	5.50	4.29	82	0.28	0.09
					78	3.58	0.37	20.74	28.17	2.17						
					79	3.75	0.49	17.95	25.65	1.97						
					81	3.55	0.45	21.19	28.57	2.20						
					84	3.30	0.45	25.27	32.24	2.48						
					85	3.32	0.41	25.03	32.03	2.46						
					88	3.63	0.28	19.90	27.41	2.11						
					89	3.59	0.17	20.59	28.03	2.16						
					90	3.46	0.20	22.57	29.81	2.29						
					91	3.41	0.19	23.52	30.67	2.36						
					92	3.19	0.25	27.22	33.99	2.61						
					93	3.41	0.25	23.46	30.61	2.35						
N0003	11	N	29.00	36.00	78	3.88	0.46	16.12	24.00	1.85	82	2.84	0.56	82	0.33	0.11
					79	4.16	0.45	12.19	20.47	1.57						
					84	3.95	0.34	15.18	23.16	1.78						
					88	3.62	0.19	20.10	27.59	2.12						
					89	3.67	0.15	19.37	26.94	2.07						
					90	3.49	0.21	22.20	29.48	2.27						
					91	3.56	0.16	20.96	28.37	2.18						
					92	3.37	0.25	24.17	31.25	2.40						
					93	3.42	0.17	23.22	30.40	2.34						
N0003	3	S	16.00	18.00	77	3.40	0.52	23.70	30.83	2.37	78	5.30	1.53	78	0.33	0.11
					78	3.38	0.42	24.04	31.13	2.39						
					79	3.45	0.55	22.80	30.02	2.31						
					81	3.24	0.60	26.43	33.26	2.56						
					84	2.54	0.45	40.18	45.65	3.51						
					87	3.42	0.31	23.29	30.46	2.34						
					89	3.27	0.23	25.91	32.82	2.52						
					90	3.09	0.26	29.10	35.69	2.75						
					91	3.04	0.27	30.03	36.52	2.81						
					92	2.80	0.33	34.57	40.70	3.13						
					93	2.90	0.50	32.69	38.92	2.99						
N0003	12	S	0.00	8.00	77	3.96	0.44	15.09	23.09	1.78						
					78	4.06	0.61	13.60	21.74	1.67						
					79	4.13	0.53	12.67	20.90	1.61						
					84	3.97	0.35	14.91	22.92	1.76						
					88	3.62	0.19	20.10	27.59	2.12						
					89	3.67	0.15	19.37	26.94	2.07						
					90	3.49	0.21	22.20	29.48	2.27						
					91	3.56	0.16	20.96	28.37	2.18						
					92	3.37	0.25	24.17	31.25	2.40						
					93	3.42	0.17	23.22	30.40	2.34						
N0003	12	S	17.00	20.00	78	3.98	0.43	14.74	22.77	1.75	86	5.33	2.01	86	0.12	0.07
					79	4.17	0.37	12.11	20.40	1.57						
					84	4.13	0.20	12.69	20.92	1.61						
					89	3.57	0.24	20.92	28.33	2.18						
					90	3.27	0.30	25.82	32.74	2.52						
					91	3.19	0.31	27.22	33.99	2.61						
					92	2.91	0.38	32.40	38.65	2.97						
					93	3.16	0.33	27.80	34.52	2.66						
N0003	12	S	24.00	25.00	78	3.66	0.68	19.47	27.02	2.08						
					79	3.58	0.41	20.71	28.14	2.16						
					84	3.68	0.17	19.16	26.74	2.06						
					89	3.52	0.11	21.67	29.00	2.23						
					90	3.33	0.25	24.79	31.81	2.45						
					91	3.31	0.28	25.13	32.12	2.47						
					92	3.06	0.36	29.56	36.11	2.78						
					93	3.10	0.35	28.83	35.45	2.73						
N0004	1	W	21.00	25.00	77	3.52	0.46	21.70	29.03	2.23						
					79	3.51	0.48	21.86	29.17	2.24						
					82	3.86	0.42	16.50	24.35	1.87						
					87	3.35	0.52	24.49	31.54	2.43						
					89	3.26	0.37	26.03	32.92	2.53						
					90	3.07	0.33	29.42	35.97	2.77						
					91	3.14	0.35	28.20	34.88	2.68						
					92	3.01	0.45	30.44	36.89	2.84						
					93	3.03	0.50	30.16	36.64	2.82						

Where:

Year = Indicates the year in which the measurement was conducted.

Ave PSI = The average riding quality in PSI obtained for section.

Std Deviat = The standard deviation of the riding quality for the section.

QIr = The average Quarter Car Index value calculated from PSI by using equation developed by Visser(1982).

QIm = The average Quarter Car Index value after conversion QIr for incorporation into HDM-III model.

Ave IRI = The average International Roughness Index (IRI) value (QIm/13).

Table B.4: Structural number and subgrade CBR values used in study.

Route	Section	Direction	Kilometre distance		Structural number					Subgrade CBR	Structural number	Modified Structural
			From	To	Wearing	Base	Subbase	Top select	Bot select			
N0001	3	N	25.00	30.00	0.32	1.12	0.78	0.66	None	18.00	2.88	4.52
N0001	4	N	10.00	15.00	0.32	1.12	0.78	1.10	None	15.50	3.32	4.86
N0001	4	N	60.00	65.00	0.32	1.12	0.78	1.10	None	35.00	3.32	5.28
N0001	5	N	20.00	25.00	0.32	1.12	0.52	1.10	None	32.00	3.06	4.99
N0001	6	N	20.00	25.00	0.32	1.12	0.52	1.10	None	22.50	3.06	4.82
N0001	7	N	20.00	25.00	0.32	1.12	0.78	1.10	None	31.50	3.32	5.24
N0001	7	N	40.00	45.00	0.32	1.12	0.78	1.10	None	25.00	3.32	5.14
N0001	8	N	20.00	25.00	0.32	1.12	0.78	1.10	None	10.00	3.32	4.55
N0001	8	N	65.00	70.00	0.32	1.12	0.78	1.10	None	18.50	3.32	4.97
N0001	9	N	11.00	16.00	0.32	1.12	0.52	1.10	None	14.00	3.06	4.54
N0001	9	N	80.00	85.00	0.32	1.12	0.52	1.10	None	21.00	3.06	4.78
N0001	10	N	10.00	15.00	0.32	1.12	0.78	1.10	None	14.50	3.32	4.82
N0001	10	N	40.00	45.00	0.32	1.12	0.78	1.10	None	26.00	3.32	5.15
N0001	11	N	30.00	35.00	0.32	0.84	0.84	1.10	None	30.00	3.10	5.00
N0001	15	N	31.00	39.00	0.80	1.32	0.84	0.54	None	21.00	3.50	5.22
N0001	18	N	70.00	77.00	0.64	1.15	1.68	0.45	0.45	21.00	4.37	6.09
N0001	21	N	19.00	25.00	0.46	1.76	0.84	0.60	0.54	19.00	4.20	5.86
N0001	21	N	29.00	33.00	0.96	1.76	0.56	0.50	0.54	16.00	4.32	5.88
N0001	21	N	35.00	40.00	0.46	1.76	0.84	0.84	0.30	23.00	4.20	5.97
N0001	22	N	0.00	4.00	0.46	1.76	0.84	0.70	0.30	13.50	4.06	5.51
N0001	22	N	18.00	22.00	0.25	1.60	0.84	0.54	None	17.00	3.23	4.83
N0001	23	N	14.00	28.00	0.64	1.02	1.76	0.84	0.54	12.10	4.80	6.18
N0001	1	S	20.00	23.00	0.25	1.60	0.60	0.60	0.36	12.10	3.41	4.78
N0001	12	S	4.00	10.00	0.32	1.04	0.60	0.45	0.36	15.10	2.77	4.30
N0001	12	S	20.00	25.00	0.32	1.12	0.60	0.45	0.36	27.00	2.85	4.70
N0001	14	S	29.00	48.00	0.32	1.44	0.84	1.00	0.36	14.50	3.96	5.46
N0001	15	S	10.00	20.00	0.32	1.44	0.84	1.08	None	13.00	3.68	5.11
N0001	16	S	67.00	78.00	0.32	1.32	1.68	0.54	0.54	15.00	4.40	5.92
N0002	6	E	1.00	10.00	0.72	1.12	0.60	0.45	None	25.00	2.89	4.71
N0002	6	E	15.00	22.00	0.32	1.12	0.60	0.45	None	13.00	2.49	3.92
N0002	6	E	40.00	45.00	0.32	1.12	0.60	0.90	None	12.20	2.94	4.32
N0002	6	E	60.00	65.00	0.32	1.12	0.60	1.00	None	14.50	3.04	4.54
N0002	7	E	20.00	25.00	0.32	0.84	1.68	0.54	0.54	19.50	3.92	5.60
N0002	10	E	0.00	8.00	0.32	1.12	0.60	1.00	0.54	28.00	3.58	5.45
N0002	10	E	13.00	25.00	0.32	1.12	0.60	1.00	0.54	14.50	3.58	5.08
N0002	10	E	40.00	52.00	0.64	1.32	1.68	0.60	0.54	27.50	4.78	6.64
N0002	10	E	61.00	65.00	0.46	1.12	0.60	1.20	0.54	14.50	3.92	5.42
N0002	11	E	24.00	30.00	0.46	1.12	0.60	1.08	None	20.00	3.26	4.95
N0002	11	E	31.00	32.00	0.46	1.92	0.60	1.08	None	19.50	4.06	5.74
N0002	11	E	43.00	45.00	1.06	1.12	0.60	1.08	None	6.50	3.86	4.72
N0002	11	E	60.00	68.00	0.25	0.60	0.60	0.90	None	31.00	2.35	4.26
N0002	16	E	0.00	5.00	0.46	1.92	0.84	1.00	None	22.00	4.22	5.97
N0002	16	E	9.00	14.00	0.46	1.92	0.84	1.00	0.90	15.00	5.12	6.64
N0002	16	E	16.00	22.00	0.44	1.12	0.72	1.00	0.90	28.00	4.18	6.05
N0002	16	E	50.00	60.00	0.46	0.62	1.00	0.90	None	23.00	2.97	4.75
N0002	23	E	7.00	13.00	0.80	1.54	1.68	0.36	None	16.00	4.38	5.94
N0002	23	E	33.00	41.00	0.64	1.54	1.68	0.54	0.36	14.50	4.76	6.26
N0002	24	E	14.00	18.00	0.80	1.41	1.68	0.54	0.36	9.50	4.79	5.98
N0002	29	E	0.00	5.00	0.42	0.80	0.60	0.60	None	10.00	2.42	3.65
N0002	30	E	66.00	74.00	0.13	1.44	0.66	0.60	None	22.50	2.83	4.59
N0002	6	W	85.00	90.00	0.72	1.12	0.60	0.45	None	8.00	2.89	3.94
N0002	23	W	27.00	32.00	0.80	1.54	1.68	0.54	0.36	11.00	4.92	6.22
N0002	25	W	18.00	22.00	0.61	1.92	1.68	0.84	0.54	12.50	5.59	6.99
N0002	26	W	4.00	10.00	0.61	1.15	1.68	1.40	None	9.50	4.84	6.03
N0003	1	N	9.00	16.00	0.64	1.60	1.68	0.36	None	9.70	4.28	5.49
N0003	1	N	20.00	25.00	0.64	1.60	1.68	0.45	None	7.00	4.37	5.30
N0003	1	N	25.00	30.00	0.64	1.60	1.68	0.45	None	10.00	4.37	5.60
N0003	2	N	12.00	20.00	0.42	1.12	0.60	1.08	None	9.00	3.22	4.37
N0003	4	N	53.00	58.00	0.80	1.44	0.84	1.08	0.36	18.50	4.52	6.17
N0003	11	N	29.00	36.00	0.42	1.44	0.84	0.60	0.54	19.00	3.84	5.51
N0003	3	S	16.00	18.00	0.61	1.12	0.80	0.48	None	19.00	3.01	4.68
N0003	12	S	0.00	8.00	0.61	1.32	1.68	0.54	0.54	15.50	4.69	6.23
N0003	12	S	17.00	20.00	0.42	1.92	0.84	0.70	0.54	11.00	4.42	5.72
N0003	12	S	24.00	25.00	0.80	1.60	0.98	0.84	1.14	10.00	5.36	6.59
N0004	1	W	21.00	25.00	0.25	1.20	0.56	0.56	0.95	18.00	3.52	5.16

Where:

Wearing = Refers to the actual contribution of wearing coarse to structural number in mm. Value obtained by multiplying thickness of layer with its material strength coefficient. Base, Subbase, Top select and Bot select the same as above, only for the different pavement layers this time.

Subgrade CBR = Refers to the in-situ California Bearing Ratio of the subgrade calculated from Falling Weight Deflection measurements.

Struct Number = Structural number of pavement in mm, without subgrade.

Modified SNC = Same as above, except contribution of subgrade included.

Table B.5: General information on traffic used in study.

Route	Section	Direction	Kilometers distance		TAWC	Construct	Maintenan	E80 ref	Evaluation	Number of axles in weight group									Total Axels	Total Axels	Growth rate of axels		Initial Axels	Initial axels	Total	Total	E80 growth rate		Initial E80's	Initial E80's
			From	To	Position	Date	Date	used	Date	<2	2 - 4	4 - 6	5 - 8	8 - 10	10 - 12	12 - 14	14 - 16	per day	for year	Assumed	Calculated	first year	axels day	E80's/DAY	E80's(year)	Assumed	Calculated	first year	E80/day
N0001	3	N	25	30		65	93	N1 - 4	89.92	1017	163	443	400	188	17	1	0	2229	813585	0.07		576543.3	3159.141	678.649	247706.9	0.03		213715.6	1171.044
N0001	4	N	10	15	52	84		N1 - 4	89.92	1017	163	443	400	188	17	1	0	2229	813585	0.07		537565.4	2945.564	678.649	247706.9	0.03		207399.3	1136.435
			60	65		83	85	N1 - 4	89.92	1017	163	443	400	188	17	1	0	2229	813585	0.07		501222.6	2746.425	678.649	247706.9	0.03		201269.8	1102.848
N0001	5	N	20	25		75		N1 - 4	89.92	1017	163	443	400	188	17	1	0	2229	813585	0.07		286302.9	1568.783	678.649	247706.9	0.03		158324.4	867.531
N0001	6	N	20	25		78	86	N1 - 4	89.92	1017	163	443	400	188	17	1	0	2229	813585	0.07		353205.6	1935.373	678.649	247706.9	0.03		173234.5	949.2301
N0001	7	N	20	25		75	86	N1 - 8	90.92	952	153	305	259	154	41	4	0	1866	681820	0.07		223713.4	1225.827	616.6698	225614.5	0.03		140066	767.4849
N0001			40	45		75	86	N1 - 8	90.92	952	153	305	259	154	41	4	0	1866	681820	0.07		223713.4	1225.827	616.6698	225614.5	0.03		140066	767.4849
N0001	8	N	20	25	90.7	80	86	N1 - 8	90.92	952	153	305	259	154	41	4	0	1866	681820	0.07		317464.4	1739.531	616.6698	225614.5	0.03		162733.5	891.6902
N0001			65	70		83	86	N1 - 11	89.75	665	122	270	252	130	10	0	0	1449	528885	0.07		329729	1805.734	438.0986	159906	0.03		130593	715.5783
N0001	9	N	11	16		82		N1 - 11	89.75	665	122	270	252	130	10	0	0	1449	528885	0.07		307437.3	1684.588	438.0986	159906	0.03		126733.4	694.4298
N0001			80	85		87		N1 - 11	89.75	665	122	270	252	130	10	0	0	1449	528885	0.07		436274.2	2390.544	438.0986	159906	0.03		147243.3	806.6123
N0001	10	N	10	15		80		N1 - 11	89.75	665	122	270	252	130	10	0	0	1449	528885	0.07		267273.1	1464.51	438.0986	159906	0.03		119353.1	653.9894
N0001			40	45		80		N1 - 11	89.75	665	122	270	252	130	10	0	0	1449	528885	0.07		267273.1	1464.51	438.0986	159906	0.03		119353.1	653.9894
N0001	11	N	30	35	70.8	88		N1 - 11	89.75	665	122	270	252	130	10	0	0	1449	528885	0.07		467907.7	2563.878	438.0986	159906	0.03		151727.5	831.3834
N0001	15	N	31	39	59.6	77	87		82.6667	740	133	234	172	87	24	3	0	1393	508445					384.8579	140473.1				
					40.2	77	87	N1 - 13	88.583	1592	125	410	375	348	75	2	0	2927	1068355					1111.06					
					29.6	77	87	N1 - 15	91.1667	1855	430	574	477	47	3.3	0.1	0	3386.4	1236036		0.10451	281223.1	1540.949	484.2952	176767.7		0.02704	120518.3	660.3744
N0001	18	N	70	77	6.5	78	86	N1 - 19	88.25	2452	143	272	187	107	11	1	0	3173	1158145					377.5451	137804				
					60.2	78	86	N1 - 19	89.417	2319	148	209	158	78	4	0	0	2916	1064340	0.055		568030.5	3112.496	273.812	99941.39	0.02		79536.72	435.8286
N0001	21	N	29	33	28	75	88		84.25	25162	1089	1300	539	320	101	12	0	28543	1E+07					1542.271	562929.1				
					30.6	75	88		91.1667	41881	1513	1840	1058	329	120	1.1	0	46742.1	2E+07	0.07		5502037	30148.15	1993.89	727770		0.03713	399287.6	2187.877
N0001	21	N	19	25	19.8	75	88		80.25	12795	892	1133	462	283	82	7	0	15654	5713710	0.07		3956535	21679.64	1284.995	469023.3	0.037		386218.2	2116.264
			35	40	40	75	88		80.25	12680	892	1133	462	275	82	7	0	15531	5668815	0.07		3925446	21509.3	1272.322	464397.4	0.037		382400	2095.392
N0001	22	N	0	4	23.8	76	88		84.083	5559	353	363	320	217	105	16	3	6936	2531640	0.055		1623042	8893.382	1107.864	404370.3	0.03		317297.9	1738.619
			16	28		76	87											0	0	0.055		1623042	8893.382			0.03		317297.9	1738.619
N0001	23	N	14	28	37.2	78	87		83.25	2584	163	156	72	18	1	0	0	2994	1092810					110.6196	40376.16				
					15.6	78	87		88.083	4734	293	385	291	117	7	0	0	5627	2126855		0.13778	530150.7	2904.935	462.935	168971.3	0.037		116356.4	637.5692
N0001	1	S	20	23		73	87																							
					22.8	73	87		86.5	14825	1740	648	393	136	19	2	0	17763	6483495	0.07		2520002	13808.23	713.6763	260491.9	0.02		198854.1	1089.612
N0001	12	S	4	10	59.6	74	87		82.75	740	133	234	172	87	24	3	0	1393	508445					351.608	128336.9				
					29.6	74	87		91.167	1663	102	292	237	192	40	2.7	0	2528.7	922976		0.07084	273660.4	1498.961	599.9239	218972.2		0.06348	73643.45	403.5258
			20	25																										
N0001	14	S	29	48	59.6	75.25	87		82.6667	961	99	184	147	125	54	12	0	1582	577430					560.8202	211999.4				
					26.6	75.25	87		91.1667	1663	102	292	237	192	40	2.7	0	2528.7	922976		0.05518	383502.6	2101.384	650.3721	237365.8		0.01331	192076.7	1052.475
N0001	15	S	10	20	59.6	75	87		82.75	961	99	184	147	125	54	12	0	1582	577430					553.5	202027.5				
					29.6	75	87		91.167	1663	102	292	237	192	40	2.7	0	2528.7	922976		0.05572	374929.7	2054.409	599.9239	218972.2		0.00957	187587.5	1027.876
N0001	16	S	67	78	59.6	74	87		82.75	2505	190	366	272	146	53	13	0	3545	1293925					676.521	246930.2				
					5	74	88		91.167	3628	357	595	645	396	75	3.6	2	5701.6	2081084		0.05646	789520.9	4326.142	1304.95	476306.8		0.07805	124730.8	683.4565
N0002	6	E	1	10		73	87		89.917	2026	238	214	125	62	9	1	2	2677	977105					249.434	91043.41				
			15	22	7.6	73	87		90.917	4613	301	269	135	73	16	3.6	0	5410.8	1974942	0.055		737200.1	4039.452	296.8256	108341.3	0.006		19399.65	106.2994
			40	45		80	86		90.917									5410.8	1974942	0.055		1083400	5935.437	296.8256	108341.3	0.006		37987.41	208.1502
			60	65		78	86		90.917									5410.8	1974942	0.055		970546.5	5318.063	296.8256	108341.3	0.006		31351.27	171.7878
N0002	7	E	20	25		88			90.917	4613	301	269	135	73	16	3.6	0	5410.8	1974942	0.055		1682203	9217.549	296.8256	108341.3	0.006		61660.01	448.6576
N0002	10	E	0	8	3.4	72	87	N2 - 9	82.917	726	92	98	31	15	3	1	0	966	352590					1345.95	66.994	25182.61		0.09315	9108.62	49.91025
			13	25	25.4	79	87	N2 - 10	89.583	1316	159	154	123	31	2	0	0	1787	652255		0.09228	245635.9	1345.95	137.666	50248.09		0.10363	16780.79	91.94956
N0002	10	E	40	52	61.6	78	87	N2 - 10	82.75	1390	91	122	79	41	11	3	0	1737	634005					1332.035	194.1613	70868.86		0.09947	44183.8	242.103
			61	65	61.6	74	87	N2 - 10	87.1667	2256	172	186	125	52	25	3	0	2818	1028570		0.10955	243096.3	1332.035	301.2702	109963.6		0.09947	29680.48	162.6328
N0002	11	E	24	30	26.6	73	86	N2 - 11	86.917	16615	600	634	355	202	41	2	0	18449	6733885					835.1408	304826.4	0.06517		93170.53	510.5235
					33.8	71	86	N2 - 11	89.583	23338	1491	1277	541	224	19	1	0	26891	9815215		0.14133	710084.2	3890.672	1048.025	382529.1	0.06517			510.5235
N0002	11	E	43	45	36.6	71	87		86.833	6616	636	686	321	204	11	0	0	10478	3824470	0.07		1262520	6917.919	699.2049	255209.8	0.06517		66260.19	363.0695
			60	68	47	71	87		86.9167	3204	357	476	264	67	3	0	0	4371	1595415					370.145	19247.54				
					63	71	87	N2 - 11	89.5833	3726	448	491	246	75	6	0	0	4992	1822080		0.04982	721945.9	3955.868	388.3107	20192.16		0.01797	14460.3	79.23453
N0002	16	E	0	5	16.8	77	87		84.333	8863	380	151	80	44	3	0	0	9521	3475165	0.07		2079925	11396.85	179.4398	9330.871	0.017		8237.256	45.13565
			9	14		78	87		84.333									0	0			2079925	11396.85	179.4398	9330.87	0.017		8378.486	45.90951
			18	22		75	87		84.333									0	0	0.07		2079925	11396.85	179.4398	9330.87	0.017		7961.896	43.62683
			50	60	36.7	73	87		88.333	1922	122	161	66	47	9	0	0	2327	849355	0.07		290373.3	1591.086	177.9025	9250.931	0.017		7128.232	39.0588
N0002	23	E	7	13	19.4	79	87		88.0833	4375	366	485	369	135	11	0	0	5741	2095465	0.055		1271496	6957.1	569.831	29631.21	0.06		17181.45	94.14492
			33	41	39.2	79	87		88.667	7176	507	746	580	373	44	1	0	9427	3440855	0.055		2021895	11078.87	1239.349	64446.17	0.06		36082.58	197.7128
N0002	24	E	14	18		72	87	N2 - 24	83.75	11200	729	925	646	312	14	1	0	13827	5046855	0.07		2217245	12149.29	1126.123	58568.39	0.06		28934.2	158.5436
N0002	29	E	0	5	3.1	65	87		83.5	1707	298	237	69	38	6	0	0	2356	859575					173.4243	9018.066	0.02		6229.068	34.13199
						65	87		87.25	2166	327	315	127	59	4	0	0	2998	1094270		0.06437	261258	1431.551	249.0165	12948.86	0.02		8297.943	45.46818
N0002	30	E	66	74		74	87		87.25	2166	327	315	127	59	4	0	0	2998	1094270	0.055		527998.1	2893.14	249.0165	90891.03	0.02		69732.14	382.0939
N0002	6	W	65	90		73			90.917	4613	301	269	135	73	16	3.6	0	5410.8	1974942	0.055		737200.1	4039.452	296.8256	108341.3	0.006		19399.65	106.2994
N0002	23	W	27	32	39.2	75	87		88.667	7071	756	809	328	287	37	2	0	9290	3390850	0.055		1590027	8761.794	955.8828	49705.91	0.025		35319.98	193.5341
N0002	25	W	18	22	8	76	87		88.75	35934	3148	1102	652	233	81	27	4	41181	2E+07	0.07		6157181	33737.98	1597.029	83045.49	0.05		43898.87	240.5417
N0002	26	W	4	10	2	78	87		87.583	11200	729	925	646	287	14	1	0	13802	5037730	0.055		2973949	16295.61	1087.15	56531.62	0.05		35010.7	191.8394
N0003	1	N	9	16	13.6	74	85	N3 - 01	83.75	21912	2080	2017	1201	382	24	2	0	27618	1E+07	0.07		5094237	27913.62	1853.647	96389.65		0.1075	33793.35	185.169
N0003	1	N	20	25		82			83.75	21912	2080	2017	1201	382	24	2	0	27618	1E+07	0.07		8918340	48867.62	1853.647	96389.65		0.1075	79859.76	437.5877
			25	30		85			83.75	21912	2080	2017	1201	382	24	2	0	27618	1E+07	0.07		11002360	60286.9	1853.647	96389.65		0.1075	110252.7	604.1244
N0003	2	N	12	20	7.6	72	86	N3 - 2	83.67	13575	1285	1513	880	353	32	0	0	17638	6437870					1506.043	78314.24				
					16.2	72	86	N3 - 2	88.917	16007	1692	1660	1273	858	53	1	0	21544	7863560		0.03812	4125860	22607.56	2647.31	137660.1		0.1075	22335.81	122.388
N0003	4	N	2	5	3	70	87	N3 - 4	81.583	8631	863	985	628	180	18	6	0	11311	4128515	0.055		2183333	11963.47	965.7268	50217.79	0.085		18761.64	102.8035
						70	87											0	0										
			53	58	13.1	75	88	N3 - 4	81.583	6316	806	885	645	142	14	4	0	8812	3216360					866.9931	45083.64				
					5	75	86	N3 - 5	83.75	8166	432	692	537	235	46	8.1	1.4	10119.5	3693618		0.06384	2112711	11576.5	1064.934	55376.59		0.09489	24138.93	132.2681
N0003	11	N	29	36	7.2	73	87		87.417	3901	242	562	315	219	50	3	0	5292	1931580	0.055		874068.4	4789.416	829.4202	43129.85	0.08		13610.69	74.57911
N0003	3	S	16	18	20.2	75	87	N3 - 3	83.75	9522	988	1162	517	147	17	2	0	12355	4509575					854.2367	44420.31				
					22.2	75	87		87.667	12303	657	1300	1100	617	93	2	0	16072	5866280		0.06715	2505930	13731.12	2211.519	114999	0.096		34066.15	186.7734
N0003	12	S	0	8	9.4	76	87	N3 - 12	85.583	8017	871	869	472	151	36	6	0	10422	3804030	0.055		2245652	12304.94	867.9295	45132.33	0.1		17310.25	94.85069
			17	20																										
			24	25	27.6	75	88		89.333	79302	0	4192	1908	1013	172	8	0	86595	3E+07	0.07		11589205	63502.5	4212.971	219074.5	0.1		52253.75	286.3219
N0004	1	W	21	25	52.6	73	87		85.917	3612	318	257	196	43	2	0	0	4426	1616220					250.7397	13068.47				
					9.1	73	87		87.417	6689	250	239	179	122	9	0	0	7486	2733120	0.07		998260.8	5458.963	387.83	20167.16	0.04		11329.11	62.07732

Table B.6: Determination of environmental coefficient(m) for semi-arid areas.

Route	Section	Direction	Kilometre distance		Pavement	Roughness			Rm-Rp	(Rm + Ri)x(T/2)
			From	To	Age (T)	Ri	Rm	Rp		
N0001	3	N	25	30	5	32.00	36.11	33.90	2.21	170.28
N0001	4	N	10	15	7	32.00	38.14	33.80	4.34	245.49
N0001	4	N	60	65	7	38.50	42.84	39.30	3.54	284.69
N0001	5	N	20	25	16	27.50	39.54	34.50	5.04	536.32
N0001	6	N	20	25	13	28.50	31.51	31.40	0.11	390.07
N0001	7	N	20	25	16	28.00	38.14	34.70	3.44	529.12
N0001	7	N	40	45	16	25.00	35.94	31.80	4.14	487.52
N0001	8	N	20	25	10	25.00	33.05	27.20	5.85	290.25
N0001	8	N	65	70	9	28.00	34.64	29.80	4.84	281.88
N0001	9	N	11	16	8	26.00	31.51	27.90	3.61	230.04
N0001	9	N	80	85	4	29.20	33.05	30.70	2.35	124.50
N0001	10	N	10	15	10	25.00	30.31	26.80	3.51	276.55
N0001	10	N	40	45	10	25.00	32.12	26.60	5.52	285.60
N0001	11	N	30	35	3	31.80	32.89	33.10	-0.21	97.04
N0001	15	N	31	39	5	21.44	23.02	22.70	0.32	111.15
N0001	12	S	4	10	8	32.10	35.28	33.90	1.38	269.52
N0001	12	S	20	25	17	28.00	38.83	36.10	2.73	568.06
N0001	14	S	29	48	9	35.80	38.08	37.40	0.68	332.46
N0001	15	S	10	20	8	30.00	33.28	31.70	1.58	253.12
N0001	16	S	67	78	14	30.00	35.68	34.60	1.08	459.76
								Sum	56.06	6223.40
									m	0.009
									Kge	0.392

Table B.7: Determination of environmental coefficient(m) for subhumid areas.

Route	Section	Direction	Kilometre distance		Pavement	Roughness			Rm-Rp	(Rm + Ri)x(T/2)
			From	To	Age (T)	Ri	Rm	Rp		
N0001	18	N	70	77	15	16.40	27.86	21.70	6.16	331.95
N0001	21	N	19	25	9	16.00	20.25	18.20	2.05	163.13
N0001	21	N	29	33	9	23.00	25.76	25.30	0.46	219.42
N0001	21	N	35	40	4	25.00	27.90	26.30	1.60	105.80
N0001	22	N	0	4	10	22.50	32.12	25.50	6.62	273.10
N0001	22	N	18	22	8	18.20	22.56	21.00	1.56	163.04
N0001	23	N	14	28	10	17.50	22.64	19.00	3.64	200.70
N0001	1	S	20	23	10	20.00	28.81	23.60	5.21	244.05
N0002	10	E	0	8	12	22.20	31.85	23.30	8.55	324.30
N0002	10	E	13	25	5	28.50	32.52	29.60	2.92	152.55
N0002	10	E	40	52	13	28.00	35.28	30.20	5.08	411.32
N0002	10	E	61	65	4	30.00	32.77	31.10	1.67	125.54
N0002	11	E	24	30	9	27.00	29.07	29.10	-0.03	252.32
N0002	11	E	31	32	6	27.00	30.17	28.20	1.97	171.51
N0002	11	E	43	45	7	20.00	25.79	21.60	4.19	160.27
N0002	11	E	60	68	18	24.50	44.81	40.50	4.31	623.79
N0002	16	E	0	5	2	26.20	27.65	27.00	0.65	53.85
N0002	16	E	9	14	4	28.50	30.70	29.30	1.40	118.40
N0002	16	E	16	22	9	19.50	28.87	20.50	8.37	217.67
N0002	16	E	50	60	18	26.10	36.56	36.50	0.06	563.94
N0003	11	N	29	36	11	19.00	23.90	21.60	2.30	235.95
N0003	12	S	0	8	12	20.00	27.59	21.90	5.69	285.54
N0003	12	S	17	20	9	18.50	24.13	19.90	4.23	191.84
N0003	12	S	24	25	16	20.00	32.12	26.30	5.82	416.96
N0004	1	W	21	25	4	26.80	29.03	28.10	0.93	111.66
								Sum	85.41	6118.58
									m	0.014
									Kge	0.607

Table B.8: Determination of environmental coefficient(m) for humid areas.

Route	Section	Direction	Kilometre distance		Pavement	Roughness			Rm-Rp	(Rm + Ri)x(T/2)
			From	To	Age (T)	Ri	Rm	Rp		
N0002	6	E	1	10	10	20.00	27.12	21.40	5.72	235.60
N0002	6	E	15	22	6	24.80	27.38	26.30	1.08	156.54
N0002	6	E	40	45	13	20.00	40.43	22.80	17.63	392.80
N0002	6	E	60	65	15	23.90	41.16	29.20	11.96	487.95
N0002	7	E	20	25	3	33.00	38.14	34.10	4.04	106.71
N0002	23	E	7	13	16	20.00	29.54	26.40	3.14	396.32
N0002	23	E	33	41	8	19.00	24.00	20.00	4.00	172.00
N0002	24	E	14	18	9	28.90	34.76	28.00	6.76	286.47
N0002	29	E	0	5	6	28.90	32.92	30.40	2.52	185.46
N0002	30	E	66	74	7	27.50	30.67	28.80	1.87	203.60
N0002	23	W	27	32	12	20.00	30.64	21.90	8.74	303.84
N0002	25	W	18	22	11	22.00	26.98	23.10	3.88	269.39
N0002	26	W	4	10	11	19.70	27.40	21.30	6.10	259.05
N0003	1	N	9	16	7	22.80	28.06	24.00	4.06	178.01
N0003	1	N	20	25	11	28.20	35.45	31.30	4.15	350.08
N0003	1	N	25	30	8	28.20	33.99	29.70	4.29	248.76
N0003	2	N	12	20	3	26.50	28.45	28.50	-0.05	82.43
N0003	4	N	53	58	10	25.10	32.03	26.30	5.73	285.65
N0003	3	S	16	18	6	30.00	33.28	31.30	1.98	189.84
								Sum	97.60	4790.48
									m	0.020
									Kge	0.886

Where:

T = Number of years between roughness measurement date and construction date.

Ri = Initial roughness at date of construction.

Rm = Measured roughness.

Rp = Predicted roughness with Kge = 0 = m.

m = Environmental coefficient.

Kge = Environmental roughness calibration factor (m/0,023).

APPENDIX C

Results from comparison and calibration

NOTE THAT ALL ROUGHNESS VALUES ARE IN QI_m
SEE CHAPTER 4

Table C.1: Calibration values for pavement sections evaluated.

Route	Section	Direction	Kilometre distance		Calibration factor values				
			From	To	kci	kcp	krp	kge	kgp
N0001	03	N	20	25	1,17	0,22	-	0,39	1,06
N0001	04	N	10	15	1,33	0,20	-	0,39	0,98
N0001	04	N	60	65	1,29	0,25	-	0,39	1,04
N0001	05	N	20	25	2,00	0,19	-	0,39	0,96
N0001	06	N	20	25	2,29	0,19	-	0,39	1,17
N0001	07	N	20	25	2,50	0,16	-	0,39	0,97
N0001	07	N	40	45	2,38	0,22	-	0,39	1,06
N0001	08	N	20	25	2,33	0,21	-	0,39	0,92
N0001	08	N	65	70	1,00	0,15	-	0,39	1,17
N0001	09	N	11	16	1,57	0,23	-	0,39	1,00
N0001	09	N	80	85	1,86	0,22	-	0,39	1,04
N0001	10	N	10	15	2,14	0,26	-	0,39	0,99
N0001	10	N	40	45	1,38	0,25	-	0,39	1,23
N0001	11	N	30	35	1,86	0,05	-	0,39	0,79
N0001	15	N	31	39	1,63	0,25	0,47	0,39	0,96
N0001	18	N	70	77	0,80	0,23	1,52	0,61	0,93
N0001	21	N	19	25	1,50	0,22	1,25	0,61	0,61
N0001	21	N	29	33	1,00	0,22	1,50	0,61	0,86
N0001	21	N	35	40	1,00	0,13	1,50	0,61	0,73
N0001	22	N	0	4	1,17	0,43	1,61	0,61	1,07
N0001	22	N	18	22	1,80	0,16	1,49	0,61	1,28
N0001	23	N	14	28	0,99	0,53	1,55	0,61	1,04

Where:

kci = Cracking initiation calibration factor.

kcp = Cracking progression calibration factor.

krp = Rut depth progression calibration factor.

kge = Roughness environmental related calibration factor.

kgp = Roughness age calibration factor.

kvi = No calibration values calculated for ravelling initiation.

kpp = No calibration values calculated for pothole progression.

Table C.1: Continued.

Route	Section	Direction	Kilometre distance		Calibration factor values				
			From	To	kci	kcp	krp	kge	kgp
N0001	01	S	20	23	1,17	0,31	-	0,61	1,38
N0001	12	S	4	10	1,29	0,24	0,92	0,39	1,06
N0001	12	S	20	25	2,63	0,16	-	0,39	1,37
N0001	14	S	29	48	0,75	0,23	1,53	0,39	0,81
N0001	15	S	10	20	1,00	0,20	1,46	0,39	0,87
N0001	16	S	67	78	1,38	0,16	1,63	0,39	0,92
N0002	06	E	1	10	1,33	0,20	1,59	0,87	0,73
N0002	06	E	15	22	1,50	0,16	1,57	0,87	1,20
N0002	06	E	40	45	1,75	0,19	-	0,87	0,98
N0002	06	E	60	65	2,00	0,19	-	0,87	1,16
N0002	07	E	20	25	1,25	0,19	-	0,87	1,08
N0002	10	E	0	8	1,00	0,27	1,67	0,61	1,12
N0002	10	E	13	25	0,33	0,31	1,51	0,61	0,84
N0002	10	E	40	52	0,64	0,12	-	0,61	0,99
N0002	10	E	61	65	1,22	0,14	1,74	0,61	0,80
N0002	11	E	24	30	1,00	0,09	1,70	0,61	0,83
N0002	11	E	31	32	1,40	0,15	1,62	0,61	1,16
N0002	11	E	43	45	1,75	0,31	1,57	0,61	0,70
N0002	11	E	60	68	2,39	0,23	1,69	0,61	0,96
N0002	16	E	0	5	2,30	0,19	-	0,61	0,81
N0002	16	E	9	14	0,42	0,43	2,46	0,61	0,82
N0002	16	E	16	22	0,82	0,18	1,70	0,61	1,28

Where:

kci = Cracking initiation calibration factor.

kcp = Cracking progression calibration factor.

krp = Rut depth progression calibration factor.

kge = Roughness environmental related calibration factor.

kgp = Roughness age calibration factor.

kvi = No calibration values calculated for ravelling initiation.

kpp = No calibration values calculated for pothole progression.

Table C.1: Continued.

Route	Section	Direction	Kilometre distance		Calibration factor values				
			From	To	kci	kcp	krp	kge	kgp
N0002	16	E	50	60	0,95	0,19	1,71	0,61	0,65
N0002	23	E	7	13	0,60	0,19	1,65	0,87	0,89
N0002	23	E	33	41	0,99	0,19	1,84	0,87	0,72
N0002	24	E	14	18	1,00	0,34	-	0,87	1,35
N0002	29	E	0	5	2,80	0,18	-	0,87	1,16
N0002	30	E	66	74	1,38	0,15	1,64	0,87	0,85
N0002	06	W	30	35	1,25	0,19	-	0,87	1,11
N0002	23	W	27	32	0,91	0,16	-	0,87	1,14
N0002	25	W	18	22	0,99	0,32	1,62	0,87	0,94
N0002	26	W	4	10	0,90	0,43	1,48	0,87	0,98
N0003	01	N	9	16	1,33	0,07	1,10	0,87	0,98
N0003	01	N	20	25	1,25	0,18	1,10	0,87	1,15
N0003	01	N	25	30	1,38	-	-	0,87	1,05
N0003	02	N	12	20	2,60	0,19	1,75	0,87	0,81
N0003	04	N	53	58	1,10	0,20	1,88	0,87	0,74
N0003	11	N	29	36	1,20	0,25	1,53	0,61	0,90
N0003	03	S	16	18	1,38	0,13	1,89	0,87	0,89
N0003	12	S	0	8	0,55	0,21	-	0,61	1,09
N0003	12	S	17	20	1,11	0,15	1,64	0,61	0,70
N0003	12	S	24	25	1,00	0,08	-	0,61	1,15
N0004	01	W	21	25	2,60	0.18	-	0,61	0,93

Where:

kci = Cracking initiation calibration factor.

kcp = Cracking progression calibration factor.

krp = Rut depth progression calibration factor.

kge = Roughness environmental related calibration factor.

kgp = Roughness age calibration factor.

kvi = No calibration values calculated for ravelling initiation.

kpp = No calibration values calculated for pothole progression.

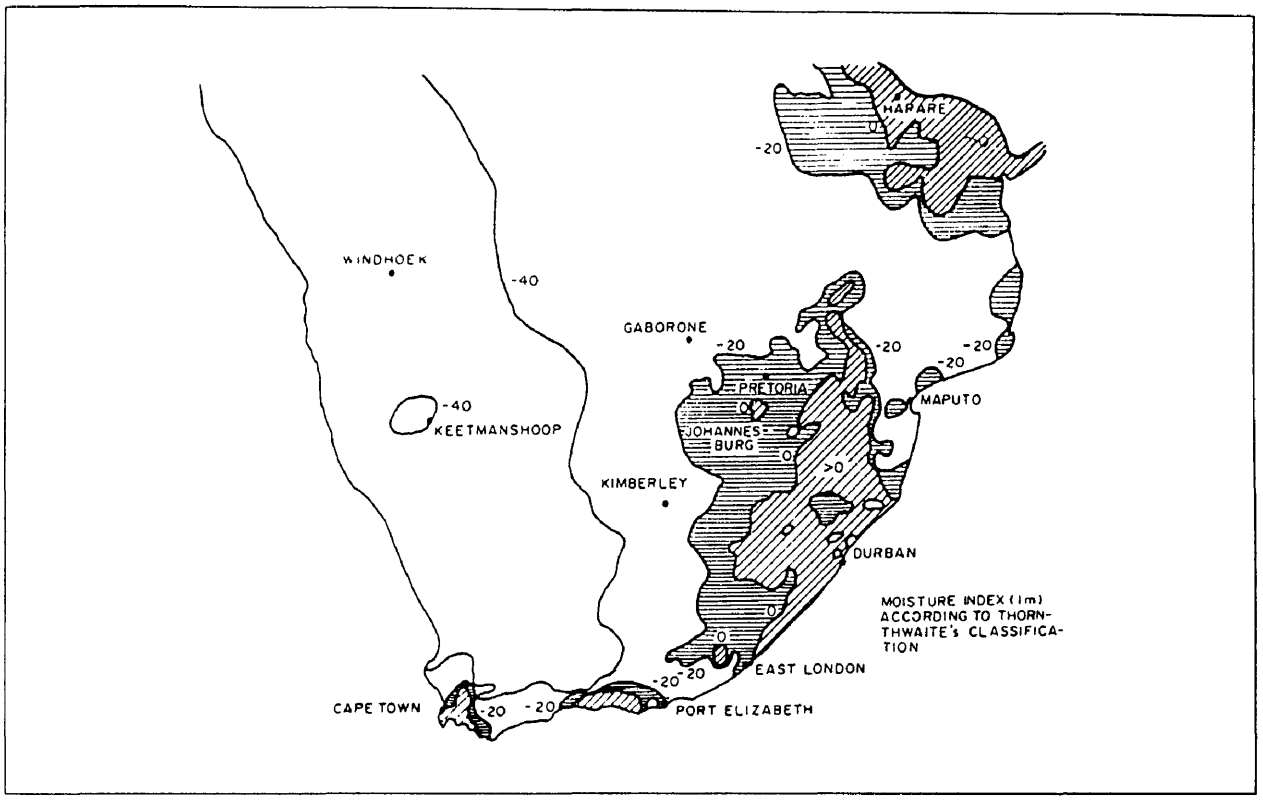

Figure C.1: Thornthwaite moisture classification for South Africa (TRH 4, 1985).

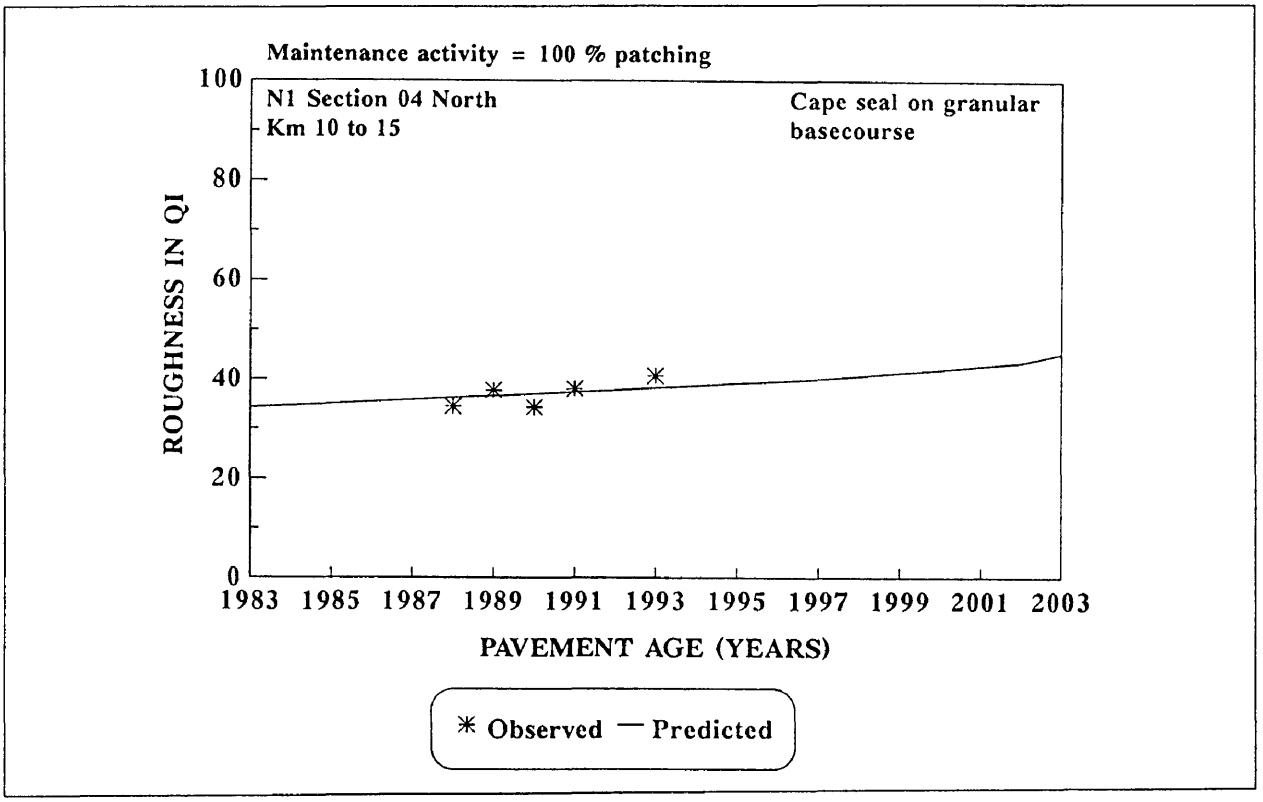

Figure C.2: National route 1 section 04 north from kilometre 10 to 15.

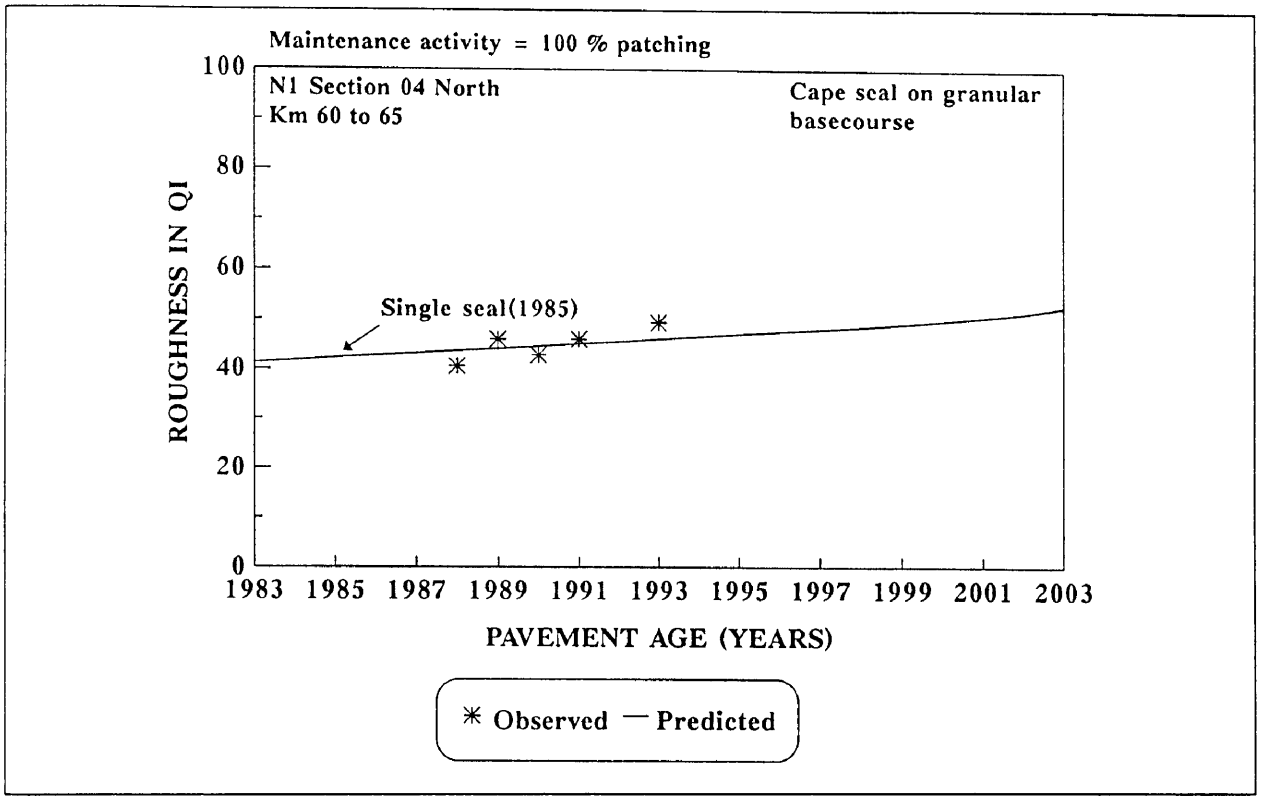

Figure C.3: National route 1 section 04 north from kilometre 60 to 65.

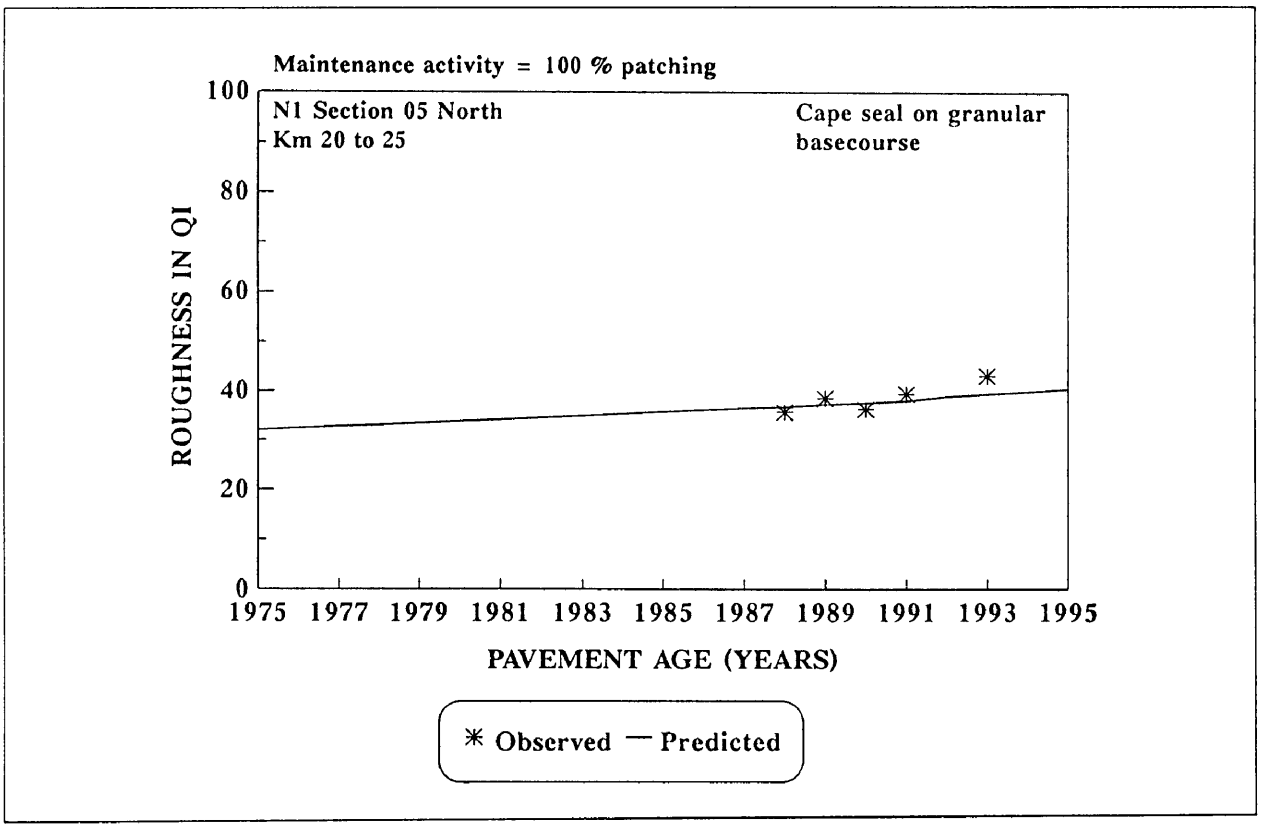

Figure C.4: National route 1 section 05 north from kilometre 20 to 25.

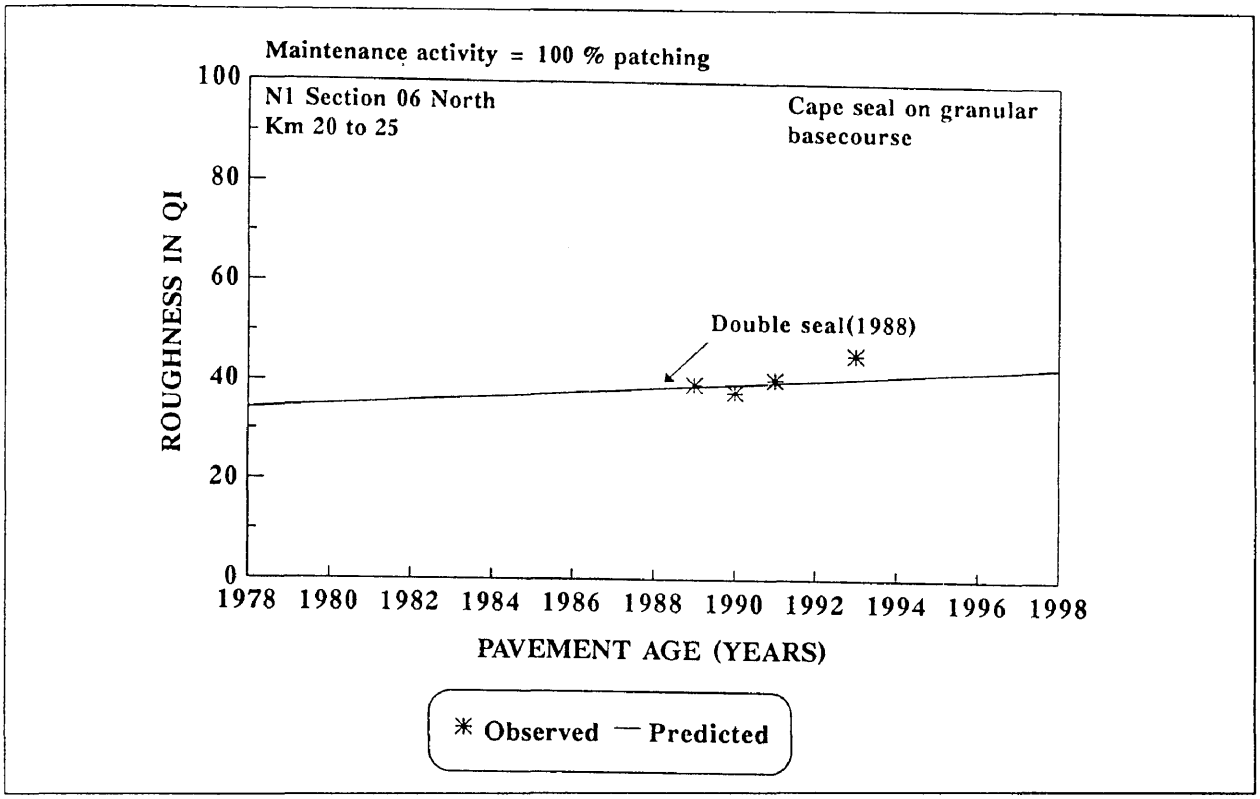

Figure C.5: National route 1 section 06 north from kilometre 20 to 25.

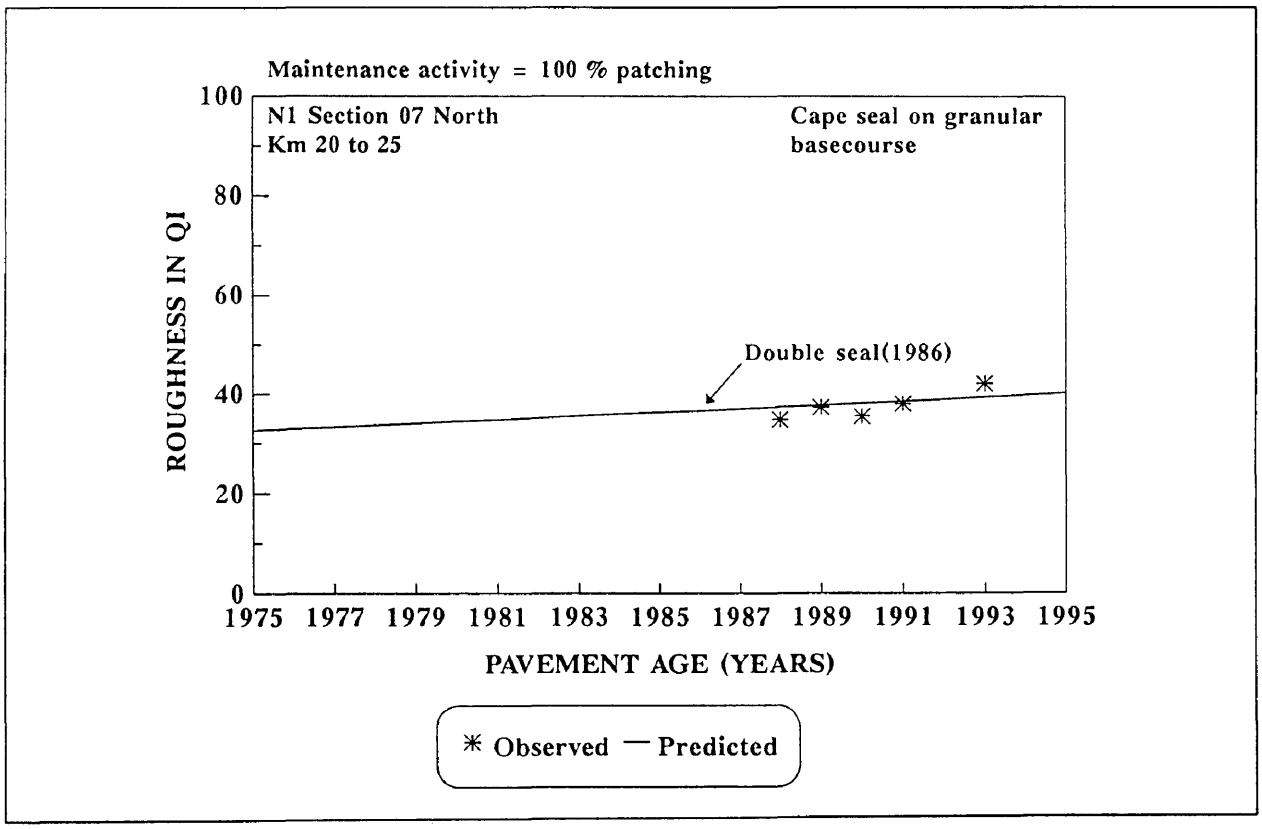

Figure C.6: National route 1 section 07 north from kilometre 20 to 25.

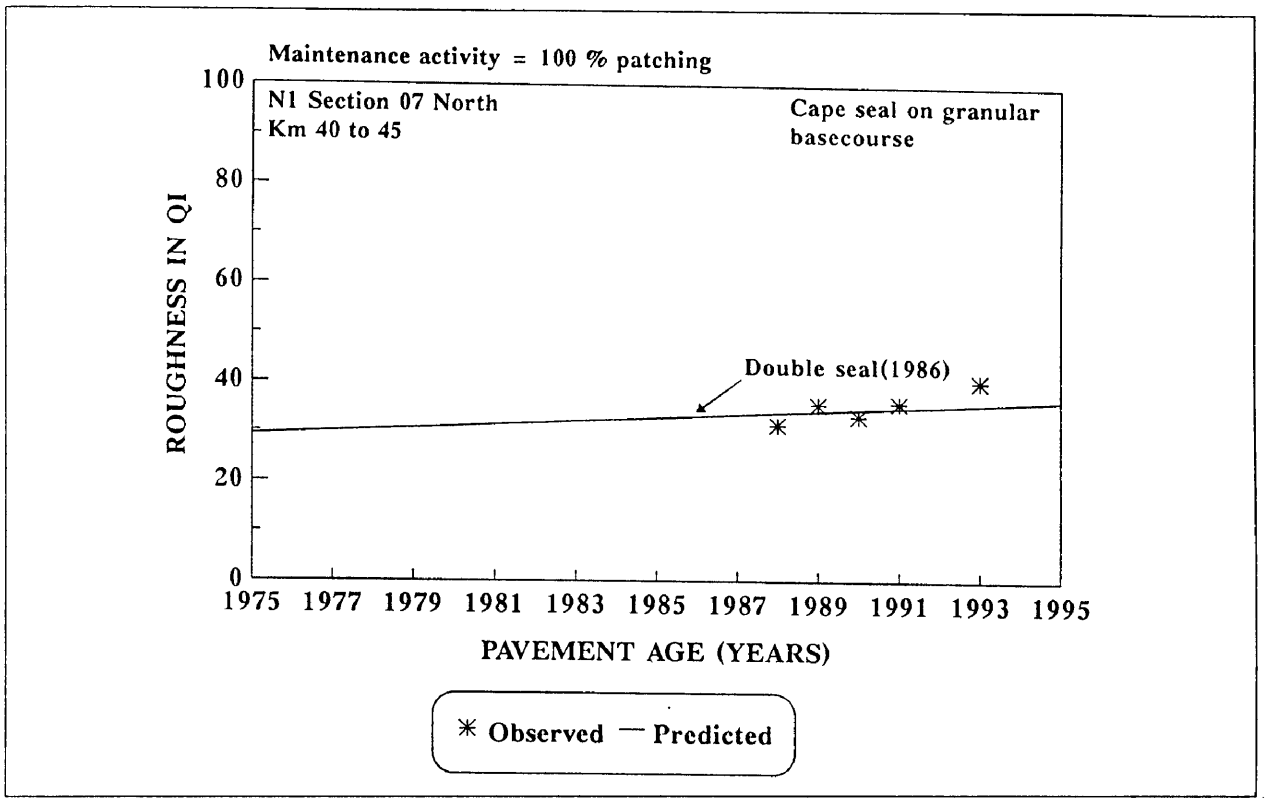

Figure C.7: National route 1 section 07 north from kilometre 40 to 45.

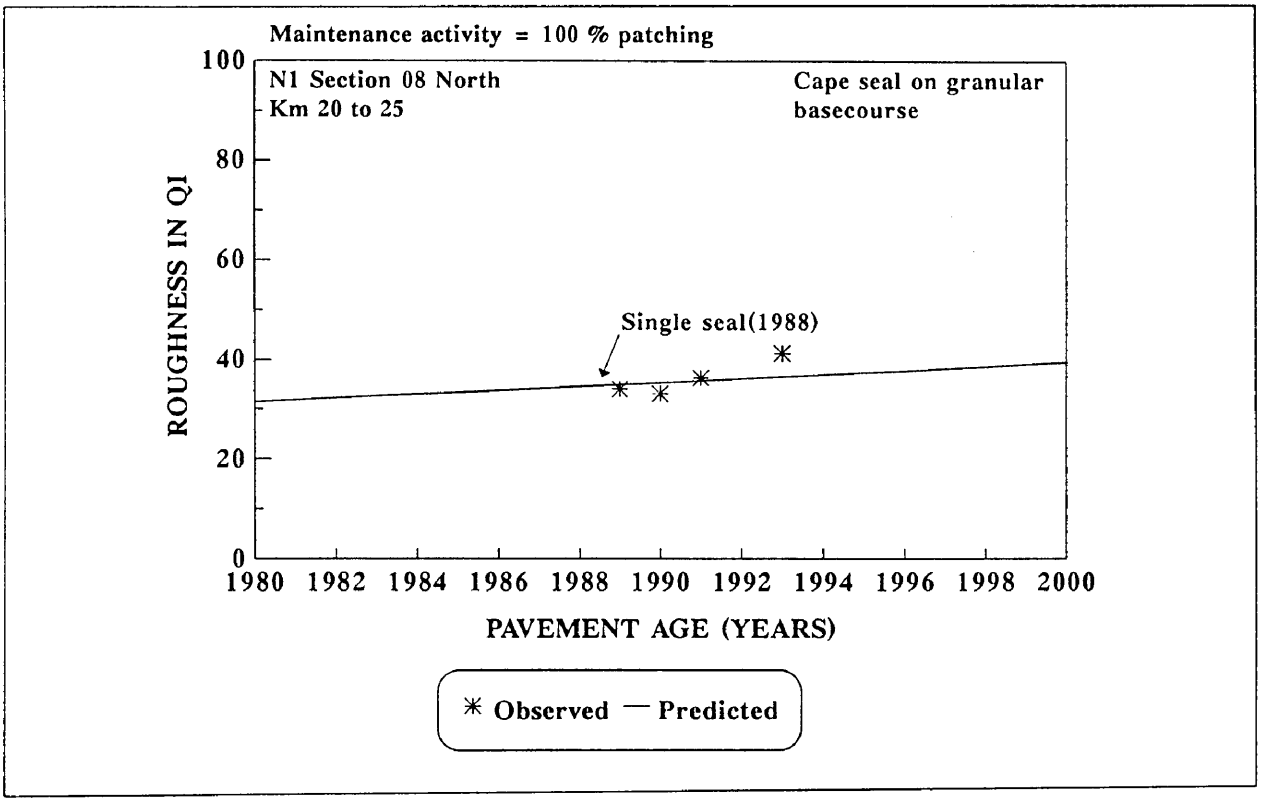

Figure C.8: National route 1 section 08 north from kilometre 20 to 25.

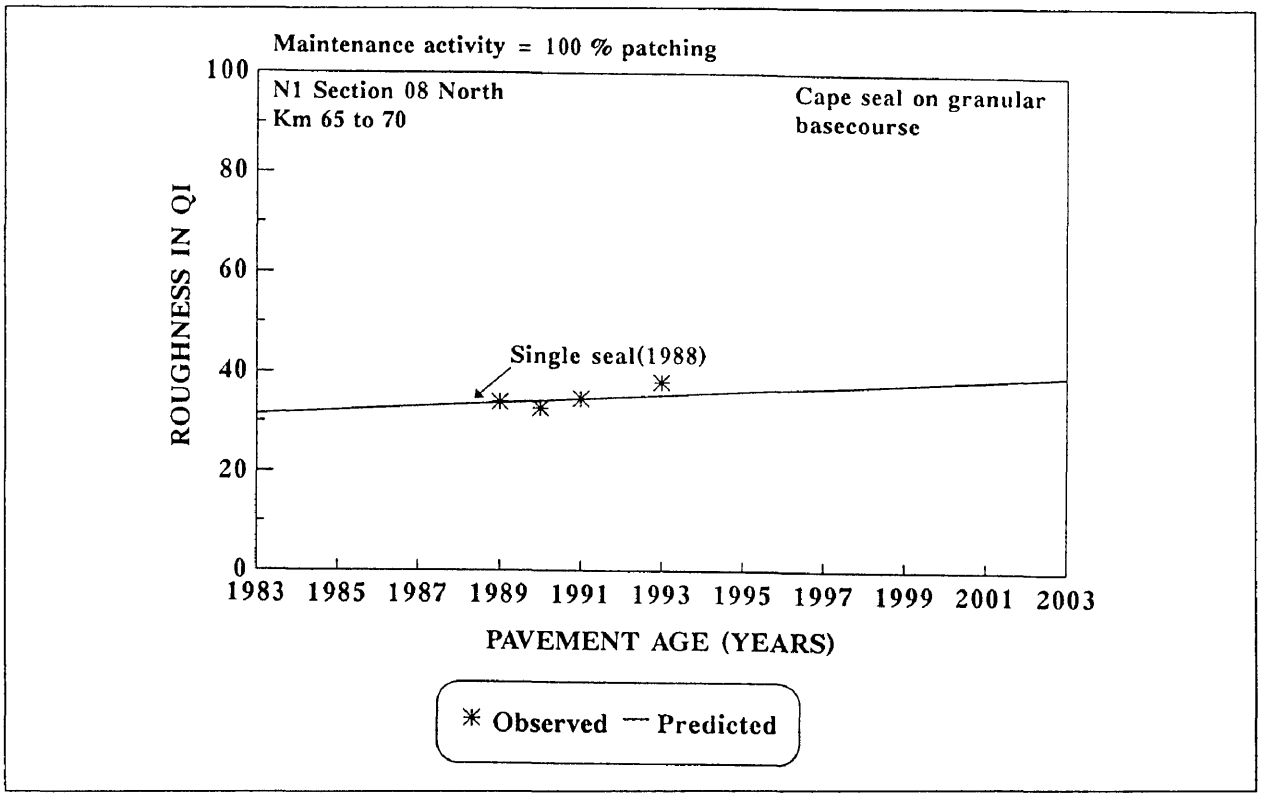

Figure C.9: National route 1 section 08 north from kilometre 65 to 70.

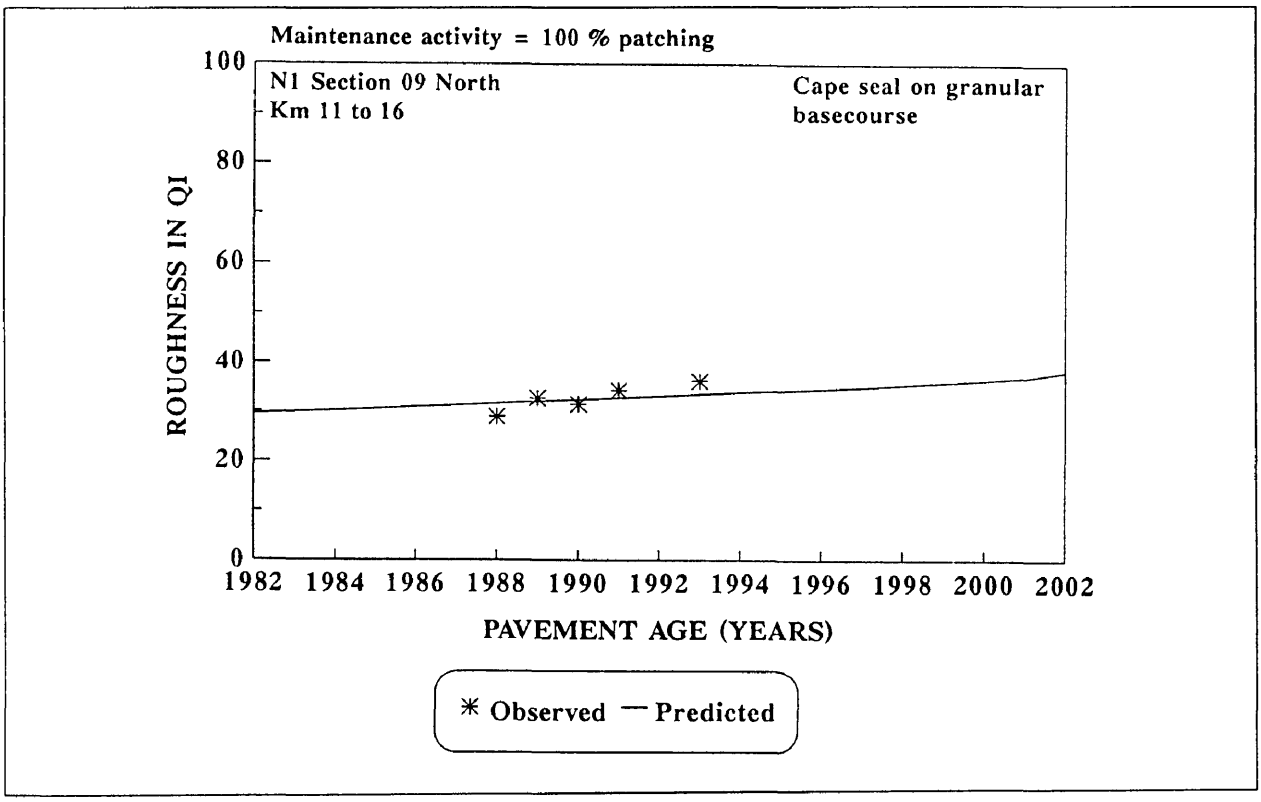

Figure C.10: National route 1 section 09 north from kilometre 11 to 16.

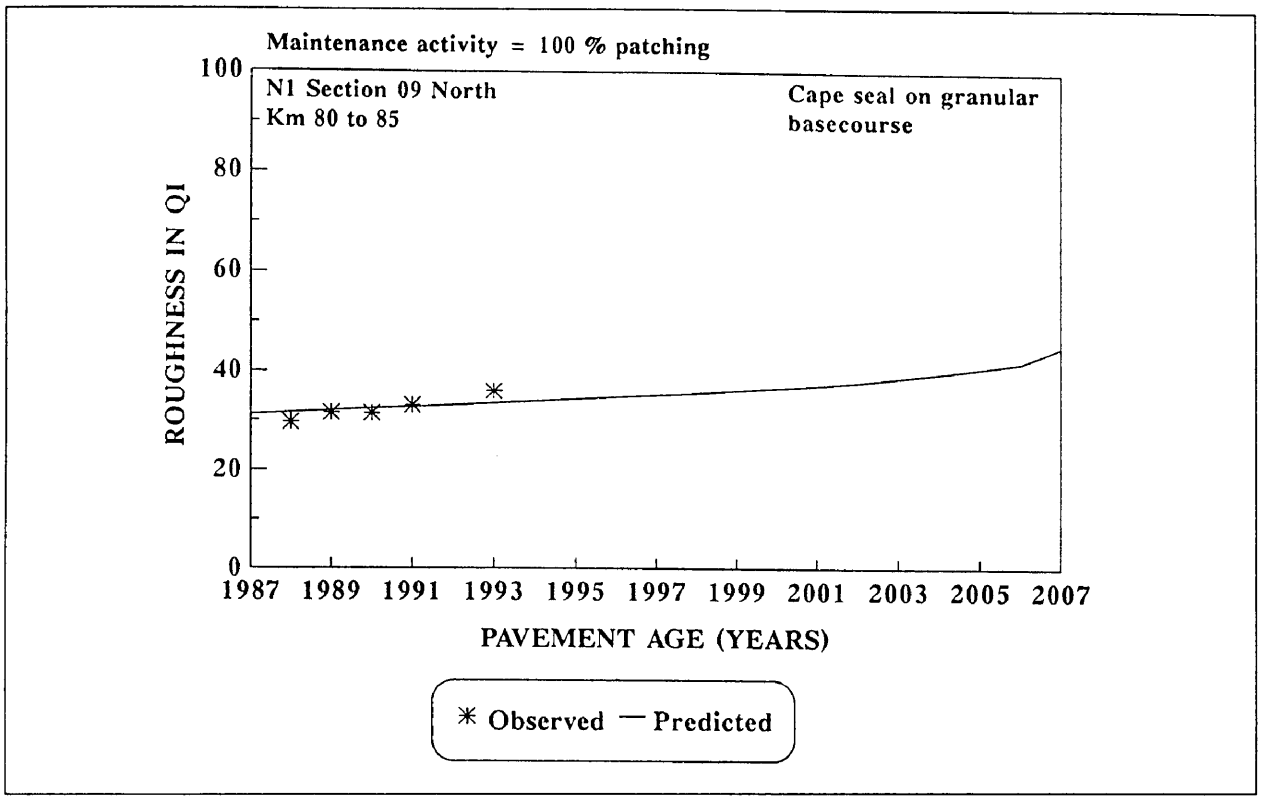

Figure C.11: National route 1 section 09 north from kilometre 80 to 85.

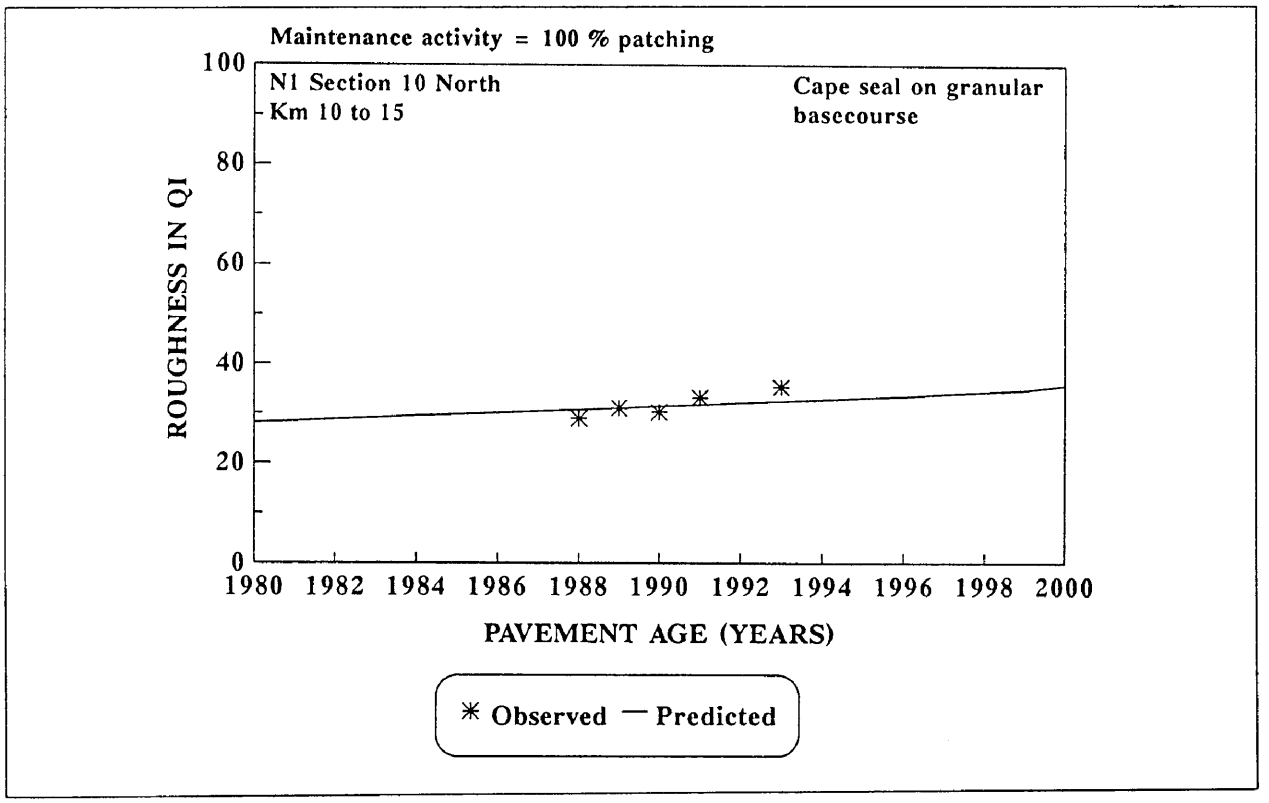

Figure C.12: National route 1 section 10 north from kilometre 10 to 15.

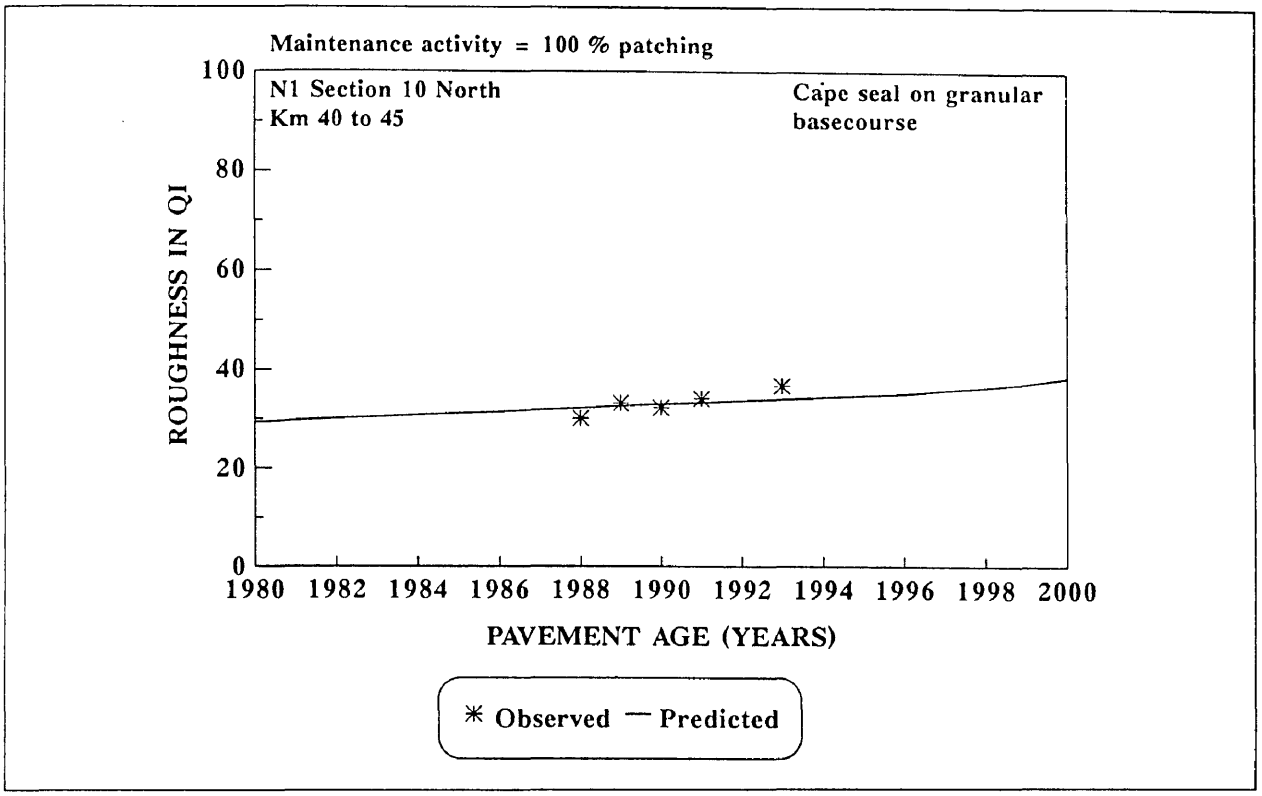

Figure C.13: National route 1 section 10 north from kilometre 40 to 45.

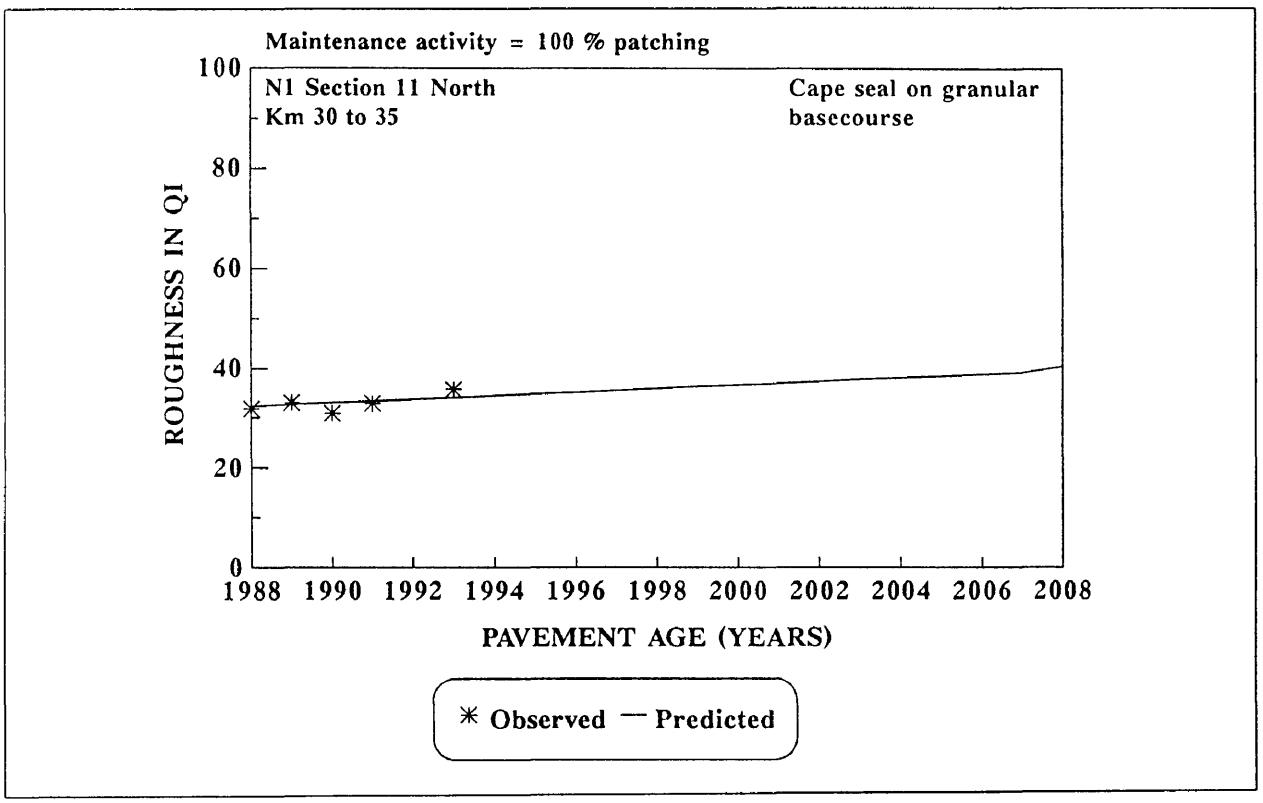

Figure C.14: National route 1 section 11 north from kilometre 30 to 35.

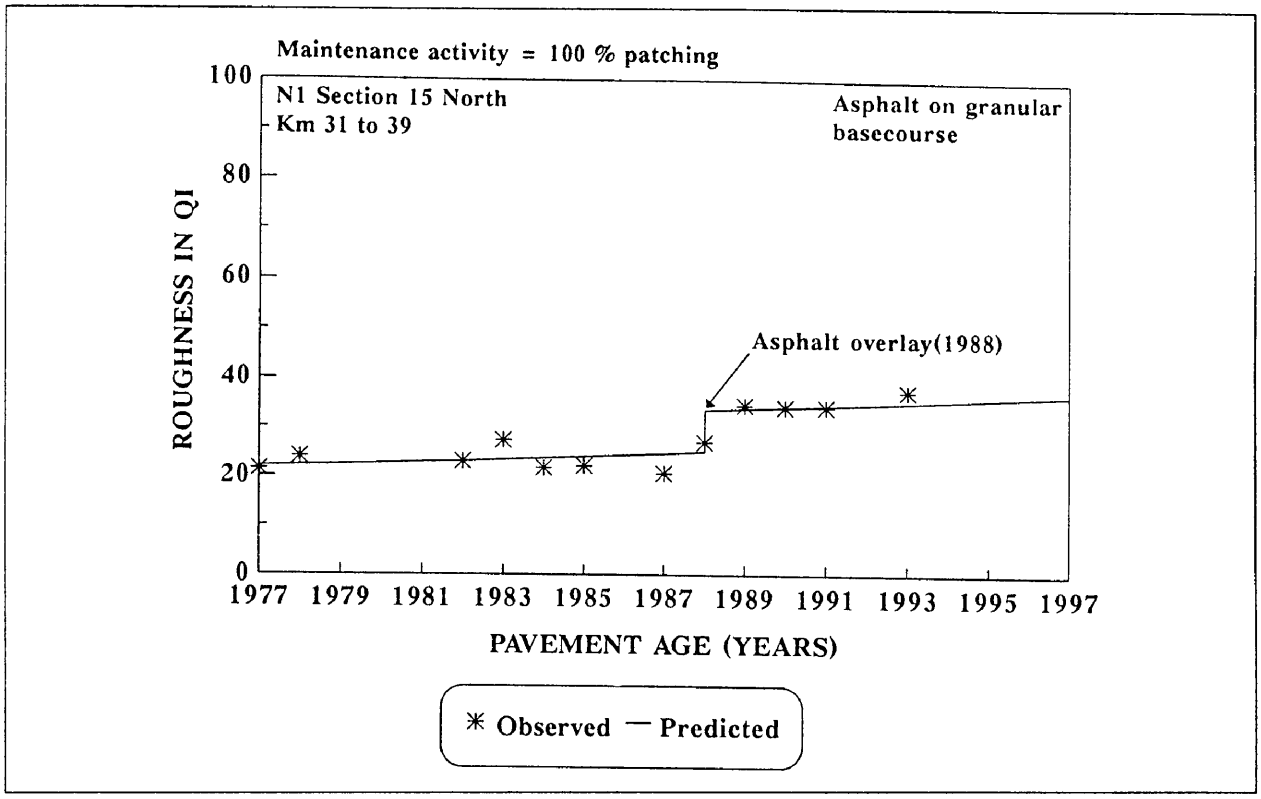

Figure C.15: National route 1 section 15 north from kilometre 31 to 39.

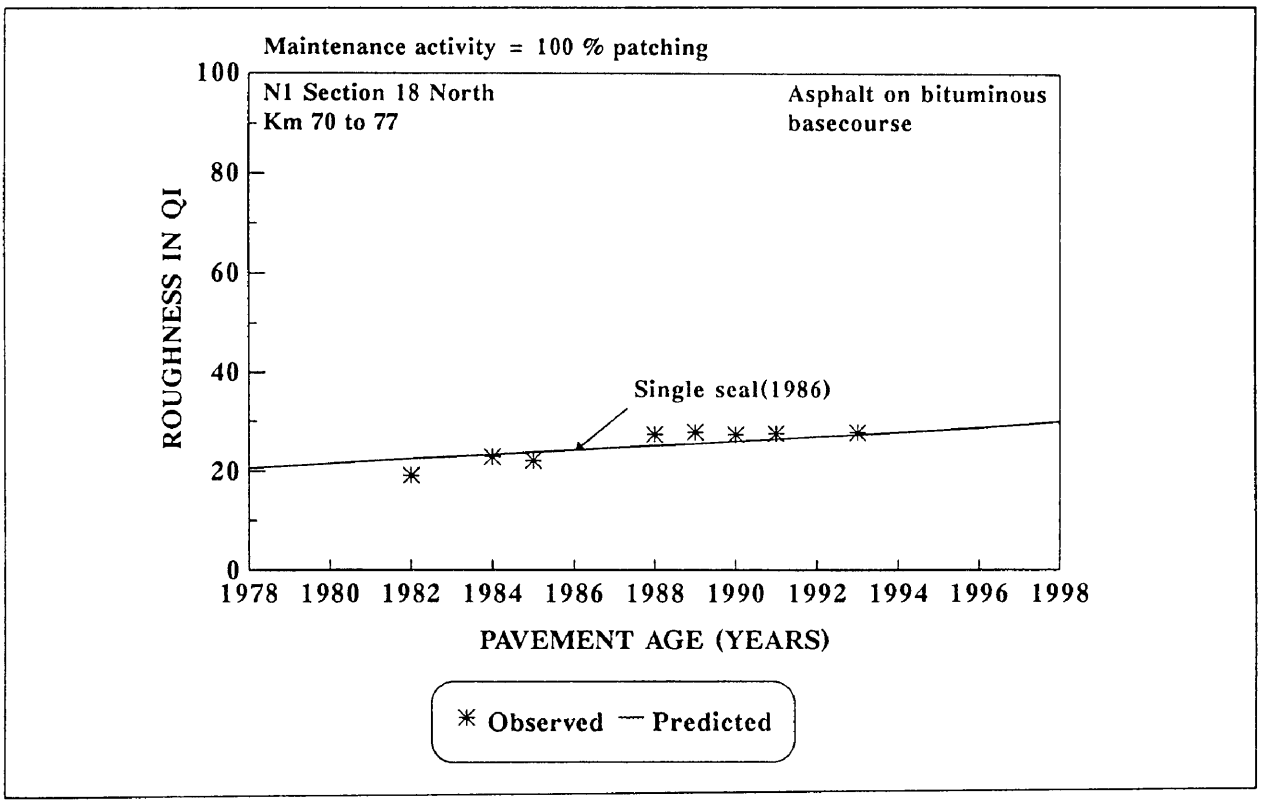

Figure C.16: National route 1 section 18 north from kilometre 70 to 77.

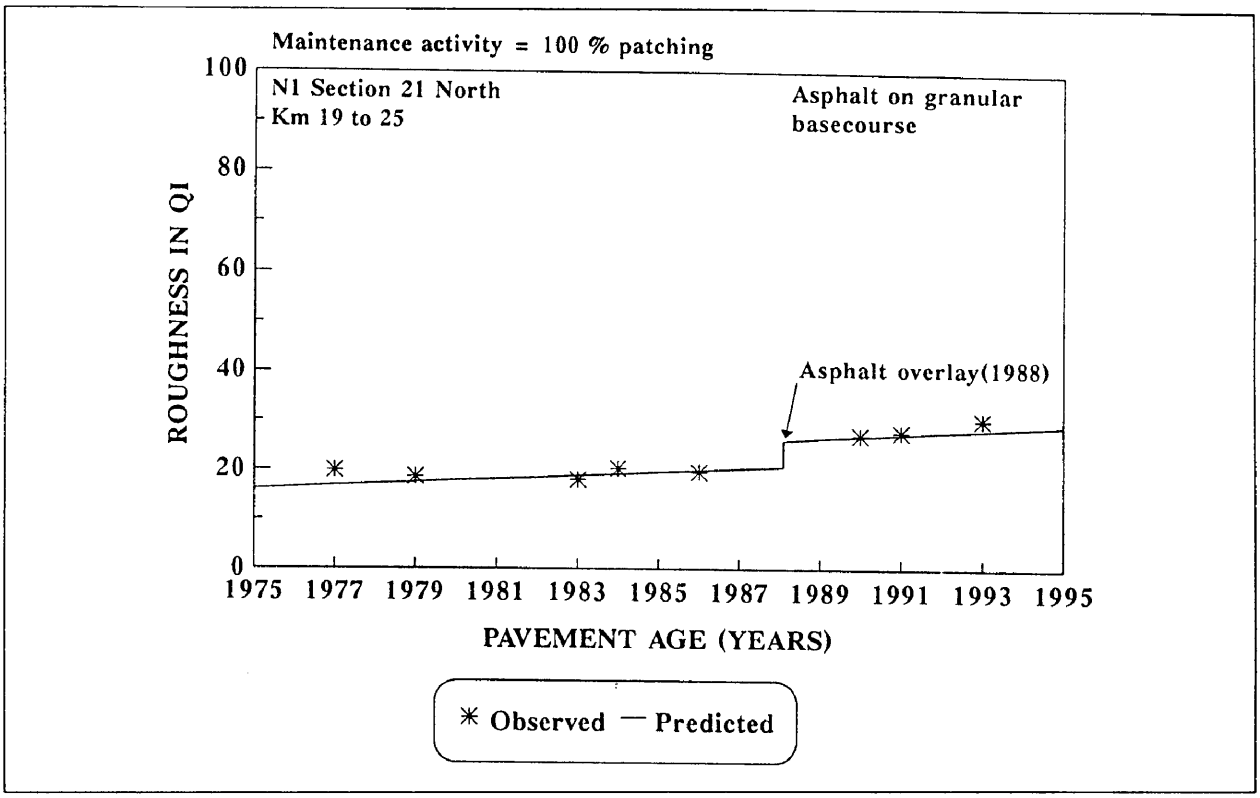

Figure C.17: National route 1 section 21 north from kilometre 19 to 25.

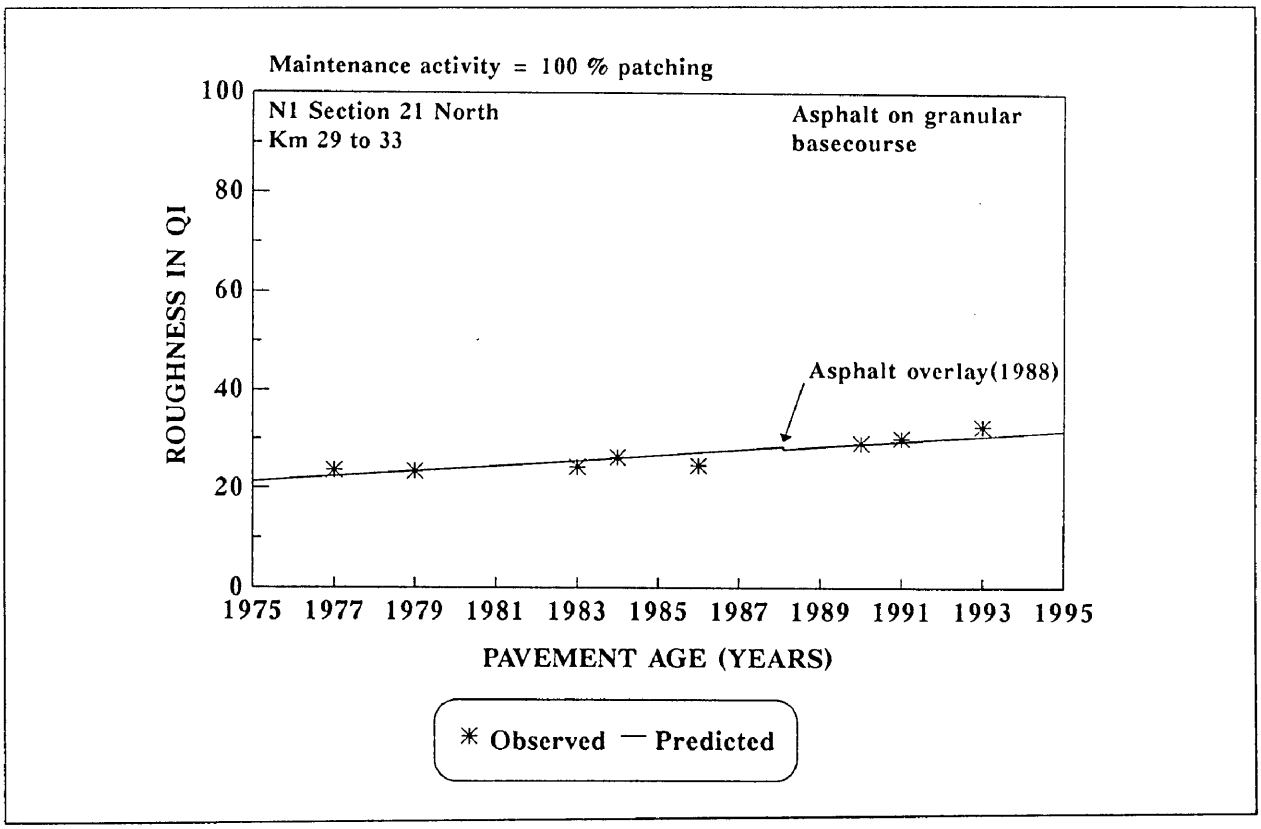

Figure C.18: National route 1 section 21 north from kilometre 29 to 33.

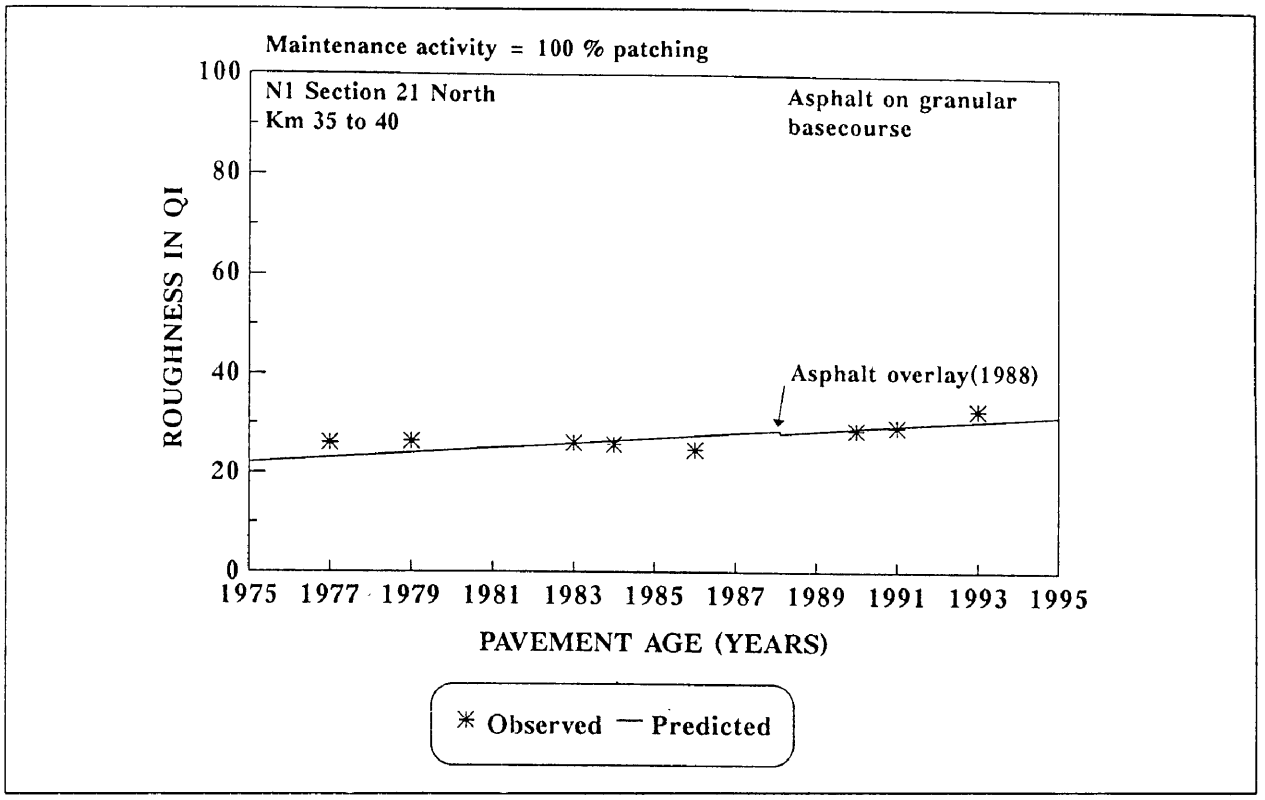

Figure C.19: National route 1 section 21 north from kilometre 35 to 40.

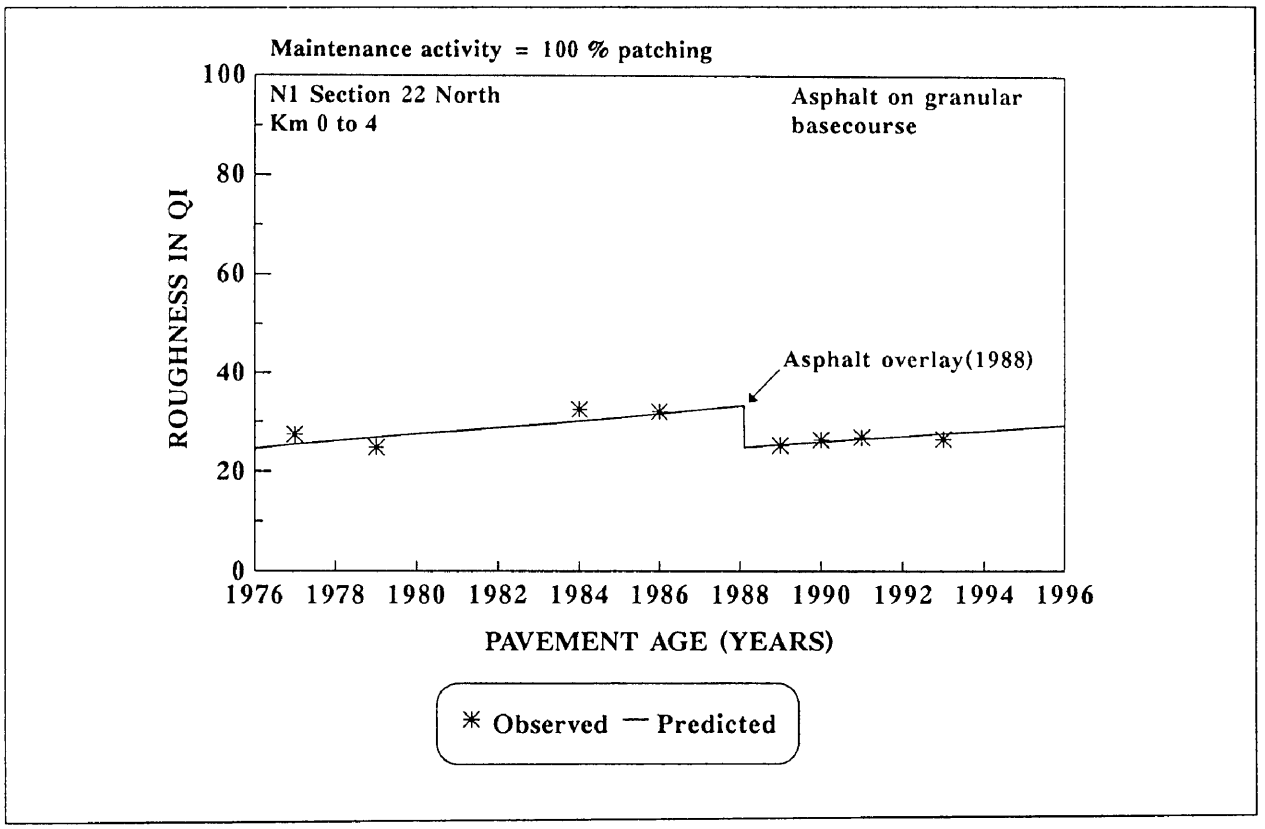

Figure C.20: National route 1 section 22 north from kilometre 0 to 4.

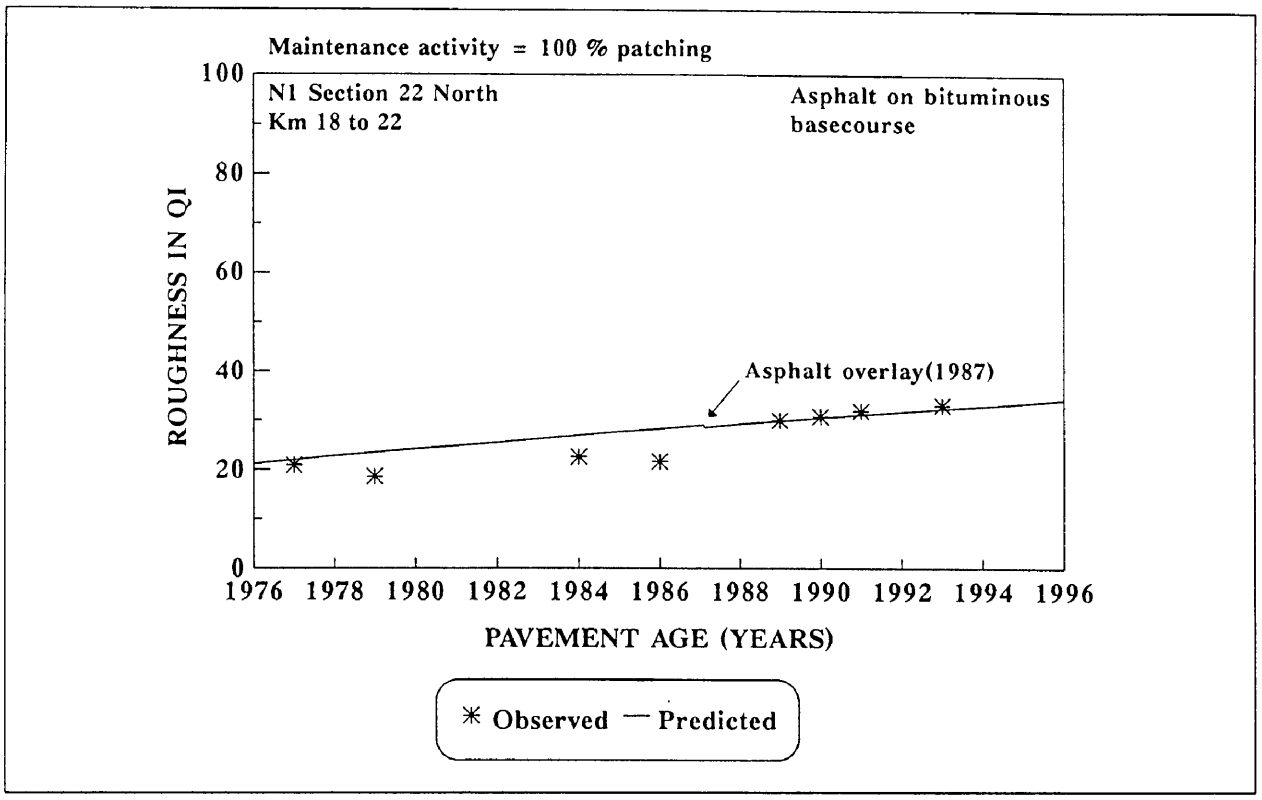

Figure C.21: National route 1 section 22 north from kilometre 18 to 22.

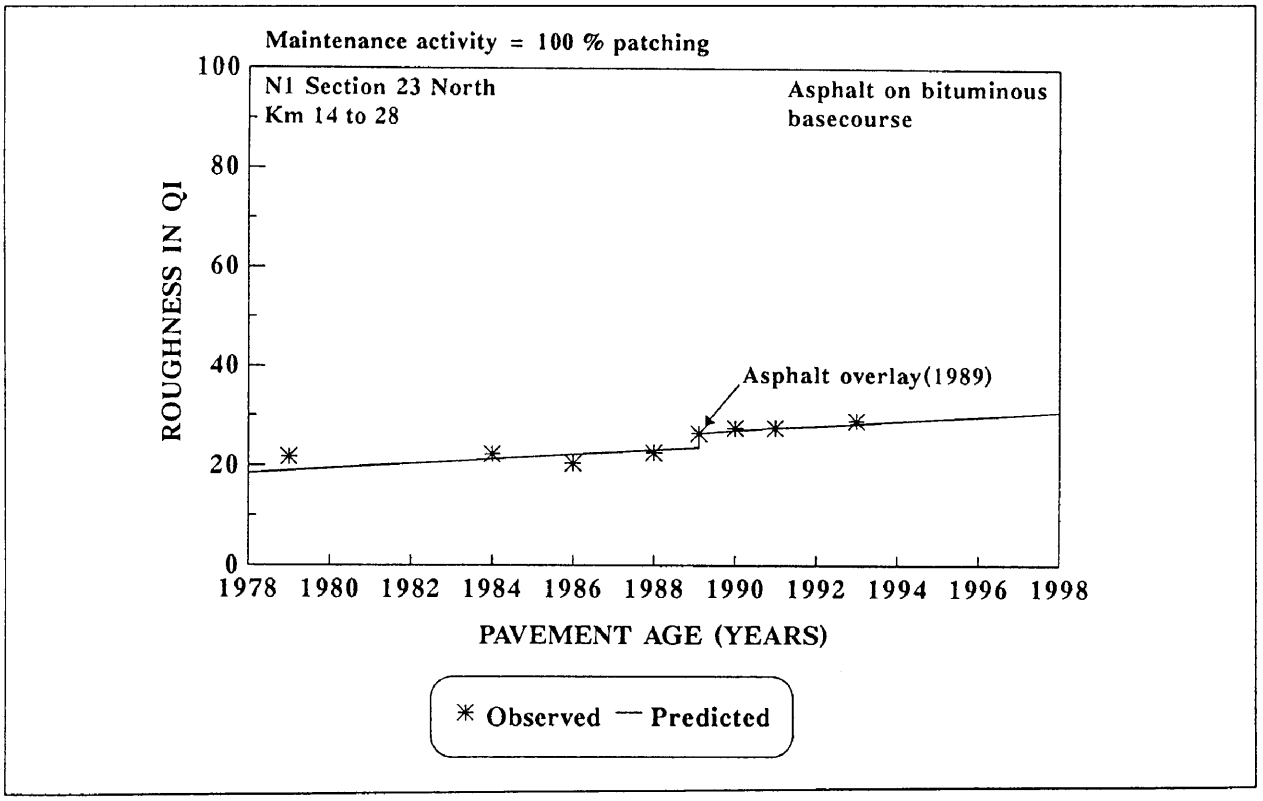

Figure C.22: National route 1 section 23 north from kilometre 14 to 28.

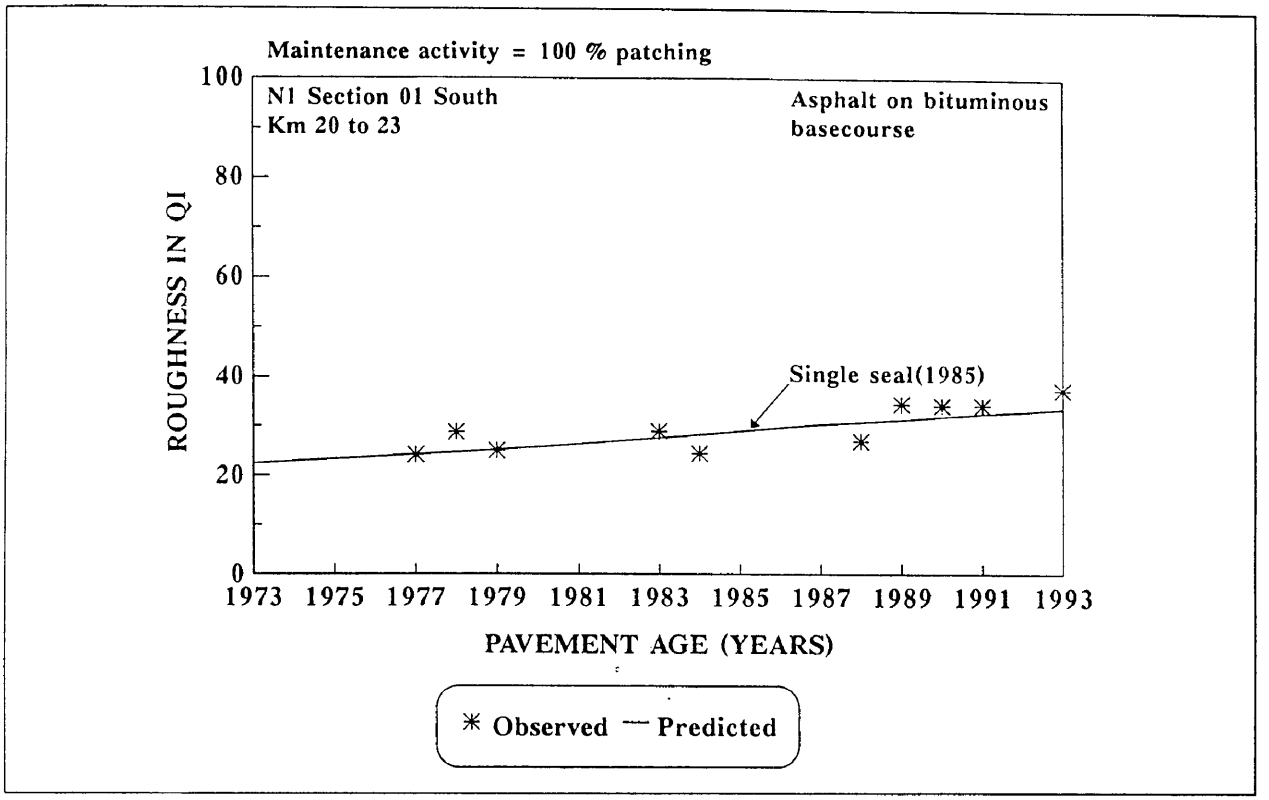

Figure C.23: National route 1 section 1 south from kilometre 20 to 23.

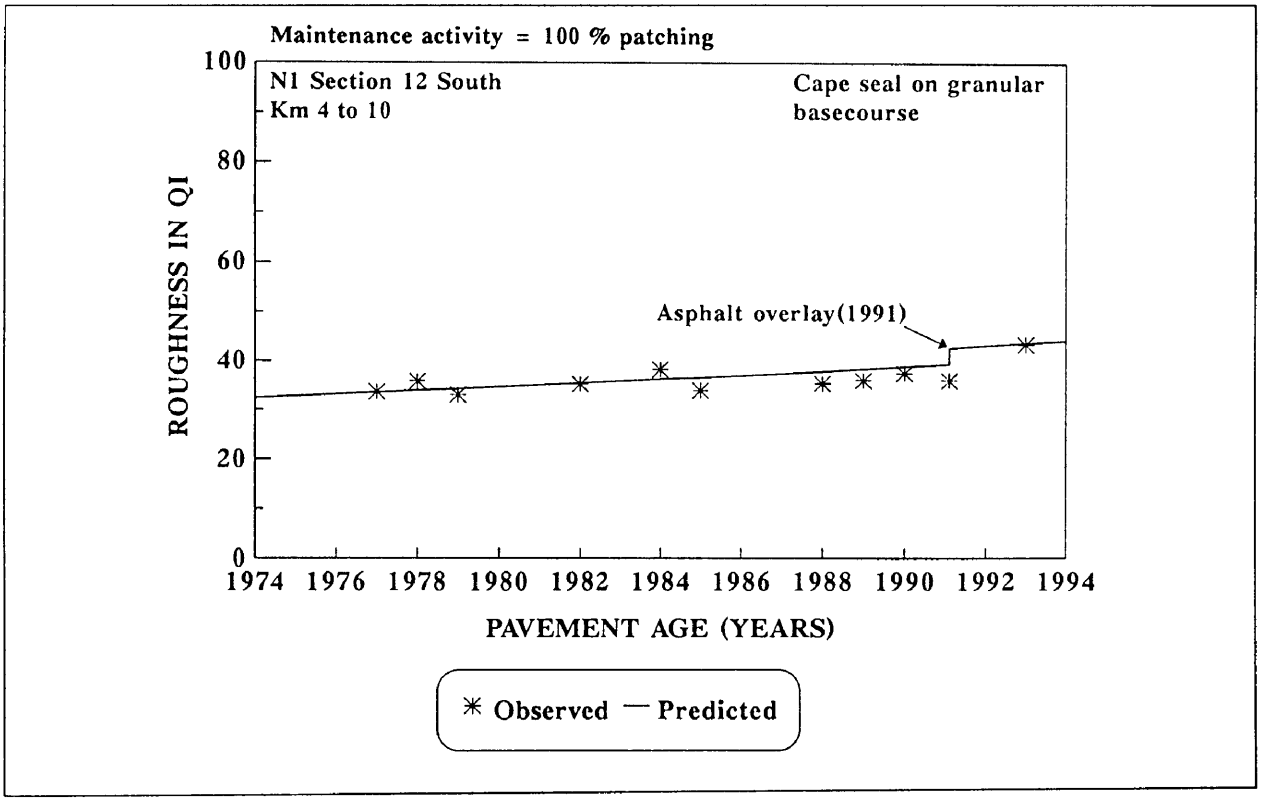

Figure C.24: National route 1 section 12 south from kilometre 4 to 10.

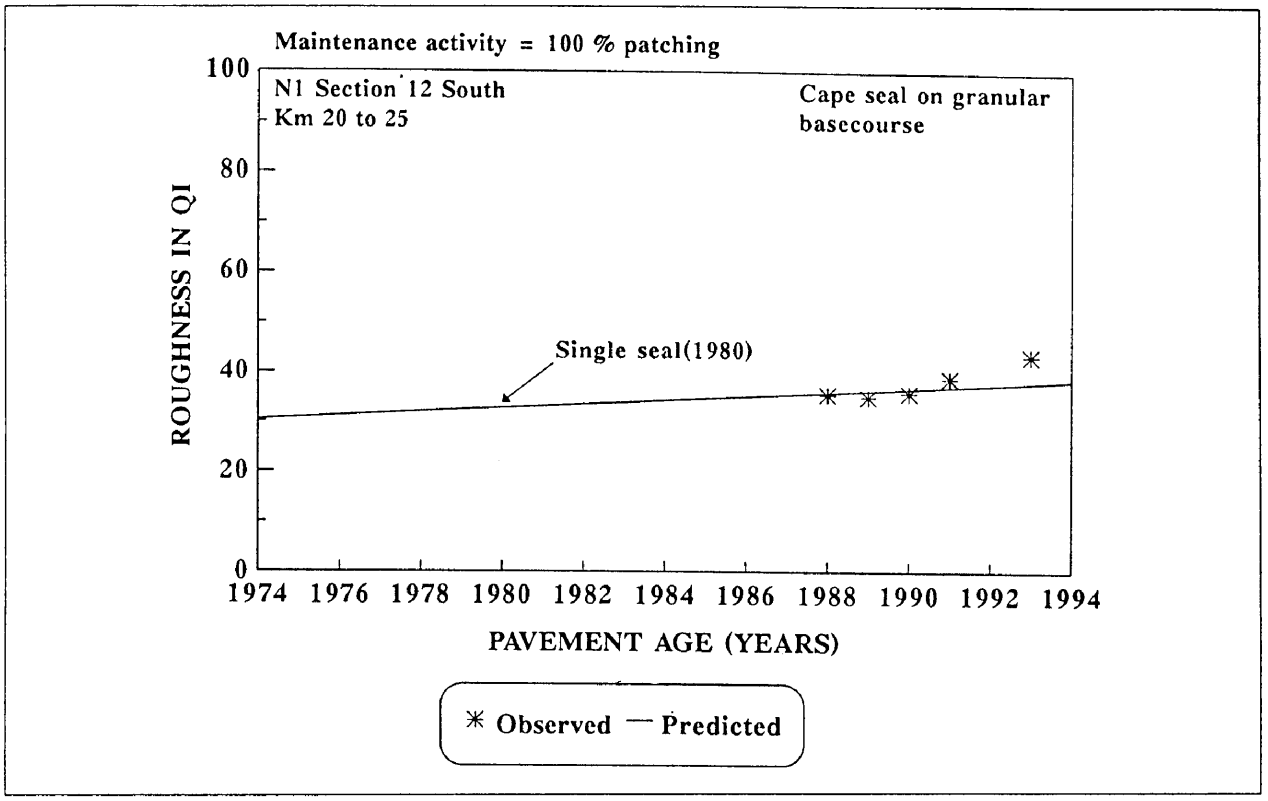

Figure C.25: National route 1 section 12 south from kilometre 20 to 25.

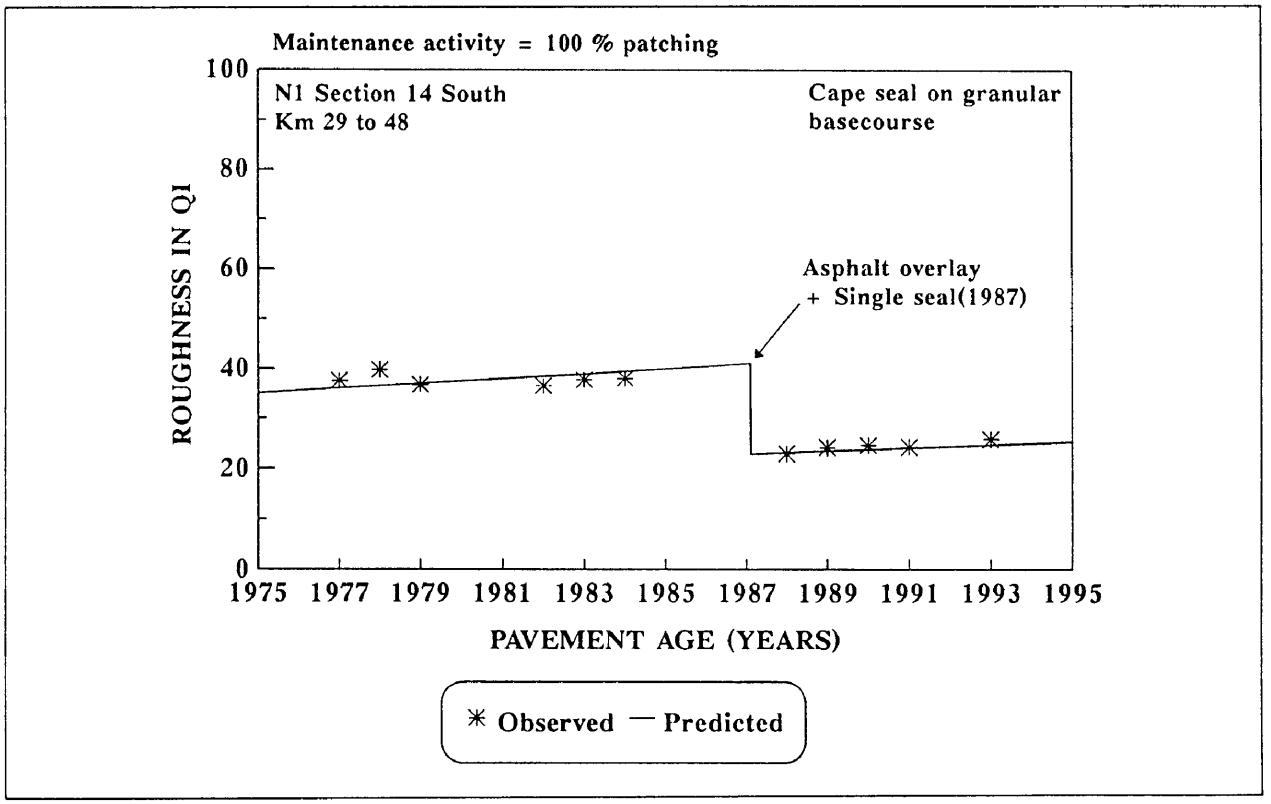

Figure C.26: National route 1 section 14 south from kilometre 29 to 48.

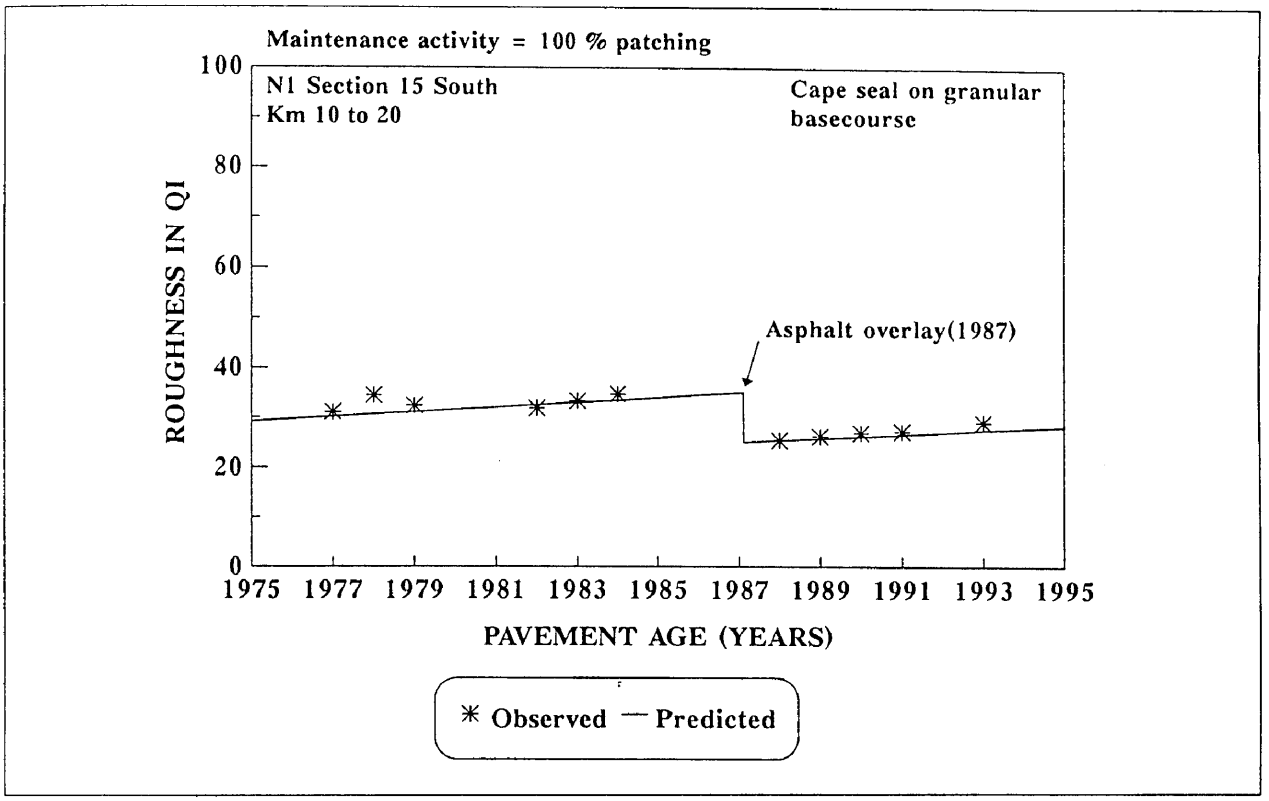

Figure C.27: National route 1 section 15 south from kilometre 10 to 20.

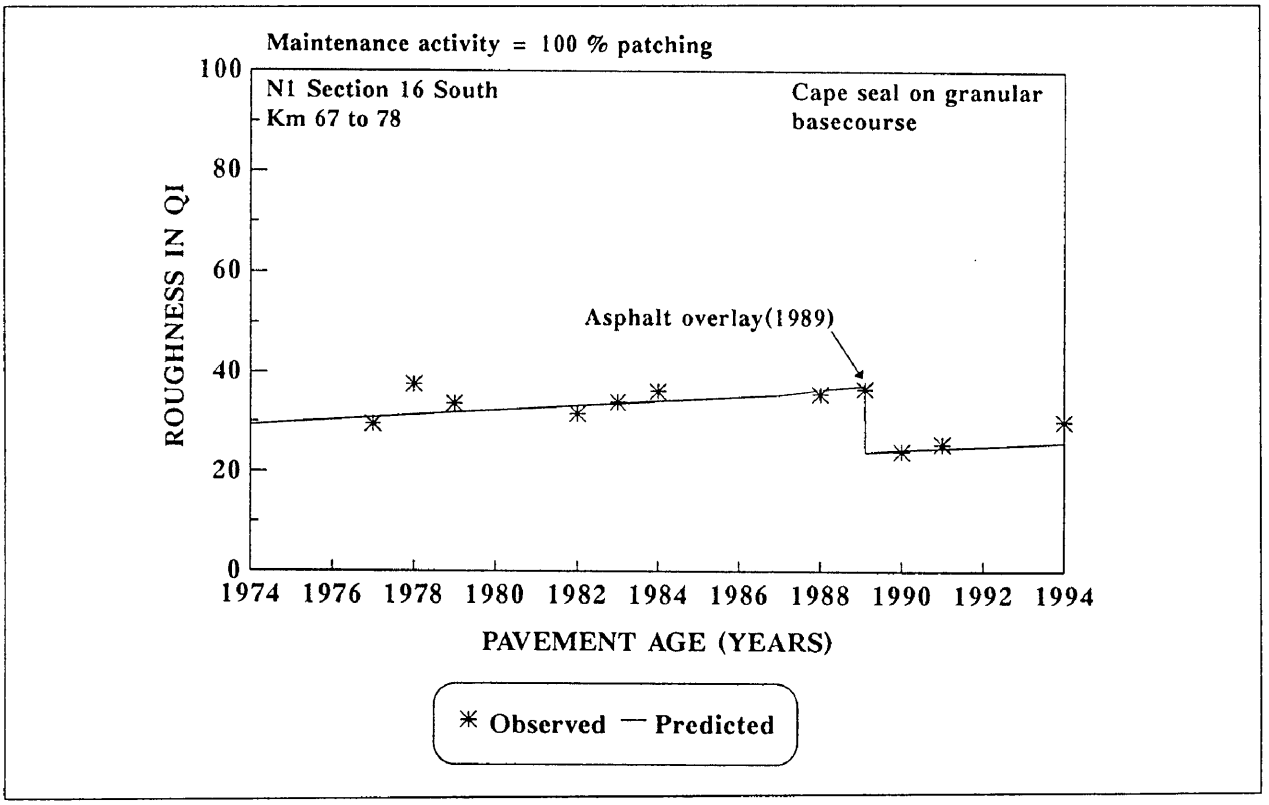

Figure C.28: National route 1 section 16 south from kilometre 67 to 78.

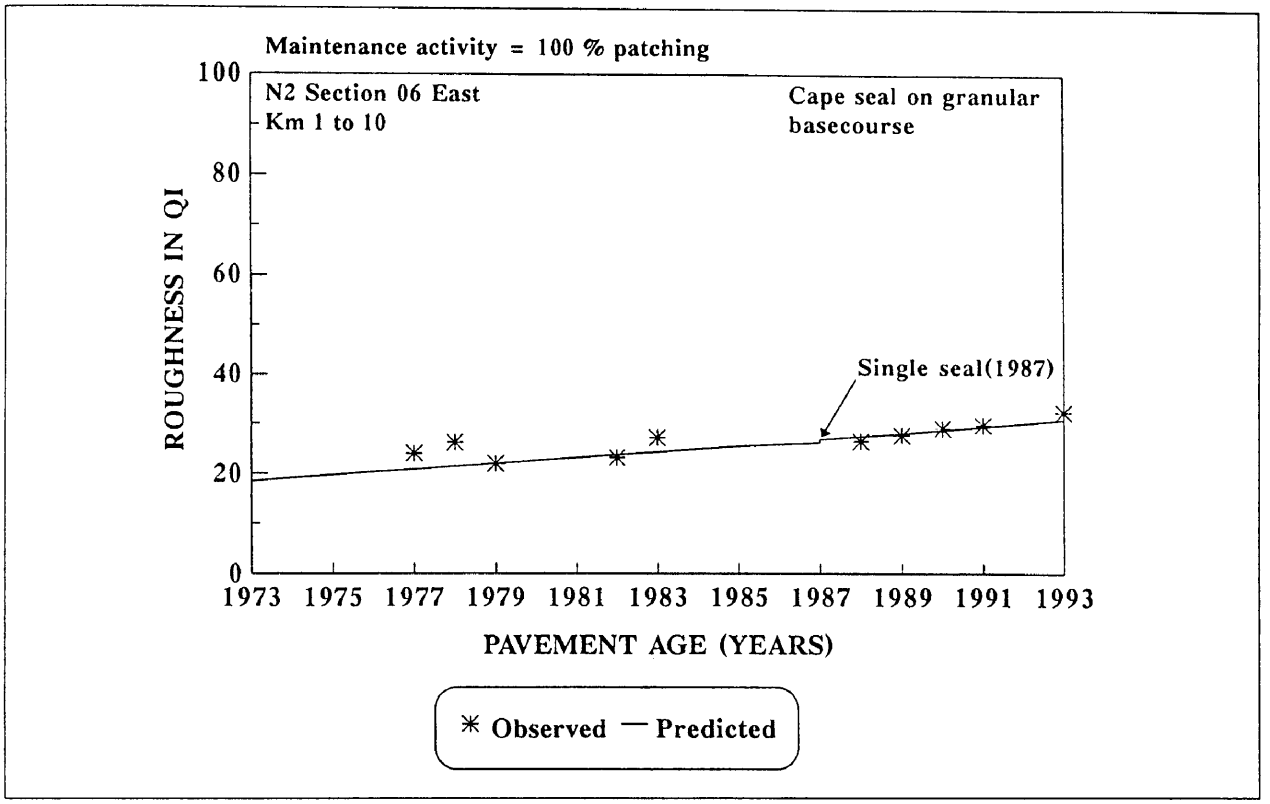

Figure C.29: National route 2 section 6 east from kilometre 1 to 10.

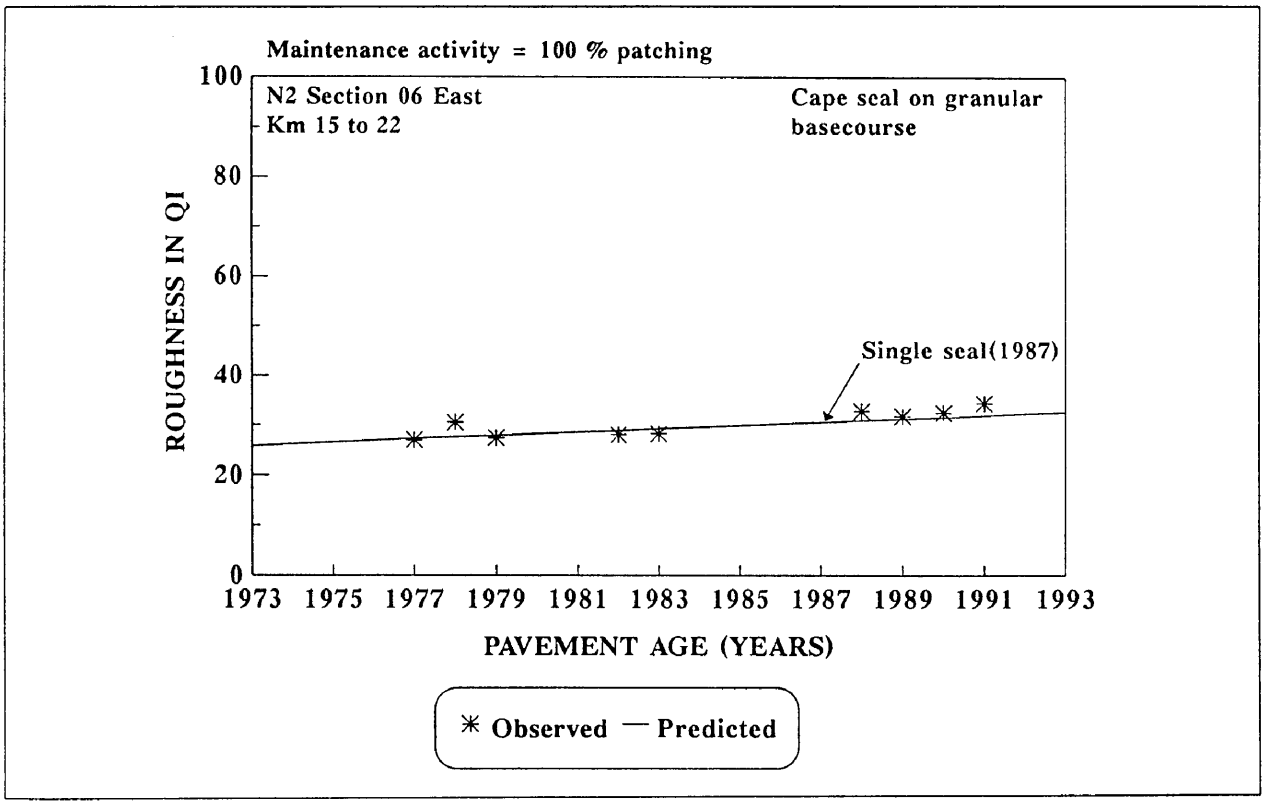

Figure C.30: National route 2 section 6 east from kilometre 15 to 22.

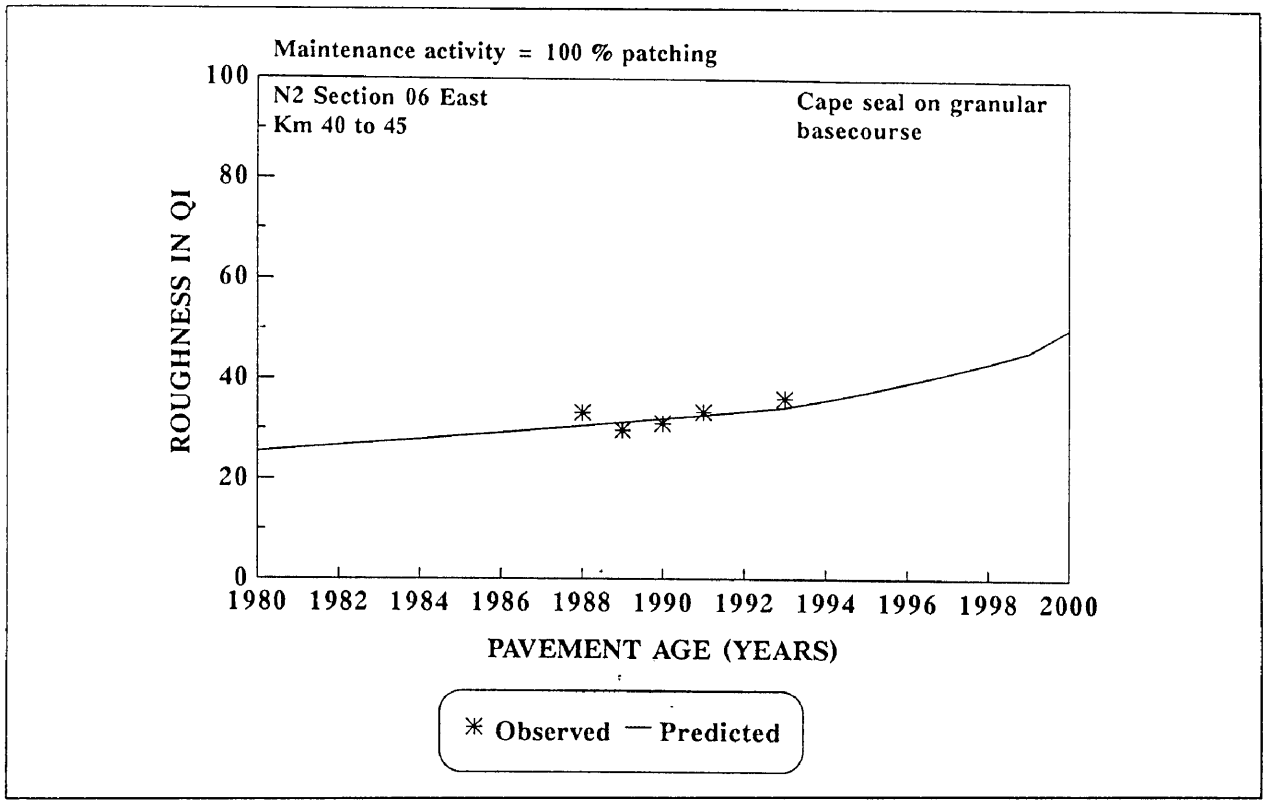

Figure C.31: National route 2 section 6 east from kilometre 40 to 45.

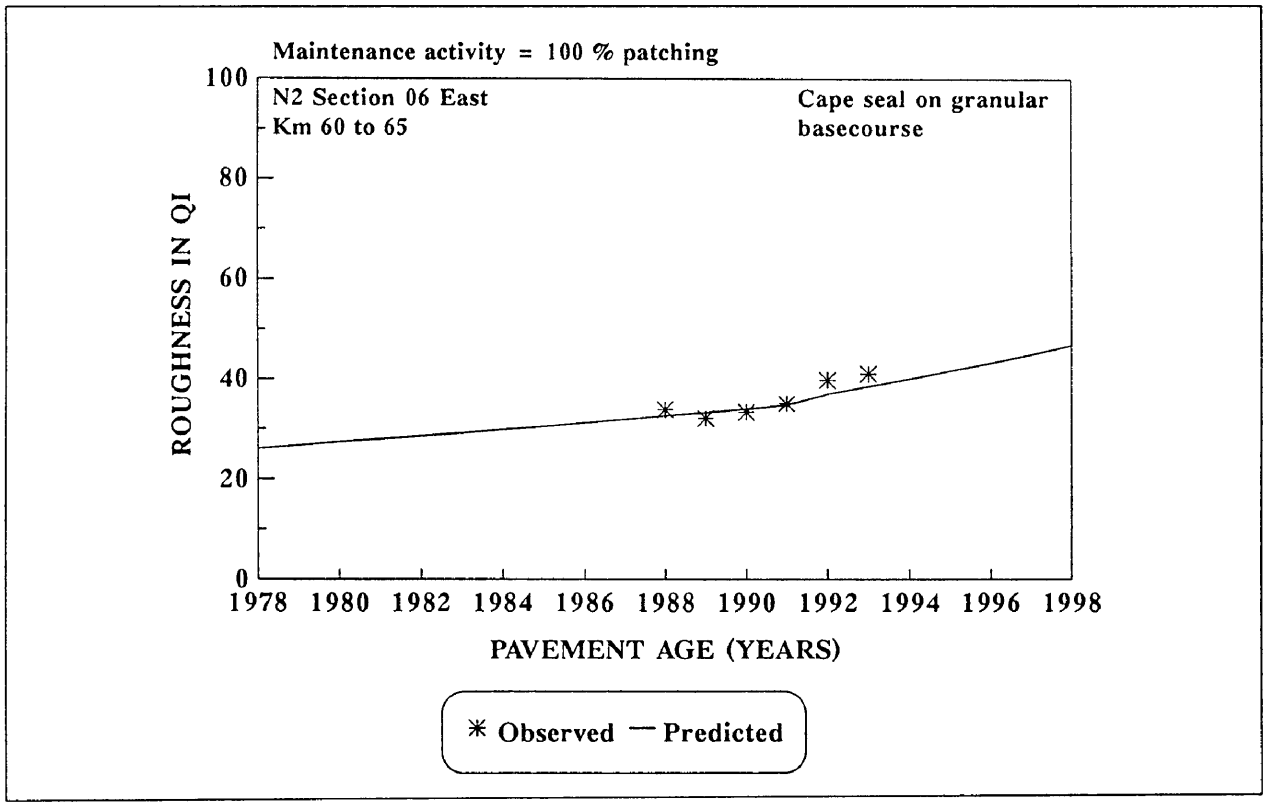

Figure C.32: National route 2 section 6 east from kilometre 60 to 65.

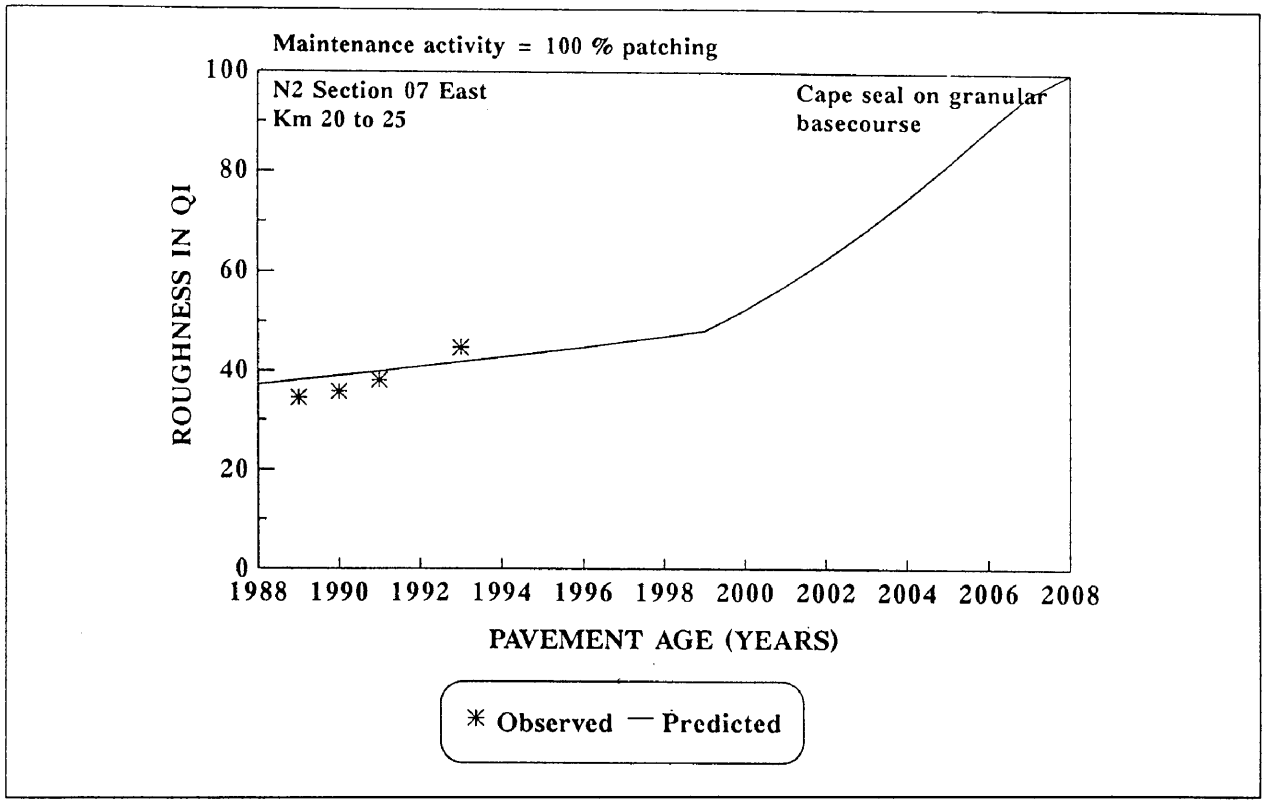

Figure C.33: National route 2 section 7 east from kilometre 20 to 25.

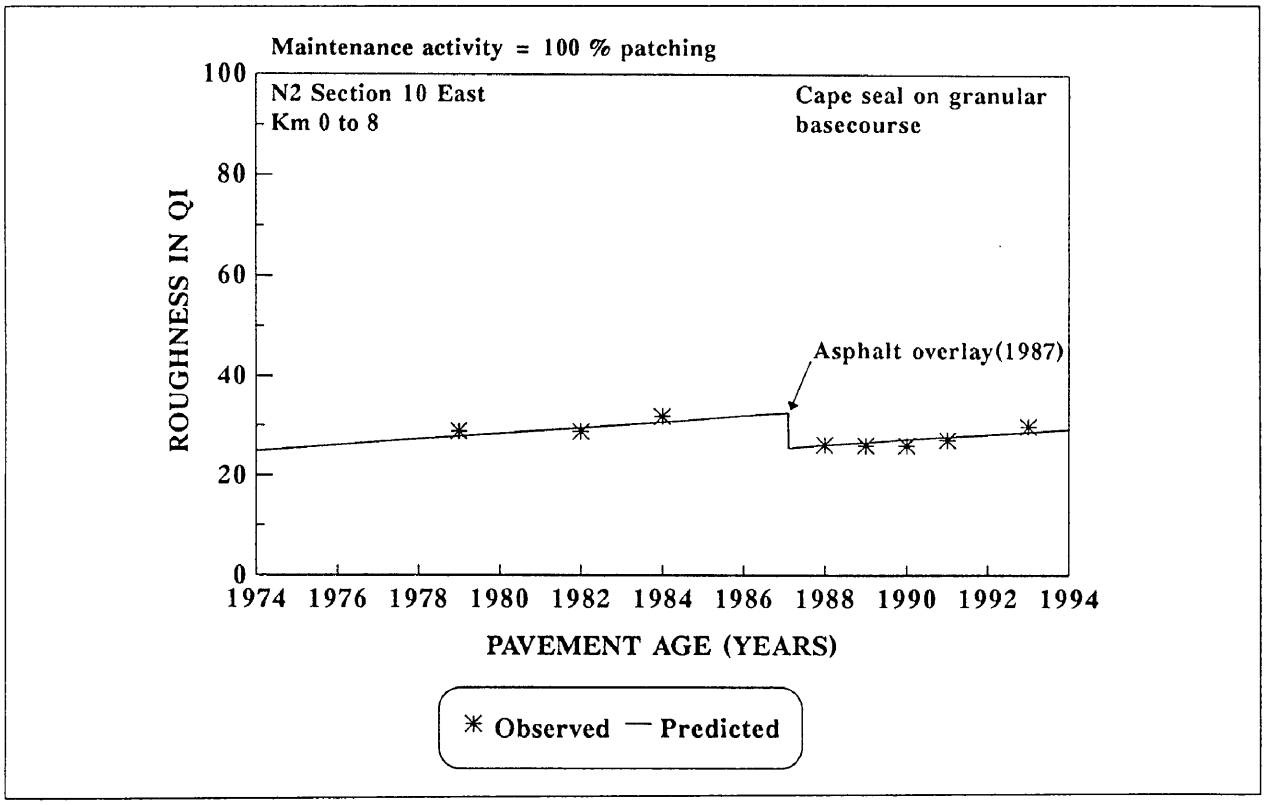

Figure C.34: National route 2 section 10 east from kilometre 0 to 8.

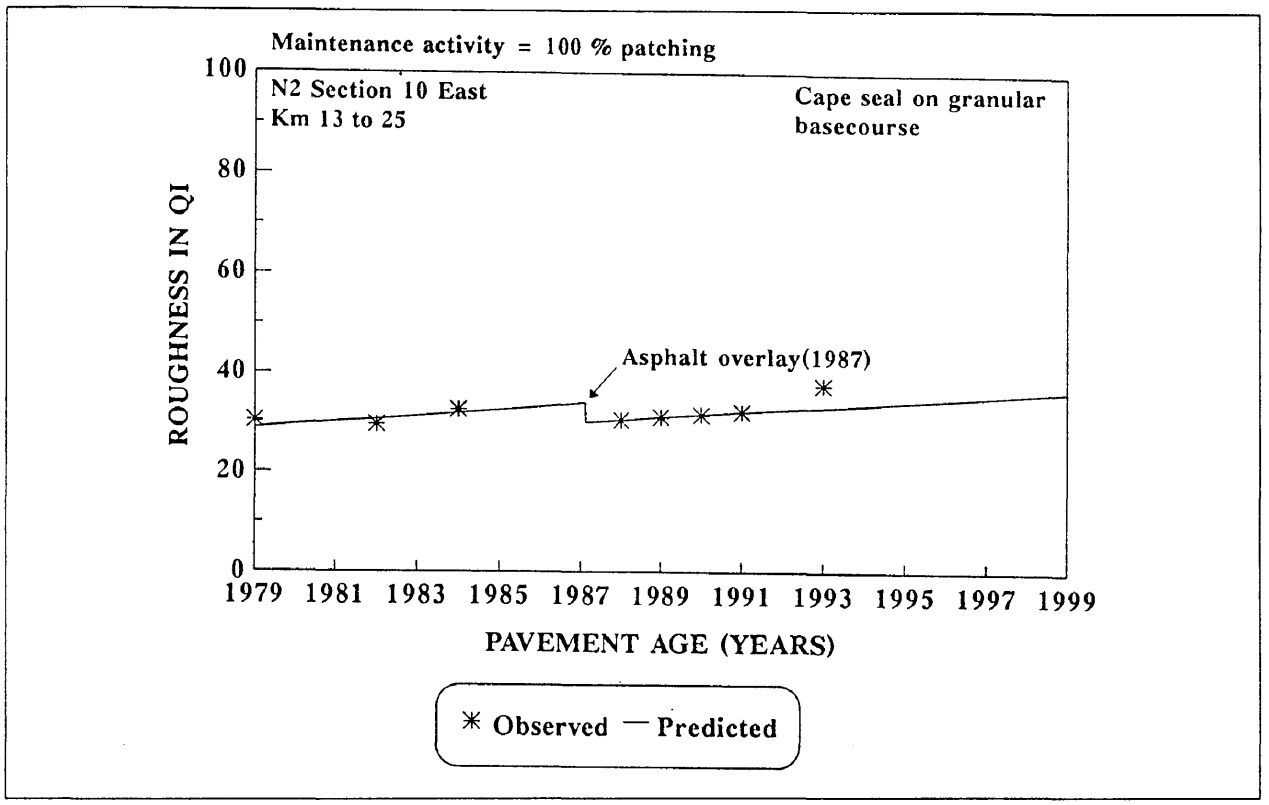

Figure C.35: National route 2 section 10 east from kilometre 13 to 25.

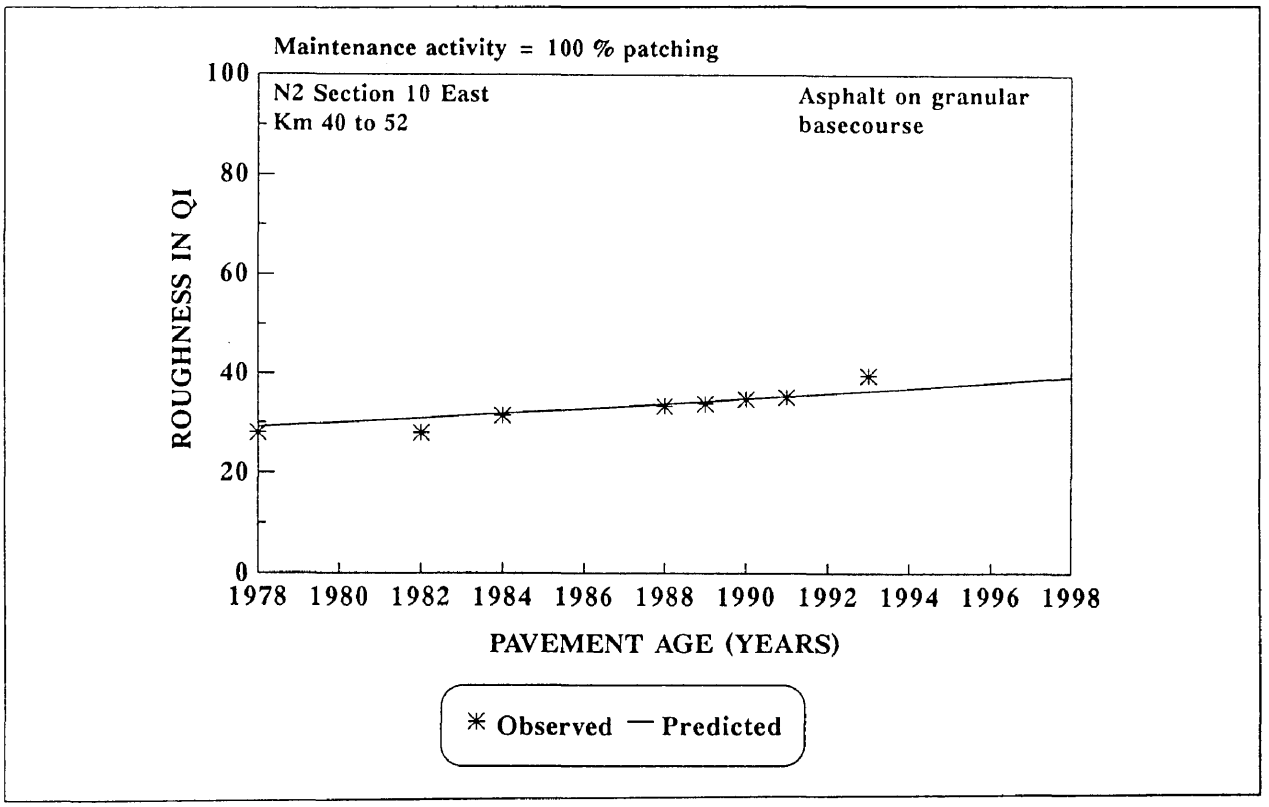

Figure C.36: National route 2 section 10 east from kilometre 40 to 52.

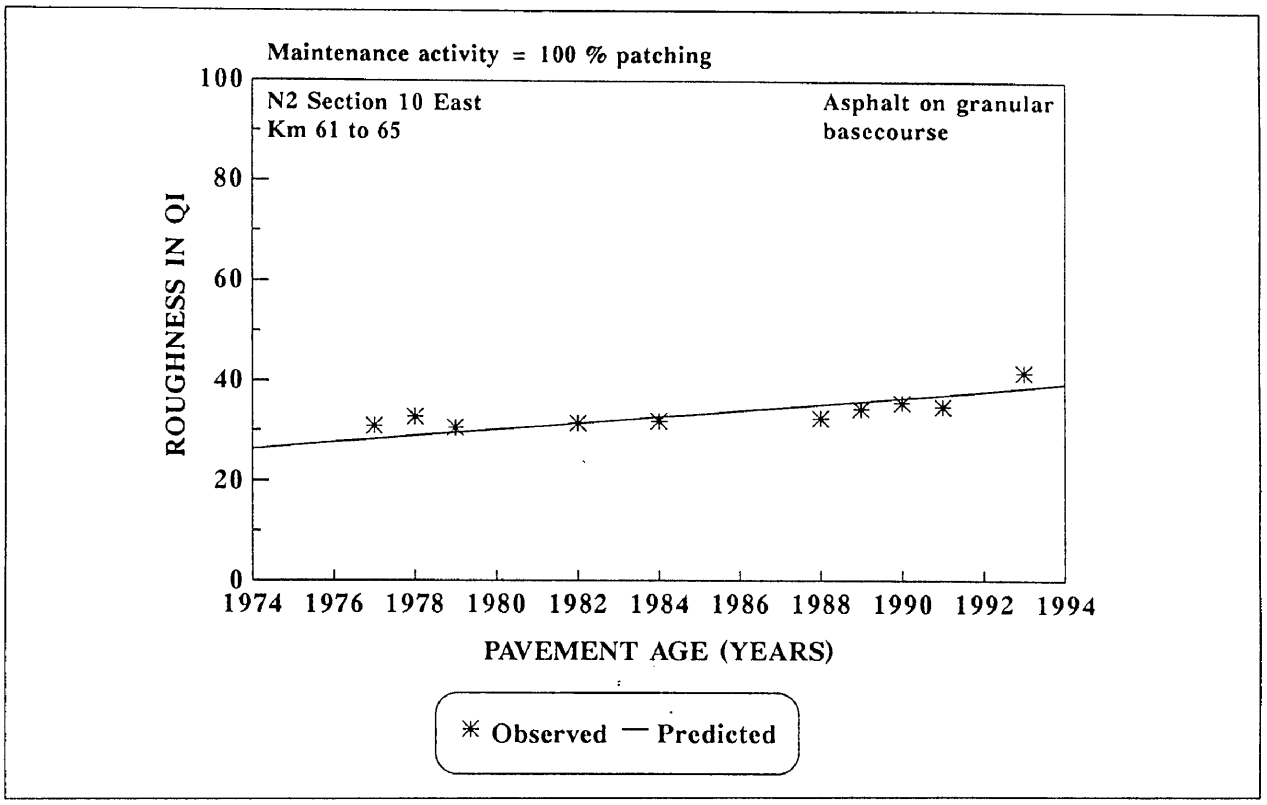

Figure C.37: National route 2 section 10 east from kilometre 61 to 65.

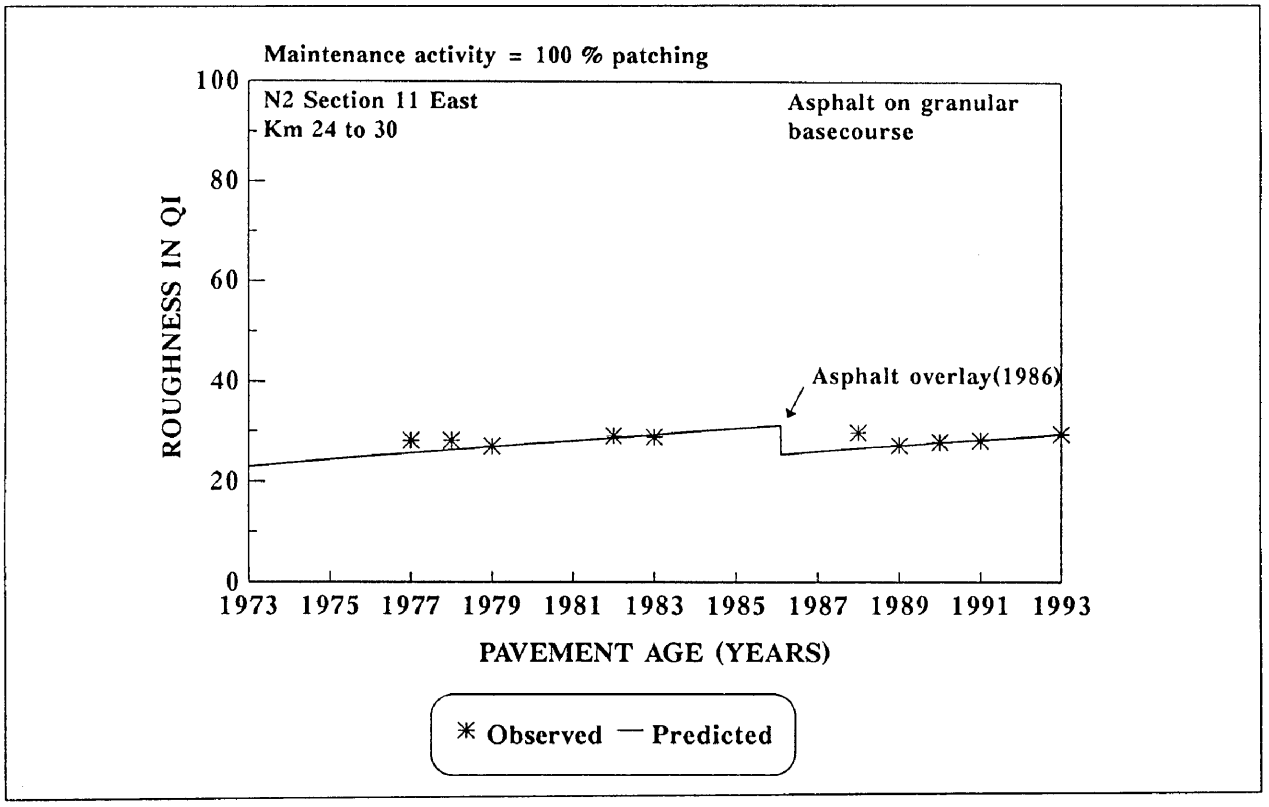

Figure C.38: National route 2 section 11 east from kilometre 24 to 30.

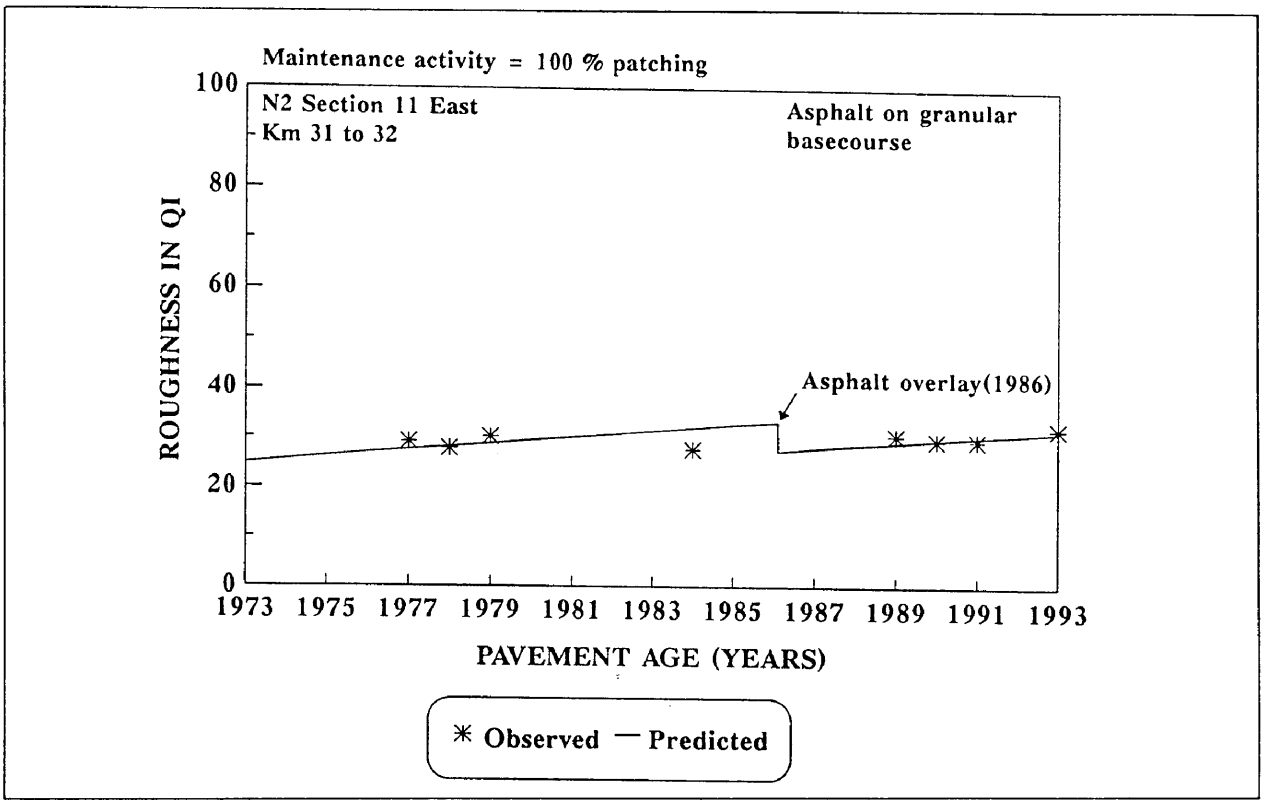

Figure C.39: National route 2 section 11 east from kilometre 31 to 32.

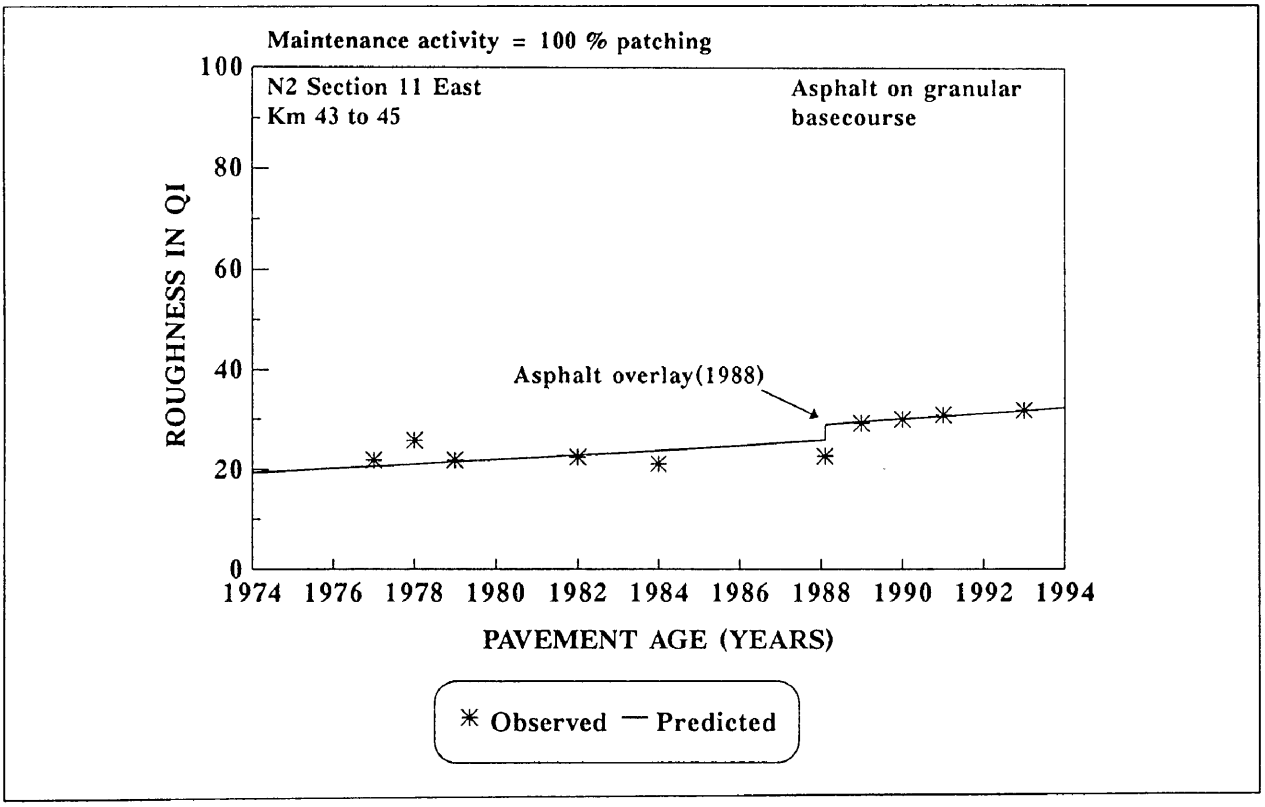

Figure C.40: National route 2 section 11 east from kilometre 43 to 45.

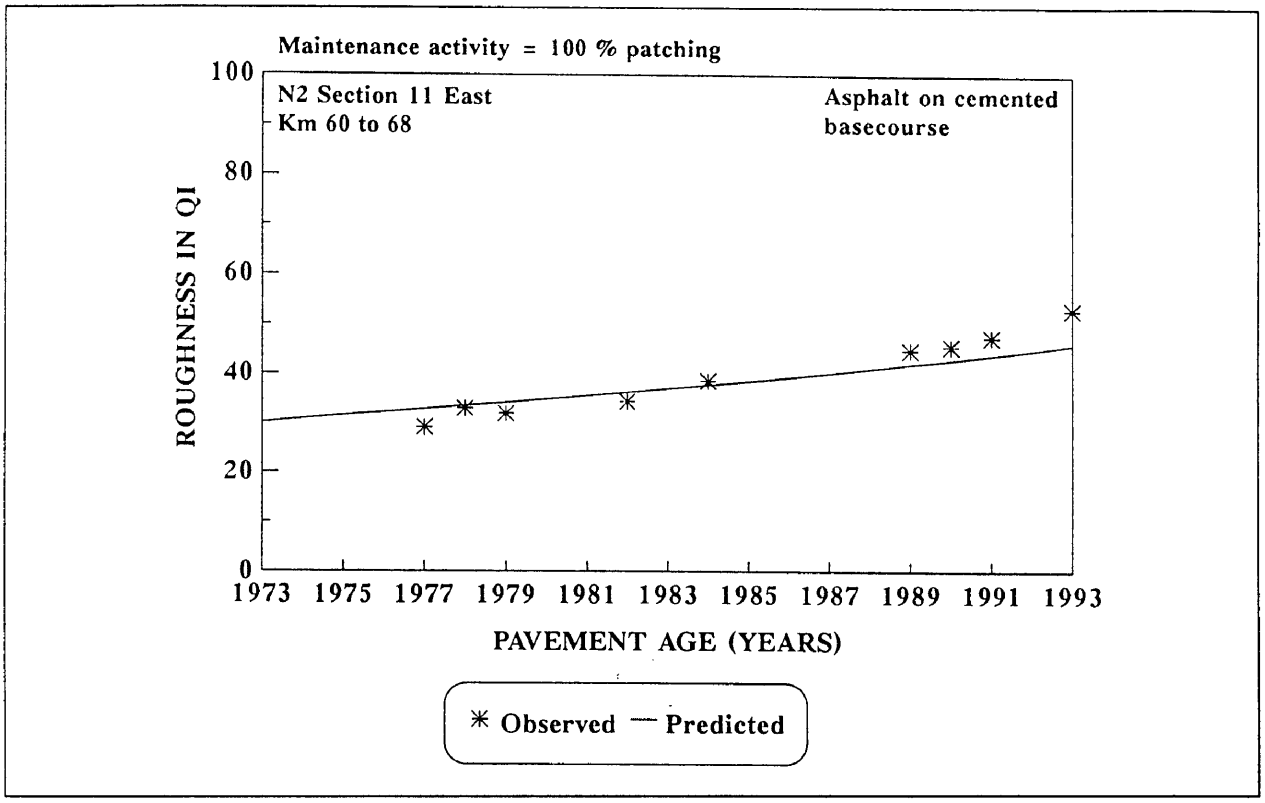

Figure C.41: National route 2 section 11 east from kilometre 60 to 68.

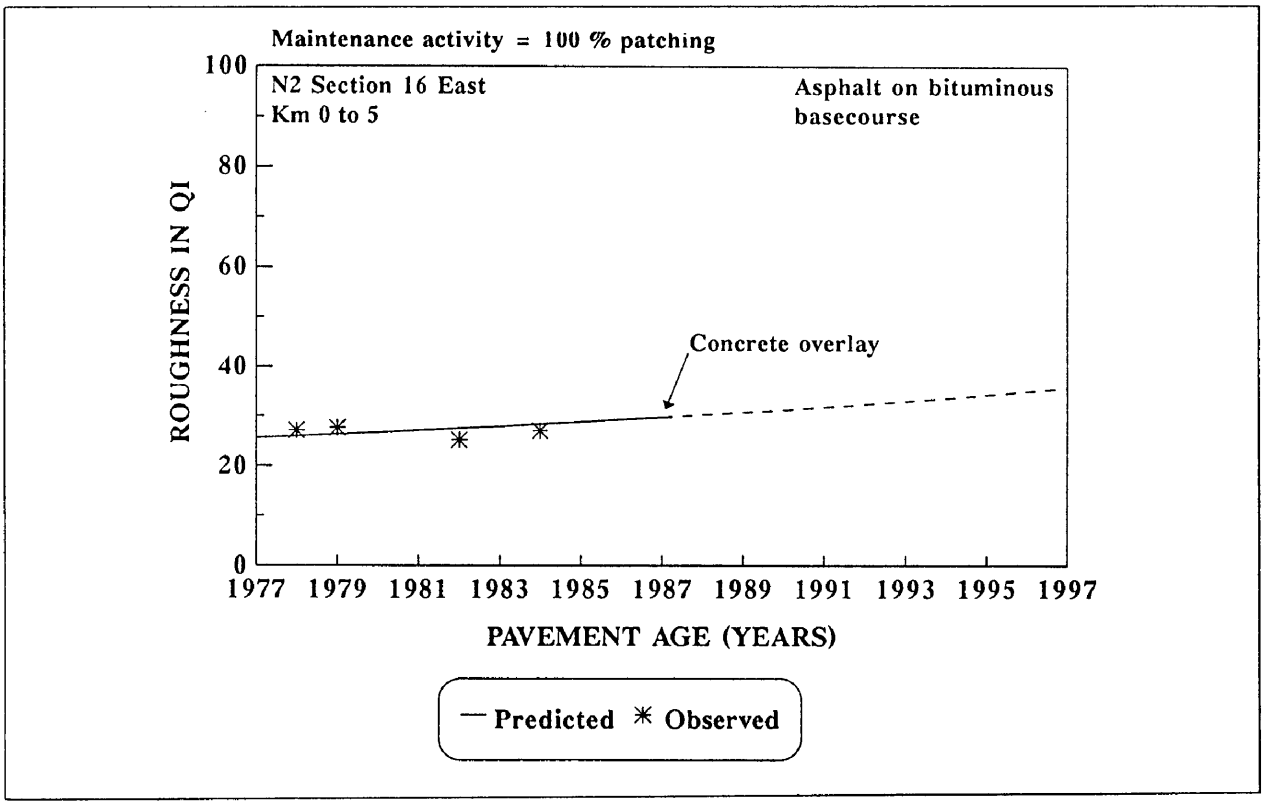

Figure C.42: National route 2 section 16 east from kilometre 0 to 5.

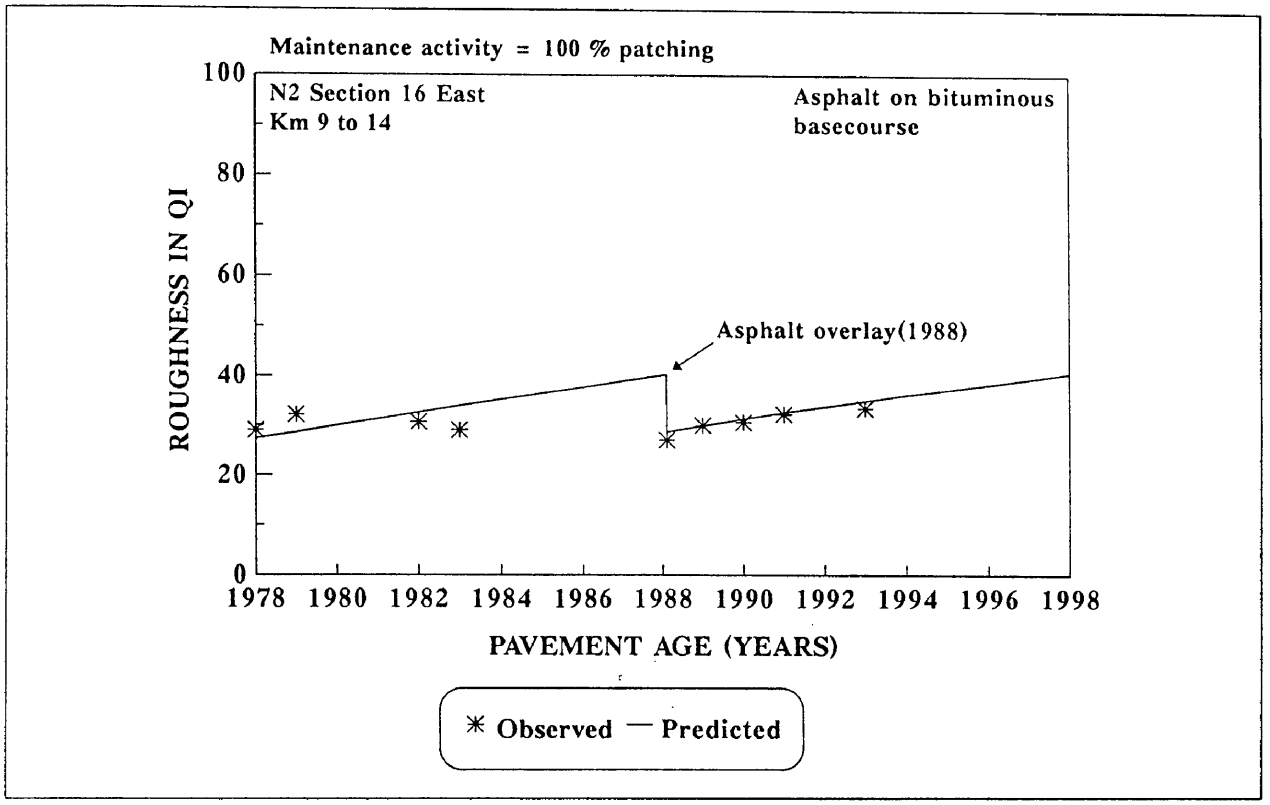

Figure C.43: National route 2 section 16 east from kilometre 9 to 14.

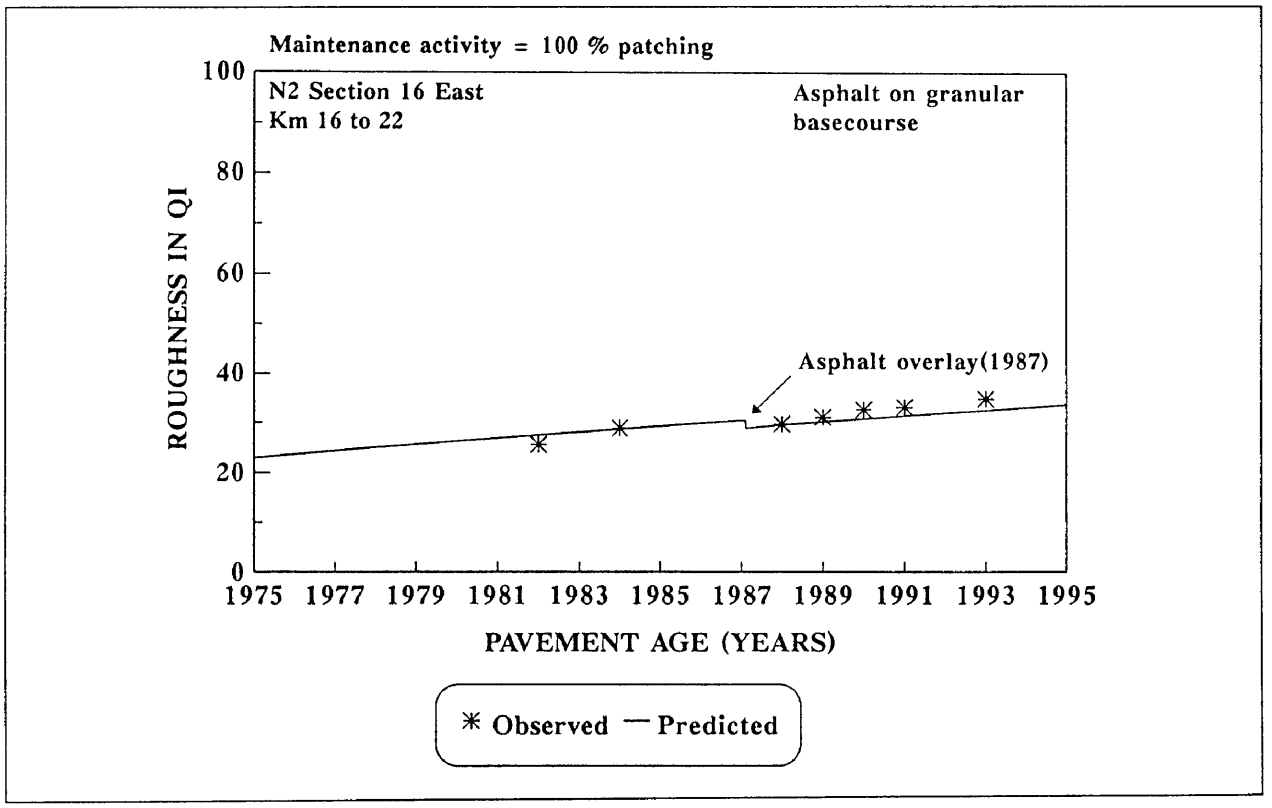

Figure C.44: National route 2 section 16 east from kilometre 16 to 22.

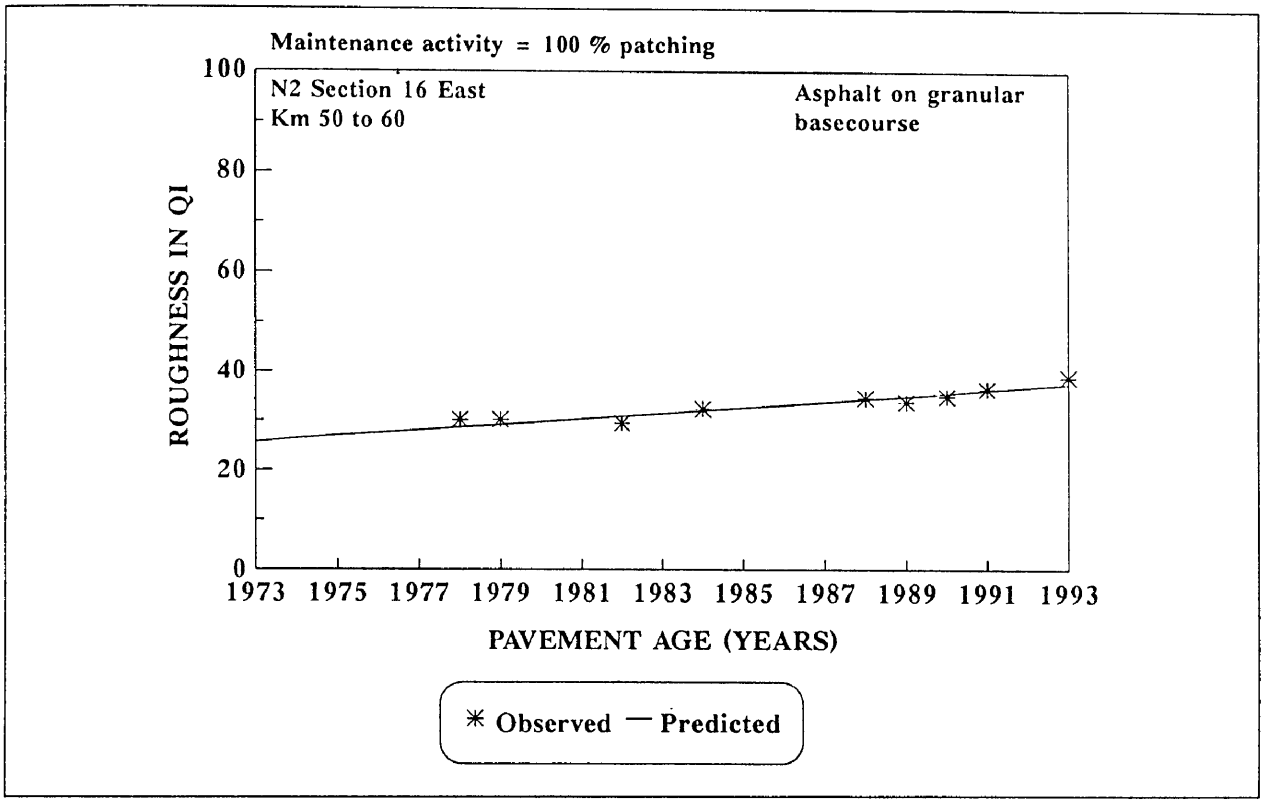

Figure C.45: National route 2 section 16 east from kilometre 50 to 60.

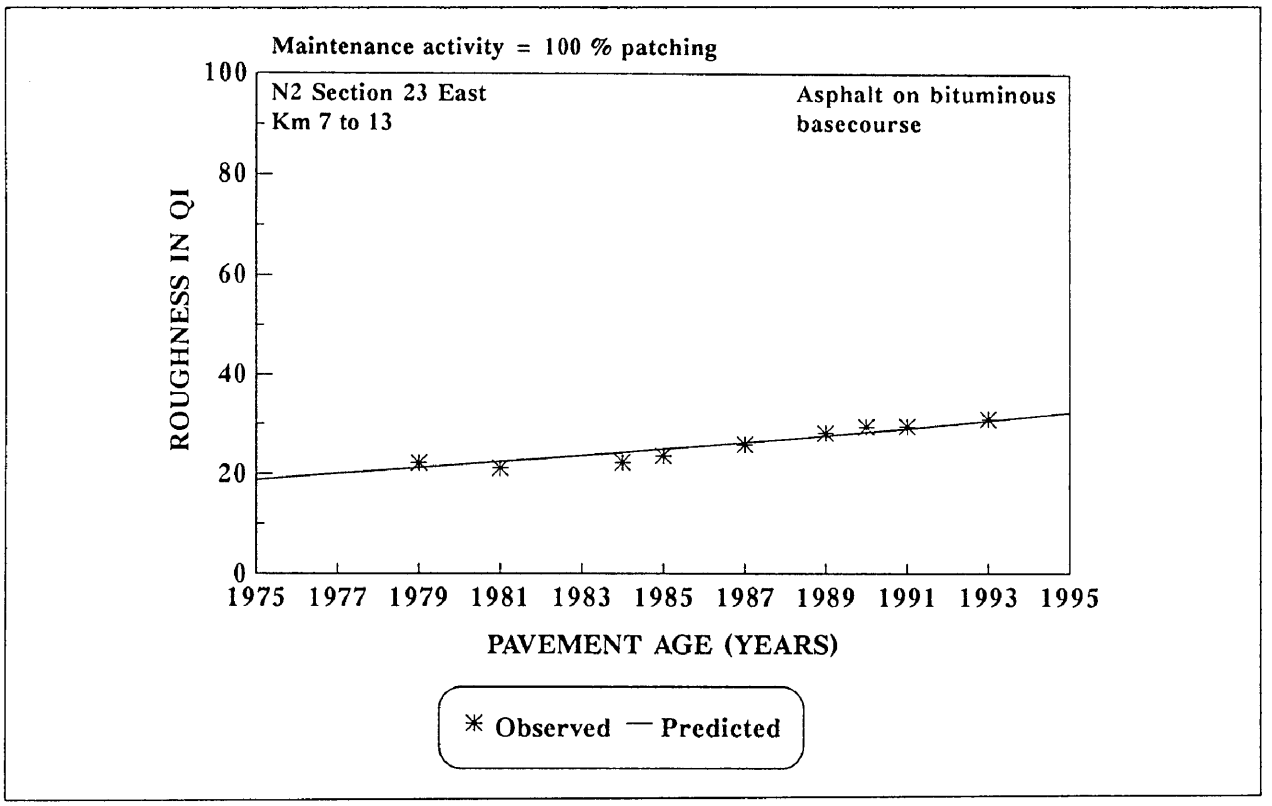

Figure C.46: National route 2 section 23 east from kilometre 7 to 13.

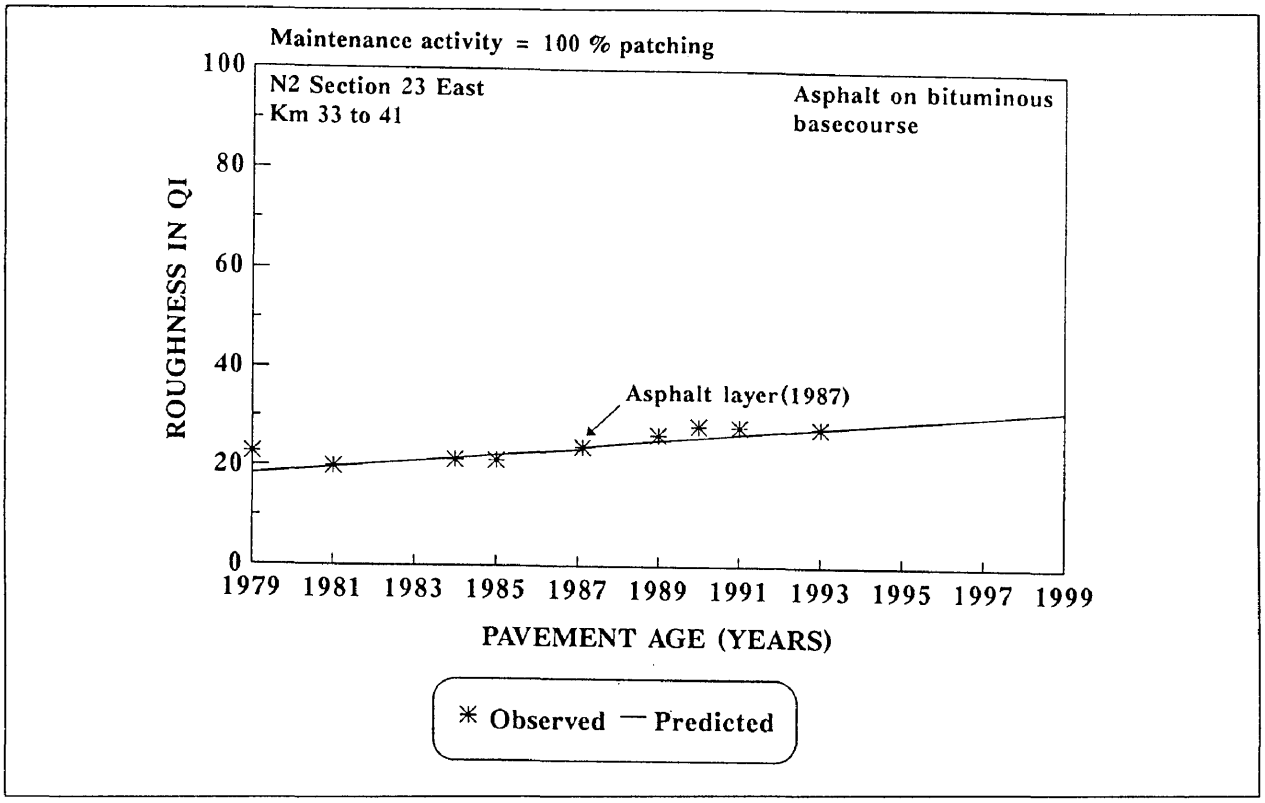

Figure C.47: National route 2 section 23 east from kilometre 33 to 41.

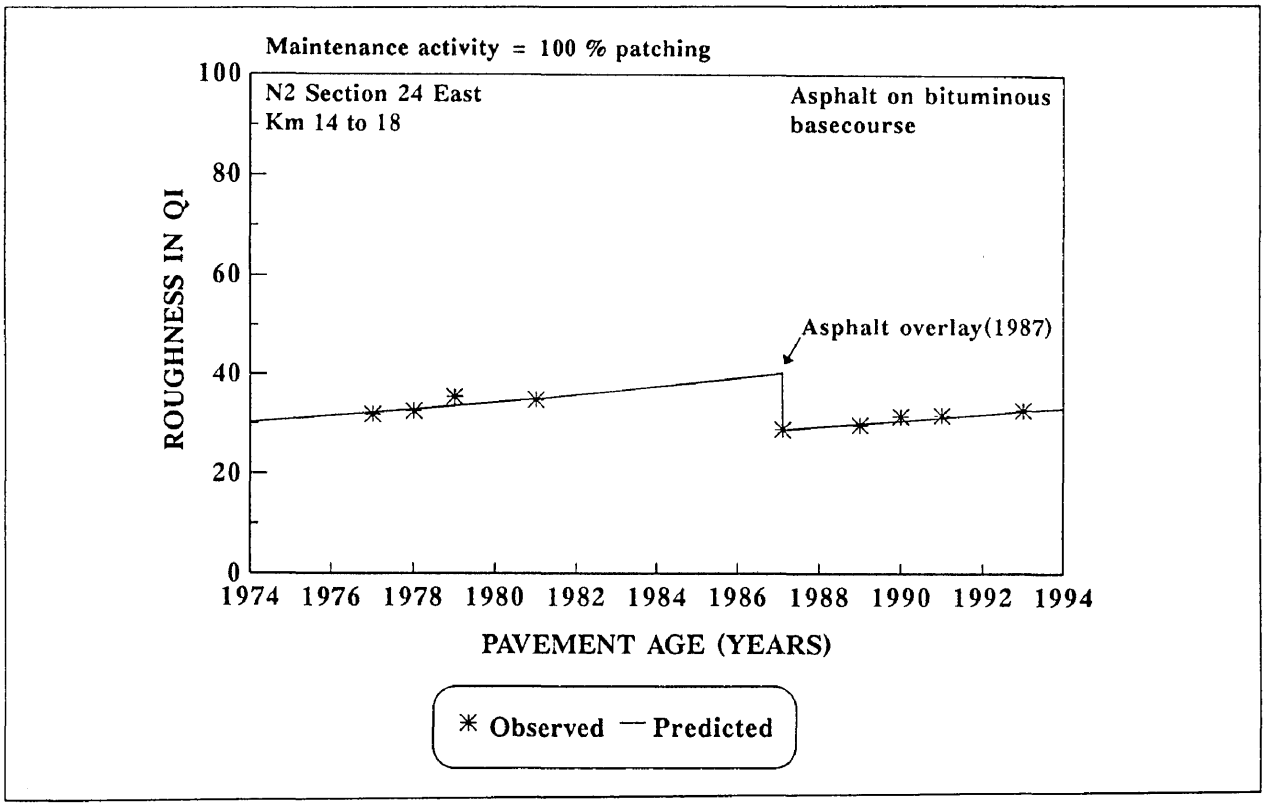

Figure C.48: National route 2 section 24 east from kilometre 14 to 18.

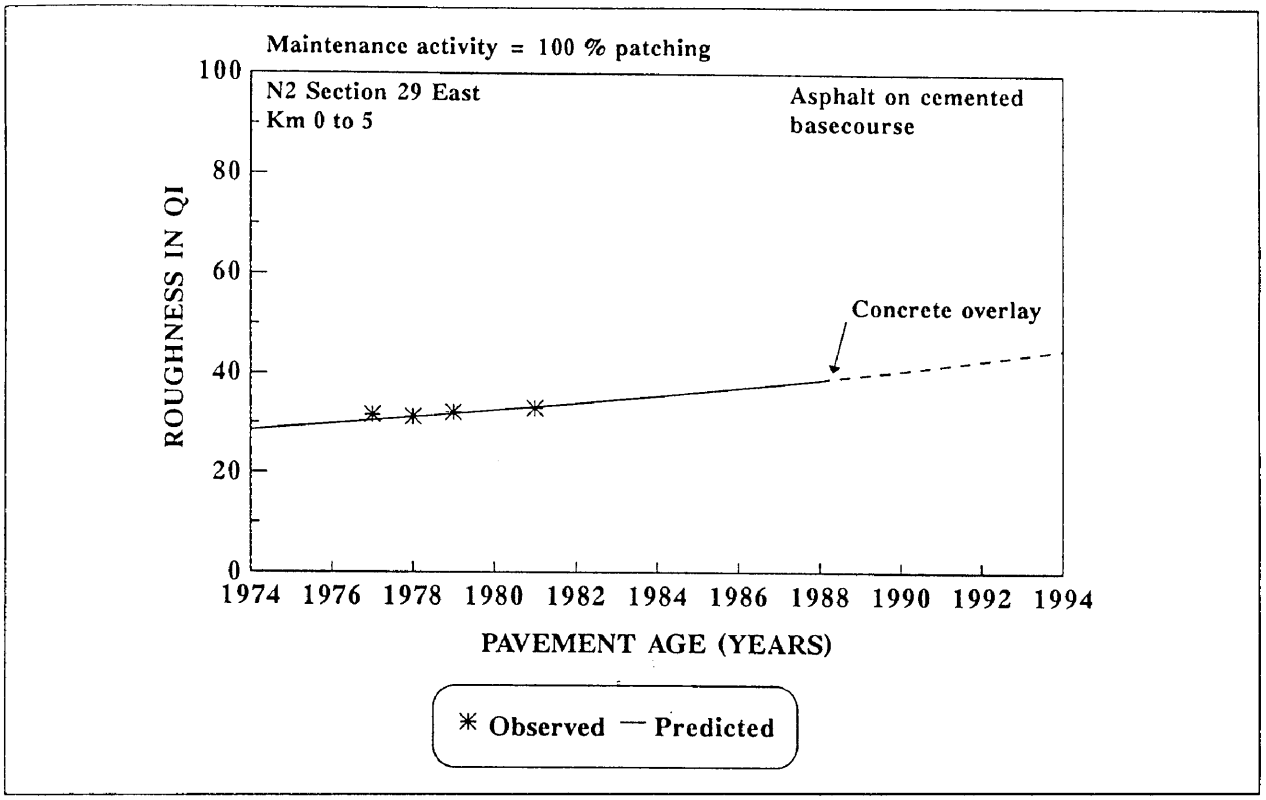

Figure C.49: National route 2 section 29 east from kilometre 0 to 5.

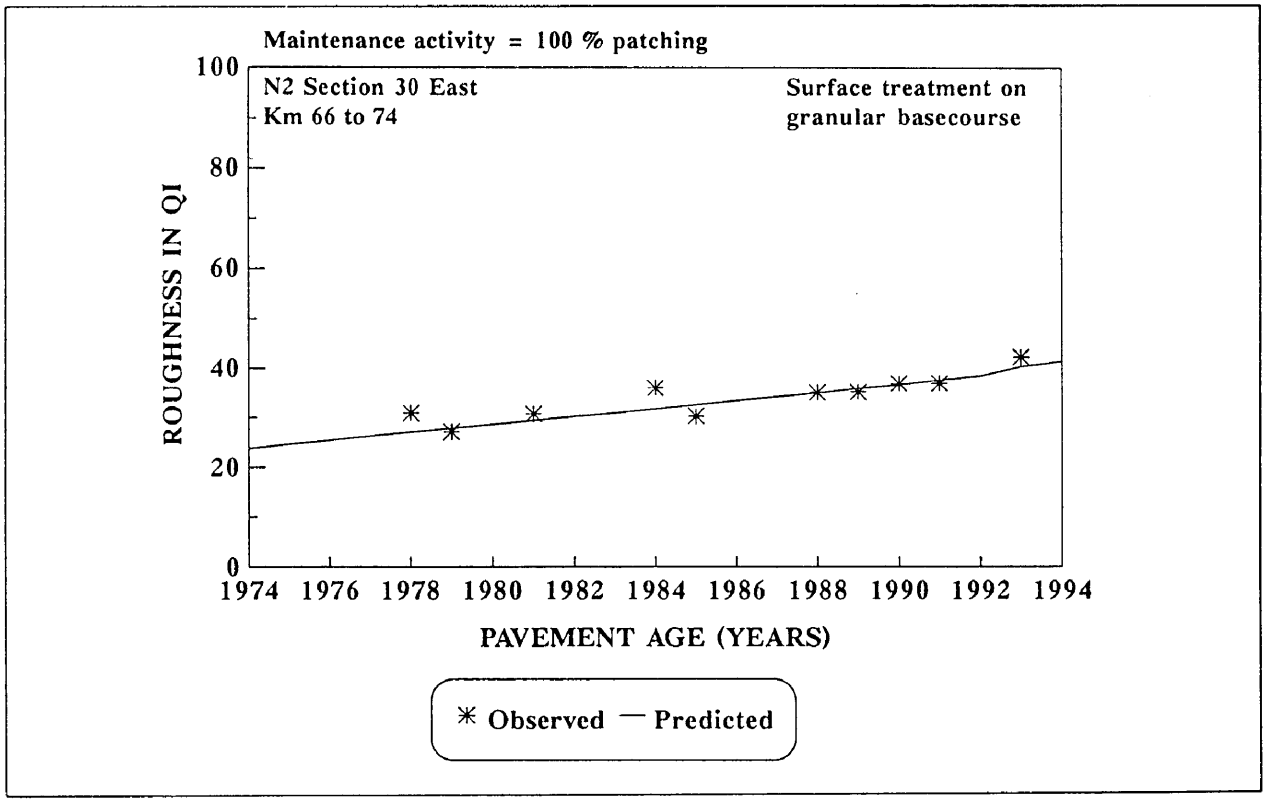

Figure C.50: National route 2 section 30 east from kilometre 66 to 74.

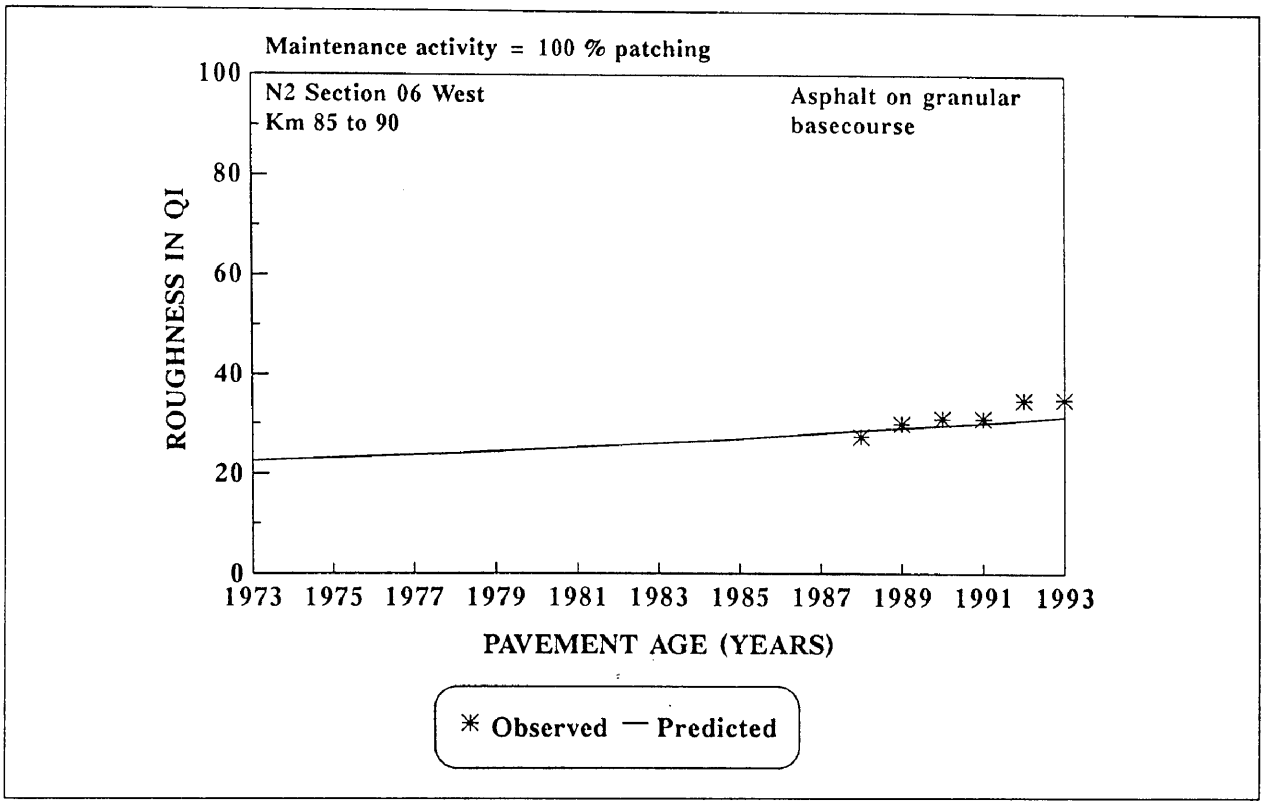

Figure C.51: National route 2 section 06 west from kilometre 85 to 90.

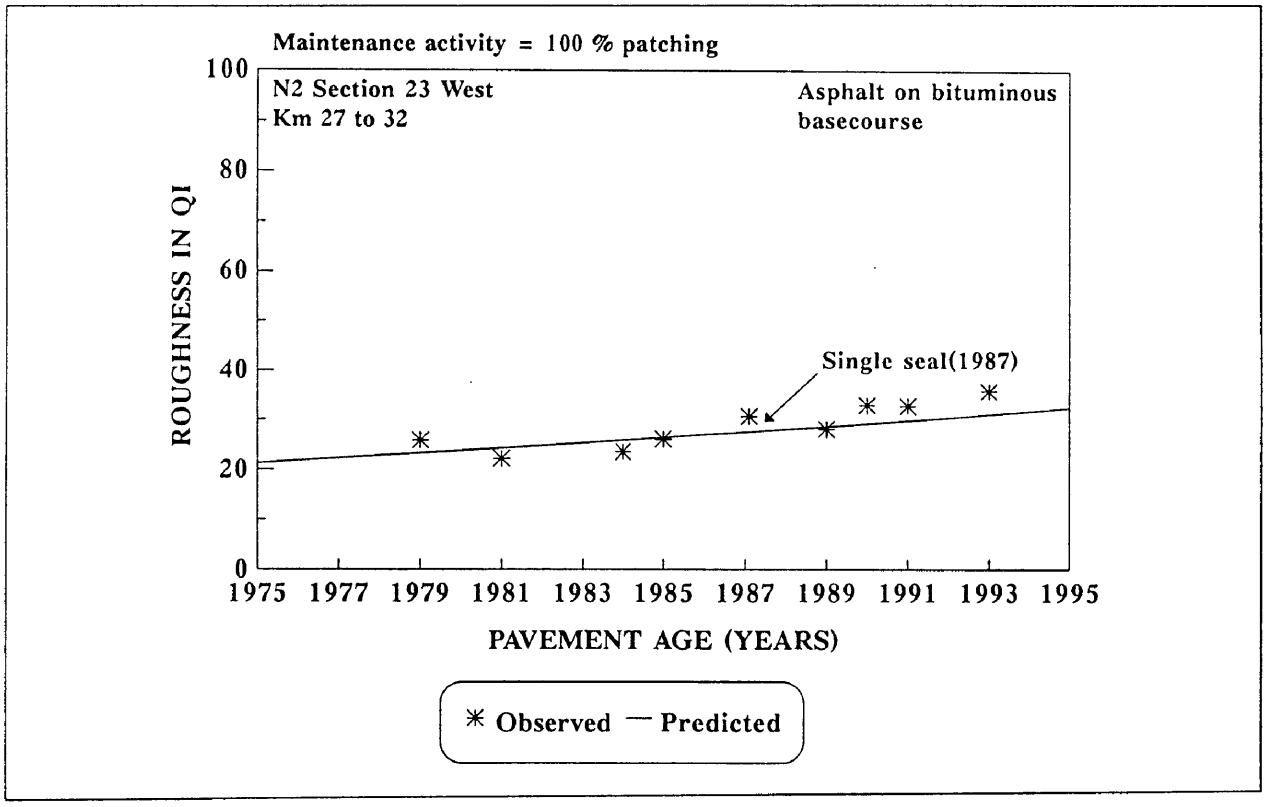

Figure C.52: National route 2 section 23 west from kilometre 27 to 32.

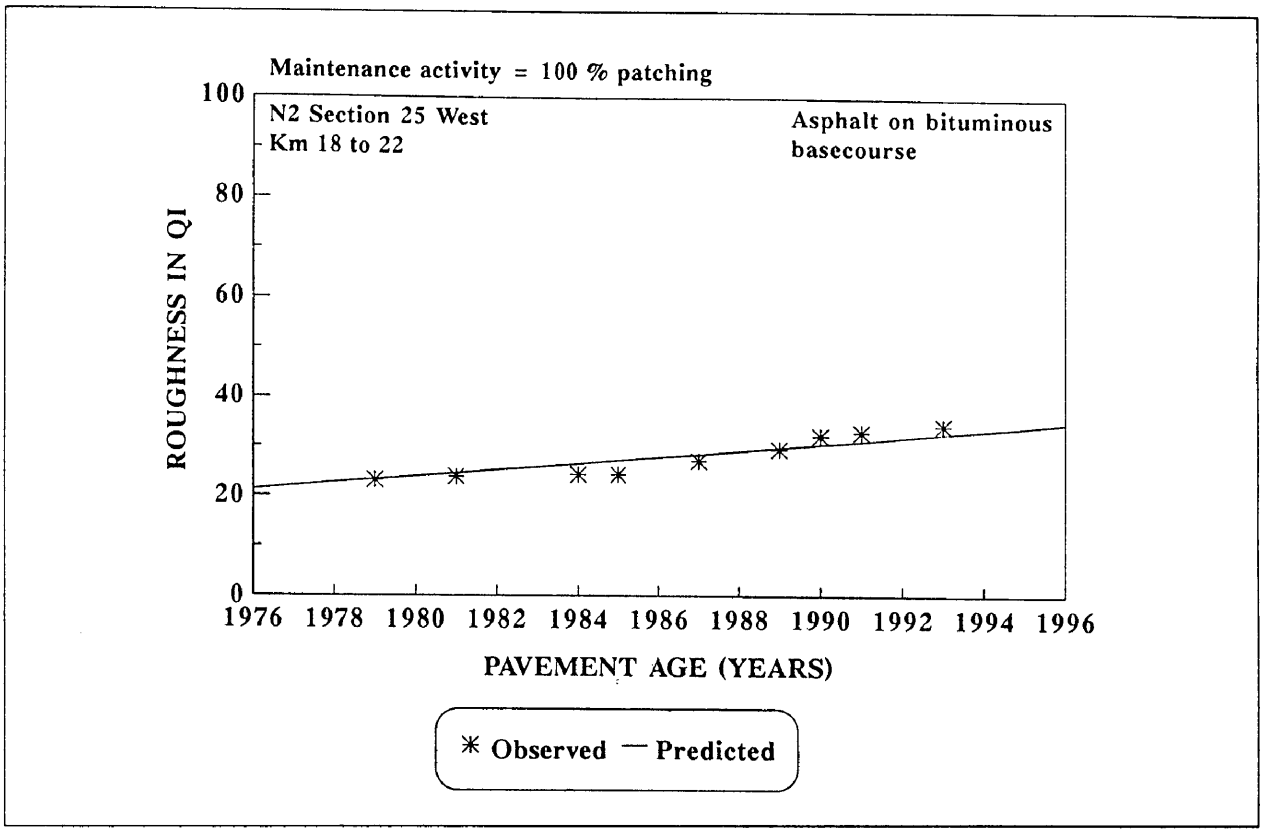

Figure C.53: National route 2 section 25 west from kilometre 18 to 22.

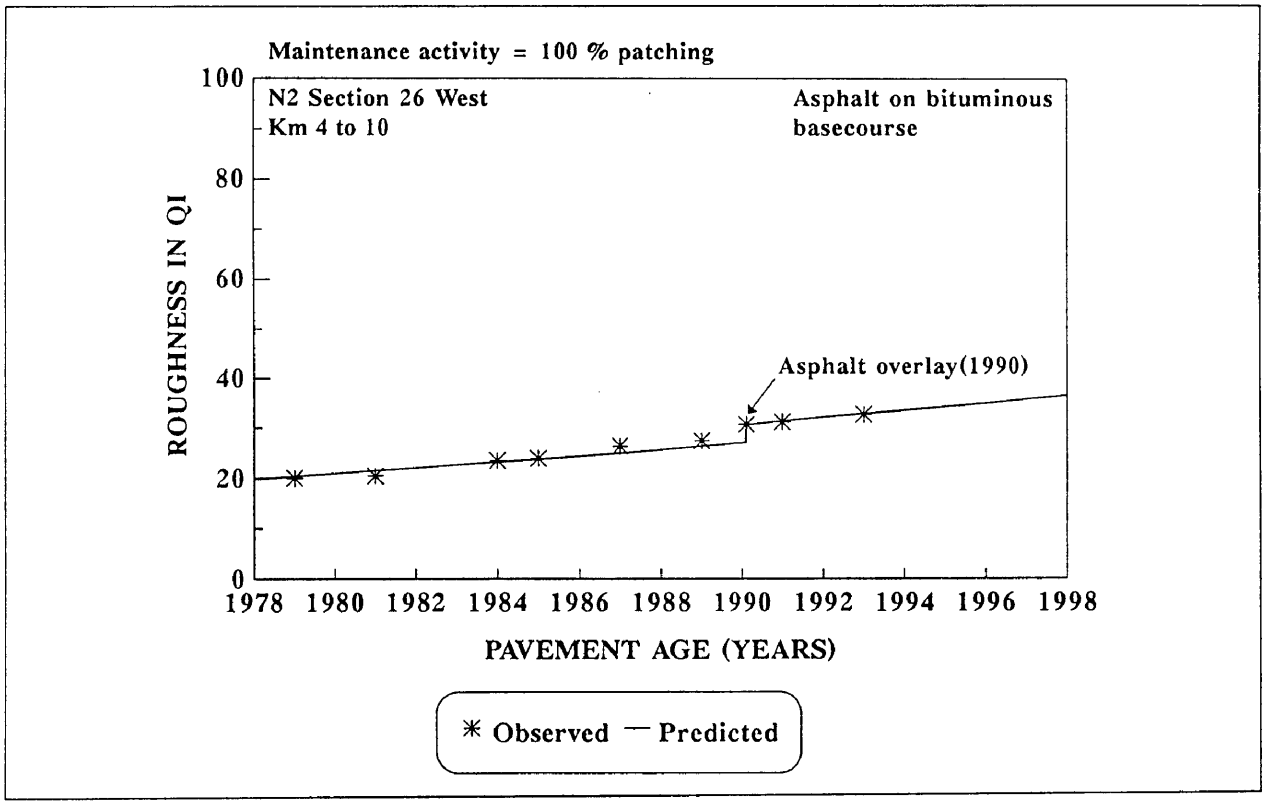

Figure C.54: National route 2 section 26 west from kilometre 4 to 10.

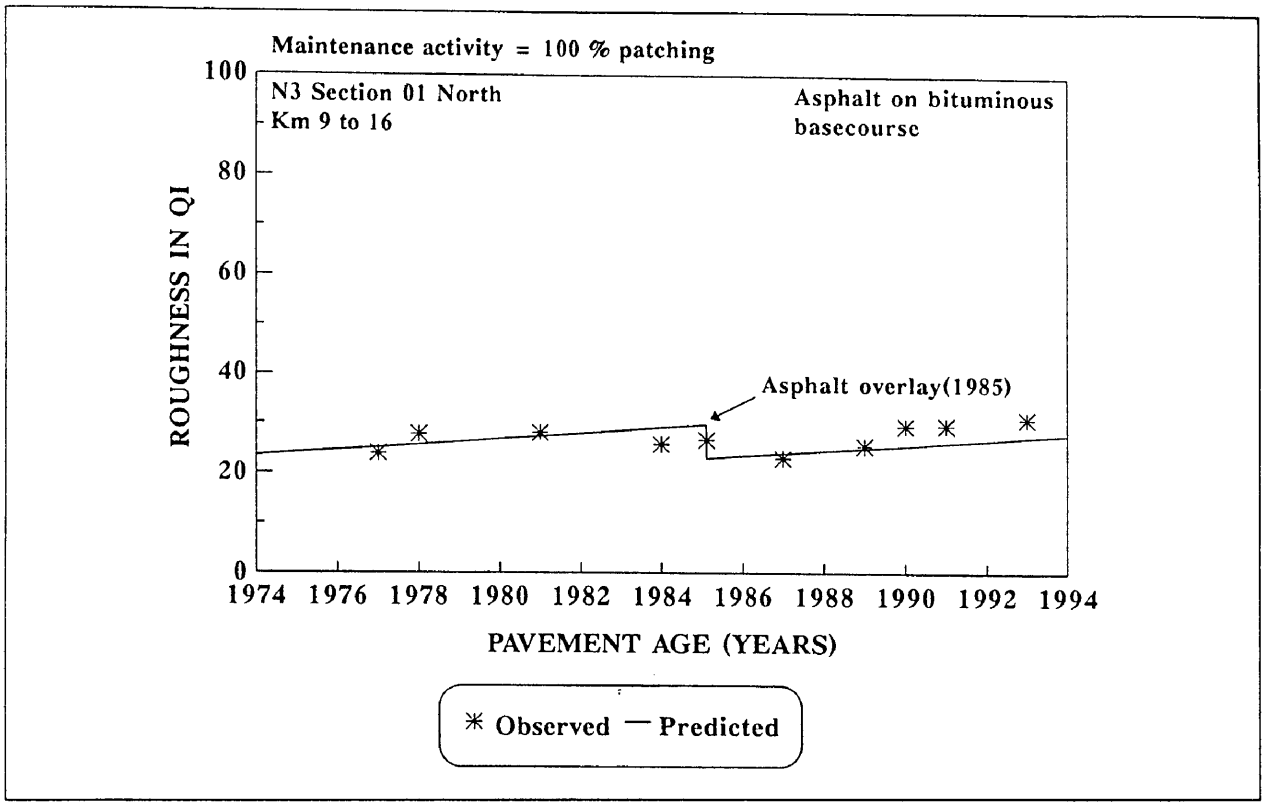

Figure C.55: National route 3 section 1 north from kilometre 9 to 16.

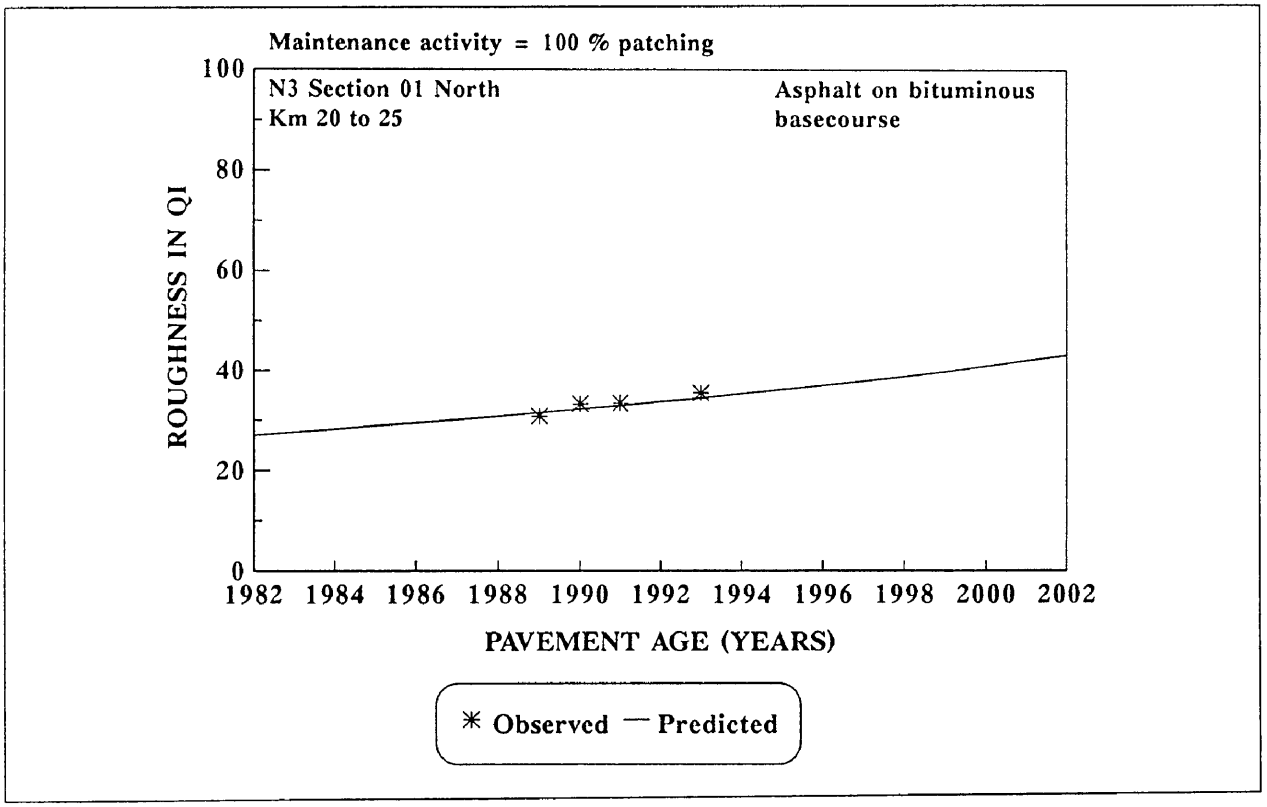

Figure C.56: National route 3 section 1 north from kilometre 20 to 25.

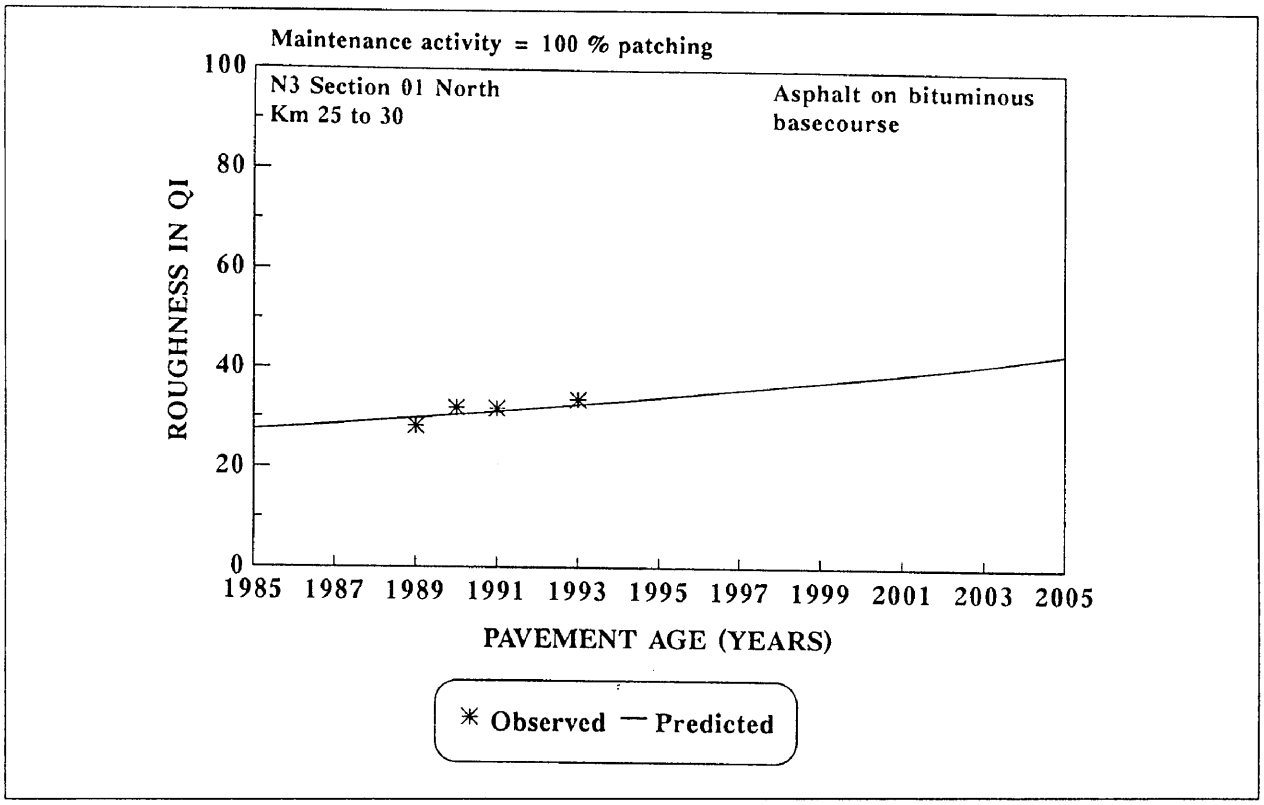

Figure C.57: National route 3 section 1 north from kilometre 25 to 30.

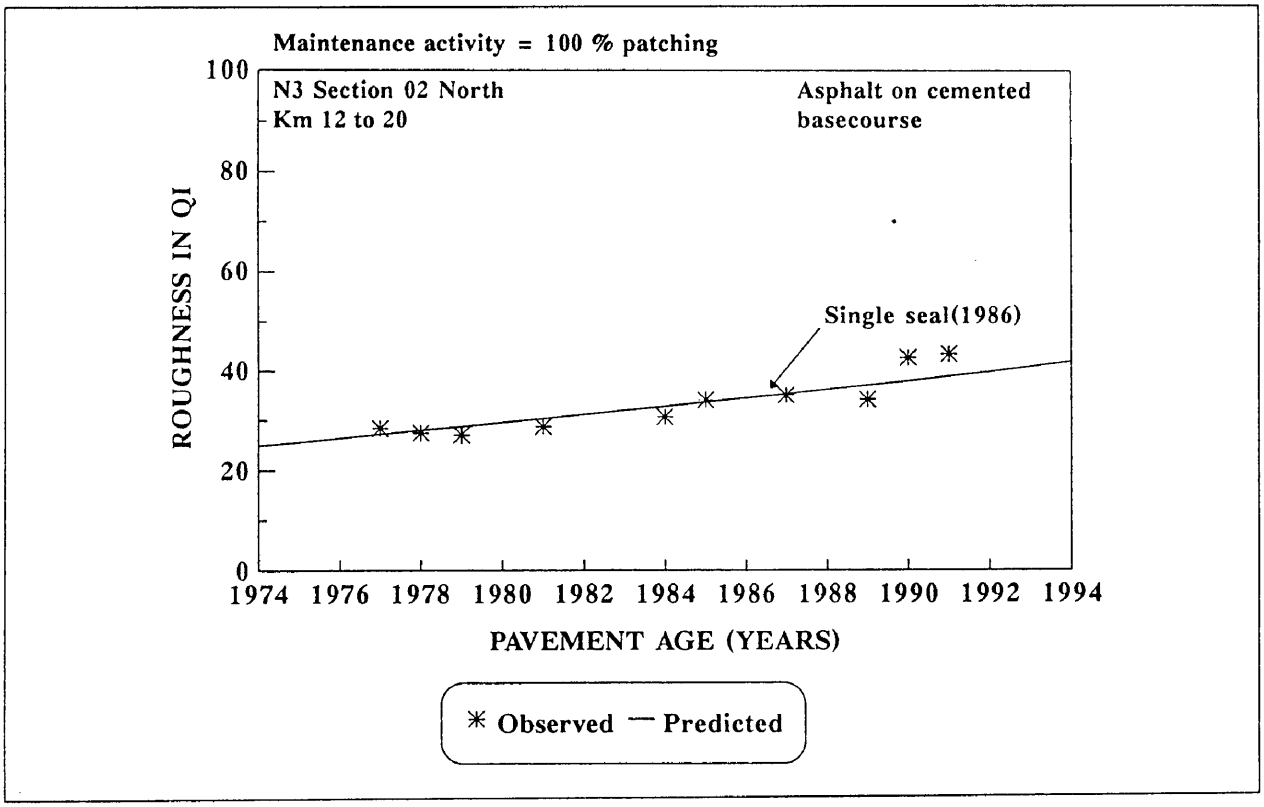

Figure C.58: National route 3 section 2 north from kilometre 12 to 20.

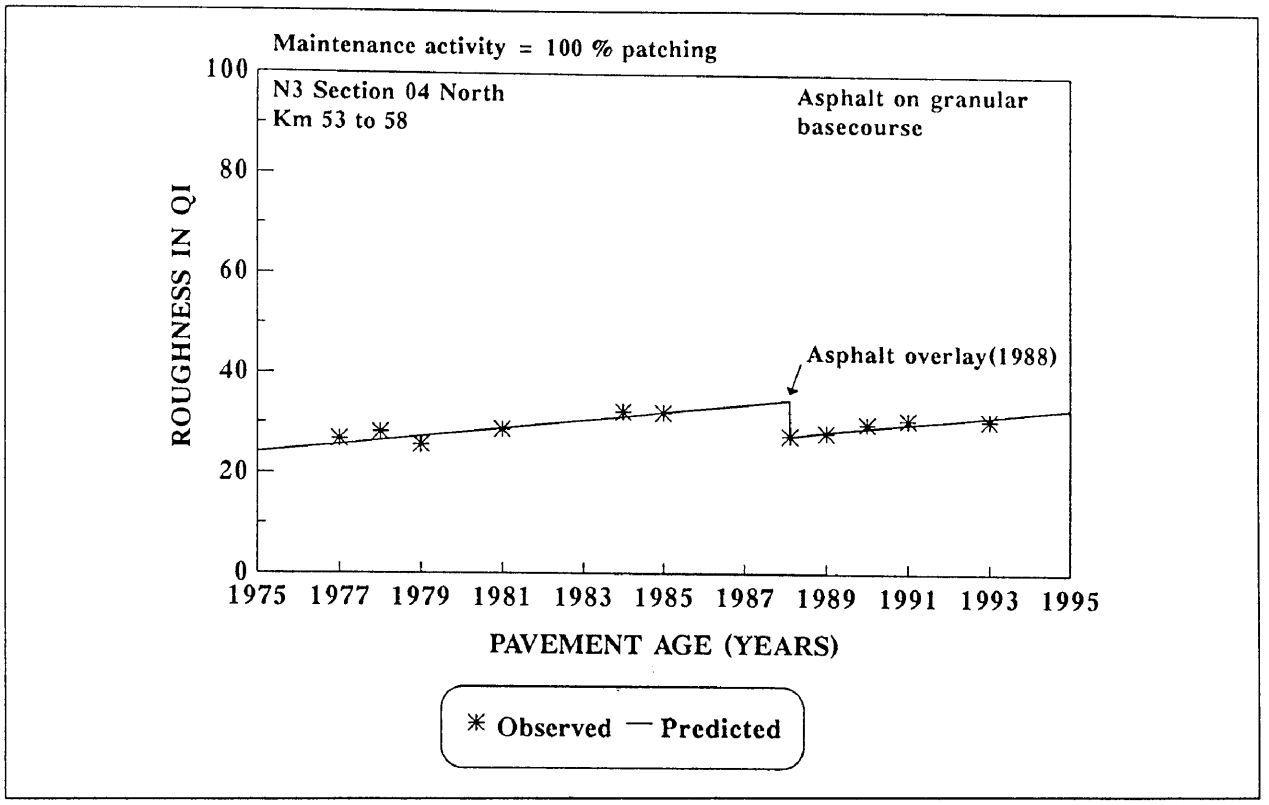

Figure C.59: National route 3 section 4 north from kilometre 53 to 58.

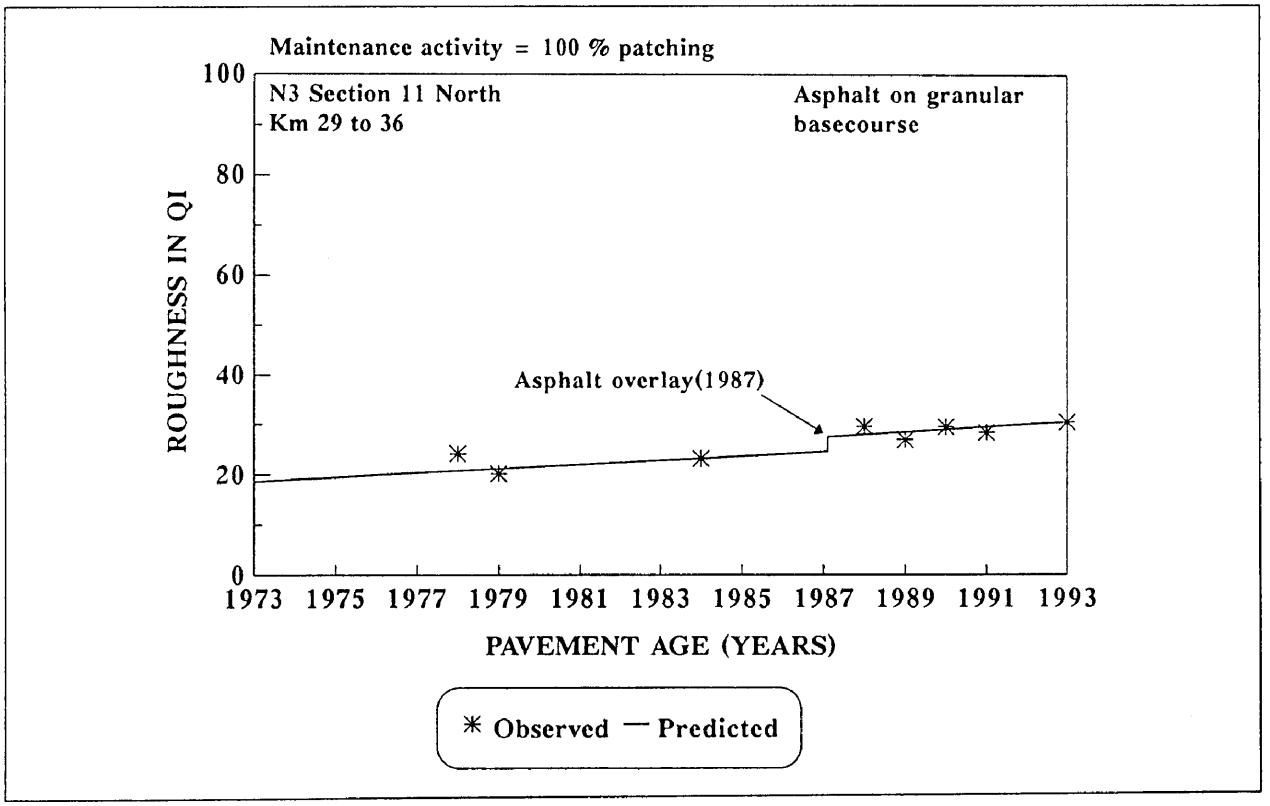

Figure C.60: National route 3 section 11 north from kilometre 29 to 36.

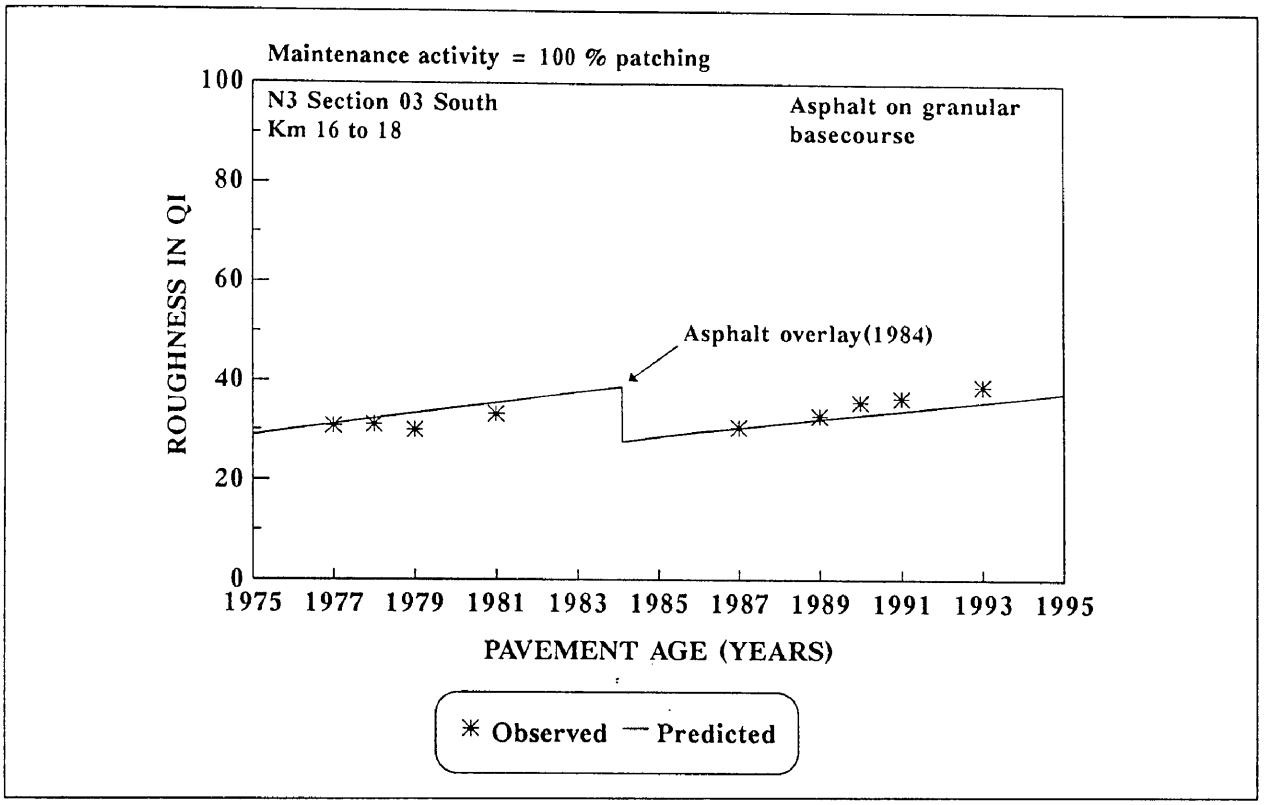

Figure C.61: National route 3 section 3 south from kilometre 16 to 18.

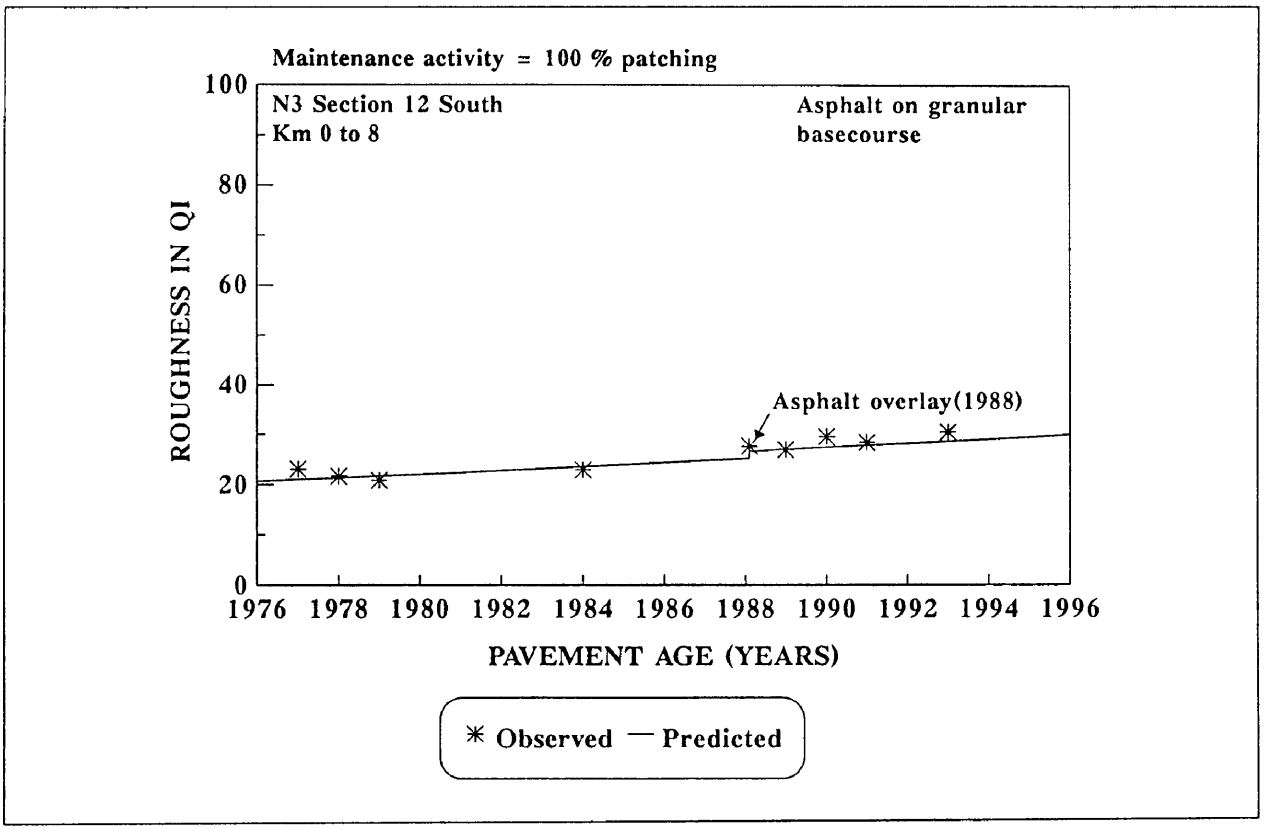

Figure C.62: National route 3 section 12 south from kilometre 0 to 8.

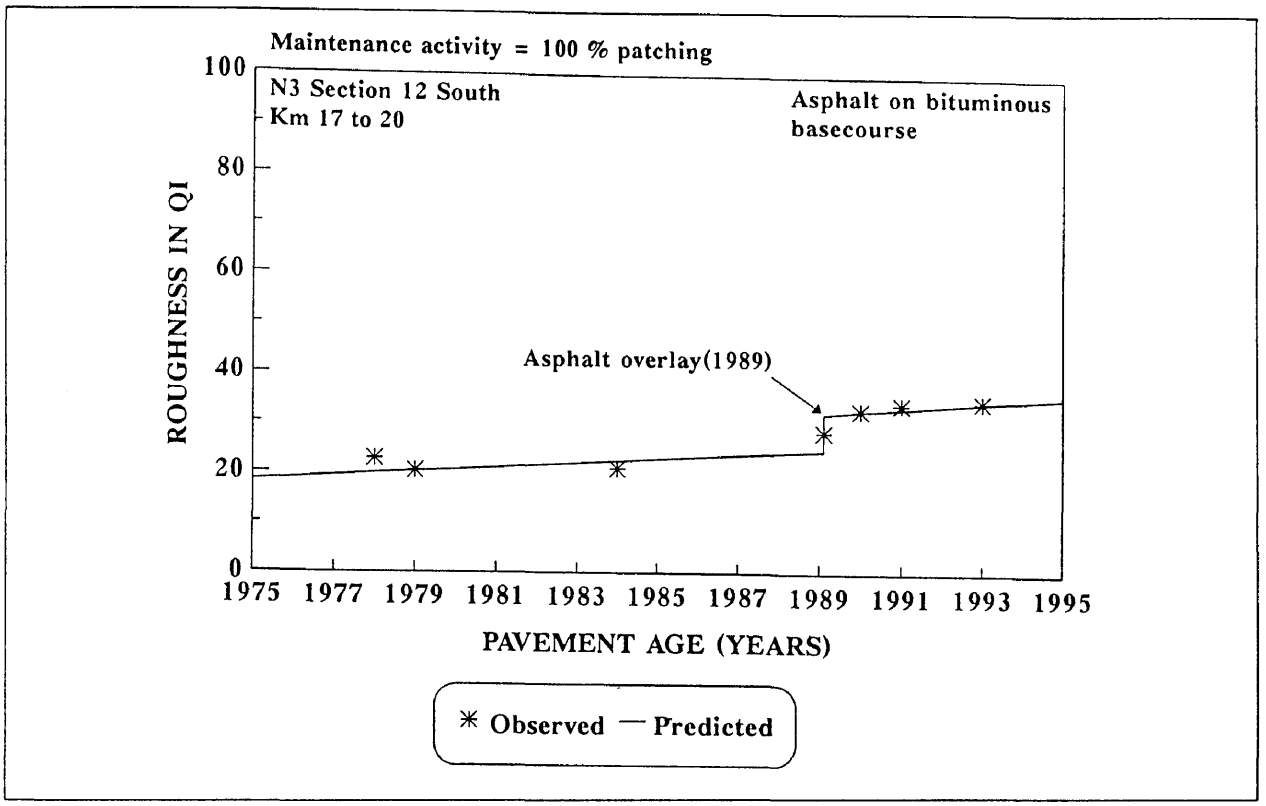

Figure C.63: National route 3 section 12 south from kilometre 17 to 20.

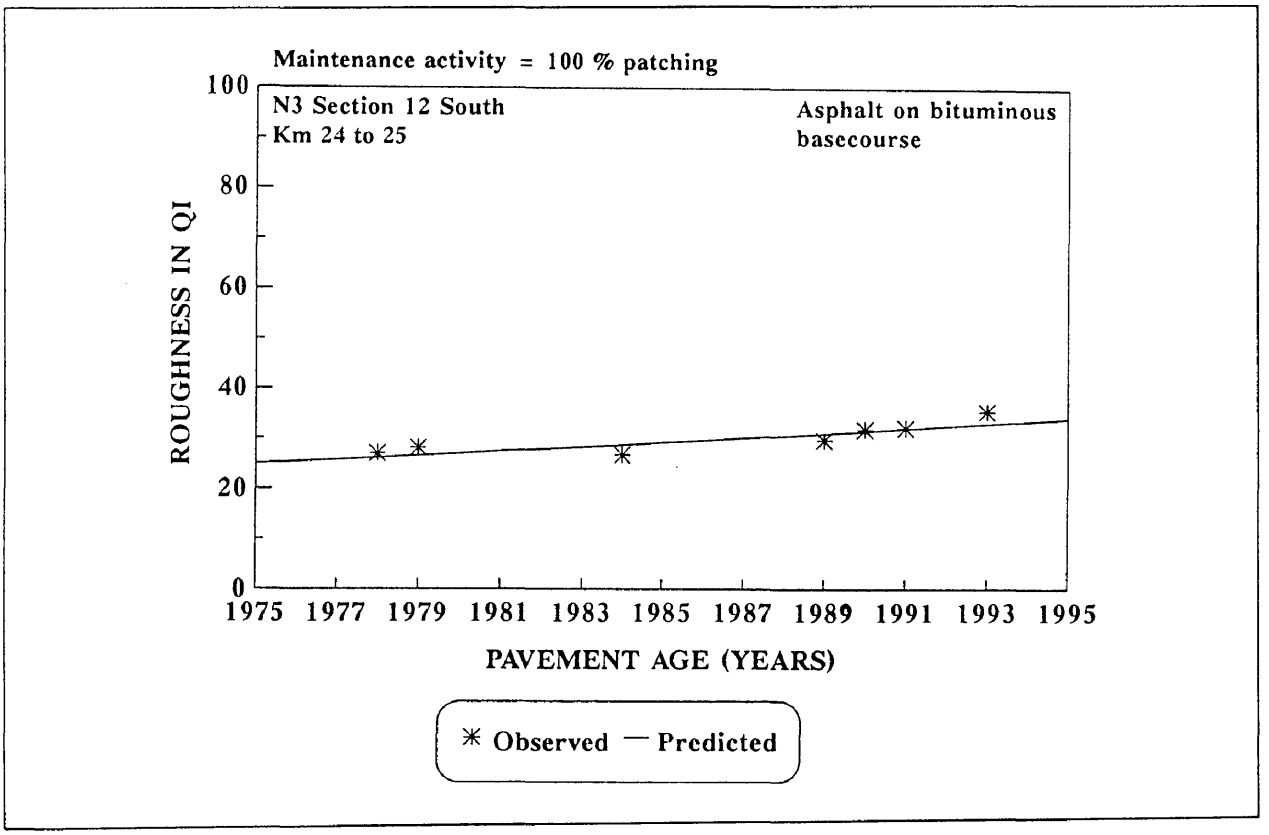

Figure C.64: National route 3 section 12 south from kilometre 24 to 25.

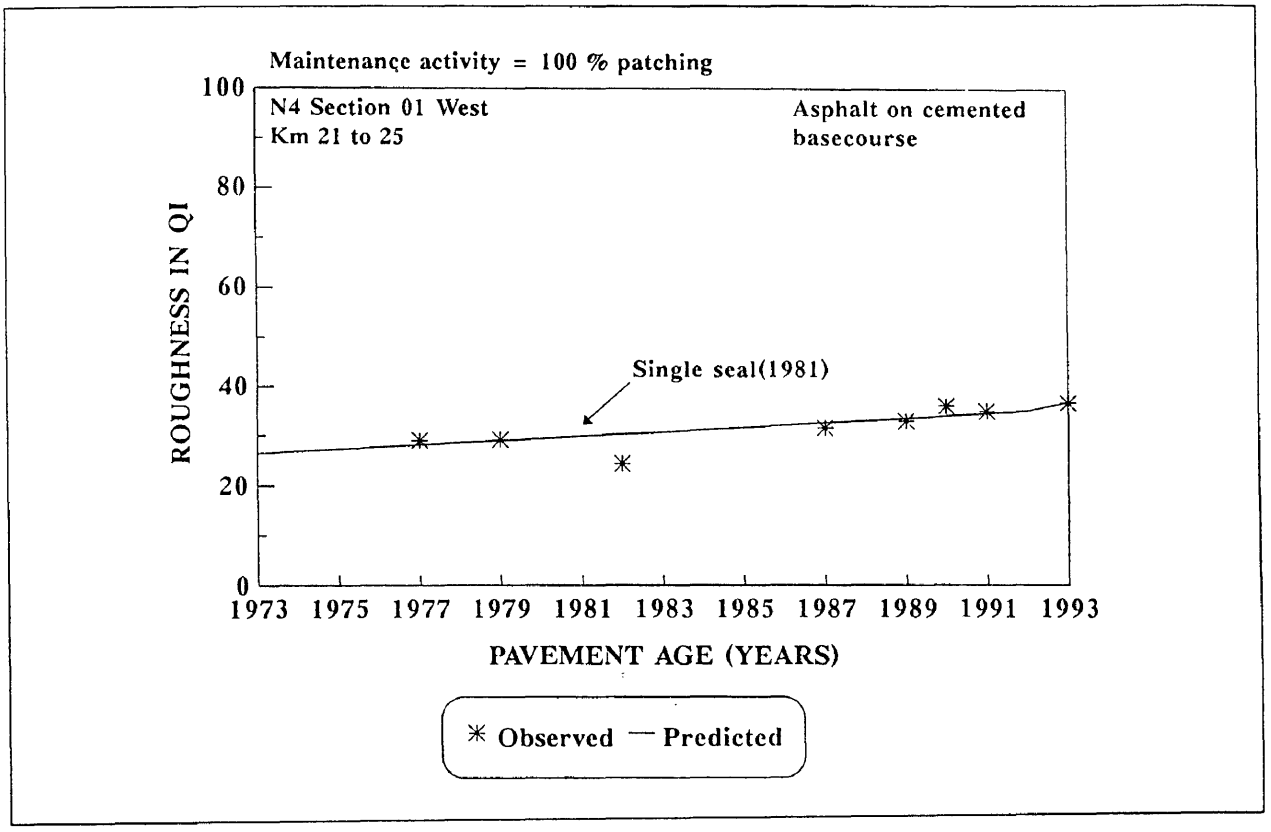

Figure C.65: National route 4 section 1 west from kilometre 21 to 25.